2nd International Energy Conference on Power Options for the Eastern Mediterranean Region

7 - 8 October 2013 | Nicosia, Cyprus

CONFERENCE PROCEEDINGS

2nd Conference on
Power Options for the Eastern Mediterranean Region

Nicosia, Cyprus, 07 - 08/10/2013

The Eastern Mediterranean region currently is facing new developments in the field of hydrocarbon reserves and renewable energy sources (RES). These developments include the licensing of the Cyprus exclusive economic zone that Cyprus Government is negotiating with international key oil and gas companies. Also, Israel is now ready to proceed with the international marketing of its hydrocarbon reserves. Furthermore, seismic data acquisition searches in the exclusive economic zone of Lebanon have shown the probability of discovering large amounts of hydrocarbon reserves. In relation to this, the Cyprus Government has undertaken a diplomatic initiative for solving the political problem of the boundaries settlement between Lebanon, Israel and Cyprus exclusive economic zones. Moreover, the possibility of the development of natural gas liquefaction terminal in Cyprus in cooperation with Noble and Israel will strengthen the cooperation with Israel for exploiting its hydrocarbon reserves and make Cyprus and Israel key players in the international natural gas market. As a result, new industries are expected to be developed in Cyprus, such as chemical industries, by using natural gas as a raw material and this will result in the opening of new jobs with a positive impact in the Cyprus economy.

Regarding RES the new developments concern the discussion for the development of the EuroAsia submerged electric cable which will connect Israel with Cyprus and Europe via Greece that could help the further penetration of RES in the power generation systems of Israel and Cyprus by selling this excess electricity to Europe. Moreover, the introduction of

net metering schemes for households will help the further penetration of photovoltaics in Cyprus and help households to reduce their high electricity bills.

In view of the above developments, the 2nd Conference on Power Options for the Eastern Mediterranean Region (POEM 2013) is already established as an important meeting point for ideas and knowledge sharing on the technical, economic and regulatory implications of energy production in the Eastern Mediterranean region. In an international dimension, the Conference aims to act as a catalyst on the transfer of oil, gas and RES technology advancements and best practices from developed energy markets to the region. Moreover, the Conference hopes to facilitate the exploration of future business opportunities between international and regional energy sector enterprises, in the fields of oil and gas energy infrastructure and RES projects. Finally, the Conference aims to highlight the necessity of research and development in the further advancement of the energy sector in the Eastern Mediterranean region.

Focusing on a regional and local dimension, the Conference aims to provide insights into how local energy players can accommodate the sustainable use of the potential Eastern Mediterranean region's hydrocarbon reserves together with the penetration of solar energy systems in the power electricity generation industry. Moreover, local business representatives will have a chance to be updated on the latest developments in RES technologies, to evaluate the commercial and financial aspects of these technologies as well as to be updated on the energy projects which are expected to be developed in Cyprus during the following years.

Special sessions on solar energy technologies have been integrated within POEM 2013 Conference. These sessions, which are focusing on the cogeneration of desalinated water with renewable energy sources electricity production, are part of the research program STEP-EW that is funded by the Cross-border Cooperation Program Greece-Cyprus 2007-2013. These sessions include topics regarding desalination methods as well as operational plants in the Eastern Mediterranean region, thermal storage technologies with renewable energy sources and cogeneration techniques for desalination with renewable energy sources.

Prof. Andreas Poullikkas
Nicosia, Cyprus
October 2013

Conference Chair

Conference Chairman
Prof. Poullikkas Andreas
American University of Sharjah and Electricity Authority of Cyprus

Secretary
Mr. Hadjipaschalis Ioannis
Electricity Authority of Cyprus

Treasurer
Mr. Kourtis George
Electricity Authority of Cyprus

Conference Steering Committee

- Dr. Christodoulides Christos, *Director, Transmission System Operator*
- Prof. Christofides Costas, *Rector, University of Cyprus*
- Mr. Christofides Costas, *Assistant Director General OEB*
- Dr. Efthimiou Venizelos, Executive *Networks Manager, Electricity Authority of Cyprus*
- Prof. Onoufriou Toula, *Vice Rector for Academic Affairs, Cyprus University of Technology*
- Prof. Papanastasiou Panos, *Dean of School of Engineering, University of Cyprus*
- Prof. Papanicolas Costas, *President, Cyprus Institute*
- Mr. Patsalis Antonis, *Executive Generation Manager, Electricity Authority of Cyprus*
- Mr. Shammas George, *Chairman, Cyprus Energy Regulatory Authority*
- Dr. Stylianou Stelios, *General Manager, Electricity Authority of Cyprus*

Conference Scientific Committee

- Dr. Bonanos Aris, *Cyprus Institute, Cyprus*
- Prof. Charalambides Alexandros, *Cyprus University of Technology, Cyprus*
- Ms. Charalambous Anthi, *Cyprus Energy Agency, Cyprus*
- Prof. Charalambous A. Charalambos, *University of Cyprus, Cyprus*
- Prof. Christodoulou Christodoulos, *Frederick University, Cyprus*
- Prof. Demokritou Philip, *Harvard University, USA*
- Dr. Fokaides Paris, *University of Cyprus, Cyprus*
- Prof. Georghiades John, *University of Illinois, USA*
- Prof. Georghiou George, *University of Cyprus, Cyprus*
- Prof. Hadjiargyriou Nicos, *National Technical University of Athens, Greece*
- Prof. Kalogirou Soteris, *Cyprus University of Technology, Cyprus*
- Prof. Karageorgis George, *Frederick University, Cyprus*
- Prof. Kyriakides Elias, *University of Cyprus, Cyprus*
- Prof. Michaelides Ioannis, *Cyprus University of Technology, Cyprus*
- Prof. Mitsos Alexandros, *Aachen University, Germany*
- Dr. Peteves Efstathios, *Institute for Energy, Joint Research Center, EC*
- Prof. Sourkounis Constantinos, *Ruhr-University of Bochum, Germany*
- Dr. Tzimas Evangelos, *Institute for Energy, Joint Research Center, EC*
- Dr. Tzamtzis George, *Cyprus Institute, Cyprus*
- Prof. Zachariades Theodoros, *Cyprus University of Technology, Cyprus*

Invited Speakers

Cyprus's Energy Strategy - The views of Cyprus Political Parties

- **Mr. Prodromos Prodromou**, Member of Parliament, Democratic Rally of Cyprus
- **Mr. Andros Kyprianou**, General Secretary of the Central Committee, Progressive Party for the Working People
- **Mr. Angelos Votsis**, Member of Parliament, Democratic Party
- **Mr. Pambis Christodoulides**, Member of Central Committee, Socialists Democratic Party
- **Mrs. Eleni Chrysostomou**, Press Officer, Cyprus Green Party
- **Mr. Demetris Syllouris**, President, European Party Cyprus
- **Mr. Alexandros Michaelides**, Press Officer, Citizens Alliance Party

Invited Speakers

- **Prof. Mohamed Gadalla**, American University of Sharjah, UAE, *The large scale integration of solar energy in UAE*
- **Prof. Soteris Kalogirou**, Cyprus University of Technology, Cyprus, *Building Integration of Solar Thermal Systems (BISTS)*
- **Prof. Constantinos Sourkounis**, Ruhr University Bochum, Germany, *Developments in power trains for wind energy converters*
- **Dr. Stelios Stylianou**, Electricity Authority of Cyprus, Cyprus, *EAC planning for renewable energy sources generation*
- **Mr. Marios Tannousis**, Cyprus Investment Promotion Agency, Cyprus, *Cyprus an attractive investment destination*
- **Prof. Theodoros Zachariades**, Cyprus University of Technology, Cyprus, *Analyzing energy policy options in Cyprus with a suite of energy-economy models*

Conference Program

Monday, 07 October 2013	
08:30	**Registration**
	Opening Ceremony
09:15	**Welcome coffee and Welcome notes** *Chairperson: Prof. Ioannis Michaelides*
	Mr. Constantinos Yiorkadjis, *Mayor of Nicosia* Mr. George Shammas, *Chairman of Cyprus Energy Regulatory Authority* Mr. Charalambos Tsouris, *Chairman of Board of Directors, Electricity Authority of Cyprus* Prof. Costas Papanicolas, *President, Cyprus Institute* Mr. Akis Ellinas, *President, Cyprus Wind Energy Association* Mr. Philios Zachariades, *Chairman of Cyprus Employers and Industrialists Federation* Prof. Andreas Poullikkas, *Conference Chairman, American University of Sharjah and Electricity Authority of Cyprus*
10:20	**Plenary session I (Cyprus's Energy Strategy - The views of Cyprus Political Parties)**
	Chairperson: Prof. Christodoulos Christodoulou
10:20	Mr. Prodromos Prodromou, *Member of Parliament, Democratic Rally of Cyprus*
10:35	Mr. Andros Kyprianou, *General Secretary of the Central Committee, Progressive Party for the Working People*
10:50	Mr. Angelos Votsis, *Member of Parliament, Democratic Party*
11:05	Mr. Pambis Christodoulides, *Member of Central Committee, Socialists Democratic Party*
11:20	**Coffee Break**
11:40	**Plenary session II (Cyprus's Energy Strategy - The views of Cyprus Political Parties)**
	Chairperson: Prof. Christodoulos Christodoulou
11:40	Mrs. Eleni Chrysostomou, *Press Officer, Cyprus Green Party*
11:55	Mr. Demetris Syllouris, *President, European Party of Cyprus*
12:10	Mr. Alexandros Michaelides, *Press Officer, Citizens Alliance Party*
12:25	**Lunch Break**
13:30	**Keynote lecture** *Chairperson: Prof. George Karageorgis* **EAC planning for renewable energy sources generation** ***Dr. Stelios Stylianou**, Electricity Authority of Cyprus, Cyprus*

Conference Program

Monday, 07 October 2013		
14:00	**Plenary session III**	
	Special session: Energy policy and security aspects in Eastern Mediterranean *Chairpersons: Prof. Achilles Emilianides, Prof. Paris Fokaides*	
14:00	Energy security in the Eastern Mediterranean regional security complexes (Paper No. POEM13/168) *C. Adamides, O Christou (Cyprus)*	
14:15	The Cypriot hydrocarbons and the European financial crisis (Paper No. POEM13/169) *C. Ioannou, A Emilianides (Cyprus)*	
14:30	The feasibility and impact of the Turkish-Israeli "Rapprochement" on the geopolitics of the Eastern Mediterranean (Paper No. POEM13/170) *T. Tsakiris (Cyprus)*	
14:45	Escapades at sea: sovereignty, legality and machismo in the Eastern Mediterranean (Paper No. POEM13/171) *C. Constantinou (Cyprus)*	
15:00	European roadmap for energy and the role of Cyprus hydrocarbons (Paper No. POEM13/173) *P. Fokaides (Cyprus)*	
15:15	**Coffee Break**	
15:45	**Keynote lecture** *Chairperson: Prof. Paris Fokaides* **Cyprus an attractive investment destination** ***Marios Tannousis**, Cyprus Investment Promotion Agency, Cyprus*	
16:15	**Technical sessions**	
	Special session: The use of data for power system monitoring and control *Chairperson: Prof. Elias Kyriakides*	**Special session: Impacts of climate change on electricity needs in the Mediterranean** *Chairperson: Prof. Manfred Lange*
16:15	From sensors and measurements, to data and applications in power systems (Paper No. POEM13/183) *I. Ciornei, P. Mavroeidis, G. Pieri, E. Kyriakides (Cyprus)*	Anticipated impacts of climate change of electricity demand of Athens, Greece (Paper No. POEM13/174) *C. Giannakopoulos (Greece)*
16:30	A power system controlled islanding scheme for emergency control (Paper No. POEM13/184) *J. Quirós-Tortós, V. Terzija (United Kingdom)*	Small scale thermal solar district units for Mediterranean communities - The STS-MED project (Paper No. POEM13/175) *N. Fylaktos (Cyprus)*
16:45	Measurement data aggregation in power systems – challenges and opportunities (Paper No. POEM13/185) *A. M. Dumitrescu, M. Calin, M. Albu (Romania)*	Climate change and expected enhanced urban heat-island effects (Paper No. POEM13/176) *P. Hadjinicolaou (Cyprus)*
17:00	Application of synchronized measurement technology in the Cyprus power transmission system (Paper No. POEM13/151) *M. Asprou, Y. Yiasemi, E. Kyriakides, Y. Ioannou, A. Petousis, M. Michael, S. Stavrinos (Cyprus)*	Assessment of increasing electricity demand for space cooling under climate change condition in the Eastern Mediterranean (Paper No. POEM13/177) *M. Lange (Cyprus)*
17:15	Dynamic fault studies of an offshore four-terminal VSC-HVDC grid utilizing protection means through AC/DC circuit breakers (Paper No. POEM13/186) *M. Hadjikypris, V. Terzija (United Kingdom)*	A review of innovative measures to reduce energy consumption in the urban built environment (Paper No. POEM13/178) *M. Santamouris (Greece)*
17:30	**End of Day 1**	

Conference Program

<table>
<tr><th colspan="3">Tuesday, 08 October 2013</th></tr>
<tr><td>08:00</td><td colspan="2">Registration</td></tr>
<tr><td>08:45</td><td colspan="2">Conference announcements</td></tr>
<tr><td>09:00</td><td colspan="2">Keynote lecture
Chairperson: Dr. Andreas Stavrou

Developments in power trains for wind energy converters
Prof. Constantinos Sourkounis, Ruhr-University of Bochum, Germany</td></tr>
<tr><td>09:30</td><td colspan="2">Technical sessions</td></tr>
<tr><td></td><td>Special session: Solar thermal cogeneration of electricity and water: The STEP-EW project
Chairperson: Prof. Aris Bonanos</td><td>Energy systems I
Chairperson: Prof. Theodoros Zachariades</td></tr>
<tr><td>09:30</td><td>Design of a solar thermal co-generation demonstrator (Paper No. POEM13/179)
G. Tzamtzis (Cyprus)</td><td>Impact of the Euro-Asia Interconnector project on the economic operation of Crete and Cyprus power systems (Paper No. POEM13/153)
A. Antoniou, N. Theodorou (Cyprus), A. Tsikalakis, K. Kalaitzakis, G. Stavrakakis (Greece)</td></tr>
<tr><td>09:45</td><td>Optical design of an integrated receiver and storage system (Paper No. POEM13/180)
C. Marakkos (Cyprus)</td><td>Action steps for refining the Cyprus national action plan on RES penetration for electricity generation – Should we reconsider? (Paper No. POEM13/158)
A. Nikolaidis, C. Charalambous (Cyprus)</td></tr>
<tr><td>10:00</td><td>Cost-benefit analysis for the installation of cogeneration CSP technology in Cyprus (Paper No. POEM13/166)
A. Poullikkas, G. Kourtis, I. Hadjipaschalis (Cyprus)</td><td>A software tool to evaluate the total ownership cost of distribution transformers (Paper No. POEM13/160)
A. Lazari, C. Charalambous (Cyprus)</td></tr>
<tr><td>10:15</td><td>Techno-economic analysis of a co-generation solar thermal plant (Paper No. POEM13/181)
N. Fylaktos (Cyprus)</td><td>Integration of quick charging stations for e-mobility in power grids of weak infrastructure and high impact of renewable energies (Paper No. POEM13/162)
C. Sourkounis, N. Becker, A. Broy, F. Einwächter (Germany)</td></tr>
<tr><td>10:30</td><td>Thermal desalination performance analysis (Paper No. POEM13/182)
M. Georgiou (Cyprus)</td><td></td></tr>
<tr><td>10:45</td><td colspan="2">Coffee Break</td></tr>
<tr><td>11:15</td><td colspan="2">Keynote lecture
Chairperson: Dr. George Tzamtzis

The large scale integration of solar energy in UAE
Prof. Mohamed Gadalla, American University of Sharjah, UAE</td></tr>
</table>

Conference Program

Tuesday, 08 October 2013		
11:45	**Technical sessions**	
	Special session: Current research at Archimedes solar energy laboratory *Chairperson: Prof. Soteris Kalogirou*	**Energy Systems II** *Chairperson: Prof. Alexandros Charalambides*
11:45	Experimental investigation of the thermosiphonic phenomenon in domestic solar water heaters (Paper No. POEM13/187) *S. Kalogirou, G. Panayiotou, G. Florides, G. Roditis, N. Katsellis, A. Constantinou, P. Kyriakou, Y. Vasiades, A. Michaelides (Cyprus), T. Parisis (Greece), J. E. Nielsen (Denmark)*	Design rules for autonomous hybrid energy supply systems for various types of buildings in central Europe (Paper No. POEM13/163) *A. Broy, I. Vasileva, C. Sourkounis (Germany)*
12:00	Theoretical study of the application of Phase Change Materials (PCM) on the envelope of a typical dwelling in Cyprus (Paper No. POEM13/188) *G. Panayiotou, S. Kalogirou, S. Tassou (Cyprus)*	Concept of energy extraction from sludge of a clarification plant (Paper No. POEM13/161) *N. Becker, C. Sourkounis (Germany)*
12:15	Experimental evaluation of Phase Change Materials (PCM) for energy storage in solar water heating systems (Paper No. POEM13/189) *S. Kalogirou, G. Panayiotou, V. Antoniou (Cyprus)*	Storage solutions for power quality problems of the distribution network (Paper No. POEM13/165) *A. Poullikkas, S. Papadouris, G. Kourtis, I. Hadjipaschalis (Cyprus)*
12:30	Experimental investigation of the performance of a parabolic trough collector (PTC) installed in Cyprus (Paper No. POEM13/190) *S. Kalogirou, G. Panayiotou (Cyprus)*	Technical and feasibility analysis of gasoline and natural gas fuelled vehicles (Paper No. POEM13/154) *C. Chasos, G. Karagiorgis, C. Christodoulou (Cyprus)*
12:45	Optimization of Thermosiphon Solar Water Heaters working in a Mediterranean Environment (Paper No. POEM13/191) *S. Kalogirou, R. Agathokleous (Cyprus)*	
13:00	Evaluation of the solar cooling and heating system of the CUT mechanical engineering laboratories (Paper No. POEM13/167) *S. Kalogirou, F. Francou, G. Florides (Cyprus)*	
13:15	**Lunch Break**	
14:30	**Keynote lecture** *Chairperson: Prof. Constantinos Sourkounis* **Analyzing energy policy options in Cyprus with a suite of energy-economy models** ***Prof. Theodoros Zachariades**, Cyprus University of Technology, Cyprus*	

Conference Program

Tuesday, 08 October 2013		
15:00	**Keynote lecture** *Chairperson: Prof. Constantinos Sourkounis* **Building Integration of Solar Thermal Systems (BISTS)** ***Prof. Soteris Kalogirou**, Cyprus University of Technology, Cyprus*	
15:30	**Technical sessions**	
	RES systems *Chairperson: Prof. Charalambos Chasos*	**Special session: Current research at Cyprus Energy Agency** *Chairperson: Ms. Anthi Charalambous*
15:30	On the power control techniques of DFIG: From conventional to a novel BELBIC scheme (Paper No. POEM13/155) *M. Valikhani, C. Sourkounis (Germany)*	Increase of energy efficiency in 25 low income houses in Cyprus – a holistic approach (Paper No. POEM13/192) *G. Panayiotou, A. Charalambous, S. Vlachos, O. Kyriacou, E. Theofanous, T. Filippou (Cyprus)*
15:45	Operation of wind energy conversion systems with Doubly-Fed induction generators during asymmetrical voltage dips (Paper No. POEM13/159) *P. Tourou, C. Sourkounis (Germany)*	Promotion of PV energy through net metering optimization (Paper No. POEM13/193) *M. Hadjipanayi (Cyprus)*
16:00	Over-irradiance due to the presence of clouds (Paper No. POEM13/152) *R. Tapakis, A. Charalambides (Cyprus)*	Production of biodiesel from microalgae in selected Mediterranean countries (Paper No. POEM13/194) *A. Charalambous (Cyprus), N. Gamal (Egypt)*
16:15		Towards low carbon homes through energy renovations (Paper No. POEM13/195) *G. Panayiotou, M. Ioannidou, A. Charalambous (Cyprus)*
16:30	**End of Conference**	

Special Sessions on Solar Energy Technologies

Special sessions on solar energy technologies will be integrated within POEM 2013 Conference. These sessions, which are focusing on the cogeneration of desalinated water with renewable energy sources electricity production, are part of the research program STEP-EW which is funded by the Cross-border Cooperation Program Greece-Cyprus 2007-2013.

The STEP-EW project (www.step-ew.eu) examines the possibility of cogeneration of desalinated water and electricity. In detail, the project's objective is to build a pilot solar thermal cogeneration unit in Cyprus, which will be based on a feasibility study already carried out by the Cyprus Institute for a similar plant. The construction will confirm the technical feasibility of the innovative idea of cogeneration of desalinated water and electricity by using concentrated solar energy on a small scale and realistic environmental and operating conditions. The proposed technology is extremely important, particularly for areas that are isolated from continental electricity networks and with limited water resources, such as the Mediterranean islands. The cogeneration unit will have the ability to reliably and consistently produce water and electricity according to specific needs. The construction and operation of the unit will confirm that the technology is mature enough to be commercially used and will highlight potential need in subsystems that need further development.

The Special Sessions are:

- Energy policy and security aspects in Eastern Mediterranean
- Impacts of climate change on electricity needs in the Mediterranean
- Solar thermal cogeneration of electricity and water: The STEP-EW project
- The use of data for power system monitoring and control
- Current research at Archimedes solar energy laboratory
- Current research at Cyprus Energy Agency

Το Πρόγραμμα συγχρηματοδοτείται από την Ευρωπαϊκή Ένωση (ΕΤΠΑ) και από Εθνικούς Πόρους της Ελλάδας και της Κύπρου
ΕΛΛΗΝΙΚΗ ΔΗΜΟΚΡΑΤΙΑ ΕΥΡΩΠΑΪΚΗ ΕΝΩΣΗ ΚΥΠΡΙΑΚΗ ΔΗΜΟΚΡΑΤΙΑ
Πρόγραμμα Διασυνοριακής Συνεργασίας Ελλάδα - Κύπρος 2007-2013
ΕΠΕΝΔΥΟΥΜΕ ΣΤΟ ΚΟΙΝΟ ΜΑΣ ΜΕΛΛΟΝ
ΗΠΗΝ Ηλιοθερμική Παραγωγή Ηλεκτρισμού & Νερού

Conference Subject Areas

- Advanced seismic data acquisition, processing and interpretation techniques
- Advances in oil and gas separation
- Carbon capture and storage technologies and enhanced oil recovery for deepwater
- Concentrated solar power technologies
- Conventional and non-conventional hydrocarbons energy development
- Deepwater drilling and completions technologies
- Deepwater structures and system integration
- Desalination methods
- Distributed generation
- Energy economics
- Energy policy issues
- Energy storage systems
- Environment and climate change issues
- Exploration geohazards and sea bed service
- Global natural gas market outlook
- Hydrogen production, storage and use
- Hydrocarbons exploration strategies
- Natural gas liquefaction technologies
- Natural gas pipeline transportation technologies
- Natural gas policy issues
- Oil and gas reserves and economics by region
- Oil and gas transportation cost and infrastructure development
- Photovoltaic technologies
- Power generation technologies
- Power system economics
- Renewable energy sources technologies
- Renewable generation scheduling
- Subsea completions and well testing and economics
- Sustainable cities and regions
- Wind technologies

List of Papers

Paper Ref. No.	Author(s)	Title
POEM13/151	Markos Asprou, Yiasoumis Yiasemi, Elias Kyriakides, Yiannakis Ioannou, Antreas Petousis, Michalis Michael and Stavros Stavrinos	*Application of synchronized measurement technology in the Cyprus power transmission system*
POEM13/152	Rogiros Tapakis and Alexandros Charalambides	*Over-irradiance due to the presence of clouds*
POEM13/153	Antonis Antoniou, Nikolas Theodorou, Antonis Tsikalakis, Kostantinos Kalaitzakis and George Stavrakakis	*Impact of the Euro-Asia Interconnector project on the economic operation of Crete and Cyprus power systems*
POEM14/154	Charalambos Chasos, George Karagiorgis and Chris Christodoulou	*Technical and feasibility analysis of gasoline and natural gas fuelled vehicles*
POEM13/155	Mona Valikhani and Constantinos Sourkounis	*On the power control techniques of DFIG: From conventional to a novel BELBIC scheme*
POEM13/158	Alexandros Nikolaidis and Charalambos Charalambous	*Action steps for refining the Cyprus national action plan on RES penetration for electricity generation - Should we reconsider?*
POEM13/159	Pavlos Tourou and Constantinos Sourkounis	*Operation of wind energy conversion systems with doubly-fed induction generators during asymmetrical voltage dips*
POEM13/160	Antonis Lazari and Charalambos Charalambous	*A software tool to evaluate the total ownership cost of distribution transformers*
POEM13/161	Nora Becker and Constantinos Sourkounis	*Concept of energy extraction from sludge of a clarification plant*
POEM13/162	Constantinos Sourkounis, Nora Becker, Alexander Broy and Fredrik Einwächter	*Integration of quick charging stations for e-mobility in power grids of weak infrastructure and high impact of renewable energies*
POEM13/163	Alexander Broy, Izabella Vasileva and Constantinos Sourkounis	*Design rules for autonomous hybrid energy supply systems for various types of buildings in Central Europe*
POEM13/165	Andreas Poullikkas, Savvas Papadouris, George Kourtis and Ioannis Hadjipaschalis	*Storage solutions for power quality problems of the distribution network*
POEM13/166	Andreas Poullikkas, George Kourtis and Ioannis Hadjipaschalis	*Cost-benefit analysis for the installation of cogeneration CSP technology in Cyprus*
POEM13/167	Soteris Kalogirou, Foivos Francou and Georgios Florides	*Evaluation of the solar cooling and heating system of the CUT mechanical engineering laboratories*
POEM13/168	Constantinos Adamides and Odysseas Christou	*Energy security in the Eastern Mediterranean regional security complexes*

List of Papers

Paper Ref. No.	Author(s)	Title
POEM13/169	Christina Ioannou and Achilles Emilianides	*The Cypriot hydrocarbons and the European financial crisis*
POEM13/170	Theodoros Tsakiris	*The feasibility and impact of the Turkish-Israeli "Rapprochement" on the geopolitics of the Eastern Mediterranean*
POEM13/171	Costas Constantinou	*European roadmap for energy and the role of Cyprus hydrocarbons*
POEM13/173	Paris Fokaides	*Parameters of European energy policy framework related to the hydrocarbons exploration in Cyprus*
POEM13/174	Christos Giannakopoulos	*Anticipated impacts of climate change of electricity demand of Athens, Greece*
POEM13/175	Nestoras Fylaktos	*Small scale thermal solar district units for Mediterranean communities - The STS-MED project*
POEM13/176	Panos Hadjinicolaou	*Integration of quick charging stations in power grids of weak infrastructure areas*
POEM13/177	Manfred Lange	*Assessment of increasing electricity demand for space cooling under climate change condition in the Eastern Mediterranean*
POEM13/178	Manthos Santamouris	*A review of innovative measures to reduce energy consumption in the urban built environment*
POEM13/179	George Tzamtzis	*Design of a solar thermal co-generation demonstrator*
POEM13/180	Christos Marakkos	*Optical design of an integrated receiver and storage system*
POEM13/181	Nestoras Fylaktos	*Techno-economic analysis of a co-generation solar thermal plant*
POEM13/182	Marios Georgiou	*Thermal desalination performance analysis*
POEM13/183	Irina Ciornei, Petros Mavroeidis, Georgia Pieri and Elias Kyriakides	*From sensors and measurements, to data and applications in power systems*
POEM13/184	Jairo Quirós-Tortós and Vladimir Terzija	*A power system controlled islanding scheme for emergency control*
POEM13/185	Ana Maria Dumitrescu, Mihai Calin and Mihaela Albu	*Measurement data aggregation in power systems – challenges and opportunities*
POEM13/186	Melios Hadjikypris and Vladimir Terzija	*Dynamic fault studies of an offshore four-terminal VSC-HVDC grid utilizing protection means through AC/DC circuit breakers*

List of Papers

Paper Ref. No.	Author(s)	Title
POEM13/187	Soteris Kalogirou, Gregoris Panayiotou, Georgios Florides, George Roditis, Nasos Katsellis, Andreas Constantinou, Paraskevas Kyriakou, Yiannis Vasiades, Thomas Parisis, Alexandros Michaelides and Jan Erik Nielsen	*Experimental investigation of the thermosiphonic phenomenon in domestic solar water heaters*
POEM13/188	Gregoris Panayiotou, Soteris Kalogirou and Savvas Tassou	*Theoretical study of the application of Phase Change Materials (PCM) on the envelope of a typical dwelling in Cyprus*
POEM13/189	Soteris Kalogirou, Gregoris Panayiotou and Vasiliki Antoniou	*Experimental evaluation of Phase Change Materials (PCM) for energy storage in solar water heating systems*
POEM13/190	Soteris Kalogirou and Gregoris Panayiotou	*Experimental investigation of the performance of a parabolic trough collector (PTC) installed in Cyprus*
POEM13/191	Soteris Kalogirou and Rafaela Agathocleous	*Optimization of Thermosiphon Solar Water Heaters working in a Mediterranean Environment*
POEM13/192	Gregoris Panayiotou, Anthi Charalambous, Savvas Vlachos, Orestis Kyriacou, Elisavet Theofanous and Thomas Filippou	*Increase of energy efficiency in 25 low income houses in Cyprus – a holistic approach*
POEM13/193	Maria Hadjipanayi	*Promotion of PV energy through net metering optimization*
POEM13/194	Anthi Charalambous and Nagwa Gamal	*Production of biodiesel from microalgae in selected Mediterranean countries*
POEM13/195	Gregoris Panayiotou, Maria Ioannidou and Anthi Charalambous	*Towards low carbon homes through energy renovations*

2nd Conference on Power Options for the Eastern Mediterranean Region
07-08 October 2013, Nicosia, Cyprus (Paper No. POEM13/151)

Application of Synchronized Measurement Technology in the Cyprus Power Transmission System

Markos Asprou, Yiasoumis Yiasemi, Elias Kyriakides, Yiannakis Ioannou, Antreas G. Petousis, Michalis Michael and Stavros Stavrinos

Abstract-- **Synchronized Measurement Technology (SMT) is rapidly deployed in the measurement layer of the electric utilities as the real time monitoring and control of the power systems operation becomes an imperative need. The key element of SMT is the Phasor Measurement Unit (PMU) that provides, among other quantities, synchronized voltage and current phasor measurements at high reporting rates. The capabilities of PMUs can enhance the accuracy and robustness of several contemporary applications of the power system control center and lead to the evolution of the conventional control center to a Wide Area Monitoring and Control (WAMC) center. In this paper, the benefit of including PMUs in the Cyprus power system for enhancing state estimator performance will be discussed. Further, potential PMU placements in the transmission system of Cyprus will also be shown for minimizing state estimator variance.**

Index Terms-- **PMU, real time monitoring and control, SCADA, synchronized phasor measurements.**

I. Introduction

The operation of the power systems to their physical limits by the electric utilities in order to satisfy the ever increasing electricity demand, along with the increasing complexity of the power systems due to the penetration of renewables, have led to the vulnerability of the power systems to severe faults. At the same time, the electric utilities should be competitive in the deregulated electricity market by providing reliably and continuously electricity to the end users. Based on the above, the real time monitoring and control of the power systems is increasingly becoming a necessity.

The Supervisory Control and Data Acquisition (SCADA) systems that are widely used for maintaining the power system operation orderly, present potential weaknesses to provide to the power system operators timely and accurately the visualization of the power system operating condition. This is mainly because the contemporary applications of the SCADA system are based on conventional measurements, which have inherently slow reporting rate and encompass high uncertainty.

With the advent of the SMT and the installation of PMUs incrementally by the electric utilities the abstract idea of real time monitoring and control of the power system operation has started to become a reality. The SMT can find direct application in several SCADA functions, such as state estimation, voltage and frequency stability assessment, and contingency analysis. Further, an intense research effort is performed for the development of hybrid methodologies that use both synchronized and conventional measurements. Although many monitoring and control applications can benefit from the presence of synchrophasors in the control center, state estimation is considered as one of the original applications of SMT [1].

The aim of state estimation is to provide an estimation of the network relevant quantities (i.e., bus voltage magnitudes and bus voltage angles), using redundant measurements. The measurements that are incorporated in the measurement vector of the contemporary state estimator are the real and reactive power injections, real and reactive power flows and bus voltage magnitudes. The corresponding measurements are expressed using non-linear functions in relation to the power system states and therefore an iterative state estimation scheme is followed. Prior to state estimation, an observability analysis should be executed for ensuring that the power system is fully observable by the installed measurement devices. A fully observable system guarantees a unique and reliable state estimation solution [2].

With the presence of synchrophasors in the power system control centers, new concepts have been raised regarding the formulation of the state estimator. A linear state estimator can be applied to a power system fully observable by PMUs. Although this could be the ideal case, the cost and communication requirements of the PMUs are the main obstacles for rendering a large scale power system fully observable by PMUs. Thus, electric utilities install PMUs incrementally. As power systems become partially observable by synchronized measurements, a hybrid state estimator that uses both conventional and synchronized phasor measurements for estimating the states of the system seems to be the most convenient solution. Even though, the presence of conventional measurements imposes a non-linear state estimator scheme, the synchronized phasor measurements improve the performance of the hybrid state estimator considerably [3], [4].

In addition, the problem for determining the optimal PMU locations for improving certain PMU applications is also addressed by many researchers. The PMUs can be optimally

This work was co-funded by the European Regional Development Fund and the Republic of Cyprus through the Research Promotion Foundation (Project TIIE/OPIZO/0311/20)"

M. Asprou, Y. Yiasoumis, E. Kyriakides are with the KIOS Research Center for Intelligent Systems and Networks and the Department of Electrical and Computer Engineering, University of Cyprus, Nicosia, Cyprus (e-mail: asprou.markos@ucy.ac.cy, yiasemi.yiasoumis@ucy.ac.cy, elias@ucy.ac.cy).

Y. Ioannou is with the Electricity Authority of Cyprus, Nicosia, Cyprus (e-mail: yioannou@eac.com.cy).

A. G. Petoussis, S. Stavrinos, and M. Michael are with the Transmission System Operator Cyprus, Nicosia, Cyprus (e-mail: apetoussis@dsm.org.cy, mmichael@dsm.org.cy, sstavrinos@dsm.org.cy)

placed for ensuring power system observability, increasing measurement redundancy, monitoring voltage instability in particular buses (i.e., tie-line buses), and increasing state estimator accuracy. Therefore, electric utilities should include the PMUs in their measurement layer according to their short term goals, but in a manner that can accommodate future applications. The improvement of state estimation accuracy is among the priorities of electric utilities. The state estimation accuracy improvement increases the situational awareness of the stakeholders regarding the operating condition of the power system. The precise estimation of the states enables operators to take the correct preventive actions avoiding the false triggered alarms. Moreover, among the various applications that make use of the state estimator results is the calculation of power flow. Thus, the state estimator accuracy improvement has significant impact in the financial aspects of the electric utilities since the calculation of the power losses will be more precise and will facilitate the cost-effective unit commitment [5].

Several techniques are proposed to determine the optimal PMU placement for improving the state estimator accuracy. In [6], the PMU placement algorithm performs critical measurement analysis and state estimation for creating two sets of candidate PMU buses. The first set contains all the buses that are present in critical measurements and the second contains the buses whose estimated states have the largest variance. The optimal PMU placement is determined by choosing from the intersection of the two created sets, the bus with the most branches connected to it. In [7], an iterative exhaustive search is performed for finding each time the PMU bus combinations with the largest contribution to the minimization of the state estimation residual error. For each combination a state estimation is performed and its residual error associated with each combination is obtained. The combination that causes the smallest state estimation residual error is chosen as the optimal. Although this is a trivial methodology, the computational burden associated with the formation and the examination of all the combinations and the performance of a state estimation for each combination, especially for large systems, is considerably huge. In [8], the optimal PMU placements are obtained by minimizing or maximizing accordingly some condition indicators related to the condition number of the gain matrix.

In this paper, the improvement of the state estimator accuracy applied to the Cyprus transmission power system, as well as the optimal locations of the PMUs for minimizing the state estimator variance are presented. More specifically, a comparison of the state estimator accuracy before and after the inclusion of the PMU measurements in the measurement vector of the state estimator is performed. It should be noted that in this paper the hybrid state estimator that was proposed in [3] will be used. Further, the determination of the locations of the Cyprus power system substations where the PMUs can be installed for improving state estimation accuracy will be shown by applying the methodology proposed in [9].

This paper is organized as follows. In Section II, the theory behind the conventional and the state estimator used in this paper will be presented, while the theory behind the optimal PMU placement methodology will be shown in Section III. The accuracy comparison of the conventional and the hybrid state estimator when are applied to the Cyprus power transmission system as well as the optimal PMU locations for minimizing state estimator variance will be shown in Section IV and the paper concludes in Section V.

II. Conventional and Hybrid State Estimator

In this section the formulations of a conventional and a hybrid state estimator are presented. Both estimators formulated in the weighted least squares (WLS) framework are shown here for completeness. Further information can be found in [2] and [3].

A. *Conventional state estimator*

The concept of state estimation was introduced for the first time in the late 1960s [10]. The inclusion of the state estimation function had extended the capabilities of the SCADA system. Since then, power system state estimation constitutes the core of the SCADA system, facilitating accurate and efficient monitoring of the power system.

The objective of state estimation is to determine the most likely state of the system (i.e., bus voltage magnitudes and phase angles) based on the acquired measurements. The procedure for determining the state of the system is based on different approaches but the most commonly used approach is the WLS. According to WLS theory, the state vector $\mathbf{x}$ of the system is determined by minimizing the weighted residuals between the estimated and the actual acquired measurements,

$$J(\mathbf{x}) = [\mathbf{z} - \mathbf{h}(\mathbf{x})]\mathbf{R}^{-1}[\mathbf{z} - \mathbf{h}(\mathbf{x})], \quad (1)$$

where $\mathbf{z}$ is a vector including the acquired measurements from the system, $\mathbf{h}(\mathbf{x})$ is a vector containing the non-linear equations that relate the state variables to the measurements, and $\mathbf{R}$ is the measurement error covariance matrix. Thus, since the objective of the state estimation problem is to minimize (1) by determining the states of the system, the derivative of $J(\mathbf{x})$ with respect to the state variables must be set to zero. Expanding the derivative of $J(\mathbf{x})$ using the Taylor series and neglecting the higher order terms, leads to an iterative solution scheme known as the Gauss-Newton method [1],

$$\mathbf{x}^{k+1} = \mathbf{x}^{k} + [\mathbf{G}(\mathbf{x}^{k})]^{-1}\mathbf{H}^{T}(\mathbf{x}^{k})\mathbf{R}^{-1}[\mathbf{z} - \mathbf{h}(\mathbf{x}^{k})], \quad (2)$$

where $\mathbf{H}(\mathbf{x})$ is the Jacobian matrix and is equal to $\frac{\partial \mathbf{h}(\mathbf{x})}{\partial \mathbf{x}}$ and $\mathbf{G}(\mathbf{x})$ is the gain matrix and is equal to $\mathbf{H}^{T}(\mathbf{x})\mathbf{R}^{-1}\mathbf{H}(\mathbf{x})$. The state vector $\mathbf{x}$ of the power system is determined by applying (2) in an iterative manner. The iterative process should stop when the element of $\Delta\mathbf{x}^{k+1}$ with the maximum absolute value is smaller than a predefined threshold.

It should be noted that some assumptions are made regarding the statistical properties of the measurement errors when the WLS approach is used. The measurement errors are assumed to be independent; hence, the error covariance matrix $\mathbf{R}$ is a diagonal matrix having as diagonal elements the variance of the measurements. Additionally, it is assumed that the network topology and parameters are known prior to state estimation.

State estimation is an overdetermined problem, implying that the number of measurements should be greater than the number of the state variables that must be estimated. Therefore, a higher measurement redundancy improves the accuracy of the state estimation. Moreover, for obtaining reasonable results the power system should be completely

observable by the measurements contained in vector **z**.

B. Hybrid state estimator

A generalized formulation of a hybrid state estimator utilizes both conventional and synchronized phasor measurements for estimating the states of the system. The structure of the measurement vector **z** of a generic hybrid state estimator is,

$$\mathbf{z}=\begin{bmatrix}\mathbf{P_{flow}}\\ \mathbf{P_{inj}}\\ \mathbf{Q_{flow}}\\ \mathbf{Q_{inj}}\\ \boldsymbol{\theta}_{\mathbf{Vpmu}}\\ \mathbf{V_{pmu}}\\ \boldsymbol{\theta}_{\mathbf{Ipmu}}\\ \mathbf{I_{pmu}}\end{bmatrix}. \tag{3}$$

The measurements used in state estimation must be related to the state variables by the equations included in vector **h**(**x**). With reference to Fig. 1 and assuming known network parameters, the real and reactive power flows and injections measurements are expressed as follows [1]:

- Real and reactive power injection at bus *i*

$$P_i = V_i \sum_{j\in\aleph_i} V_j (G_{ij}.\cos\theta_{ij} + B_{ij}\sin\theta_{ij}) \tag{4}$$

$$Q_i = V_i \sum_{j\in\aleph_i} V_j (G_{ij}.\sin\theta_{ij} - B_{ij}\cos\theta_{ij}) \tag{5}$$

- Real and reactive power flow from bus *i* to bus *j*

$$P_{ij} = V_i^2 (g_{si} + g_{ij}) - V_i V_j (g_{ij}\cos\theta_{ij} + b_{ij}\sin\theta_{ij}) \tag{6}$$

$$Q_{ij} = -V_i^2 (b_{si} + b_{ij}) - V_i V_j (g_{ij}\sin\theta_{ij} - b_{ij}\cos\theta_{ij}), \tag{7}$$

where,

V_i, θ_i is the voltage magnitude and phase angle at bus *i*

$\theta_{ij}=\theta_i-\theta_j$

$G_{ij}+jB_{ij}$ is the *ijth* element of bus admittance matrix

$g_{ij}+jb_{ij}$ is the series admittance of the branch connecting bus *i* and bus *j*

$g_{si}+jb_{si}$ is the shunt admittance that is connected to bus *i*

$\aleph_i$ is the set of buses directly connected to bus *i*

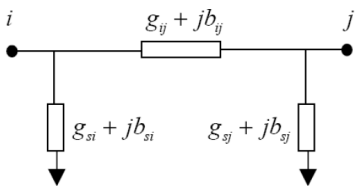

Fig. 1. Transmission line representation in a pi model

The voltage phasor measurements are directly related to the state variables; therefore, no equations are needed to express them as a function of the state variables. This is not valid however with the current phasor measurements. Thus, with reference to Fig. 1 the current phasor that flows from bus *i* to bus *j* is expressed as:

$$\bar{I}ij = \bar{V}_i (g_{si} + jb_{si}) + (\bar{V}_i - \bar{V}_j)(g_{ij} + jb_{ij}) = C + jD, \tag{8}$$

where,

$\bar{V}_i$ and $\bar{V}_j$ are the voltage phasors of buses *i* and *j*

$$C = V_i\cos\theta_i(g_{si}+g_{ij}) - V_i\sin\theta_i(b_{si}+b_{ij}) + b_{ij}V_j\sin\theta_j - g_{ij}V_j\cos\theta_j \tag{9}$$

$$D = V_i\cos\theta_i(b_{si}+b_{ij}) + V_i\sin\theta_i(g_{si}+g_{ij}) - b_{ij}V_j\cos\theta_j - g_{ij}V_j\sin\theta_j . \tag{10}$$

The current magnitude and the current phase angle are obtained by,

$$I_{ij} = \sqrt{C^2 + D^2} \tag{11}$$

$$\theta_{ij} = \tan^{-1}(D/C). \tag{12}$$

The measurement Jacobian **H(x)** is formed by taking the derivatives of the equations stated above with respect to the state variables. It must be noted that the elements of the Jacobian corresponding to voltage magnitude and phase angle are 1 in the columns that correspond to the bus which the voltage phasor is measured from and 0 in all the other columns.

The measurement error covariance matrix **R** is a diagonal matrix having as elements the variances of the measurements which are determined by the maximum uncertainty of the measurement device when Gaussian distribution is considered over the entire range of the uncertainty.

The above hybrid state estimator has certain drawbacks with respect to convergence, as stated in [4]. In particular, the elements of the Jacobian corresponding to current measurements become undefined for a certain range of terminal voltage and phase angle. Thus, the gain matrix **G** of the state estimator becomes ill-conditioned and the results obtained by the state estimator diverge from the real state of the power system.

1) Hybrid state estimator including pseudo power flows

In order to overcome the issue of having an ill conditioned gain matrix due to the presence of current phasors in the measurement vector **z**, a different formulation of a hybrid state estimator is proposed in [3]. Based on Fig. 1, and by assuming that a PMU is connected at bus *i*, then the voltage phasor of bus *i* as well as the current phasor flowing from bus *i* to bus *j* are available. Hence, the active and reactive power flows from bus *i* to bus *j* are obtained by using (13) and (14) respectively. The power flows can be calculated for all the branches connected to the PMU bus since, without loss of generality, it is assumed that the channels of the PMU that correspond to current phasors are enough to measure all the currents flowing from the PMU bus. Since the power flows of the incident branches are not measured directly, these are called pseudo measurements. The avoidance of including direct current phasor measurements is accomplished by incorporating pseudo power flows in the measurement vector **z** of the hybrid state estimator.

$$P_{ij_{pseudo}} = V_i I_{ij}\cos(\theta_i - \theta_{ij}) \tag{13}$$

$$Q_{ij_{pseudo}} = V_i I_{ij}\sin(\theta_i - \theta_{ij}) . \tag{14}$$

The structure of the measurement vector *z* becomes,

$$\mathbf{z}=\begin{bmatrix}\mathbf{P_{flow}}\\ \mathbf{Pflow_{pse}}\\ \mathbf{P_{inj}}\\ \mathbf{Q_{flow}}\\ \mathbf{Qflow_{pse}}\\ \mathbf{Q_{inj}}\\ \boldsymbol{\theta}_{\mathbf{Vpmu}}\\ \mathbf{V_{pmu}}\end{bmatrix}. \quad (15)$$

The pseudo power flow measurements are related to the state variables of the power system similar to the conventional real and reactive power flow measurements using (6) and (7). The uncertainties of the pseudo flow measurements have to be calculated by combining the standard uncertainties of the measurements used to calculate them. The uncertainty propagation of the exact measurements in the pseudo real and reactive power flows can be obtained utilizing the classical theory of uncertainty propagation and are given by,

$$u(P_{ij_{pseudo}})=\sqrt{\sum_{k=1}^{4}[\partial P_{ij_{pseudo}}/\partial\mathbf{p}(k)]^2.[u(\mathbf{p}(k))]^2} \quad (16)$$

$$u(Q_{ij_{pseudo}})=\sqrt{\sum_{k=1}^{4}[\partial Q_{ij_{pseudo}}/\partial\mathbf{p}(k)]^2.[u(\mathbf{p}(k))]^2}, \quad (17)$$

where,

$\mathbf{p}(k)=[V_i,\theta_i,I_{ij},\theta_{ij}]$

$u(\mathbf{p}(k))$ is a vector containing the standard uncertainties of the measurement $\mathbf{p}(k)$.

III. Optimal PMU Placement Methodology

The integration of PMUs in a power system has a great impact in the improvement of the state estimator accuracy. For the proposed methodology, and without loss of generality, it is assumed that the power system is fully observable by the conventional measurements; thus, PMUs are included in the measurement system in order to minimize the variance of the hybrid state estimator calculated as,

$$\sigma_s{}^2=\frac{1}{M}\sum_{i=1}^{M}\sum_{k=1}^{N}(\mathbf{x}(k)-\hat{\mathbf{x}}(k)_{(i)})^2, \quad (18)$$

where,

M is the number of the Monte Carlo trials

N is the number of the state variables of the power system

$\mathbf{x}$ is the state vector containing the state variable

$\hat{\mathbf{x}}_{(i)}$ is the estimated state vector in the i^{th} Monte Carlo trial.

Moreover, finding the optimal PMU placement for improving state estimator accuracy implies that the number of PMUs that are used will be the minimum for achieving a specific variance. For the determination of the optimal PMU placement a binary integer linear programming is formulated as follows,

$$\begin{aligned}&Min\ \ \mathbf{G(b)}=\mathbf{c^T b}\\ &subject\ to\ \ \mathbf{b(radial\ bus)}=\mathbf{0}\\ &\qquad\qquad\mathbf{Pb}=1\end{aligned} \quad (19)$$

where,

c = A.Var

b is a $N\times1$ vector comprising N-1 zeros and 1 one.

N is the number of buses

The vector **c** is obtained by calculating the product between the connectivity matrix **A** and the vector **Var**. It essentially contains the weights for the buses. The connectivity matrix **A** is an $N\times N$ symmetric matrix, determined by the network topology. Its ijth and jith elements are equal to one, all the diagonal elements are equal to one and all the other elements are equal to zero. The vector **Var** with dimensions $N\times1$ contains the variance for each bus, calculated by the covariance matrix of the state variables (V_i and θ_i). The procedure for calculating the vector **Var** is shown below for a two bus system.

In state estimation the covariance matrix **C** is symmetric and can be obtained by,

$$\mathbf{C}=(\hat{\mathbf{x}}-\mathbf{x})(\hat{\mathbf{x}}-\mathbf{x})^T \quad (20)$$

It is formulated as,

$$\mathbf{C}=\begin{bmatrix}\sigma^2_{\theta_1,\theta_1} & \sigma^2_{\theta_1,\theta_2} & \sigma^2_{\theta_1,V_1} & \sigma^2_{\theta_1,V_2}\\ \sigma^2_{\theta_2,\theta_1} & \sigma^2_{\theta_2,\theta_2} & \sigma^2_{\theta_2,V_1} & \sigma^2_{\theta_2,V_2}\\ \sigma^2_{V_1,\theta_1} & \sigma^2_{V_1,\theta_2} & \sigma^2_{V_1,V_1} & \sigma^2_{V_1,V_2}\\ \sigma^2_{V_2,\theta_1} & \sigma^2_{V_2,\theta_2} & \sigma^2_{V_2,V_1} & \sigma^2_{V_2,V_2}\end{bmatrix} \quad (21)$$

Based on the theory of random variables, the summation of the variances of two or more variables can be obtained by [11],

$$\sigma^2_{(V_1+\theta_1)}=\sigma^2_{\theta_1,\theta_1}+2\sigma^2_{\theta_1,V_1}+\sigma^2_{V_1,V_1} \quad (22)$$

Therefore, the vector **Var** for a two bus system has the structure shown below,

$$\mathbf{Var}=\begin{bmatrix}\sigma^2_{(V_1+\theta_1)}\\ \sigma^2_{(V_2+\theta_2)}\end{bmatrix}. \quad (23)$$

When a PMU is installed at a bus, it has as an effect to minimize the variance of the particular bus as well as the variances of its adjacent buses. Hence, for finding the PMU placement that minimizes the variance of the state estimator, it is sufficient to find the bus, which has the largest variance aggregately (i.e., summation of its variance and the variances of its adjacent buses). Therefore, the aggregate variance of each bus could be obtained by the product between the connectivity matrix **A** and the vector **Var**.

Moreover, the optimization function **G(b)** is subjected to two constraints, hence a binary integer linear programming is used for solving the minimization problem. The first constraint ensures that a PMU is not installed at a radial bus because a possible loss of the branch connecting the radial bus to the network leads to the immediate loss of the PMU. The second constraint ensures that only one element of the vector **b** will be one and all the other elements zero (i.e., one PMU is installed at each iteration). Thus, the vector **P** in the second constraint has dimensions $1\times N$ containing ones. The procedure for determining the optimal PMU placement is iterative and comprises the following steps:

Step 1. Run the conventional state estimator for 1000 Monte Carlo simulations to obtain the covariance matrix **C**.

Step 2. Form the vector **Var**.

Step 3. Calculate the vector **c**.

Step 4. Obtain the vector **b** for minimizing **G(b)** using binary integer linear programming.

Step 5. Find the index that corresponds to the nonzero

element of vector **b**, which denotes the next PMU bus.

Step 6. Add the chosen bus to the set of PMU buses.

Step 7. Run the hybrid state estimator for 1000 Monte Carlo analysis to obtain the updated covariance matrix **C**.

Step 8. Calculate the variance of the hybrid state estimator using (18).

Step 9. If the hybrid state estimator variance is below a certain threshold (in this paper, $1x10^{-5}$) stop, else go to step 2.

IV. Simulation Results

The conventional and the hybrid state estimator are applied to the transmission system of Cyprus after being implemented in Matlab software. The measurements that are used in both estimators are created using the power flow solution of the Cyprus power system using the Digsilent software. For a more realistic scenario, the simulated measurements are subjected to Gaussian noise due to the measurement error that is introduced by the measurement device. Hence, in this paper the measurements used in both state estimators are created as,

$$P/Q_{flow} = P/Q_{flow}^{exact} + unc_{flow}.P/Q_{flow}^{exact}.GN(0,1) \quad (24)$$

$$V_{PMU} = V_{PMU}^{exact} + unc_{Vpmu}.V_{PMU}^{exact}.GN(0,1) \quad (25)$$

$$I_{PMU} = I_{PMU}^{exact} + unc_{Ipmu}.I_{PMU}^{exact}.GN(0,1) \quad (26)$$

$$\theta_{PMU} = \theta_{PMU\ exact} + unc_{\theta pmu}.GN(0,1), \quad (27)$$

where,

unc is the maximum error for each measurement type tabulated in Table I

GN(0,1) is the additive Gaussian noise with mean 0 and standard deviation 1.

The Cyprus transmission power system consists of 65 high voltage buses (66, 132 kV) and 109 transmission lines connecting the buses between them. All the power that flows from the transmission lines (sending and receiving ends) can be measured through the SCADA system. Since the Cyprus power system is fully observable through the power flow measurements, in this case study all the power flows are used in both state estimators as measurements for obtaining the power system states. In the case of the hybrid state estimator, PMU measurements are also used in its measurement vector. The locations of the PMUs for minimizing the variance below the predefined threshold ($1x10^{-5}$) are determined by the methodology that is presented in Section III and are shown in Table II.

The voltage magnitude and the voltage angle residuals for all the buses of the power system in the case of the conventional and the hybrid state estimator are shown in Figs. 2 and 3 respectively in stacked form. It should be noted that both the voltage and angle residuals are calculated by finding the absolute difference between the actual states of the power system (voltage and angle) and the estimated states provided by the two types of the state estimators. As it is illustrated, the voltage and angle residuals of the hybrid state estimator are much smaller than the corresponding residuals of the conventional state estimator. This indicates that the installation of the 6 PMUs in the substations tabulated in Table II will improve the state estimator accuracy considerably.

Further, the variance of the conventional and the hybrid estimator shown in Table III, underlines the benefit of incorporating PMU measurements in the measurement vector of the stat estimator, since the variance of the hybrid state estimator is almost 100% smaller than the one of the conventional state estimator

TABLE I
MEASUREMENT DEVICES MAXIMUM ERRORS

Real/reactive power flow (%)	Voltage magnitude PMU (%)	Current magnitude PMU (%)	Phase angle PMU (degrees)
±3	±0.02	±0.03	±0.57

TABLE II
OPTIMAL PMU LOCATIONS IN CYPRUS POWER SYSTEM

Bus Number	Bus Name
4	Anatolikos 132 kV
35	Polemidia 132 kV
6	Athalassa 132 kV
45	Vasilikos 132 kV
17	FIZ 132 kV
27	Moni 132 kV

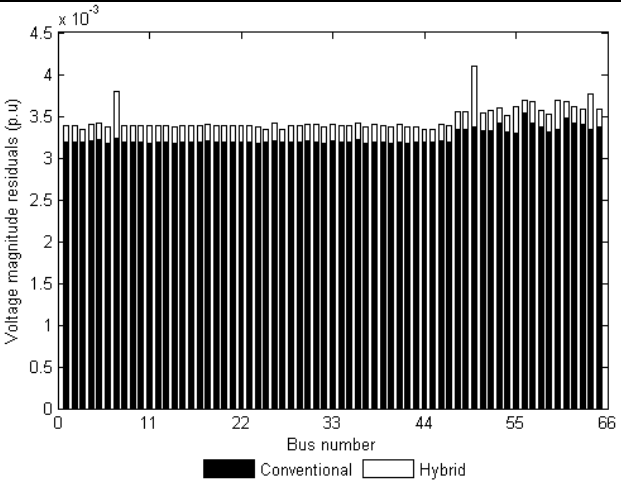

Fig. 2. Voltage magnitude residuals

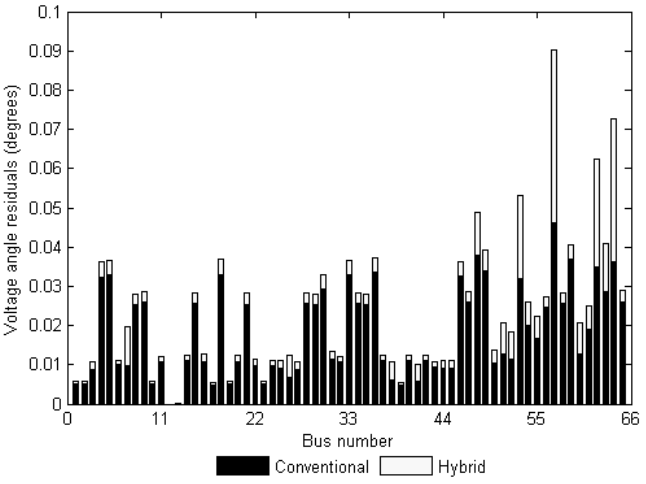

Fig. 3. Voltage angle residuals

TABLE III
VARIANCE OF THE TWO TYPES OF STATE ESTIMATORS

Conventional state estimator	Hybrid state estimator
$1.102x10^{-3}$	$6.687x10^{-6}$

V. CONCLUSIONS

The presence of Synchronized Measurement Technology (SMT) in the power systems enables the upgrade of the existing SCADA system to a Wide Area Monitoring and Control system that will provide accurately and timely the power system operating condition. In this evolutionary SCADA system, the state estimator will play a crucial role in the monitoring aspect of the power system. In this paper, the improvement of the state estimator accuracy was shown when 6 PMUs were assumed that are installed in selected substations in the Cyprus transmission power system. The PMU locations were selected for minimizing the state estimator variance using the methodology proposed in [9]. As it is shown in the simulation results, the accuracy of the state estimator can be improved considerably when PMU measurements are present in the measurement vector of the state estimator.

The application of the SMT in the measurement layer of the Cyprus power systems will provide high capabilities in the monitoring and control functions of the existing SCADA system. This will enhance the situational awareness of the power system operators for taking protective actions in the case of an evolving contingency and prevent a possible blackout. To this attempt, a clearly defined roadmap should be developed to give directions for the deployment of SMT in the Cyprus power system for the implementation of a future Wide Area Monitoring and Control system.

VI. REFERENCES

[1] A. G. Phadke and J. S. Thorp, "Synchronized phasor measurements and their applications," New York: Springer, 2008.

[2] A. Abur and A. G. Exposito, "Power system state estimation: Theory and Implementation," New York: Basel, 2004.

[3] M. Asprou and E. Kyriakides, "Enhancement of hybrid state estimation using pseudo flow measurements," IEEE Power and Energy Society General Meeting, Detroit, MI, USA, paper no. 1022, pp. 1-7, July 2011.

[4] S. Chakrabarti, E. Kyriakides, G. Ledwich, and A. Ghosh, "On the inclusion of phasor measurements in a power state estimation," IET Generation, Transmission, and Distribution, vol. 4, no. 10, pp. 1104-1115, Sep. 2010.

[5] KEMA, "Metrics for determining the impact of phasor measurement on power system state estimation," *Eastern Interconnection Phasor Project,* Mar. 2006.

[6] W. Jiang and V. Vittal, "Optimal placement of phasor measurements for the enhancement of state estimation," *Power System Conference and Exposition*, Atlanta, USA, pp. 1550-1555, Feb. 2007.

[7] N .H. El-Amary, Y. G. Mostafa, M. M. Mansour, S. F. Mekhamer, and M. A. L. Badr, "Effect of synchronized phasor measurement units locations on power system state estimation," *International conference on computer engineering and* systems, Cairo, Egypt, pp. 309-314, Feb. 2009.

[8] M. Rice and G. T. Heydt, "Enhanced state estimator: Part III: Sensor location strategies," PSERC, Tempe, AZ, Final Project Report, Nov. 2006.

[9] M. Asprou and E. Kyriakides, "Optimal PMU placement for improving hybrid state estimator accuracy," *IEEE PowerTech 2011*, Trondheim Norway, pp. 1-7, Jun. 2011.

[10] F. C. Schweppe and D. B. Rom, "Power System Static-State Estimation, Part II: Approximate Model," *IEEE Transactions on Power Apparatus and Systems*, vol. 89, pp. 125-130, Jan. 1970.

[11] A. L. Garcia, "Probability and random processes for electrical engineering," Addison Wesley Longman, 1994.

VII. BIOGRAPHIES

Markos Asprou obtained the B.Sc. degree in Electrical Engineering from the University of Cyprus in 2009. Currently he is a Ph.D. candidate in the Department of Electrical and Computer engineering at the University of Cyprus. He is also working as a researcher in the KIOS Research Center for Intelligent Systems and Networks. His research interests include monitoring and state estimation of power systems and fault location detection in power system transmission lines based on synchronized measurements. He is the Chair of the IEEE PES student branch at the University of Cyprus.

Yiasoumis Yiasemi received his B.Sc. degree (2010) and his M.Sc. (2012) in Electrical Engineering from the University of Cyprus. He is currently working as a researcher in the KIOS Research Center for Intelligent Systems and Networks.

Elias Kyriakides is from Nicosia, Cyprus. He received the B.Sc. degree from the Illinois Institute of Technology in Chicago, Illinois in 2000, and the M.Sc. and Ph.D. degrees from Arizona State University in Tempe, Arizona in 2001 and 2003 respectively, all in Electrical Engineering. He is currently an Assistant Professor in the Department of Electrical and Computer Engineering at the University of Cyprus, and a founding member of the KIOS Research Center for Intelligent Systems and Networks. He is the Action Chair of the ESF-COST Action IC0806 "Intelligent Monitoring, Control, and Security of Critical Infrastructure Systems" (IntelliCIS) (2009-2013). His research interests include synchronized measurements in power systems, security and reliability of the power system network, optimization of power system operation techniques, and renewable energy sources.

Yiannakis Ioannou BEng in Electrical and Electronics Eng. from Brunel Univ. and MSc in Electrical Energy Systems from the Univ. of Manchester. He is working at the Electricity Authority of Cyprus since 1994, and he is PhD candidate in the Department of Electrical and Computer Engineering at University of Cyprus.

Andreas G. Petoussis is a Consultant Electrical Engineer with the TSO of Cyprus. He received the PhD degree in Electrical Engineering at the University of Warwick in 2009. His research interests include electricity markets, dynamic modeling of isolated power systems, and grid-connected RES.

Stavros M. Stavrinos received his B.Sc. (Hons) in Electrical Engineering from Salford University, UK and his M.Sc. degree in Telecommunications and Information Systems from Essex University, UK. Since 2004 he has been working with the TSO in the System Operation section.

2nd Conference on Power Options for the Eastern Mediterranean Region
07-08 October 2013, Nicosia, Cyprus (Paper No. POEM13/152)

Over-irradiance due to the presence of clouds

Rogiros D. Tapakis and Alexandros G. Charalambides

Abstract--**During the transition of solar radiation through the atmosphere of the earth, the intensity of solar irradiance is attenuated due to the absorption and scattering by atmospheric particles. Thus, during cloudy conditions, the presence of clouds results to the attenuation of global irradiance that result to a respective decrease in the power output of Photovoltaic (PV) modules and the Electricity Generation of PV Parks. However, it is observed that when suitable conditions of partial cloudy sky exist, the positive correlation of different factors can enhance the value of solar irradiance instead of attenuating it. This paper presents measurements of enhanced global irradiance from data obtained in Cyprus (latitude 34.75° N, longitude 32.62° E), during the spring and summer of 2010. In seven different occasions during five days of May and June 2010, the measured value of global irradiance exceeded 1500W/m^2 that corresponds to almost 150% of the theoretical value computed by Bird and Hulstrom clear sky computational model for those specific occasions. Moreover, it is noteworthy that in more than 20 days of April, May and June, the one minute and sometimes even the ten minute average global horizontal irradiance exceeded 1200W/m^2 (enhanced by 125% compared to the theoretical ensembled averaged value for those specific occasions) showing a long lasting period of the effect. These long periods of over-irradiance, along with the temperature drop due to clouds (approximately 15-20°C compared to 30-40°C in the summer period of Cyprus) might boost the performance of photovoltaic modules and cause irreparable damage to photovoltaic inverters. However, although this additional power output is desirable, it may be rejected by the inverter if it is larger than the inverter's AC rating or if the value of the Current-Voltage exceeds the operating range of the inverter.**

Index Terms-- **Cloud Enhancement, Global horizontal irradiance, Over-irradiance, Photovoltaics**

I. Introduction

SOLAR Irradiance is the feedstock for various Renewable Energy Source (RES) technologies, either by exploiting global solar irradiance such as Photovoltaics (PV), commercial solar updraft towers and residential/commercial solar heating and cooling systems or by exploiting only the Direct Normal Irradiance (DNI), such as solar troughs, solar tower plants and solar dish technologies.

DNI is the amount of solar radiation that comes directly from the sun and is incident on a surface that is always perpendicular to the direction of the sun rays. Global Irradiance is the total amount of the incident irradiance on a surface and is the sum of the DNI and the diffuse irradiance. Diffuse irradiance is the part of irradiance that is scattered or reflected by atmospheric components of the sky or by the surface of the earth (in the case of tilted surface only). Global irradiance is usually measured on a horizontal surface, (Global Horizontal Irradiance, GHI) or on an inclined surface concerning specific applications. Global Irradiance on an inclined surface can be estimated from other meteorological data using mathematical formulas [1][2].

Various models have been proposed for the estimation of GHI either with no exogenous inputs using only the extraterrestrial radiation (solar constant), solar declination, sunshine duration, geographical location and date/time, or with additional exogenous parameters such as air temperature, earth surface albedo, relative humidity, cloudiness, precipitation, evaporation, atmospheric composition, aerosol optical depth and soil temperature [3][4][5]. From these parameters, the most profound parameter for solar irradiance variations is cloudiness, because although it can be predicted, the spatial and temporal resolution of the predictions is very low, resulting to an uncertainty in solar energy generation prediction, especially for Solar Power Systems without energy storage, such as PV parks [6].

The solar constant (1367 W/m² ± 3.3%) is the intensity of solar irradiance that is incident to the earth's atmosphere [7] and during the transition of solar radiation through the earth's atmosphere, the intensity of irradiance is attenuated due to absorption and scattering by atmospheric particles such as clouds and aerosols. Thus, during cloudy conditions, the presence of clouds results in the attenuation of DNI that consequences in a corresponding decrease in the intensity of global irradiance. Nevertheless, occasionally, the combination of the above different parameters leads to a perfect storm which may result in the enhancement of global irradiance, thus achieving irradiance values even higher than the solar constant [8].

The enhancement of solar irradiance occurs under specific partial cloudy conditions. Piacentini et al. [8] proposed that the following conditions should coexist:

1. Presence of Cumulus clouds around the sun disk with the sun unobstructed, i.e. the clouds should not be present between the sun disk and the measurement point on the ground. The direct sun's radiation should be reflected by the edges of the clouds.
2. The minimum cloud coverage should be not less than 50% and the maximum not more than 90%, thus, allowing patches of clear-sky between clouds.
3. Clouds should be very thick in order to scatter solar radiation and increase the intensity of diffuse irradiance.

Additionally to these, Yordanov et al. [7] proposed that irradiance enhancement may be also attributed to strong

R. Tapakis is with Cyprus University of Technology, Department of Environmental Science and Technology, Lemesos, 3603, Cyprus, (e-mail: rd.tapakis@edu.cut.ac.cy).

A. G. Charalambides is with Cyprus University of Technology, Department of Environmental Science and Technology, Lemesos, 3603, Cyprus, Tel: +357 25 002306 (e-mail: a.charalambides@cut.ac.cy).

forward Mie scattering of light inside the clouds within a narrow angle around the solar disk. As they have shown in their research, during Mie scattering, 51% of all scattered photons concentrated within 5° in the forward directions, thus contributing to the enhancement of irradiance. Thus, in some cases, when the sun is obscured by clouds, strong light is emitted within the clouds caused by Mie scattering (Figure 1). A similar statement was presented earlier by Rouse [9] proposing that if the cloud top albedo is small and the cloud base and the terrestrial surface albedos are high, most of the radiation is to be transmitted through the cloud and strongly enhanced by multiple reflections between the surface of the earth and the cloud base.

Fig. 1. Solar Irradiance emission through the clouds

Although the weather conditions that cause irradiance enhancement are not rare, exceptionally high values of irradiance occurrences are not often mentioned in the bibliography. This is mainly due to the long response time of the pyranometers used, thereby ignoring instantaneous fluctuations of irradiance or because the recorded data include the average value of irradiance only and not the maximum one [10]. The pyranometers used in various bibliographic references have a response time of 18 seconds which is very long compared to modern pyranometers with response times less than 5 seconds, as those used for the measurements presented in the following sections [7][11].

Nevertheless, short term enhancements of GHI may exceed 1500 W/m^2, whereas peaks reaching 2000 W/m^2 may be observed in mountainous regions near the equator. Piacentini et al. (2003) [12] reported a maximum value of GHI of 1528 W/m^2 at an altitude of 3900m in Argentina and, in a subsequent study at sea level near the equator, a maximum intensity of 1477W/m^2 was recorded [7].

Emck and Richter [11] presented a study regarding 4 year measurements of GHI in the southern Ecuadorian Andes Mountains near the equator, at an altitude of over 1900m, where they observed multiple occurrences of GHI exceeding 1700W/m^2, while the maximum recorder value reached 1832W/m^2. Cede et al. [13] recorded enhanced values of total irradiance at four sites in Argentina. Overall, at the four sites, the maximum recorded values of total irradiance were enhanced by 135% with respect to the very clear sky situation; the maximum measurements of 15-min average and 60 min average were 123% and 120% respectively.

The aim of this paper is to measure GHI in Cyprus, compare the measurements to the theoretical values of GHI for clear-sky conditions, calculate the percentage of measurements higher than the modeled ones, and evaluate the reason for these events and when they occur (i.e. middays, summer period, etc.). In Section 2, the equipment used for the measurements and the irradiance model used to calculate the clear-sky irradiance are described. In Section 3, a statistical analysis of the measurements is presented, and the recorded data are compared to the computed values of irradiance. The discussion of the results, with relevance to their effect on PVs, is presented in Section 4 and the conclusions in Section 5.

II. Equipment and Computational Model

The equipment used for the measurements is a remote meteorological station based on Geónica's Meteodata 3000 data transmission system positioned in Paphos, Cyprus (34.75°N, 32.62°E). The station consists of various measuring sensors, such as a pyrheliometer for measuring DNI, pyranometers for measuring GHI and diffuse irradiance, anemometer and wind vane and air temperature and humidity sensors. The pyrheliometer for measuring DNI and the pyranometer for measuring diffuse irradiance are positioned on a solar tracker.

The pyranometers (model MS-802) are ISO 9060 Secondary Standard with response time 5s and the pyrheliometer (model DN01) is ISO 9060 first class, with response time 18s. Since the response time of the pyranometers is 5 seconds, thus only intensities lasting over 5 seconds were recorded. The temperature sensor's range and accuracy are -30°C to +70°C and ±0.1°C respectively. The solar tracker (Model SunTracker-3000) is a two axis tracker (360° Azimuth, 90° elevation) with ±0.1° accuracy. The measurements from the sensors were recorded and stored on the datalogger and transferred to a computer server and then to a workstation for further processing. The measurements were taken from November 2009 to November 2010. The sensors of the meteorological station recorded the maximum and average values of the various parameters over a 10-minute period.

In order to be able to evaluate the measurements from the meteorological station, the theoretical values of the irradiance for any given instance were first computed and then compared to the measurements. The computational model used for the estimation of solar irradiance is that developed by Bird and Hulstrom in 1981 [23]. The model computes hourly values of direct normal, direct horizontal, global and diffuse irradiance for every day of the year. The parameters of the model were modified regarding the geographical location of the meteorological station and the atmospheric parameters of the site. Great attention was given to the parameter regarding the albedo of the specific site, quantified to 0.4 since the surrounding surface is semi-desert with high reflectivity [14][21]. Since the Bird's model computes the average hourly values of the irradiance, the calculations were interpolated to the intermediate 10-minute and 1-minute values using cubic interpolation. All the calculations were computed by an algorithm developed in MATLAB based on the mathematical formulas proposed by Bird and Hulstrom [23]. The daily ten-minute average GHI of thirty cloudy free days were used for the comparison of the measured GHI and computed GHI to validate both the model and the equipment accuracy and the results of the model agree well with measured clear-sky GHI (both the

slope and R^2 of the best-fit line approximate 1).

III. Results

All the enhanced values of GHI were recorded only during the period April-July 2010, thus, the analysis presented in this Section will be with respect to the measurements of this four month period.

Figure 2 presents the distribution of the measured GHI for different times of the day for all data recorded (diamond points), compared to the average theoretical value (solid line); (a) presents the maximum measured GHI and (b) presents the average GHI.

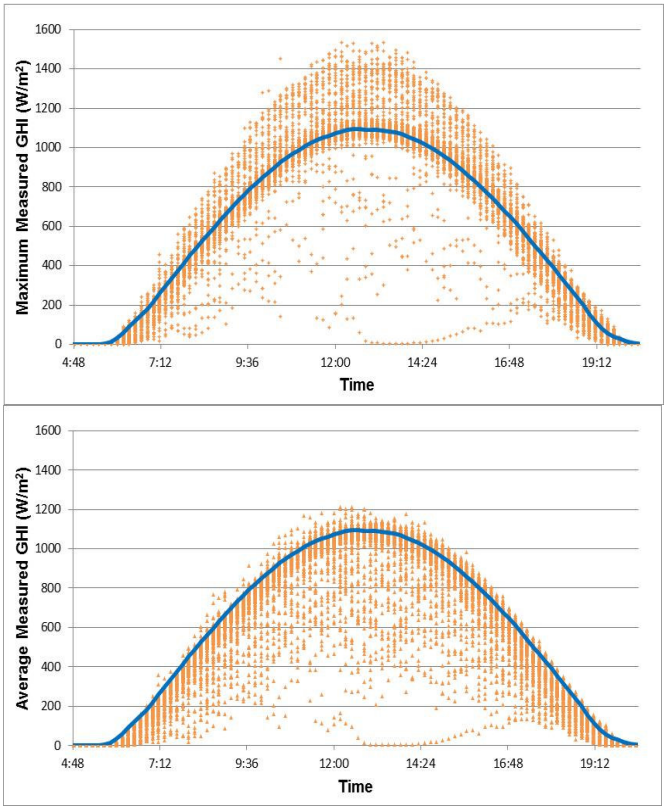

Fig. 2. Diurnal distribution of (a) maximum and (b) ten minute average values of GHI. The solid line represents the maximum theoretical GHI as computed by the clear sky model

During the aforementioned period, the maximum intensity of GHI measured was 1533W/m^2 on the 25th of June 2010, at 11:10 local time, which corresponds to 151% of the value of GHI with respect to the modeled clear-sky GHI at the same time. Overall, on seven different occurrences over five different days, the measured GHI exceeded 1500W/m^2. This value exceeds by far the value of the extraterrestrial irradiance outside the Earth's atmosphere (i.e. Solar Constant). Generally, on 25 different days, the measured GHI exceeded the value of the Solar Constant.

What is equally surprising is that while normally this enhancement of solar irradiance lasts for a short period, depending on the motion of clouds, on 5 different days of May and June 2010, the ten minute average GHI was above 1200W/m^2 (125% of the modeled clear-sky GHI value for the same time). As it will be discussed in Section 4, these long periods of enhanced irradiance can boost the power output of PV modules and increase the Solar Electricity Generation (SEG) of PV parks. However, although this additional power output is desirable, it may be rejected by the inverter if it is larger than the inverter's AC rating or if the current (I) - voltage (V) intensity exceeds the operational range of the inverter or even cause irreversible damage to PV inverters if the levels of I or V exceed the upper threshold.

It has to be mentioned that all these occurrences were recorded only during April-July 2010 despite the fact that during this period the Solar Constant is at the lower range of 1321-1367W/m^2.

Figure 3 presents the occurrences of high recorded intensities of maximum GHI during the period April – July 2010. The red bars of the graph represent the intensities of GHI that exceeded the theoretical threshold of the average value of the Solar constant (1367 W/m^2), despite the fact that since the measurements were recorded during the summer months at the Northern Hemisphere, the Solar Constant has lower values. The blue bars represent the intensities lower than 1367W/m^2.

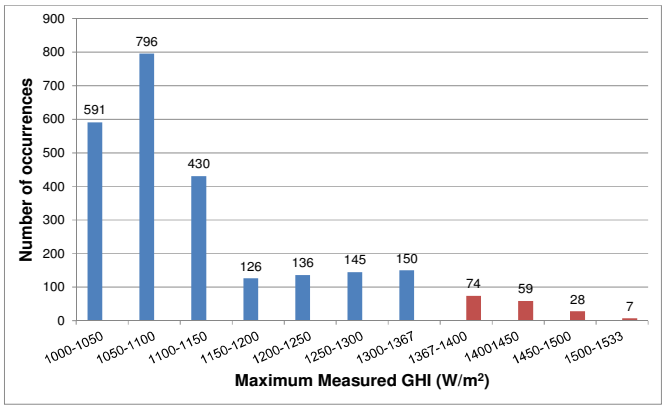

Fig. 3. Number of occurrences of maximum GHI over 1000W/m^2.

Figure 4 presents the corresponding occurrences of the ten-minute averaged GHI measured for the same period that exceeds 1000W/m^2. This shows that the duration of the irradiance enhancement lasted at least for several minutes and not just for a few seconds. Such long duration of irradiance enhancement, ranging from 20 to 140 seconds was also stated by Schade et al. [15]. The importance of recording data at small time intervals is also shown, since otherwise, important data/results might be lost.

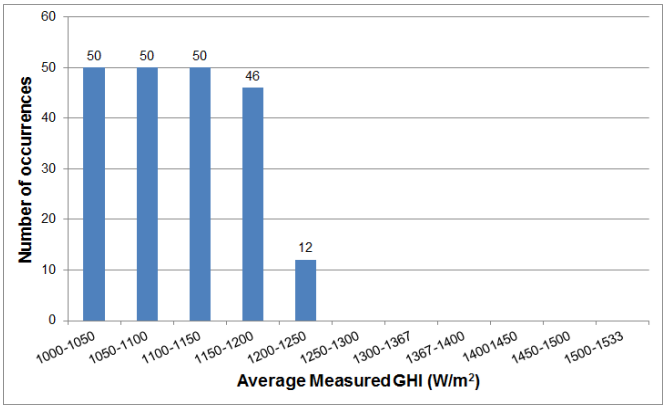

Fig. 4. Number of occurrences of average GHI over 1000W/m^2.

IV. Discussion – Effect on PV Inverters

The I-V characteristic curves defined in the Standard Testing Conditions (STC) for PV modules have a rating maximum irradiance value 1000W/m^2 which approximates the theoretical maximum clear sky global irradiance [22]. Most PV inverters integrate a Maximum Power Point Tracking (MPPT) device that regulate the I-V characteristics of the PV modules (varying either I or V) at fixed time intervals, in order to obtain the maximum power output from the modules. Modern MPPT inverters have very short intervals (less than 5 seconds) thus, they are able to take advantage of the very fast fluctuations of solar irradiance [16].

During the fluctuations of the irradiance, and at constant temperatures, the voltage output remains approximately the same whereas the current fluctuates linearly resulting in a relevant variation of the power output of the PV module.

Under clear sky conditions at mid and low latitude sites (like Cyprus), when incident irradiance exceeds the threshold of 1000W/m^2, the PV module temperature also increases, resulting in a decrease of the PV solar conversion efficiency by about 15% [17]. Nevertheless, the presence of clouds with low base height (such as Cumulus clouds) may reduce the surface air temperature up to 50% during warm and dry seasons compared to clear sky conditions [18][19]. This is demonstrated in Figure 5 that presents typical examples of one cloudy and one cloudy free day, during partial cloudy conditions, the ambient temperature is lower than 25^{o}C for long periods during which the GHI is also higher than the computed value. Thus, the positive correlation of the temperature drop and GHI enhancement leads to a further enhancement of the power output of the PV modules.

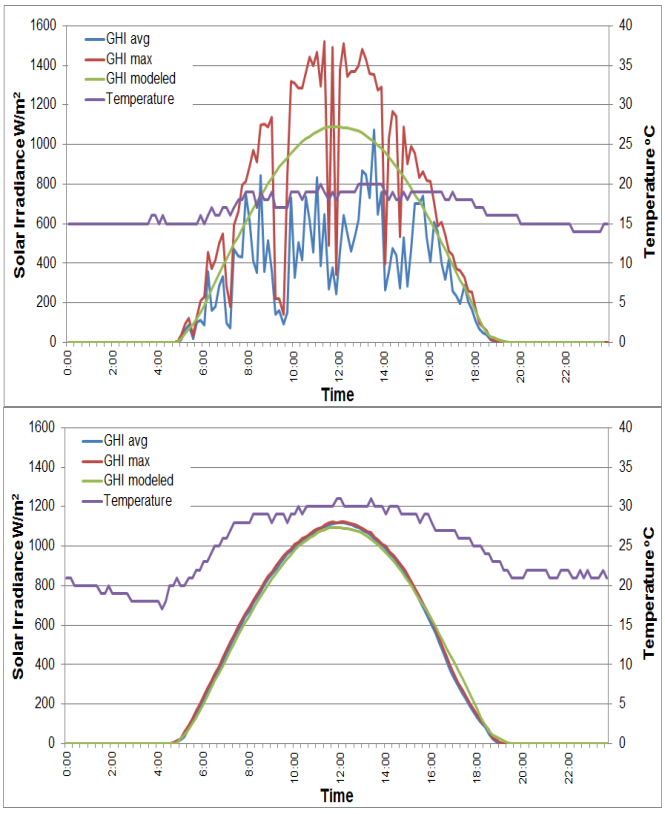

Fig. 5. Temperature variation during cloudy and partial cloudy days for (a) 23rd May 2010, (b) 30th May 2010

Since the instantaneous enhancement of solar irradiance has limited duration, it may affect only slightly the overall SEG of a PV Park due to the short duration of this effect. Only long durations of enhanced irradiance, even at lower absolute values may result on substantial supplementary SEG from the PV Parks. As presented in Section 3, long intervals of enhanced GHI were recorded at the meteorological station; in various cases the one minute average and in rarer cases the ten minute average GHI exceeded 1200W/m^2 which corresponds to 120% over the STC of the PV modules. Furthermore, in all these cases, the weather conditions were relatively invariant, the ambient temperature always lower than 25^{o}C and in most cases under 20^{o}C, which is relatively low for the summer in Cyprus during daytime. These two coinciding parameters would in theory increase the overall SEG of the PV Park.

However, this additional power output of the PV modules may not always result in additional SEG from the PV Park, but it may lead to energy losses due to inverter saturation [17]. Inverter saturation occurs when the inverter rejects the electricity from the PV modules because the DC input power is larger than the inverter AC rating [24]. Depending on the inverter technology, the inverter drifts from the MPP by increasing the voltage, thus reducing DC current and power.

Regardless of the ability of the inverter to regulate the input power, there are limits that cannot be overcome. If the DC input power to the inverter exceeds the maximum DC power threshold of the inverter, then it may cause irreparable damage to the inverter. Similarly, if the value of I primarily (or V in more extreme scenarios) exceeds the maximum threshold defined by the inverter producer, irreparable damage may be caused to the inverter. For example, since an increase of solar irradiance leads to a linear increase of I [20], using linear extrapolation, the maximum measured value of GHI (1533W/m^2 in our case) will result in a value of I 150% greater than the design value of the PV string, which may exceed the upper safety threshold of the inverter.

It should be noted here, that the irradiance measurements presented in this paper regard GHI and not global irradiance on the inclined surface recommended for PV installation in Cyprus and hence variations will exist. Several researchers have proposed mathematical formulas based on statistical or Artificial Intelligence techniques [1][2] to compute the global irradiance on an inclined surface using measurements of GHI.

V. Conclusions

Very high intensities of GHI were measured by a remote meteorological station in Cyprus during April – July 2010, a period of usually low cloud coverage (0-1 oktas) [25]. The highest intensity of GHI measured was 1533W/m^2 at noon of the 25th of June 2010 corresponding to values of 150% of the theoretical clear sky value for the same period. Of equal significance is that in various occasions, the one-minute average GHI and the ten-minute average exceeded 1200W/m^2, corresponding to additional 120% over the theoretical clear sky value in most cases. Such exceptionally high values of irradiance have also been mentioned in the literature, although in most cases they were recorded at very high latitudes (over 1600m) or near the equator, where higher irradiance occurs. These periods of enhanced

irradiance, along with the temperature drop due to the presence of clouds might boost the performance of photovoltaic modules and cause irreparable damage to photovoltaic inverters. Future objectives consist of detailed irradiance measurements on site at a PV park and association of possible enhanced irradiance measurements with the power output of the PV Park as well as to correlate enhanced irradiance measurements to cloud classification and cloud classes using ground based cameras.

VI. References

References are important to the reader; therefore, each citation must be complete and correct. References should be readily available publications.

List only one reference per reference number. If a reference is available from two sources, each should be listed as a separate reference. Give all authors' names; do not use *et al.* except if the authors are more than six.

Samples of the correct formats for various types of references are given below.

Periodicals:

[1] C. Demain, M. Journée, and C. Bertrand, "Evaluation of different models to estimate the global solar radiation on inclined surfaces," *Renew. Energ*, vol. 50, pp. 50:710-721, 2013.

[2] A. M. Muzathik, M. Z. Ibrahim, K. B. Samo, and W. B. Wan Nik, "Estimation of global solar irradiation on horizontal and inclined surfaces based on the horizontal measurements," *Energy*, vol. 36, pp. 36:812-8, 2011.

[3] V. Badescu, C. A. Gueymard, S. Cheval, C. Oprea, M. Baciu, A. Dumitrescu, F. Iacobescu, I. Milos, and C. Rada, "Accuracy analysis for fifty-four clear-sky solar radiation models using routine hourly global irradiance measurements in Romania," *Renew. Energ.* vol. 55, pp. 85-103, 2013.

[4] M. J. Ahmad and G. N. Tiwari, "Solar radiation models - A review," *Int. J. Energ. Res*, vol. 35, pp. 271–290, 2011.

[5] K. Ulgen, and A. Hepbasli. "Solar Radiation Models. Part 1: A Review," *Energ. Sources*, vol. 26, pp. 507–520, 2004.

[6] R. Tapakis, and A. G. Charalambides. "Equipment and Methodologies for Cloud Detection and Classification: A review," *Sol. Energy* [Online] 2013. Available: http://dx.doi.org/10.1016/j.solener.2012.11.015.

[7] G. H. Yordanov, O. M. Midtgård, T. O. Saetre, H. K. Nielsen, and L. E. Norum, "Overirradiance (Cloud Enhancement) Events at High Latitudes," *IEEE J Photovolt*, vol. 3, pp. 271-277, 2013.

[8] R. D. Piacentini, G. M. Salum, N. Fraidenraich, and C. Tiba, "Extreme total solar irradiance due to cloud enhancement at sea level of the NE Atlantic coast of Brazil," *Renew. Energ,* vol. 36, pp. 409-412, 2011.

[9] W. R. Rouse, "Examples of enhanced global solar radiation through multiple reflection from an Ice-Covered Arctic Sea," *J. Clim. Appl. Meteorol*, vol. 20, pp. 670-674, 1987.

[10] H. Suehrcke, and P. G. McCormick, "The frequency distribution of instantaneous insolation values," *Sol Energy*, vol. 40, pp. 413–422, 1988.

[11] P. Emck, and M. Richter, "An upper threshold of enhanced global shortwave irradiance in the troposphere derived from field measurements in tropical mountains." *J. Appl. Meteorol. Clim*, vol. 47, pp. 2828–2845, 2008.

[12] R. D. Piacentini, A. Cede, and H. Bárcena, "Extreme solar global and UV irradiances due to cloud effect measured near the summer solstice at the high altitude desertic plateau Puna of Atacama (Argentina)," *J. Atmos. Sol-Terr. Phys*, vol. 65, pp. 727-731, 2003.

[13] A. Cede, M. Blumthaler, E. Luccini, R. D. Piacentini, and L. Nuñez, "Effects of clouds on erythemal and total irradiance as derived from data of the Argentine Network," *Geophys. Res. Lett*, vol. 29, GR015708, 2002.

[14] B. P. Briegleb, P. Minnis, V. Ramanathan, and E. Harrison, "Comparison of Regional Clear-Sky Albedos Inferred from Satellite Observations and Model Computations," *J. Appl. Meteorol*, vol. 25, pp. 214-226, 1986.

[15] N. H. Schade, A. Macke, H. Sandmann, and C. Stick. "Enhanced solar global irradiance during cloudy sky conditions," *Meteorol. Z.,* vol. 16, pp. 295–303, 2006.

[16] J. J. Delaunay, M. Rommel, and J. Geisler. "The importance of the sampling frequency in determining short-time-averaged irradiance and illuminance for rapidly changing cloud cover," *Sol. Energy*, vol. 52, pp. 541–545, 1994.

[17] J. Luoma, J. Kleissl, and K. Murray, "Optimal inverter sizing considering cloud enhancement," *Sol. Energy*, vol. 86, pp. 421–429, 2012.

[18] A. Dai, K. E. Trenberth, and T. R. Karl, "Effects of Clouds, Soil Moisture, Precipitation, and Water Vapor on Diurnal Temperature Range," *J. Climate*, vol. 12, pp. 2451-2473, 1999.

[19] S. H. Schneider, "Cloudiness as a Global Climatic Feedback Mechanism: The Effects on the Radiation Balance and Surface Temperature of Variations in Cloudiness," *J. Atmos. Sci*, vol. 29, pp. 1413–1422, 1972.

[20] Y. Tsuno, Y. Hishikawa, and K. Kurokawa, "Modeling of the I–V curves of the PV modules using linear interpolation/extrapolation," *Sol. Energ. Mat. Sol. C*, vol. 93, pp. 1070–1073, 2009.

Books:

[21] J. A. Coakley Jr., "Reflectance and albedo, surface," in *Encyclopedia of Atmospheric Sciences* 1st ed., R. Holton, J. Pyle and J. A. Curry, Ed. Academic Press, 2003, pp. 1914-1923.

[22] A. Goetzberger, and V. U. Hoffmann. *Photovoltaic Solar Energy Generation*, Springer Series in optical sciences, Springer-Verlag Berlin Heidelberg; 2005.

Technical Reports:

[23] R. E. Bird, and R. L. Hulstrom. "Simplified Clear Sky Model for Direct and Diffuse Insolation on Horizontal Surfaces," Golden, CO. Solar Energy Research Institute, TR SERI/TR-642-761, 1981.

Papers from Conference Proceedings (Published):

[24] M. Zehner, T. Weigl, M. Hartmann, S. Thaler, O. Schrank, M. Czakalla, et al. "Energy loss due to irradiance enhancement," in Proc. 2012 *26th EU PVSEC*, pp. 3935-3938.

Private Communication:

[25] Private communication with Meteorological Service of Cyprus; 2012.

VII. Biographies

Rogiros Tapakis is currently a PhD candidate, in the field of Renewable Energy Systems, at the Department of Environmental Science and Technology at the Cyprus University of Technology (CUT). He has conducted his studies in Mechanical Engineering specializing at Energy at National Technical University of Athens (NTUA) in Greece and has graduated in 2006. He also carries an MSc from NTUA on “Power Generation and Distribution” and has graduated in 2008.

After the completion of his studies up to 2010, he has worked as a mechanical engineer in Greece in the Solar-Desalination section, He is a member of mechanic chamber in Cyprus and Greece and is a certified inspector of Energy Efficiency on Buildings in Cyprus.

Following that, in February 2011, he was admitted at the CUT as a trainee and PhD candidate at the Department of Environmental Management on “Computational Calculations of Solar Intensity in Cyprus”. His research interests lie in the domains of Renewable Energy Systems, Power Generation and Distribution, Computer Simulation Models and energy conservation in buildings.

Dr Alexandros Charalambides is a full-time Lecturer at the Department of Environmental Management of the Cyprus University of Technology in Cyprus since 2009. He is primarily interested in establishing a viable and sound energy policy based on research outcomes. He holds a PhD from Imperial College London on combustion and his PhD work was sponsored by Honda R&D, Japan. As a lecturer at CUT, he has written and has/is currently supervising various research grants (worth over €260,000 for CUT benefit). His work focuses on image processing, optical techniques and combustion. He is also working on the production of biofuels from algae and on the treatment of sewage/ wastewater. He has 2 active PhD

students, and has also supervised 2 research associates in successfully completed projects. He has also written various publications on his work and is actively promoting renewable energy sources in Cyprus. In 2011, he came 3rd in the Cyprus Famelab competition, a national talent competition to find the best new talent in science communication. He has also won a scholarship from the Japanese Society for Promoting Science, was a finalist in the House of Commons Special Annual Reception for Britain's Younger Engineers Competition and won the Cyprus Entrepreneurship Competition 2005 organized by the University of Cyprus.

2nd Conference on Power Options for the Eastern Mediterranean Region
07-08 October 2013, Nicosia, Cyprus (Paper No. POEM13/153)

Impact of the Euro-Asia Interconnector project on the economic operation of Crete and Cyprus power systems

Antonis Antoniou, Nikolas Theodorou, Antonis Tsikalakis, Kostantinos Kalaitzakis, George Stavrakakis

***Abstract*—Cyprus and Crete are the largest autonomous power systems in the Mediterranean Sea. Euro-Asia Interconnector project is about to interconnect both power systems with Israel and in future with the Mainland Greece. The impact on the economic operation of both power systems, the expected flow between these two power systems and the final savings stemming from their interconnection are presented in this paper.**

***Index Terms*—Euro-Asia Interconnector, Autonomous Power Systems, Economic scheduling,**

I. Introduction

CYPRUS and Crete are the 3rd and the 5th largest islands in the Mediterranean Sea, respectively. However, they are the 1st and the 2nd largest autonomous power systems of the Mediterranean Sea. They both have abundant solar resources, Crete has also favourable wind conditions, but both have significant share of thermal units running on important fuel oil byproducts.

Euro-Asia Interconnector [1] is a very ambitious project for interconnecting three countries, Israel, Cyprus and Greece via submarine High Voltage Direct Current (HVDC) cables. In the second stage interconnection with mainland Greece via Peloponnese is foreseen. The total length will be 540 nautical miles even at depth 2000m and capacity of 2000MW making the interconnection one of the largest in the world.

Such interconnection will create significant difference in the operation of the power systems. The scope of this paper is to present the impact of considering only Crete-Cyprus interconnection of the Euro-Asia Interconnector. The main differences in operation autonomously and interconnected are going to be pinpointed. In section II the necessary estimations about demand, production units both thermal and Renewable Energy Sources (RES) are presented. This will give an idea of the size of the new Power System created. For our analysis we have used actual data from both island power systems for year 2010. The reasons for selecting this year are:

A) All units in both island power systems were in operation. In 2011 that would have been more recent, there was the tragic disaster at Mari [2] that would have created a much different Power System, affecting also 2012 operation.
B) The estimations for future demand increase cannot be clear within the financial crisis environment that currently affects both countries.
C) We desired to have a base case scenario of the Interconnected Power System on which future scenarios about production expansion, including new types of RES can refer to
D) We desired to examine the expected financial benefits if now these two power systems were interconnected.

Section III presents the methodology followed for our analysis. Operation scheduling of the power systems was made from scratch for both autonomous and interconnected operation of the power systems. The unified power system is still an autonomous power system.

Section IV presents the simulation results and mainly the comparison between autonomous operation and interconnected operation. The comparison focus on the effects on the operation of the thermal units before and after the interconnection with emphasis to intermediate or peaking units, the flow between the two interconnected power systems and the operation of RES considered in our scenarios. The corresponding change in fuel consumption and the corresponding cost change is considered. Last but not least, a load flow analysis can show us whether new transmission works are required additionally to the HVDC interconnection. A first insight of the network losses is also provided. Finally conclusions are drawn in section V regarding potential actions based on these results.

II. Characteristics Of The Two Power systems to Be Interconnected

Some characteristics of the two interconnected systems

The paper title should be in uppercase and lowercase letters, not all uppercase.

A. Antoniou, N. Theodorou, are with the Department of Electronics and Computers engineering of the Technical University of Crete, Kounoupidiana, 73100 Chania, Crete, Greece (e-mail: antonisanton@hotmail.com, nitheodorou@hotmail.com)

A. G. Tsikalakis is with the Department of Electronics and Computers engineering, Technical University of Crete and the Department of Electrical Engineering of the Technological Educational Institute of Crete Kounoupidiana, 73100 Chania, Crete, Greece (e-mail: atsikalakis@isc.tuc.gr).

K.Kalaitzakis is professor at the Technical University of Crete, Department of Electronics and Computers engineering, Kounoupidiana, 73100 Chania, Crete, Greece (kkalaitzakis@isc.tuc.gr)

G.Stavrakakis is professor at the Technical University of Crete, Department of Electronics and Computers engineering, Kounoupidiana, 73100 Chania, Crete, Greece (gstavr@electronics.tuc.gr)

regarding demand pattern, thermal stations synthesis and expected RES contribution are presented in the following sub-sections.

A. Demand Characteristics

Both islands share in common increased demand during summer. Crete demand clearly presents two peaks during a summer day while Cyprus presents one as shown in Fig.1.

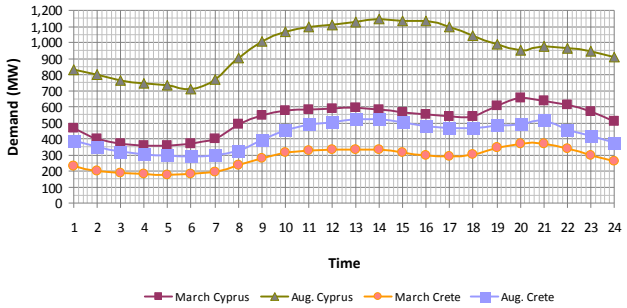

Fig. 1. Typical demand curves for each system alone for low and high demand periods.

However, the peak demand in both islands is strongly correlated. The correlation factor (ε) is 1.035 and during summer months this may be as low as 1.013. The load factor (lf) is expected to be 54.38% compared to 51.8% for Cyprus alone. Another challenge is the minimum to maximum ratio, which even though it is increased, is as low as 28.1% on annual base but can be as high as 45% for the summer period. This is much higher compared to 21% of the Cretan Power System for the year of study 2010.

Clearly, the demand in Cyprus is significantly higher compared to Crete in both peak and energy demand as Table I illustrates.

TABLE I
SUMMARY OF DEMAND CHARACTERISTICS FOR THE INTERCONNECTED POWER SYSTEMS

Power System	Demand (GWh)	Peak Demand (MW)	Min Demand (MW)
Cyprus	5189,18	1143.2	308,50
Crete	2732,64	577.9	126
Unified	7921,82	1662.9	467.25

34.5% of the demand comes from Crete and the rest from Cyprus

The typical demand curves for peak and low loading periods for the unified power system is shown in Fig.2.

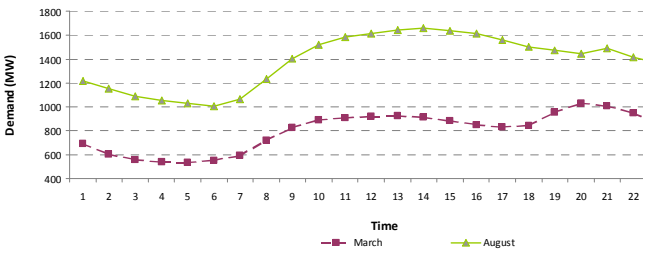

Fig. 2. Typical demand curves for the unified power system for low and high demand periods.

B. Thermal Power Station Characteristics

Interconnection of the two Power Systems will create one Power System with 6 Power Stations consuming fuel oil using a variety of units technologies such as Steam Turbines (ST), Internal Combustion Engines (ICE), Gas Turbines (GT) and Combined Cycle Units (CC). A summary of the power stations is provided in Table II with the installed capacity per unit type. On Cyprus the power stations are owned and operated by the Electricity Authority of Cyprus (EAC), while the power stations on Crete are operated by the Public Power Corporation (PPC).

TABLE II
INSTALLED CAPACITY (MW) PER UNIT TYPE AND POWER STATION

Power Station	ST	ICE	GT	CC	Installed Capacity (MW)
Vasilikos	390	-	37.5	220	647,5
Dekelia	360	104.8	-	-	464,8
Moni	180	-	150	-	330
Linoperamata	106	44	115	-	265
Chania	0	0	216	132	348
Atherinolakos	102	88		-	190
Total Capacity	1138	236.8	518.5	352	2245.3

All stations consume heavy fuel oil (HFO) for the steam turbine units and ICE and diesel oil for the gas turbine units and the Combined Cycle units. Interconnection will create a power system with 66.4% of the installed capacity coming from must run units ST and CC. This may decrease the operating cost imposing however significant challenges in co-operation with RES, especially wind power [3].

C. Renewable Energy Sources (RES) status

Both islands enjoy favourable conditions for exploiting solar energy. PVs are much more widespread on the island of Crete compared to Cyprus. Crete already meets 20% of the energy needs using Wind and PVs. Since 2000, Crete steadily meets 10% of the demand with wind power with clear benefits in both economics and operational terms [4]. In March 2013, 26.4% of the produced energy on Crete came from RES [5].

Details from the operation of the largest PV plant on the island are described in [6] while the expected impact of PV operation in Cyprus and Crete has been described in [7] and [8] respectively.

The installed capacity in both islands is currently slightly below 450MW and is summarized in Table III.

TABLE III
INSTALLED RES CAPACITY (MW) PER TYPE AND ISLAND

Power System	Wind (MW)	PV(MW)	Other RES (MW)
Cyprus	146.7	16.4	8.7
Crete	183.54	91.41	1
Unified	330.24	107.81	9.7

There are significant plans for installing additional capacity on both islands. Proposals and feasibility studies for Solar thermal power stations in Cyprus have been also made[9], their potential impact has been assessed [10], and 77MW have been granted authorization. On Cyprus there have been applications for 950MW of wind power and significant number of large-scale applications of PVs is also foreseen. The Cypriot Energy Regulatory Authority (CERA) frequently issues details on the applications and the authorizations received [11].

On the island of Crete, about 1000MW of Wind power had been granted authorization expected to be installed as soon as Crete is interconnected to other power systems.

These plans foresee also Hybrid Solar-thermal power stations on Crete in the order of 200 MW. Regarding PVs, there will not be authorizations unless the island gets interconnected. No more than 15MW have been authorized but not installed yet. On Crete there are also plans for Pumped-Hydro units.

III. Simulation Methodology

A. Economic Operation Simulation

The economic operation of both Power Systems either running autonomously or operating interconnected is simulated using the common methodology described below.

1) Import of Demand, RES Data and error-checking of input Data.

RES units are priority dispatched according to the legislation in both countries. The rest of the demand is to be met by the thermal units of the power systems. As realistic availability of the thermal units as possible has been also taken into account for our simulations. Data from the SCADA systems of both power systems, regarding demand and RES production were used and are checked for potential errors, such as failure of storing reasonable values.

Neither in Cyprus nor in Crete, was the production of PVs recorded during 2010. Thus, the demand records from SCADA already included PV production. This was taken into account in the considered PV capacity in the simulations being the difference of currently installed capacity and the capacity installed in 2010 Thus, the PV capacity on Crete for our simulations was considered 44 MW while in Cyprus 11 MW.

2) Demand and RES forecasting error information utilization.

This step is essential in order to determine the expected range of the demand to be met by the thermal units of either each of the power systems or the interconnected ones. This is required not only to determine the load to be met by the thermal units, but also to determine RES production to be injected to the grid without violating the technical minima constraints of the thermal units committed.

The utilization of information about forecasting errors is based on probabilistic techniques presented in [12]. It is assumed that demand forecasting errors are statistically independent random variables (rv) [13] and thus the probability density functions of load forecasting $l_e(t)$ and RES forecasting $w_e(t)$ can be convoluted to produce the $lw_e(t)$ probability density function as described in (1)

$$lw_e(t) = l_e(t) - w_e(t). \quad (1)$$

Having calculated the $lw_e(t)$ pdf, confidence intervals for the expected uncertainty of the load to be distributed to the thermal units can be derived, expressed as the interval between p and q percentiles.

The q percentile, $perc(q,lw_e(t))$, of the cumulative distribution function (cdf), $F_{lwe(t)}(lw_e(t))$, of the $lw_e(t)$ pdf is the solution of the following equation:

$$F_{lwe(t)}(lw_e(t)) = q. \quad (2)$$

The solution of (2) depends on the pdf that is derived according to the available information on the forecasting error functions. According to the desired confidence interval, the economic scheduling functions identify which units operate, their production and if there is any need for RES curtailment. Even though with regards to curtailment, all RES are considered equivalent in our simulations, usually curtailment refers to wind since this is much easier implemented compared to hundreds of low capacity PVs scattered in the Distribution grid.

3) Solving the Unit Commitment problem

The next step is to determine which thermal units should operate. The units to be committed should meet, *Ld2Units(t)*, at each time interval *t*, which is the maximum of the following two values as described in (3)

$$Ld2Units(t)=max\{UCload\_1(t), UCload\_2(t)\} \quad (3)$$

a) The demand left to the thermal units considering uncertainties on Demand and RES production denoted as *Ucload_1(t)* in equation (4).

$$UCload\_1(t)=perc(q,lw_e(t))+load(t)-WP(t)-PVP(t) \quad (4)$$

The highest values of $F_{lwe(t)}(lw_e(t))$, correspond to overestimation of RES and underestimation of load, the case the system might be inadequate. Therefore, q is selected high (e.g. 98.5%), so that the risk of insufficient committed capacity is less than 1-q (e.g. 1.5%). Variables *load(t), WP(t),PVP(t)* denote respectively the demand, the Wind Power production and the considered PV production of the Power system under study.

b) The demand left to the thermal units considering however loss in the greatest operating unit ($Pg_i(t-1)$) is denoted as *UCload_2(t) in* equation (5). In this case forecasts have been considered perfect.

$$UCload\_2(t)=load(t)-WP(t)-PVP(t)+max\{Pg_i(t-1)\} \quad \mathbf{(5)}$$

The minimization function for selecting *unno* thermal units, using the following formulation for each time interval is described in equation (6) with the constraints(7)and (8), for each time step.

$$Min(OC(t)) = Min(\sum_{i=1}^{unno}(u_{i,t}\cdot FC(Pg_i(t)) + u_{i,t}\cdot(1-u_{i,t-1})\cdot SUC_i(t)) \quad (6)$$

OC(t) is the operating cost, FC is the fuel cost function (cubic cost function) of unit *i* depending on its production $Pg_i(t)$, $u_{i,t}$ is the unit status (0 if unit is OFF, 1 if unit is ON). $SUC_i(t)$ denotes the start up cost of the *i*-th unit here considered constant.

$$P_i^{\min}(t) \le Pg_i(t) \le P_i^{MAX}(t) \quad (7)$$

$$\sum_{i=1}^{unno} u_{i,t} \cdot P_i^{MAX} \ge Ld2Units(t) \quad (8)$$

where $P_i^{\min}$ and P_i^{MAX} are the technical minimum and maximum of unit *i*, respectively.

In order to solve this problem a Priority List method with merit to base units (i.e ST and CC Units) is developed. The routine developed for this purpose assumes the available base units operating all the time even if one of them could have been switched off if it was a faster unit.

4) Economic Dispatch

Based on the schedule in step 3, the Economic Dispatch of the Power Systems should take place. However, it should be checked whether the sum of the technical minima of the units committed will be larger than the expected minimum load to be served in case of simultaneous overestimation of load and underestimation of wind as (9) describes.

$$\sum_{j \in IN(t)} P_j^{\min} \ge load(t) - WP(t) - PVP(t) + perc(p, lw_e(t)) \quad (9)$$

IN(t) is the set of the committed units and *p* is the value of the percentile, usually very small, e.g. *p*=2.5%, meaning that the probability of violating the technical minima is less than *p%*. If inequality (9) is satisfied, then some RES should be curtailed in order to satisfy (10):

$$WP(t) + PVP(t) = -\sum_{j \in IN(t)} P_j^{\min} + perc(p, lw_e(t)) + load(t) \quad (10)$$

The set-points of the committed units are finally calculated from the economic dispatch (ED) problem. This is formulated as the minimization of the fuel cost (FC) in (11), meeting the load as described in (12), without violating the technical limits of the units in (7).

$$\min \sum_{j \in IN(t)} FC(Pg_j(t)) \quad (11)$$

$$\sum_{j \in IN(t)} Pg_j(t) = load(t) - WP(t) - PVP(t) \quad (12)$$

In order to solve the ED optimization problem, the sequential quadratic programming method is used. This is a generalization of the Newton's optimization method, which uses a quadratic approach of the non-linear objective function of fuel costs and linear approximations for the technical constraints. This method guarantees that the solution is the global optimum in the feasible space, if the objective function is convex[14],[15].

5) Calculation of results

After the simulation is complete, we have used hourly steps for each month of the year, to take into account maintenance of the units, the following results are saved in *.txt files for further process.

a) Production per thermal unit, plant, unit type and Island
b) Fuel Consumption and cost calculation
c) Final production and curtailment of RES units.
d) Calculation of the flow between the two power systems.

B. Simulation of the Transmission System

Based on the results when methodology in subsection A is applied, a load flow is run in order to identify potential issues regarding losses and voltage profile. For this purpose the extended educational version of the PowerWorld Simulator [16], allowing 40-buses was used. A 37-bus network was built in order to simulate the interconnected power system. Additionally to the existing lines, two HVDC lines and four transformers, two at each side were added to simulate the interconnected power systems. The actual data on reactive power capacity curve and the installed shunt capacitors on both systems had been taken into account. The results regarding the Transmission network reinforcement is described in the results section.

IV. Simulation Results

As described above data on 2010 were used from both islands. Even though the fuel prices does not affect significantly the commitment of units within the same power systems, when these get interconnected different fuel prices in each systems may lead to increase of production at the other regardless the actual efficiency of the units. The fuel Prices considered based on actual data are described in Table IV.

TABLE IV
Fuel Prices For Each Power System

Source	Price (€/Tn)
HFO -Crete	415
Diesel-Crete	698
HFO -Cyprus	359
Diesel- Cyprus	539

Results refer to A) Thermal production and Power Exchange, B) RES Integration, C) Fuel Consumption and Economic Results and D) Initial estimations of Transmission Systems upgrades.

A. Thermal Production and Power Exchange

1) Flow Exchange

The increased fuel prices on the island of Crete, the fact that there is significant capacity in Steam Units on Cyprus and the interconnection of the two power systems clearly, leads to increase of thermal production on the island of Cyprus and significant flow from Cyprus to Crete. Very seldom, only 58 hours, does Crete export energy to Cyprus. This is mainly during low load periods with high RES production on Crete, low demand in both islands and maintenance of the base units in Vasilikos Power Plant. The maximum flow on the cable is 308.77 MW from Cyprus to Crete, in June. When Cyprus imports from Crete the flow is below 100 MW. For the whole year 987.8 GWh are imported to Crete and 0.8 GWh to Cyprus. June presents the highest monthly flow with 118.74GWh.

The duration curve of the flow between the two power systems is shown in Fig.3. Negative values mean that active power is imported to Cyprus from Crete. Crete would meet 33% of the energy needs with imports from Cyprus. In November more than half the demand of Crete comes from import from Cyprus.

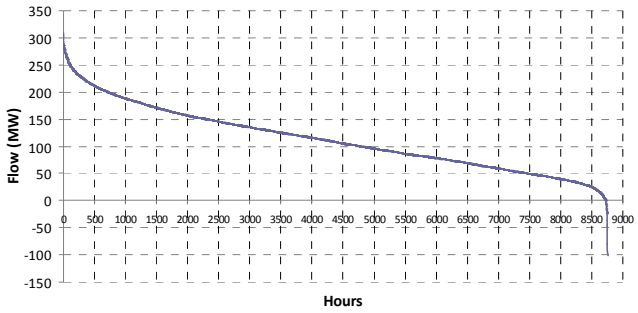

Fig. 3. Duration curve of the Power Flow in the interconnecting HVDC cables (Positive values mean flow from Cyprus to Crete).

2) Units production

Both the thermal and the total production per island system before and after the interconnection are summarized in Fig. 4. Additionally, the percentage change compared to independent operation is shown. Clearly production on Cyprus increases significant compared to Crete. RES help in decreasing total production change on Crete.

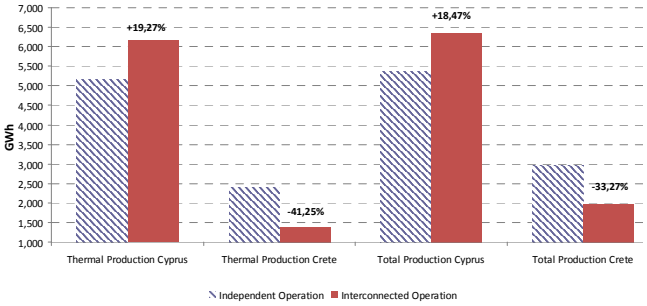

Fig. 4. Change in both thermal and total production

An analysis of the production at Power Station level before and after the interconnection is shown in Fig. 5. Vasilikos power station is the most important power station meeting more than half of the demand allocated to the thermal units of the interconnected power systems. Atherinolakos units, decrease their production by 50%, mainly due to the reduced operating hours of the ICE units. However, this is still the most important Power Station on Crete increasing even more the flow from East to West on the island of Crete.

More details on the production, regarding production of each type of units is shown in Fig.6. Interconnection leads to a power system with 84.7% of the demand met by must run units like Steam turbines and Combined Cycle units compared to 79% when these two systems run independently. This may create issues co-operation with RES as described in sub-section B.

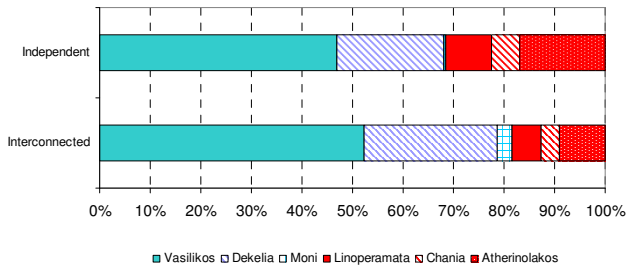

Fig. 5. Production at Power Station level before and after the interconnection

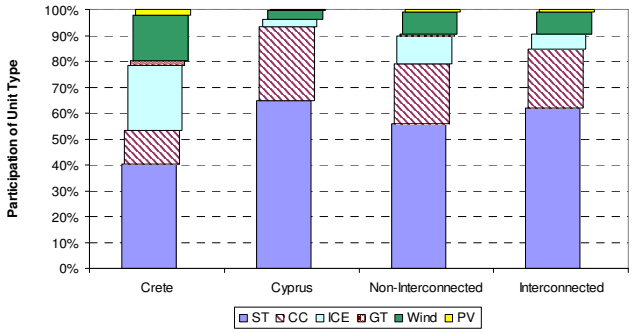

Fig. 6. Production at Power Station level before and after the interconnection

Further details on the impact on the operation of intermediate and peaking load units are provided in the following paragraph.

3) Operation of intermediate and peaking load units

Even though the correlation of demand between Crete and Cyprus is rather high, interconnecting these two power systems leads to reduction of operation of intermediate and peaking load units such as Internal Combustion Engines and mainly Gas turbines. Reduction is mainly for the units on Crete. Fig.7 shows the change in the operating hours of various intermediate and peaking load units. Their contribution from 11.49% in independent operation drops to 5.83% in interconnected operation.

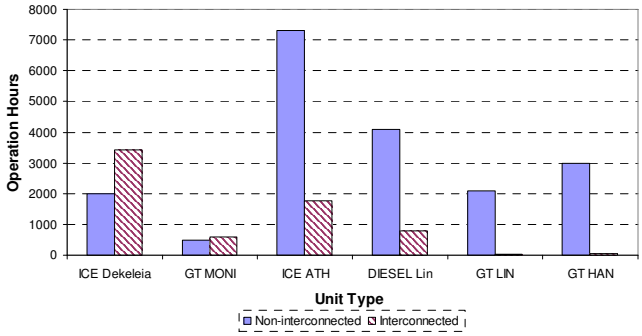

Fig. 7. Operation of Peaking and intermediate units

None of the units operates for more than half of the year while Gas Turbines in Chania (HAN) and Linoperamata (LIN).

B. RES Integration

When Cyprus Power System operates autonomously, 3.69% of RES production is expected to be curtailed. This curtailment comes almost inclusively from wind power resulting in curtailment of 4.13% of the expected wind power production may be required to be curtailed. This is even worse during November when 12% of the expected wind power production may be curtailed. RES penetration in Cyprus reaches 3.6% and monthly penetration in February exceeds 6%. On Crete, RES curtailment is 0.55% with highest curtailment during January at 4%. RES penetration reaches 19.6% with July penetration at 26%. The estimated curtailed RES production from both power systems is 11.3 GWh or 1.5% of the estimated production.

When these two power systems get interconnected, RES share is 9.35% and the allocation among the various types of RES and islands is shown in Fig. 8. The wind parks on Crete

account for the 65.3% of the production in the interconnected power system.

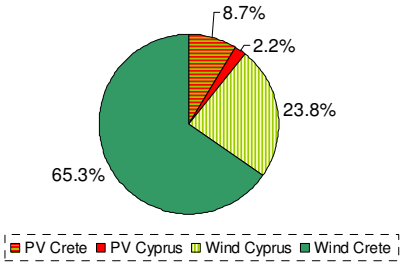

Fig. 8. Allocation of RES production per type and island

When the systems get interconnected, RES curtailment should be re-arranged according to the expected production. This is favourable for wind power owners in Cyprus, since curtailment is reduced by 53% but for wind power owners on Crete the curtailment increases by 175%. The curtailed RES production is increased by 6.2% reaching 12.1 GWh annually. However, the percentage of RES production curtailed is still limited accounting for 1.51% of RES production.

In both case curtailment is expected during early morning hours, i.e. about 5.00am and is significantly increased during Spring, when demand is low. This could be exploited for providing power to Desalination loads already existing on Cyprus acting as flexible loads [17].

C. Economic Results

Due to a) the operation of the most economic units in both systems b) reduction of intermediate and peaking units production and c) the most efficient operating point of the operating units, heavy fuel oil consumption is slightly increased and diesel oil is reduced by higher percent.

This has as impact reduction of the operating cost of the unified power systems by 15million € compared to even the most economic operation of the separate power systems. RES remuneration leads to slight reduction of the annual benefits to 14.9 million €.

The operational cost takes into account RES remuneration described in Table V.

TABLE V
CONSIDERED REMUNERATION FOR RES

Source	Remuneration (€/MWh)
Wind Power on Crete	99.45
PV on Crete	305.6
Wind Power on Cyprus	129
PV on Cyprus	340

A summary of the operating cost per island and the fuel consumption is shown in Table VI.

TABLE VI
SUMMARY OF THE FUEL CONSUMPTION AND COST

Power System	HFO (tn)	Diesel (klt)	Fuel Cost (mil. €)	Operational Cost (mil. €)
Cyprus	936628	249092	470.6	499.7
Crete	488629	143191	281.04	352.85
Total Independent Operation	1385294	392284	751.6	852.61
Interconncected operation	1432687	361363	736.6	837.67
Percentage Difference	3.42%	-7.88%	-2.00%	-1.75%

Average thermal cost when two power systems are interconnected is 97.48€/MWh which is by 2 €/MWh lower than the one for independent operation of the power systems. This is very beneficial for the island of Crete where the average cost when running independently is 117.89 €/MWh, in contrast with Cyprus where the related cost is 91.03 €/MWh. If RES remuneration is taken into account the average energy cost for the interconnected power system is 100.45€/MWh, by 1.73€/MWh lower compared to independent operation.

Due to higher emissions level of HFO for CO_2, 3.2 kg/Kg compared to 2.45kg/kg of diesel, the CO_2 emissions of the unified power system are slightly increased. Since production in Cyprus is substantially increased, there should be a significant revision of the emissions quota for the EAC by 800 thousand Tons.

D. Preliminary load flow results

Based on the 37-bus system of Cyprus and Crete, an analysis of the expected voltage profile and the losses of both power systems is performed. Even with the initial simulations performed it was apparent that:

a) At least two transformers at island equal to the capacity of each one of the DC cables used are required. On Crete these will be 400 kV/150 kV, while on Cyprus this will be 400 kV/132 kV. Otherwise, the voltage drop will be significant in the interconnection cable, the transformer losses will be increased and the reliability will be decreased.

b) There is requirement for building a new double transmission line on Cyprus between Vasilikos and the interconnection point near Paphos preferably at 400kV. Also a line between Moni and Paphos would improve significantly the voltage profile and the transfer capability on Cyprus.

c) On Crete there will be significant flow from East to West due to the economic units of the Atherinolakos Power Station and the significant RES capacity sited there (more than 50% of the installed capacity). Additionally, in the most Eastern part of the island the demand is significantly low. The flow will be much higher when Cyprus and Crete are interconnected compared to non-interconnected operation due to the significantly reduced production at Chania Power Station. This may create issues in the voltage level on Western Crete due to increased flow to this area and the limited reactive power supply especially during summer. Therefore, reactive power support would be required on Western Crete with flexible shunt capacitors or more sophisticated devices like FACTS.

For presentation reasons each island has been separated into western and eastern part with center Vasilikos and Linoperamata Power Stations respectively. The losses per area are summarized in the diagram of Fig. 9. 63.99GWh are lost and 0.7% of the transferred energy between the two power systems is lost in the Interconnection.

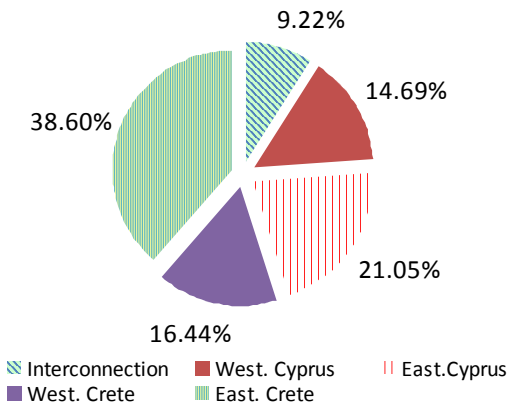

Fig. 9. Allocation of losses in various parts of the Cretan and Cyprus network.

Maximum value of active power losses during August is 28.79MW. The maximum active power losses are 22.26MW on Crete in June while on Cyprus the maximum losses are 8.14MW. It should be noted that no reactive flow between these two systems is foreseen.

Due to c) the losses on the eastern Part of Crete constitute the largest portion of losses, especially in double circuit line of 150kV between Atherinolakos and Heraklion.

V. Discussion And Conclusions

Interconnection of the largest Autonomous Power systems in the Mediterranean Sea is a very ambitious project. This will create a power system with significant base units capacity with rather slow response, 1660MW peak demand and 450MW RES capacity already installed on the islands. Interconnection may be also a reason for further deployment of RES on both islands where investors have already shown interest.

From our simulations for both independent and interconnected operation, it is clear that there will be significant flow from Cyprus to Crete, accounting for 33% of the annual demand on Crete. Interconnection will have as result, higher usage of HFO compared to diesel oil and as a consequence, slight decrease in CO_2 emissions quota required for both systems. EAC will definitely due to increased production in Cyprus have to buy additional CO_2 emissions quota. Since HFO is cheaper and the fact of using efficient units at more efficient operating points, the operating cost of the unified power system by 14.9 million €, or 1.75% of the operating cost if RES remuneration is taken into account. This money would suffice for 209 million € investment on the cable at 30 years basis and 6% interest rate.

RES penetration is not expected to change significantly since interconnection does not reduce RES curtailment. Scenarios with increased RES capacity and even greater diversity of units, including decommissioning of some old Steam Units (perhaps in Moni and Linoperamata power stations) in favour of ICE will be the topic of a future paper. Some very preliminary analysis show that if must run units are kept in the order of 75%-80% and not exceeding 80% of the demand as expected, will reduce RES curtailment

Further RES installation should focus on producing during the summer peak periods. Thus, the value of RES for the interconnected islands will be increased bringing the maximum benefits. To the same direction shifting of the demand, to morning hours could provide substantial aid for RES integration.

What is clear from the initial load flow scenarios is that an upgrade in the Transmission System of Cyprus from Vasilikos to Western part of Cyprus would be essential for supporting the project. There may be the case, when demand on Western Crete is high, mainly summer, that Chania Power station should operate at higher level in order to maintain higher voltage profile and provide voltage support. A proposal could have been to increase RES capacity on Western Crete to support demand locally.Transmission system reinforcement including interconnection to mainland Greece can use similar methodology with [18].

VI. Acknowledgment

The remarks of Dr. Emm.Thalassinakis and Dr.Andreas Poulikkas during the simulations held are gratefully acknowledged.

VII. References

[1] Euro-Asia Interconnector Website. [Online]. Available http://www.euroasia-interconnector.com/Index.aspx

[2] T. Zachariadis, and A. Poullikkas, "The costs of power outages: A case study from Cyprus". *Energy Policy*, Vol 51, Dec.2012, pp 630-641

[3] P. S. Georgilakis, "Technical challenges associated with the integration of wind power into power systems," *Renewable and Sustainable Energy Reviews*, Vol 12, Issue 3,pp 852-863, Apr. 2008.

[4] A.Tsikalakis, N. Hatziargyriou, K. Papadogiannis, A.Gigantidou, J. Stefanakis and E. Thalassinakis, "Financial Contribution of Wind Power on the Island System of Crete," *in Proc of RES for islands conference, Crete, May 2003*, pp 21-31

[5] Report for Non-Interconnected Islands operation of the Distribution System Operator (DEDDHE). [Online].Available www.deddie.gr (in Greek)

[6] E. Kymakis, S. Kalykakis and Th. Papazoglou, "Performance analysis of a grid connected photovoltaic park on the island of Crete" *J.Energy Conversion and Management,* Vol. 50, Issue 3, pp 433-438, March 2009.

[7] A. Poulikkas, A. Tsikalakis and N.D. Hatziargyriou, "Economic evaluation of low Photovoltaics (PV) penetration in island power systems, application to Cyprus," *In proc DISTRES Conference (Conference on the promotion of Distributed Renewable Energy Sources in the Mediterranean region) Cyprus 11-12 December 2009*, Paper no 108.

[8] A. G. Tsikalakis, N. D. Hatziargyriou, E. Karapidakis, and E. Kymakis, "Economic evaluation of low Photovoltaics (PV) penetration in island power systems, application to Crete," presented at the DEMSEE conference, Sitia, Crete, Greece, Sept. 2010.

[9] A Poullikkas, "Economic analysis of power generation from parabolic trough solar thermal plants for the Mediterranean region—a case study for the island of Cyprus. *Renewable and Sustainable Energy Reviews*, Vol.13, Issue 9,pp 2474-2484. Dec. 2009.

[10] A. Poullikkas, I. Hadjipaschalis, and G. Kourtis, "The cost of integration of parabolic trough CSP plants in isolated Mediterranean power systems". *Renewable and sustainable energy reviews*, Vol 14, issue 5,pp 1469-1476, June 2010.

[11] Cypriot Energy Ragulatory Authority. Authorization statistics. [Online]. Available, http://www.cera.org.cy/main/default.aspx?tabid=127

[12] A. G. Tsikalakis, N.D. Hatziargyriou, Y. A. Katsigiannis and P.S. Georgilakis, "Impact of wind power forecasting error bias on the economic operation of autonomous power systems", *J.Wind Energy*, Vol. 12 Issue 4, pp 315 –331,May 2009.

[13] B. Parsons, M. Milligan, B. Zavadil, D. Brooks et al., "Grid impacts of wind power: a summary of recent studies in the United States". *J. Wind Energy* ,Vol 7, Issue 2, pp 87–108, Apr. 2004

[14] XS Han, HB Gooi, DS Kirschen, "Dynamic economic dispatch: feasible and optimal solutions". *IEEE Trans. on Power Systems* Vol 16,,Issue 1pp 22-28, Feb. 2001

[15] Rao SS. *Engineering Optimization: Theory and Practice*, 3rd Ed.. John Willey & sons, 1996.

[16] PowerWorld Simulator 16GSO Edition. [Online},Available: http://www.powerworld.com/gloversarmaoverbye

[17] A. G. Tsikalakis, N.D. Hatziargyriou, G. Caralis, A. Zervos, E. Zoulias, E. Stamatakis et al., "Impact of different applications of Storage Systems in island power systems," *in proc of the DISTRES Conference (Conference on the promotion of Distributed Renewable Energy Sources in the Mediterranean region). Cyprus 11-12 December 2009*, paper no 131.

[18] E. Loukarakis and G. Stavrakakis, "Adaptive enumeration method for the optimal interconnection planning of isolated power systems, *IET Generation, Transmission & Distribution,* Vol 7, Issue 3, pp235-243,March 2013.

VIII. BIOGRAPHIES

Antonis Antoniou was born in Frenaros, Cyprus in 1985. He graduated from the Department of Electronics and Computer Engineering in Technical University of Crete in 2013 and his Diploma thesis was entitled "The effects on the Economic Operation of Power Systems of Cyprus and Crete because of their interconnection". His research interests include programming and Economic Analysis of Power Systems.

Nikolas Theodorou was born in Larnaca, Cyprus, in 1987. He graduated from the Department of Electronics and Computer Engineering in Technical University of Crete in 2013 and his Diploma thesis was entitled "The effects on the Steady state operation of Power Systems of Cyprus and Crete because of their interconnection". His research interests include programming and Power Systems Analysis under steady state.

Antonis G. Tsikalakis was born in Greece in 1979. He received his diploma in Electrical and Computer Engineering from NTUA. He received his PhD on "Distributed generation especially under high RES share and storage devices" from the same school in 2008. His research interests include optimization of power system operation, Dispersed Generation and energy storage. He currently is Adjunct Lecturer at the Department of Electronics and Computer Engineering in the Technical University of Crete and Research associate of the Technological Educational Institute of Crete. Mr. Tsikalakis is a student member of IEEE and member of the Technical Chamber of Greece.

Dr. Kostas Kalaitzakis was born in Chania-Crete-Greece in 1954. He received his B. Eng. degree in Electrical and Mechanical Engineering from the National Technical University of Athens/Greece (NTUA) in 1977 and his Ph.D. in electrical engineering from the Democritus Univ. of Thrace/Greece in 1983. He is currently a Professor at the Technical Univ. of Crete/Greece. He served as Adjunct Assistant Professor in the Georgia Institute of Technology/USA. His current R&D areas are in renewable energy sources, energy saving in buildings, power electronics, sensors and measurement systems, bioengineering and biomedical etc.He has published more than 40 papers in international journals, more than 40 papers in international conferences, one book and 2 chapters in books. He has participated in more than 25 national and international research projects, either as principal investigator or as researcher.

Dr.George S. Stavrakakis received his first degree in Electrical Engineering from the N.T.U.A. (National Technical University of Athens), Athens, in 1980. His D.E.A. in Automatic Control and Systems Engineering was obtained from I.N.S.A., Toulouse, France in 1981 and his Ph.D. in the same area was obtained from "Paul Sabatier"- Toulouse-III University, Toulouse, France in 1984. He was Vice President of the Hellenic Centre of Renewable Energy Sources(CRES) , Octob..2000-April 2002. He is currently a Full Professor at the Electronic and Computer Engineering Dpt., Technical University of Crete, Chania, Crete, Greece.His research interests include industrial and space technology applications of control theory and estimation theory, production and power systems automation, Neural Networks and Fuzzy Logic technology, optimization theory and applications, Decision Support Systems, Renewable Energy Sources , energy management, "smart" buildings.

.

2nd Conference on Power Options for the Eastern Mediterranean Region
07-08 October 2013, Nicosia, Cyprus (Paper No. POEM13/154)

Technical and feasibility analysis of gasoline and natural gas fuelled vehicles

Charalambos A. Chasos, George N. Karagiorgis and Chris N. Christodoulou

Abstract-- **There is recent interest for the utilisation of natural gas for empowering the internal combustion engines (ICE) of vehicles. The production of novel natural gas ICE for vehicles, as well as the conversion of existing gasoline fuelled ICE of vehicles to natural gas fuelled ICE are new technologies which require to be analysed and assessed. The objective of the present study is to examine the adaptation of natural gas as vehicle fuel and carry out a technical analysis and an economical feasibility analysis of the two types of ICE vehicles, namely gasoline and natural gas fuelled vehicles. The technical model uses the physical properties of the two fuels and the performance factors of internal combustion engines including brake thermal efficiency. The resulting exhaust gas emissions are also estimated by the technical model using combustion calculations which provide the expected levels of exhaust gas emissions. Based on the analysis with the technical model, comparisons of the two types of engines are performed. Furthermore, the estimated performance characteristics of the two types of engines, along with local statistical data on annual fuel imports and annual fuel consumption for transportation and data on the vehicles fleet for the case study of Cyprus are used as input in the economical model. For the base year 2012, data of natural gas price is also used in the economical model. The economical model estimates the capital cost, the carbon dioxide emissions avoidance of fines, the net present value and the internal rate of return of the investment of large scale adaptation of natural gas fuelled vehicles for the case study. From the results and comparisons, conclusions are drawn and recommendations are provided for the adaptation of natural gas vehicles which can provide improved performance with reduced pollutant emissions.**

Index Terms-- **Feasibility analysis, internal combustion engines (ICE), ICE performance, gasoline fuel, natural gas fuel, technical analysis.**

I. Nomenclature

a	Annual
C	Carbon. Cost
CF	Cash flow
E	Energy
f	Fuel
G	Gasoline
I	Income
i	Year index
ICE	Internal combustion engine
IRR	Internal rate of return
LHV	Lower heating value of the fuel
n	Efficiency
N	Number
NG	Natural gas
NPV	Net present value
th	Thermal
Q	Quantity

C. A. Chasos is with the Department of Mechanical Engineering, Frederick University, Nicosia 1036, Cyprus (e-mail: eng.cca@fit.ac.cy).

G. N. Karagiorgis is with the Department of Mechanical Engineering, Frederick University, Nicosia 1036, Cyprus (e-mail: eng.kg@fit.ac.cy).

C. N. Christodoulou is with the Department of Mechanical Engineering, Frederick University, Nicosia 1036, Cyprus (e-mail: eng.cc@fit.ac.cy).

II. Introduction

THE natural gas can be used in combustion systems for power generation and for propulsion purposes. Natural gas can be explored from large fossil fuel reserves, and can also be produced from biomass, waste treatment and hydrogen electrolysis with methanisation. The natural gas main ingredient is methane CH_4 which has low carbon content and is considered as less environmentally harmful fuel than conventional fossil fuels which are currently used in internal combustion engines. Compressed natural gas is mainly used in spark-ignition engines [6], but is also tested in Diesel engines where the soot production is negligible. Recently, a European standard [20] was published which describes the fuel quality for compressed natural gas vehicles.

Natural gas internal combustion engines (ICE) have been produced and are used in vehicles. There are engines with port fuel injection system and engines with direct injection system. Direct injection of fuel into the cylinder of the engine can supply the exact amount of fuel for the corresponding engine speed and load. The direct injection system is considered to produce better quality of air-fuel mixture in the cylinder than the mixture which is produced with port fuel systems [1]. The fuel injection timing as well as the quality of the air-fuel mixture (stoichiometric or weak in fuel) affect the engine performance and emissions [5]. The emissions of unburnt hydrocarbons produced by natural gas vehicles are found to be lower than the emissions of gasoline fueled vehicles [4]. The NOx emissions were reduced when the engine operated for a weak in fuel mixture [2], but variations from cycle to cycle of the engine operation were high resulting in unstable engine operation.

Conventional internal combustion engines of vehicles fueled with gasoline can be modified in order to operate with natural gas. The main modifications include the natural gas tank, equipped with special safety components and valves, the engine control unit, the gas filter, special sensors and the gas injection unit. The modifications should be performed

by licensed automotive stations and regulated by the law. However, there is a cost related with the modifications which dependents on the age of the conventional vehicle which is to be modified. The feasibility of the modification for the expected period of usage of the vehicle, and furthermore the modifications on vehicle fleet at national level for large scale adaptation of natural gas should be investigated. Also, there are modified engines which can operate with dual fuel systems in order to switch to different fuel according to the operating conditions and engine load demand. It should be mentioned that existing ICE are designed and optimized for using liquid fossil fuels, and the utilization of natural gas is expected to affect the performance behavior of the engine. Thus, research is required in order to design new ICE with increased efficiency when natural gas is used.

Considerable amounts of natural gas fuel are required for large scale adaptation of natural gas vehicles. Recently, at the area of the exclusive economic zone (EEZ) of the Republic of Cyprus a commercial discovery has been identified. The discovery can be exploited commercially after consideration of all pertinent operating and financial data collected during the performance of the appraisal work programme for natural gas recoverable reserves, sustainable production levels and other relevant technical and economic factors, according to generally accepted international petroleum industry practice [11].

Pipelines and related transport and storage facilities will be required for transportation of hydrocarbons that will be produced in the EEZ to the storage systems and delivery points. However, there will be also high associated costs for the supply of natural gas from the terrestrial storage systems to the vehicle filling stations which will be required to be erected, via a network of natural gas pipelines, compressors and auxiliary equipment.

The natural gas can be stored as compressed natural gas (CNG) or liquefied natural gas (LNG). However, the infrastructure is not yet fully developed and there will be need for development of natural gas filling stations for the supply of natural gas. CNG requires four times the volume of gasoline for the same energy content [6]. CNG can be liquefied at -162°C into LNG, but liquefaction requires energy consumption. The storage capacity of LNG is approximately by factor of three greater than the storage capacity of CNG [6].

Natural gas fuel supply to vehicles can be provided by special fuel stations. In some cities there exist few distribution points of natural gas [8], but the change from conventional fossil fuels to natural gas is expected to be slow with high associated costs [8]. This will require national and European planning with substantial technical and economical investigations for the new technology to be adapted, including both the vehicles technologies and the infrastructure for the supply of natural gas fuel. In Europe, in 2013 approximately 1 million vehicles were fuelled with CNG and around 3000 filling stations were operating [9]. Italy has developed an infrastructure for natural gas fuelling stations, with increased development in the north of Italy. Also, the legislation of Italy allowed the construction of multi-fuel stations with CNG or small CNG stations next to conventional petrol and Diesel fuel stations, as well as providing the possibility to install self-service refuelling systems at the CNG filling stations [9]. The average cost of natural gas stations in Italy was 300000 Euro and related funding schemes for the installation of new stations have been provided by the state [9].

The price of natural gas per energy content is lower than gasoline and Diesel fuel according to published market data [17]. Also, economically viable adaptation of natural gas vehicles could materialise with the intervention of the European Union (EU) and local governments, in order to avoid fragmented EU level markets and enable EU-wide mobility for NGVs [10].

The present paper investigates the vehicles with spark-ignition engine, namely gasoline internal combustion engines and natural gas internal combustion engines. The technical analysis calculates the required annual fuel consumption by the total number of vehicles using SI engine and using either gasoline or natural gas fuel. The resulting amounts of carbon dioxide emissions are also calculated. An economical analysis is performed using statistical data on annual fuel imports and annual fuel consumption for transportation and data on the vehicles fleet for the case study of the Cyprus Republic. The economical analysis examines the scenario of investment from the local government on the infrastructure for the supply of natural to filling stations and the erection of filling stations at national scale, while the local government will own and sell the natural gas to consumers.

III. Methodology

Here, the methodology for the technical and economical analyses is described. First the technical model is presented and then the linkage between the technical and economical model is explained, followed by the presentation of the economical model.

A. Technical model

The technical model uses the physical properties of the two fuels and the thermal efficiency of ICE. The resulting exhaust gas emissions are also estimated by the technical model using using the equation of combustion.

For the purposes of the present study, data on the fuel imports for transportation is used, along with an average thermal efficiency of gasoline ICE [7] and natural gas ICE. The quantity of gasoline fuel imported per year, Q_f, and the thermal efficiency of ICE are used in the analysis. The total energy of the imported fuel for gasoline vehicles and the amount of energy produced by all gasoline vehicles empowered with ICE are calculated from the following equations:

$$E_f = Q_f LHV_f$$

where Ef is the annual total energy of the imported fuel, Q_f is the annual total quantity of gasoline fuel imported for transportation in Kg and LHV_f is the lower heating value of gasoline in KJ/Kg, and,

$$E_V = E_f n_{th,ICE}$$

where E_V is the annual energy produced by all the vehicles, and $n_{th,ICE}^{V}$ is the thermal efficiency of gasoline ICE.

The quantity of mass of the required natural gas in Kg per year which is to be supplied to the natural gas fuelled vehicles is calculated from,

$$Q_{NG} = \frac{E_V}{n_{th,NG} LHV_{NG}}$$

The amount of CO_2 emitted from vehicles is calculated by the combustion equation of fuel with air using the chemical compound of the fuel and its molecular weight. The amount of CO_2 emitted is estimated as:

$$Q_{CO2,i} = \frac{N_C M_{CO2}}{M_f} Q_{f,i}$$

where N_C is the number of carbon atoms for the fuel, M_{CO2} is the molecular weight of carbon dioxide, and M_f is the molecular weight of the fuel considered. $Q_{f,i}$ is the quantity of the fuel in Kg, and refers to the fuels, namely gasoline and natural gas, which are used for fuelling the gasoline and natural gas vehicles, comprising the vehicle fleet of the case study. The quantity of CO_2 emissions, $Q_{CO2,i}$ is calculated in Kg per year from the above expression and the produced emissions for the two different fuels are calculated, which sum to the total amount of CO_2 emissions from spark-ignition vehicles. The CO_2 emissions avoidance from the usage of natural gas is found as the difference of the two estimated values for gasoline and natural gas, respectively.

B. Economical model

The estimated performance characteristics of the two types of engines from the technical analysis, along with local statistical data on annual fuel imports and annual fuel consumption for transportation and data on the vehicles fleet are used for the case study calculations. Data of natural gas prices is also used in the economical model. The economical model estimates the capital cost of the investment in the new technology, the amount of income because carbon dioxide emissions avoidance and the income from selling natural gas. The annual cashflow and the capital cost are used for the estimation of the net present value (NPV) and the internal rate of return (IRR) of the investment of large scale adaptation of natural gas fuelled vehicles for the case study.

The capital cost of the investment by the Cyprus Republic consists of the funding cost of erection of natural gas fuelling stations, the funding cost for the installation of the piping system for the supply of natural gas to the fuelling stations and the funding cost for the the purchase of natural gas vehicles by the consumers. The capital cost in Euro, Cc, is estimated by:

$$C_c = C_s + C_P + C_{NGV}$$

where *Cs* is the cost for funding of fuelling stations, Cp is the cost for the piping network and C_{NGV} is the cost for funding the new natural gas vehicles. The cost for funding the fuelling stations is calculated by,

$$C_s = F_S N_S P_S$$

where F_S is the funding percentage, N_S is the total number of new natural gas fuelling stations and P_S is the cost for erection of a new natural gas station. The cost for the installation of the piping network is estimated by,

$$C_P = L_P P_P$$

where L_P is the total length of the piping network in Km and P_P is the cost of the pipe installation in Euro per Km. The cost for funding of the new natural gas vehicles is given by,

$$C_{NGV} = F_{NGV} N_{NGV} P_{NGV}$$

where F_{NGV} is the funding percentage for a new natural gas vehicle, N_{NGV} is the total number of new natural gas vehicles and P_{NGV} is the average cost for a new natural gas vehicle.

It is assumed that the amount of natural gas which is consumed on annual basis is the income for the Cyprus Republic which is considered to be the investor in the new technology. The selling price of natural gas is estimated using current average selling price of natural gas in Europe, found from market source [17] and it is equal to 26 Euro/MWh which results in 0.325 Euro/Kg of natural gas. However, the erection of liquefaction plant and the storage of natural gas as well as relevant operation and maintenance costs are not considered in the present economical model.

The income from the investment in the new technology is considered to be the annual cash flow which is calculated from,

$$CF_i = I_{a,i} + I_{CO2,i}$$

where i is the running year index, $I_{a,i}$ is the annual income from the natural gas fuel sales, and $I_{CO2,i}$ i is the annual savings in CO_2 emissions fines imposed by the emissions trading scheme of EU [13], from avoiding using gasoline fuel in transportation and using natural gas because of the introduced number of natural gas vehicles.

The annual income from the natural gas fuel sales is calculated by,

$$I_{a,i} = Q_{NG} P_{NG} (1 + IR)^i$$

where Q_{NG} is the annual consumption of natural gas in Kg by the natural gas vehicles, P_{NG} is the current selling price of natural gas in Euro/Kg for the base year and IR is the inflation rate.

The annual avoidance of cost because of fines is given by,

$$I_{CO2,i} = (Q_{CO2,G} - Q_{CO2,NG}) P_{CO2} (1 + IR)^i$$

where $Q_{CO2,G}$ is the quantity of CO_2 emissions emitted by the number of vehicles with gasoline in Kg/year, $Q_{CO2,NG}$ is the quantity of CO_2 emissions of the same number of vehicles fueled with natural gas, instead, which substitute the gasoline vehicles in the scenarios of the present study. P_{CO2} are the fines for the produced CO2 in Euro/ton for the base year.

The NPV is calculated over the operation period of the new technology, and it is calculated by,

$$NPV = \sum_{i=1}^{n} CF_i \left(\frac{1}{1+R_d} \right)^i - C_c$$

where n is the number of years for the operation of the investment and R_d is the discount rate.

Finally, the IRR is calculated with a function which considers the cash flow of each year of operation of the technology and the capital cost for the new technology. IRR is the interest rate at which the incomes are equivalent to the costs of the investment.

IV. Results and Discussion

For the analysis of the two types of vehicles, three scenarios are investigated for the technical and economical analysis.

- At the first scenario, 25 % of the gasoline ICE vehicles fleet to be replaced by new natural gas vehicles
- At the second scenario, 50 % of the gasoline ICE vehicles fleet to be replaced by new natural gas vehicles
- At the third scenario, all 100% of the gasoline ICE vehicles fleet to be replaced by new natural gas vehicles

The analysis is performed on an annual basis and a 25 years period of operation of the new technology from the base year is examined. For the base year 2013, average data for a year to present was used.

For the economical analysis, the effect of the selling price of natural gas on the investment is also studied by examining the reduction of the selling price by 25 % and 50% compared to the base year average selling price.

A. Case study

In the Republic of Cyprus, there is a huge prospect with the exploration and exploitation of natural gas resources [12], and the subsequent erection of a liquefaction plant, within five years [11]. Thus, research activities should be directed towards the applications of natural gas and investigate the feasibility of adaptation of natural gas vehicles. Figure 1 shows the hydrocarbon exploration blocks at the area of EEZ of Cyprus. If it is proved that natural gas reserves are exploitable, then Cyprus Republic can switch to wide range of natural gas applications including the introduction of natural gas vehicles at large scale.

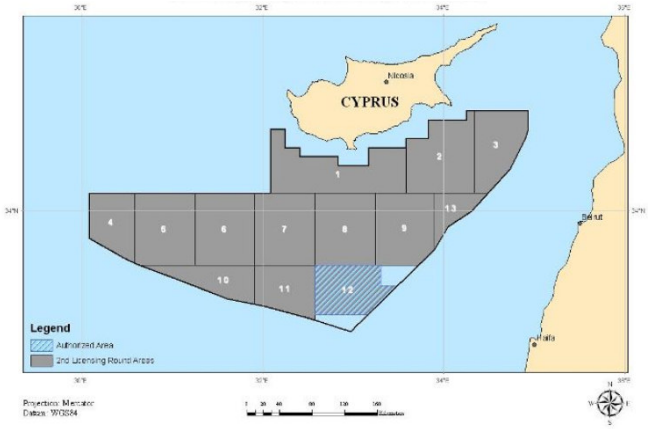

Fig. 1. Offshore Cyprus hydrocarbon exploration blocks at the area of the EEZ (from [ministry]).

Many activities will be involved including the drilling of wells other than exploration wells and appraisal wells, the deepening, plugging, completing and equipping of such wells, along with the design, construction and installation of equipment. Equipment includes pipeline installations, production units and all other systems in conformity with sound oilfield and generally prevailing environmental practices in the international petroleum industry [11]. However, these factors and the associated costs are not considered in the present study.

The cost of installation of pipelines is enormous, and for inland installation of natural gas pipelines an average cost of 750000 Euro per installed Km length of pipe is estimated from contract data [13] for a natural gas pipeline network development on the south coast of Cyprus, as shown in Figure 2.

Fig. 2. Natural gas pipeline network development on the south coast of Cyprus (from [13]).

For the present study, the statistical data is collected from the Statistical Service of the Republic of Cyprus [15], and includes the fuel imports for the years 2007, 2008 and 2009, the number of vehicles and their types registered in Cyprus Republic. Table I includes the quantity of imported fuel in tons per year for transportation with different fossil fuels (95 RON petrol, 100 RON petrol and Diesel with low sulphur), as well as the total amount of fossil fuels imported.

TABLE I

Fossil fuel imports for the years 2007, 2008 and 2009

Fuel	Fuel Quantity imported in tons		
	2007	2008	2009
Unleaded gasoline 95RON	313535	334079	343907
Unleaded gasoline 98RON	38317	38597	39561
Diesel (gas oil low sulphur)	350037	365982	348841
All fossil fuels	2985841	3086409	2936121

From the data for fuel imports contained in Table I, it is found that 23.5, 23.9 and 24.9 % for years 2007, 2008 and

2009, respectively, of the total amount of fossil fuels imported and consumed in Cyprus is used for transportation [19]. In the present study, the total amount of 350000 tons of gasoline assumed to be consumed for transportation with gasoline vehicles, for the base year of the analysis. Table II contains the number of vehicles according to their type which are registered in the Republic of Cyprus for the year 2008.

TABLE II

REGISTERED PASSENGER VEHICLES IN THE REPUBLIC OF CYPRUS FOR THE YEAR 2008

Vehicle type	Number of registered passenger vehicles
Petrol ICE	402435
Diesel ICE	40248
Electric	834
Total	443517

As can be seen in Table II, the total number of vehicles is 443517 and the majority is gasoline vehicles, which is the candidate technology to be substituted by natural gas technology.

Table III includes the yearly amount of CO_2 emissions emitted from transportation, as well as the total amount of CO_2 for the years 2006 and 2007. The amount of CO2 emissions as a percentage of the total amount of CO2 emitted from all activities is 25.6 and 26.7 % for the years 2006 and 2007, respectively. The statistical data on CO_2 emissions suggests that finding solutions such as the introduction of reduced carbon dioxide transportation technologies is required. Furthermore, the EU limit for the CO_2 emissions allowed for the Republic of Cyprus is much lower than the total amount that is currently emitted. For the years 2008 – 2012, the allowed limit is 5.48 million tons per year [14,15].

TABLE III

CO2 EMISSIONS FOR THE YEARS 2006 AND 2007

Activity	Yearly amount of CO2 emissions (thousand tons)	
	2006	2007
Transportation	2053.63	2193.70
All	8025.12	8167.26

B. Data for the technical and economical analysis

The data used for the technical and economical analysis is summarised in Table IV and Table III, respectively.

TABLE IV

DATA FOR THE TECHNICAL ANALYSIS OF GASOLINE AND NATURAL GAS FUELLED VEHICLES

Parameter	Value
Quantity of imported gasoline for the base year (Kg)	350 million
LHV of gasoline for ICE (KJ/Kg)	44000
LHV of natural gas (KJ/Kg)	50000
Thermal efficiency of gasoline ICE (%)	25
Thermal efficiency of natural gas ICE (%)	25

The total number of gasoline vehicles is assumed 400000, and for the three scenarios 100000, 200000 and 400000 vehicles are used in the analysis, respectively. The thermal efficiency of gasoline ICE and natural gas ICE are assumed 25 % as shown in Table IV.

The data which is used for the economic analysis is included in Table V. It includes the cost for the erection of new natural gas fuelling stations, the number of the natural gas filling stations to be erected around the state, the cost of installation of the gas piping network and the approximate length of the piping network. For the estimation of the cost of the emission fines the current rate of 10 Euro per ton of emitted CO_2 is the average over the last two years, from the emissions trading system [13].

TABLE V

DATA FOR THE ECONOMICAL ANALYSIS OF THE INVESTMENT IN NATURAL GAS VEHICLES

Parameter	Value
Cost of the natural gas fuelling station	300000 Euro
Number of new stations	100
Cost for the installation of the natural gas piping network	750000 Euro/Km
Length of piping network	300 Km
Natural gas spot price	26 Euro/MWh
EU emission allowance price	10 Euro/t CO_2

C. Technical analysis and comparisons

For the three scenarios examined, the required amount of natural gas can be found from Figure 3, including the data of scenarios of 25%, 50% and 100 % replacement of SI engine vehicles, respectively.

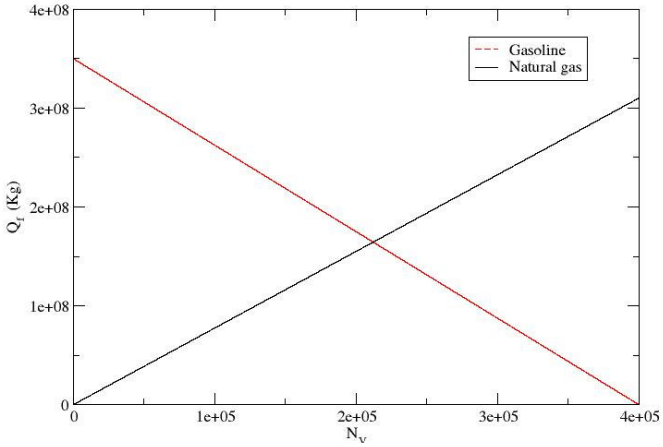

Fig. 3. Quantity of fuel as function of the number of introduced natural gas vehicles.

From the data shown in Figure 3, it can be seen that the mass quantity of natural gas for fuelling the 400000 vehicles is lower than the amount of mass of gasoline.

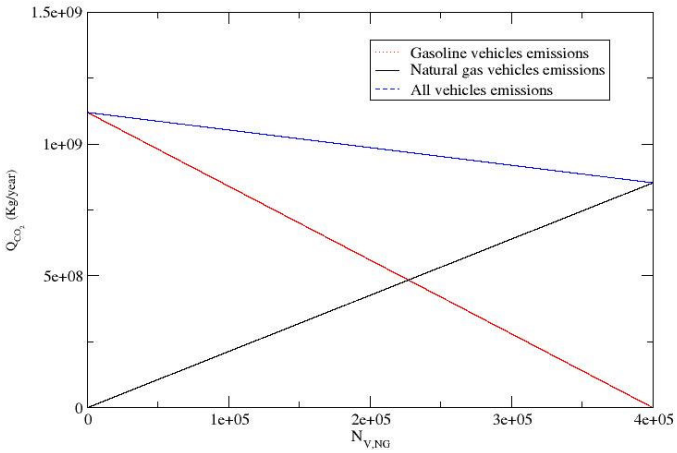

Fig. 4. Quantity of emitted CO_2 from gasoline and natural gas vehicles as function of the number of introduced natural gas vehicles.

Figure 4 shows the total CO_2 emitted from the number of vehicles examined. When all the vehicles operate with gasoline then the amount of CO_2 emissions is higher than the amount emitted when all the vehicles operate with natural gas. It can be seen that using natural gas vehicles instead of gasoline vehicles reduces CO_2 emissions.

D. Economical analysis and comparisons

When large scale adaptation of natural gas vehicles is going to happen, then a huge investment by the government will be required. It is important to examine the number of vehicles which are going be introduced in order to identify whether the investment in infrastructure will be feasible. A criterion for feasibility can be considered as the lower limit of the IRR should be higher than the discount rate and around 10 %. The investment in infrastructure is not expected to be dependent on the number of new natural gas vehicles. An inflatio ratio of 2 % and a discount rate of 6 % were used in the economical analysis.

From the economical analysis, the NPV of the investment is shown in Figure 5. It can be seen that because of the increase of the number of natural gas vehicles the income from the sales of fuel will increase accordingly.

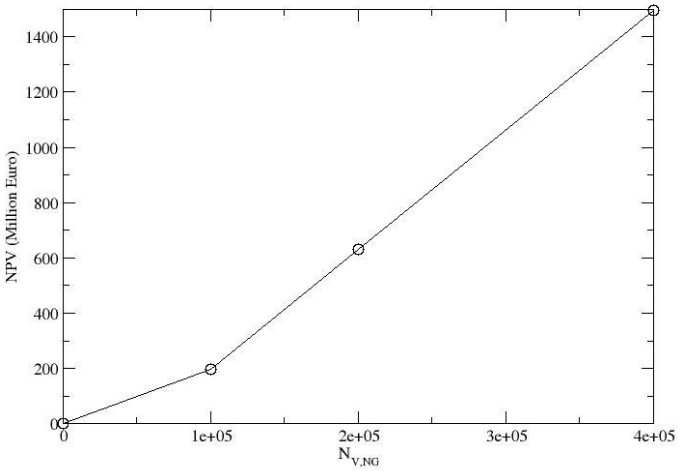

Fig. 5. Net present value of the investment as function of the introduced number of natural gas vehicles for each scenario.

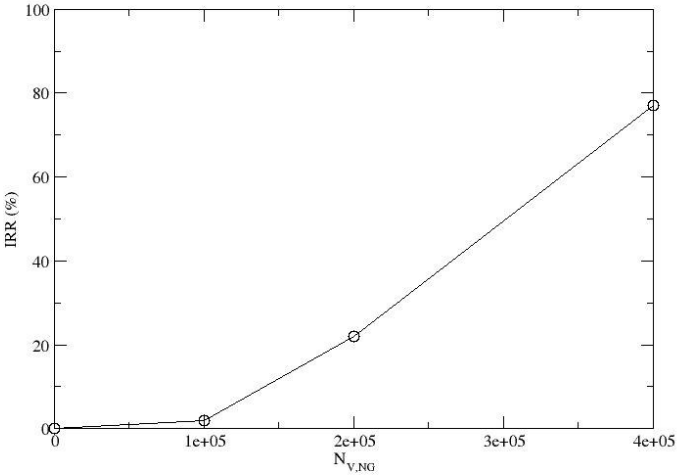

Fig. 6. Internal rate of return of the investment as function of the introduced number of natural gas vehicles for each scenario.

The estimated IRR is presented in Figure 6, where it can be seen that the introduction of increased number of natural gas vehicles results in profitable investment when the current market selling price of natural gas is utilized. The scenario of 25 % replacement gasoline vehicles with natural gas vehicles provides unfeasible investment, while the 50 % replacement is promising and the complete 100 % replacement is expected to be very profitable, along with the fact that harmful greenhouse effect carbon dioxide emissions will be reduced.

Further analysis was carried out for the case of 50 % replacement of gasoline vehicles, ie. introduction of 200000 new natural gas vehicles. For the analysis, the selling price of natural gas of 0.325 Euro/Kg which was used for the three scenarios already presented was reduced by 25 % and 50 %, in order to investigated the possibility for reduced fuel prices in the future.

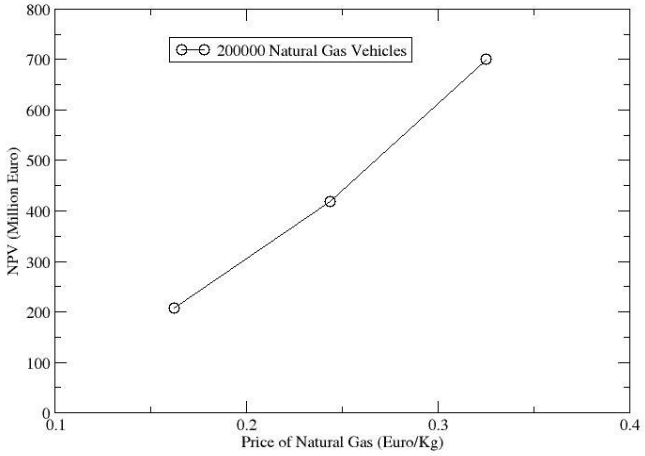

Fig. 7. Net present value of the investment as function of natural gas selling price for the scenario of the introduction of 200000 natural gas vehicles.

The NPV of the investment for the three fuel prices is shown in Figure 7. It can be seen that when the fuel price increases, then the NPV of the investment increases which suggests that the investment is highly dependent on the fuel price.

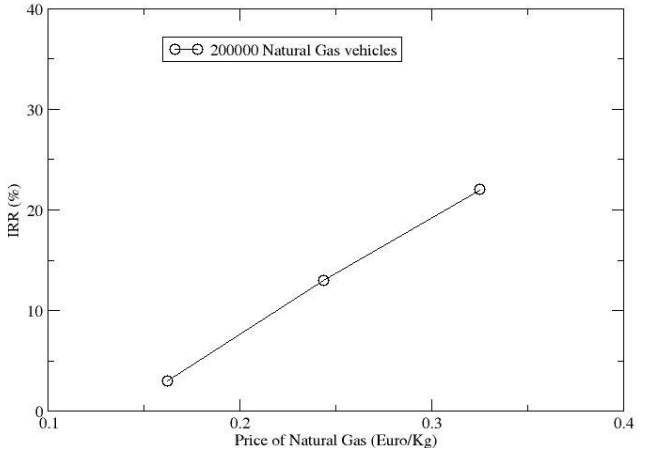

Fig. 8. Internal rate of return of the investment as function of natural gas selling price for the scenario of the introduction of 200000 natural gas vehicles.

Figure 8 shows the IRR of the investment for the scenario of 200000 vehicles when the natural gas selling price is varying. It can be observed that if the price of natural gas is reduced by 50 %, then the investment is expected to be unfeasible.

V. Conclusions and Recommendations

When natural gas fuel is employed, then the mass of fuel required to empower vehicles is slightly reduced.

Introducing natural gas vehicles will result in reduced carbon dioxide emissions, thus the new technology will contribute to the reduction of the greenhouse effect.

Introducing natural vehicles at large scale will result in avoiding the imports of fossil fuel for transportation applications and the Cyprus national economy will be benefited, since almost 25 % of fuel imports are used for transportation.

The investment in large scale adaptation of natural gas vehicles will require a complete new infrastructure which will rely on other technologies such as liquefaction plants and natural gas storage and transportation system.

The investment is expected to be feasible, given that substantial number of new natural gas vehicles are introduced.

The adaptation of the new technology is expected to be gradual and incentives by the EU and the local government and should be given to the consumers, in order to achieve large scale adaptation of natural gas vehicles.

Further investigations of natural gas ICE are required in order to achieve improved engine designs optimised to operate with natural gas which is expected to improve thermal efficiency and life expectancy of the engine. The investigations include experiments, simulations and analysis of direct-injection natural gas ICE operating at increased compression ratio and with advanced supercharging systems.

Further economical analysis is recommended including examination of operation and maintenance costs of the infrastructure of natural gas fuelling, as well as associated costs for the utilization of the envisaged liquefaction plant.

VI. Acknowledgment

Data and information provided from the Statistical Service of the Republic of Cyprus on fuel imports, emissions and registered vehicles is acknowledged.

VII. References

Periodicals:

[1] Abdullah, S., Kurniawan, W. H., Khamas, M. and Ali, Y. "Emission analysis of a compressed natural gas direct-injection engine with a homogeneous mixture". International Journal of Automotive Technology, Vol. 12, No. 1, pages 29-38, 2011.

[2] Cho, H. M. and He, B. Q. "Combustion and emission characteristics of a lean burn natural gas engine". International Journal of Automotive Technology, Vol.92, No. 4, pages 415-422, 2008.

[3] Wang, M. "Fuel Cycle Analysis of Conventional and Alternative Fuel Vehicles". Encyclopedia of Energy, Pages 771–789, 2004.

[4] Ristovski, Z., Morawska, L., Ayoko, G. A., Johnson, G., Gilbert, D. and Greenway, C. "Emissions from a vehicle fitted to operate on either petrol or compressed natural gas". Science of The Total Environment, Vol. 323, Issues 1-3, Pages 179-194, 2004.

[5] Bysveen, M. "Engine characteristics of emissions and performance using mixtures natural gas and hydrogen". Energy, Vol. 32, Issue 4, Pages 482 – 489, 2007.

Books:

[6] Bosch Automotive Handbook, 6th Edition. Bentley Publishers, USA, 2004.

[7] Heywood, J. B. "Internal Combustion Engines Fundamentals". New York, McGraw-Hill Book Company, 1988.

[8] Pulkrabek, W. M. *Engineering fundamentals of the Internal Combustion Engine.* 2nd Edition. Pearson Prentice Hall, New Jersey, 2004.

Technical Reports:

[9] E3M-Lab National Technical University of Athens. "Assessment of the implementation of a European alternative fuels strategy and possible supportive proposals". Project MOVE/C1/497-1-2011. August, 2012. Available: http://ec.europa.eu/transport/themes/urban/studies/doc/2012-08-cts-implementation-study.pdf

[10] European Commission. "Clean Power for Transport: A European alternative fuels strategy". Available: http://eur-lex.europa.eu/LexUriServ/LexUriServ.do?uri=COM:2013:0017:FIN:EN:PDF

[11] Government of the Republic of Cyprus. "Notice from the Government of the Republic of Cyprus concerning Directive 94/22/EC of the European Parliament and of the Council on the conditions for granting and using authorisations for the prospection, exploration and production of hydrocarbons". Official Journal of the European Union. C38/24, 2012.

[12] Government of the Republic of Cyprus, Ministry of Commerce Industry and Tourism. "2nd Licensing round – hydrocarbon exploration". Available: http://www.mcit.gov.cy/mcit/mcit.nsf/dmlhcarbon_en/dmlhcarbon_en?OpenDocument. Cyprus, 2012.

[13] Natural Gas Public Company (DEFA). "Projects: Construction of natural gas pipeline network". Available: http://www.defa.com.cy/en/projects.html, Cyprus, 2013.

[14] European Commission, DG Energy. "Quarterly report on European Gas Markets". Volume 6, issue 1, First quarter, 2013. Available: http://ec.europa.eu/energy/observatory/gas/doc/20130611_q1_quarterly_report_on_european_gas_markets.pdf

[15] European Commission. "Emissions trading: Commission adopts decision on Cyprus' national allocation plan for 2008-2012". Press Release, IP-07-1131, Brussels, July 2007. Available: http://europa.eu/rapid/press-release_IP-07-1131_en.htm

[16] European Commision. "The EU emission trading sytem EU ETS". Brussels, 2013. Available: http://ec.europa.eu/clima/publications/docs/factsheet_ets_2013_en.pdf

[17] The European Energy Exchange (EEX). "Market data on Natural Gas Spot prices and trading volumes", Frankfurt, Germany, 2013. Available: http://www.eex.com/en/EEX

[18] Statistical Service of the Cyprus Republic. "*Statistical Themes: Energy, Environment*". Available: http://www.mof.gov.cy/mof/cystat/statistics.nsf/energy_environment_81main_gr/energy_environment_81main_gr?OpenForm&sub=1&sel=2

Papers from Conference Proceedings (Published):

[19] Chasos, C. A., Karagiorgis G. N. and Christodoulou, C. N. "Utilisation of solar/thermal power plants for production of hydrogen with applications in the transportation sector". Proceedings of the 7th Mediterranean Conference and Exhibition on Power Generation, Transmission, Distribution and Energy Conversion (MEDPOWER 2010). Agia Napa, Cyprus, 7 – 10 November, 2010.

Standards:

[20] Cyprus Organisation for Standardisation (CYS), CYS EN ISO 15403-1:2008: Natural gas – Natural gas for use as compressed fuel for vehicles – Part 1: Designation of the quality. (2008)

VIII. BIOGRAPHIES

Chasos Antoniou Charalambos graduated from the National Technical University of Athens in 1997 from where he obtained a Diploma in Mechanical Engineering, following the courses of the energy cycle programme of studies. He obtained a PhD from the University of London, Imperial College in 2006, and his research focused in the development and application of two-phase flows models and of the computational fluid dynamics (CFD) methodology for the prediction and validation of flow processes in the cylinders of internal combustion engines. He is currently Lecturer at Mechanical Engineering Department of the Frederick University Cyprus. For many years, he worked as a consultant and research fellow for various organisations and universities, in the fields of internal combustion engines, energy and CFD, and dealt with technological and development programmes of the European Union.

Giorgos Nikou Karagiorgis holds a B.Eng. degree in mechanical engineering and a Ph.D. degree in Computational Fluid Dynamics related to thermal energy, from City University, U.K. He is a Member of The Institute of Mechanical Engineers (IMechE), and Technical Chamber of Cyprus (ETEK). His present employment is with Frederick University Cyprus where he holds the position of Associate Professor in the Mechanical Engineering Department; he is also, a Visiting Senior Researcher at the Chemical Engineering Department of Imperial College of Science Technology and Medicine UK. In his professional career he has worked for engineering companies and academic institutions, before joining Frederick University Cyprus. He has over 15 years experience on research and development projects related to renewable energy sources, energy storage systems, and systems for hydrogen storage. He is the author of various publications in scientific journals and conference proceedings.

Christodoulos Neophytou Christodoulou is of Greek Nationality and was born in the city of Paphos in the island of the Republic of Cyprus in September 15, 1959. He received the B.Sc. (5-year study) in Chemical Engineering (1984) from the Polytechnic School of Thessaloniki, Aristotle University of Thessaloniki, Greece, the M.Sc. in Chemical Engineering (1987) from Kansas State University, Manhattan, KS, USA, and the Ph.D. in Metallurgical Engineering & Materials Science (1990) form Carnegie Institute of Technology, Carnegie-Mellon University in Pittsburgh, PA, USA. Presently, he is a tenure Professor in the Mechanical Engineering Department of Frederick University Cyprus, where he joined the Faculty of Engineering in 1995. He also serves as the Director of the Frederick Research Center since 1995. Prior to these appointments, he served as Research and Teaching assistant (1985-1987) in the Department of Chemical Engineering and the Department of Physics in Kansas State University (USA), as Research and Teaching Assistant (1987-1990) in the Department of Metallurgical Engineering & Materials Science in Carnegie Mellon University, Pittsburgh, PA, USA, and as Research Associate (1990-1995) in the Central Research Institute of Mitsubishi Materials Corporation in Japan. Dr. Christodoulou has an Industrial experience working in many Industries, such as "TITAN" Cement Industry, Thessaloniki, Greece, Hellenic Sugar Industry, Thessaloniki, Greece and the Central Research Institute of Mitsubishi Materials Corporation in Japan. His research interests and activities are in the fields of Energy and Materials: Hydrogen Production and Purification Technologies, Hydrogen Storage Technologies (metal-hydrides, compressed gas), Renewable Energy Sources (RES, Solar, Wind, Hydrogen), H_2/Fuel Cells, Hydrogen Compression based on Metal-Hydrides, Electricity Production from Low-Temperature Waste Heat with the use of Metal-Hydrides, Integrated Hydrogen/RES systems, Distributed Energy Resources (DER), Materials Processing & Characterization, Micro- and Nano-crystalline Materials, Hydrogen Storage Materials, Magnetic Materials (Permanent Magnets). Dr. Christodoulou has carried out more than 6 EU and 11 National research projects and has over 60 publications

2nd Conference on Power Options for the Eastern Mediterranean Region
07-08 October 2013, Nicosia, Cyprus (Paper No. POEM13/155)

On the power control techniques of DFIG: From conventional to a novel BELBIC scheme

Mona Valikhani and Constantinos Sourkounis

Abstract- **Many hard and soft control techniques have been presented for the DFIG-based systems, in which vector control(VC) and direct power control(DPC) methods have been analyzed and applied widely. This paper deals thus with a comparative study of the common DFIG conventional control techniques. A multilevel control scheme is developed which covers the most challenging and common control and modulation strategies: PWM-based-VC, Hysteresis-based-VC, Rotor flux position-based-DTC.**
Modern control strategies including artificial intelligent methods have been also successful especially in nonlinear structures but they demand fast computer processing besides lacking a complete solution for stability and robustness issues. In recent years, a new artificial intelligent controller has been introduced which imitates the brain emotional learning computational process, called BELBIC in the literature. This paper develops a novel BELBIC-based model as a complement of PWM-based-VC for the DFIG power control and remarkable results have been obtained.

***Index Terms*— Doubly fed induction generator, DFIG, Voltage source inverter, VSI, Vector control, VC, Direct power control, DPC, brain emotional learning based intelligent control, BELBIC, emotional cue, EC, Orbitofrontal Cortex, OFC.**

I. Nomenclature

Parameter	Definitions	Parameter	Definitions
r_s, l_{ls}	Stator resistance and leakage inductance	ω_r	Rotor electrical speed
r_r, l_{lr}	Rotor resistance and leakage inductance	ω_s	Synchronous speed
l_m	Magnetizing inductance	P_p	Pairs of poles
l_s, l_r	Total Stator and rotor inductance	ω_m	Rotor mechanical speed
λ	Flux linkage	θ_m	Rotor angular position
s,r	Stator, rotor	θ_r	Rotor electrical angular position
u, i	voltage and current	P_s, Q_s	Stator active and reactive power

II. Introduction

The rapid depletion of traditional sources of energy, basically referred to as fossil fuels, beside their unwilling effects of air pollution and production of high amount of green-house gases, has been one of the major threatening factors, which has prompted the distribution networks to find alternative energy resources, mainly referred to as renewable energy resources, which as a result leads to future changes in the distribution system infrastructure, moving from the centralized generation structures to distributed ones. Wind energy, as one of the most promising alternatives among other renewable sources of energy, have drawn more interests in recent years. Wind-based generators, being divided into two categories for constant and variable speed applications, offer more flexible and reliable electricity production compared to the other renewable sources.

To have a reliable and stable contribution of electricity generation based on distributed generation, the system has to be continuously controlled so as to satisfy the power demands no matter as to whether supplying a small load or being in the active mode while interconnected to the main grid. The main focus in this paper is to compare different power control strategies applied so far to the doubly fed induction generator (DFIG) as a wind-based generator. Figure 1.1 shows diagram of the grid connected DFIG using back to back voltage source inverters (VSI).

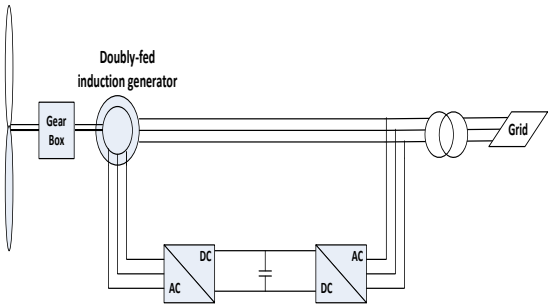

Fig. 1.1 Diagram of grid connected DFIG

In this paper, vector control and direct power control methods as mostly common and challenging conventional control procedures in the field of induction machines beside a novel artificial intelligence-based control strategy (BELBIC) will be studied and simulated. In this way, this paper can be structured as following:

1- PWM-based vector control method(PWM-VC)
2- Hysteresis (Bang-Bang)-based vector Control method (Hysteresis-VC)
3- Rotor flux position-based direct power control method (DPC)
4- BELBIC-based PWM-VC

Figure 1.2 shows a multilevel control structure of the DFIG system.

The authors are with the Research Institute for Power Systems Technology and Power Mechatronics, Ruhr-University Bochum, 44780 Bochum, Germany.
(e-mail: valikhani@enesys.rub.de ; sourkounis@enesys.rub.de).

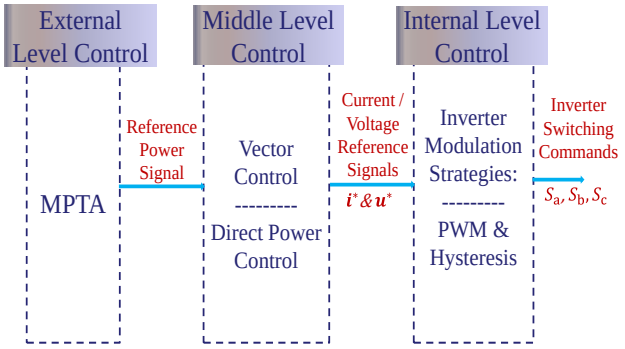

Fig. 1.2 A Multilevel Control Scheme of a Wind-based DFIG System

III. Power Control Strategies of DFIG-based Wind System

Prior to addressing the control design of a system, an appropriate mathematical model based on the existent physical laws in the system is required. In this paper, the T-representation of the induction machine will be used and to make the dynamic model easier to be solved by the digital processor, the d-q model would be of interest.

A. Vector Control (VC)

This method, also known as field oriented control method resembles the simplicity in torque control method of separately excited DC machines through manipulations in the axis of coordinates. In this regard, different schemes of vector control method have been developed.

A.1 PWM-based VC

In dealing with the vector control method, it's been common to adopt the dynamic dq equations of the machine in order to perform the desired orientation. For this purpose, stator flux has to be aligned with the d-axis of a synchronously rotating dq system of coordinates. This alignment forces the q component of the stator flux to be zero:

$$\underline{\boldsymbol{\lambda}}_s^{\angle\omega_s} = \sqrt{\boldsymbol{\lambda}_{ds}^{\angle\omega_s 2} + \boldsymbol{\lambda}_{qs}^{\angle\omega_s 2}} \qquad (1)$$

Since $\boldsymbol{\lambda}_{qs}^{\angle\omega_s} = 0$ then $\underline{\boldsymbol{\lambda}}_s^{\angle\omega_s} = \boldsymbol{\lambda}_{ds}^{\angle\omega_s}$.

Stator flux and stator flux position can be obtained directly using flux and position sensors. However, mathematical calculations have been attempted to be replaced, removing the requirement and drawbacks of flux and position sensors [1]. In some researches it has been also recommended to apply stator voltage frame [2] instead of the stator flux frame, since in the latter the stator flux position has to be accurately detected. On the other hand, the electrical rotor angle θ_r which is the angle between the rotor axis and the d axis of coordinates will be also needed for frame transformation requirements. Several methods have been developed for this issue. One of the most common way is to use an encoder coupled to the rotor which gives the mechanical rotor angle. However in practice, utilizing an encoder wouldn't be cost effective and on the other hand, it is vulnerable against noise which as a result influences its preciseness. Rotor position estimators have been also proposed which lead to the sensorless operations [3]. In [4] a short review of stator and rotor flux estimation methods is given.

In order to simplify the expressions under stator flux orientation, two approximations are taken into account:

1- Stator resistance is to be neglected, since its voltage drop is negligible compared to the voltage drop across leakage and mutual inductances.
2- Derivative of stator flux d component is thought to be zero, because of the stator connected directly to the relatively constant voltage and frequency grid, which provides nearly constant stator flux in amplitude and phase.

Dynamic equations of the machine can be thus written considering the above approximations:

$$\boldsymbol{u}_{ds}^{\angle\omega_s} = 0 \qquad (2)$$

$$\boldsymbol{u}_{qs}^{\angle\omega_s} = r_s \boldsymbol{i}_{qs}^{\angle\omega_s} + \frac{d\boldsymbol{\lambda}_{qs}^{\angle\omega_s}}{dt} + \omega_s \boldsymbol{\lambda}_{ds}^{\angle\omega_s} \qquad (3)$$

$$\boldsymbol{u}_{qs}^{\angle\omega_s} \approx \omega_s \boldsymbol{\lambda}_{ds}^{\angle\omega_s} \approx \underline{\boldsymbol{u}}_s^{\angle\omega_s} \qquad (4)$$

From the above equations it can be deduced that:

$$\boldsymbol{i}_{qs}^{\angle\omega_s} = -\frac{l_m}{l_s} \boldsymbol{i}_{qr}^{\angle\omega_s} \qquad (5)$$

$$\boldsymbol{i}_{ds}^{\angle\omega_s} = \frac{\underline{\boldsymbol{\lambda}}_s^{\angle\omega_s}}{l_s} - \frac{l_m}{l_s} \qquad (6)$$

$$\boldsymbol{u}_{dr}^{\angle\omega_s} = r_r \boldsymbol{i}_{dr}^{\angle\omega_s} + (l_r - \frac{l_m^2}{l_s}) \frac{d\boldsymbol{i}_{dr}^{\angle\omega_s}}{dt} - g\omega_s (l_r - \frac{l_m^2}{l_s}) \boldsymbol{i}_{qr}^{\angle\omega_s} \qquad (7)$$

$$\boldsymbol{u}_{qr}^{\angle\omega_s} = r_r \boldsymbol{i}_{qr}^{\angle\omega_s} + (l_r - \frac{l_m^2}{l_s}) \frac{d\boldsymbol{i}_{qr}^{\angle\omega_s}}{dt} + g\omega_s (l_r - \frac{l_m^2}{l_s}) \boldsymbol{i}_{dr}^{\angle\omega_s} + g\frac{l_m}{l_s} \underline{\boldsymbol{u}}_s^{\angle\omega_s} \qquad (8)$$

Where $g = \frac{\omega_s - \omega_r}{\omega_s}$.

It can be deduced that the stator active and reactive powers can be controlled by means of rotor currents.

$$P_s = -\frac{3}{2}\frac{l_m}{l_s} (\underline{\boldsymbol{u}}_s^{\angle\omega_s} \boldsymbol{i}_{qr}^{\angle\omega_s}) \qquad (9)$$

$$Q_s = \frac{3}{2}\frac{\underline{\boldsymbol{u}}_s^{\angle\omega_s}}{l_s} (\underline{\boldsymbol{\lambda}}_s^{\angle\omega_s} - l_m \boldsymbol{i}_{dr}^{\angle\omega_s}) \qquad (10)$$

It comes from the above expressions that, the current references to be injected to inner control loops can be generated by the power error signals between reference and actual powers. This approach is also referred to as indirect control of the stator powers due to the power regulations through the rotor current d-q components.

For this purposes two cascaded sets of PI controllers will be utilized in order to fulfill the task of generating the current and voltage references, respectively. Based on the aforementioned discussions, a schematic diagram of the overall PWM-based vector control scheme is illustrated in Figure 1.3.

A.2 Hysteresis-based VC

Vector control has been known as the most common control method of DFIGs. As shown in previous section, PI regulators standing at the most critical and important point of the control block play key role in regulating desired parameters such as power, torque or flux quantities. Accordingly, the cascaded PI controllers have been utilized such that in the case of power control, the outer loop is in charge of P, Q control and the inner loop is in charge of controlling fast dynamic response parameters such as rotor

current. However, vector control implementation using PI current regulators, has its own drawbacks, in that the system is so highly dependent on the operating conditions of the system that any variation in operating points results in deviations in response thus leading to a non-optimal control scheme.

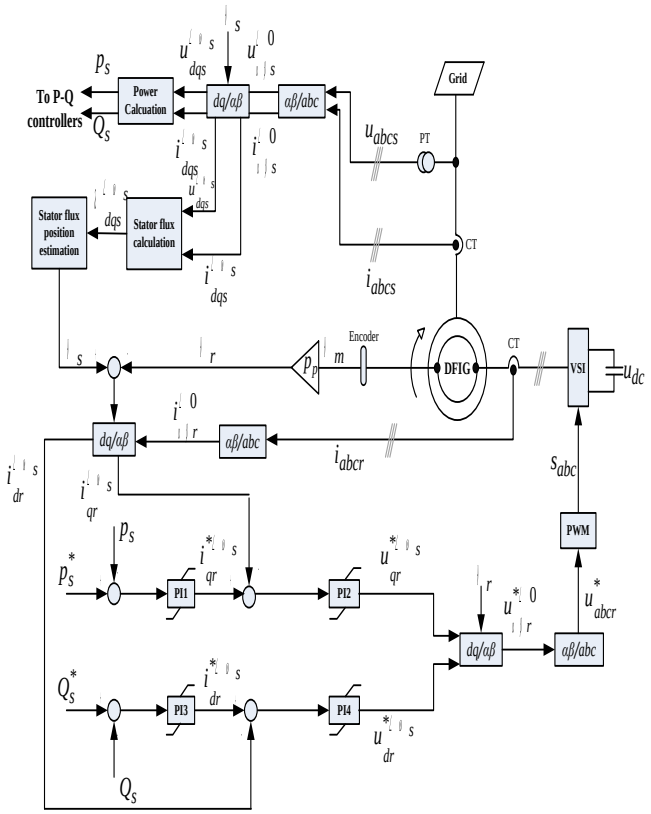

Fig. 1.3 An overall scheme PWM-based vector control

This becomes particularly critical in wind turbine applications. In this regard, researches have been done to eliminate the current control loop [5], but on the other hand, eliminating these current control loops will deteriorate the system performance that imbalances appear in flux and current. Some other methods have been proposed directly to handle the problems related to PI controllers without eliminating the current control loops [6]. In [7] a neuro-fuzzy based vector control technique is proposed considering the effect of saturation in leakage and main fluxes. In this scheme, the proportional and integral gains of the PI controllers which are fixed. In conventional VC method can be now varied in different operating modes owing this method. In [8] a direct-current vector control approach is introduced so that the process of reference voltage generation is omitted in this method. This controller outputs d and q tuning rotor currents.

Current controllers can be classified as hysteresis controllers, linear PI or predictive dead-beat controllers, variable structure controllers, intelligent controllers and non-linear and adaptive regulators. In [9] and [10] a general study over conventional and modern current control techniques have been brought, respectively. Hysteresis current controllers also called on-off or bang-bang controllers have been compatibly used in vector control applications for DFIGs. In this way, they are used to control the rotor currents providing considerably well transient performance and stability. However, the random selection of the switching vectors in the conventional hysteresis controllers which results in high switching losses beside high oscillations in the output current are important matters which cannot be neglected.

In this method, the d-q components of the rotor current, which have been produced via the current decoupling procedure in the stator flux oriented vector control of the DFIG, have to be transformed into three phase components to be forced into the hysteresis comparator, in which Bang-Bang switching of the VSI switches makes the actual wave track its sine reference wave within hysteresis boundary so as to generate the proper VSI control command pulses. This method forces the currents to be kept within hysteresis bandwidth. In this study, a fixed-band hysteresis comparator is put into practice. An overall scheme of the hysteresis-based vector control is depicted in Fig 1.4.

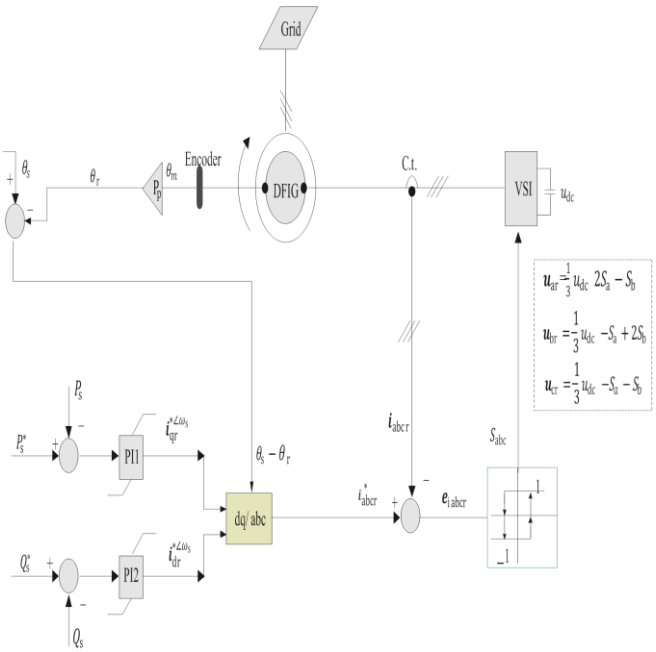

Fig. 1.4 An overall scheme of hysteresis-based vector control

This method is referred to as the conventional hysteresis control applied to the vector control of the DFG which needs less computational effort rather PWM-based vector control and can perform an excellent transient behavior but still the power vector oscillations are obvious in the steady state performance and it is extremely willing to become unstable due to parameter variations. On the other hand, high switching frequency which is due to redundant switching results in high switching losses which consequently associates with thermal stability concerns of VSI. Hysteresis control of the DFIG has slided itself recently to current error space vector based hysteresis control, which employs the advantages of both SVPWM and conventional hysteresis method as a solution to improve the drawbacks of the conventional hysteresis controller, while simultaneously taking advantage of its strength point in transient behavior. The space phasor quantities are injected to the controller, that is, a single error space vector is built and applied to the inverter instead of three current errors used in conventional hysteresis methods. In this scheme

current error space vector position should be determined [11]. In [12], it has been reported that by using the space vector based hysteresis control within a parabolic boundary, constant switching frequency can be achieved. In [2] equidistant-band vector-based hysteresis current regulators have been proposed for vector control applications of DFIG for limiting the instantaneous variations of switching frequency and to reduce the maximum switching frequencies experienced in the converters.

B. Rotor Flux Position-based Direct Power Control (DPC)

Since the mid-1980s the ac drives have gone through direct control techniques: Direct torque control (DTC) and direct power control (DPC). Direct torque control of DFIG was first developed in [13]. Today, direct control strategies are more and more demanded in high dynamic performances, since they offer superior dynamic response while decoupling control signals such as active and reactive power in case of DPC. On the other hand, these methods are independent of the machine parameter variations as was inevitable in conventional vector control methods. However, the variable switching frequency can be the main drawback of direct control methods. This deficiency can cause more complicated effects particularly in power converter and ac filter designs. On the contrary, PWM-based vector control can be implemented with a constant switching frequency and suitable to digital controllers. More recently, DPC based predictive controls have been developed resulting in constant switching frequency operation [14,15].

B.1 Stator active and reactive power formulation based on the flux functionality

From the basic power equations, it can be understood that stator active and reactive powers can be obtained directly from the measured stator current and voltage as follows:

$$P_s = \frac{3}{2}\mathrm{Re}\{\underline{\boldsymbol{u}}_s \underline{\boldsymbol{i}}_s^*\} \qquad (11)$$

$$Q_s = \frac{3}{2}\mathrm{Im}\{\underline{\boldsymbol{u}}_s \underline{\boldsymbol{i}}_s^*\} \qquad (12)$$

With the stator voltage being rather constant, it follows from the above equations that the stator current takes over in power control task such that changes in the stator current will have effects on active and reactive power values. However, stator current itself can be altered by the rotor voltage vectors. In a more general form, by injection of different rotor voltage vectors, stator active and reactive powers are controlled. However, this assertion needs to be more clarified, since the last two expressions don't provide enough information. In this regard, the power equations of (11), (12) can be rewritten as below:

$$P_s = \frac{3}{2}\frac{l_m}{\sigma l_s l_r}\omega_s \, \underline{\boldsymbol{\lambda}}_s \, \underline{\boldsymbol{\lambda}}_r \, sin\delta \qquad (13)$$

$$Q_s = \frac{3}{2}\frac{\omega_s}{\sigma l_s} \, \underline{\boldsymbol{\lambda}}_s \, \frac{l_m}{l_r} \, \underline{\boldsymbol{\lambda}}_s - \underline{\boldsymbol{\lambda}}_r \, cos\delta \qquad (14)$$

Where δ is the phase angle between rotor and stator flux vectors, which depending on the generating or motoring mode it adopts positive or negative values. These equations show the stator active and reactive power dependency on the fluxes. Since the stator voltage and frequency are kept constant and the stator resistance being also neglected, it will lead thus to a constant stator flux. Therefore, it is just needed to keep $\underline{\boldsymbol{\lambda}}_r \, sin\delta$ and $\underline{\boldsymbol{\lambda}}_r \, cos\delta$ under control to achieve active and reactive power regulation purposes. In other words, that either the rotor flux amplitude or the flux angle has to be varied in order to control the stator powers.

B.2 Rotor Flux Definition based on the Rotor Voltage Vector

To determine the rotor flux, the voltage model [13] will be used, considering the rotor reference frame as follows:

$$\underline{\boldsymbol{u}}_{\mathrm{r}}^{\angle \mathrm{r}} = r_{\mathrm{r}} \underline{\boldsymbol{i}}_{\mathrm{r}}^{\angle \mathrm{r}} + \frac{\mathrm{d}\underline{\boldsymbol{\lambda}}_{\mathrm{r}}^{\angle \mathrm{r}}}{\mathrm{d}t} \qquad (15)$$

Neglecting the drop voltage over rotor resistance, we may have the final rotor flux in terms of rotor voltage injected by the converter at the h time interval of the voltage injection as can be seen in Eq. 16.

$$\underline{\boldsymbol{\lambda}}_{\mathrm{rf}}^{\angle \mathrm{r}} - \underline{\boldsymbol{\lambda}}_{\mathrm{ri}}^{\angle \mathrm{r}} \cong - \int_0^{\mathrm{h}} \underline{\boldsymbol{u}}_{\mathrm{r}}^{\angle \mathrm{r}} \mathrm{d}t \qquad (16)$$

The first two terms of Eq. (16) are final and initial rotor flux amplitudes respectively. If the converter injects constant rotor voltage during the injection time interval, the equation above can be simplified as:

$$\underline{\boldsymbol{\lambda}}_{\mathrm{rf}}^{\angle \mathrm{r}} - \underline{\boldsymbol{\lambda}}_{\mathrm{ri}}^{\angle \mathrm{r}} \cong -\underline{\boldsymbol{u}}_{\mathrm{r}}^{\angle \mathrm{r}} \mathrm{h} \qquad (17)$$

It follows from the Eq. (17) that injecting different rotor voltage vectors influences the rotor flux, thus from Eq.(13), (14) leading to changes in stator active and reactive powers.

However, in [36], it has been proved that, the impact of initial rotor flux amplitude and position on the active and reactive power changes can be neglected.

As a final result, the appropriate choice of each of the rotor voltage vectors depend not only on the rotor flux position but also on the active and reactive power errors.

In Table 1.1, the relation between rotor flux position, power error on-off values and rotor voltage vector selection (the converter switching states) is well depicted.

Table 1.1 Rotor Voltage Vector Selection based on the power errors and rotor flux position (k=section)

		ΔP_s	
		1	0
ΔQ_s	1	$\boldsymbol{u}$(k+1)	$\boldsymbol{u}$(k-1)
	0	$\boldsymbol{u}$(k+2)	$\boldsymbol{u}$(k-2)

However, some methods have been also proposed to ease the procedure of rotor voltage vector selection. In [16], it is proposed to use the virtual flux position instead of using rotor and stator flux position, which can be estimated by integration of converter output voltage. In [17] a method of direct calculating the rotor voltage vector based on the stator flux, rotor position, actual values of active and reactive powers and their corresponding errors is proposed in which the constant switching frequency beside transient performance improvement without using any current control loop and frame transformation is achieved.

A schematic diagram of an overall scheme of a conventional DPC method based on the rotor flux position is illustrated in Figure 1.5.

DPC is known to be a robust and fast power control method, which doesn't involve any difficulties related to the

current regulating or numerous frame transformations as in vector control methods. Beside these positive points, direct control method can be effectively used for fast dynamics, that is, fast responses can be obtained under transients. In [18] this feature is highlighted using a sliding mode approach in which the robustness and effectiveness are proved during the active and reactive power variations. As mentioned earlier, the non-constant switching frequency in DPC methods has prompted the researchers to find solutions for this major drawback. In [19] it is reported that incorporating SVM strategy in direct control methods can result in constant switching frequency.

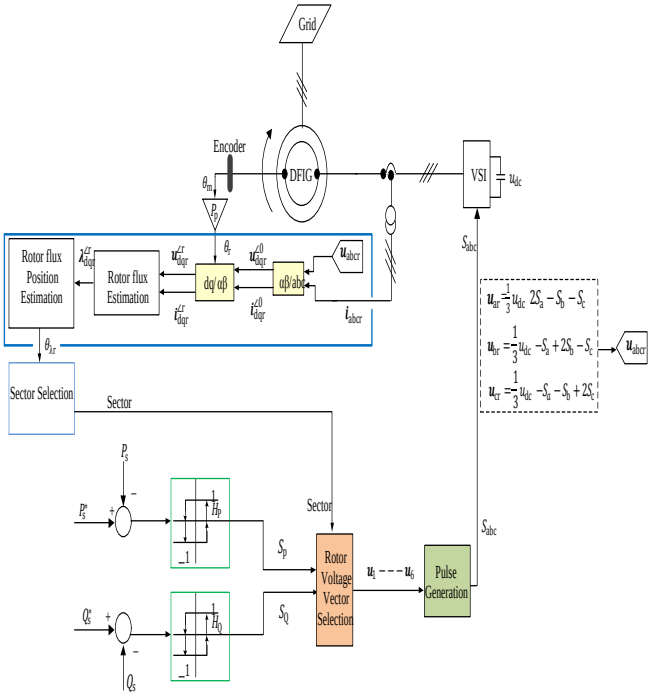

Fig. 1.5 An Overall scheme of the DPC method based on the rotor flux position

Since 2006, there has been more interest on using stator flux position in DPC methods instead of rotor flux position [20]. The reason behind this can be due to the fact that since the stator voltage is rather fixed in frequency and harmonics-free, hence the accuracy of the estimated stator flux is no more susceptible. In [21], a modified DPC strategy has been developed based on the stator flux oriented control in synchronous reference frame in which the constant switching frequency has been reported. However, this method seems to have drawbacks associated with parameter variations especially magnetizing inductance. Therefore, the use of a rotor voltage limiter in transients seems essential. On the other hand, the estimation of the rotor flux position together with stator flux calculation seems a great deal and this might require high computation efforts.

C. Simulations and Comparative Study

Due to the simulation results, a comparative study can be done and advantages and disadvantages of each method can be described.

Simulation of a 40 KW DFIG was carried in Matlab/Simulink. The performance of this control design is investigated for different active and reactive power commands shown in Figure 1.6.

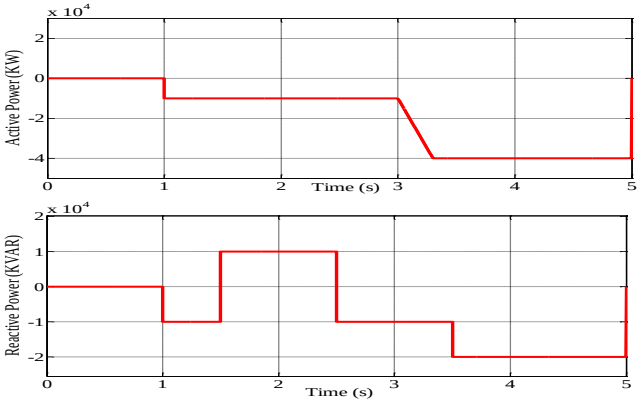

Fig. 1.6 Active and reactive power references, respectively

Figure 1.7 shows a general review on the active and reactive power curves of each method:

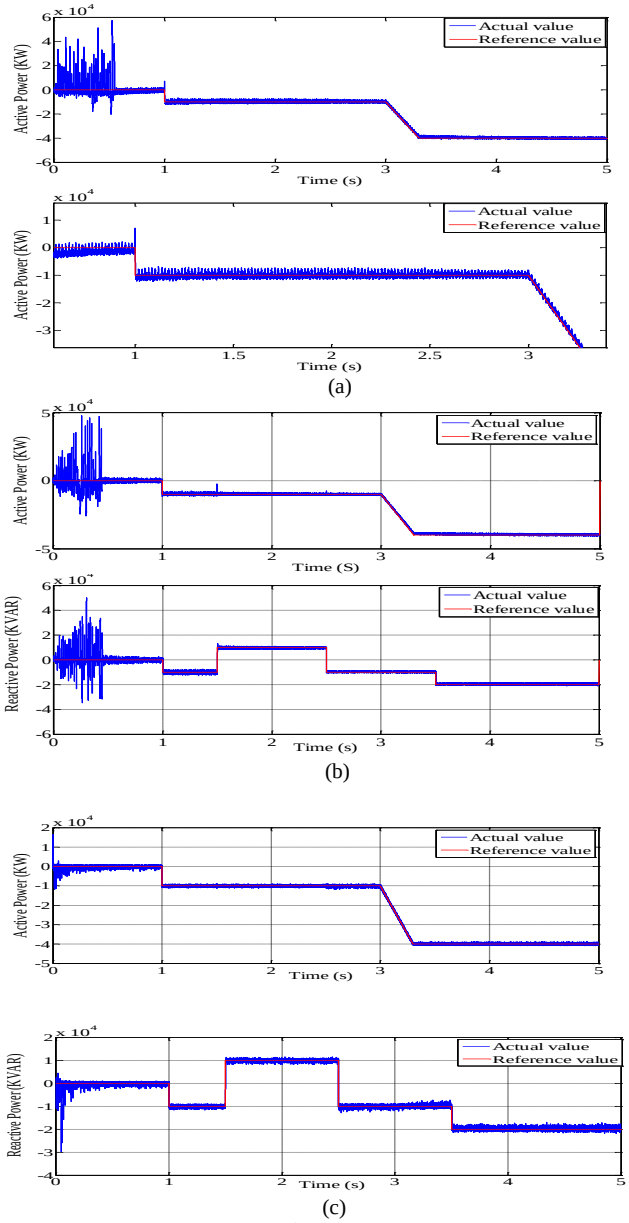

Fig. 1.7 Active and reactive power reference tracking curves a) PWM-VC b) Hysteresis-VC c) DPC

Since the stator power control of the DFIG is relatively confined to the vector control and direct power control methods, it is required to count the strength and weakness of

each method according to the simulation results. This is structured as below:

C.1 Decoupling behavior

According to the decoupling analysis results, the hysteresis-based vector control has proved to be the worst among other control techniques. This feature is highlighted in Figure 1.8, where DPC is totally regardless to the reactive power transition at t=1.5s and t=2.5s, while PWM-based vector control tries to maintain totally decoupled or at least with a minimum coupling effect.

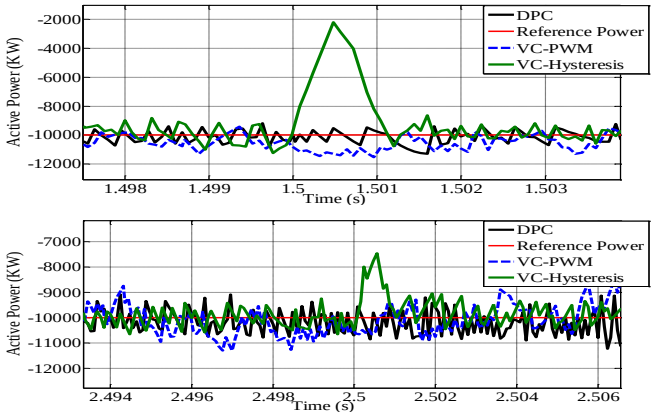

Fig. 1.8 Comparison of decoupling behavior: a) t=1.5s b) t=2.5s

C.2 Dynamic Response

Dynamic response is another important feature to be evaluated. As can be seen in Figure 1.9 DPC method provides a superior dynamic response than vector control methods. Among vector methods, hysteresis-based shows a better transient response than PWM-based vector control.

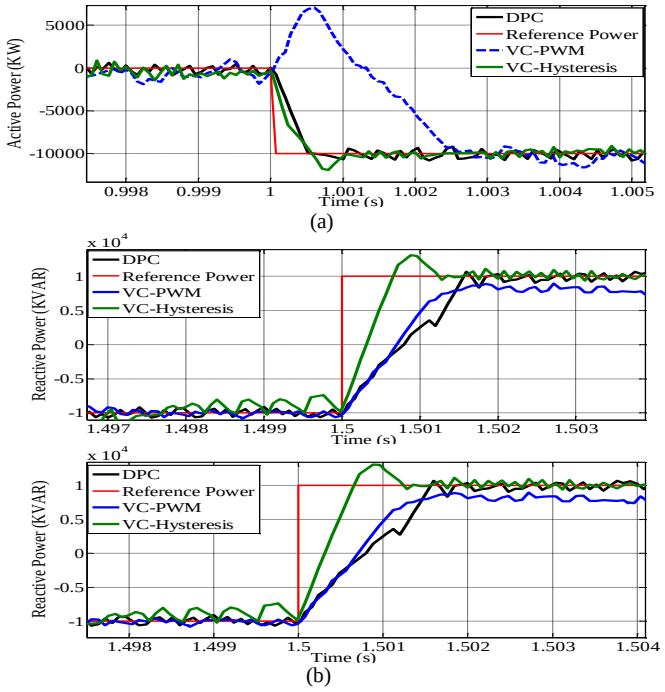

Fig. 1.9 Comparison of dynamic response: a) active powers b) reactive powers

C.3 Robustness

One of the important factors for evaluating a control scheme is robustness of the system against parameter variations. The control design is thus examined incorporating parameter variation effect by changing the stator resistance to 50% and 150% of its nominal value. Since the stator resistance plays a key role in stator flux measurement it would then be important to consider its effect on the system performance. Stator resistance variation arises mainly from frequency and temperature changes. Which in case of a wound rotor induction generator connected directly to the grid, it would arise thus mainly due to the temperature increase rather than frequency. As can be seen in Figure 1.10 DPC can easily tackle this obstacle while PWM vector control encounters small disturbances but still acts firmly. Unlike DPC and PWM vector control, the hysteresis vector method becomes to a large extent oscillatory.

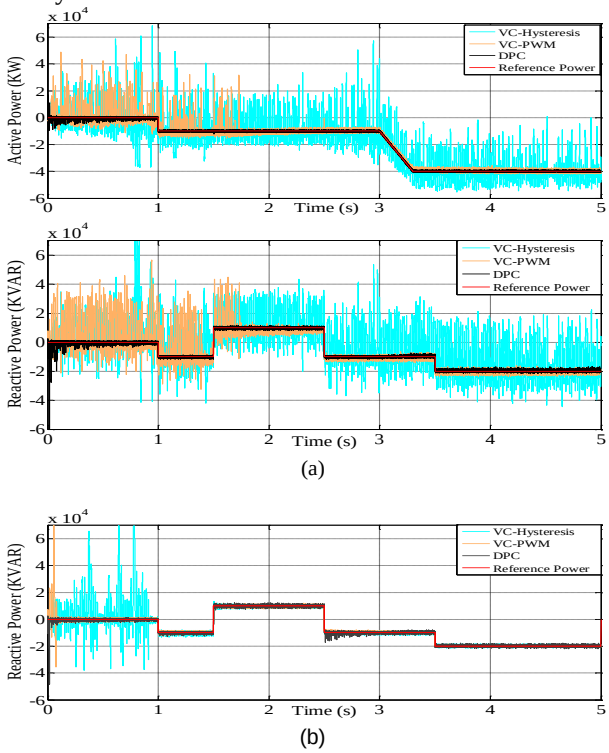

Fig. 1.10 Comparison of robustness of active and reactive power at: a) 50% r_sb) 150% r_s

PWM-based vector control has proved to be a fast and decoupled active and reactive power control method in which the constant switching frequency is obtained which doesn't exist in other proposed control schemes. On the other side, the high computational actions and complexities relevant to the numerous reference frame transformations beside its model-based nature might be counted as the major drawbacks of PWM control method. However PWM-based vector control method performs more and more satisfactory results than hysteresis-based vector method, in which although the power ripples are reduced and the transient response is very fast but the decoupling problem beside high performance degradation during parameter variation still exist.

Direct power method unlike vector control methods is independent from machine parameters. Fast and accurate response is obtained within this control scheme, that is, a remarkable match between actual and reference signals is achieved. On the other hand it performs a very good decoupling behavior. In this method, there exists the least frame transformation requirement which means omitting too

much measurements of some electrical signals which have brought complexities in VC methods.

Although DPC has an excellent transient performance, high power ripples in steady state performance beside non-constant switching frequency debase its advantages. On the other hand, lack of any current controllers in the system seems to have deteriorating effects as mentioned earlier which can be regarded as another deficiency of this method.

D. Vector Control of DFIG with Brain Emotional Learning-based Intelligent Controller (BELBIC)

So far, vector control and direct power control methods have been implemented for the DFIG-based systems. Advantages and disadvantages of each method have been declared based on the simulation results. Lack of enough decoupling behavior as power references change, high dependency on the machine parameters, high computational issues, non-constant switching frequency, high power oscillations, position estimating issues, current regulation concerns, presence or absence of sensors or estimators, etc. These are the challenging issues addressing directly the variable speed operation applications which have propelled the researchers to find solutions for each of the aforementioned problems. Among those problems, some developments address the controllers, some focusing on the power electronic structures and modulation strategies, some investigate the sensor less operation, etc.

The advent of intelligence-based control techniques have been developed in recent years, to overcome some analytical and computational problems which exist in classical controllers. Due to this, the control of wind-based systems can be divided into two general categories of hard and soft control techniques [22]. The first category, stands mostly for the conventional or high computation-based control techniques such as: PID control, Optimal control, Robust control, adaptive control, sliding mode control and predictive control approaches, while the second category involves mainly the modern control techniques addressing the drawbacks in conventional methods which are mainly referred to intelligence-based control techniques such as fuzzy control, neural networks control, etc.

Although the modern control techniques including artificial intelligent methods have been successful in nonlinear structures and there have been too much interest to utilize them in industrial and practical applications, they demand fast computer processing and they have not yet provided a complete solution for stability and robustness issues. In recent years, a new artificial intelligent controller has been introduced which imitates the computational process of the medial brain emotional learning action. This method is also known as brain emotional learning-based intelligent control (BELBIC) in the literature. BELBIC application in industry was first introduced in which was inspired from **Moren-Balkenius**'s proposed brain computational model in [23,24]. In [25], the first application of BELBIC controller in electrical machine drives was tested by **Lucas**. It has been proved that the BELBIC controller is fast and more robust against parameter variation and can be simply implemented in comparison with those of PID controllers or other artificial intelligence methods.

In [26] BELBIC controller was applied to implement the simultaneous speed and flux control in induction motors. It has been shown that the control system was properly working regardless of variations in parameters.

BELBIC method stems from the computational model of the brain limbic system where the emotions are controlled. In general, the task of the human emotional control is taken on the limbic system, which is considered as one of the various functionalities of the limbic system. The emotional control system of the brain is the system of several IOs with two main processors. Amygdala is the main emotional processing unit in the limbic system which is bidirectionally connected to the orbitofrontal cortex (OFC). Its main inputs can be referred to as sensory input (SI) which is injected indirectly via the Thalamus and the other input which is common with the orbitofrontal cortex is emotional cue (EC) referred to as reinforcing signal or also in some literatures, Reward signal. Emotional cue is thought to be an internal signal possibly brought by Pre frontal cortex which is not shown here. However, amygdala establishes extra connections with other parts of limbic system such as sensory cortex unit and receives other signals in order to compliment the emotional processing action. Sensory cortex itself is the receiver of thalamus output signal, and manipulating the sensed input, it gives the sensory cortex signal out. The system of processing emotions in the brain is depicted in Figure 1.10:

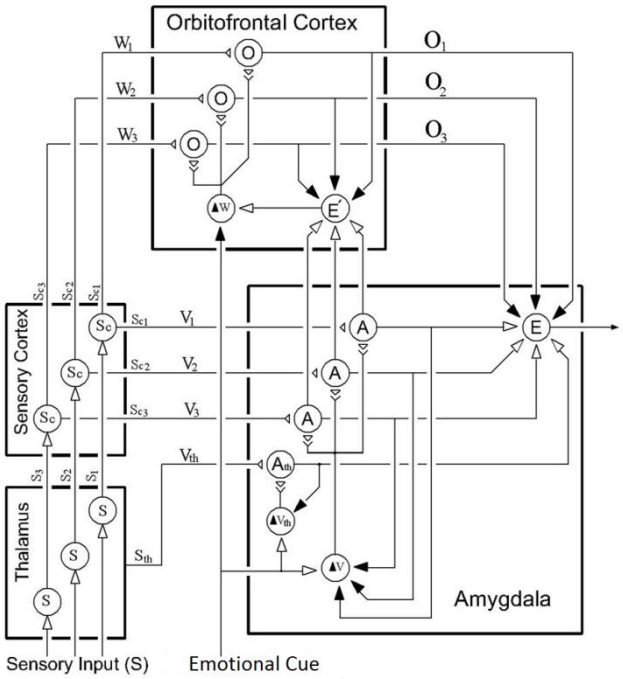

Fig. 1.10 The brain emotional processing system [55]

According to Figure 1.10 each input signal entering the amygdala and orbitofrontal cortex is weighted with V and W gains, respectively. For each of the amygdala, thalamus and the orbitofrontal cortex, there are three nodes of *A*, *Ath* and *O* which converge to the output *E* node of the brain emotional processing closed-loop model. The *E* node simply sums the outputs from the *A* nodes, and *Ath* and then subtracts the inhibitory outputs of the *O* nodes.

The mathematical relation pertaining to the above model can be defined as:

$$E = \ {}_i A_i + A_{th} - \ {}_i O_i \qquad (18)$$

The internal area outputs are computed as:

$$A_i = S_i V_i \quad (19)$$

$$O_i = S_i W_i \quad (20)$$

Where *Ai* and *Oi* are the output signals of amygdala and orbitofrontal cortex. *S* is the stimuli and *i* is the *i*th input. Since the sensory input is not directly injected to amygdala, the maximum value of this signal would be considered as the thalamus input of the amygdala, as shown below:

$$A_{th} = V_{th}\ max(S_i) = S_{th}\} \quad (21)$$

Where *Sth* is the output of Thalamus unit.

The incremental adjustments of each gain (the learning rates of the connection V and W weights) pertaining to amygdala and OFC are proportional to the sensory input *Si* and emotional cue *EC*:

$$\Delta V_i = K_1\ S_i\, max(0, EC - {}_i A_i \quad (22)$$

$$\Delta W_i = K_2\ S_i(\ {}_i A_i - {}_i O_i - EC) \quad (23)$$

Where *K1* and *K2* are amygdala and OFC learning rate coefficients (learning steps). Eq. (22) yields a monotonic learning change, which implies that the decisions (also from biological point of view called emotional reactions) which are made via amygdala with respect to any sensory input are innately permanent if they have been learnt for the first time. In case of similar sensory signals being injected to amygdala, amygdala chooses the same emotional reaction which was learnt before. On the other hand, orbitofrontal cortex comes to correct the decisions which are made via amygdala if they have been inappropriately chosen. According to the introduced equations, the BELBIC diagram is depicted in Figure 1.12.

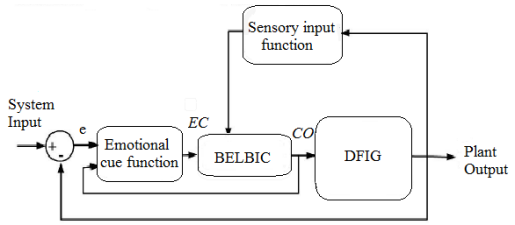

Fig. 1.12 Control System Configuration using BELBIC

The functions of emotional cue *EC* and the sensory input *Si* blocks can be obtained as below:

$$EC = W_1 \quad edt + W_2.CO \quad (24)$$

$$S_i = W_3.PO + W_4.PO \quad (25)$$

Where CO and PO are controller and plant output (stator active and reactive power), and *W1- W2* are controller gains like PID controller constants and *e* is the error signal. Each gain must be so accurately tuned that satisfactory results are obtained. In this regard, tuning *W1* will manipulate the overshoot level, while the gain *W2* is responsible for adjusting the settling time. The steady state error will be tuned by the gain *W3* and finally the gain *W4* is tuned to achieve a more smooth response at its initial moments.

Figure 1.13 shows an overall scheme of PWM-based vector control incorporating BELBIC controller in which one set of PI regulators is replaced by BELBIC controllers.

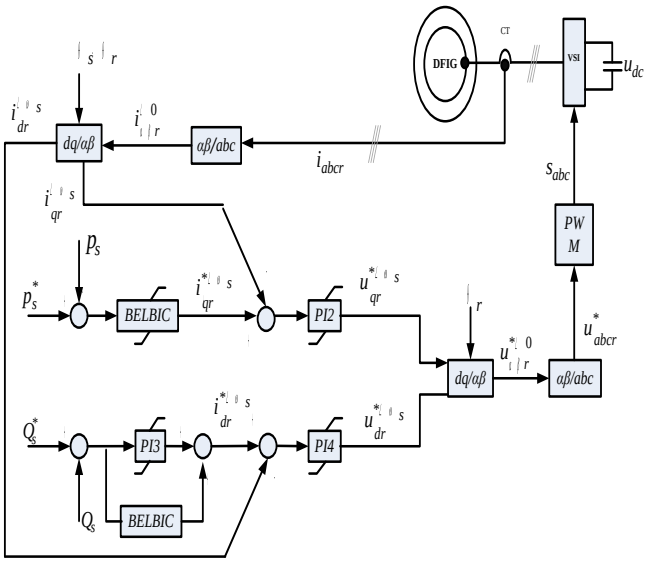

Fig 1.13 An overall scheme of incorporating BELBIC controllers into PWM-based vector control

Simulation results show that in the PWM-based vector control involving BELBIC controllers the transient behavior have been remarkably improved (see Figure 1.14-1.16).

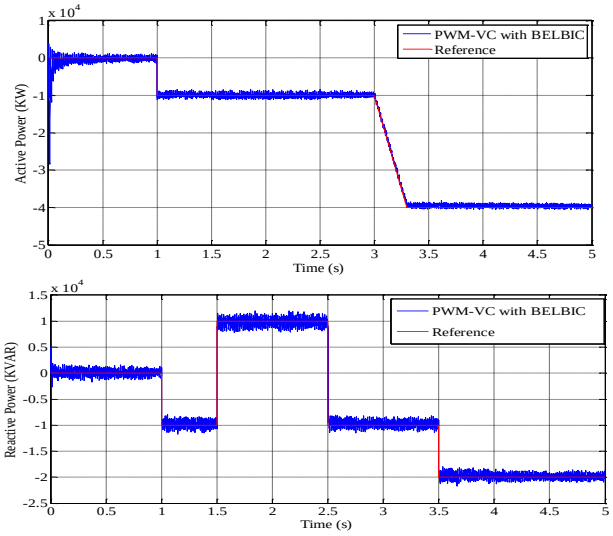

Fig. 1.14 Active and reactive power

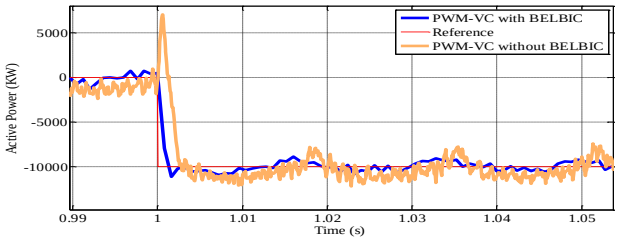

Fig. 1.15 Active power curves of PWM-vector control with and without BELBIC controllers

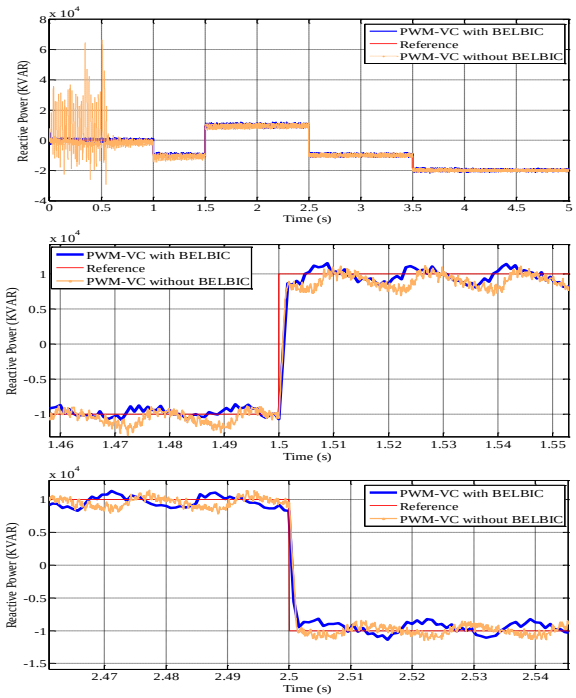

Fig. 1.16 Reactive power curves of PWM-vector control with and without BELBIC controllers

As comes from the above results, the power ripples have been highly improved. According to the active and reactive power curves, it can be concluded that BELBIC controller can be successfully used and can be thought of as one of the alternatives of conventional PI regulators in future.

IV. Conclusions

In this paper different active and reactive power control schemes have been developed for distributed generator in wind turbine applications. In this way, three different control schemes have been implemented and analyzed in a DFIG-based wind turbine using Matlab/Simulink. The first control scheme adopted the common vector control technique under stator flux orientation which was accomplished using PWM strategy. Fast and decoupled active and reactive power control beside excellent decoupling behavior and constant switching frequency are the most salient features of this method. Since vector control is a model-based method, lack of robustness has been reported in case of machine parameter variations. The excessive computational efforts and rather high power ripples are challenging concerns in this method. Moreover, tuning fixed-gain current regulators is itself a great deal. The vector control under stator-flux orientation was then examined omitting one set of PI current regulators and replacing them with conventional hysteresis current controllers. It has been reported that, in comparison with the PWM-based vector control this scheme gives fast dynamic response and the power ripples were improved. The reference power tracking behavior was to some extent degraded nevertheless reasonable results are acquired. The main drawback of this method could be found decoupling active and reactive powers. The last power control method also referred to as direct power control method (DPC) is so structured that no current regulating loop exists in this scheme. In this way, the inverter switching pulses are obtained using hysteresis controllers and an optimal switching table. The inputs of this switching table are not only active and reactive power errors but also the rotor flux position in order that an optimum result is yielded. It has been found out that this method shows superior dynamic response relative to that of vector control method. DPC has shown firm and robust operation against parameter variations. However, high power ripples were obvious in the power curves which would be problematic in ac filter and converter designs. At the end a novel controller based on the brain emotional learning-based intelligent system has been incorporated into PWM-VC and remarkable results were obtained.

V. Appendix

Table 1.2 DFIG Parameters

Parameter of DFIG	
Rated Power	40 kW
Stator Voltage	400 V
Stator Resistance	01.733 Ω
Referred Rotor Resistance	1.99 Ω
Stator Inductance	6.94 mH
Rotor Inductance	6.94 mH
Magnetizing Inductance	163.73 mH
Pole Pair	2
Rotor Inertia	0.1 Kg.m2
Simulation Time	5s

VI. References

[1] P. Vas,'' Sensorless Vector and Direct Torque Control'', *Oxford University Press, United States of America*, 1998.

[2] M. Mohseni, S. Islam, ''Enhanced Hysteresis-Based Current Regulators in Vector Control of DFIG Wind Turbines'', *IEEE Transactions on Power Electronics*, January 2011.

[3] G.D. Marques, D.M. Sousa, ''New Sensorless Rotor Position Estimator of a DFIG Based on Torque Calculations-Stability Study'', *IEEE Transactions on Energy Conversion*, March. 2012.

[4] S. Engelhardt, ''Direkte Leistungsregelung einer Windenergieanlage mit doppelt gespeister Asynchronmaschine, Shaker'', *Aachen*, 2011.

[6] J. Hu, L. Shang, ''Direct Active and Reactive Power Regulation of Grid-Connected DC/AC Converters Using Sliding Mode Control Approach'', *IEEE Transactions on Power Electronics*, January 2011.

[7] F.P. Bouaouiche, M. Machmoum, ''Advanced control of a doubly-fed Induction Generator for Wind Energy Conversion'', *Electric Power Systems Research*, July, 2009.

[8] H.M. Jabr, D.Lu, ''Design and Implementation of Neuro-Fuzzy Vector Control for Wind-Driven Doubly-Fed Induction Generator'', *IEEE Transactions on sustainable energy*, October. 2011.

[9] H. Li, T.Haskew, R. Swatloski, ''Control of DFIG Wind Turbine with Direct-Current Vector Control Configuration'', *IEEE Transactions on Sustainable Energy*, January 2012.

[10] M. Kazmierkowski, L. Malesani, ''Current Control Techniques for Three-Phase Voltage Source PWM Converters: A Survey'', *IEEE Transactions on Industrial Electronics*, October 1998.

[11] D. Holmes, B. McGrath, S.Parker, '' Current Regulation Strategies for Vector-Controlled Induction Motor Drives'', *IEEE Transactions on Industrial Electronics*, October 2012.

[12] T. Ghennam, E.M. Berkouk, ''A Novel Space-Vector Current Control Based on Circular Hysteresis Areas of a Three-Phase Neutral-Point-Clamped Inverter'', *IEEE Transactions on Industrial Electronics*, August 2010.

[13] Ch. Patel, R. Ramchand, ''A Rotor Flux Estimation During Zero and Active Vector Periods Using Current Error Space Vector From a Hysteresis Controller for a Sensor less Vector Control of IM Drive'', *IEEE Transactions on Industrial Electronics*, June 2011.

[14] R. Datta, V.T. Ranganathan, ''Direct Power Control of Grid-Connected Wound Rotor Induction Machine without Rotor Position Sensors'', *IEEE Transactions on Power Electronics*, May 2001.

[15] L. Xu, d. Zhi, Williams, B.W., ''Predictive current control of doubly fed induction generators'', *IEEE Transactions on Industrial Electronics*, October 2009.

[16] G. Abad, M. Rodr´ıguez, J. Poza, ''Three-level NPC converter-based predictive direct power control of the doubly fed induction machine at low constant switching frequency'', *IEEE Transactions on Industrial Electronics*, December 2008.

[17]M.Malinowski, M.P.Kazmierkowski, S.Hansen, F.Blaabjerg, '' Virtual-flux-based direct power control of three-phase PWM rectifiers'', *IEEE Transactions on Industrial Applications*, July-August 2001.

[18] S.Y. Liu, V.F.M.S. Silva, F.Runcos, ''Analysis of Direct Power Control Strategies Applied to Doubly Fed Induction Generator'', *Power Electronics Conference (COBEP)*, 2011.

[19] H.G. Jeong, W.S. Kim, K.B. Lee, B.C. Jeong, ''A Sliding-Mode Approach to Control the Active and Reactive Powers for A DFIG in Wind Turbines'', *Power Electronics Specialists Conference IEEE PES*, 2008.

[20] N.R.N. Idris, A.H.M. Yatim, ''Direct Torque Control of Induction Machines with Constant Switching Frequency and Reduced Torque Ripple'', *IEEE Transactions on Industrial Electronics*, August. 2004.

[21] L. Xu, P. Cartwright, ''Direct active and reactive power control of DFIG for wind energy generation'', *IEEE Transactions on Energy Conversion*, September 2006.

[22] L. Xu, D. Zhi., L.Yao, ''Direct Power Control of Grid Connected Voltage Source Converters'', *Power Engineering Society General Meeting IEEE Digital Object Identifier* , 2007.

[23] H.M. Nguyen, S. Naidu, ''Advanced Control Strategies for Wind Energy Systems: An Overview'', *IEEE PES Power Systems Conference & Exposition*, March, 2011.

[24] J. Moren, C. Balkenius, ''A computational model of emotional learning in the amygdala'', *in Proc. 6th Int. Conf. Simul. Adapt. Behav., Cambridge,* MA, 2000, pp. 411–436.

[25] J. Moren, ''Emotion and learning: A computational model of the Amygdala'', *Ph.D. dissertation, Lund Univ.*, Lund, Sweden, 2002.

[26]M.A.Rahman, , M.Milasi, , C.Lucas, B.N.Arrabi, , T.S. Radwan, ''Implementation of emotional controller for interior permanent magnet synchronous motor drive'', *IEEE Transactions on Industrial Applications*, September/October 2008.

[27]G.R. Markadeh, , E. Daryabeigi, , C. Lucas, A. Rahman, ''Speed and Flux Control of Induction Motors Using Emotional Intelligent Controller'', *IEEE Transactions on Industrial Applications*, May/June 2011.

2nd Conference on Power Options for the Eastern Mediterranean Region
07-08 October 2013, Nicosia, Cyprus (Paper No. POEM13/158)

Action steps for refining the Cyprus national action plan on RES penetration for electricity generation - *Should we reconsider*?

A.I. Nikolaidis and C.A. Charalambous[1]

Abstract-- **The Cyprus power system has certain peculiarities arising from its isolated nature, the geographic concentration of its conventional power plants and the use of underground cables, in high proportion. These specific conditions dictate certain operational and controlling challenges with regards to voltage and frequency stability of the system. Moreover, the system is expected to face major technical and financial challenges when integrating substantial proportions of Renewable Energy in the generation mix. Thus, this paper investigates past and current trends in power system planning processes and discusses possible action steps in order to ensure a secure and effective integration of Renewable Energy. The discussion accounts for the specifics of the power system in Cyprus.**

Index Terms— **Energy policy, power system planning, renewable energy sources, flexible generation.**

I. Introduction

THE Cyprus power system is characterized by specific conditions arising from its electrically isolated nature, the geographic concentration of its conventional power plants and the use of underground cables, in high proportion. These specific conditions enforce certain operational and controlling challenges with regards to voltage and frequency stability of the system. Moreover, the system is expected to face major technical and financial challenges when integrating substantial proportions of Renewable Energy in the generation mix.

However, Cyprus has the obligation to comply with the EU directives and policies [1] that aim to transform Europe into a low-carbon, highly energy-efficient economy. The road map to reach these targets is defined through the *National Action Plan* (NAP). More specifically this plan sets certain targets for the final use of energy regarding heating and cooling as well as electricity generation and transportation.

To this extend the Cyprus Energy Regulation Authority (CERA) is periodically redefining the "strategic plan" for the promotion of renewable energy sources in the Cyprus electricity generation system by issuing certain updates. These updates mainly reflect on the fluctuating capital costs of RES technology.

It is therefore prudent to effectively address any arising challenges under a comprehensive planning process. Thus the main objective of this paper is a) to identify the key issues that relate to reliably maximizing the R.E.S penetration and b) to raise awareness regarding the complexities that need to be thoroughly addressed bearing in mind the specific characteristics of the Cyprus System.

The paper is organized as follows: Section II describes the framework for power system capacity planning studies. It further discusses the new challenges that have to be addressed in order to integrate large proportions of RES generation in existing power systems. Section III introduces the flexibility adequacy studies. These studies complement capacity adequacy studies in order to successfully manage the inherent generation fluctuation of RES. Section IV provides a brief description of the Cyprus Power System. It further presents a case study that investigates the effect of varying the relative penetration proportions of wind and PV generation. This is done in an effort to maximizing the benefit from an aggregate RES mix. Finally, section V summarizes the key points by providing a set of recommendations.

II. Power system capacity planning studies

Power system planning is defined as a decision making process to ensure that the system will reliably satisfy the demand in a specified future horizon [3]. Thus, the ultimate goal of the planning process is to ensure that adequate capacity will be available to serve the demand at any given time. In the past few decades, numerous methodologies have been developed to ensure an optimum system expansion at the lowest possible cost. To this extend the reliability of the system is a dominant factor in both the planning studies and operational procedures. There exist several methods for evaluating power system reliability, both deterministic and probabilistic [4-5]. Deterministic methods include the *generation reserve margin*, the *percentage of demand* and/or the *loss of largest unit.* These have been implemented in the past with satisfying results.

On the other hand probabilistic methods take into account the stochastic behavior of the power system elements and equipment by relying on appropriate risk models. These models account for reliability indices such as the *loss of load probability/expectation* (LOLP/LOLE) and the *expected energy not served* (EENS).They are, in essence, providing more thorough estimations about the system's potential to serve its demand [4-5].

Furthermore, an indirect reliability index is used in capacity expansion studies [6]. This is often classified as the capacity credit. It reflects on the generators' contribution in the system's overall adequacy. In other words, it is the generators' (conventional or renewable) ability to reliably serve the load demand.

The capacity credit of RES has drawn much of the research community attention in the last decade in an effort to quantify the contribution of intermittent sources in the system's capacity. Within this framework, the Load Duration Magnitude Capacity (LDMC) metric is an approximation method that capitalizes on the load duration

[1] A.I. Nikolaidis and C.A. Charalambous are with the Department of Electrical and Computer Engineering of University of Cyprus, PO Box 20537, 1687, Nicosia, Cyprus e-mail: (nikolaidis.alexandros@ucy.ac.cy, cchara@ucy.ac.cy).

curve (LDC) [7]. It is calculated as the mean RES output for all loads greater than the LDMC threshold. The LDMC threshold is defined as the utility's peak load L, minus the installed RES capacity X, as given in (1).

$$LDMCthreshold = L(1-p) \quad (1)$$

where L is the system peak load and p is the RES penetration fraction which is defined by the ratio *X/L*. A graphic illustration of the LDMC method is shown in Fig. 1.

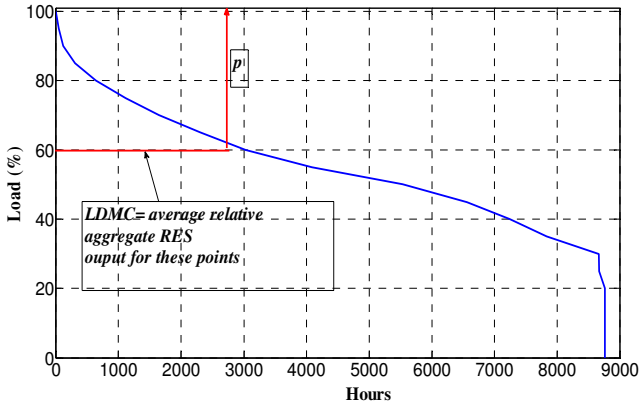

Fig. 1: Illustration of the LDMC method.

A. Discussion

The aforementioned reliability indicators, although very useful and frequently utilized, are becoming less adequate to fully address the true operational challenges that high levels of RES penetration introduce in the system.

This is mainly due to the volatile contribution of RES in the system's capacity adequacy. This contribution is usually low-to-medium compared to the nameplate capacity of RES. This means that RES can potentially cover a substantial share of the system's energy needs but not necessarily of its capacity needs. Consequently, in the energy-only market that exists today, conventional generators might face difficulties to recover all their costs (as they need to account for an unpaid capacity). This could lead to a loss of investment interest [8]-[9]. Several capacity remuneration mechanisms have been proposed so far, each with pros and cons, in order to prevent such a situation.

Finally, the inherent variability and large forecasting uncertainties that characterize renewable energy sources entail a certain management risk. These challenges are now being addressed through system *flexibility* studies. The following section discusses the relevant framework of these flexibility studies.

III. Flexibility Adequacy Studies

Flexibility is defined in [10] as the ability of a system to cope with any variations and uncertainties in a specified time horizon. A similar definition is given in [11] and [12] where flexibility means the ability of a system to deploy its resources to respond to changes in the net demand[2].

The options for flexibility provision in power systems and their applicability in the Cyprus case (May 2013), are shown in Table I [11].Table I can be interpreted as follows: Given the same demand and RES characteristics, a system with more flexibility options is more likely to securely integrate larger amounts of RES.

It may be well understood that for the case of Cyprus not all flexibility options are available (especially the lack of interconnections). In fact, the available options include controlling conventional generators and RES curtailment. With regards the latter, the circumstance is rather abstract since the publicly available rules, for RES curtailment in Cyprus, are constructively ambiguous [13].

TABLE I
Power System Flexibility Options [11]

	Availability in Cyprus	
Option	2013	2020
Conventional generators	Yes	Yes
RES curtailment	Yes	Yes
Interconnections	No	Unknown
Energy storage	No	Unknown
Demand-side resources	No	Unknown

Moreover, it is well accepted that flexibility options are more associated with the operational characteristics of a power system. However, flexibility must be taken into consideration at the planning stage. This concern has been addressed as early as in the 1980's. However, it has gained more of the planners' attention in the last few years since RES generation has strongly entered the electricity sector. In [14] it is suggested that the potential gain in capacity from RES could be, in some cases, eliminated by the cost of altering the conventional generation portfolio to include more flexible generation sources with higher operating costs.

Flexibility metrics can be found in recent literature [10-12]. These metrics aim to complement current capacity adequacy studies in order to ensure the effective integration of variable generation in existing systems. The interpretation of such metrics is explained through a parallelism to capacity adequacy metrics. That is when a system's LOLE is higher than the acceptable limit then new generation sources have to be added to the system to increase its reliability. Similarly, when the flexibility metrics are higher than acceptable limits, new flexibility options must be adopted in order for the system to be able to withstand all expected or unexpected fluctuations.

A. Conventional generators flexibility provision

Conventional generators provide flexibility, mostly through spinning reserve. Spinning reserve is defined as the unused capacity which can be activated by the decision of the system's operator. It is provided by devices which are synchronized to the network and are able to affect the active power [15].

The general approach in spinning reserve quantification includes: Primary reserve is procured based on the largest credible contingency event. Secondary and tertiary reserves are procured based on probabilistic calculations with regards

[2] Net demand is defined as the residual of the demand minus the RES generation and net generation import/export.

to each system's generation, demand and market characteristics. This requires searching for the optimal trade-off between the cost of procuring an additional MW of spinning reserve and the cost of shedding a certain amount of load [16-18].

Several studies have investigated the impact of RES generation on the conventional generation fleet of a system. This impact will be eminent on the system's unit commitment, generation cycling and economic dispatch (which may be performed under increased uncertainty). A method to deal with this uncertainty is to procure larger amounts of flexibility options. Thus, there is a consensus in the research community that the spinning reserve requirements should increase as RES penetration increases. The studies that have been performed clearly show that variable RES generation leads to lower load factors in thermal units as well as to extended start-up and shut-down costs due to increased cycling [19]. They also suggest that this inherent RES generation variability is more likely to have an effect on the secondary and tertiary reserve needs rather than on the primary reserve. This is because RES variability usually takes place at a slower rate rather than faults and failures in generation units or transmission lines [20]. This has been confirmed for the Cyprus power system in [21].

B. RES curtailment flexibility provision

As previously mentioned, RES curtailment can act as a flexibility option in maintaining the system's balance. However, the current practice in Cyprus provides a priority access to R.E generation in the transmission system [13]. This leaves RES curtailment up to the TSO's daily judgments to maintain the system's security.

In [22] it is suggested that RES curtailment could be performed as a market operation practice, based on the disposition of power producers to curtail their generation if they are given compensating options. This could prove to be a fair option for RES curtailment since it will clarify, in advance, the process both for the TSO and RES producers.

IV. Current status of the Cypriot electricity sector

Cyprus is an island located in the south-eastern part of the Mediterranean Sea. Its population is approximately 850.000. However, in the summer this number reaches more than 1.5 million due to the tourist influx. Hence, the peak load of the system takes place in the summer (this is also due to the climate conditions) rather than in winter. The annual demand pattern is characterized by two high demand seasons (summer and winter) and two low demand seasons (spring and autumn) [23].

Furthermore, the Cyprus power system is a small-to-medium-sized isolated system with an almost exclusive dependence on fossil fuels, namely heavy oil, diesel and natural gas (as a future part of the fuel mix). The thermal generation fleet is owned by the Electricity Authority of Cyprus (E.A.C). In addition, 146.7 MW of wind generation have been installed by independent power producers as of late 2011-early 2012.

The installed capacity of conventional and wind generation in Cyprus in May 2013, is shown in Table II and Table III respectively.

TABLE II
Current Cyprus thermal generation fleet (May 2013) [21]

No. of units	2	6	4	5
Fuel type	Gasoil	HFO	HFO	Gasoil
Efficiency (%)	50	31	30	29
Pmax (MW)	220	60	30	37,5
Pmin(MW)	113	30	18	4
Ramp rate(MW/min)	8	2	1	5
Min. time on (h)	12	4	2	0,5
Min. time off (h)	6	8	6	3
Primary Reserve (MW)	44	8	5	12
Secondary Reserve (MW)	80	18	5	34
Tertiary Reserve (MW)	107	30	30	37,5

TABLE III
Wind parks currently installed in Cyprus (May 2013) [24]

Location	Installed Capacity (MW)
Orites	82
Alexigros	31.5
Agia Anna	20
Koshi	10.8
Kambi	2.4

A. National Action Plan of Cyprus

The Cyprus National Action Plan, as per the Directive 2009/28/EC [1], can be found in [25]. It is briefly described in Table IV. In particular, for the electricity sector, 16% of the final energy consumption must come from renewable energy sources. Specifically, the target for the aggregate wind and PV energy yield should be approximately 12% of the total energy demand in 2020. The proposed aggregate PV-wind penetration would reach approximately 500 MW. The documented/proposed PV to wind penetration ratio is 40%-60% (see Table IV).

TABLE IV
Proposed National Action Plan for the Cyprus electricity sector

	2010		2020	
	MW	GWh	MW	GWh
Demand	1100	5300	1730	6805
Wind	82	31,4	300	499
PV	6	6,46	192	309
Biomass	6	30	17	143
CSP	0	0	75	224

Table V shows the revised demand forecasts for 2020 that were utilized for this case study [24].

TABLE V
REVISED FORECASTS FOR THE CYPRUS ELECTRICITY SECTOR [24]

	2013		2020	
	MW	GWh	MW	GWh
Demand	1000	4820	1210	6130
Wind	146,7	31,4	To be revised	To be revised
PV	~10	~11	To be revised	To be revised
Biomass	6	30	To be revised	To be revised
CSP	0	0	To be revised	To be revised

B. Case study results

In this section a case study concerning the integration of RES generation in the Cyprus power system has been performed. The revised demand forecasts (see Table V) have been utilized and the proposed aggregate RES penetration of the NAP is examined. The aim is to investigate the effect of the RES penetration proposed by the NAP on the system. In addition, an examination of alternative PV to wind penetration ratios is performed.

The fundamental approach of the case study is illustrated in Fig. 2. This shows an ideal (and thus proposed) power system planning framework. Fig. 2 can be interpreted as follows: the ultimate planning goal is to ensure the optimal trade-off between reliability, required RES capacity penetration, corresponding installation location and expected overall costs. In simple words, if RES penetration is to reach high levels without jeopardizing the current system reliability, then the expected costs are very likely to increase as well. This will result from the need to steer conventional generation investments towards more flexible generators with higher operating costs that can cover for the inherent RES variability [14]. A first attempt to evaluate the installation location of RES through a set of indices is given in [26].

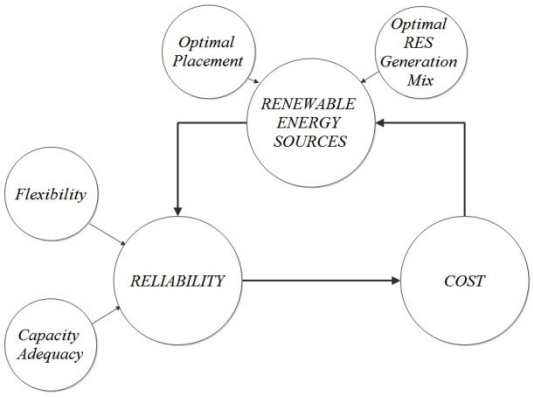

Fig. 2. Current power system planning approach.

The approach in Fig. 2 focuses its attention on three very important aspects of RES integration, namely average load level penetration (i.e. RES energy penetration), capacity contribution and flexibility requirements. Nevertheless, in order to fully comprehend the nature of this case study, the special characteristics of RES generation, both wind and solar, should be addressed.

One should note that RES generation is not controllable. Therefore, it is considered as a non-dispatchable generation source[3]. Moreover, it is evident that its correlation and relative coincidence with the demand is of crucial importance. These will define the potential energy and capacity benefits as well as the needs for flexibility provision. The relative coincidence of demand and RES generation can be macroscopically captured by calculating the correlation between them.

The correlation coefficient is a single number that describes the degree of linear relationship between two variables. If its value is close to ±1, then there exists a strong linear relationship between the two variables (positive or negative). If its value is close to zero, then there is no such relationship. Therefore, by utilizing available historical demand and RES generation daily patterns for each month of the year, their correlation coefficients can be calculated. The respective correlation coefficients between demand, wind and PV generation are shown in Table VI.

It is shown that PV generation has a positive correlation with the demand, especially during the summer months when the peak load takes place during the day (as opposed to winter months when it takes place in the evening).

On the other hand, wind generation presents diverse correlations with the demand. This indicates a relative difficulty to match wind generation with the demand thus implying an additional need for conventional generators cycling (through spinning reserve).

Moreover, the correlation between wind and PV generation is negative through most of the year. This fact can be seen as encouraging since the two technologies can act as a complement to each other thus reducing the overall need for flexibility options.

TABLE VI
CORRELATION COEFFICIENTS BETWEEN THE DEMAND, WIND AND PV GENERATION PROFILES

	Demand/Wind	Demand/PV	Wind/PV
Jan	0,1756	0,2039	0,6913
Feb	0,3992	0,2460	0,6283
Mar	-0,5009	0,3596	-0,2676
Apr	-0,1524	0,5088	-0,6364
May	0,6010	0,5970	0,5951
Jun	0,1134	0,6616	-0,4057
Jul	-0,4150	0,6550	-0,6572
Aug	-0,1240	0,5557	-0,6196
Sep	0,0917	0,6205	-0,5177
Oct	-0,4822	0,5173	-0,7214
Nov	0,5838	0,4181	0,2939
Dec	0,0899	0,1964	-0,3367

Fig. 3 shows the wind generation distribution for Cyprus for the year 2012 while Fig. 4 illustrates the PV generation distribution. It is shown that the wind potential in Cyprus is rather limited (approximately 90% of the time the wind generation is less than 40% of its rated capacity). This leads to a rather low capacity factor which in conjunction with the negative correlation with demand leads to a very low capacity contribution.

[3] This term is used interchangeably with the term *negative load*.

Nevertheless, this is not the case for PV generation. Although PVs are not generating during the night (that is why 55% of the time the generation level is zero), they present a positive correlation with the demand. Also, their generation pattern is more predictable since they closely follow the solar irradiation profile.

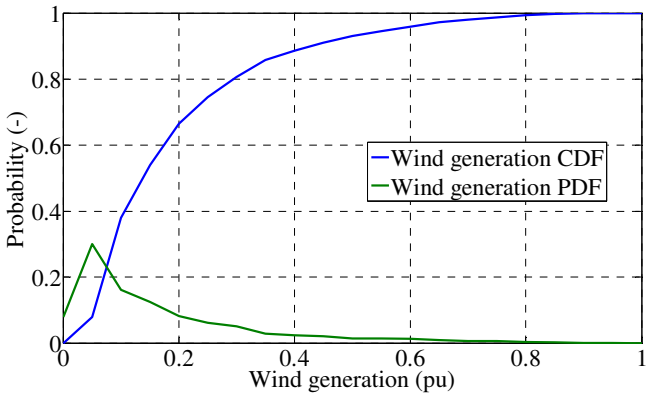

Fig. 3. Wind generation distribution (PDF and CDF) for Cyprus in 2012.

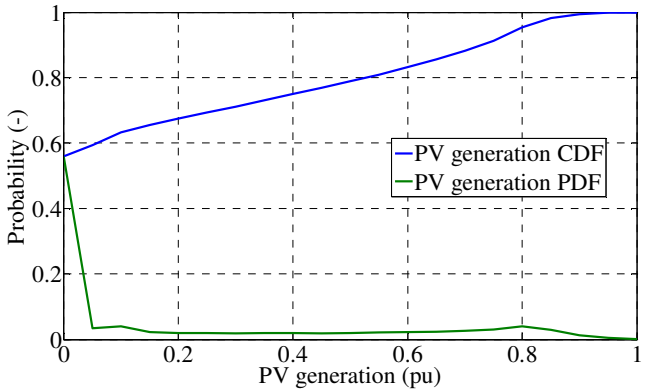

Fig. 4. PV generation distribution (PDF and CDF) for Cyprus.

In the next subsections a set of indicative results is provided for an aggregate RES penetration of 500 MW. This exercise is performed in order to investigate the effect on the three aspects stated above, namely average load level penetration, capacity contribution and flexibility requirements. It is noted that the proposed 500 MW RES penetration may exceed the requirements of the EU directive (provided that the targets of biomass and CSP penetration remain unchanged and will be fully implemented). This is due to the financial recession that currently takes place in Cyprus and has caused a rapid decrease in the electricity demand [24].

1) Average load level penetration

In Fig. 5 the monthly average load level penetration for different aggregate RES mixes is presented while the annual average load level penetration is shown in Fig. 6. The two graphs show that, as PV penetration increases, the average load level penetration increases as well. This proves that even though PVs are not generating during the night, this does not mean they cannot provide a substantial share of the energy demand - bearing in mind that the demand is low during nights.

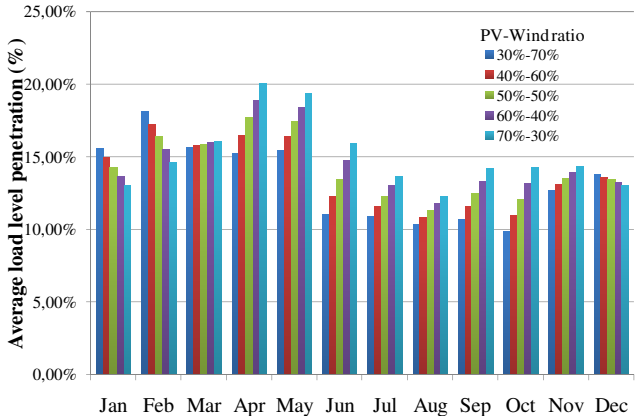

Fig. 5. Monthly average load level penetration for different aggregate RES mixes.

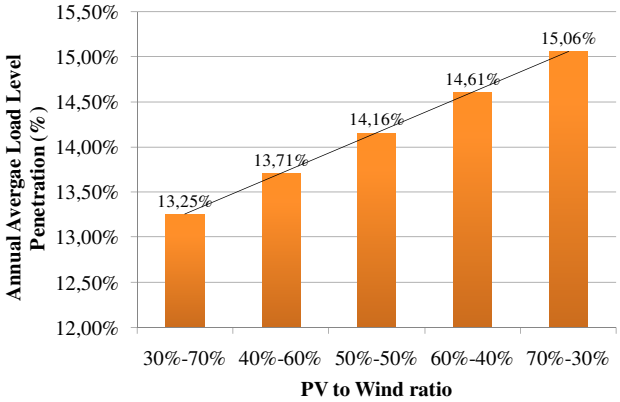

Fig. 6. Annual average load level penetration for different aggregate RES mixes.

2) Capacity contribution

Fig. 7 presents the aggregate RES capacity contribution by utilizing the LDMC method that also accounts for the relative RES penetration level (in this case study, this level is approximately *p=40%*). It is clear that PV generation provides a larger contribution in the capacity adequacy of the system as a result of its positive correlation with the system's peak demand.

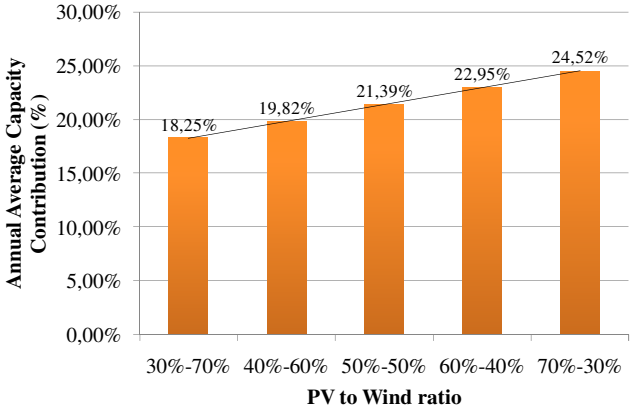

Fig. 7. Annual average capacity contribution for different aggregate RES mixes.

3) Flexibility requirements

By utilizing historical, real-measured per unit patterns for the demand, wind and PV generation of the Cypriot system and by scaling them according to their forecasted values in the future, a simulation of the future system state can be achieved. This provides key indications concerning both expected and unexpected real-time fluctuations for each

scenario of aggregate RES mix that will have to be addressed through the system's flexibility options.

It should be noted that the average values of these fluctuations cannot be utilized for the day-to-day operational decisions. However, they provide an indication as to which scenario requires less flexibility. Thus, the planners can include flexibility options in the system's studies by comparing each proposed scenario at the planning stage and determine which scenario of aggregate RES mix is more suitable for the system specifics.

In Fig. 8 the comparative results for different scenarios of aggregate RES generation mix and the aggregate RES mix scenario that is proposed in the Cyprus NAP (40%-60% PV to wind ratio) are shown. It is shown that the output of each scenario is relatively similar to each other. This is because the correlation between PV and wind generation is negative through most of the year. However, as PV penetration gets larger (e.g. 70%) there would be a reduction (4.25%) in flexibility requirements when compared to the proposed 40%PV-60% wind current plan. The net cost effect of this reduction will be quantified, as part of our future work.

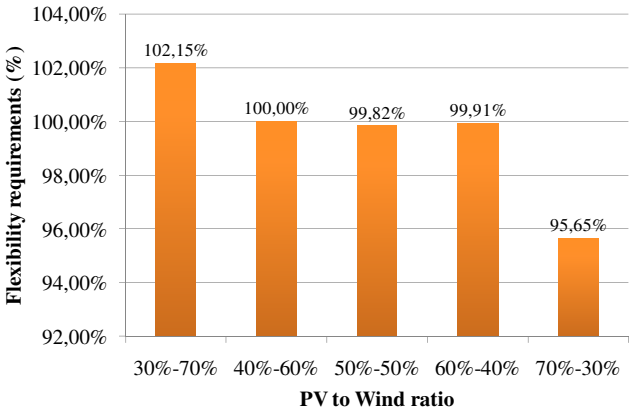

Fig. 8. Flexibility requirements for different aggregate RES mixes compared to the aggregate RES mix proposed in the Cyprus NAP. (40%-60% PV to wind ratio).

V. Recommendations

In this work some of the planning challenges for maximizing RES penetration in existing power systems have been addressed. A case study for the isolated system of Cyprus has also been performed in an effort to raise awareness and briefly address some of the major technical issues that concern RES integration. The associated remarks and recommendations are as follows:

i. Integrating large shares of intermittent RES generation in Cyprus is limited by the lack of interconnections and/or large-scale storage. This proves the eminent need to include flexibility option studies during the planning stages in order to ensure that the system's capabilities will meet the system's requirements.

ii. PV generation is undoubtedly well-suited for Cyprus due to its positive correlation with the demand patterns, especially during the high demand periods.

iii. Wind generation does not present a steady relationship with the demand thus making its associated integration more difficult than PV generation. However, due to Cyprus' relatively low wind potential, wind generation levels remain low in most of the time. This can be more easily controllable. Of course, the negative correlation with demand might sometimes translate into high wind generation levels at low demand periods (high wind generation during nights). This jeopardizes the system's stability and may force TSO to curtail some of the generation in order to maintain the system's balance.

iv. Even though wind generation is relatively low during most of the year, its fluctuations require the increase of conventional generators cycling and the procurement of larger shares of spinning reserve at times of high wind speed fluctuations. The associated costs for these services should be alleviated from conventional generators (through an ancillary services market) in order to ensure a fair market competition. It is noted that these costs should not be transferred only to the end-consumers but to the RES producers as well thus making the process rational.

v. It is a fact that PV generation requires large portions of land. This effectively limits the large-scale PV plant installation capability. However, rooftop-PVs could be the answer to the extensive land requirements. Therefore, rooftop-PVs should also be included in the planning stages but as a different category than large-scale PV plants because of several differences; connection voltage levels, distribution network capacity, congestion management and small-scale storage.

vi. Financial incentives such as the feed-in tariffs or net-metering can stimulate RES investments by minimizing the RES producers' revenue risk [9]. However, a common market framework for all kinds of producers should be gradually implemented to increase market efficiency and level out the rules in order to maintain investment interest in all kinds of generation.

vii. The NAP should not act as a binding constraint on the related RES investments but merely act as an indicator to the degree that each RES technology is suitable for the system current and future state. The main difficulty, but first priority, should be to design a solid market framework with clear rules for each participant, either conventional, RES or hybrid. This could be accomplished by introducing well defined capacity remuneration and penalty schemes depending on the services that each producer provides.

VI. Conclusion

This paper has highlighted some of the current challenges arising from the increasing RES penetration in existing, classically designed power systems. It has been established that capacity adequacy studies are no longer sufficient to capture the full effects of intermittent RES penetration. Therefore, the inherent variability of such technologies should be addressed through flexibility adequacy studies to complement the current practices. This will ensure that the system capabilities will not lag the system requirements in the future.

Cyprus is an (electrically) isolated island. This exacerbates the difficulties of integrating large shares of RES generation in the system. However, the NAP should be a result of informed decisions and well-refined actions in order to effectively integrate RES in elastically defined proportions.

VII. References

[1] T. E. Parliament and the Council of the European Union, "Directive 2009/28/EC of the European parliament and of the council on the promotion of the use of energy from renewable sources and amending and subsequently repealing directives 2001/77/EC and_2003/30/EC," *Official Journal of the European Union*, vol. L140, pp. 17-62, 2009.

[2] Cyprus Energy Regulatory Authority. "A strategic plan for the promotion of renewable energy sources in the Cyprus electricity generation system: Update for PV systems early deployment" Tech. Rep. September 2011.

[3] H. Seifi and M. S. Sepasian, *Electric Power System Planning: Issues, Algorithms and Solutions.* Springer, 2011.

[4] R. Billinton and R. N. Allan, *Reliability evaluation of power systems*. Vol. 2. New York: Plenum Press, 1984.

[5] M. Cepin, *Assessment of Power System Reliability: Methods and Applications.* Springer-Verlag London Limited, 2011.

[6] G. R. Pudaruth and F. Li, "Capacity credit evaluation: A literature review," in *Proc. Third International Conference on Electric Utility Deregulation and Restructuring and Power Technologies, 2008.* pp. 2719-2724.

[7] T. Hoff, R. Perez, J. Ross, and M. Taylor, "Photovoltaic capacity valuation methods," Solar Electric Power Association, Tech. Rep., 2008.

[8] S. Stoft, *Power System Economics: Designing Markets for Electricity*, S. V. Kartalopoulos, Ed. John Wiley & Sons, Inc., 2002.

[9] L.J. De Vries, "Generation adequacy: Helping the market do its job," *Utilities Policy, Elsevier*, vol. 15(1), pp. 20-35, 2007.

[10] J. Ma, V. Silva, R. Belhomme, D.S. Kirschen and L.F. Ochoa, "Exploring the use of flexibility indices in low carbon power systems," in *Proc. 3rd IEEE PES International Conference and Exhibition on Innovative Smart Grid Technologies (ISGT Europe), 2012*, pp.1-5.

[11] E. Lannoye, D. Flynn and M. O'Malley, "The role of power system flexibility in generation planning," in *Proc. IEEE Power and Energy Society General Meeting, 2011*, pp.1-6, 2011.

[12] E. Lannoye, D. Flynn and M. O'Malley, "Evaluation of Power System Flexibility," *IEEE Trans. Power Systems,* vol.27, no.2, pp.922-931, 2012.

[13] Transmission System Operator of Cyprus. "Transmission and Distribution rules, version 3.0.2" Tech. Rep. October 2012. [Online] Available: http://www.dsm.org.cy/media/attachments/Transmission%20and%20Distribution%20Rules/KMD_3_0_2_-_October_2012.pdf

[14] S.T. Lee and Z.A. Yamayee, "Load-Following and Spinning-Reserve Penalties for Intermittent Generation," *IEEE Trans. Power Apparatus and Systems,* vol. PAS-100, no.3, pp.1203-1211, 1981.

[15] Y. Rebours and D.S. Kirschen, "What is spinning reserve?" The University of Manchester, Tech. Rep., 2005.

[16] M.A. Ortega-Vazquez and D.S. Kirschen, "Optimizing the Spinning Reserve Requirements Using a Cost/Benefit Analysis," *IEEE Trans. Power Systems,* vol. 22, no.1, pp.24-33, 2007.

[17] F. Bouffard and F.D. Galiana, "Stochastic Security for Operations Planning with Significant Wind Power Generation," *IEEE Trans. Power Systems*, vol.23, no.2, pp.306-316, 2008.

[18] M.A. Ortega-Vazquez and D.S. Kirschen, "Estimating the spinning reserve requirements in systems with significant wind power generation penetration," *IEEE Trans. Power Systems,* vol.24, no.1, pp.114-124, Feb. 2009.

[19] N. Troy, E. Denny and M. O'Malley, "Base-load cycling on a system with significant wind penetration," *IEEE Trans. Power Systems,* vol. 25, no. 2, pp. 1088–1097, 2010.

[20] J. Restrepo and F. Galiana, "Secondary reserve dispatch accounting for wind power randomness and spillage," *in Proc. Power Engineering Society General Meeting,* 2007. *IEEE*, pp. 1–3.

[21] K. D. Vos, A. G. Petoussis, J. Driesen, and R. Belmans, "Revision of reserve requirements following wind power integration in island power systems," *Renewable Energy*, vol. 50, pp. 268 – 279, 2013.

[22] L.J. De Vries, "Mandatory long-term contracts for renewable energy: The best of both worlds?," in *Proc. 8th International Conference on the European Energy Market (EEM), 2011,* pp.586-591.

[23] I. Ciornei and E. Kyriakides, "Impact of variable generation on the dispatch operation in isolated power systems," *International Journal of Electrical and Electronics Engineering*, vol. 6, no.1-4, pp. 66-73, 2012.

[24] Transmission System Operator of Cyprus. [Online] Available: www.dsm.org.cy

[25] National action plan for renewable energy sources based on the directive 2009/28/EC. Republic of Cyprus, Ministry of Commerce, Industry and Tourism. [Online]. Available: ec.europa.eu/energy/renewables/

[26] A.I. Nikolaidis, F.M. Gonzalez-Longatt, and C.A. Charalambous, "Indices to Assess the Integration of Renewable Energy Resources on Transmission Systems," *Conference Papers in Energy*, vol. 2013, Article ID 324562, 8 pages, 2013. [Online]. Available: http://www.hindawi.com/cpis/energy/2013/324562/

VIII. BIOGRAPHIES

Alexandros I. Nikolaidis was born in Ptolemaida, Greece in 1986. He received his Diploma in Electrical & Computer Engineering from the Democritus University of Thrace, Greece, in 2010 and his MSc degree in Energy Technologies and Sustainable Design from the University of Cyprus in 2012. He is currently pursuing his PhD degree at the University of Cyprus. His main research interests include power system planning and operation, power system reliability and renewable energy sources integration.

Charalambos A. Charalambous was born in Nicosia, Cyprus in 1979. He received a Class I BEng (Hons) degree in Electrical & Electronic Engineering in 2002 and a PhD in Electrical Power Engineering in 2005 from UMIST, UK (The University of Manchester). Currently, he is an Assistant Professor, in the Department of Electrical and Computer Engineering, at the University of Cyprus. He was formerly with the National Grid High Voltage Research Center at the University of Manchester, UK. His research interests include transformer finite element modeling, Ferroresonance transient studies, the electrical control and analysis of DC corrosion and the dynamic - life cycle - evaluations of power system operation and losses.

2nd Conference on Power Options for the Eastern Mediterranean Region
07-08 October 2013, Nicosia, Cyprus (Paper No. POEM13/159)

Operation of Wind Energy Conversion Systems with Doubly-Fed Induction Generators During Asymmetrical Voltage Dips

Pavlos Tourou and Constantinos Sourkounis

***Abstract*-- Asymmetrical voltage conditions in the grid can have significant negative effects on the performance of wind energy conversion systems (WECS) equipped with doubly-fed induction generators (DFIG). Transient peaks as well as steady-state second-order and higher frequency harmonics are introduced in the active and reactive output powers, in the Dc-link voltage and in the toque produced by the WECS. These effects can decrease the lifetime of the system and in extreme cases the can lead to violation of the grid code requirements as the system will not be able to ride-through the fault. Therefore protective measures must be taken so that the WECS remains connected to the grid and fulfills the (low voltage ride-through (LVRT) requirements, without putting the reliability of the system at risk. In this paper the dynamic behavior of the DFIG-based WEC in the case asymmetrical voltage dips is analyzed. A control strategy is presented, which minimizes the negative effects of the voltage dips on the WECS and enables it to 'ride-through' the fault safely. With this strategy the WEC can support the voltage recovery during and after the fault and it can fulfill the relevant grid code requirements.**

***Index Terms*—wind energy, doubly-fed induction generator, DFIG, asymmetrical faults, low voltage ride through, reactive power, voltage support, wind power integration.**

I. Nomenclature

$\overrightarrow{v_s}, \overrightarrow{v_r}$ - stator and rotor voltage vectors

$\overrightarrow{e_r}, \overrightarrow{e_r}^r$ - induced rotor emf in the static and rotor reference frames respectively

$\overrightarrow{\imath_s}, \overrightarrow{\imath_r}$ - stator and rotor currents vectors

$\overrightarrow{\psi_s}, \overrightarrow{\psi_r}$ - stator and rotor flux (or flux linkage) vectors

R_s, R_r - stator and rotor resistances

ω - rotating speed of the arbitrary reference frame

ω_r - rotor electrical angular speed

L_m - magnetizing inductance

L_s, L_r - stator and rotor self-inductances

J - moment of inertia of the rotor

p - number of pole pairs in the generator

T_m - mechanical torque applied at the generator shaft

T_e - electromechanical torque of the generator

PavlosTourou and Constantinos Sourkounis and are with the Enesys Institute for Power System Technology and Power Mechatronics, Ruhr-University Bochum, Germany (e-mail: tourou@enesys.rub.de, sourkounis@enesys.rub.de).

II. Introduction

WIND energy conversion systems have nowadays become a proven and mature technology. They are currently generating most of the electricity produced by renewable energy sources. In 2011 they have provided about 3.5% of the global electricity demand and this figure is expected to rise to 16% by 2030 under moderate scenarios [1]. As the penetration of wind power and other renewable energy sources in the electrical grids increases, WECS and wind farms are expected to behave more like conventional power plants by fulfilling stricter grid code requirements. One of the most important requirements for the grid stability in the case of grid faults is the low voltage ride through (LVRT), by which the WECS must remain in operation during symmetrical and asymmetrical voltage dips and they must support the voltage recovery by supplying reactive current[2].

The LVRT requirement is particularly challenging for WECS with doubly-fed induction generators (DFIG). Most of the WECS in the Megawatt range installed around the world are DFIG-based, currently occupying close to 50% of the wind energy market. Their popularity is mainly due to the partial rating of the power electronic converters (about 30% of the nominal power), which allows for a variable speed range that is sufficient for maximum power conversion, while the investment costs are significantly lower compared to WECS with fully-rated power electronic converters.

As the stator terminals of the DFIG are connected directly or through a transformer to the grid, significant disturbances in the grid voltage induce very high electromotive forces and currents in the rotor circuit which can damage the power electronic converters if the system remains connected to the grid. In the case of asymmetrical grid voltages, the rotor-side converter can saturate and significant power and torque oscillations can arise. Therefore protective measures must be taken so that the WECS remains connected to the grid and fulfills the LVRT requirements, without putting the power electronic converters at risk. In this paper a detail analysis of the dynamic behavior of the DFIG-based WEC in the case of asymmetrical voltage dips is provided. A control strategy is presented, which minimizes the negative effects of the voltage dips on the WECS and enables it to 'ride-through' the fault safely. With this strategy the WEC can support the

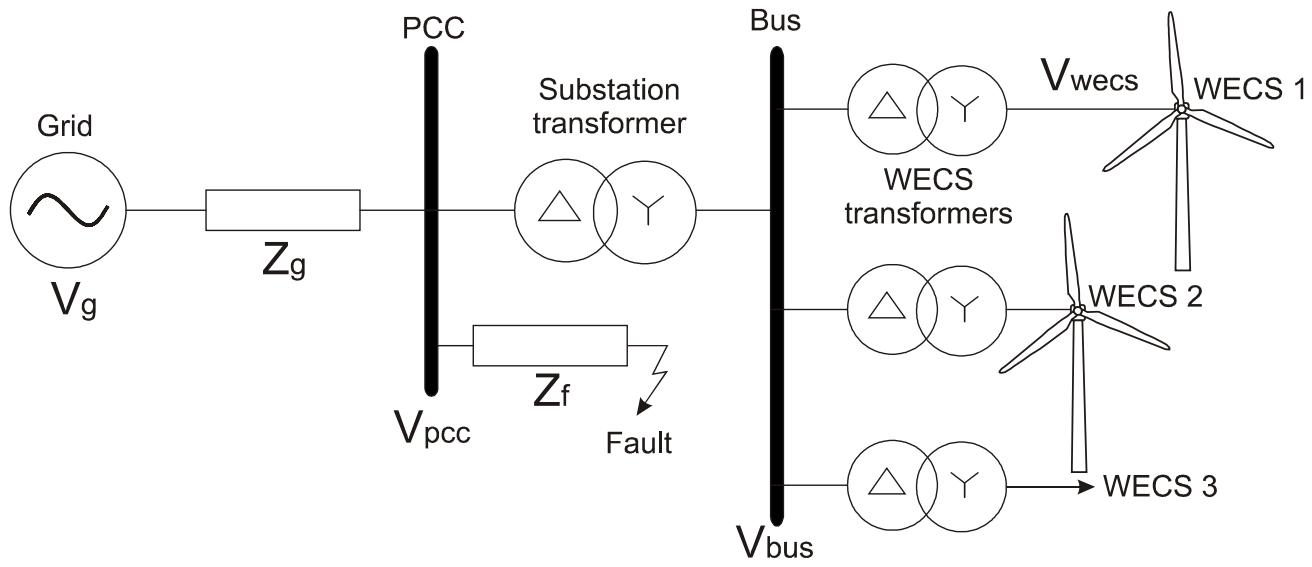

Figure 1: Typical wind farm configuration

voltage recovery during and after the fault and it can meet the demanding grid code requirements of the LVRT.

III. Asymmetrical voltage dips

The main cause of voltage dips experienced by wind farms is due to short-circuits and earth faults in the grid. These types of voltage dips have a short duration, usually in the ms range, and they last until circuit breakers disconnect the faulted lines. Other causes of less severe dips but with possibly longer duration include load faults, motor starting, energizing of transformers and capacitors which may occur nearby the wind farm. Four different types of faults that can occur in a three-phase power system:

- Single-phase-to-ground (1φ)
- Phase-to-phase (φφ)
- Two-phase-to-ground (2φ)
- Three-phase-to-ground (3φ)

Fault types 1φ, 2φ and φφ result in 'asymmetrical' (also called 'unbalanced') voltage dips, where the voltage magnitude of the three phases is not the same. In asymmetrical dips the phase difference in can also be different from 120° as it is the case during normal operation. Furthermore the voltage dip, as seen by the WECS, can be influenced by the configuration of the wind farm and the way it is connected to the grid.

IV. Wind farm configuration and propagation of asymmetrical dips

In the case of asymmetrical voltage dips in the grid, the actual voltage seen by the WECS will depend on the wind farm configuration. In most cases a step-up WECS transformer is used to increase the low-voltage of the WECS to the medium-voltage level. In large wind farms the voltage can be further stepped-up to the distribution voltage level through a substation transformer before it is connected to the point of common coupling (PCC), as shown in Figure 1.

The magnitude and phase of the voltages at the PCC are determined by the source impedance Z_g of the grid and the impedance Z_f between the PCC and the fault location. Referring to Figure1 the resulting complex voltage is:

$$V_{PCC} = V_g \frac{Z_f}{Z_g + Z_f} \quad (1)$$

Where V_g is the grid voltage, V_{PCC} is the PCC voltage, Z_g is the source impedance and Z_f is the fault impedance.

As the distance between the fault location and the PCC increases, the severity of the voltage dip will decrease. If the fault is symmetrical, the voltage dip experienced at the PCC will propagate largely unaffected thought to the terminals of each WECS, influenced only by the impedance of the interconnecting lines.

The situation is quite different In the case of asymmetrical dips. The actual magnitudes and phases of the 3-phase voltages at the terminals of the WECS (V_{wecs}) can be very different from the corresponding magnitudes and phases of the voltages at the PCC. They will not only depend on the type of asymmetrical voltage at the PCC but also on the winding connections of the transformers, as well as on the winding connection of the stator [3]. (table with phasor equations)The stator of the DFIG is normally ungrounded. In this case a zero-sequence voltage will reach the terminal of the DFIG only if there is no substation transformer and a YGyg transformer (star-star connection with both star points grounded) is used for the WECS tranformer. All other possible types of WECS transformers will block the zero-sequence and only positive-sequence and negative-sequence voltages propagate to the terminals of the WECS. A common type of WECS transformer used in commercial wind power systems is Dy [4]. Even if a YGyg is used the zero-sequence will reach the terminals of the WECS only if the substation transformer is also of type YGyg [5]. Consequently, in the subsequent studies it is assumed that the WECS experienced only positive-sequence and negative-sequence voltages in all cases of asymmetrical grid faults.

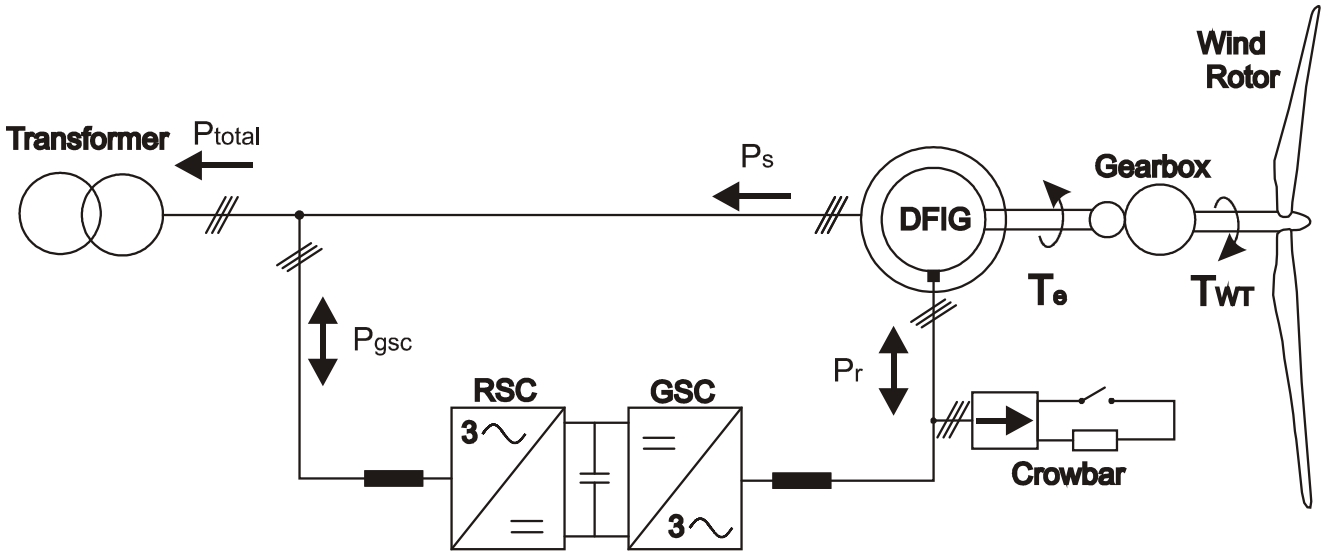

Figure 2: Wind energy conversion system with a doubly-fed induction generator and crowbar circuit

V. Description of the DFIG-based WECS

The doubly-fed induction generators are currently the most widely used type of electrical generators for wind turbine systems in the Megawatt range, occupying close to 50% of the wind energy market [6]. The DFIG technology has proven to be an efficient and cost-effective solution for variable speed wind turbines.

The wind rotor is in most cases connected to the rotor shaft of the generator through a gearbox that increases the rotational speed at the generator side as shown in Fig. 2. The stator windings are directly connected to the grid. The rotor windings are connected to the grid through two voltage source converters (VSC) connected back-to-back. Each VSC is usually the common two-level type, consisting of the six insulated gate bipolar transistors (IGBTs) and their respective antiparallel diodes. The rotor-side converter (RSC) is used to apply three-phase voltages at the rotor windings (usually via slip rings) with the appropriate amplitude, phase and frequency, the flow of currents and consequently the active and reactive power at the stator terminals is controlled. Similarly, the grid-side converter (GSC) can control the active and reactive power exchange between the rotor and the grid. The DC-link capacitor acts as an energy buffer between the two converters, smoothing the voltage variations. No additional devices for reactive power compensation or soft-starting are required.

This converter configuration decouples the rotor electrical frequency from the grid frequency, and as a result the rotor can have a variable speed, normally in a range ±30% around the synchronous speed. Variable-speed wind turbines can harvest much more energy compared to fixed-speed wind turbines because depending on the wind speed, they can operate at the optimum rotational speed at which the aerodynamic efficiency of the wind rotor is maximum [7], [8].

During normal operation the stator power flows from the stator to the grid, while the flow of rotor power over the DC-link is bidirectional; power flows from the grid to the rotor at under-synchronous speeds and in the opposite direction at over-synchronous speeds. The maximum rotor power depends on the slip, and since the rotational speed range is limited, the rotor power is only a fraction of the stator power. This allows significant cost savings as the power electronic converters can be partially rated to only 25-30% of the total power of the generator. Furthermore the power efficiency of the system is higher because there are lower switching and conduction losses in the partially rated back-to-back converter.

The active power flow during normal operation is displayed by the arrows in Figure 2. The stator power flows from the stator to the WECS transformer. The rotor power direction depends on the generator speed. During under-synchronous speeds the rotor absorbs active power, while during over-synchronous speeds it transfers active power to the WECS transformer through the back-to-back converter. A crowbar circuit is usually connected to the rotor. Its purpose is to protect the power electronic switches of RSC in the case of severe grid faults by choking any transient over-currents into its power resistor.

The maximum rotor power depends on the slip, and since the rotational speed range is limited, the rotor power is only a fraction of the stator power. This allows significant cost savings as the power electronic converters can be partially rated to only 25%–30% of the total power of the generator. Furthermore, the power efficiency is higher because there are lower switching and conduction losses in the converters because the power electronic components block and conduct lower voltages and currents.

VI. Modeling of the DFIG

A. Normal operation

The DFIG is modeled in a static reference frame using the following dynamic equations:

$$\overrightarrow{v_s} = R_s\overrightarrow{i_s} + \frac{d}{dt}\overrightarrow{\psi_s} \tag{2}$$

$$\overrightarrow{v_r} = R_r\overrightarrow{i_r} + \frac{d}{dt}\overrightarrow{\psi_r} + j\omega_r\overrightarrow{\psi_s} \tag{3}$$

The stator and rotor flux vectors can be expressed in terms of the stator and rotor current vectors and the magnetizing and leakage inductances:

$$\overrightarrow{\psi_s} = L_s\overrightarrow{i_s} + L_m\overrightarrow{i_r} \quad (4)$$

$$\overrightarrow{\psi_r} = L_r\overrightarrow{i_r} + L_m\overrightarrow{i_s} \quad (5)$$

In the above equations all the rotor quantities are referred to the stator based on the stator-to-rotor turns ratio. The rotor mechanical speed can be described dynamically in terms of the external mechanical torque (e.g. from the wind rotor) and the electromechanical torque using the equation of motion:

$$J\frac{d}{dt}\omega_m = T_e - T_m \quad (6)$$

$$T_e = 1.5 \cdot p \cdot Re\{j\overrightarrow{\psi_s}.\overrightarrow{i_s}\} = -1.5 \cdot p \cdot Re\{j\overrightarrow{\psi_r}.\overrightarrow{i_r}\} \quad (7)$$

The rotor flux can be written in terms of the stator flux and rotor current using (4) and (5)

$$\overrightarrow{\psi_r} = \frac{L_m}{L_s}\overrightarrow{\psi_s} + \sigma L_r\overrightarrow{i_r} \quad (8)$$

where σ is the leakage factor

$$\sigma = 1 - \frac{{L_m}^2}{L_s L_r} \quad (9)$$

From (3) and (6)

$$\overrightarrow{v_r} = \frac{L_m}{L_s}\left(\frac{d}{dt} - j\omega_r\right)\overrightarrow{\psi_s} + \left(R_s + \sigma L_r\left(\frac{d}{dt} - j\omega_r\right)\right)\overrightarrow{i_r} \quad (10)$$

The rotor voltage consists of the first term that is voltage induced by the variation of stator flux and the second term that is the voltage drop across the rotor resistance and the rotor transient inductance. If the rotor is open-circuited the rotor voltage will be equal to the induced emf.

$$\overrightarrow{e_r} = \frac{L_m}{L_s}\left(\frac{d}{dt} - j\omega_r\right)\overrightarrow{\psi_s} \quad (11)$$

The induced emf. depends only on the variation of the stator flux. In the case of a grid-connected DFIF the stator flux variation is imposed by the grid voltage. Therefore any change in the grid-voltage will affect the stator flux and consequently the induced emf in the rotor voltage will be affected.

At normal operation

$$\overrightarrow{v_s} = Ve^{j\omega_s t} \quad (12)$$

If the stator resistance is ignored the stator flux space vector is

$$\overrightarrow{\psi_s} = V\frac{V}{j\omega_s}e^{j\omega_s t} \quad (13)$$

B. Behavior under dips in the grid voltage

During asymmetrical voltage conditions the stator voltage will contain both positive and negative sequence components

$$\overrightarrow{v_s} = V_1 e^{j\omega_s t} + V_2 e^{-j\omega_s t} = \overrightarrow{v_{s1}} + \overrightarrow{v_{s2}} \quad (14)$$

During steady-state the "forced" stator flux will be made of two components corresponding to the positive and negative sequences of the stator voltage. Although the voltage can change instantaneously at the start and end of the dip, the stator flux is a continuous variable and an abrupt decrease in the flux is not physically possible. If the total stator flux immediately after the fault is not equal to the stator flux immediately before the fault, then a transient flux exists, called "natural" flux. The initial value of this transient flux depends on the type and timing of the fault, while the decay rate is depended on the transient time constant of the stator (in the rotor open-circuit case). Therefore the total stator flux is made of two steady-state and one transient component.

$$\overrightarrow{\psi_s} = \overrightarrow{\psi_{s1}} = \overrightarrow{\psi_{s1}} + \overrightarrow{\psi_{s2}} + \overrightarrow{\psi_{sn}}$$

$$= \frac{V_1}{j\omega_s}e^{j\omega_s t} + \frac{V_2}{-j\omega_s}e^{-j\omega_s t} + \psi_{sn}.e^{-t/\tau_s} \quad (15)$$

Similarly, the total emf induced by the variation of stator flux in in the rotor terminals can be calculated:

$$\overrightarrow{e_r} = \overrightarrow{e_{r1}} + \overrightarrow{e_{r2}} + \overrightarrow{e_{rn}}$$

$$= \frac{L_m}{L_s}V_1.s.e^{j\omega_s t} + \frac{L_m}{L_s}V_2.(s-2).e^{-j\omega_s t}$$

$$= \frac{L_m}{L_s}\left(\frac{1}{\tau_s} + j\omega_r\right)\psi_{sn}.e^{-t/\tau_s} \quad (16)$$

In the rotor reference frame the induced emf is

$$\overrightarrow{e_r}^r = \frac{L_m}{L_s}V_1.s.e^{js\omega_s t} + \frac{L_m}{L_s}V_2.(s-2).e^{-j(s-2)\omega_s t}$$

$$-\frac{L_m}{L_s}\left(\frac{1}{\tau_s} + j\omega_r\right)\psi_{sn}.e^{-\left(\frac{1}{\tau_s} + j\omega_r\right)t} \quad (17)$$

The first term of the equation rotates with slip frequency and it is proportional to the positive sequence voltage and to the slip. This voltage is also present during normal operation. The RSC is normally designed so that it can produce voltages large enough to counteract this emf and to regulate the rotor currents. The third term is a transient emf that appears at the start and end of the dip and it can occur in both symmetrical and asymmetrical dips. The second term appears only in the presences of asymmetrical voltage. It is proportional to the negative sequence voltage and to (s-2). At severe unbalance this emf can be larger than the rated RSC voltage, leading to loss of current regulation.

C. Calculation of powers and torque

The apparent power at the stator is given by

$$\overrightarrow{S_s} = 1.5 \cdot \overrightarrow{v_s}\overrightarrow{i_s}^* = P_s + jQ_s \quad (18)$$

The active and reactive powers are given by

$$P_s = 1.5\left[P_{so} + P_{s,cos}\cos(2\omega_s t) + P_{s,sin}\sin(2\omega_s t)\right] \quad (19)$$

$$Q_s = 1.5\left[Q_{so} + Q_{s,cos}\, cos(2\omega_s t) + Q_{s,sin}\, sin(2\omega_s t)\right] \quad (20)$$

The components of the powers expressed in positive and negative rotating reference frames are

$$\begin{bmatrix} P_{so} \\ P_{s,cos} \\ P_{s,sin} \\ Q_{so} \\ Q_{s,cos} \\ Q_{s,sin} \end{bmatrix} = \begin{bmatrix} v_{sd}^{+} & v_{sq}^{+} & v_{sd}^{-} & v_{sq}^{-} \\ v_{sd}^{-} & v_{sq}^{-} & v_{sd}^{+} & v_{sq}^{+} \\ v_{sq}^{-} & -v_{sd}^{-} & -v_{sq}^{+} & v_{sd}^{+} \\ v_{sq}^{+} & -v_{sd}^{+} & v_{sq}^{-} & -v_{sd}^{+} \\ -v_{sd}^{-} & -v_{sq}^{-} & v_{sd}^{+} & v_{sq}^{+} \end{bmatrix} \cdot \begin{bmatrix} i_{sd}^{+} \\ i_{sq}^{+} \\ i_{sd}^{-} \\ i_{sq}^{-} \end{bmatrix} \quad (21)$$

Similarly the electromagnetic toque is given by

$$T_e = 1.5p\left[T_{eo} + T_{e,cos}\, cos(2\omega_s t) + T_{e,sin}\, sin(2\omega_s t)\right] \quad (22)$$

$$\begin{bmatrix} T_{eo} \\ T_{e,\cos} \\ T_{e,\sin} \end{bmatrix} = \frac{L_m}{L_s} \begin{bmatrix} -\psi_{sq}^{+} & \psi_{sd}^{+} & -\psi_{sq}^{-} & \psi_{sd}^{-} \\ \psi_{sd}^{-} & \psi_{sq}^{-} & -\psi_{sd}^{+} & \psi_{sq}^{+} \\ -\psi_{sq}^{-} & \psi_{sd}^{-} & -\psi_{sq}^{+} & \psi_{sd}^{+} \end{bmatrix} \cdot \begin{bmatrix} i_{sd}^{+} \\ i_{sq}^{+} \\ i_{sd}^{-} \\ i_{sq}^{-} \end{bmatrix} \quad (23)$$

VII. CONTROL SYSTEM

The proposed system is designed so that the rotor-side converter can control independently the active and reactive components of both the positive and negative sequence rotor currents. In this way different control targets can be implemented in order to remain connected to the grid during asymmetrical faults while minimizing at the same time the negative effects which the grid voltage unbalance has on the wind turbine system. The grid-side converter can be control to supply reactive current if it is required by the Grid Codes. As a result the wind turbine can safely ride through asymmetrical faults and it can fulfill the relevant Grid Code requirements.

A. Rotor-side converter control

The RSC control system is designed to control the positive and negative sequences of the currents in the DFIG. The main control system is show in Figure 3. The sequence extraction and synchronization block extracts the angle of the positive sequence voltage which is used for the vector orientation. It also extracts the positive sequence of the stator voltage indicated by the subscript 1 i.e. V_{sd1} and V_{sq1} and the negative sequence of the stator voltage indicated by the subscript 2 i.e. V_{sd2} and V_{sq2}.

In traditional field-orientated electrical drive applications as well as in many DFIG studies the control system is implemented using a stator flux vector reference frame. In this paper a stator-voltage vector orientation (or grid-flux orientation) is preferred, in which the stator voltage (or the virtual grid flux) is aligned with the direct axis. This type of orientation exhibits a better current-loop stability and damping compared to the stator-flux vector orientation [9]. Furthermore the need for stator flux angle estimation is avoided. The angle of the positive sequence stator voltage is obtained using the same synchronization employed for the GSC. It should be noted, that in medium and high power WECS with large generators, the voltage drop across the relatively small stator resistance is negligible and the stator-flux frame is practically aligned to the stator-voltage frame [10],[11], [12].

The extracted voltage sequences are fed to the rotor reference sequence calculation block where the reference rotor sequences are calculated based on the control target.

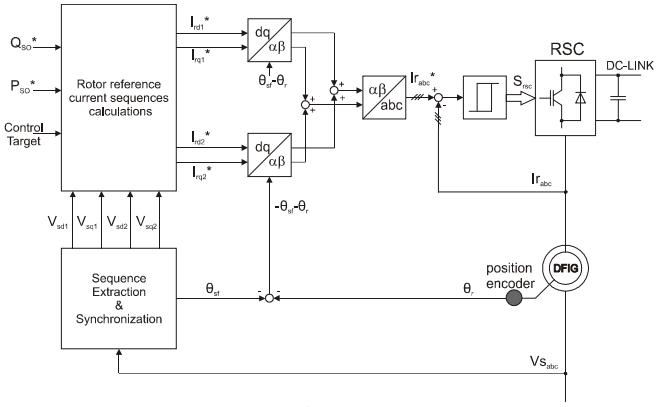

Figure 3: Proposed control system for the rotor-side converter

The positive sequence reference currents I_{sd1} and I_{sq1} are then transformed to the stationary α-β reference frame using the positive stator voltage angle and the rotor angle. Similarly the negative sequence reference currents I_{sd2} and I_{sq2} are transformed to the stationary α-β reference frame using the negative stator voltage angle and the rotor angle. The α and β components are then added together and they are transformed to the abc components using the inverse Clarke transform. The reference abc rotor currents are finally fed to the hysteresis controller. The hysteresis controller compares the reference currents with the measured currents and produces the switching signals for the gates of the rotor-side converter. The hysteresis controller has a very fast transient performance and it can control effectively both positive and negative sequence currents. An advantage of this approach is that only one current controller is required and no additional modulation is needed. Furthermore no extraction of the positive and negative current sequences are required which adds significant delays in the current loop and can make the system unstable.

B. Control targets

As the proposed system can control four components of the rotor currents different control targets can be chosen. The following control targets can be chosen:

1. **Balancing of the stator and rotor currents:** if a low unbalance is present in the grid voltage for a long period then uneven heating in the stator and rotor can be minimized by balancing the respective currents (i.e. when the voltage dip is smaller than the fault definition of the Grid Codes and therefore the wind turbine cannot disconnect from the grid). To achieve this, the negative sequences of the rotor current in equation (21) are both nullified.
2. **Minimization of torque oscillations:** due to the interaction of the positive and negative sequence fluxes in the generator, significant torque oscillations can arise. These oscillations are a strain for the mechanical drive-train of the wind turbine and the gearbox and can be minimized. Oscillations between the generating and motoring operation

must be definitely avoided as they can damage the gearbox i.e. the torque must remain in the same direction despite the oscillations. To minimize the torque oscillations the oscillating components in equation (23) are regulated to zero.

3. **Minimization of the rotor voltage and DC-Link oscillations:** At high grid voltage asymmetry, the negative sequence flux induces a high voltage in the rotor which can saturate the RSC and as a result the current control can be partially lost. This rotor voltage can be minimized up to a certain degree in order to avoid saturation of the RSC and to control effectively the currents.

Only one control target can be implemented at a given time therefore the target should be chosen based on the required performance.

VIII. Investigation Results

In the following simulations the worst-case operating conditions for the wind turbine were tested i.e.:

- over-synchronous speed at maximum slip
- operating at rated active power i.e. Ps=1 p.u.
- the asymmetrical voltage dip occurs at the high-voltage side of the WECS transformer
- instantaneous voltage drop at the start of the fault
- instantaneous voltage increase at the end of the fault

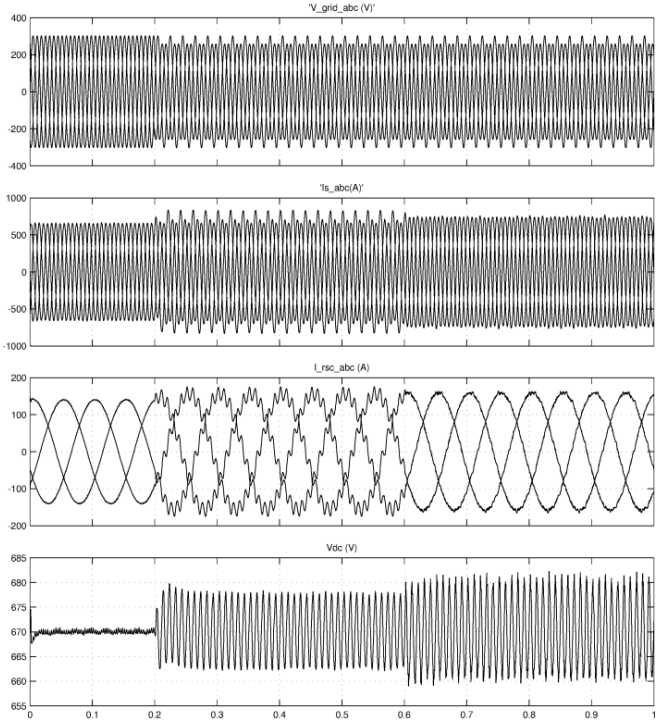

Figure 4: Phase-to-phase dip at t=0.2, Control Target 1 activated at t=0.6

In Figure 4 the conventional system is in operation for the time period t=0-0.6 s. A phase-to-phase dip starts at t=0.2 s. The normal control system cannot regulate the negative current sequences. Small high frequency oscillations at 100 Hz appear in the DC-Link voltage. The negative sequence appears as high frequency oscillations in the rotor currents superimposed on the positive sequence currents. Also the stator currents become unbalanced as the dip begins. At t=0.6 the proposed system is activated with the **Control Target 1.** It is clear from Figure 4 that the control system eliminates the negative sequence oscillations in the rotor current and balances also the stator currents. A side-effect of this method is a slight increase in the DC-Link voltage oscillations. This control target may be useful during small voltage dips e.g. less than 10%. In such case the wind turbine must not disconnect and it may operate under asymmetrical conditions for a long period of time. Using Control Target 1 can limit the unbalanced overheating in the generator.

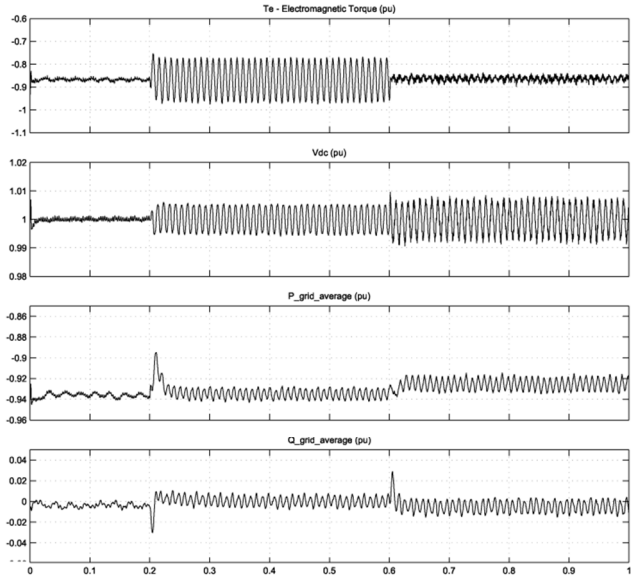

Figure 5: Phase-to-phase dip at t=0.2, Control Target 2 activated at t=0.6

In Figure 5 a similar phase-to-phase dip is considered. At t=0.6 s **Control Target 2** is activated. The system in this case eliminates the torque oscillations down to zero and limits the mechanical stresses on the gearbox and the drive-train of the wind turbine. A side-effect is again an increase in the DC-Link voltage oscillations.

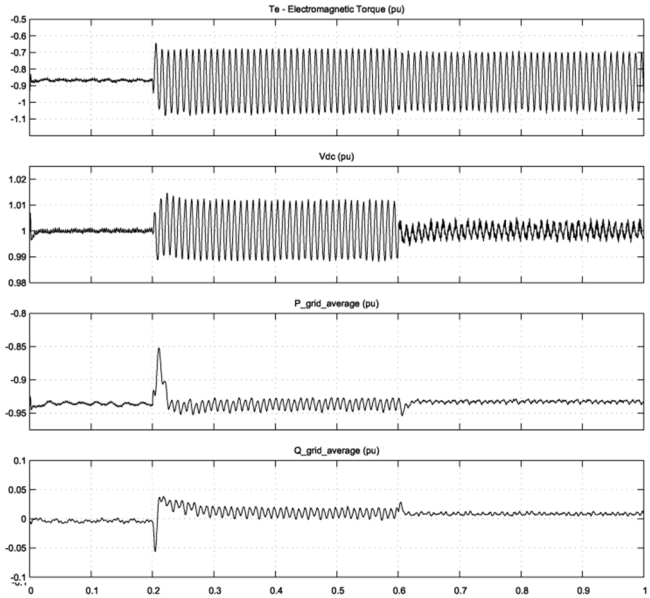

Figure 6: Phase-to-phase dip at t=0.2, Control Target 1 activated at t=0.6

In Figure 6 the effect of activating **Control Target 3** at t=0.6 s is shown. With this target the rotor voltage seen by the RSC is minimized (not shown) and the current sequences in the rotor can be better controlled. As a result the oscillations in the DC-Link voltage are eliminated.

The transient currents at the start and clearance of the asymmetrical voltage dips are lower than the currents observed during three-phase symmetrical dips. The voltage disturbances in the DC-Link are low and they can be completely eliminated by the control system as long as the current capacity of the rotor-side converter is not exceeded As a result the crowbar is not triggered except in extremely asymmetrical dips e.g. > 70%.

IX. Conclusion

Asymmetrical voltage dips in the grid can degrade the performance of WECS with doubly-fed induction generators. A detailed analysis of the DFIG behavior during in the presence of asymmetrical voltages has been carried out. The negative sequence component in the voltage creates a component in the stator flux that rotates in the opposite direction of the normal flux. This introduces double frequency oscillations in the WECS variables which can damage components of the system (e.g. gearbox) and they limit the lifetime of the WECS. The proposed control system can implement different control strategies based on the desired performance of the wind turbine during the asymmetrical voltage dip i.e. to balance rotor and stator currents (Target 1), to limit torque oscillations (Target 2) or to minimize the induced rotor voltage and the DC-link voltage oscillations (Target 3). All the targets can be implemented as long at the induced emf in the rotor is not greater than the maximum voltage that can be imposed by RSC.

X. References

[1] GWEC, “Global wind energy outlook 2012,” 2012.

[2] C. Sourkounis and P. Tourou, “Grid Code Requirements for Wind Power Integration in Europe,” *Conference Papers in Energy*, vol. 2013, pp. 1–9, 2013.

[3] M. H. Bollen, *Understanding power quality problems: Voltage sags and interruptions*. New York: IEEE Press, 2000.

[4] L. Wang, T.-H. Yeh, W.-J. Lee, and Z. Chen, “Analysis of a Commercial Wind Farm in Taiwan Part I: Measurement Results and Simulations,” *IEEE Transactions on Industry Applications*, vol. 47, no. 2, pp. 939–953, Mar. 2011.

[5] E. Muljadi, N. Samaan, V. Gevorgian, J. Li, and S. Pasupulati, “Different Factors Affecting Short Circuit Behavior of a Wind Power Plant,” *IEEE Transactions on Industry Applications*, vol. 49, no. 1, pp. 284–292, Jan. 2013.

[6] M. Liserre, R. Cárdenas, M. Molinas, and J. Rodríguez, “Overview of multi-MW wind turbines and wind parks,” *IEEE Transactions on Industrial Electronics*, vol. 58, no. 4, pp. 1081–1095, 2011.

[7] B. Ni and C. Sourkounis, “Energy yield and power fluctuation of different control methods for wind energy converters,” *IEEE Transactions on Industry Applications*, vol. 47, no. 3, pp. 1480–1486, 2011.

[8] C. Sourkounis and B. Ni, “Influence of Wind-Energy-Converter Control Methods on the Output Frequency Components,” *IEEE Transactions on Industry Applications*, vol. 45, no. 6, pp. 2116–2122, 2009.

[9] A. Petersson, L. Harnefors, and T. Thiringer, “Comparison between stator-flux and grid-flux-oriented rotor current control of doubly-fed induction generators,” in *2004 IEEE 35th Annual Power Electronics Specialists Conference (IEEE Cat. No.04CH37551)*, pp. 482–486.

[10] R. Datta and V. T. Ranganathan, “Decoupled control of active and reactive power for a grid-connected doubly-fed wound rotor induction machine without position sensors,” in *Conference Record of the 1999 IEEE Industry Applications Conference. Thirty-Forth IAS Annual Meeting*, 1999, vol. 4, pp. 2623–2630.

[11] F. Poitiers, T. Bouaouiche, and M. Machmoum, “Advanced control of a doubly-fed induction generator for wind energy conversion,” *Electric Power Systems Research*, vol. 79, no. 7, pp. 1085–1096, Jul. 2009.

[12] F. K. A. Lima, A. Luna, P. Rodriguez, E. H. Watanabe, and F. Blaabjerg, “Rotor Voltage Dynamics in the Doubly Fed Induction Generator During Grid Faults,” *IEEE Transactions on Power Electronics*, vol. 25, no. 1, pp. 118–130, Jan. 2010.

XI. Biographies

Pavlos Tourou received his M.Eng. degree in electrical and electronic engineering from the University of Bristol, UK in 2010. Since 2011 he works as a Research Assistant in the Institute of Power Systems Technology and Power Mechatronics at Ruhr University Bochum, Germany. His research interests include control and grid integration of renewable energy systems.

Constantinos Sourkounis received the Dipl.-Ing. and Dr.-Ing. degrees from the Technische Universität (TU) Clausthal, Clausthal-Zellerfeld, Germany, in 1989 and 1994, respectively, and the Habilitation degree from TU Clausthal, Clausthal- Zellerfeld, Germany, in 2003. After he received the Dr.-Ing. degree, he occupied the position of Chief Engineer at TU Clausthal. Since 2003, he has been a Professor at Ruhr-University Bochum, Germany, heading the Power Systems Technology and Power Mechatronics Research Group. His main research areas are mechatronic drive systems, renewable energy sources, decentralized energy systems supplied by renewable energy sources, and energy supply systems for transportation systems.

2nd Conference on Power Options for the Eastern Mediterranean Region
07-08 October 2013, Nicosia, Cyprus (Paper No. POEM13/160)

A software tool to evaluate the total ownership cost of distribution transformers

Antonis L. Lazari and Charalambos A. Charalambous[1]

Abstract-- **The software tool described in this paper reflects on a holistic management approach to accurately appraise the energy and the demand component of the cost of losses for Electricity Authority of Cyprus (E.A.C). The demand (*D* - *€/kW*) and the energy (*E* - *€/kWh*) components are utilised in evaluating the Total Ownership Cost (*T.O.C*) of distribution transformers. Specifically, the tool is used to dynamically evaluate the levelized annual cost of losses of transformers, by incorporating actual financial data and system characteristics through built-in techno-economic models as well as statistical evaluations for future fuel pricing.**

Index Terms-- **Demand Component of Losses, Energy Component of Losses, System and Cost Parameters, Risk Assessment and Forecasting.**

I. Introduction

IN the light of the continuous increase on power system investment and energy costs, the stakeholders are attempting to strike a balance between capital/operating expenditures and systems' losses. It is therefore necessary to elaborate on methodologies that could systematically evaluate the cost of losses encountered in power systems, e.g. in transformers.

The total losses in a transformer are in principle, power losses both no load and load loss. Each type of loss is evaluated on the basis of its demand (*D*) and energy component (*E*). As clearly explained in the IEEE C57.120-1991 [1], the demand component of losses is the cost of installing system capacity expressed in *€/kW* to serve the power used by the losses. The energy component of losses is the present value of the energy that will be used by one kilowatt of loss during the life-cycle of the power plant under study, expressed in *€/kWh*.

To this extent, the demand (*D* - €/kW) and the energy component (*E* - €/kWh) of losses are the prevailing factors in the process of establishing the cost value of the electric power and services needed to supply the life-cycle losses of transformers. The transformers' users can use a loss evaluation method to determine the relative economic benefit of a high-first-cost, low-loss unit versus one with a lower first cost and higher losses. Loss evaluation endeavors can further inform a user regarding the optimum time to retire or replace existing units. They, further, enable a user to determine the total cost of ownership of different units. Finally, they enable utilities to compare the offerings of two or more manufacturers to facilitate the best purchase choice and the relative merits among competing transformers.

The software tool developed is based on a thorough calculation method proposed by the authors [2], [3], for establishing the demand (*D* - €/kW) and the energy component (*E* - €/kWh) of transformer losses at generation, transmission and distribution level. This classification is essential for augmenting the process of establishing the cost value of the electric power needed to supply the life-cycle losses of transformers which may be installed at different kV levels. This paper specifically addresses the application of the method on distribution transformers, through the developed software. The software tool incorporates certain adaptability factors that allow extensive and friendly user intervention. It can be used in Tender Evaluations e.g. for distribution transformer purchases.

II. Brief Description of Method

The needs and the means to reflect on a comprehensive process that derives a complete and sustainable model for evaluating the life-cycle losses of power transformers are detailed in [2] and [3].

In this paper the demand (*D*) and the energy (*E*) costs are categorized and defined as follows:

$\boldsymbol{D_{g\_peak}}$ is the annuitized demand cost per *kW* associated with the generation level related expenses. It is the annual fixed cost required to serve a *kW* of loss occurring at the time of the system's peak demand.

$\boldsymbol{D_{t\_peak}}$ is the annuitized demand cost per *kW* associated with the transmission level related expenses. It is the annual fixed cost required to serve a *kW* of loss occurring at the time of the system's peak demand.

$\boldsymbol{D_{d\_peak}}$ is the annuitized demand cost per *kW* associated with the distribution level related expenses. It is the annual fixed cost required to serve a *kW* of loss occurring at the time of the system's peak demand.

$\boldsymbol{E_{g\_peak}}$ is the annuitized energy cost per *kWh* associated with the generation level related expenses. It is the annuitized variable cost required to serve the energy consumed by the losses occurring at the time of the system's peak demand, over the life cycle of a transformer.

$\boldsymbol{E_{t\_peak}}$ is the annuitized energy cost per *kWh* associated with the transmission level related expenses. It is the annuitized variable cost required to serve the energy consumed by the losses occurring at the time of the system's peak demand, over the life cycle of a transformer.

$\boldsymbol{E_{d\_peak}}$ is the annuitized energy cost per *kWh* associated with the distribution level related expenses. It is the annuitized variable cost required to serve the energy consumed by the losses occurring at the time of the system's

A.L. Lazari and C.A. Charalambous are with the Department of Electrical and Computer Engineering, Faculty of Engineering, of the University of Cyprus, PO Box 20537, 1687, Nicosia, Cyprus (e-mail: alazar01@ucy.ac.cy, cchara@ucy.ac.cy).

peak demand, over the life cycle of a transformer.

The demand and the energy factors are subsequently utilized in the derived formulas [2] for evaluating the total cost of losses (*TCL*) for power transformers (TCL_{pt}) and distribution transformers (TCL_{dt}) as given by (1) and (2) respectively. The nomenclature used, in these equations can be found in Appendix A.

$$TCL_{pt} = \left[D_{p\_Base} + 8760 \cdot AF \cdot E_{p\_Base}\right] \cdot NLL + \left[D_{p\_Peak} \cdot PRFS^2 \cdot PEQO^2\right] \cdot LL + \left[8670 \cdot LLF \cdot E_{p\_Peak} \cdot PEQE^2\right] \cdot LL + \left[D_{p\_Peak} + 8760 \cdot FOW \cdot E_{p\_Peak}\right] \cdot AUX \quad (1)$$

$$TCL_{pt} = \left[D_{dt\_Base} + 8760 \cdot E_{dt\_Base}\right] \cdot NLL + \left[D_{dt\_Peak} \cdot PRFS^2 \cdot PEQO^2\right] \cdot LL + \left[8670 \cdot LLF \cdot E_{dt\_Peak} \cdot PEQE^2\right] \cdot LL \quad (2)$$

The aggregate annuitized cost components for power transformers are given by (3) and (4).

$$D_{p\_Base} = D_{p\_Peak} = D_{g\_Peak} + D_{t\_Peak} \quad (3)$$

$$E_{p\_Base} = E_{p\_Peak} = E_{g\_Peak} + E_{t\_Peak} \quad (4)$$

The aggregate annuitized cost components for distribution transformers are given by (5) and (6). For simplicity, it is assumed that the base generation components are equal to the peak generation components as shown by the referred equations.

$$D_{dt\_Base} = D_{dt\_Peak} = D_{g\_Peak} + D_{t\_Peak} + D_{d\_Peak} \quad (5)$$

$$E_{dt\_Base} = E_{dt\_Peak} = E_{g\_Peak} + E_{t\_Peak} + E_{d\_Peak} \quad (6)$$

Finally, the Total Ownership Cost (*TOC)* of a transformer is defined by the purchase price (*PP*) of the transformer plus the total cost of losses *(TCL)* as illustrated by (7).

$$TOC = PP + TCL \quad (7)$$

A. Allocation of Cost Items to Demand and Energy Components & Size Factors

If losses are seen as a load to the system it is apparent that additional system capacity is required to meet them. Therefore, it is necessary to determine the impact a change in losses would have on future capacity additions, as detailed in [3].

To this extend, the software tool incorporates the suggestion of EPRI Guide [4] which considers that a change in losses will not affect the scheduling of new facilities but may affect their size. The recommendation is that the demand component of losses should be evaluated at the incremental cost of increasing the size of new facilities which is typically two thirds of the average cost; these are termed in the software as "size factors". For the transmission level related cost items the size factor is $SFcc_t$ = 2/3 and for the distribution level relevant costs the size factor is $SFcc_d$ =2/3. For the generation level cost items, the size factor given by (8) is used:

$$SFcc_g = \frac{2}{3} \cdot (1 + RM) \quad (8)$$

Where, *RM* is the reserve margin in per unit of the system available generation capacity.

Moreover, the allocation of any relevant cost items (e.g. operation, repairs and maintenance, etc.) to their demand and energy components is based on weight factors, extracted from historical data [7], [8]. However, the weight factors should be under systematic review using the screening curve approach [2], especially when there is a substantial change in the plant mix and/or system load factor [1].

The procedure of weighting the costs items in their demand and energy components as well as assigning an appropriate size factor, for use in loss evaluation endeavors is shown in Fig. 1. The allocation of the relevant cost items to their equivalent components, for E.A.C specifics, is shown in Table I, Appendix B.

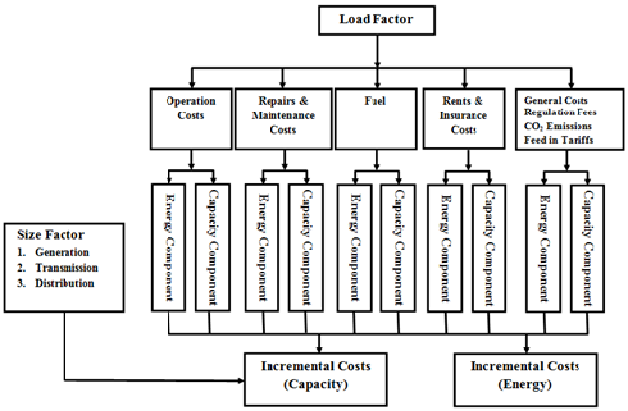

Fig. 1. Allocation of Costs to Demand/Capacity and Energy Components & Size Factor

Fig. 1 shows that the cost of fuels should not be in total allocated to energy component, because part of the fuel is consumed to meet the "zero load" generation losses. In the context of this study, the zero load losses are assumed to depend on the type and size of the generating plant and therefore should be related to the demand component of the cost of losses. Therefore, a rigorous method [2] is adopted using (9) that characterize the actual power station fuel consumption.

$$Actual\_Fuel\_Consumption = A \cdot B + C \cdot D \quad (9)$$

Where *A* is Total "Sent Out" units from the Power Station machines burning the same fuel (MWh), *B* is the machines' corresponding incremental fuel rate (MT/MWh), *C* is the sum of machines running hours burning the same fuel (hour) and *D* is the machines' corresponding zero load fuel rate (MT/hour). Fig. 2 illustrates the fundamental structure of the methodology followed, to weight the fuel costs to utility to their equivalent demand and energy components.

Furthermore, Fig. 3 shows the theoretical background for the demand incremental cost component derivation for each cost item. As detailed in [2], [3], once the financial data are obtained and classified, these are associated to the maximum demand (MW) for each corresponding year. The cost figures

are then adjusted to consider the inflation of each corresponding year. By associating the various financial costs to the corresponding system's maximum demand it is then possible to extract, *b* - €/MW, by applying the method of least squares on the set of referred data (Cost vs. Peak Demand). This figure, *b*- €/MW, is the increase/decrease trend of the relevant cost per MW, as obtained from the historical data available.

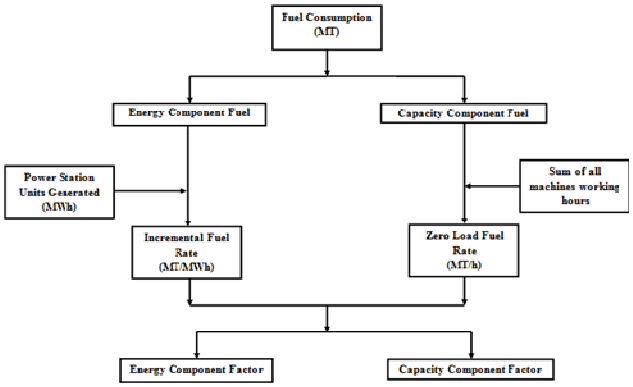

Fig. 2. Allocation of Fuel Costs to Demand/Capacity and Energy Components

Once the incremental cost value is determined i.e. the slope of the graph (*b*), the demand component of losses attributed to the specific account item is calculated as detailed in [2] and [3].

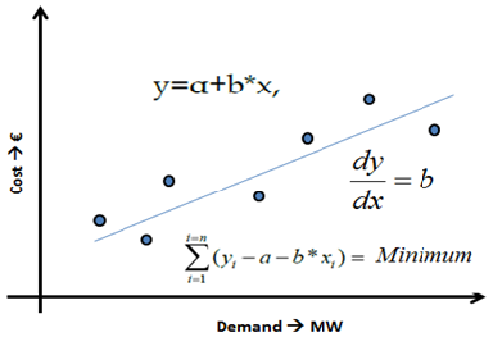

Fig. 3. Demand Cost Component Calculation (€/MW)

Fig. 4 shows the background for deriving the energy incremental cost component for each cost item. As with the demand case, once the costs data are obtained and classified, these are de-inflated according to the annual inflation factor of each tabulated year. Consequently, for each corresponding year the ratio (€/MWh) of the de-inflated costs (€) to the total energy generated (MWh) per year is determined and subsequently plotted over its corresponding year. A straight line is then fitted as shown in Fig. 4. However, in order to bias the calculated energy component of the cost of losses towards the latest cost figures and to a lesser extent towards costs valid in previous years, *y* is calculated for the latest year for which data is available [2], [3].

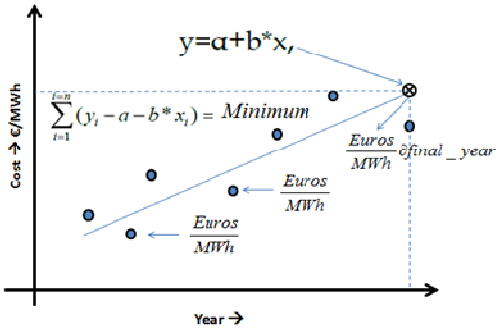

Fig. 4. Energy Cost Component Calculation (€/MWh)

III. Software Description

The software tool is based on executable files by using *C* programming language to evaluate the algorithms and methods that have been determined in [2], [3]. The executable files are incorporated in the software as evaluation engine modules. These modules serve the scope of calculating the numerical factors necessary to formulate the holistic loss evaluation equations on a case by case scenario, i.e. according to different input data. There exist 5 different executable files, all contributing to the formulation of (1) and (2). The executable files specifically calculate the following: a) the incremental energy and demand cost components, b) the weighted multiplying factors, c) the system load characteristics, d) the Total Cost of Losses & the Ownership Cost of the evaluated transformer. There exist two sets of the four executable files, one tailored for power transformers and the other tailored for distribution transformers, as evident by Fig. 5.

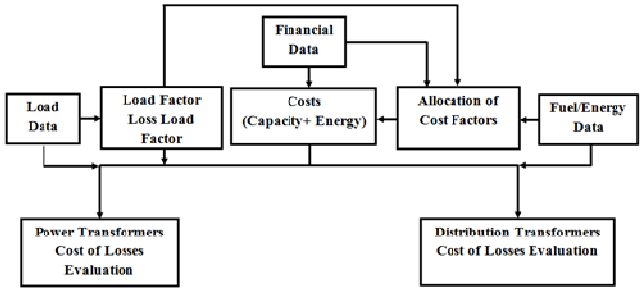

Fig. 5. Interaction of software modules

Furthermore, the developed software benefits from 4 different main modules, namely the Graphical User Interface (GUI), the Data Base, the Evaluation Engine, and the Postprocessor. The fundamental logic of the Software Architecture is illustrated by Fig. 6.

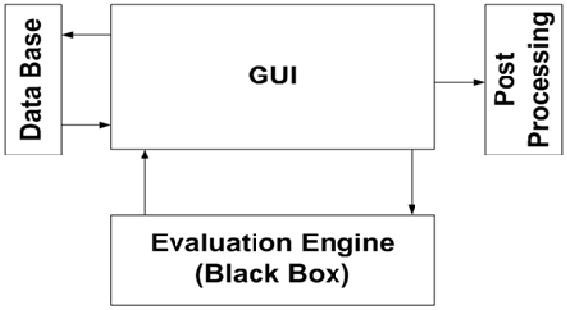

Fig. 6. Software Architecture

Firstly, the *GUI* (Graphical User Interface) is the module that allows an extensive and user friendly intervention for: a) importing the required data from the data base, b)

retrieving previous stored parameters for comparison and c) storing evaluation results for post processing. In general the GUI can be used to compare several evaluation scenarios e.g. in tender evaluation procedures. It, also, graphically illustrates the evaluation results and generates log reports for each evaluation scenario. More specifically, the GUI consists of three main categories, specified by appropriately named tabs, allowing the user to interact easily with the software. These categories would be divided into the "Input" tab category, the "Results" tab category and "Reports" tab category.

In the "Input" category the user has the opportunity to set the input parameters required for a specific evaluation, to initialize the process. The evaluation pertains to the executable files, as previously explained. Furthermore, there is a provision for storing the input parameters onto the database for future retrieving. The stored parameters provide the user with the opportunity to run the process under a combination of set parameters from different scenarios to extract useful information. The user friendly and guiding nature of the software is reinforced by the display of tooltips that inform the user about the parameters' range of valid values limits and formats, and the underlying standard or reference for such evaluations. Lastly, prior to initialization of the evaluation process, the software perform checks for the accuracy of the input parameters setting and informs the user accordingly.

Moreover, the "Results" tab category will be initially disabled and would be activated as soon as the user proceeds with an evaluation test. The evaluation test run in the background and the software concurrently informs the user about the evaluation progress (using progress bars and messages). After the evaluation finalizes, the extracted results are briefly presented providing an option to store them in the database. If the evaluation progress ends unexpectedly (for example due to an out of memory exception), messages are displayed in order to inform the user accordingly.

The third category, "Reports" tab, allows the user to preview reports or graphs of the computed results as well as viewing comparison reports graphs and tables between two or more stored evaluation scenarios. The user has the opportunity to select between several types of graphs (CPF, PDF etc.). All the reports and graphs are available for printing or exporting to file options.

Moving further, the Database module is implemented in order to firstly store all the information required (e.g. Financial Data, SCADA Recordings, Substation Information and Manufacturers Data) to run an evaluation scenario (evaluation parameters) and secondly to store all the evaluation results for future processing. Each record of the database is mapped with a GUID (Global Unique IDentity), allowing them to be transferred in a supplement machine which will run the software. This prevents the mixing up of existing and newly imported records in the database.

As previously stated, the Evaluation Engine module would perform all the calculations during the evaluation process, by hosting the executable files developed. This module will interact with the GUI by importing the input parameters from it, and it will subsequently perform the evaluation processes. Following the evaluation the module will be sending back to the GUI all the computed results.

Finally, the Post Processing module of the software will allow the user to print or to export to files (pdf, doc, xls) the selected reports and/or graphs that would be generated by the GUI.

IV. Post Processing Results

Following the analysis and procedure detailed in (2) - (9), the Total Cost of Losses (TCL) and the Total Ownership Cost (TOC) of transformers for the Cyprus Power System may be evaluated. The following sections provide a brief discussion regarding the influence of a) fuel pricing variation, b) reserve margin variation, c) discount rate variation and d) different fuel usage on the demand and energy components of losses.

A. The Influence of Fuel Pricing Variation and Predictions

Firstly, it is well understood that some form of uncertainty exists with future fuel price forecasts; uncertainty that increases with longer time horizons [3]. It should be noted that any predictions should be used with caution as market prices change in an unpredictable mode, over time, according to the financial and political circumstances. It is, however, imperative to depend on future energy price estimates when it comes to life-cycle loss evaluations.

Fig. 7 shows the diesel and crude oil forecasted prices up to 2040. The forecasted price figures result from Regime Switching methods as described in [3]. It shows diesel and crude oil projected prices for the 30th, the 40th and the 50th percentiles.

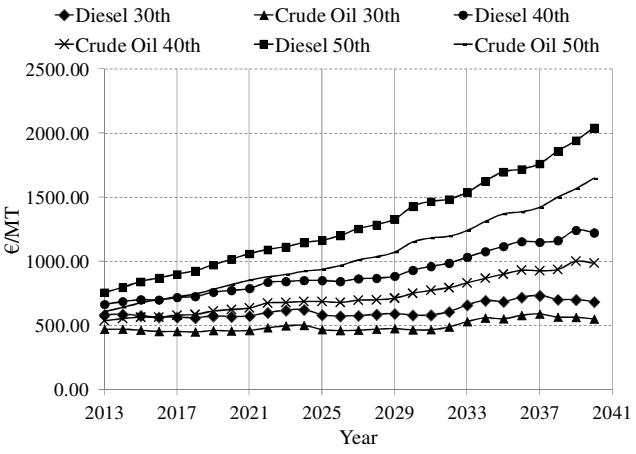

Fig. 7. Fuel Forecasted Data

Fig. 8 illustrates the impact on the demand and energy components of losses, under the three percentiles considered.

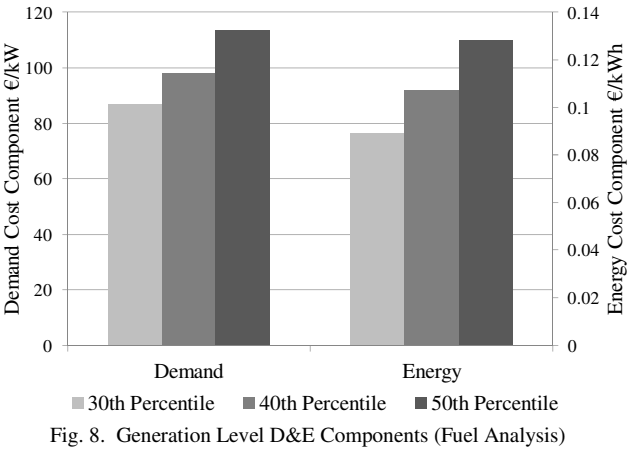

Fig. 8. Generation Level D&E Components (Fuel Analysis)

The results refer to the generation level only, since the transmission and distribution levels are not significantly affected by the varying fuel prices. The sensitivity analysis for different fuel prices showed that the energy component (*E)*, as opposed to demand component (*D*), is heavily dependent on future fuel prices.

B. Reserve Margin

A sensitivity analysis regarding the effect of a varying reserve margin is also provided. Fig. 9 presents the analysis using a reserve margin of 2%, 5.46 % and 23%. The demand and energy components of the total cost of losses are presented for the generation category only. The evaluation has shown that the energy component of losses, E_{g_peak}, remains unaffected. On the other hand, the demand component of losses, D_{g_peak}, is heavily influenced by the reserve margin.

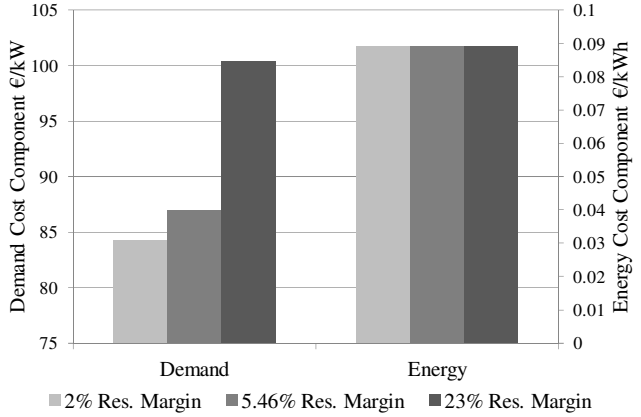

Fig. 9. Generation Level D&E Components (Reserve Margin Analysis)

C. The effect of Discount Rate

Another important factor that needs to be correctly evaluated in loss evaluations procedures is the discount rate (%) for calculating the present worth (*pw*) of future costs and the capital recovery factor (*crf*). The discount rate is the minimum acceptable rate of return from the investment and thus is should be above the interest rate (about 2% higher) [5], [6] which applies to the overall objectives of the business. It is proposed that the discount rate employed, should be based on the interest rate paid by a utility in the last 5 years [6].

Fig. 10 illustrates the effect that different discount rates have on the demand and energy component of losses for the generation level. As an example, the discount rates used are 5%, 10% (benchmark scenario) and 12%.

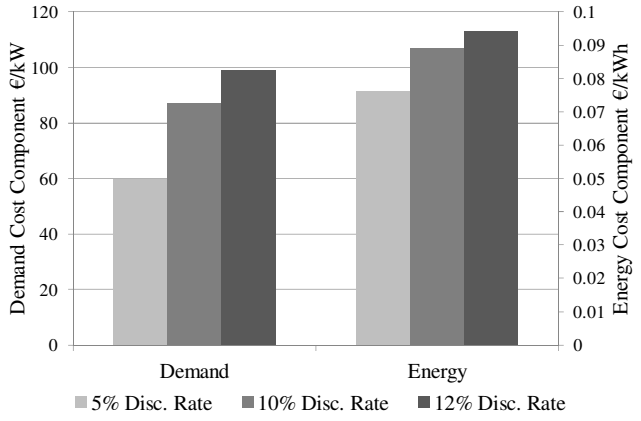

Fig. 10. Generation Level D&E Components (Discount Rate Analysis)

The % difference of D_{g_peak} and E_{g_peak} components by assessing the 5% discount factor and the 10% discount factor is more clear in D_{g_peak} that is -31.27 % since E_{g_peak} deviates by -14.5 %. This reflects the higher cost value of the utility plant premises and equipment over the cost of the energy generated, thus giving greater impact of the *crf* and *pw* to the demand component of the cost of losses.

D. Influence of Different Fuel Usage

E.A.C's current generating cycles are capable of delivering power using Liquid Natural Gas (LNG). However, only crude oil and diesel are used until LNG is available to the island. Current fuel forecasting trends suggest that LNG prices would be lower than diesel and crude oil. The predicted LNG prices for the evaluation period were performed by using linear regression on the forecasted Brent fuel prices [3]. Fig. 11 presents the influence on the demand and energy component of losses based on which year (e.g. 2013, 2016, and 2040) LNG will be added in the generation mix of the system. The obvious conclusion is that the soonest the LNG will be added the greater would be the reduction in the demand and energy component of losses.

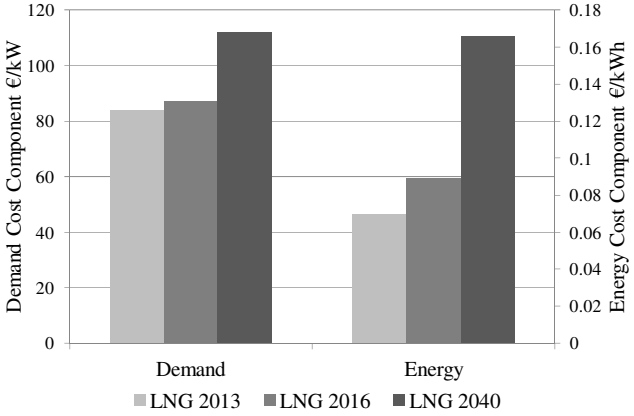

Fig. 11. Generation Level D&E Components (LNG Introduction Analysis)

V. Conclusion

The software tool described in this paper reflects on a holistic management approach to thoroughly appraise the demand and energy component of the cost of losses for power and distribution transformers. The developed model provides a dynamic, adaptive and sustainable approach for evaluating the life-cycle losses of a transformer. The referred software tool is currently available to E.A.C.

VI. Appendix A

$\boldsymbol{D_{p\_Peak}}$ – Aggregate annuitized demand cost per kW evaluated for power transformers - peak load (€/kW).

$\boldsymbol{D_{p\_Base}}$ - Aggregate annuitized demand cost per kW evaluated for power transformers - base load (€/kW).

$\boldsymbol{D_{dt\_Peak}}$ - Aggregate annuitized demand cost per kW evaluated for distribution transformers – peak load (€/kW).

$\boldsymbol{D_{dt\_Base}}$ - Aggregate annuitized demand cost per kW evaluated for distribution transformers – base load (€/kW).

$\boldsymbol{E_{p\_Peak}}$ – Aggregate total levelized cost per kWh of fuel and any other energy related operating expenditure that is associated to the energy output of the generating units for power transformers – peak load (€/kWh).

$\boldsymbol{E_{p\_Base}}$ -Aggregate total levelized cost per kWh of fuel and any other energy related operating expenditure that is

associated to the energy output of the generating units for power transformers – base load (€/kWh).

E_{dt_Peak} -Aggregate total levelized cost per kWh of fuel and any other energy related operating expenditure that is associated to the energy output of the generating units for distribution transformers – peak load(€/kWh).

E_{dt_Base} -Aggregate total levelized cost per kWh of fuel and any other energy related operating expenditure that is associated to the energy output of the generating units for distribution transformers – base load (€/kWh).

NLL - No Load Losses (kW).

LL - Load Losses (kW).

AUX - Auxiliary Losses (kW).

PRFS - Peak Responsibility Factor System (p.u.).

PEQO - Levelized Annual Peak Load no Inflation (p.u.).

PEQE - Levelized Annual Peak Load with Inflation (p.u.).

LLF - Loss Load Factor (p.u.)

FOW - Average hours per day (or per year) the transformer cooling is operated (p.u.).

AF – Availability Factor, the proportion of time that a transformer is predicted to be energized (p.u.).

VII. Appendix B

TABLE I
ALLOCATION OF COST FACTORS

Cost Item	Demand Component (%)	Energy Component (%)
Depreciation	100	0
Operation	84	16
Repairs &Maintenance	69	31
Rents & Insurances Costs	100	0
Energy Regulation Authority Fees	100	0
T.S.O Fees	100	0
Green House Emission Rights	0	100
Renewable Energy Purchase	0	100
General Costs	100	0
Fuel Storage Fees (COSMOS)	100	0

VIII. Acknowledgment

The Electricity Authority of Cyprus for their technical and financial support.

IX. References

[1] IEEE std C57.120.1991, “IEEE Loss Evaluation Guide for Power Transformers and Reactors”, August 12, 1991.

[2] Charalambous, C.A.; Milidonis, A.; Lazari, A.; Nikolaidis, A.I., "Loss Evaluation and Total Ownership Cost of Power Transformers—Part I: A Comprehensive Method," *Power Delivery, IEEE Transactions on* , vol.28, no.3, pp.18720 - 1880, July 2013

[3] Charalambous, C.A.; Milidonis, A.; Hirodontis, S.; Lazari, A., "Loss Evaluation and Total Ownership Cost of Power Transformers—Part II: Application of Method and Numerical Results," *Power Delivery, IEEE Transactions on* , vol.28, no.3, pp.1881 - 1889, July 2013

[4] Technical Assessment Group, “Technical Assessment Guide”, EPRI PS0866-SR Special Report, Electric Power Research Institute, Palo Alto, CA, June 1978.

[5] D.L. Nickel, H.R. Braunstein, “Distribution transformer loss evaluation: I – Proposed Techniques”, IEEE Transactions on Power Apparatus and Systems, vol. 100, no. 2, pp. 788-797, Feb. 1981.

[6] D.L. Nickel, H.R. Braunstein, “Distribution transformer loss evaluation: II – Load Charasteristics and System Cost Parameters”, IEEE Transactions on Power Apparatus and Systems, vol. 100, no. 2, pp. 798-811, Feb. 1981.

[7] A.L. Theophanous, “Manual for Distribution Transformer Tender Evaluation”, EAC Engineering Department, System Development and Forward Planning Section Head Office, May 1988.

[8] Optimum Resources Utilisation for Generation Development Expansion, EAC Internal Report – by LAHMEYER 2006.

X. Biographies

Antonis Lazari was born in Nicosia, Cyprus in 1988. He studied M.Eng. (Hons) in Electrical and Electronic Engineering and graduated in 2010 from the University of Bristol, UK. Since January 2011 he has been with the Department of Electrical and Computer Engineering, at the University of Cyprus as a PhD student in the field of Electrical Power Engineering. His research interests include Losses Evaluation in the light of increasing penetration of renewable energy generation.

Charalambos A. Charalambous was born in Nicosia, Cyprus in 1979. He received a Class I BEng (Hons) degree in Electrical & Electronic Engineering in 2002 and a PhD in Electrical Power Engineering in 2005 from UMIST, UK (The University of Manchester). Currently, he is an Assistant Professor, in the Department of Electrical and Computer Engineering, at the University of Cyprus. He was formerly with the National Grid High Voltage Research Center at the University of Manchester, UK. His research interests include transformer finite element modeling, Ferroresonance transient studies, the electrical control and analysis of DC corrosion and the dynamic operation and loss evaluations

2nd Conference on Power Options for the Eastern Mediterranean Region
07-08 October 2013, Nicosia, Cyprus (Paper No. POEM13/161)

Concept of energy extraction from sludge of a clarification plant

Nora Becker, Constantinos Sourkounis

[1]***Abstract*-- Along with the increasing quality of life, the demand of fresh water grows continuously which may result in a shortage of water in warmer regions. In summer times, the water demand is particularly raised by the tourism. The consequence is that clarification plants become overloaded which leads to odor nuisance for townships and holiday villages. In order to avoid this, investigations have been made on the energy extraction from organic sludge particles on the basis of digestive processes.**

Index Terms--Clarification plant, energy extraction from organic sludge, biogas.

I. Introduction

The increasing water demand in line with a growing standard of living provides new challenges for regions with warmer climates, particularly with respect to the construction and operation of water supply and treatment systems. Clarification plants in such regions are subject to extra operating conditions resulting from the special climate conditions. Water consumption is directly coupled to the seasonal temperatures so that a considerable increase is recorded during summer months. In addition, the number of tourists is very high in summertime which raises the water consumption even more. This leads to an overloading of the clarification plants which has the consequence of ecological and economical restrictions for those areas.

As an example, the aeration system may overflow in summer months with heavy inflow when the clarification plants are overloaded, so that odor emissions in the area of the clarification plant itself but also in adjacent dwellings and tourist areas are the consequence. Furthermore, the sludge itself places a continuous problem.

In case of the clarification plant under investigation, located in Cyprus, the sludge is dewatered by two centrifuges and two mechanical dryers and features therefore a proportion of dry substances of 20 to 22 pc. The share of organic substances still amounts to 75 p.c., so that at storage in a non-air tight space, fouling processes take place which entail odor emission.

Within the scope of these investigations, emphasis has been placed on the energy extraction of organic components of the sludge to avoid odor emission.

N. Becker is with the Faculty of Electrical Engineering and Information Sciences, Ruhr-Universität Bochum, 44801 Bochum, Germany (email: becker@enesys.rub.de)

C. Sourkounis is with the Faculty of Electrical Engineering and Information Sciences, Ruhr-University Bochum, 44801 Bochum, Germany (e-mail: sourkounis@enesys.rub.de)

II. Current structure and Operation of the clarification plant

On the basis of the available key data and basic function principle of the clarification plant, a concept for an expansion of the plant has been established with the aim to achieve energy extraction from the sludge. The loading of the investigated plant is subjected to fluctuations varying with the season. This difference is due to the increased tourist numbers on the one hand, and due to the hygienic behavior of the residents and tourists during summer months since the water consumption per capita increases by multiple shower taking and washing. Inflows in summer and winter and their composition depend on the actual number of residents including tourists.

Since the existing clarification plant does not own a primary clarifier, no energy-rich primary sludge is extracted prior to the aeration step, i.e. the entire sludge is subjected to the second cleaning step and loses energy due to aerobic processes.

The sludge production is based on the inflow and therefore is subject to seasonal fluctuations.

Table I Sludge Quantity

	Summer		Winter	
	m³/d	DS	m³/d	DS [g/l]
Primary Sludge	0	0 g/l	0	0
Secondary	800	4 g/l	150	3
After Drying	32	20-22 %	5	20-22 %

Due to the overloading during the summer months, the operating concept of the clarification plant under investigation needs to be revised: at first, due to the overflowing of the aeration plant during summer months with heavy inflow, and then because of the resulting odor emissions in the vicinity of the clarification plant but also in adjacent dwelling areas. Moreover, the energetic usage of the sludge requires a process-specific reconstruction of the clarification plant.

At present, the sludge is drained by two centrifuges and two mechanic dryers and features therefore a dry particle proportion of 20 to 22 p.c. The share of organic substance still amounts to

75 p.c., so that at storage in a non-air tight space fouling processes take place which entail odor emission. Part of the potentially usable energy gets lost.

A durable expansion of the clarification plant must be based on a prognosis on the quantity of water to be cleared in future. The clarification plant under investigation has to anticipate increasing inflows due to rising tourist numbers. Another important aspect is that Cyprus becomes more and more a retirement place for seniors from middle Europe.

Therefore, the following prognoses have been made for the inflow values of the clarification plant (table 2):

TABLE II: SLUDGE QUANTITY IN 2020

	Summer	Winter
Inflow [m³/d]	21000	7500
Dry Substance [%]	20 - 22	20 - 22
After Drying [t/d]	55	15

The mere consideration of the inflow prognoses follows that an expansion of the plant is necessary, because the inflow values increase by 45 p.c. as compared with the inflow of summer 2010.

Increasing inflow affects the entire system, all parts of the plant must therefore be checked for their loading and be extended, if necessary. For the currently available mechanic preliminary treatment range, i.e. coarse or fine screen and the grit chamber, no rated values are available; therefore it is not possible to evaluate them within the scope of these investigations.

However, it must be emphasized that further costs may occur since an adaptation to the other systems of the plant must be considered.

The same applies to the wastewater treatment which is carried out separately by the two villages as reported.

III. CONCEPT OF SLUDGE TREATMENT

The sludge treatment in the existing clarification plant only applies to the sludge originating from the aeration since a preliminary treatment is not available so that no preliminary sludge can be taken. The sludge proportion which is separated from wastewater in the final clarification is then redirected into the aeration in order to maintain the bacteria concentration of the activated sludge.

The surplus sludge (=sludge from the activation) is fed to an aerated dryer at first and then conducted to a drying unit consisting of two mechanic dryers and two centrifuges.

Since there are no further details available for these systems, it is not possible to make any further comments in this respect.

The dried sludge is then stored in containers. Since there are still water proportions and organic substances contained in the sludge (the sludge is not fully digested), odor emissions occur due to the storage under non air-tight conditions.

For the energetic treatment of the sludge a concept has been worked out which entails the expansion of the existing clarification plant.

The planned concept of sludge treatment is shown in the flow chart of the system (Fig. 1).

The primary sludge extracted from the primary sedimentation basin is conducted from the activation into a buffer basin, same as the surplus sludge. An agitator mixes the sludge in order to get a homogenous mass from the different sludge types – also called raw sludge.

Afterwards this mass is conducted to a thickener which shall be realized by a band filter. In the thickener, the sludge is generally converted to a dry substance content between 4 and 6 p.c. [3, p. 330]. At the plant under investigation, a dry substance content of 4 p.c. is sufficient so that a comprehensive circulation system can be avoided and available circulation pumps be used which means a lower cost factor.

Prior to the fouling process, the thickened sludge is guided to a tank feeding the digester.

A digester feeding pump (eccentric screw pump) supplies the digester with the treated sludge as necessary. The duration time in the digester varies between 15 and 30 d at around 33 to 37 °C (mesophil) [3, p. 329; 4, p. 408].

The sludge leaves the digester fully digested and is thus stabilized. In order to save possible transportation costs and storage space, the digested sludge is subsequently thickened. This could be realized by the existing drying systems (two mechanic dryers and two centrifuges). The subsequently thickened digested sludge can now be stored for agricultural utilization in a quasi-odor-emission-free condition.

IV. ASSESSMENT BASIS FOR THE TREATMENT OF THE SLUDGE

The evaluation of the necessary expansion and the system quantities for digester gas recovery, has been based on the population equivalent used in Sanitary Environmental Engineering. It refers to wastewater of industrial and home origin and is an essential quantity for the layout of the clarification plant.

Basis for the determination of the population equivalent is the daily inflow of the plant under assessment [l/d], , the biochemical oxygen demand for five days (BSB_5) in [mg/l] as well as an average consumption value in [g BSB_5/(EW·d)].

The forecast inflow for the summer 2020 amounts to 21 000 000 l/d. Therefore, a value of 11 025 g/d follows from a BSB_5 content of 525 mg/l for the daily BSB_5 load.

With the BSB_5 load and an average daily consumption of BSB_5 per inhabitant of 60 g BSB_5/(EW·d) follows for the population equivalent in summers:

$$EGW = \frac{\mathrm{BSB_5\text{-}Fracht}}{\mathrm{BSB_{5\text{-}d}/EW}} = 183750\,E \qquad \textbf{(1)}$$

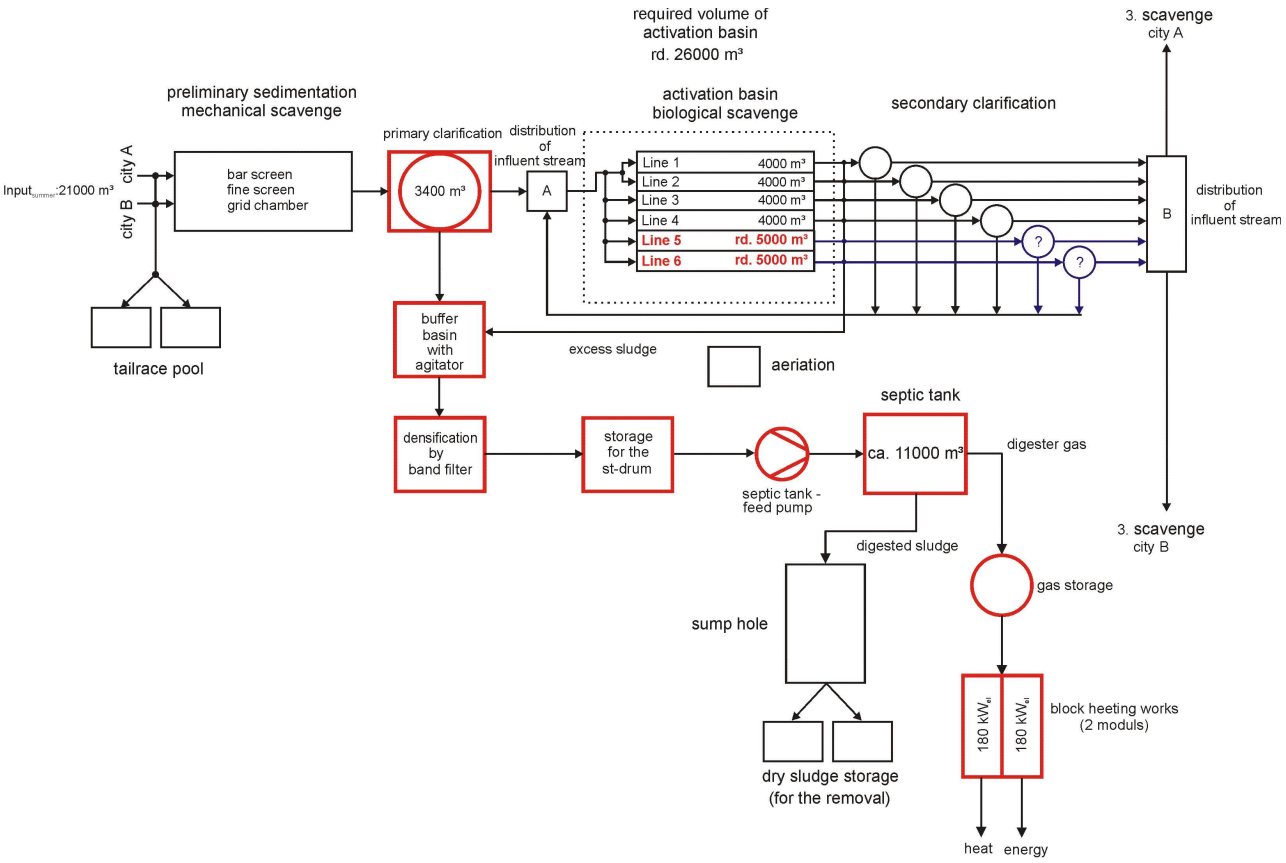

Fig. 1 Flow Chart of the extended clarification plant with energy extraction from the sludge

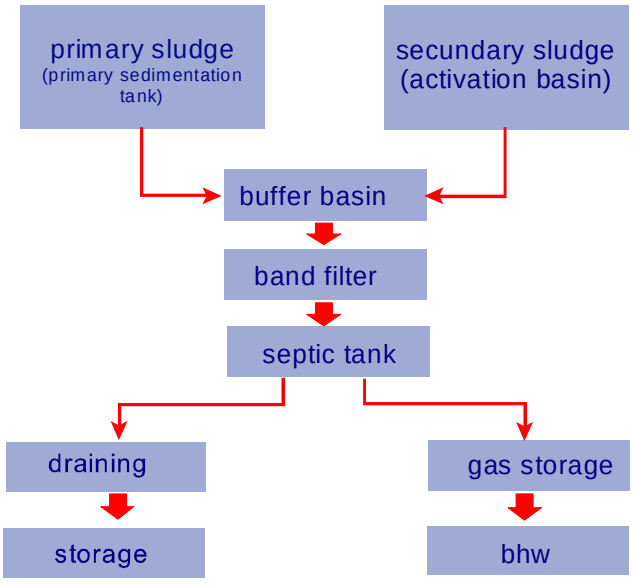

Fig 2 Concept of Sludge Treatment

Similarly, the population equivalent can be calculated for the winter. At an inflow of 312,5 5 m³/h and a BSB_5 content of 575,66 mg/l follows for the BSB_5 load a value of 4 317 450 g/d and therefore for the population equivalent 71 957,5 E.

For further considerations, a population equivalent of 200 000 E for the summer and 75 000 E for the winter is assumed.

V. Digester Gas Extraction

Digester gas develops in the digester of a clarification plant. The thickened sludge (primary and surplus sludge) is fermented under anaerobic conditions (exemption from oxygen) at a mesophile temperature range (33 – 35 °C [1, p. 423] by microorganisms intro gas-type particles (methane, carbon dioxyde, ammoniac and hydrogene sulfide), digested sludge and non-degradable components.

The sludge can be classified into three main components: fats, carbohydrates and proteins.

In the first phase of digester gas extraction, the hydrolysis, exoenzyme separate high-molecular in low-molecular compounds (fats in fatty acids, i.e. palmitic acid) and glycerines, carbohydrates in monosacchrides and proteins in amino acids.

In the acido genesis – also called acid fermentation - ” [1,p. 426 Fig 1] – i.e. the second phase – the hydrolysis products are converted by facultative anaerobic life bacteria (bacteria which can survive both with or without oxygen), mainly in short-chained fat acids (i.e. carbon acid), alcohols, carbon dioxides, ammoniac, hydrogen and hydrogen sulfides.

In the aceto genesis, organic acids and alcohols are transformed by acetorogenous bacteria into acetic acid, where also hydrogen and carbon dioxides are generated (third phase).

Finally, in the fourth phase – the methano genesis – carbon

dioxide and hydrogen are reduced to methane and acetic acid separated in methane and carbon dioxides. This is realized by methanogenic bacteria.[1] (Fig. 3).

Decisive for the calculation of the gas yield per day is the BSB5 load which depends on the kind of operation, the sludge age and the population equivalent. According to the classification, the gas yield per day can be calculated for summer and winter. Calculation basis is a parameter of the relevant DWA data sheet. [3].

Since for the investigated clarification plant BSB_5-load 45 g BSB_5/(EW·d) shall be relevant, an average gas yield value is calculated for the summer:

$$V_{Gas} = V_{Gas,av(2)} + \frac{\Delta V_{Gas}}{\Delta BSB_{5-Fracht}} \Delta BSB_{5-Fracht,plant}$$

with

$$V_{Gas,av(2)} = 13,2 \frac{l}{EW \cdot d} \;,\; \Delta V_{Gas} = 5,1 \frac{l}{EW \cdot d}$$

$$\Delta BSB_{5-Fracht} = 13 \frac{g}{EW \cdot d} \qquad (2)$$

$$\Delta BSB_{5-Fracht,plant} = 3 \frac{g}{EW \cdot d}$$

$$V_{Gas} = 14,38 \frac{l}{EW \cdot d}$$

Depending on a population equivalent of 200.000 EW, the gas yield per day in summer amounts to 2 876 m^3/d. Since a lower aeration must be considered for the winter so that the biology is progressed further, the surplus sludge is less fertile compared with the summer. For the gas yield in winters, a value of around 20 p.c. below the yield in summer is assumed. For the specific gas yield in winter therefore a value of 11,5 l/(EW·d) is obtained and thus for a population equivalent of 75.000 E, a daily gas yield of 862,5 m^3/d.

For the consideration of a whole year, a certain number of days of the year must be allocated to the summer as well as to the winter classification. Since a meteorological temperature limit of 25°C is given for a summer day, this is used as parameter within the scope of this research work.

Calculation criteria are the average temperatures per year in Cyprus (table 3):

TABLE 3 AVERAGE TEMPERATURE IN CYPRUS

Month	Jan.	Feb.	March	April	May	June
Temp.	17 °C	17 °C	23 °C	25 °C	27 °C	30 °C
Month	July	Aug.	Sep.	Okt.	Nov.	Dez.
	31 °C	32 °C	33 °C	27 °C	22 °C	19 °C

Herewith, the "summer" is defined to the months of April to October which corresponds to 214 days of the year. Accordingly, the "winter" counts for 151 days from the months of November to March.

In agreement with the specification of the duration of summer and winter, the gas yield for the summer amounts to 615 464 m^3 and for the winter to 130.237 m^3.

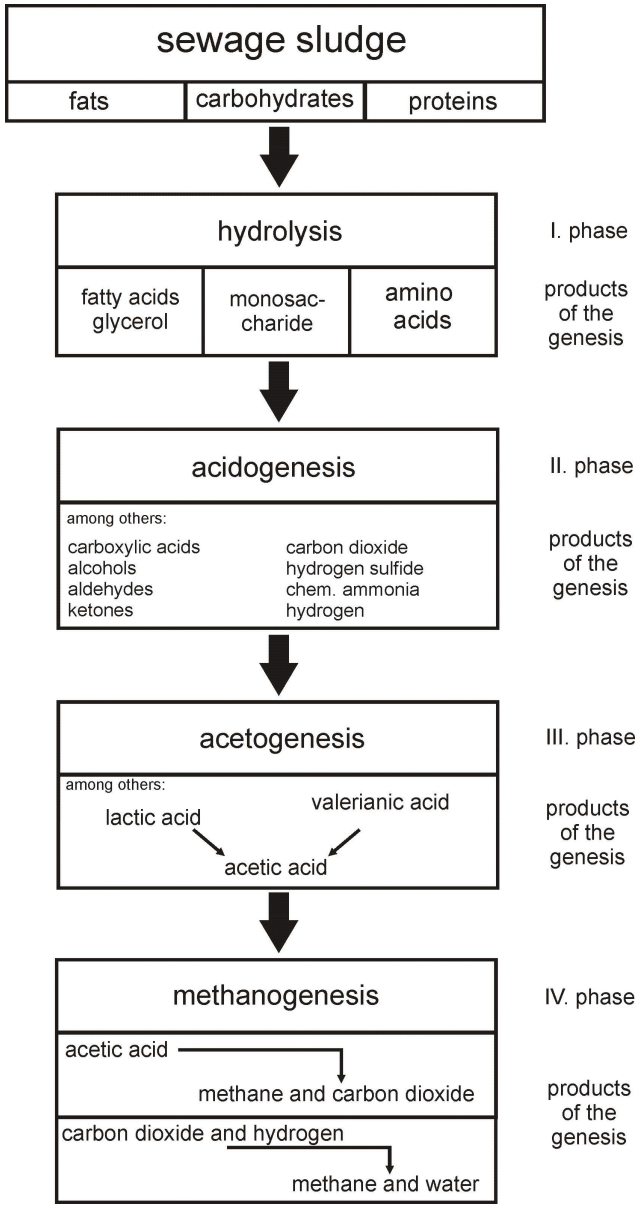

Fig. 3 Anaerobic sludge stabilization

The sum of both gas quantities provides a prognosis of the yearly gas yield (summer and winter) of 745.701 m^3.

The recoverable energy quantity is calculated from the calorific value for biogas from sludge digestion plants and the forecast gas quantity.

The calorific value can be taken from DWA data sheets and is defined to 6 to 7 kWh/m³ for digester gas with an average methane content of 60 – 70 Vol p.c. [2; p. 9].

For the calculation of the energy extraction, an average value is assumed, i,e. 6,5 kWh/m³. From this follows an energy quantity of 4 487 060 kWh/a.

VI. Conclusion

Together with the increasing quality of life the demand for fresh water rises which leads to shortages in water supply in warmer regions. Particularly the tourism is a reason for the increasing water demand in such regions in summer. This has the result that clarification plants become overloaded and odor nuisances for the near by population and holiday villages are the consequence. In order to avoid this, investigations on the energy utilization of organic particles of the sludge on the basis of digestion processes have been carried out.

Several methods of sludge treatments are possible. Bearing in mind the prohibition to use sludge in agriculture in Switzerland (in Germany strong requirements apply (AbfKlärV), this paper describes a method where the proportion of sludge for use in agriculture is only low. Therefore, the chosen methods of anaerobic digestion with preliminary thickening and subsequent dehydration are widely accepted in many European countries.

Based on a prognosis for the quantity of water to be cleared in the future, a concept for the energetic extraction from sludge has been developed. By determining the seasonal *population equivalent*, the necessary expansions have been evaluated and the expected quantities of digester gas per day have been determined.

At a population equivalent of 200.000 EW, a gas yield of 2.876 m^3/d results for the summer. A lower digestion process yield is expected for the winter. The gas yield in winter has been estimated to be around 20 p.c. lower than the one for the summer. The gas yield per day in winter therefore amounts to 862,5 m^3/d at a population equivalent of 75.000 E. With an average calorific value of 6,5 kWh/m^3 of the digested gas, this results to an energy quantity of 4 487 060 kWh/a.

VII. References

[1] KOPPE, Paul; [STOZEK, Alfred]: Kommunales Abwasser. Seine Inhaltstoffe nach Herkunft, Zusammensetzung und Reaktionen im Reinigungsprozesse einschließlich Klärschlämme. 4. Auflage. Essen: Vulkan-Verlag, 1999.

[2] DWA-Merkblatt 363: Herkunft, Aufbereitung und Verwertung von Biogasen. Hennef: DWA Deutsche Vereinigung für Wasserwirtschaft, Abwasser und Abfall e. V., November 2011.

[3] IMHOFF, Karl; [IMHOFF, Klaus R.; JARDIN, Norbert]: Taschenbuch der Stadtentwässerung. 31. Auflage. München: Oldenbourg Verlag, 2009.

[4] GOYA, Willi: Siedlungswasserwirtschaft. 3., bearbeitete Auflage. Berlin, Heidelberg:Springer Verlag, 2007.

[5] DWA-Arbeitsblatt ATV-DVWK-A 198: Vereinheitlichung und Herleitung von Bemessungswerten für Abwasseranlagen. Hennef: DWA Deutsche Vereinigung für Wasserwirtschaft, Abwasser und Abfall e. V., April 2003.

[6] GÖRISCH, Uwe; [HELM, Markus (Hrsg.)]: Biogasanlagen. 2. Ausgabe. Stuttgart: Eugen Ulmer KG, 2007.

[7] RES Legal/Bundesministerium für Umwelt, Naturschutz und Reaktorsicherheit: http://www.res-legal.de/suche-nach-laendern/zypern.html; Stand: 28.06.2011

[8] Universität für Bodenkultur Wien, Department für Wasser - Atmosphäre -Umwelt , Institut für Siedlungswasserbau, Industriewasserwirtschaft und Gewässerschutz. Stand: 01/2010: http://www.wau.boku.ac.at/fileadmin/_/H81/H811/Skripten/811352/811352_01 _SO.pdf; Stand: 01.06.2011

[9] MÜLLER, Ernst A.: Handbuch der Energie in Kläranlagen. Hrsg.: Ministerium für Umwelt, Raumordnung und Landwirtschaft des Landes Nordrhein- Westfalen. Düsseldorf, 1999.

[10] MUDRACK, Klaus; [KUNST, Sabine]: Biologie der Abwasserreinigung. 5. Auflage. Heidelberg/Berlin: Spektrum Akademischer Verlag GmbH, 2003.

VIII. Biographies

Dipl.-Ing. Nora Becker received her Dipl.-Ing. from the Ruhr-University Bochum at the facultiy of Enviromental Technology and Resource Management in 2012. Her majoring is the mechanical engineering with the area of concentration in renewable energies, sustainable energy supply, materials and materials testing and recycling of technical products.

Since October 2012 she is research assistant at the Institut of Power System Technology and Power Mechatronics at the Ruhr-University Bochum. Her main research area is the integrated electromobility in the logistics of urban agglomeration areas.

Prof. Dr.-Ing Constantinos Sourkounis received his Dipl.-Ing and his Dr.-Ing degrees from the TU Clausthal in 1989 and 1994 respectively. After he received his Ph. D. at the Institute of Electrical Power Engineering at the TU Clauthal, he occupied the position of the chief engineer. In 2003 Dr.-Ing. Sourkounis received his habilitation. Since 2003 he is professor at the Ruhr-University Bochum, heading the Power System Technology Research Group. His main research areas are mechatronic drive systems, renewable energy sources, decentralised energy systems supplied by renewable energy sources, and energy supply systems for transportation systems.

2nd Conference on Power Options for the Eastern Mediterranean Region
07-08 October 2013, Nicosia, Cyprus (Paper No. POEM13/162)

Integration of Quick Charging Stations for E-Mobility in Power Grids of Weak Infrastructure and High Impact of Renewable Energies

Constantinos Sourkounis, Nora Becker, Alexander Broy, Fredrik Einwächter

[1]***Abstract*-The social acceptance of electro-mobility increases as the capacity of electric vehicle batteries is improved and technical solutions for a short charging time become available.**
For this reason, the charging of even a few number of electric vehicles may pose a significant additional load on the respective grid section. In the case of a grid load near the nominal capacity by the households and industry or in case of remote low-supply areas, the increased power demand can lead to an overload. Besides the voltage variations, unwanted harmonics can be emitted into the grid.
Therefore examinations have been carried out to investigate the installation of quick charging stations in remote low-supply areas together with the necessary grid integration. In this context, different concepts for the grid integration of quick charging stations in low-supply regions have been taken into consideration.

Index Terms– Quick charging station, electric mobility, mains pollution by charging stations

.

I. Introduction

In the worldwide discussion on reducing CO_2-emissions, the utilization of electric vehicles is considered to be a reasonable approach. Facing the fact that electrically powered vehicles were introduced even before vehicles based on internal combustion engines, and that between 1892 and 1940 they were considerably formative for the development of mobility in many countries, like the USA, the mentioned approach is obvious.

The social acceptance of electro-mobility increases as the capacity of electric vehicle batteries is improved and technical solutions for a short charging time become available. This results in a series of requirements regarding the power demand due to the charging of the electric vehicles, the charging infrastructure as well as their integration in the energy supply systems.

For this reason, the charging of even a few number of electric vehicles may pose a significant additional load on the respective grid section. In the case of a grid load near the nominal capacity by the households and industry or in case of remote low-supply areas, the increased power demand can lead to an overload. In addition, there are restrictions on the disturbances that are introduced into the grid by the fast charging stations. Besides the voltage variations, unwanted harmonics can be emitted into the grid.

Therefore examinations have been carried out to investigate the installation of quick charging stations in remote low-supply areas together with the necessary grid integration. In this context, different concepts for the grid integration of quick charging stations in low-supply regions, for example at motorway service areas have been taken into consideration.

Besides the charging technology and the integration of the electric vehicles into the electrical power supply grid the current discussion deals with the issue of the potential of reducing CO_2- emissions.

In the scope of this paper, different possible applications of electric vehicles with their resulting CO_2 reduction will be discussed and compared to each other. Furthermore, new approaches for the integration of electric vehicles will be introduced, which will allow the charging of electric vehicles primarily from the intermittent energy supply of renewable energy sources. These approaches are validated with the help of simulations.

II. Application Cases and Integration Scenarios

Based on the necessity for mobility of a private person, from the current point of view the application of vehicles can be divided into two categories. The first category of mobility necessity covers first and foremost the application cases of long distances. The classic demand of this vehicle application can be described by carrying four persons plus luggage, traveling at a speed of 120km/h for a distance of 250km [4]. The second category results from the application for transportation duties for local or commuter traffic (driving the children to school, shopping, etc.). In contrast to the first application category the second category allows for partially charging the vehicle battery in between trips during the day without having a negative effect on the driving flexibility.

In contradiction to the above described scenario, when for the first application category the planned traveling distance is larger than the maximum range of the electric vehicle, then an interruption of the trip has to be accepted. In this case a

C. Sourkounis is with the Institute for Power Systems Technology and Power Mechatronics, Faculty of Electrical Engineering and Information Sciences, Ruhr-University Bochum, 44801 Bochum, Germany (e-mail: sourkounis@enesys.rub.de)

N. Becker is with the Institute for Power Systems Technology and Power Mechatronics, Faculty of Electrical Engineering and Information Sciences, Ruhr-University Bochum, 44801 Bochum, Germany (e-mail: becker@enesys.rub.de)

A. Broy is with the Institute for Power Systems Technology and Power Mechatronics, Faculty of Electrical Engineering and Information Sciences, Ruhr-University Bochum, 44801 Bochum, Germany (e-mail: broy@enesys.rub.de)

F. Einwächter is with the Institute for Power Systems Technology and Power Mechatronics, Faculty of Electrical Engineering and Information Sciences, Ruhr-University Bochum, 44801 Bochum, Germany (e-mail: einwaechter@enesys.rub.de)

recharge of the storage system is necessary in order to continue the trip. By using of quick charging stations a 80% recharging an accumulator with a 16 kWh capacity takes about 20 minutes. A recharge process based on the standard charging technology needs up to eight hours. Therefore for the long distance application an acceptance of the electric vehicle can be only reached in combination with quick charging stations.

Under the condition that in the future more and more electric vehicles are designed to support quick charging, the integration of electric vehicles into the electrical grid results in significant requirements. Depending on the integration scenario, there are different load profiles throughout the day, which influence directly the electrical grid.

In principle, the grid perturbation of quick charging station for electric vehicles depends on many different characteristics; the short circuit power of the distribution grid in relation to the power of the charging station and the topology, the switching frequency and the control method of the accumulator charger. Based on the most commonly used concepts for charging stations, the grid perturbations will be investigated and discussed with analytical methods in the next section.

An obvious integration scenario is allowing the electric vehicles to access to the electrical grid and therefore to draw electrical energy for recharging without any restrictions, just like normal private consumers. The result will be that on working days, after office hours the majority of the electric vehicles will be connected to the electrical grid for recharging. Based on this scenario it can be achieved that the CO_2-emissions will be avoided at the location where the vehicles are used, like in city centers or urban agglomerations. At the same time the power demand between 17:00 and 22:00 o'clock will be significantly increased, so that the demand for power reserves in centralized power stations has to be extended in order to meet the power peaks. Furthermore it will be necessary to extend the capacity of the distribution network and depending on the number of electric vehicles even capacity shortages in the transmission grid will evolve.

From a global point of view, the described integration scenario will not really lead to a reduction in CO_2-emission. Furthermore major investments will be necessary to adapt the energy supply infrastructure to the new load profile.

The mentioned investments that are directly linked to the integration of electric vehicles can be avoided, and at the same time the utilization ratio of the energy supply infrastructure can be achieved, if the electric vehicles are integrated into the infrastructure as controlled loads. In this case the charging of the vehicle accumulators is realized in such a way that an even load on the electrical grid can be achieved. The electric vehicles can be charged during night time, while the power demand from the standard consumers, who have first priority, is low. This can be attained either by control signals which start the charging process or by price incentives. The charging stations ("filling stations") have to be able to interpret the control and price signals respectively, and to start the charging process according to the presets. It would be possible to set a maximum kWh-price for charging the accumulator and at what time the charging must to be completed. Thereby the charging will be shifted to time periods with low load on the electrical grid, triggered by the pricing policy.

A different integration scenario, which applies a similar charging procedure for the electric vehicles, targets to basically utilize the energy from renewable sources for charging of the electric vehicles [4], [6], [7]. With an appropriate grid and energy management the charging process can be organized in such a way, that a timely correlation between power availability from renewable sources and the power demand for charging the electric vehicles can be achieved. Therefore it is made possible to even utilize stochastically fluctuating energy sources, like wind energy, for charging. This integration scenario possesses the highest CO_2- reduction potential. At the same time a higher utilization of integrated stochastically fluctuating energy sources can be achieved, especially for decentralized power supply, while it will not be necessary to upgrade the capacity of the grid nor the coupling to the superior transportation grid.

III. Grid Pollution by the Integration of Quick Charging Stations

A. *Charger with Mains Commutated Converters*

The charging devices with mains commutated converters cause harmonics with the frequencies

$$f_\nu = f_N \cdot (6k \pm 1) \quad \text{with } k = 1, 2, 3, \ldots \qquad (1)$$

This results in harmonics with five, seven, eleven, and so on, times the grid frequency f_N.

The amplitude depends on the short circuit power of the grid connection or the grid impedance $Z_{i,N}$ and the size of the additionally installed commutation inductivityies respectively. It can be determined with following equation:

$$I_{\nu L} \cdot \sqrt{2} = C_\nu = \sqrt{A_\nu^2 + B_\nu^2}$$

$$\text{with } A_\nu = \frac{1}{\pi} \int_0^{2\pi} i_L(\omega t) \cdot \cos \nu\omega t \cdot d\omega t \qquad (2)$$

$$B_\nu = \frac{1}{\pi} \int_0^{2\pi} i_L(\omega t) \cdot \sin \nu\omega t \cdot d\omega t$$

Because the wave shape of the branch current does not depend on the control angle α, the relation between the amplitude of the harmonics and the basic frequency stays constant for any duty cycle. Hereafter, at stationary operation of a mains commutated converter the following harmonics can be measured

Under consideration of the compatibility level for urban distribution grids described in [2], the unwanted emission of

$$\hat{I}_{\nu;L} = \sqrt{2} \cdot I_{\nu,L} = \frac{\sqrt{2}}{\nu} \cdot I_{1,L} = \frac{\sqrt{2}}{\nu} \cdot \frac{\sqrt{6}}{\pi} \cdot I_d \qquad (3)$$

harmonics will be judged. Table 1 shows a list of the compatibility levels for different voltage harmonics.

TABLE I
COMPATIBILITY LEVEL $U_{N,VT}$ FOR SINGLE VOLTAGE HARMONICS IN THE LOW VOLTAGE GRID

Ordinal number ν[-]		compatibility level $u_{ν,VT}$[%]
odd, not containing multiples of 3, ordinal numbers	5	6
	7	5
	11	3,5
	13	3
	17	2
	19	1,5
	23	1,5
	25	1,5
	>25	0,2+0,5*25/ν
odd, multiple of 3 ordinal numbers	3	5
	9	1,5
	15	0,3
	21	0,2
even ordinal numbers	4	1
	6	0,5
	8	0,5
	10	0,5
	>10	0,2

By calculating the relation between the voltage harmonic $u_ν$ and the relevant compatibility level $u_{ν,VT}$, a harmonics interference factor $B_ν$ results. It describes the relation between the nominal apparent power $S_{LG,nenn}$ and the short circuit power S_{kV}. for charging devices being operated at a particular coupling point of the grid.

$$B_ν = \frac{u_ν}{u_{ν,VT}} = \frac{k_{Pν}\, ν\, I_{ν,L}}{u_{ν,VT}} \cdot \frac{S_{LG,nenn}}{S_{kV}} \qquad (4)$$

$$\text{with } \angle Z_{iN} \geq 80°$$

With kPν being the harmonics weighting factor (see Table 2). The highest value B_{max}

$$B_{max} = \max\{B_ν\} \quad \text{for } ν = 1...25 \qquad (5)$$

will be considered for the evaluation. According to [2], the necessary $k_{Pν}$-values to calculate $B_ν$ can be taken from table 2.

TABLE 2
VALUES OF FACTOR K_{PN}

ν	3	5	7	11	13	17	19
	0,3	0,1	0,1	0,1	0,1	-	-
	0,4	0,3	0,2	0,1	0,1	0,1	-
	0,6	0,5	0,3	0,2	0,2	0,1	0,1
	0,7	0,7	0,5	0,4	0,4	0,3	0,2
	0,9	0,8	0,7	0,6	0,6	0,5	0,5
	1	1	1	1	1	1	1

The necessary short circuit power of the grid connection point S_{kV} can be determined according to

$$S_{kV} \geq \frac{k_{Pν}\, ν\, I_{νL}}{u_{νVT}} \cdot \frac{S_{LG,nenn}}{B_{max}} \qquad (6)$$

In a similar way, the highest allowable power rating of the charging device at the grid coupling point can be determined.

$$S_{LG,nenn} \leq \frac{u_{νVT} B_{max}}{k_{Pν}\, ν I_{νL}} \cdot S_{kV} \qquad (7)$$

The harmonic interference factor is maximally allowed to amount up to $B_{max} = 0.02$.

B. Charger with Self Commutated Converters

Charging devices with self-commutated rectifier cause harmonic voltage components of different spectra, contrary to charging devices with mains-commutated rectifier; this is directly dependent on the control method. Three different methods can be used for the control of a mains-operated rectifier taking into account the demand for lower mains pollution:

- sine-delta modulation
- space vector modulation, and
- current hysteresis procedure.

In case of sine-delta and space vector modulations, a continuous switching frequency f_p can be selected taking into account the semi-oscillation symmetry as multiple of the basic frequency which corresponds to a mains frequency of 50 Hz, so that the generation of intermediate harmonics is basically avoided. This procedure reduces the demands on the mains-side filter and the height of the short-circuit power at the mains connection point, because the maximal admissible values of the intermediate harmonics are considerably lower than the admissible values of the harmonic components.

Nowadays available electronic switching elements allow for very high switching frequencies as compared with the first harmonic frequency ($f_p/f_1 > 21$), so that the low-frequency harmonic components are suppressed as far as possible. With these procedures, high-frequency harmonic components with ordinal numbers $ν = f_p/f_1$ occur in packages only. Harmonic components of order ν can then be determined according to

$$U_{νWR} = \left(1 + 2\sum_{n=1}^{N} (-1)^n \cos ν\alpha_n\right) \frac{\sqrt{2}}{νπ} U_d \qquad (8)$$

$$\text{with } N = \frac{ν-1}{2} \text{ and } ν = \frac{f_P}{f_1}$$

α_n describes the switching angles within a quarter of the cycle duration. Different to the hitherto described control methods, a switching frequency is not preset in case of the current hysteresis method. A tolerance band around the desired course of the mains current is defined in this procedure. As long as the actual value of the current remains inside the tolerance band, no switching action happens. When the upper limits are exceeded, the “high-side” electronic switch is switched-off in the phase, and the “low-side” switch is engaged, vice versa when the lower limits of the tolerance band are undercut. Since the desired sine shape of the current features different gradients within one cycle duration, the switching frequency varies accordingly. Furthermore, the switching frequency is directly connected with the effective inductivity in the respective phase on the mains side. The tolerance band determines the maximal harmonic component content of the mains current directly, so that an alteration of the short-circuit power of the circuit or of the internal mains impedance or an alteration of the filter impedance would entail a change of the switching frequency accordingly. This makes it necessary to lay out the inductivity of the mains filter in such a way that not too high switching frequencies occur. The switching frequency is limited by the resulting switching losses of electronic switches. The average switching frequency can be derived by the following equation:

$$\overline{U}_d - U_B = i\left(R_K + R_{iN}\right) + \left(L_K + L_{iN}\right)\frac{di}{dt}$$

$$\text{with } R_K, R_{iN} << \Rightarrow \quad Z_{iN} \approx \omega L_{iN}, \quad Z_F \approx \omega L_K \tag{9}$$

$$\Rightarrow \bar{f}_P = \frac{1}{2\Delta t} = \frac{\overline{U}_d - U_B}{2\left(L_K + L_{iN}\right)}$$

From this equation, the dependency of the switching frequency on the internal mains impedance or accordingly the inductivity at the mains connection point and the inductivity of a mains filter, which can be assumed to be an inductance as the first approximation, can be clearly seen. The site-specific layout is necessary because of the direct interrelation between the harmonic component propagation and the internal impedance of the mains connection.

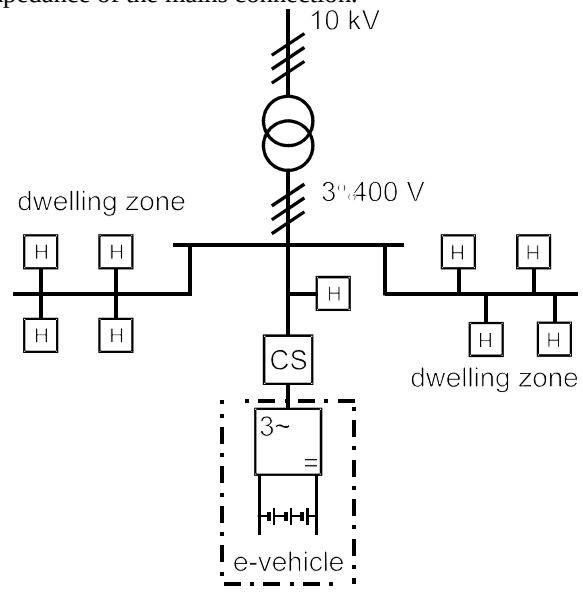

Fig. 1 Grid topology for the simulation examinations

Based on analytical considerations, a number of different scenarios for high power charging of electric vehicles have been examined by means of simulation.

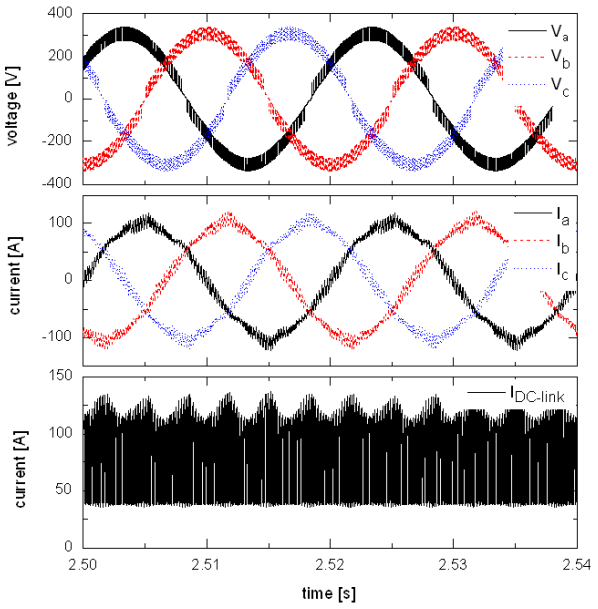

Fig 2 Voltage and current ant connection point

The dynamical behaviour of the low-voltage supply grid and the influence of the high-power charging device on the grid were subject of the examinations.

The applied charging device uses the sine-delta modulation procedure, a classical control method and features advantages with regard to the spectrum of emitted voltage harmonic components. At high switching frequencies (f_p/f_1>21), the first harmonic components occur at a switching frequency with sidebands of lower amplitudes: One disadvantage is that a direct influence on the current ripple is not possible during operation.

A higher short circuit power, and therefore lower internal grid impedance, leads to lower amplitudes of the harmonics [10].

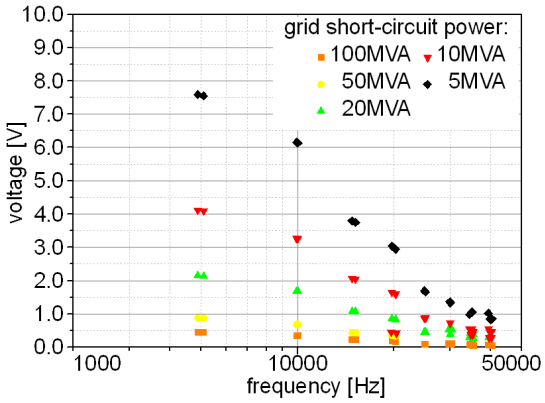

Fig. 3 Harmonics introduced by quick charging station

IV. Integration Scenarios of Electric Vehicles into Decentralized Power Supply Systems

Generally, for the large scale integration of electric vehicles into decentralized power supply systems, avoiding additional power peaks by the charging process and using power from renewable energy sources is the major concern, as described earlier. The first measure, like in centralized power supply systems, is to shift the charging process to time periods with low load on the grid.

As indicated above, this can be realized by means of price incentives, configuration and/or by a central release of the charging station with favourable energy rates. Here the long-term energy supply flexibility is rewarded by an applicable tariff configuration and fixed by contract for certain periods of time. The price incentives which shall have the effect of an adjustment of the consumers to the energy offer without long-term contracting, can be formulated on the basis of prognoses for the energy requirement and the energy supply by renewable energy sources in the long run or as direct reaction on actual condition of the supply net (energy supply and requirement) in the short-run or rather dynamically. Consumers or prosumers can then get this information via the socalled electronic energy maket (e-energy-market) which presumes intelligent meters (smart metering) with information resp. communication interfaces (ICT gateway, Fig. 4).

The prosumer can now connect the devices or in general consumers manually at times of favourable tariffs or by means of programmable reference managements. In the given case of electric vehicles this can be realized by a charging station, which is able to inquire price incentives via ICT-gateway and enter criteria for the start of the accumulator charging.

The particular challenge to use the power from intermittent energy sources (like wind energy, for example) integrated in decentral energy supply systems comprises a considerable contribution to a minimisation of the CO_2-output by electric vehicles. Aggravating in this respect is the fact that the fluctuation of the energy offer of the sources mentioned does not feature a time correlation to the energy requirement (load profile). Generally the energy requirement is at its lowest at night. Therefore it is available for the loading of vehicles, in this case of the electrical vehicles, which is favored by the mentioned decrease in energy requirement of other consumers, like households, trades a.s.o.

At night, fluctuations of renewable energy sources can be utilized on the basis of similar procedures like in the case of alterations in the energy requirements, that means that at high energy availabilities the loading of electric vehicles can be animated temporally by price incentives. Over the day, the availability is differing, varying with the application category, but in any way time-confined for loading and thus for utilization resp. intermediate storage of stochastically fluctuating energy.

A condition for realizing the described scenarios for the integration of electric vehicles in power supply systems is the possibility for quick charging. The integration of quick charging stations, with 50 kW nominal power can load significantly a well constructed electrical grid. Therefore it is necessary to generate technical concepts for the grid integration of quick charging stations in areas with a weak grid infrastructure. Two basic strategies are considered: the hybrid energy supply concept by using an energy storage to support the grid in case of quick charging and the direct energy solution by expanding the grid in concerned areas.

The integration scenarios mentioned have been examined and compared on the basis of simulation procedures.

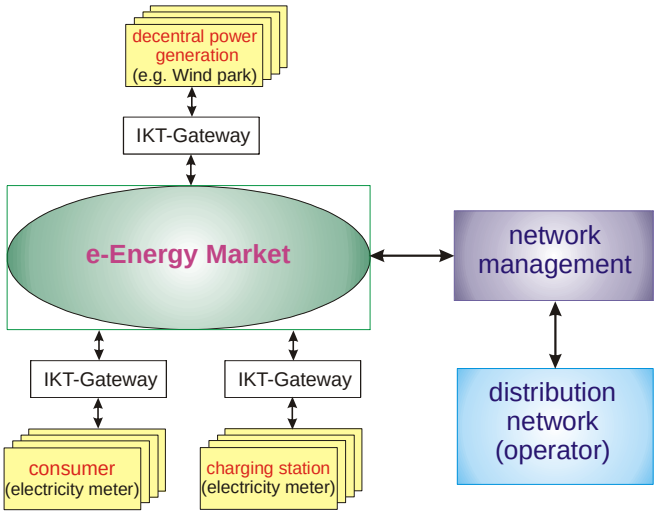

Fig. 4 Integration principle of consumer with energy demand flexibility like electric vehicles

V. Integration of Electric Vehicles in a Model Region

The influence of electric vehicles on the energy supply in a model region has been investigated by simulation on the basis of the already described integration scenarios. These examinations were based on the consumer behaviour of a region consisting of a city with a population of 88.000 people, further surrounding cities with populations of between 10.000 and 20.000 and some smaller villages (Fig.5). The total population of the region amounts to 162.000. This region features an annual load peak of 119 MW. The average annual electrical power demand amounts to 48 MW. The load frequency is shown in Fig. 6. Most of the time a power of 80 MW is consumed from the energy supply grid. Due to high fluctuations in the energy demand part of the electrical energy is fed back into the superposed transmission grid by wind energy converters or rather wind parks installed in that region.

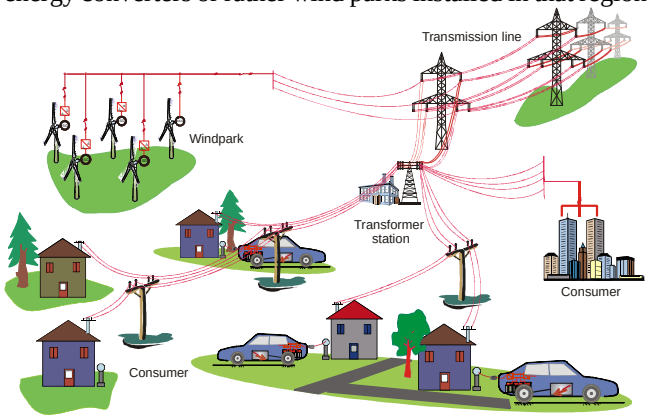

Fig. 5 Integration of electrical cars in a model region with high share of wind energy

A fleet of 6000 electric vehicles has been supposed for the examinations. This equates to approx. 15 %. of the private vehicles of that region. The different power classes have been taken into account when modeling the electric vehicles. This results in a power consumption during charging of between 2 kW and 50 kW per vehicle, depending on the type of vehicle.

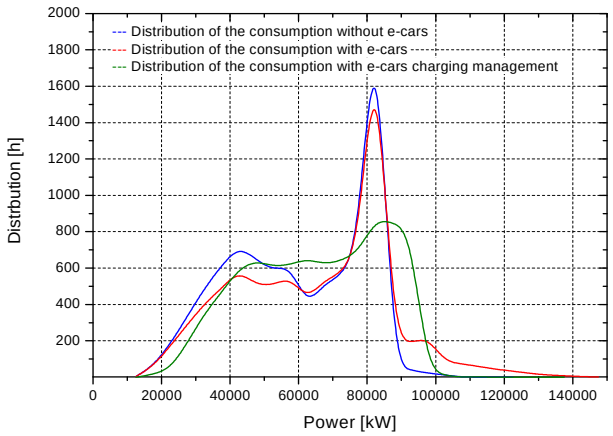

Fig. 6 Frequence distribution of the load (consumption) in the regional distribution network

Initially, the electric vehicles were examined as first priority consumers, that means that the vehicles can be connected to the charging station and loaded at any time. As already mentioned in chapter IV, presumes the scenario that the electric vehicles are charged immediately after work finishing time. This is particularly applicable to the user category with long travelling distances and commuters with vehicles of higher power classes.

The results of the simulation show an increase of the load peaks in the energy supply grid up to 150 MW. That means an increase of at least 25 %.

At the integration scenario featuring a priorization of the electric vehicles recharging at times with high energy availability from renewable energy sources integrated in the energy supply grid and low loads, an increase of the load peaks could generally be avoided in time elapsed of the power demand from transmission line. The distribution of the power consumption shows power peaks of only 108 MW (see Fig. 6).

From this can be derived, that by timely priorisation of the charging process a regional integration of the electric vehicles with a maximal loading capacity of 60 MW in the energy supply infrastructure can be realized without major investments. A timely priorization of the charging procedure can be achieved by long-term and short-term price incentives.

When modeling the integration scenario it has been assumed that the electric vehicles of the application category with long traveling distances can only be recharged during night times (after work closing time till the next morning). This has led to load peaks at early morning times in nights with low energy availability from wind parks, since the vehicles must be fully loaded each morning, for example, to be ready for drives to work [8]. A more exact and more long-term prognosis for the wind energy supply can avoid this deficiency for integration of electric vehicles. In the simulation model a prognosis of 4 hours in advance and an exactness of 10 %. has been implemented.

In both cases for integration of quick charging station, the hybrid energy supply as well as the direct energy supply, it is necessary to analyse the arising expenses. The question in this context is, whether it is economically sensible to use a low-voltage connection, and to relieve the grid by using a flywheel energy storage system, or if a medium-voltage grid expansion is the most economical option.

For economical investigations of quick charging stations installation an already existing low-voltage port is assumed. At this connection point a power of 30 kW is not in use. In case of using a flywheel storage has to be generated that way, so a quick charging station can charge an electric vehicle as fast as possible without exceeding the maximum power of the connection point. In case of a directly power supply from the grid an grid extension to the nominal power of the quick charging station has to be realized.

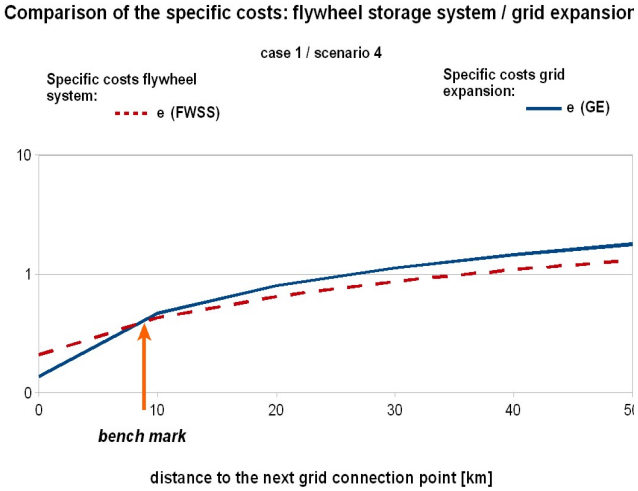

Fig. 7: Comparison of the specific costs of the concepts for the integration of quick charging stations

The hybrid energy supply system entails special fixed investment costs, due to the flywheel system. The variable investment costs depending on the distance to the nearest connection point have a lower impact on the overall cost, because the existence of low voltage connection is assumed. The grid expansion incurred mainly variable investment costs, because mainly the distance to the nearest connection point is crucial. The bench marks in the different scenarios of investigation depend mainly on the applied operating life and the applied rate. The higher the operating life and the higher the applied rate, the longer it is more economical to expand the grid instead of using a energy storage [9].

VI. Conclusion

Different integration scenarios of the large-scale integration by quick charging stations of electric vehicles in existing energy supply systems has been presented and analysed. For the future utilization of electric mobility in everyday life, the technical and economical conditions have been determinated. This means on the one hand, that technical restrictions according to the current available range and the required charging time has to be solved and on the other hand the charging infrastructure needs to be improved.

The examinations proved, that an integration of electric vehicles as first priority consumers - like any other household device - leads to considerable load peaks in the regional energy supply grids and to load peaks over the consumption period from the transmission grid. This necessitates corresponding investments into an expansion of the power capacities of electric power substations.

At the integration scenario featuring a priorization of the electric vehicles charging by long-term and dynamical price incentives recharging at times with high energy availability from renewable energy sources integrated in the energy supply grid and low loads, an increase of the load peaks can generally be avoided in time elapsed of the power demand from transmission line.

VII. References

[1] C. Sourkounis , B. Heusler-Sourkounis, J. Koppe; “Software to Design Autonomous Power Supply Systems Based on Renewable Energies with a Mathematic Optimisation Algorithm Tool” EWEC 2006-European Wind Energy Conference, Athens Greece

[2] A. Soni, C. S. Ozveren; “Improved Control of Isolated Power System by the Use of Feeding Technique”, Proceedings of the 41st International Universities Power Engineering Conference, 2006. UPEC '06. Volume 3, 6-8 Sept. 2006 Page(s):974 - 977

[3] C. Sourkounis, F. Richter, “Increase of the Quality of Energy from Stochastic Fluctuation Sources by Dynamic Power Conditioning” International Journal of Energy Technology and Policy, Vol. 5, No. 3 (2007) pp. 271-279.

[4] T. Engel; “Plug-In Hybrids: Studie zur Abschätzung des Potentials zur Reduktion der CO2-Emissionen im PKW-Verkehr bei verstärkter ds: Studie zur Abschätzung des Potentials zur Reduktion der CO2-Emissionen im PKW-Verkehr bei verstärkter”, Verlag Dr. Hut, ISBN 978-3-89963-327-6

[5] W. Kempton and K. Toru; “Electric-drive Vehicles for Peak Power in Japan”, Energy Policy 2000, 28(1): 9-18

[6] W. Kempton and J. Tomić; "Vehicle to Grid Implementation: from stabilizing the grid to supporting large-scale renewable energy". Journal of Power Sources Volume 144, Issue 1, 1 June 2005, Pages 280-294.

[7] W. Kempton and A. Dhanju, “Electric Vehicles with V2G: Storage for Large-Scale Wind Power”, Windtech International 2 (2), March 2006, pp 18-21

[8] C. Sourkounis,, F. Einwächter.,“Large scale integration of electric cars in decentralised power supply systems” 6th Conference on the promotion of Distributed Renewable Energy Sources in the Mediterranean region (DISTRES 2009), 11-12 Dec. 2009, Nicosia, Cyprus

[9] C. Sourkounis, N. Becker,“Integration of Quick Charging Stations in Power Grids of Weak Infrastructure Areas” Power Options for the Eastern Mediterranean Conference (POEM 2012), 19 - 21 November 2012, Limassol, Cyprus

[10] A. Broy, C. Sourkounis,”Influence of charging electric vehicles and on the quality of the distribution grids”, Electrical Power Quality and Utilisation (EPQU), 11th International Conference on, (Lissabon, Portugal), pp. 01.04.2012, oct.2011.

VIII. Biographies

Prof. Dr.-Ing Constantinos Sourkounis received his Dipl.-Ing and his Dr.-Ing degrees from the TU Clausthal in 1989 and 1994 respectively. After he received his Ph. D. at the Institute of Electrical Power Engineering at the TU Clauthal, he occupied the position of the chief engineer. In 2003 Dr.-Ing. Sourkounis received his habilitation. Since 2003 he is professor at the Ruhr-University Bochum, heading the Institute for Power Systems Technology and Power Mechatronics. His main research areas are mechatronic drive systems, renewable energy sources, decentralised energy systems supplied by renewable energy sources, and energy supply systems for transportation systems.

Dipl.-Ing. Nora Becker received her Dipl.-Ing. from the Ruhr-University Bochum at the faculty of Mechanical Engineering Environmental Technology and Resource Management in 2012. Her majoring is the Environmental Technology and Resource Management with the area of concentration in renewable energies, sustainable energy supply, materials and materials testing and recycling of technical products.

Since October 2012 she is research assistant at the Institute for Power Systems Technology and Power Mechatronics at the Ruhr-University Bochum. Her main research area is the integrated electromobility in the logistics of urban agglomeration areas.

Dipl.-Ing. Alexander Broy received his Dipl.-Ing. degree in Electrical Engineering and information technology from the Ruhr-University Bochum in 2009. Since 2009 he is a scientific coworker at the Institute for Power Systems Technology and Power Mechatronics Research Group at the Ruhr-University Bochum. His main research area is the integration of electric vehicles in decentral supplied distribution grids.

Dipl.-Ing. Frederik Einwächter received his Dipl.-Ing degree in Electrical Engineering and Information Technology from the Ruhr-University Bochum in 2009. Since 2009 he is a scientific assistant at the the Institute for Power Systems Technology and Power Mechatronics at the Ruhr-University Bochum. His main research area is management of decentralized energy systems.

2nd Conference on Power Options for the Eastern Mediterranean Region
07-08 October 2013, Nicosia, Cyprus (Paper No. POEM13/163)

Design Rules for Autonomous Hybrid Energy Supply Systems for Various Types of Buildings in Central Europe

Alexander Broy, Izabella Vasileva, Prof. Dr.-Ing. Constantinos Sourkounis

***Abstract*—The autonomous supply of buildings with renewable energies is a great challenge. The main topic is the link between the demand- und the supply side at any time. Renewable generated electricity is subjected to the natural fluctuation. On the other hand there is the bad predictability of the user. To ensure a secure supply, the use of energy storage systems is required.**
In this paper, a guideline is developed to design an autonomous hybrid system based on renewable energies and an energy storage system for buildings. The guideline is applicable for every type of building and considers the user load. the location with its solar- and wind conditions, as well as economic aspects.

***Index Terms*—Autonomous power supply, hybrid energy supply system, renewable energy supply**

I. Nomenclature

A	Area	$[m^2]$
a	Availability	-
a	Average availability (coverage)	-
A_F	Factor autonomy of the battery	$[Tage]$
c_p	Power coefficient of the wind energy converter	-
C_N	Nominal capacity of the battery	$[kWh]$
E	irradiance	$\frac{W}{m^2}$
E_0	Irradiance at STC	$1000\ \frac{W}{m^2}$
g	Simultaneity factor	-
GA	Annual average of the daily exposure	$\frac{kWh}{m^2}$
G_{dim}	Dimensioning - Irradiation	$\frac{kWh}{m^2}$
I_{MPP}	Maximum Power Point current	$[A]$
I_{sc}	short circuit current	$[A]$
P	Power	$[W]$
P_{total}	Total installed power	$[W]$
P_{pk}	Nominal peak power of the solar cell at STC	$[W]$
PR	Performance Ratio of the pv-plant	-
PR_0	Performance Ratio of the solar cell	-
$P_{pk.opt}$	Optimal peak power (PV - system)	$[W]$
PV	Photovoltaic	-
STC	Standard Test Conditions of P_{pk}	-
t	Time	$h\ ;\ Tag$
U_{MPP}	Maximum Power Point voltage	$[V]$
v	speed	$\frac{m}{s}$
v	Mean speed	$\frac{m}{s}$
W_a	Annual energy demand of the consumer	$[kWh]$
W_d	Daily energy demand of the consumer	$[kWh]$
W_{el}	Theoretical energy yield of the PV - system	$[kWh]$
$W_{a.PV}$	Annual energy yield of the PV - system	$[kWh]$
$W_{d.PV}$	Daily energy yield of the PV - system	$[kWh]$
W_{diff}	difference in yield	$[kWh]$
W_{PV}	Energy yield of the PV - system	$[kWh]$
W_{WEK}	Energy yield of the wind energy converter	$[kWh]$
η	efficiency	-
η_{Batt}	Energy efficiency of the battery	-
η_{rel}	relative efficiency	-
η_{WR}	Efficiency of the inverter	-
ρ	air density	$\frac{kg}{m^3}$
δ	Standard deviation of the irradiation	$\frac{kWh}{m^2}$

A. Broy is scientific coworker with the institute for Power Systems Technology and Power Mechatronics of the Ruhr-University Bochum, Bochum, 44801 Germany (e-mail: broy@enesys.rub.de).

I. Vasileva is master student at the institute for Power Systems Technology and Power Mechatronics of the Ruhr-University Bochum, Bochum, 44801 Germany (e-mail: izabella_86@mail.ru).

Prof.Dr.-Ing. C. Sourkounis is the head of the institute for Power Systems Technology and Power Mechatronics of the Ruhr-University Bochum, Bochum, 44801 Germany (e-mail: office@enesys.rub.de).

II. Introduction

Island-systems or so called off-grid-systems are autonomous power systems that are operation in areas, were no public grid connection is available or the supplied system needs a special voltage or a special frequency.
The design depends on the energy demand, the location of operation and especially on the available energy at this location. The aim is an appropriate combination of the components of an off-grid-system, which provides not only from a technical but also from an economic point of view an optimal result. These systems can have a power range between some kilowatts of to several megawatts.
As energy sources, several energies can be used. In general, there are pv-systems with an additional generator or a combination of different energy producers. In this work only renewable energy sources are considered, but it is to mention that are auxiliary sources such as diesel- or gas engines as generators could be used as well. In general, it can be distinguished between island-system with – and without electrical storage as well as systems supplied by more than one sources. so called hybrid systems. Systems without electrical storage are usually used for irrigation systems for example but are no longer considered in this work. The main objectives of this work are hybrid systems based on renewable sources. The question of the benefits of renewable energy use can be answered relatively easy. First, the renewable supply exceeds the amount of energy that is needed. Another key advantage is the fact that in contrast to conventional (fossil) energy sources, renewable energy sources are inexhaustible and also available everywhere.

III. Hybrid systems Architecture

In addition to the above listed benefits of environmentally friendly, low-emission and low-cost energy, power exclusively generated by the sun - or by wind energy also has its disadvantages.

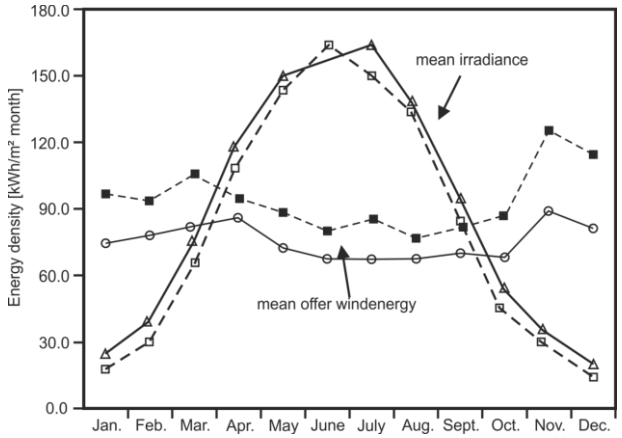

Fig. 1 Monthly mean wind speed and solar irradiance in two different cities (first one dashed lines, second one solid lines)

Thus, for example, at night the sun is not available. Similarly, it is usually windless sunny days and in cloudy winter weather, there is hardly any sun, but strong wind. The interaction of sun and wind, a combination that is ideal for decentralized power supply (Fig. 1).

The main advantage of this combined energy is the increase of the overall performance. Thus, the individual system components, such as an expensive battery system or a solar generator, must not be significantly oversized. It is not only a higher overall system availability achieved, but also a longer backup time of the hybrid system.

A. Hardware design of hybrid systems

The hardware design of a hybrid system is dependent on the needed current and voltage (AC or DC).

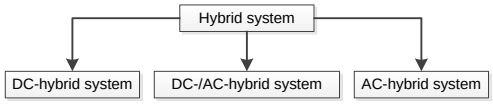

Fig. 2 Classification of hybrid systems according to their construction principle

Here a short introduction to the principal hardware design and their fields of operation are given.

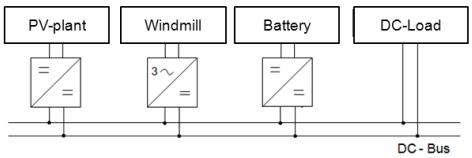

Fig. 3 Example structure of a DC - Hybrid System

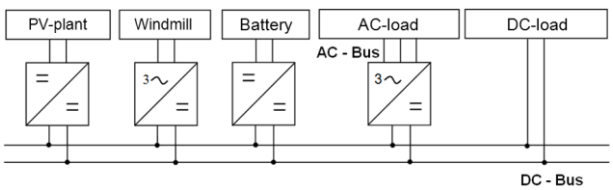

Fig. 4 Example structure of a AC/DC - Hybrid System

DC-hybrid systems are usually used in combination with dc-loads, for example lightning (Fig. 3). The subsystems are connected on the voltage level of the battery system or on the level the DC-load needs.

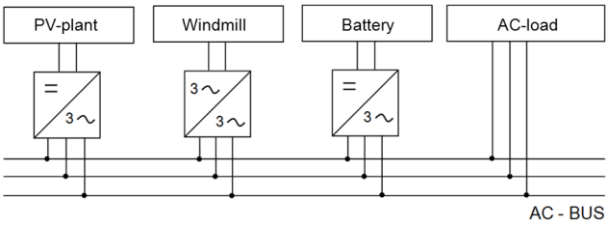

Fig. 5 General block diagram of an AC - hybrid system

AC/DC-hybrid systems have advantages if there are a small number of AC-loads that has to be supplied in combination with DC-loads (Fig. 4).

The concept that is basis for this work is an AC-hybrid system. In this concept, the sub-systems are connected to a 3-Phase AC-Bus (230V/400V). This concept is due to the fact, that in the considered buildings the loads are normal ac-loads, like washing machines and so on, so an AC-hybrid system is the most useful concept.

The coupling of the renewable sources is shown in Fig. 5. Dependent on the actual load balance the energy goes direct to the load or to the battery. in the case of more load than generated power, there is an additional feed from the battery.

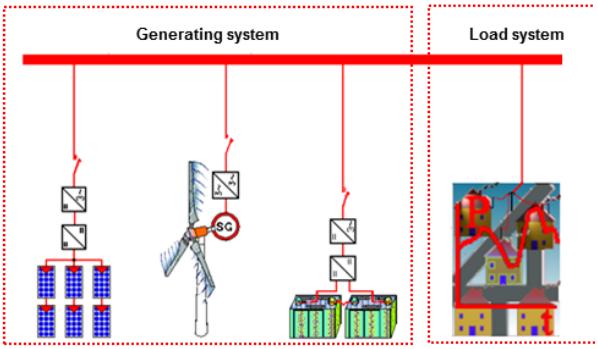

Fig. 6.. Overview considered concept

IV. Concept to replicate the load side

The consumption behavior of a household and a supermarket is different fundamentally. While the power consumption in a supermarket on the day (and consequently over the week and throughout the year) remains almost constant, the energy requirements of a household is very unsteady. This irregularity is expressed in high load spikes that typically occur in the morning, in the afternoon or in the evening hours and is caused by factors such as, for example, number of persons in the household, electrical equipment and user behavior.

In a supermarket, the power consumption is mainly dominated by the freezers and artificial lighting. Due to the uninterrupted operation of the refrigeration systems during weekdays and on weekends, the results in the mentioned constancy power consumption. Lighting, which is not necessarily on at night or on Sundays drops, based on the annual load curve is negligible.

The load curve and the expected energy demand of loads is a deciding factor for the dimensioning of the generation side and related components and subsystems. A general statement regarding the typical energy consumption is impossible at this point of the discussion. This is why the

knowledge of the specific load profile of the consumer or the load systems is of great importance.

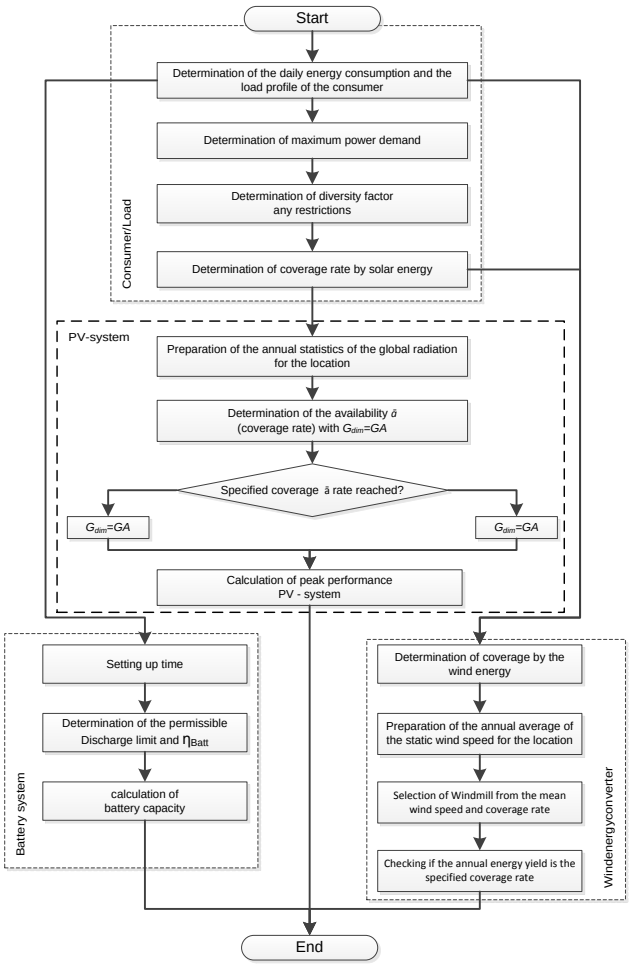

Fig. 7 Flowchart of the decision process

The decision process starts with the calculation of the load system. There are load profiles provided by the BDEW (National association of energy providing companies) but these profiles are made for estimation of the load flow for to steer centralized power plants. These curves are averaged over several households, so these profiles are not usable for the case of single supply.

$$W_d = \sum_{i=1}^{n} W_{di} = \sum_{i=1}^{n} P_i \cdot t_i \qquad (1)$$

Equation (1) describes the general need for electrical energy over the day.

TABLE I
DAILY DEMAND FOR ELECTRICAL POWER (2 PERSON HOUSEHOLD)

Device	No.	Power [W]	operating time [h]	energy demand [Wh/d]
Freezer (30 p.c. compressor runtime)	1	65	7.5	487.5
coffee machine	1	900	0.123	153
Washing machine (60°)	1	1400	1	1400
Dishwasher	1	1600	1	1600
TV	1	80	4	320
Radio	1	60	1	60
Cooker (2 plates)	1	4000	2	8000
Energy saving lamp	7	15	10	150
Results				**12171**

The energy demand is a key value for the design of the energy generation- and storage systems, the maximum value is the basis for the calculations.

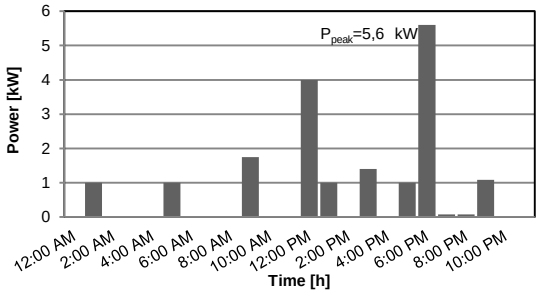

Fig. 8 Specific load-curve of a 2-person household

In fig. 8 and fig. 9 the load curves for the two examples are presented. For the household, the typical maximum (peak demand) is between 5 and 7 pm. The peak value has to be considered for the design of the inverter. The simultaneity factor takes account into the percentage of total installed capacity, which is required at the same time.

$$g = \frac{P_{peak}}{P_{total}} \qquad (2)$$

With the total installed load (P_{total}=8.21 kW). g=0.68. That leads to the consequence that the inverter usually is in part load operation. This leads to a reduced efficiency. For autonomous supplied households, a reduction of the peak power demand is recommended. This can achieved by a load management and/or by the choice of the technical devices.

TABLE II
DAILY DEMAND FOR ELECTRICAL POWER (SUPERMARKET)

Device	No.	Power [W]	operating time [h]	energy demand [kWh/d]
Island freezer	2	400	21	16.8
Frezzer (standalone)	4	245	16	15.7
Frezzer (wall cabinet)	6	600	16	57.6
Fluorescent light	100	38	12	45.6
Klima and ventilation	6	200	8	9.6
Results				**145.3**

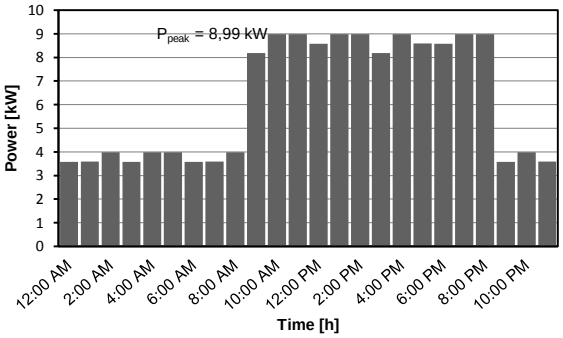

Fig. 9 Specific load-curve of a supermarket

In Fig. 9 is shown the load curve of the supermarket. The power demand is constant, the rise at 8 am. And the drop at 8 pm is due to the light that is enabled during the opening time. The simultaneity factor is g = 0.86. The load curve is nearly constant, so the inverter will operate with a high efficiency.

A. PV-System

After paying attention to the load system, according to the flowchart in fig. 7, the design of the PV-system has to be done. First of all, the location and its global irradiation has to be considered. The example city that are the basis for the two example system designs is Alghero, Italy.

Month	Global irradiation [kWh/m²d]
January	1.91
February	2.53
March	3.81
April	5.32
May	6.23
June	6.98
July	7.46
August	6.65
Septem-ber	5.31
October	3.53
November	2.21
December	1.65

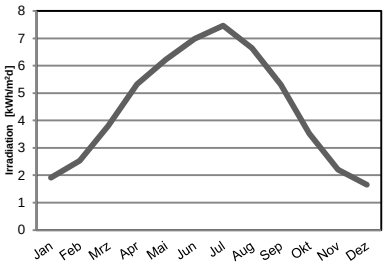

Fig. 10 Global irradiation of Alghero. Italy

To calculate the availability of the PV-system, the annual average of the daily exposure has to be calculated:

$$GA = \frac{1}{n} \cdot \sum_{i=1}^{n} G_i \tag{3}$$

$$\delta^2 = \frac{1}{n-1} * \left(\sum_{i=1} G_i^2 - n \cdot GA^2 \right) \tag{4}$$

The daily irradiation is GA = 4.46 kWh/m² and the standard deviation can be calculated by (**4**) to δ=2.12 kWh/m². The photovoltaic system is designed for a known dimensioning radiation. Hence the availability of the system depends on the daily irradiation levels. In the case that. for example, the dimensioning irradiation greater than or equal to the daily exposure, the system availability is 100 p.c.. Now, the calculated values of the average daily exposure and the standard deviation are used in the calculation of the average availability:

$$\overline{a}\ GA.\delta\ = 1 - \frac{1}{\overline{2\pi}} \cdot \frac{\delta}{GA} \tag{5}$$

For systems, that has to realize a full year operation only supplied by a pv-system, the average availability should be increased from 81 p.c. to 90 p.c.. In combination with a storage system this would be a robust and seamless energy supply over the whole year.

In case of a hybrid supply system, 90 p.c. for a PV-system would be oversized. In the question about the relation of the sun and wind share there is no unique preferred solution.

However, there is a useful benchmark of the solar share in the design of such hybrid system. It depends on the location and varies consequently. The useful guideline value of solar share for the selected location is 60 p.c..

In this regard. the irradiation optimum dimensioning is calculated:

$$G_{dim}\ a\ = GA \cdot \left(1 - \frac{a - 1 + \frac{\delta}{GA \cdot \overline{2\pi}}}{\frac{1}{2} - \frac{\delta}{GA \cdot \overline{2\pi}}}\right) \tag{6}$$

$$G_{dim}\ a = 60\%\ = 7.46\ \frac{kWh}{m^2 d}\ \textit{(household)} \tag{7}$$

A PV - system can provide the following energy over a day:

$$W_{el} = \int_d P_{max}(t)dt \tag{8}$$

Based on the definition of peak performance basis, it can be obtained:

$$W_{el} = \int_d \frac{P_{pk}}{E_0} \cdot E(t) \cdot \eta_{rel}(t)dt \tag{9}$$

Therewith P_{pk} defined as peak power according to the standard test conditions (STC according to DIN EN 60904-3). The relative efficiency of silicon - cells differs depending on the cell technology. In this work amorphous silicon-cells with the value of 0.92 are considered. In addition to that, the efficiency of the inverter has to be considered (η=0.96).

$$P_{pk.opt} = \frac{E_0 \cdot W_d}{G_{dim} \cdot \prod_i \eta_i} \tag{10}$$

Now the optimal peak power under consideration of the efficiencies and the power demand can be calculated. 30 modules of the type Millenia 50MV (BP Solar) are enough to deliver the demanded peak power in case of the household ($P_{pk.opt}$= 1.5 kW).

In case of the supermarket, $P_{pk.opt}$ is calculated to 23.8 kW. The pv-system is much bigger and consists of 180 moduls (Eurosolare PL 120A parallel).

$$W_{d.PV} = GA \cdot \frac{P_{pk.opt}}{E_0} \cdot \prod_i \eta_i \tag{111}$$

$$W_{a.PV} = \sum_{i=1}^{n=12} W_i \tag{12}$$

According to (11) the daily produced energy can be calculated. (12) delivers the yearly produced amount (32693 kWh). This value is higher than the 60 p.c.. The difference is high enough to charge the battery system during operation.

B. Windmill

The dimensioning of the WEC is based on the energy the windmill has to deliver over the year with respect to the mean wind speed at the location.

Month	Mean Wind speed [m/s]	energy density [kWh/m²d]
January	5.4	2.32
February	5.41	2.34
March	5.36	1.12
April	4.23	1.12
May	3.38	0.55
June	3.89	0.84
July	3.89	0.84
August	3.81	0.78
September	3.81	0.79
October	3.51	0.62
November	4.6	1.4
December	5.2	2.46

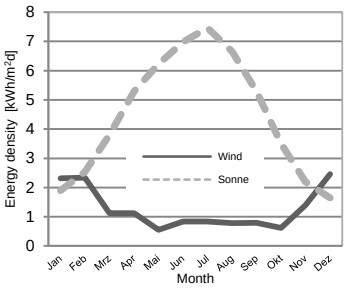

Fig. 11 Annual curve of the mean daily wind- and solar energy density. Alghero. Italy

In fig. 11 the complementary character of wind- and solar energy density can be seen. In the winter season, the wind energy rises and in the summer season the solar energy has its maximum.

In the sub-chapter above, it was described to provide

60p.c. by the pv-system. According to this, the wind-system has to provide 40 p.c. In case of the household the power the windmill has to provide is W_{wek}=1773 kWh/year. With respect to the mean wind speed over the year (4.5 m/s), two small wind turbines (for example AD REM 500W) can be chosen.

TABLE III
POWER VALUES OF THE AD REM 500W WINDMILL (HOUSEHOLD)

Wind speed [m/s]	P_{Wind} [W]	P_{WEK} [W]	c_p [-]
1	48	0	0
2	385	0	0
3	1299	200	0.15
4	3079	500	0.16
5	6013	1000	0.17
6	10391	1770	0.17
7	16500	2590	0.16
8	24630	3393	0.14
9	35069	4776	0.14
10	48106	6151	0.13
11	64029	7500	0.12
12	83127	8000	0.10
13	105688	8000	0.08
14	132002	7983	0.06
15	162357	7984	0.05
17	236344	7989	0.03
18	280553	7986	0.03
19	329957	7984	0.02
20	384846	7989	0.02

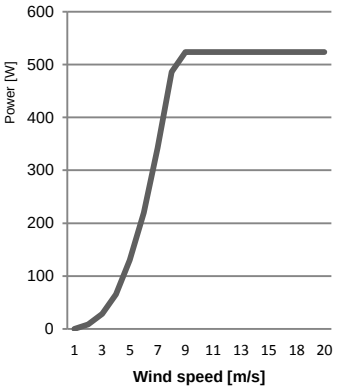

Fig. 12 Power curve in relation to the wind speed

$$P_{WEK} = \frac{1}{2} \cdot \rho \cdot A \cdot v^3(t) \cdot c_p \quad (8)$$

$$W_{WEK} = \int_0^t P_{WEK}\ t\ dt \quad (9)$$

With equation (8) and (9) the monthly generated energy can calculated (Table IV).

TABLE IV
MONTHLY ENERGY YIELD OF CONSIDERED WINDMILLS

	AD REM 500W	**Windspot 7500**
Month	**energy yield [kWh/month]**	**energy yield [kWh/month]**
January	138	1279
February	130	1178
March	120	1290
April	85	687
May	42	391
June	51	556
July	55	665
August	49	635
September	44	576
October	37	468
November	84	1011
December	117	1392
Result	**952**	**10128**

In case of the household, the windmill, the produced power over the year is 952 kWh. Two of these small windmills are enough to produce the demanded 40 p.c..
In case of the supermarket, the small windmill is not enough to produce the needed 40 p.c. (20227 kWh) during the year.

In this case, a windmill has to be chosen that has more power. To deliver the demanded energy over the year, two of the Windspot 7500 are needed.

TABLE V
POWER VALUES OF THE WINDSPOT 7500 (SUPERMARKET)

Wind speed [m/s]	P_{Wind} [W]	P_{WEK} [W]	c_p [-]
1	48	0	0
2	385	8	0.021
3	1299	28	0.022
4	3079	65	0.021
5	6013	130	0.022
6	10391	220	0.021
7	16500	342	0.021
8	24630	486	0.020
9	35069	524	0.015
10	48106	524	0.011
11	64029	524	0.008
12	83127	524	0.006
13	105688	524	0.005
14	132002	524	0.004
15	162357	524	0.003
17	236344	524	0.002
18	280553	524	0.002
19	329957	524	0.002
20	384846	524	0.001

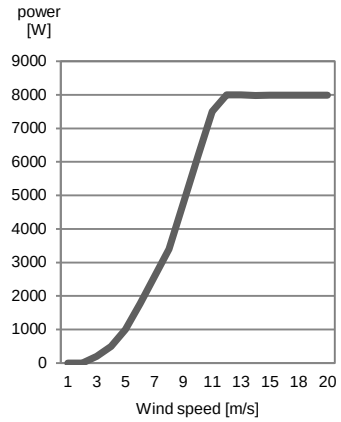

Fig. 13 Power curve in relation to the wind speed

C. Dimensioning of the storage system

When selecting a suitable type of battery in addition to its function (storing the produced energy and compensation of the energy availible), the cost aspect plays a big role. In order to achieve an economic operation, it is important to pay attention on the efficiency, the cost per kWh and especially on the investment costs (10% - 40% of total costs).

TABLE VI
COMPARISON OF KEY CHARACTERISTICS OF VARIOUS ACCUMULATOR TYPES

	Lead	NiCd	Lithium–Ionen
energy density [Wh / l]	50 … 110	80 … 200	250 … 500
energy density [Wh / kg]	25 … 50	30 … 70	95 … 200
Cell voltage [V]	2	1.2	3.6
Charge / discharge cycles	500 … 1500	1500 … 3000	500 … 10000
Operating temperaturer [°C]	0 … 55	- 40 … 55	- 20 … 55
Self-discharge rate [% / month]	5 … 15	20 … 30	< 5
Efficiency [%]	70 … 85	60 … 70	70 … 90

In this work, lead-acid batteries were used. Today, these are the most commonly used battery type in hybrid systems. due to the costs. Nickel-Cadmium batteries with the same energy storage capacity are about 3 to 5 times more expensive than lead-acid batteries. Another disadvantage of the NiCd - Accumulators is a so-called memory – Effect. These characteristics are very unfavorable for the use of this accumulator type in the Off Grid applications.

Lithium - Ion - batteries have significant advantages such as high cycle strength, durability and above all significantly higher energy density than conventional lead-acid batteries. However, these are rarely used in Off Grid applications due to the high price.

When doing the battery dimensioning, in addition to the energy demand of the consumer, the so-called autonomy time (factor) plays a major role. The autonomy time is the number of days in which the consumer is completely powered by the battery (eg bad weather). Thus, the autonomy time is a decisive factor for the availability of the overall system. The size of the battery capacity is proportional to the autonomy factor and therefore takes an immediate impact on the investment costs. How big the autonomy factor should be selected epends on the required system availability and the location. Different backup times are recommend-

ed for different latitudes. Another critical factor is the charging efficiency of the battery. The amount of energy needed to charge the rechargeable battery is greater than the amount of energy got during unloading. The charge efficiency is the ratio of the two energy amounts. In addition, it should be noted that the allowed discharge limit of the battery is 20%. Ie, the usable capacity of the battery is 80%. This is taken into account with the factor 0.8 in the calculation of the required battery capacity.

$$C_N = \frac{A_F \cdot W_d}{\eta_{Batt} \cdot 0.8} \tag{13}$$

(13) describes the needed battery capacity. The recommended autonomy time is 8 days. This leads to a needed capacity of 152.5 kWh for the household and 2.3 MWh in case of the supermarket. in case of the supermarket. the autonomy factor is chosen higher to increase the overall system availability.

V. Simulation Invetigations

Now the theoretically obtained results are checked for their applicability using a simulation program. The simulation was performed for the whole year. The parameters set in the simulation program for the individual system components were described in the previous chapters. The following tables illustrate the simulation results for a household and a supermarket. The monthly energy yields of both renewable energy sources. their sum and monthly consumer values are shown in Table VII and Table VIII.

TABLE VII
ENERGY BALANCE OF THE HOUSEHOLD OVER THE YEAR

Month	PV-system [kWh]	Wind-mill [kWh]	Sum [kWh]	Load [kWh]	Batterie [kWh]
January	120.52	259.07	379.59	376.34	3.25
February	136.79	214.27	351.06	339.92	11.14
March	180.51	221.57	402.08	376.34	25.74
April	254.55	128.36	382.92	364.2	18.72
May	306.35	72.31	378.66	376.34	2.32
June	329.97	78.56	408.53	364.2	44.33
July	337.42	83.33	420.75	376.34	44.41
August	323.96	62.87	386.84	376.34	10.50
September	286.18	80.54	366.71	364.2	2.51
October	219.23	80.10	299.33	376.64	-77.31
November	151.81	170.08	321.89	364.2	-42.31
December	127.27	259.73	386.99	376.64	10.35
Sum	**2774.57**	**1710.79**	**4485.36**	**4431.70**	**53.66**

TABLE VIII
ENERGY BALANCE OF THE SUPERMARKET OVER THE YEAR

Month	PV-system [kWh]	Windmill [kWh]	Sum [kWh]	Load [kWh]	Batterie [kWh]
January	1380.3	2613.0	3993.3	4319.79	-326.4
February	1509.1	2380.0	3889.1	3878.52	10.6
March	2100.7	2421.0	4521.7	4259.79	261.9
April	2896.5	1362.7	4259.3	4172.7	86.6
May	3540.8	785.9	4326.8	4319.79	7.1
June	3880.7	1017.4	4898.2	4112.7	785.6
July	4022.5	1028.9	5051.4	4319.79	731.7
August	3753.5	1039.5	4793.0	4319.79	473.3
September	3072.038	1060.244	4132.2	4112.7	19.6
October	2125.343	1580.518	3705.8	4319.79	-613.9
November	1614.271	1925.866	3540.1	4172.7	-632.6
December	1125.933	2685.964	3811.8	4259.79	-447.9
Sum	31022	19901	50923	50568	258.5

In the simulation, the coverage rate of the PV-system is a little bit higher (62 p.c.), for the wind-system a little bit lower (38 p.c.) than the design value. This can be explained by the fact that for the calculation, the statistic mean values are considered; the simulation is working with random values and stochastic fluctuations. In the simulation, the temperature rise of the PV-modules is considered, in the calculation only in the overall efficiency.

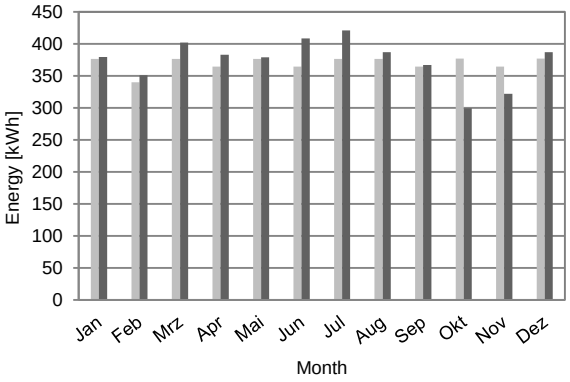

Fig. 13 Correlation between energy production and consumption for the household (light grey: load; dark grey production)

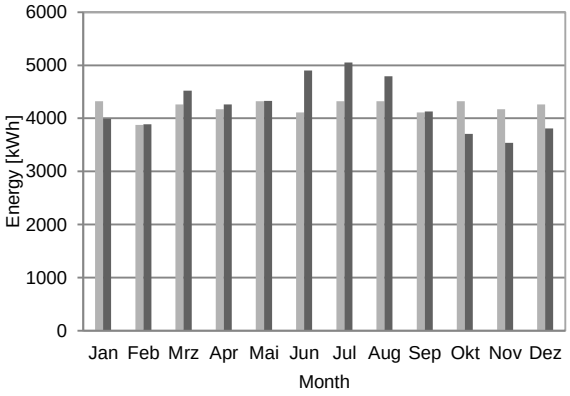

Fig. 14 Correlation between energy production and consumption for the supermarket (light grey: load; dark grey production)

VI. Conclusion

In this work, a directive to design of a hybrid system for autonomous energy supply has been developed. It was shown that it is possible to supply different types of buildings (according to different requirements) with renewable energy sources by using a hybrid system (consisting of PV – plant, wind energy converter and a storage system) year-round self-sufficient with energy. The load profiles and energy requirements of both building types were analyzed and set as the basis for sizing the generator side. With subsequent simulation of expected results were identified and thus the proof of the applicability of the theoretical results was provided.

VII. References

Books:

[1] Z. Mohr, Zukunftsfähige Energietechnologien für die Industrie: technische Grundlagen,Ökonomie, Perspektiven, Berlin Heidelberg: Springer, 1998.

[2] H. Häberlin, Photovoltaik : Strom aus Sonnenlicht für Verbundnetz und Inselanlagen, Fehraltorf: Electrosuisse, 2. Edition, 2010.

[3] U. Rindelhardt, Photovoltaische Stromversorgung, B.G. Teubner, 1. Edition, 08/2001.

[4] S. Karamanolis, Photovoltaik: Schlüßeltechnologie der Solarenergie, Weilheim i. OB: E. Karamanolos, 2009.

[5] A. Wagner, Photovoltaik Engineering: Handbuch für Planung, Entwicklung und Anwendung, Berlin-Heidelberg: Springer, 3. Extended edititon, 2010.

[6] V. Quaschning, Regenerative Energiesysteme: Technologie-Berechnung-Simulation, Munich: Hanser; 8., Extended Edition, 2013.

Papers from Conference Proceedings (Published):

Broy, A. & Sourkounis, C., Management strategies for an existing energy supply system based on wind energy untilization and a hydro-pumped storage station, in 1st Conference on Power Options for the Eastern Mediterranean Region (POEM), (Limassol, Cyprus), pp. , 2012.

.

VIII. Biographies

Dipl.-Ing. Alexander Broy received his Dipl.-Ing degrees from the Ruhr-University Bochum in 2009. He is scientific coworker with Institute for Power System Technology and Power Mechatronics at the Ruhr-University Bochum. His main research area are mechatronic drive systems of wind energy converters.

M.Sc. Izabella Vasileva received her degree from the Ruhr-University Bochum in 2013. Her master thesis was the development of the design rule for hybrid supply systems.

Prof. Dr.-Ing Constantinos Sourkounis received his Dipl.-Ing and his Dr.-Ing degrees from the TU Clausthal in 1989 and 1994 respectively. After he received his Ph. D. at the Institute of Electrical Power Engineering at the TU Clauthal, he occupied the position of the chief engineer. In 2003 Dr.-Ing. Sourkounis received his habilitation. Since 2003 he is professor at the Ruhr-University Bochum, heading the Institute for Power System Technology and Power Mechatronics. His main research areas are mechatronic drive systems, renewable energy sources, decentralized energy systems supplied by renewable energy sources, and energy supply systems for transportation systems.

2nd Conference on Power Options for the Eastern Mediterranean Region
07-08 October 2013, Nicosia, Cyprus (Paper No. POEM13/165)

Storage solutions for power quality problems of the distribution network

Andreas Poullikkas, Savvas Papadouris, George Kourtis and Ioannis Hadjipaschalis

Abstract-- **In this work, a prediction of the effects of introducing energy storage systems on the network stability of the distribution network of Cyprus and a comparison in terms of cost with a traditional solution is carried out. In particular, for solving possible overvoltage problems, several scenarios of storage units' installation are used and compared with the alternative solution of extra cable connection between the node with the lowest voltage and the node with the highest voltage of the distribution network. The results indicated that the performance indicator of each solution depends on the type, the size and the position of installation of the storage unit. Also, as more storage units are installed the better the performance indicator and the more attractive is the investment in storage units. The best solution, however, still remains the alternative solution of extra cable connection between the node with the lowest voltage and the node with the highest voltage of the distribution network, due to the lower investment costs compared to that of the storage units.**

Index Terms—**Batteries, distribution network, overvoltage, power quality, storage.**

I. Introduction

According to the European Union (EU) Directive 28/2009/EC [1], Cyprus as an EU Member State has an overall target that the share of energy from renewable sources in gross final consumption of energy by 2020 will be 13%. In order to accomplish this target, Cyprus has established a national renewable energy action plan on how to reach this target. Based on this action plan [2], there is the need of large integration of photovoltaic (PV) systems in the distribution network.

The large integration of PV systems and other distributed energy resources (DER), like small wind turbines, in the distribution network will produce a number of power quality problems, such as overloading of network components, overvoltage and undervoltage situations, voltage dips and harmonic distortion. The network problems can be solved by using storage systems, like batteries and flywheel systems, in combination with power electronics (i.e., the use of inverters) and energy management systems [3].

In this work, a prediction of the effects of introducing energy storage systems on the network stability of the distribution network of Cyprus and a comparison of these storage systems in terms of cost with a traditional solution in the local network infrastructure is carried out. In particular, the structure of the Cyprus distribution network is described and the PLATOS software tool [3], which was used for the comparison, is presented. In order to investigate the possible overvoltage effects in the distribution network of Cyprus, on both a technical and economical point of view, several scenarios of storage units' installation are used and compared with the alternative solution of extra cable connection between the node with the lowest voltage and the node with the highest voltage of the distribution network. For the comparison, a case study of a typical low voltage (LV) distribution feeder of Cyprus is used.

In section II, the Cyprus distribution network is described. The PLATOS software tool is presented in section III, whereas the simulation results, which include the case study, the investigated scenarios, the input data and the discussion of the results, are provided in section IV. Finally, the conclusions are summarized in section V.

II. The Cyprus distribution network

The power system is typically hierarchical and is divided by functional areas depending on the voltage levels. These levels, which are the transmission network, the high/middle voltage (HV/MV) substations, the MV distribution network, the MV/LV transformer substations and the LV network, are shown on Fig. 1.

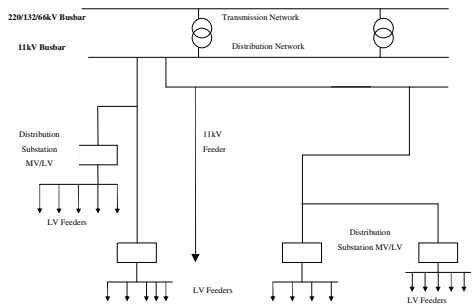

Fig. 1. Hierarchical structure of the electricity network

The distribution network in Cyprus is designed and constructed according to the international common practice and maintained to high levels of performance and efficiency. The network configuration in the urban areas is designed in ring configuration allowing interconnection between the MV feeders having multiple connections to other points of

This work has been partially funded by the by the Sixth Framework Program of Research and Development of the European Union, Contract No: SES6-CT-2007-038665.

A. Poullikkas is with American University of Sharjah, P.O. Box 26666, Sharjah, UAE and with Electricity Authority of Cyprus, P.O. Box 24506, 1399 Nicosia, Cyprus (e-mail: apoullik@eac.com.cy) (corresponding author).

S. Papadouris is with Electricity Authority of Cyprus, P.O Box 24506, 1399 Nicosia, Cyprus (e-mail: spapadou@eac.com.cy).

G. Kourtis is with Electricity Authority of Cyprus, P.O Box 24506, 1399 Nicosia, Cyprus (e-mail: georgekourti@eac.com.cy).

I. Hadjipaschalis is with Electricity Authority of Cyprus, P.O Box 24506, 1399 Nicosia, Cyprus (e-mail: ioannishadjipashalis@eac.com.cy).

supply. Radial connection is limited to long, mainly rural lines with isolated load areas. Most of the connection points are normally open allowing supply only from one point at a time, but easily can be closed in order to provide alternative point of supply if this is needed or required due to contingency. In urban areas the MV network is usually facilitated with underground construction utilizing cables and indoor substations, while for the LV network there is a mix of overhead line construction utilizing wooden poles and wire conductors and underground construction with cables. In rural areas, the overhead constructions are employed for both the MV and the LV network. The underground substation break point switches used in ring main units of the MV network are either oil-insulated or gas-insulated and those break points of the overhead network are usually of D-Fuse type that can be connected or disconnected on-load. Air-brake isolators and auto-recloser units are increasingly installed also, in overhead arrangements. EAC is in line with all recent developments in the modern distribution network practices and tries to adopt all the new developments in the area [4].

EAC utilizes analytical software tools like DigSilent [5], in order to perform the design and expansion of the distribution network. The voltage drop and the loading of the conductors are among the key factors that are taken into consideration for expansion of the network. Regarding the voltage drop, especially in long MV feeders in which voltage cannot be regulated using the tap changer of the transformers, EAC used to install voltage regulators. This was not considered as an effective measure, thus now EAC introduces higher MV distribution voltage (22kV) in order to reinforce the network and also reduce the losses, thus effectively eliminating the problem of voltage drop. Regarding the maximum current in conductors, EAC derives its annual network expansion based on the findings of software analysis studies which employ actual measurements taken throughout the year from the network. Just to outline some limits regarding the current in conductors, EAC performs expansion in a region of the distribution network, when a MV feeder is loaded near to 70% of its rated capacity, when a distribution substation is loaded near the 70% of its rated capacity and when a MV feeder is connected to more than 8-10 distribution substations. The LV feeders are reinforced when they reach the 60% of their rated capacity.

EAC regularly performs power quality examinations with frequent monitoring of the supply. The observations show that the power quality of the supply in the grid is within the normal operating parameters. Since in Cyprus there is only light industry there are no serious issues on the power quality of the supply. In the unlikely event that a discrepancy occurs related to power quality issues, immediate corrective measures are taken to resolve the issues. In a number of limited cases some problems occurred related to voltage dip and voltage drop situations which easily have been eliminated with the necessary reinforcement of the distribution grid. On the other hand, in a few cases harmonics distortion has been identified in the power supply of large commercial consumers which has been corrected with the installation of suitable power supplies [4].

III. The PLATOS software tool

In order to predict the effects of introducing energy storage systems on the network stability of the distribution network of Cyprus and make comparisons in terms of cost with a traditional solution in the local network infrastructure, the PLATOS software tool has been used for all simulations. This tool, which was produced within the GROW-DERS project [5] by the project partner KEMA, is a planning tool for optimization of modular storage applications in power systems and it was programmed in DigSilent PowerFactory by using DPL modeling language [6]. The optimization concerns the location, type and size of modular storage systems as a combinatorial problem with many possible solutions. The combinatorial problem is solved by the application of an artificial evolution, in particular using a genetic algorithm, as illustrated in Fig. 2, by following the steps (a) create random solutions, (b) analyze all solutions, (c) select the best solutions, (d) create new solutions based on the best ones and (e) if the performance convergence objective is not satisfied go to step (b).

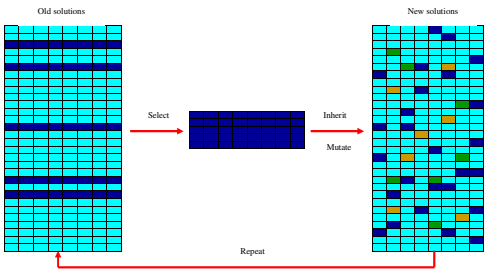

Fig. 2. Genetic algorithm process

For the simulations the following input data is required, (a) load patterns, (b) component data, (c) network topology, (d) generation patterns, (e) number, location and size of fixed storage units, (f) power system components to be monitored, (g) data required for assessment of solutions, (h) number of storage systems, (i) type of storage systems, and (k) size of storage systems. Also, the solution spaces could be defined by the user with the (a) desired number of solutions to be investigated, (b) extent of each solution space, (c) optimization objectives, (d) simulation period, and (e) data required for solution assessment.

As illustrated in Fig. 3, PLATOS tool automatically assesses the alternative solutions to the network problems, such as other tap changer settings, replacement of the power connections or additional power connections. The result of this assessment is used as a starting point for the assessment of the storage based solutions. Then the PLATOS automatically generates the storage solutions, which are influenced by the calculated performance indicator of the previous solutions and rejects the bad solutions (i.e., solutions that have too high investment costs, too small storage capacity, too small and too large charging and discharging power).

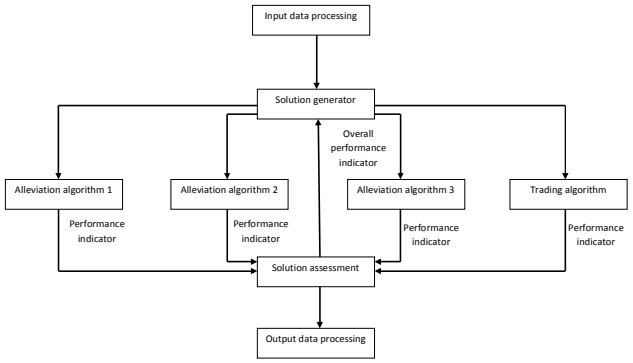

Fig. 3. Basic design of optimization model

In the case of overload, undervoltage and/or overvoltage in a LV distribution network, the overload and voltage alleviation algorithms of the software automatically determine the overload locations and overload severity or the locations with undervoltage and/or overvoltage conditions, the required storage capacity to solve the overloading or voltage problems, the power setpoints for storage inverters by taking into account operating constraints (minimum and maximum state of charge), and the performance indicator by taking into account the (a) effect of storage on overload or voltage, (b) investment costs, (c) energy losses, and (d) user storage cycles.

In order that the PLATOS tool finds the optimum solution, a performance indicator is used as an objective function, which takes into account the costs and benefits of a particular solution and it is expressed as the net present value (NPV) of the storage system, which is the value of all future cash flows discounted in today's currency. The costs include investments and operational costs, such as network losses and charging/discharging cycles. The benefits include the improvement of voltage quality, the decrease of overloading levels and the avoided claims or penalties. The results of the PLATOS software include (a) optimal locations of storage systems, (b) optimal number and type of storage systems, (c) required specifications for storage systems, (d) optimal set points for storage systems, and (e) performance indicators for each storage management algorithm [3], [7].

IV. Simulation Results

For the investigation of the possible overvoltage effects in the distribution network of Cyprus, on both a technical and economical point of view, several scenarios of storage units' installation are used and compared with the alternative solution of extra cable connection between the node with the lowest voltage and the node with the highest voltage of the distribution network. For the comparison, a case study of a typical LV distribution feeder of Cyprus is used.

A. Case study input data

In order to validate the PLATOS software on the effects of introducing energy storage systems on the network stability, a typical LV distribution underground (cable Al 300mm^2 XLPE) feeder of the Cyprus distribution network was designed in the Digsilent PowerFactory, as shown in Fig. 4. It consists of radial lines with seven nodes, general loads and two PV systems, with the first one installed in node 3 (J2) and the second one in node 7 at the end of the feeder (J6). Also, in Fig. 4 are provided (a) the voltage magnitude from line to line in kV of each node, (b) the magnitude of the voltage in per unit (p.u.) of each node, (c) the angle of the voltage in degrees of each node, (d) the active power in MW of each branch, (e) the reactive power in MVAr of each branch, (f) the loading in % of each branch, (g) the magnitude of the current in kA of each branch, (h) the active power in MW of the external grid, (i) the reactive power in MVAr of the external grid, (k) the power factor of the external grid, (l) the active power in MW of the general load at each node, and (m) the reactive power in MVAr of the general load at each node.

The magnitude of the voltage in p.u. for twenty four hours of each of the six nodes (J1-J6) of the LV distribution feeder is illustrated in Fig. 5. It can be observed that some nodes have overvoltage problem between 10:00 and 15:00 hour, as the magnitude of the voltage is over the upper limit of 1.1p.u. The loading in % of the transformer 11kV/400V and the loading in % of the connection LS1 of the feeder for twenty four hours are illustrated in Fig. 6 and in Fig. 7, respectively. It can be observed that during evening peak both experience overloading problems (over 100%). Also, the typical daily PV system load curve used in this analysis is illustrated in Fig. 8.

B. Investigated scenarios

In order to predict the effects of introducing energy storage systems on the network stability of the distribution network of Cyprus, especially overvoltage effects, and to compare them in terms of cost with a traditional solution in the local network infrastructure, four scenarios have been investigated using the PLATOS software tool. These scenarios are (a) Scenario 1, the use of one storage unit to overcome overvoltage problem in the nodes of the LV distribution feeder, (b) Scenario 2, the use of two storage units to overcome overvoltage problem in the nodes of the LV distribution feeder, (c) Scenario 3, the use of three storage units to overcome overvoltage problem in the nodes of the LV distribution feeder and (d) Scenario 4, the use of extra power connection between the node LV PILLAR and node J6 as an alternative solution to solve overvoltage problem in the nodes of the LV distribution feeder.

C. Input data in PLATOS software tool

For all the above scenarios the network topology of the case study for the LV distribution network of Cyprus with the component data, the load and the generation patterns of each node have been insert into the PLATOS software tool. Also, the software takes into account an undervoltage limit of 0.94p.u. or 0.376kV, an overvoltage limit of 1.06p.u. or 0.424kV, an overloading limit of 100% and maximum depth of the voltage dips to be alleviated 0.1p.u.

Furthermore, 10 types of storage units with discharging and charging power and 10 sizes of storage units between 2kWh up to 60kWh, as shown in Table I, have been used for the simulations.

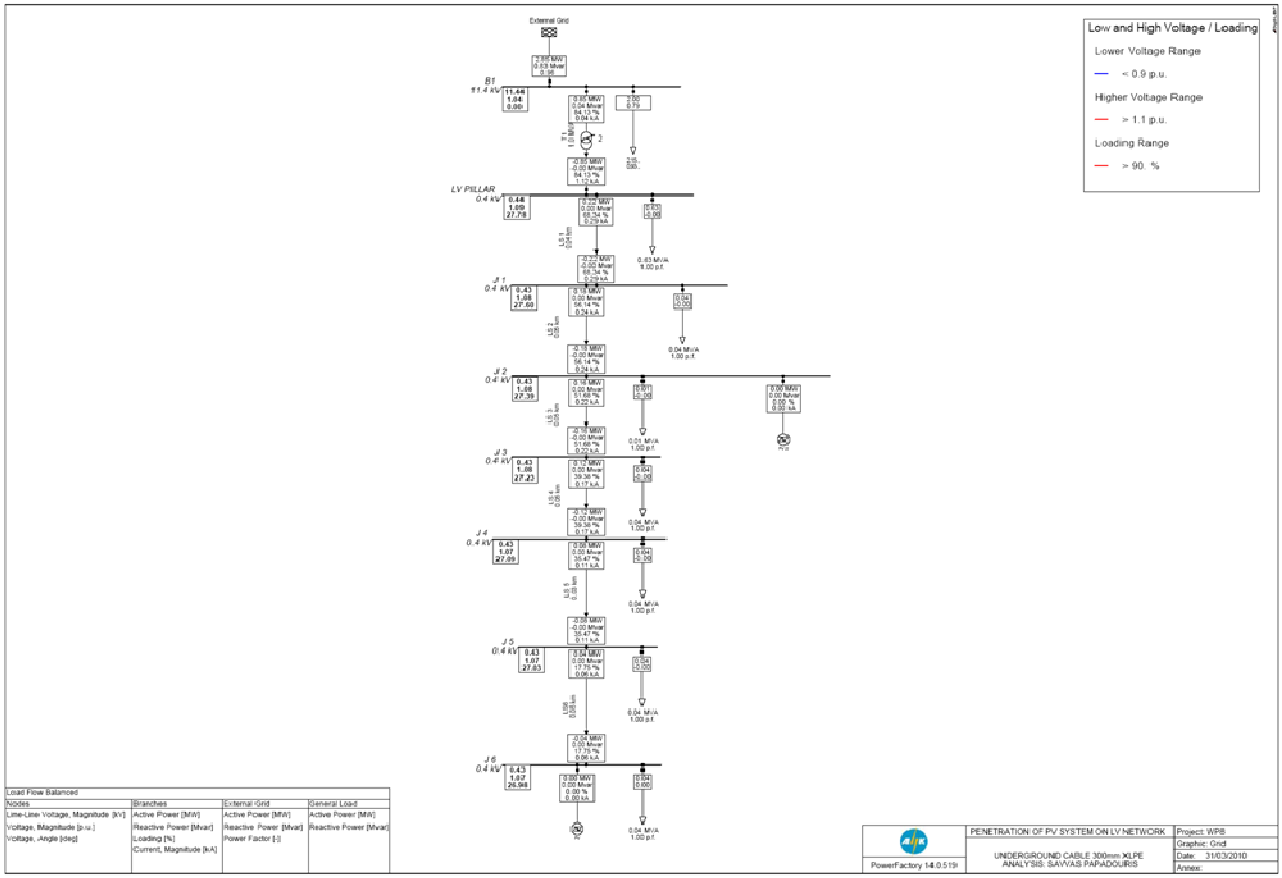

Fig. 4. Typical LV distribution feeder of Cyprus

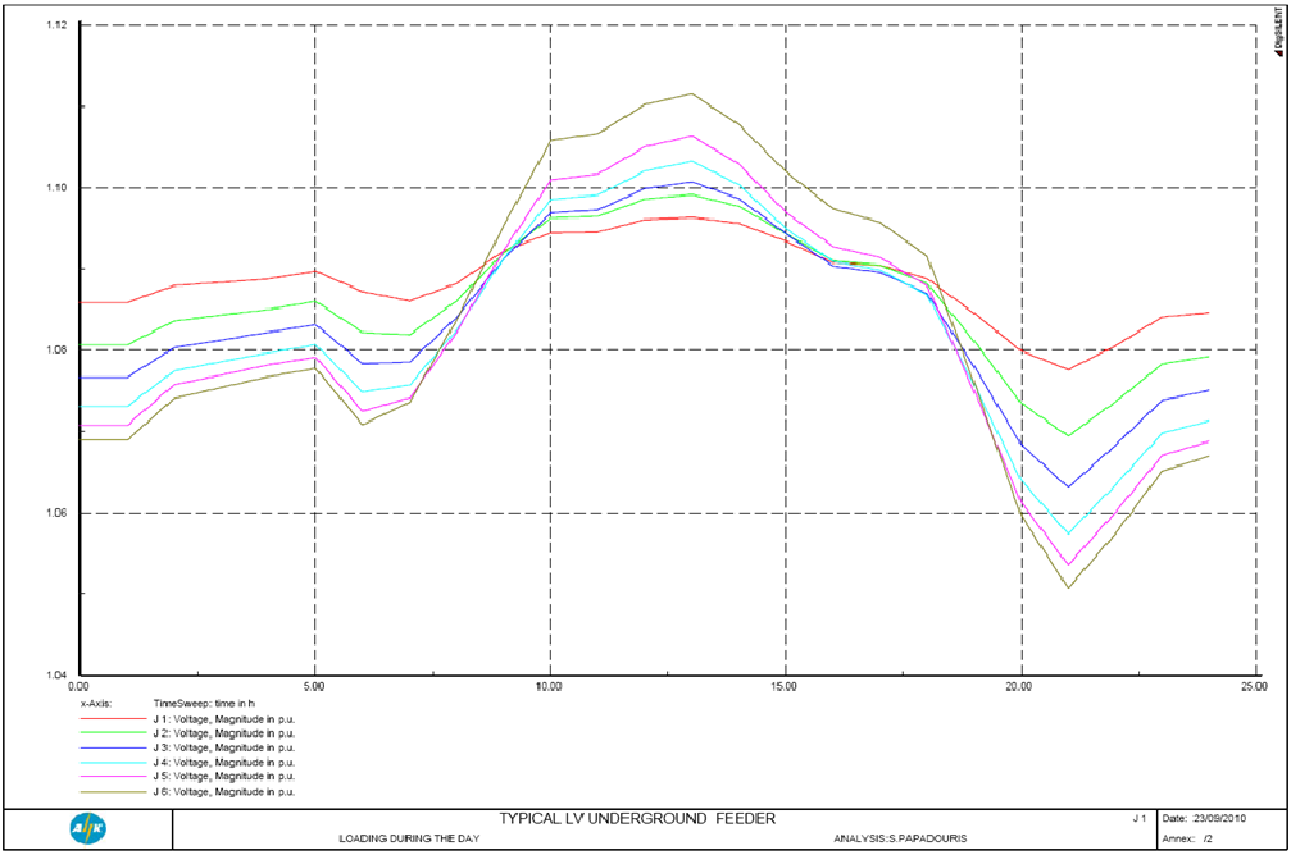

Fig. 5. Daily voltage magnitude of each node

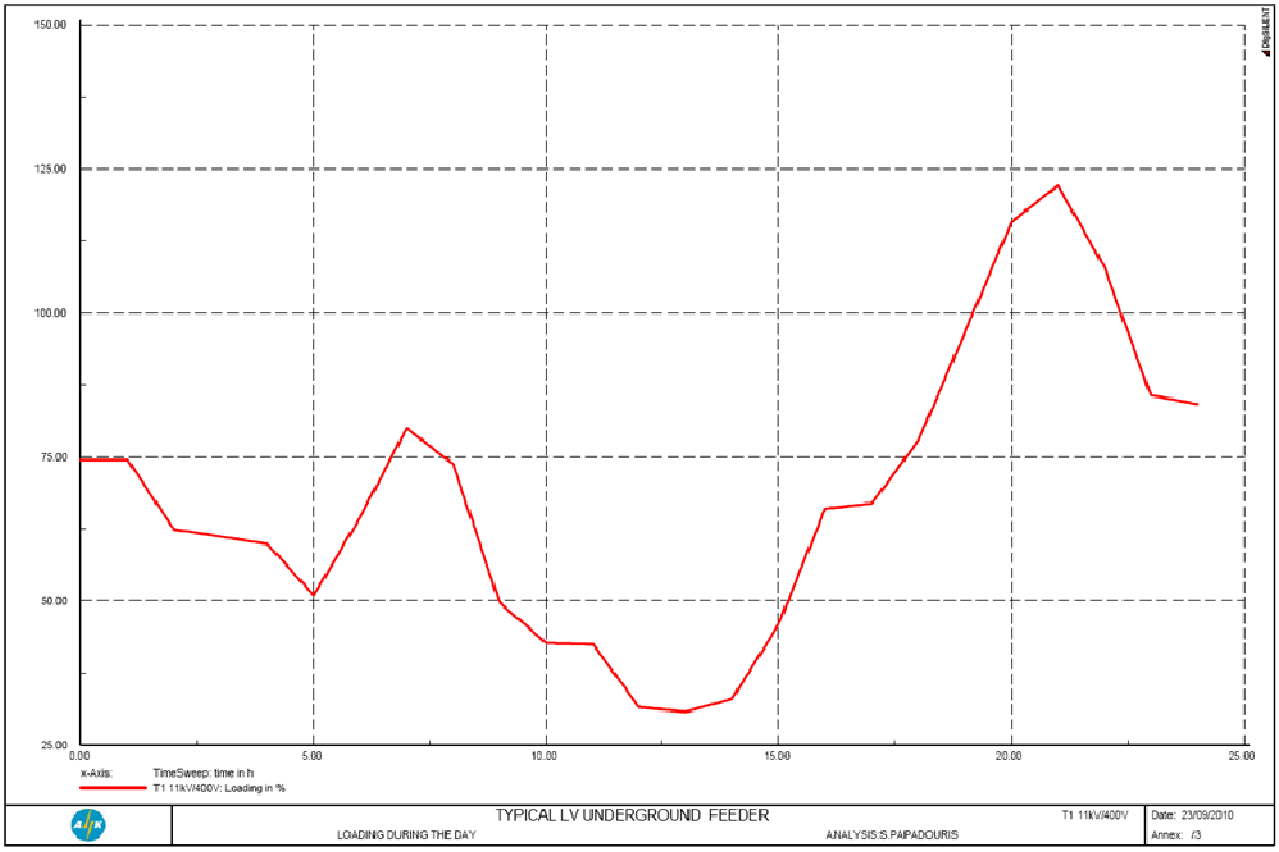

Fig. 6. Daily transformer 11kV/400V loading

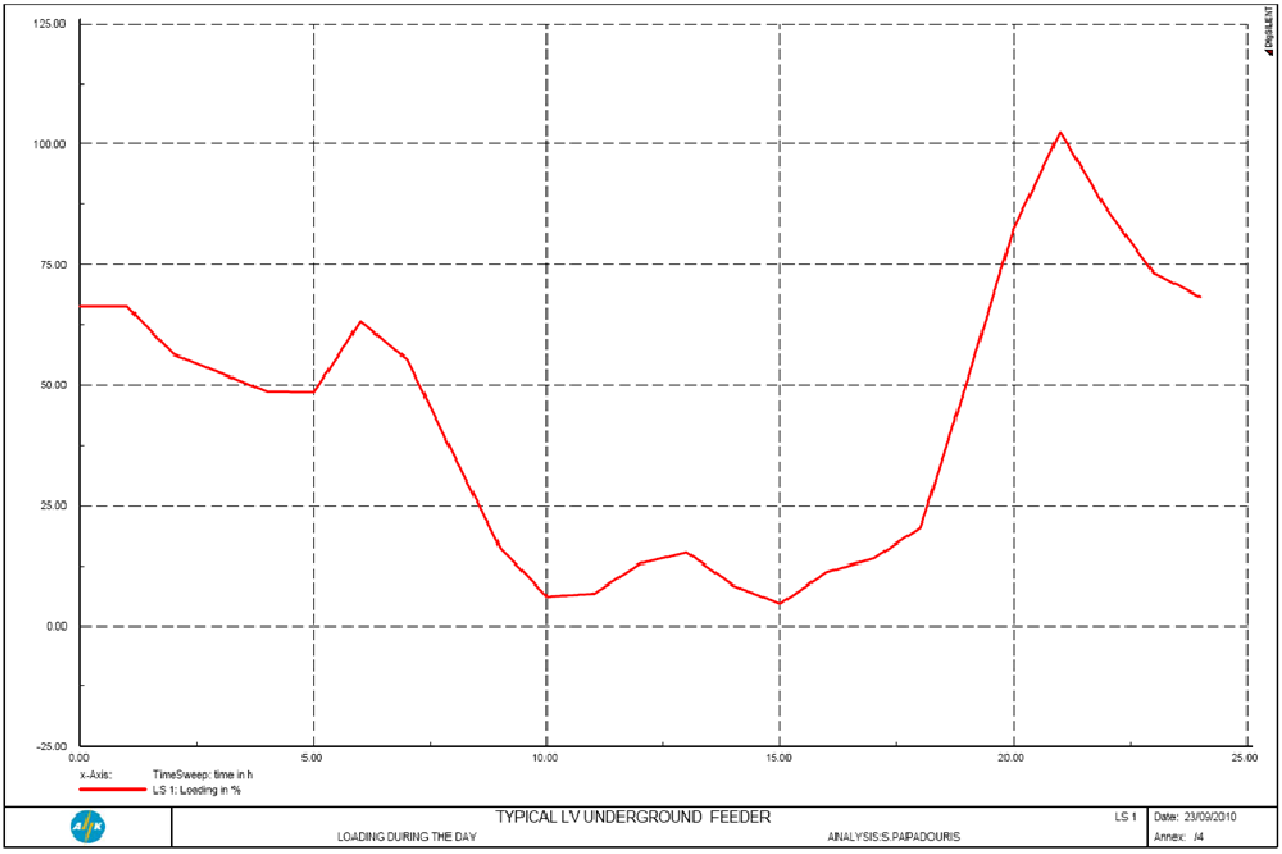

Fig. 7. Daily LS1 connection loading

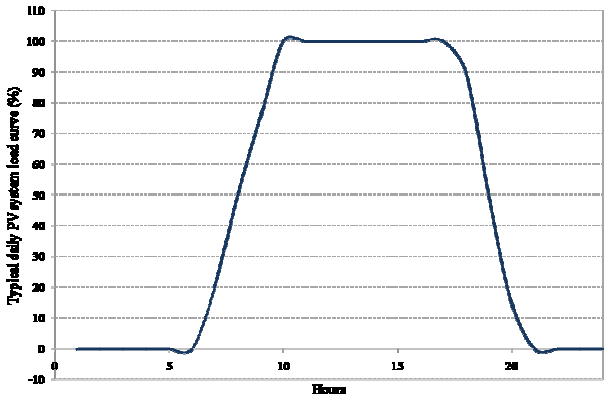

Fig. 8. Typical daily PV system load curve

TABLE I
TYPES AND SIZES OF STORAGE UNITS

No.	Charging power of storage unit (kW)	Discharging power of storage unit (kW)	Sizes of storage units (kWh)
1	-2	2	2
2	-4	4	4
3	-6	6	6
4	-8	8	8
5	-10	10	10
6	-20	20	20
7	-30	30	30
8	-40	40	40
9	-50	50	50
10	-60	60	60

For the first three scenarios, the Lithium Ion (LiIon) battery has been used with relative installation cost of 1204.1€/kWh and average maximum active power increment 10%/min [3]. For the fourth scenario, a typical cable with relative cost of 39000€/km and length of connection 0.331km has been used.

D. Discussion of the results

For all scenarios investigated, overvoltage occurs between 11:00 and 14:30 hour, as shown in Table II. The problem is identified in one node from 11:00-12:00 hour, in four nodes from 12:00-13:00 hour, in five nodes from 13:00-14:00 hour and in 2 nodes from 14:00-15:00 hour.

For the first three scenarios, 4 generations with 20 genes each are being used, accounting for 80 possible solutions (called nucleotides). In order that the simulations converge to an optimum solution, a minimum performance objective boundary has been used, which was 350000€ for the first scenario, 600000€ for the second scenario and 800000€ for the third scenario with a performance convergence objective of 0.01%. For the first scenario, only 40 solutions were needed by PLATOS to find the optimum solution which was solution number 36, as illustrated in Fig. 9, whereas for the second scenario and the third scenario, 60 solutions were needed and the optimum solutions were solution number 56 and solution number 42 respectively, as illustrated in Fig. 10 and Fig. 11. From these three figures, it can be observed that for some solutions the performance indicator is negative, which means that for these solutions the storage system, although it solves the problem of overvoltage, is not economically viable.

TABLE II
LV VIRTUAL DISTRIBUTION FEEDER OVERVOLTAGE PROBLEMS

Time	Node with lowest voltage	Lowest voltage (kV)	Node with highest voltage	Highest voltage (kV)	Number of nodes with overvoltage
10:00	J6	0.4088	J6	0.4237	0
10:30	J6	0.4088	J6	0.4237	0
11:00	J6	0.4088	J6	0.4241	1
11:30	J6	0.4088	J6	0.4241	1
12:00	J6	0.4088	J6	0.4267	4
12:30	J6	0.4088	J6	0.4267	4
13:00	J6	0.4088	J6	0.4274	5
13:30	J6	0.4088	J6	0.4274	5
14:00	J6	0.4088	J6	0.4274	2
14:30	J6	0.4088	J6	0.4274	2
15:00	J6	0.4088	J6	0.4274	0
15:30	J6	0.4088	J6	0.4274	0
16:00	J6	0.4088	J6	0.4274	0
16:30	J6	0.4088	J6	0.4274	0
17:00	J6	0.4088	J6	0.4274	0
17:30	J6	0.4088	J6	0.4274	0
18:00	J6	0.4088	J6	0.4274	0
18:30	J6	0.4088	J6	0.4274	0
19:00	J6	0.4074	J6	0.4274	0
19:30	J6	0.4074	J6	0.4274	0
20:00	J6	0.3959	J6	0.4274	0
20:30	J6	0.3959	J6	0.4274	0
21:00	J6	0.3959	J6	0.4274	0
21:30	J6	0.3959	J6	0.4274	0
22:00	J6	0.3959	J6	0.4274	0
22:30	J6	0.3959	J6	0.4274	0
23:00	J6	0.3959	J6	0.4274	0
23:30	J6	0.3959	J6	0.4274	0

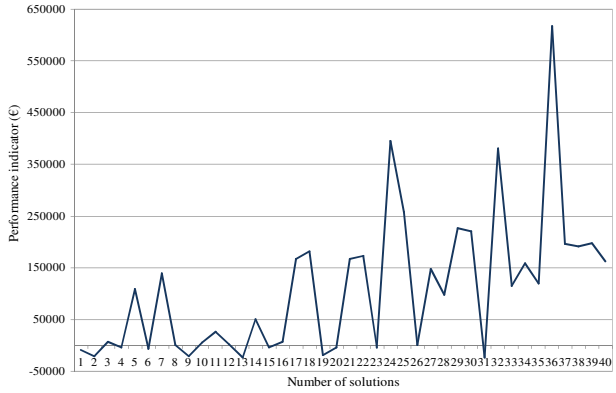

Fig. 9. Solutions for scenario 1

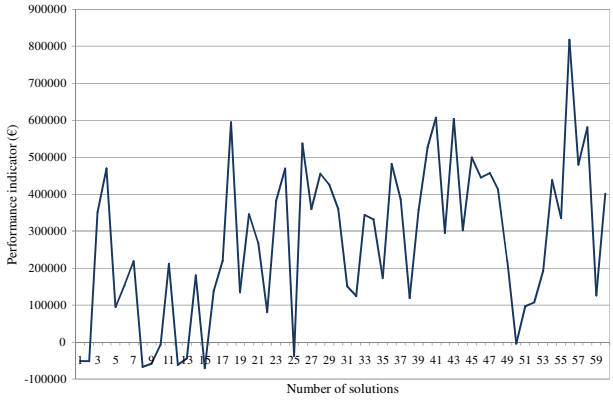

Fig. 10. Solutions for scenario 2

Table III gives an overview of the solutions for the first scenario, regarding the position node of the LV distribution feeder of Cyprus, illustrated in Fig. 4, where the storage unit will be installed to solve the overvoltage problem, the type of the storage unit that will be installed, with the relative charging and discharging power, the size of the storage unit that will be installed, the performance indicator (NPV value in €), and the payback period.

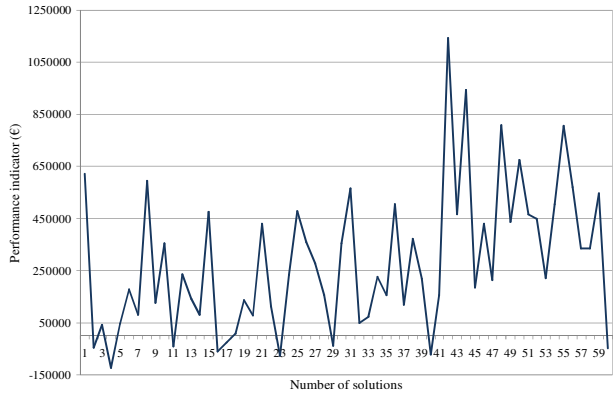

Fig. 11. Solutions for scenario 3

It can be observed that the optimum solution for the first scenario, which as mentioned above is solution number 36, concerns the installation of a storage unit with charging power -8kW, discharging power 8kW and size of 50kWh at node J5. This solution has a performance indicator of 617566€ and payback period of one year. Also, the performance indicator of a solution depends on the type, the size and the position where the storage unit will be installed. In addition, some solutions, although they provide a technical solution for the overvoltage problem, economically are not viable since the performance indicator is negative and the payback period is 100 years. For these cases an additional penalty of 4000€ is included in the performance indicator, because of the no viability.

TABLE III
OVERVIEW OF SOLUTIONS FOR SCENARIO 1

Solution number	Storage unit location node	Type of storages unit		Size of storage unit (kWh)	Performance indicator (€)	Payback period (years)
		Charging power of storage unit (kW)	Discharging power of storage unit (kW)			
1	J1	-50	50	6	-8894	100
2	J5	-50	50	20	-21431	100
3	J5	-8	8	2	6977	4
4	J5	-10	10	10	-4538	100
5	J2	-2	2	50	108896	4
6	J1	-30	30	8	-6763	100
7	J3	-10	10	40	138504	3
8	J2	-40	40	2	574	14
9	J6	-50	50	20	-21430	100
10	J6	-6	6	4	5599	6
11	J2	-2	2	6	25706	3
12	J4	-6	6	8	2041	12
13	J6	-60	60	20	-23430	100
14	J4	-2	2	8	50567	2
15	J3	-20	20	8	-4761	100
16	J5	-4	4	4	5998	6
17	J4	-8	8	20	166931	2
18	J6	-8	8	30	181827	2
19	J6	-40	40	20	-19430	100
20	J1	-8	8	10	-4141	100
21	J4	-8	8	20	166931	2
22	J5	-8	8	30	172552	2
23	J5	-8	8	10	-4138	100
24	J5	-8	8	40	395059	1
25	J2	-10	10	50	258149	2
26	J1	-4	4	4	171	15
27	J3	-10	10	30	147397	2
28	J2	-10	10	40	97315	4
29	J6	-10	10	30	225835	2
30	J6	-2	2	30	220401	2
31	J2	-20	20	30	-24326	100
32	J4	-4	4	50	380763	2
33	J6	-2	2	10	114512	1
34	J4	-8	8	30	158038	2
35	J3	-8	8	30	119126	3
36	J5	-8	8	50	617566	1
37	J4	-10	10	30	196063	2
38	J6	-8	8	20	190720	2
39	J6	-2	2	20	197401	1
40	J1	-8	8	50	161666	3

For the second scenario, the optimum solution is solution number 56, which concerns the installation of two storage units with charging power -8kW and -2kW, discharging power 8kW and 2kW, sizes of 50kWh and 30kW, respectively, at node J5 the first storage unit and at node J6 the second storage unit. The performance indicator of this solution is 818828€ with payback period of 1 year. For the third scenario, the optimum solution is number 42, which concerns the installation of three storage units with charging power -6kW, -6kW and -4kW, discharging power 6kW,

6kW and 4kW, sizes of 30kWh, 50kWh and 60kW, respectively, at node J5 the first storage unit, at node J6 the second storage unit and at node J4 the third storage unit. This solution has a performance indicator of 1142776€ and payback period of 2 years. Concerning the fourth scenario, which concerns an alternative solution to the problem of the overvoltage in the virtual LV distribution feeder of Cyprus by the installation of extra power connection between the node LV PILLAR with the node J6, the performance indicator is 1799209€ and the payback period is one year.

The performance indicator of the optimum solution of each scenario is compared to the performance indicator of the alternative solution and illustrated in Fig. 12.

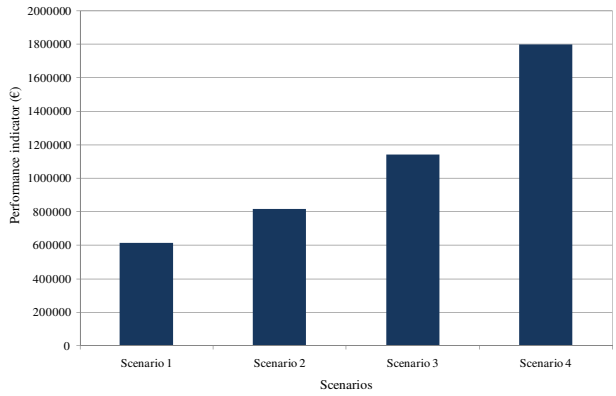

Fig. 12. Comparison of the performance indicator for the scenarios examined

It can be observed that for solving the problem of overvoltage of the LV distribution feeder of Cyprus, as more storage units are installed the better the performance indicator and, therefore, the more attractive is the investment in storage units to solve power quality problems in the distribution network. In the case where the technical requirements in voltage limitations according to distribution regulations are satisfied with one storage unit, the installation of an additional storage unit will only increase the final cost. The best solution, however, still remains the alternative solution of connecting an extra cable between the node with the lowest voltage and the node with the highest voltage of the distribution network, due to the lower investment costs compared to that of the storage units.

V. Conclusions

In this work, the structure of the Cyprus distribution network was described and the PLATOS software tool, developed within the framework of GROW-DERS, was presented. In order to investigate the possible overvoltage effects in the distribution network of Cyprus, on both technical and economical point of view, several scenarios of storage units' installation were used and compared with the alternative solution of extra cable connection between the node with the lowest voltage and the node with the highest voltage of the distribution network. For the comparison, a case study of a typical LV distribution feeder of Cyprus was used.

The performance indicator of a solution, expressed as the NPV, depends on the type, the size and the position where the storage unit will be installed. In addition, some solutions, although provide a technical solution for the overvoltage problem, are not economically viable since the performance indicator is negative and the payback period is 100 years.

The results indicated that for overcoming the problem of overvoltage of the LV distribution feeder of Cyprus, as more storage units are installed the better the performance indicator and, therefore, the more attractive is the investment in storage units to solve power quality problems in the distribution network. In the case where the technical requirements in voltage limitations according to distribution regulations are satisfied with one storage unit, the installation of an additional storage unit will only increase the final cost. The best solution, however, still remains the alternative solution of connecting an extra cable, due to the lower investment costs compared to that of the storage units.

VI. Acknowledgment

The authors gratefully acknowledge the contributions of P.de Boer, G. Bloehof, R. Cremers, and H. Colin for their work on the validation of the PLATOS software for the Cyprus case study.

VII. References

[1] European Commission, "Directive 2009/28/EC of the European Parliament and of the Council 23 April 2009 on the promotion of the use of energy from renewable sources and amending and subsequently repealing Directives 2001/77/EC and 2003/30/EC", 2009.

[2] A. Poullikkas, G. Kourtis, I. Hadjipaschalis, 2011, "A hybrid model for the optimum integration of renewable technologies in power generation systems", *Energy Policy*, 39, 926-935.

[3] M. Schreurs, P. de Boer, R. Hooiveld, "GROW-DERS; Grid reliability and operability with distributed generation using flexible storage", in *proc. 2010 China International Conference on Electricity Distribution*.

[4] Cyprus Transmission System Operator, "Transmission and Distribution Rules", 2011.

[5] growders.eu/.

[6] PowerFactory User's Manual DIgSILENT PowerFactory Version 14.0.

[7] P. de Boer, D. Gütschow, R. Cremers, "GROW-DERS; Grid reliability and operability with distributed generation using flexible storage", presented at the CIRED Workshop, Lyon, France, 2010.

VIII. Biographies

Andreas Poullikkas holds a Bachelor of Engineering (B.Eng.) degree in mechanical engineering, a Master of Phlosophy (M.Phil.) degree in nuclear safety and turbomachinery, a Doctor of Philosophy (Ph.D.) degree in numerical analysis and a Doctor of Science (D.Sc.) higher doctorate degree in energy policy and energy systems optimization from Loughborough University, U.K. He is a Chartered Scientist (CSci), Chartered Physicist (CPhys) and Member of The Institute of Physics (MInstP). His present employment is with the Electricity Authority of Cyprus where he holds the post of Assistant Manager of Research and Development; he is also, a Visiting Professor at the American University of Sharjah and at the University of Cyprus. In his professional career he has worked for academic institutions such as a Visiting Fellow at the Harvard School of Public Health, USA. He has over 20 years experience on research and development projects related to the numerical solution of partial differential equations, the mathematical analysis of fluid flows, the hydraulic design of turbomachines, the nuclear power safety, the analysis of power generation technologies and the power economics. He is the author of various peer-reviewed publications in scientific journals, book chapters and conference proceedings. He is the author of the postgraduate textbook: Introduction to Power Generation Technologies (ISBN: 978-1-60876-472-3), of the book Renewable Energy: Economics, Emerging Technologies and Global Practices, ISBN: 978-1-62618-231-8, of the book: The Cyprus Energy Future (ISBN: 978-9963-9599-4-5) and of the

book: Sustainable Energy Development for Cyprus, ISBN: 978-9963-7355-3-2. He is, also, a referee for various international journals, serves as a reviewer for the evaluation of research proposals related to the field of energy and a coordinator of various funded research projects. He is a member of various national and European committees related to energy policy issues. He is the developer of various algorithms and software for the technical, economic and environmental analysis of power generation technologies, desalination technologies and renewable energy systems.

Savvas Papadouris holds a B.Eng (Electrical Power Engineering), from Slovenská Technická Univerzita v Bratislave and a Master Degree on Power Engineering from Umist. During 1995-1998 he worked at Techmaster as Electrical Power Engineer, while during 1998-2002 he worked at Mouzouras and Associates as Building Services Consultant. He joined Electricity Authority of Cyprus in 2002, where he works at the Networks Unit as an Electrical Engineer in the department of Forward Planning.

George Kourtis holds a Diploma and a Master Degree in Electrical and Computer Engineering from the Polytechnic School of Aristoteleio University of Thessaloniki (AUTH) and a Master Degree on Electrical Engineering from the University of Cyprus. During 2007 he has worked as a technician for LOGICOM LTD, where he was responsible for the maintenance of 3G Mobile stations. He joined Electricity Authority of Cyprus Research and Development Department in 2008, where he works on European funded research programs as an electrical engineer.

Ioannis Hadjipaschalis holds a B.Eng (Electrical Engineering), from the University of Sheffield, an M.Sc from the London School of Economics and an MBA. During 1996-2000 he worked at the Electricity Authority of Cyprus as Electrical Engineer, while during the period 2001-2005 he worked at ACNielsen Market Research. He joined EAC Research and Technological Development team in 2006, where he has been working on European funded research involving RES, Distributed Generation (DG), Electricity distribution networks, Hydrogen and CO_2 capture and storage (CCS) technologies.

2nd Conference on Power Options for the Eastern Mediterranean Region
07-08 October 2013, Nicosia, Cyprus (Paper No. POEM13/166)

Cost-benefit analysis for the installation of cogeneration CSP technology in Cyprus

Andreas Poullikkas, George Kourtis and Ioannis Hadjipaschalis

Abstract-- **The purpose of this work is to investigate whether the installation of an innovative cogeneration of electricity and desalinated water (DSW) with concentrated solar power (CSP) technology in Cyprus is economically feasible. The study takes into account the following generating technologies, (a) CSP-DSW technology 4MWe, (b) CSP-DSW technology 10MWe, (c) CSP-DSW technology 25MWe and (d) CSP-DSW technology 50MWe with or without CO_2 trading for two different cases of electricity purchasing tariff. For all above cases the electricity unit cost or benefit before tax, as well as internal rate of return and payback period are calculated. The results indicate that for plants of 25MWe and 50MWe, such cogeneration technology is economically attractive even without any subsidy.**

Index Terms-- **Cogeneration desalination and electricity, concentrated solar power, electricity unit cost, renewable energy sources.**

I. Introduction

Throughout history, Cyprus has experienced long periods of water scarcity. In recent years this phenomenon occurs more due to the climate change. The overexploitation of the underground water resources and the reduction of the level of the surface water resources have brought the water resources at a critical point. The result of these factors is the shift in the desalination solution, which, although a method proven and technologically mature, still requires large amounts of energy, which in its majority is produced from conventional, polluting power plants. By increasing the water needs, there is an increase in the energy needs which are required for the operation of desalination units, which increases the impact in the environment. The cogeneration of electricity and desalinated water (DSW) by concentrated solar power (CSP) technologies is an innovative approach for solving the above problems of water scarcity and energy production from sources which are not friendly to the environment [1].

In order to tackle these problems, a research project entitled Solar Thermal Power Generation and Water (STEP-EW), has been funded by the Cross-Border Cooperation Programme Greece-Cyprus 2007-2013 [2]. The project is based on a techno-economic study carried out by the Cyprus Institute (CyI) in cooperation with Electricity Authority of Cyprus (EAC) and the Massachusetts Institute of Technology (MIT) and concerned the installation in Cyprus of CSP plants with cogeneration of electricity with desalinated water [1], [3]. The main objective of STEP-EW project is the technical confirmation of the innovative idea of the cogeneration of electricity and desalinated water by using small scale solar thermal plants in real conditions. The consortium of project partners consists of the CyI, EAC, Cyprus Water Development Department and the Act Network in Greece.

The purpose of this work is to investigate whether the installation of an innovative CSP-DSW technology in Cyprus is economically feasible. For the simulations, the IPP v2.1 software is used for calculating the electricity unit cost or benefit before tax from the selected CSP-DSW technologies [4]. For each scenario under investigation, the simulations take into account the capital cost, the fuel consumption and cost, the operation cost, the maintenance cost, the plant load factor and it calculates the electricity unit cost or benefit before tax, as well as the after tax internal rate of return (IRR) and the payback period (PBP).

Section II, gives a brief description of the CSP-DSW technology, whereas in section III, the optimization model used for the simulations, is described. Section IV, concerns the feasibility study and the results for the integration of large scale CSP-DSW technologies in the Cyprus power generation system. Finally the conclusions are summarized in section V.

II. The CSP-DSW technology

The CSP-DSW technology utilizes solar energy to generate electricity. The heat collected from converting solar energy to thermal energy is used in a conventional power cycle to generate electricity. The main components of a CSP-DSW technology are the energy collection system, the receiver system, the thermal energy storage, the desalination unit and the typical components used in conventional power cycles (e.g., steam turbines and generators), as illustrated in Fig. 1. The receiver system converts the solar energy intercepted and reflected by the collection system into thermal energy. In systems with energy storage capabilities, the thermal energy in the receiver is first stored into a heat storage medium to manage the variations in the solar energy influx. The storage system may contain sufficient thermal energy to continue the power generation overnight, or during days with overcast weather. A heat transfer fluid (HTF), possibly different from the heat storage medium, transfers

This work has been partially funded by the Cross-Border Cooperation Programme Greece-Cyprus 2007-2013, Contract No: k1_1_10.

A. Poullikkas is with American University of Sharjah, P.O. Box 26666, Sharjah, UAE and with Electricity Authority of Cyprus, P.O. Box 24506, 1399 Nicosia, Cyprus (e-mail: apoullik@eac.com.cy) (corresponding author).

G. Kourtis is with Electricity Authority of Cyprus, P.O Box 24506, 1399 Nicosia, Cyprus (e-mail: georgekourti@eac.com.cy).

I. Hadjipaschalis is with Electricity Authority of Cyprus, P.O Box 24506, 1399 Nicosia, Cyprus (e-mail: ioannishadjipashalis@eac.com.cy).

the energy from the storage medium to the steam generators in the power cycle.

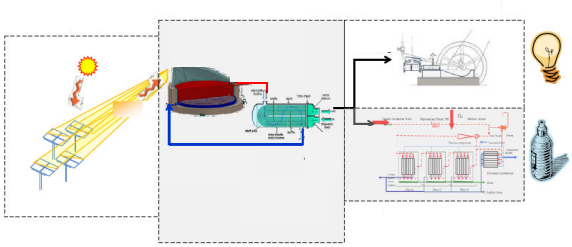

Fig. 1. Cogenerated solar thermal plant with desalinated water

The intensity of the solar energy received by the collectors is only a few kWh/m^2/day. To achieve higher intensities and ultimately higher operating temperatures, CSP technologies are used. In CSP systems, the surface area from which the heat losses occur, i.e., the receiver aperture, is significantly less than the total surface area of the collectors. In the STEP-EW project, heliostats positioned on a south-facing hill reflect the light directly onto the receiver on the ground [5], as illustrated in Fig. 2.

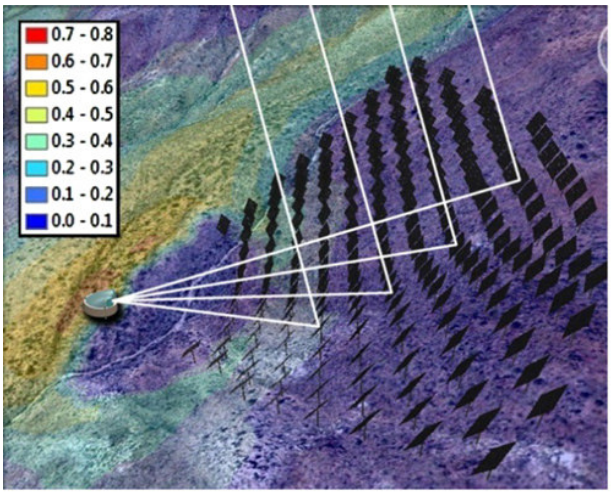

Fig. 2. Beam-down hillside heliostats

The advantages of utilizing ground-level receivers (made possible by hillsides) include the elimination of many significant costs and operating problems associated with tower systems, such as salt freezing in pipes, the capital cost and maintenance of high pressure pumps, and of course the capital cost of the tower. Additionally, terrain that is otherwise difficult to develop is suitable for hillside concentrated solar applications. As a result, the hillside heliostat field further decreases the capital cost relative to traditional CSP sites. A potential disadvantage of hillside sites is the increased cost of installing heliostats on a hillside terrain [5].

The solar receiver is the component that receives sunlight and converts it into heat. The heat is transferred through the HTF from the receiver to the storage unit, where it is accumulated for later use. The solar receiver to be used in the STEP-EW project is the CSPonD design [6]. In this design, the receiver is a salt pond which also acts as the energy storage medium. The energy storage is designed such that the radiation heat losses from the salt are predominantly absorbed by a dome structure (the lid) covering the salt pond. The lid has an opening (the aperture) that the concentrated light passes through before it is absorbed by the salt pond [6].

Both the molten salt pond and the lid will exchange heat with each other and to the environment by radiation, convection and conduction; the primary heat transfer mechanism is through radiation. The system cover will be lined with refractory firebrick and backside cooled, so the salt vapor rises and condenses on the inner surface of the cover, akin to frost collecting on evaporator coils within a refrigerator. The resulting white surface will grow until the thickness results in a thermal resistance that condenses the salt vapor, but the surface continually melts and returns liquid salt to the pond. The liquid/solid interface is expected to act as a diffuse reflector to incoming light that reflects off the surface of the salt. Solidified salt has a very high reflectivity in the visible spectrum and behaves nearly as a Lambertian reflector. Liquefied salt will be subject to grazing- angle Fresnel surface reflections and as such, much of the light impinged onto the lid will be reflected back to the pond. The energy that is transferred to the lid is from lower-temperature, longer wavelength radiation from the salt surface. Only a small fraction of incoming photon energy is converted to thermal energy at the lid [3].

The top surface of the salt needs to remain at a constant level for consistent solar absorption; hence, the tank is split into two zones with a moving barrier plate. The top zone is the hot salt side, and the bottom zone is the cold salt side. An insulated creep and corrosion resistant alloy plate divides the two sides, providing a physical and thermal barrier between the thermally stratified hot and cold layers within the tank. The light will penetrate deeply and a small fraction of it will impact the highly absorbing divider plate causing convection currents, heating the hot side to a uniform high temperature. The near neutrally buoyant divider plate is moved axially by small actuators, with negligible power consumption, to maintain the hot and cold salt volumes required for continuous operation, as illustrated in Fig. 3(A). As a result, high-temperature salt can be provided even as the average temperature in the tank decreases.

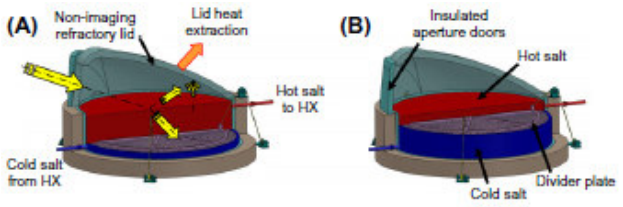

Fig. 3. Cross sections of CSPonD receiver

As the divider plate is lowered when the aperture is open and the tank is being heated by sunlight, colder salt from below moves past the annular clearance space between the barrier plate and tank wall to be reheated. Relative “blow-by” salt velocities are slow, accounting for the daily downward motion of the plate displacing fluid and pumped cold salt returning from the heat exchanger, as illustrated in Fig. 3(B).

The storage unit is designed so that the unit can operate for 24 hours at full capacity without additional energy from the sun. As a result, if there is a widespread lack of sunshine,

such as during the night or on cloudy days, the unit can continue its normal operation [3].

Extraction turbines are assumed for the electricity generation. Process steam is extracted from the turbine at various pressures. The extracted steam can be used for heating the condensed steam in the steam cycle (through open or closed feed-water heaters) and seawater desalination (both optional). The heat collected at the lid is used for pre-heating the desalination feed-water [7]. For the desalination unit, the multi-effect distillation (MED) is preferred. The MED process consists of several consecutive stages (or effects) maintained at decreasing levels of pressure (and temperature), leading from the first (hot) stage to the last one (cold), as illustrated in Fig. 4.

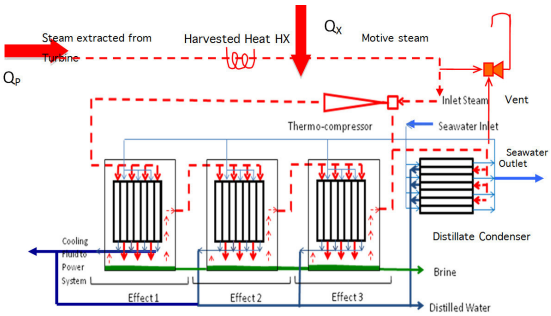

Fig. 4. Flow diagram for MED with thermal vapour compression

Each effect mainly consists of a multiphase heat exchanger. Seawater is introduced in the evaporator side and heating steam is introduced in the condenser side. As it flows down the evaporator surface, the seawater concentrates and produces brine at the bottom of each effect. The vapour raised by seawater evaporation is at a lower temperature than the vapour in the condenser. However, it can still be used as heating medium for the next effect where the process is repeated. The decreasing pressure from one effect to the next one allows brine and distillate to be drawn to the next effect where they will flash and release additional amounts of vapour at the lower pressure. This additional vapour will condense into distillate inside the next effect. In the last effect, the produced steam condenses on a conventional shell and tubes heat exchanger. This exchanger, called distillate condenser, is cooled by seawater. At the outlet of this condenser, one part of the warmed sea water is used as make-up water, while the other part is rejected to the sea. Brine and distillate are collected from effect to effect, up to the last one from where they are extracted by pumps [6].

III. Optimization Model

In order to calculate the financial indicators from the various candidate CSP-DSW technologies, each plant operation is simulated using the IPP v2.1 software [4]. The software emerged from a continued research and development in the field of software development for the needs of power industry. This user-friendly software tool, the flowchart of which is given in Fig. 5, can be used for the selection of an appropriate least cost power generation technology in competitive electricity markets. The software takes into account the capital cost, the fuel consumption and cost, the operation cost, the maintenance cost, the plant load factor, etc. All costs are discounted to a reference date at a given discount rate. Each run can handle 50 different candidate schemes simultaneously. Based on the above input parameters for each candidate technology the algorithm calculates the least cost power generation configuration in real prices and the ranking order of the candidate schemes [4], [8].

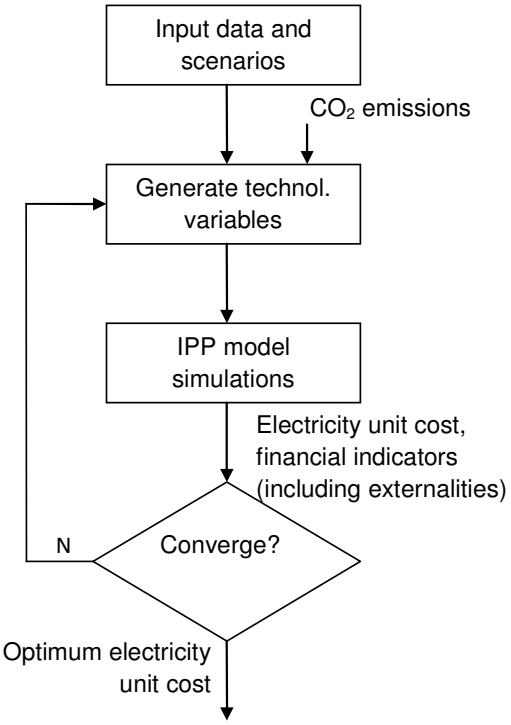

Fig. 5. Flow chart of the IPP optimization model

The technical and economic parameters of each candidate power generation technology are taken into account based on the cost function:

$$min\left(\frac{\partial c}{\partial k}\right) = min\left\{\frac{\sum_{j=0}^{N}\left[\frac{\frac{\partial C_{Cj}}{\partial k}+\frac{\partial C_{Fj}}{\partial k}+\frac{\partial C_{OMFj}}{\partial k}+\frac{\partial C_{OMVj}}{\partial k}}{(1+i)^j}\right]}{\sum_{j=0}^{N}\left[\frac{\frac{\partial P_j}{\partial k}}{(1+i)^j}\right]}\right\}, \quad (1)$$

where c is the final cost of electricity in €/kWh, in real prices, for the candidate technology k, C_{Cj} is the capital cost function in €, C_{Fj} is the fuel cost function in €, C_{OMFj} is the fixed operation and maintenance (O&M) cost function in €, C_{OMVj} is the variable O&M cost function in €, P_j is the total electricity production in kWh, j=1, 2,…N is the periods (e.g., years) of installation and operation of the power generation technology and i is the discount rate. The least cost solution is calculated by:

$$least\ \ cost\ \ solution = min\left[\frac{\partial c}{\partial k}\right], \qquad (2)$$

During the simulations procedure the following financial feasibility indicators based on the individual case examined may be calculated: (a) electricity unit cost or benefit before tax (in €/kWh), (b) after tax cash flow (in €), (c) after tax NPV (net present value: the value of all future cash flows, discounted at the discount rate, in today's currency), (d) after tax IRR (the discount rate that causes the NPV of the project to be zero and is calculated using the after tax cash flows. Note that the IRR is undefined in certain cases, notably if the project yields immediate positive cash flow in year zero) and (e) after tax PBP (the number of years it takes for the cash flow, excluding debt payments, to equal the total investment which is equal to the sum of debt and equity).

IV. Simulations and Discussion of the Results

The main objective of this work is to investigate whether the installation of an innovative cogeneration of CSP-DSW technology in Cyprus is economically feasible. For the simulations, the IPP v2.1 software is used for calculating the electricity unit cost or benefit before tax from the selected CSP-DSW technologies. Other work related to the integration of large scale CSP plants in power generation systems can be found in [9], [10], [11], [12] and in [13].

The following generating technologies have been examined, (a) CSP-DSW technology 4MWe, (b) CSP-DSW technology 10MWe, (c) CSP-DSW technology 25MWe and (d) CSP-DSW technology 50MWe with or without CO_2 trading and for two cases of electricity purchasing tariff. For each scenario under investigation, the simulations take into account the capital cost, the fuel consumption and cost, the operation cost, the maintenance cost, the plant load factor and it calculates the electricity unit cost or benefit before tax, as well as the after tax IRR and the PBP.

For all scenarios only the infrastructure required to operate the power block section is considered in the simulations. Therefore, only 80% of the total CSP-DSW plant specific capital cost and variable O&M cost is considered, assuming that the remaining 20% is required to operate the desalination unit and is not considered in this work. Regarding fixed O&M cost, 91% of the total CSP-DSW plant fixed O&M cost is considered. Furthermore, the capacity factor of the power block section is also 80% of the total capacity factor of the CSP-DSW plant.

A. Input data and assumptions

In order to compare on equal basis the electricity unit cost or benefit before tax from the selected CSP-DSW technologies, the technical and economic input data and assumptions tabulated in Table I and Table II are used.

For all scenarios, the capacity factor of the plant varies from 70-90%, in steps of 10%, due to the fact that for the CSP-DSW technologies it is assumed 24h of full daily operation. As mentioned above, the capacity factor of the power block section is 80% of the capacity factor of the CSP-DSW plant. Therefore, capacity factors of 56%, 64% and 72% are used for the power block section for all scenarios, to reflect plant capacity factors of 70%, 80% and 90%.

For the scenarios, a small plant of 4MWe, a small to medium plant of 10MWe, a medium plant of 25MWe and a large plant of 50MWe, are used with efficiencies that vary from 9.62% for the small plant up to 17% for the large plant.

TABLE I
Technical Input Data And Assumptions

Scenario	Capacity (MWe)	Efficiency (%)	Capacity factor (%)
CSP-DSW 4MWe	4	9.62	70-90
CSP-DSW 10MWe	10	11.9	70-90
CSP-DSW 25MWe	25	14.8	70-90
CSP-DSW 50MWe	50	17.0	70-90

Regarding the economic input data, the capital cost is assumed to be reduced from 5646€/kWe for the 4MWe scenario to 2795€/kWe for the 50MWe scenario. The fixed O&M cost, which includes staff salaries, insurance charges and fixed maintenance, is assumed to be reduced from 12.73€/kWe/month for the 4MWe scenario to 3.60€/kWe/month for the 50MWe scenario. As for the variable O&M cost, which includes spare parts, chemicals, oils, consumables and town water and sewage, is assumed to decrease from 37.47€/MWh for the 4MWe scenario with capacity factor 72% to 15.48€/MWh for the 50MWe scenario with the same capacity factor.

TABLE II
Economic Input Data And Assumptions

Scenario	Specific capital cost (€/kWe)	Fixed O&M (€/kWe/month)	Capacity factor (%)	Variable O&M (€/MWh)
CSP-DSW 4MWe	5646	12.73	56	48.18
			64	42.16
			72	37.47
CSP-DSW 10MWe	5090	8.05	56	34.96
			64	30.59
			72	27.19
CSP-DSW 25MWe	3364	5.09	56	25.37
			64	22.20
			72	19.73
CSP-DSW 50MWe	2795	3.60	56	19.90
			64	17.42
			72	15.48

For the environmental benefit of the plants from the CO_2 emissions trading system (ETS), two cases are examined for all scenarios, (a) the CO_2 ETS price of 10€/tCO_2 and (b) the CO_2 ETS price of 0€/tCO_2. Also, in order to calculate the financial feasibility indicators, two cases of electricity purchasing tariff are examined for all scenarios, (a) the current feed-in tariff for a CSP plant of 26€c/kWh and (b) the renewable energy sources for power generation (RES-E) purchasing tariff [14] for June 2013 (for a fuel price of 572.95€/MT and connection at 132kV/66kV) of 12.83€c/kWh, as illustrated in Fig.6.

Also, the economic life of the plants is assumed at 20 years. Throughout the simulations, a typical discount rate of 6%, a loan interest of 6%, an inflation of 2.5% and an annual tax rate of 10% are assumed.

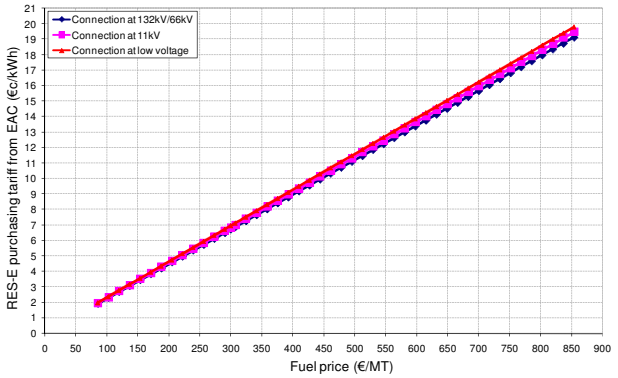

Fig. 6. RES-E purchasing tariff

B. *Results and discussion*

In order to compare on equal basis the electricity unit cost or benefit before tax from the selected CSP-DSW technologies, sixteen scenarios have been examined, which include the two cases of CO_2 ETS price and the two cases of electricity purchasing tariff. For each scenario under investigation, the simulations took into account the capital cost, the fuel consumption and cost, the operation cost, the maintenance cost, the plant load factor, etc. For each scenario, the electricity unit cost or benefit before tax, as well as after tax IRR and PBP are calculated.

The results obtained concerning the electricity unit cost benefit, which is the difference between the electricity purchasing tariff minus the electricity production cost of the plant, for electricity purchasing tariff of 26€c/kWh for all scenarios in respect to the capacity factor of the plants, are illustrated in Fig. 7.

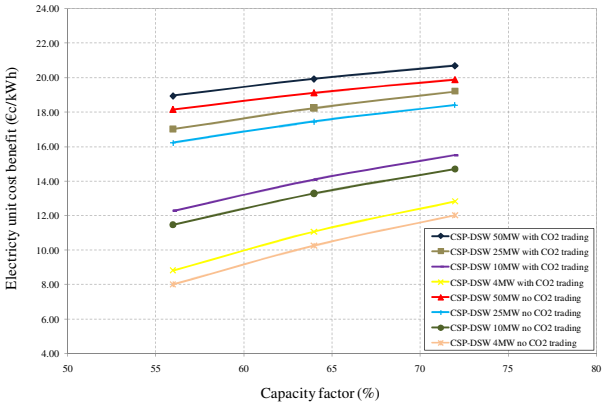

Fig. 7. Electricity unit cost benefit for electricity purchasing tariff of 26€c/kWh

It can be observed that the electricity unit cost benefit, which is the profit before tax in €c for every kWh produced by the CSP-DSW plant and delivered to the grid, increases with the increase of the capacity factor and the capacity size of the plant. Also, it can be observed that the additional benefit due to the CO_2 ETS price of 10€/tCO_2 for all scenarios is 0.8€c/kWh. Specifically, for the CSP-DSW of 4MWe with no CO_2 trading scenario and for capacity factors of the power block section of 56%, 64% and 72%, the electricity unit cost benefit is 8.03€c/kWh, 10.28€c/kWh and 12.03€c/kWh respectively. For the CSP-DSW of 4MWe with CO_2 trading, scenario and for capacity factors of 56%, 64% and 72%, the electricity unit cost benefit is 8.83€c/kWh, 11.08€c/kWh and 12.83€c/kWh respectively.

The after tax IRR and the PBP for each scenario are illustrated in Fig. 8 and Fig. 9 respectively.

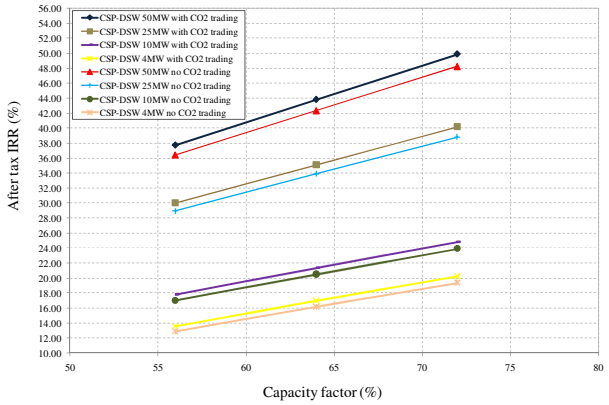

Fig. 8. After tax IRR for electricity purchasing tariff of 26€c/kWh

Specifically, for the CSP-DSW of 4MWe with no CO_2 trading scenario and for capacity factors of 56%, 64% and 72%, the after tax IRR is 12.88%, 16.19% and 19.36%, respectively. For the CSP-DSW of 4MWe with CO_2 trading, scenario and for capacity factors of 56%, 64% and 72%, the after tax IRR is 13.60%, 16.98% and 20.22% respectively.

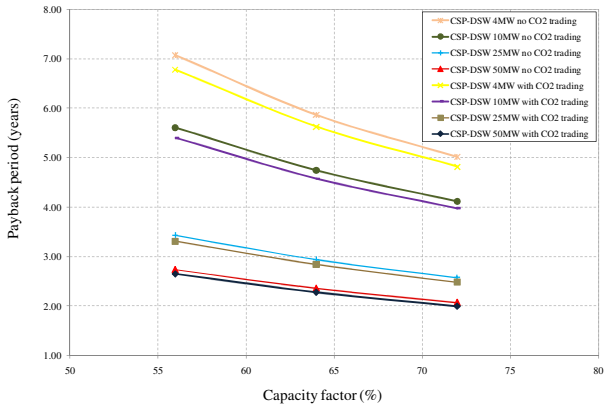

Fig. 9. After tax PBP for electricity purchasing tariff of 26€c/kWh

Concerning the after tax PBP results, it is observed that for the CSP-DSW of 4MWe with no CO_2 trading scenario and for capacity factors of 56%, 64% and 72%, the after tax PBP is almost 7 years, 6 years and 5 years respectively. For the CSP-DSW of 4MWe with CO_2 trading, scenario and for capacity factors of 56%, 64% and 72%, the after tax PBP is almost 6.8 years, 5.6 years and 4.8 years respectively.

From the above results, for the electricity purchasing tariff of 26€c/kWh case, it is obvious that the investment in CSP-DSW technology for every capacity size is very attractive.

For the electricity purchasing tariff of 12.83€c/kWh case, the electricity unit cost benefit for all scenarios is illustrated in Fig. 10.

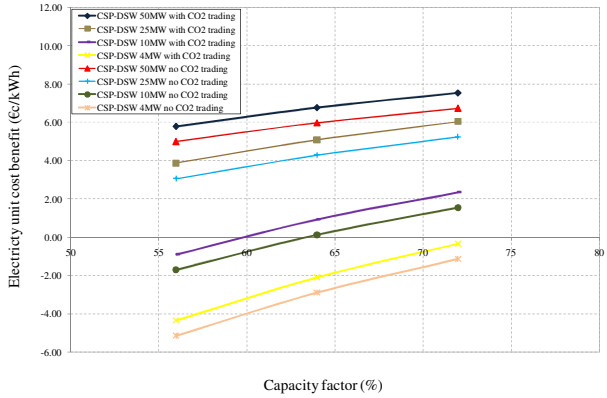

Fig. 10. Electricity unit cost benefit for electricity purchasing tariff of 12.83€c/kWh

It is observed that for this case for capacity sizes of 25MWe and 50MWe CSP-DSW plants, with or without CO_2 trading, although there is benefit for every capacity factor, this is lower than the lowest benefit observed from the previous case of electricity purchasing tariff. Especially, for capacity size of 10MWe and 4MWe with or without CO_2 trading, for some capacity factors, there is cost and not benefit. Specifically, for the CSP-DSW of 25MWe with no CO_2 trading scenario and for capacity factors of 56%, 64% and 72%, the electricity unit cost benefit is 3.07€c/kWh, 4.29€c/kWh and 5.24€c/kWh respectively. For the CSP-DSW of 25MWe with CO_2 trading, scenario and for capacity factors of 56%, 64% and 72%, the electricity unit cost benefit is 3.87€c/kWh, 5.09€c/kWh and 6.04€c/kWh respectively.

Despite the lower electricity unit cost benefit in the case of this electricity purchasing tariff, after a certain capacity size the investment in CSP-DSW technology is still attractive, as illustrated in Fig. 11. Assuming that a commercially attractive after tax IRR of a CSP-DSW project should be higher than 10%, CSP-DSW plants with capacity sizes 25MWe and 50MWe, with or without CO_2 trading, are satisfying this boundary.

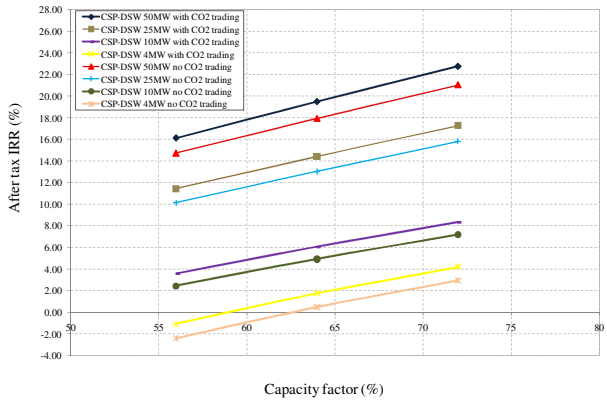

Fig. 11. After tax IRR for electricity purchasing tariff of 12.83€c/kWh

The results obtained for the after tax PBP for the electricity purchasing tariff of 12.83€c/kWh case are illustrated in Fig. 12. It can be observed that for the CSP-DSW of 25MWe with no CO_2 trading scenario and for capacity factors of 56%, 64% and 72%, the after tax PBP is almost 8.4 years, 7 years and 6 years respectively. For the CSP-DSW of 25MWe with CO_2 trading, scenario and for capacity factors of 56%, 64% and 72%, the after tax PBP is almost 7.7 years, 6.5 years and 5.5 years respectively.

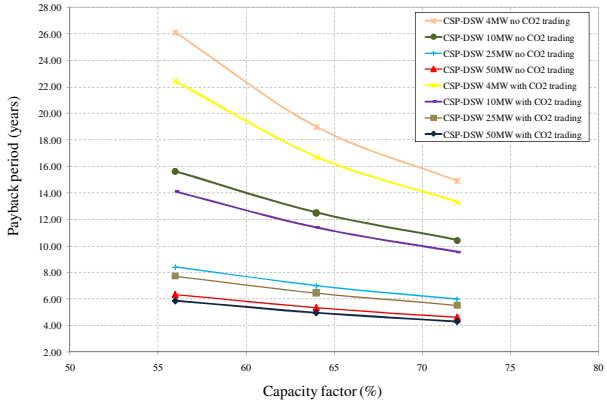

Fig. 12. After tax PBP for electricity purchasing tariff of 12.83€c/kWh

V. Conclusions

In this work, an investigation whether the installation of an innovative cogeneration of CSP-DSW technology in Cyprus is economically feasible, was carried out. In order to compare on equal basis the electricity unit cost or benefit before tax from the selected CSP-DSW technologies, sixteen scenarios have been examined, including two cases of CO_2 ETS price and two cases of electricity purchasing tariff. For each scenario under investigation, the simulations took into account the capital cost, the fuel consumption and cost, the operation cost, the maintenance cost, the plant load factor, etc. For each scenario, the electricity unit cost or benefit before tax, which is the difference between the electricity purchasing tariff minus the electricity production cost of the plant, as well as, the after tax IRR and the PBP were calculated.

The results indicated that the electricity unit cost or benefit for both cases of electricity purchasing tariff were decreased or increased with the increase of the capacity factor and the capacity size of the plant. Also, the additional benefit due to the CO_2 ETS price of 10€/tCO_2 for all scenarios was 0.8€c/kWh. Specifically, for the electricity purchasing tariff of 26€c/kWh case, the investment in CSP-DSW technology for every capacity size was very attractive, since, the CSP-DSW scenarios had high after tax IRR and low PBP.

Despite the lower electricity unit cost benefit in the case of electricity purchasing tariff of 12.83€c/kWh compared to that of the 26€c/kWh case, which in some cases there was cost and not benefit, for CSP-DSW plants of 25MWe and 50MWe, the investment in this technology was still attractive.

VI. References

[1] The Cyprus Institute, “Research and development study for a concentrated solar power - desalinization of sea water (CSP–DSW) project”, May, 2010.

[2] www.step-ew.eu/.

[3] A. Slocum, D. Codd, J. Buongiorno, C. Forsberg, T. McKrell, J. Nave, C. Papanicolas, A. Ghobeity, C. Noone, S. Passerini, F. Rojas, A. Mitsos, “Concentrated solar power on demand”, *Solar Energy*, vol. 85, pp. 1519-1529, 2011.

[4] A. Poullikkas, "A decouple optimization method for power technology selection in competitive markets", *Energy Sources*, vol. 4, pp. 199–211, 2009.
[5] C. Noone, A. Ghobeity, A. Slocum, G. Tzamtzis, A. Mitsos, "Site selection for hillside central receiver solar thermal plants", *Solar Energy*, vol. 85, pp. 839-848, 2011.
[6] A. Ghobeity, C. Noone, C. Papanicolas, A. Mitsos, "Optimal time-invariant of a power and water cogeneration solar-thermal plant", *Solar Energy*, vol. 85, pp. 2295-2320, 2011.
[7] A. Poullikkas, C. Rouvas, I. Hadjipaschalis, G. Koutis, "Optimum sizing of steam turbines for concentrated solar plants", *International Journal of Energy and Environment*, vol. 3, pp. 9-18, 2012.
[8] A. Poullikkas, "I.P.P. ALGORITHM v2.1, Software for power technology selection in competitive electricity markets", © *2000–2006*, *User Manual*, 2006.
[9] A. Poullikkas, "Economic analysis of power generation from parabolic trough solar thermal plants for the Mediterranean region - A case study for the island of Cyprus", *Renewable and Sustainable Energy Reviews*, vol. 13, pp. 2474–2484, 2009.
[10] A. Poullikkas, I. Hadjipaschalis, G. Kourtis, "The cost of integration of parabolic trough CSP plants in isolated Mediterranean power systems", *Renewable and Sustainable Energy Reviews*, vol. 14, pp. 1469–1476, 2010.
[11] A. Poullikkas, G. Kourtis, I. Hadjipaschalis, "Parametric analysis for the installation of solar dish technologies in Mediterranean regions", *Renewable and Sustainable Energy Reviews*, vol. 14, pp. 2772-2783, 2010.
[12] H. Klaiv, R. Kohne, J. Nitsch, U. Sprengel, "Solar thermal power plants for solar countries – technology, economics and market potential", *Applied Energy*, vol. 52, pp. 165–183, 1995.
[13] R. Shinnar, F. Citro, "Solar thermal energy: the forgotten energy source", *Technology in Society*, vol. 29, pp. 261–270.
[14] www.eac.com.cy/.

VII. BIOGRAPHIES

Andreas Poullikkas holds a Bachelor of Engineering (B.Eng.) degree in mechanical engineering, a Master of Phlosophy (M.Phil.) degree in nuclear safety and turbomachinery, a Doctor of Philosophy (Ph.D.) degree in numerical analysis and a Doctor of Science (D.Sc.) higher doctorate degree in energy policy and energy systems optimization from Loughborough University, U.K. He is a Chartered Scientist (CSci), Chartered Physicist (CPhys) and Member of The Institute of Physics (MInstP). His present employment is with the Electricity Authority of Cyprus where he holds the post of Assistant Manager of Research and Development; he is also, a Visiting Professor at the American University of Sharjah and at the University of Cyprus. In his professional career he has worked for academic institutions such as a Visiting Fellow at the Harvard School of Public Health, USA. He has over 20 years experience on research and development projects related to the numerical solution of partial differential equations, the mathematical analysis of fluid flows, the hydraulic design of turbomachines, the nuclear power safety, the analysis of power generation technologies and the power economics. He is the author of various peer-reviewed publications in scientific journals, book chapters and conference proceedings. He is the author of the postgraduate textbook: Introduction to Power Generation Technologies (ISBN: 978-1-60876-472-3), of the book Renewable Energy: Economics, Emerging Technologies and Global Practices, ISBN: 978-1-62618-231-8, of the book: The Cyprus Energy Future (ISBN: 978-9963-9599-4-5) and of the book: Sustainable Energy Development for Cyprus, ISBN: 978-9963-7355-3-2. He is, also, a referee for various international journals, serves as a reviewer for the evaluation of research proposals related to the field of energy and a coordinator of various funded research projects. He is a member of various national and European committees related to energy policy issues. He is the developer of various algorithms and software for the technical, economic and environmental analysis of power generation technologies, desalination technologies and renewable energy systems.

George Kourtis holds a Diploma and a Master Degree in Electrical and Computer Engineering from the Polytechnic School of Aristoteleio University of Thessaloniki (AUTH) and a Master Degree on Electrical Engineering from the University of Cyprus. During 2007 he has worked as a technician for LOGICOM LTD, where he was responsible for the maintenance of 3G Mobile stations. He joined Electricity Authority of Cyprus Research and Development Department in 2008, where he works on European funded research programs as an electrical engineer.

Ioannis Hadjipaschalis holds a B.Eng (Electrical Engineering), from the University of Sheffield, an M.Sc from the London School of Economics and an MBA. During 1996-2000 he worked at the Electricity Authority of Cyprus as Electrical Engineer, while during the period 2001-2005 he worked at ACNielsen Market Research. He joined EAC Research and Technological Development team in 2006, where he has been working on European funded research involving RES, Distributed Generation (DG), Electricity distribution networks, Hydrogen and CO_2 capture and storage (CCS) technologies.

2nd Conference on Power Options for the Eastern Mediterranean Region
07-08 October 2013, Nicosia, Cyprus (Paper No. POEM13/167)

Evaluation of the solar cooling and heating system of the CUT mechanical engineering laboratories

Soteris A. Kalogirou, Foivos Francou, Georgios Florides

Abstract-- The main objective of this paper is to describe and analyze the experimental system of solar cooling and heating, installed at the Mechanical Engineering laboratories of the Cyprus University of Technology (CUT). For this purpose, the behavior and performance of the system was studied over a period of one year, both for the cooling and heating modes using the Building Management System records. Furthermore, the performance of absorption chillers during the summer months was examined, and suggestions are made to reduce further the power consumption and to increase the overall efficiency of the system. The mean value of the coefficient of performance of the chiller was 0.68, which is quite high, even though the water entering the chiller was at a relatively low average temperature of 68°C. From the measurements it was also observed that there was excessive indirect energy consumption. Its main cause was related to the general pump over-sizing and the management of the un-used solar energy. Suggestions are given to reduce this consumption. The results of this study are very important because through our suggestions it is possible to increase efficiency, reduce energy consumption and make the system economically attractive to users.

***Index Terms*—Absorption chillers; Coefficient of performance; Solar cooling**

I. Introduction

In recent years, as reported by the Intergovernmental Panel on Climate Change (IPCC), the power consumption increased dramatically, resulting in a deterioration of the environment, which results in global warming and environmental pollution.

The negative environmental impact of climate change requires the immediate adoption of technologies that support the rational use of energy sources.

The use of solar energy for cooling of buildings is currently an attractive solution, especially for the climate of islands. The solar air conditioning, contributes positively to the energy reduction and environmental protection, while providing significant economic benefits [1].

In this paper, we will deal only with solar absorption cooling systems, and especially with the single stage lithium bromide - water absorption system that was installed in the Mechanical Engineering laboratories of the Cyprus University of Technology (CUT).

A refrigeration cycle by absorption is a process in which the cooling effect is produced through the use of two fluids and a heat source as input to the system [2].

The performance of an absorption refrigeration system depends to a significant extent on the chemical and thermodynamic properties of the fluid pair that is used [3].

There are a large number of cooling-absorbent pairs that can be used but the couple chosen should meet some important requirements such as absence of solid phase, volatility ratio, affinity, pressure, stability, corrosion, safety and latent heat.

None of the pairs meet all the requirements listed above, but the most common pair of fluids used is LiBr-H_2O (Water-Lithium Bromide) and H_2O-NH_3 (Ammonia-Water) [4].

The system employed in the CUT laboratories is of the single effect LiBr-H_2O technology. Absorption systems are similar to vapour-compression air conditioning systems but differ in the pressurisation stages. In general an absorbent on the low-pressure side (in this case the LiBr), absorbs an evaporating refrigerant (H_2O). The pressurisation is achieved by dissolving the refrigerant in the absorbent in the absorber section. Subsequently, the solution is pumped to a high pressure with an ordinary liquid pump. The addition of heat in the generator is used to separate the low-boiling refrigerant from the solution. In this way, the refrigerant vapour is compressed without the need of large amounts of mechanical energy that a vapour-compression air conditioning system demands. The remainder of the system consists of a condenser, expansion valve and an evaporator, which function in a similar way as those in a vapour-compression air conditioning system.

II. Literature Review

Literature regarding applications of absorption refrigeration systems is scarce. Bermejo et al. [5] analyzed a solar cooling system in the Faculty of Engineering of Seville in Spain. The system consists of a double effect LiBr - H_2O absorption chiller and linear concentrating collectors with a total collector area of 352 m^2. The average efficiency of the collectors was 35% and the coefficient of system performance (COP) ranged from 1.1-1.25. Also Lizarte et al. [6] analyzed a solar cooling system, applied in Madrid which consists of a single stage LiBr - H_2O absorption chiller of 4.5 kW cooling capacity and flat plate collectors

S. A. Kalogirou is with the Cyprus University of Technology, (e-mail: Soteris.Kalogirou@cut.ac.cy).
F. Francou is with the Cyprus University of Technology, (e-mail: ffrangos@hotmail.com)
G.A. Florides is with the Cyprus University of Technology, (e-mail: Georgios.Florides@cut.ac.cy).

with a total collector area of 42.2 m^2. The COP was 0.62. A similar analysis was performed by Monne et al. [7] for a solar cooling system applied in Zaragoza, Spain. The system consists of a single stage LiBr - H_2O absorption chiller of 4.5 kW cooling capacity and flat plate collectors with a total collector area of 37.5 m^2. The coefficient of performance of the system was 0.6. Furthermore Balghouthi et al. [8] analyzed a solar cooling system applied in Tunisia in a building which covers 150 m^2. The system includes a single stage LiBr - Water absorption chiller of 11 kW cooling capacity and flat plate collectors with a total collector area of 37.5 m^2. The COP of the system was 0.72. Moreover Yin et al. [9] analyzed a solar cooling system in a 50 m^2 area installed in Shanghai, China. The system consists of a single stage LiBr - H_2O absorption chiller of 8 kW cooling capacity and evacuated tube collectors with a total collector area of 96 m^2. The COP of the system was 0.31, which is very low for the solar radiation absorbed by the collectors throughout the day.

III. Description of the Building

The building was used for many years as a warehouse and its area covers 1400 m^2. In 2010, the building was renovated and is now used as classrooms and laboratories as well as a workshop (half of the building) of the Department of Mechanical Engineering and Materials Science and Engineering of the CUT. The renovation did not affect the external walls of the building, which were built in 1950 and consist of limestone blocks 50 cm in thickness. Double-glazing was fitted and the roof was rebuilt from scratch using thermal Rockwool insulation of 200 mm thickness. The building has a double pitched roof, which has a minimum height of 6m and a 20° slope. The solar panels have been installed on the two south facing areas of the building roof. The total cooling load of the building is estimated to be 250 KW [10]. In the building a solar central air conditioning system (heating and cooling) has been installed and is operating. Additionally, a cooling tower is employed to cool down the condenser of the absorption chiller. The cooling tower is also assisted by a geothermal system. The solar cooling system is installed to cover the cooling needs of the building with renewable energy and is fully monitored through the building management system, which also records all the temperatures and energy flows of the system.

The system diagram shown in Fig. 1 and Fig. 2, consists of three absorption chillers each having a cooling capacity of 95 kW, three hot water storage tanks with a total capacity of 14,100 liters, two oil fired boilers of 155 kW capacity each, a closed type water cooling tower with a capacity of 425 kW and 69 evacuated tube solar collectors having a total absorber area of 310.5 m^2 (see Fig. 3).

IV. Description of the Solar Cooling System of the Building

According to Figs. 1 and 2, solar energy is collected by the solar panels located on the roof and stored in 3 hot water storage cylinders with 4700 liters capacity each. The system is controlled by a differential thermostat, which compares the temperature of the water in the cylinders with the temperature of the water from the solar panels. When the temperature of the water from the solar panels is greater by a predetermined difference (DT) then energy is transferred from the solar panels to the storage cylinders. The hot water from the solar panels transfers the heat to the cylinders through heat exchangers located in the cylinders.

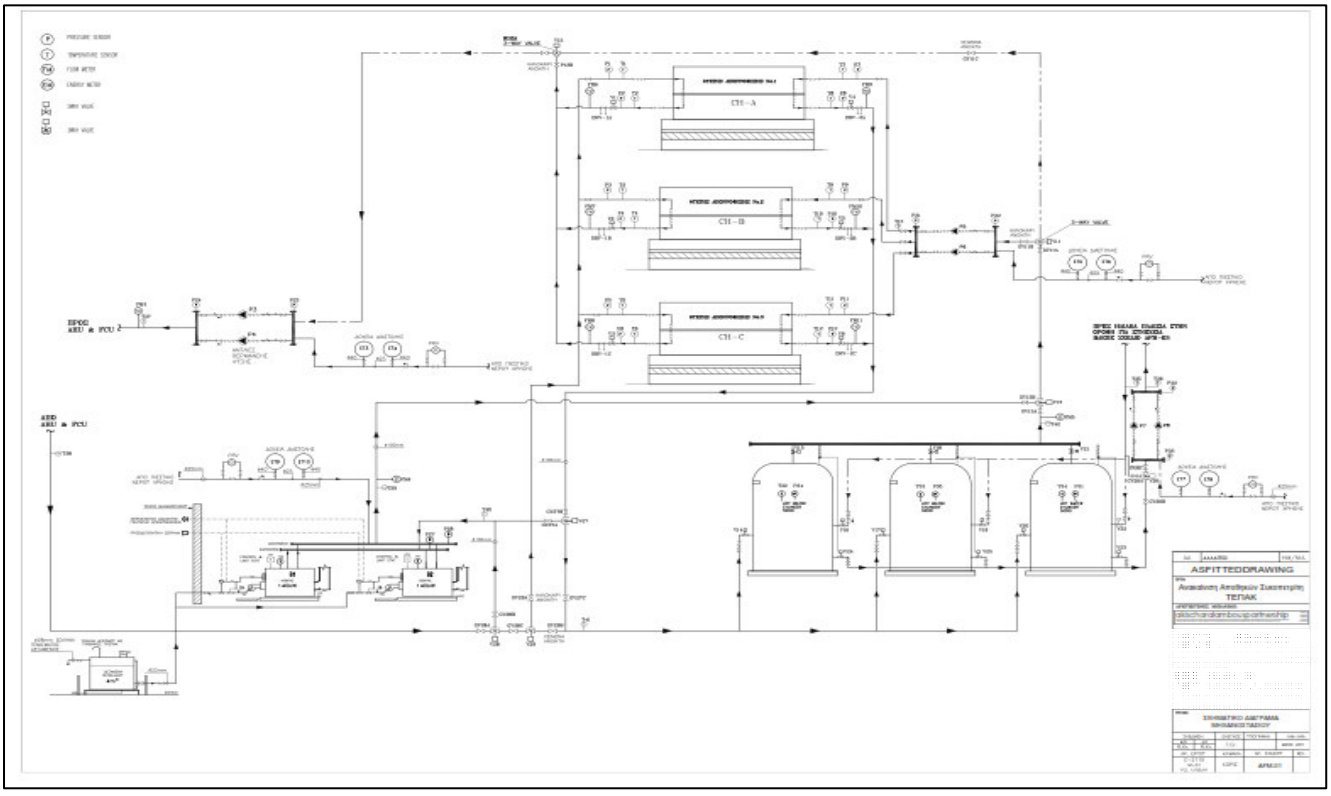

Fig. 1. Schematic diagram of the solar cooling system – connection with boilers and hot water cylinders

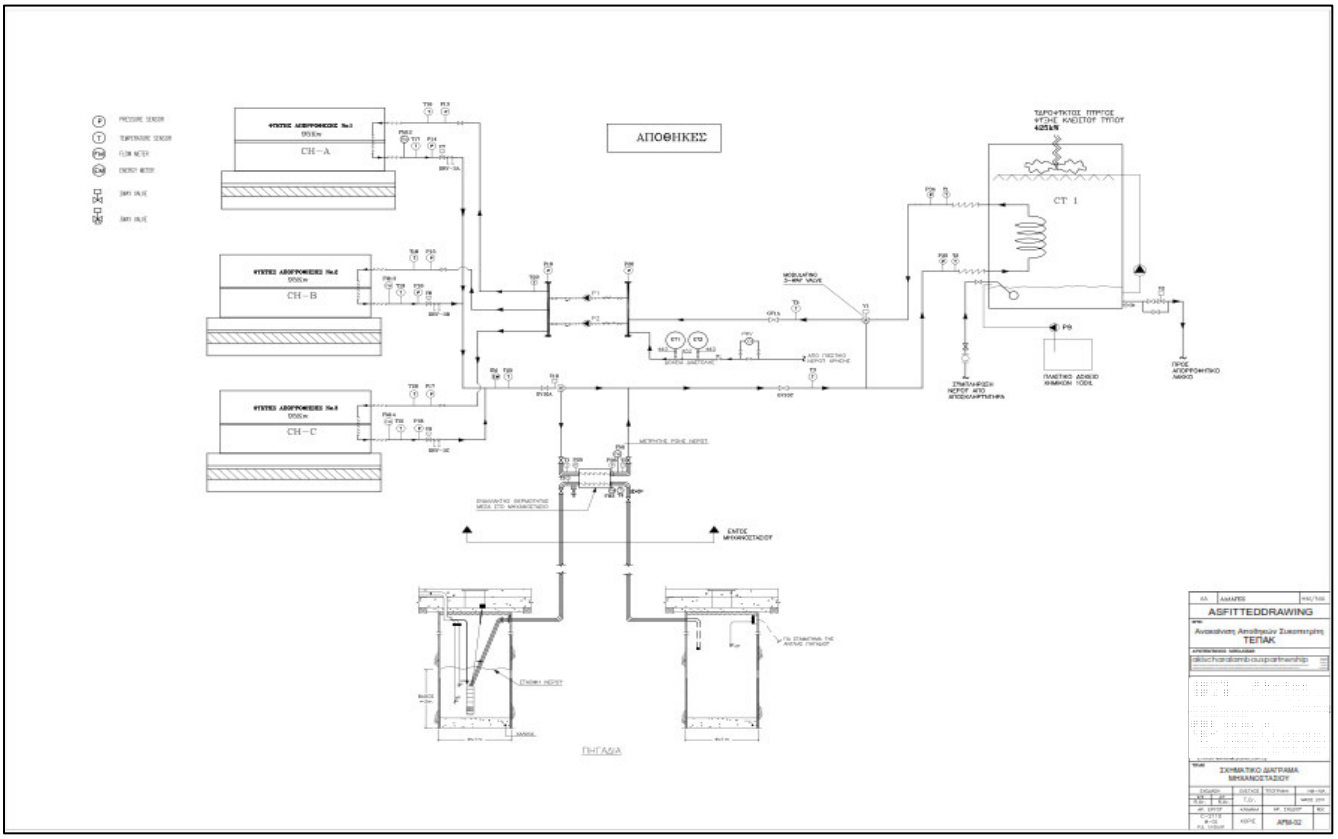

Fig. 2. Schematic diagram of the solar cooling system – connection with cooling tower and geothermal wells.

The stored hot water is circulated through pipes to the absorption chillers where the solar collected energy is used to produce refrigeration by the chillers. In the case where the stored hot water is not enough to meet the required needs of chillers, valves 4 and 5 open to allow the hot water boilers B1, B2, to give additional energy directly to the chillers (i.e., without heating the water content of the cylinders) and meet the demand.

The cold water produced by the chillers is transferred by piping to the air conditioning units (fan coil units-FCU and air handling units-AHU) which are used for cooling the building.

The hot water coming out from the chillers goes back to the hot water storage cylinders. Cold water from the cooling tower extracts heat from the absorber and the condenser of the chiller and then passes through the heat exchanger, which cools the water using two wells. This is a significant originality of the system, i.e., the combination of the cooling system with geothermal energy. Water from well 1 feeds the heat exchanger to cool the water that comes from the chillers and then is discarded in well 2. Then the water passes from the chillers of the cooling tower to further remove energy and cool it to the required temperature (Figure 2).

During the winter, chillers have no use since the demand is for heating. The solar heating system works in exactly the same manner as in summer by storing hot water in the storage cylinders.

In winter, the three way valves 6, 7 and 8 change setting so that the stored hot water does not pass through the chillers but is diverted directly to the air units (FCU and AHU) and back to the hot water storage.

In the case where the stored hot water is not enough to meet the requirements of the building, valves 4 and 9 open and hot water from the boiler is supplied directly to the air units and returns back to the boilers.

Fig. 3 Photo of one of the two banks of solar evacuated tube collectors

V. Analysis of the Solar System

A. *System analysis methodology*

The installed Building Management System (BMS) was used to record all system parameters through the whole year of study, which were then analyzed and recorded in charts using Excel. The BMS is linked with appropriate sensors and is designed to monitor, control and optimize the building installations. The system is fully monitored so as to be able to evaluate its performance as a whole and also the performance of each component of the system individually. A snapshot of the screen of the BMS, of the absorption chillers, is shown in Fig. 4. The figure shows that at that time

only the second absorption chiller was operating.

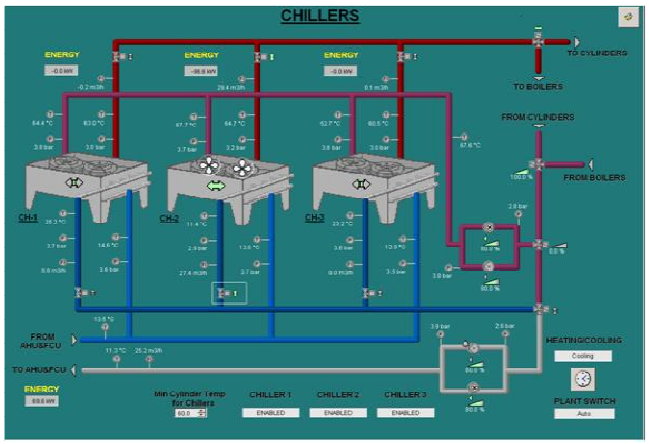

Fig. 4 BMS system showing the conditions of the absorption chillers.

To examine the performance of the absorption chillers during the summer months the records of power flow coming from the solar domestic hot water cylinders entering the chiller, and the power flow exiting the chiller and going to the air units (fun coil units and air handling units), were used. Figure 5 shows the power flow into and out of the chillers for the period of 01/06/12 to 29/06/12 on a daily basis from 8:00 in the morning until 16:00 in the afternoon. It is observed that the input power varies between 70 kW and 125 kW and the output power is between 45 kW and 90 kW. The quotient of outgoing power to the incoming one gives the performance of the chillers and as shown in the figure it varies between 52% and 73%. Additionally, Fig. 5 shows the average temperature of water entering the chiller from 8:00 in the morning until 16:00 in the afternoon, which varies between 60°C and 78°C.

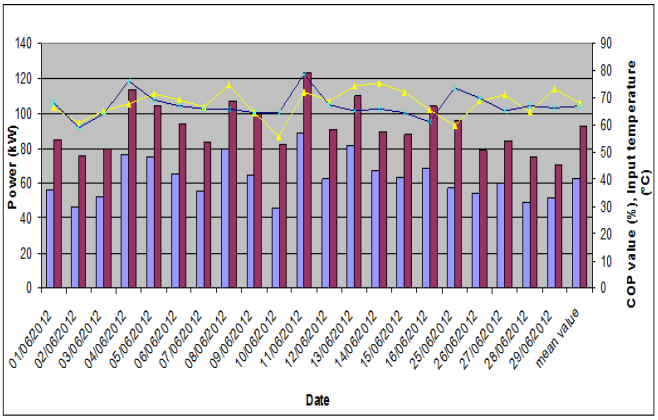

Fig. 5. Graph showing the outgoing power from chillers (blue color), the incoming power to the chillers (RED color), the incoming water temperature to the chillers (blue color line) and the coefficient of performance (yellow color line) for the period 01/06/12 – 29/06/12

B. Performance of absorption chillers during the summer months

Based on the manufacturers technical details, the absorption chillers should operate on input water temperatures of about 85°C to achieve maximum C.O.P. In our system even though the input temperatures where around 70°C, as shown in Table I, the achieved C.O.P was relatively high because the required cooling load was low compared to the size of the chiller.

Table I shows the chiller performance for May to October as well as the incoming hot water temperature to chillers. The calculated average performance (COP) of this period is 0.68 and the average incoming hot water temperature is only 67.8°C, which is low.

The system was set up in such a way as to avoid stored water temperatures to reach 75°C because there was no need for extra energy. This resulted in a low performance of the chillers. However if the whole building was operating (see section IV) the chillers would not have been able to cover the cooling load satisfactorily. Therefore, the study was focused on ways to reduce auxiliary energy consumption (e.g. electricity) but at the same time to achieve maximum system efficiency.

TABLE I
SUMMARY OF PERFORMANCE AND INLET HOT WATER TEMPERATURE OF CHILLERS DURING THE SUMMER MONTHS

Period	Chiller Performance (COP)	Incoming hot water temperature to chillers
May	0.69	71.7°C
June	0.68	67.1°C
July	0.68	67°C
August	0.68	67.1°C
September	0.69	67.3°C
October	0.66	66.3°C
Mean value	**0.68**	**67.8°C**

VI. RESULTS AND SUGGESTIONS

In general, the system as a whole is operating effectively, since during the year no fuel was needed to cover the cooling or heating loads of the building. A drawback is that the whole system is oversized, although during the examined period only half of the building was operating. In fact, the workshop part of the building, which draws half of the total load, was not conditioned during the evaluation period for various reasons.

The only energy consumed by the system was electricity and attention was given to reduce its consumption to the minimum with the suggestions that follow.

A detailed study of the technical specifications of the installed solar evacuated tube collectors proved that a much lower water flow rate than the one used was required in order to achieve higher water temperatures. Therefore, the installed pump for this purpose was oversized consuming more electrical energy than needed.

Additionally, on the same pumping system it was noted that the differential temperature controller was set up with a very small temperature differential. This caused the pump to work more often than required, thus consuming more unnecessary power and not allowing the solar system to attain high temperatures. The differential set point should have been set at 10°C.

It is suggested to correct the temperature differential and during the summer period, to account for days with low required cooling load and thus possible overheating, it is suggested to install a heat rejection system to avoid overheating. The heat rejection system operates with a much lower energy consumption rate than running the cooling

system at full load, which is what is done now to avoid this problem.

The chilled water pump installed was sized for a system where all three absorption chillers would be in operation. This means that during the operation of our system with only one chiller in operation, the pump was consuming much higher energy than a pump sized for one chiller only. Therefore, it is suggested that the pump is replaced by smaller pumps each operating with its own chiller.

An economic analysis showing the savings that would result if the current pumps are replaced with appropriate ones, is shown in Table II. As it is shown, a total cost of €4868 will be needed for the replacement of the pumps. The pay-back period for this investment will be only about eight months and the savings that would results for each year would be €7125. It should be noted that this will also increase the efficiency of the complete system.

TABLE 2
RESULTS OF ECONOMIC ANALYSIS

Pump over-sizing				
Current pump	**Suggested pump**	**Cost**	**Pay-back period**	**Saving**
Pumps circulating water in solar panels. TP 80-270/4	TP 32-320/2	**€1250**	4 months	**€4310** per year.
Pumps circulating hot water in chillers. TP 80-240/4	TP 50-240/2 for each chiller	**€1330**	7 months	**€800** per year.
Pumps circulating cold or hot water to air units. TP 80-240/4	Circulating cold water. TP 32-320/2 Circulating hot water. TP 32-200/2	**€1250** **€1038**	6 months 4 months	**€935** per year. **€1080** per year.
Total cost of the suggested pumps				**€4868**
Approximate pay-back period for all pumps				**8 months**
Savings for the operation of the suggested pumps per year				**€7125**

VII. CONCLUSION

The building in which the system was installed is not the best application for energy savings due to the nature of its operation (operating hours between 8:00 – 16:00).

Additionally, during the months of July and August, where there is maximum solar input and thus better performance of the cooling system, the building is under-utilized or closed completely due to summer holidays. In July and August, it was very important to keep the system operating to avoid overheating of the collector system, thus wasting electrical and solar power. A much better application would be in buildings with round the clock requirements for cooling and heating (e.g. hotels, airports, etc.), but the system was installed primarily for experimental reasons.

Based on the techno-economical study of the system it is suggested that all parts of the system are very carefully sized and selected to make the system viable in terms of economy and energy consumption.

It is shown that with a few simple measures the overall system performance would be improved drastically. This reduced electrical energy requirements opens also the idea of installing photovoltaics to cover this load so as to make the system 100% renewable.

VIII. REFERENCES

[1] Tsoutsos, Th., 2012. Application of solar cooling in Crete. *Building Green*, (7), pp.54–60.

[2] Srikhirin, P., 2001. A review of absorption refrigeration technologies. Renewable and sustainable energy reviews, 5, pp.343–372.

[3] Crepinsek, Z., Goricanec, D., Krope, J., 2000. Comparison of the performances of working fluids for absorption refrigeration systems. *wseas.us*, pp.59–64.

[4] Florides, G.A., Kalogirou, S.A., Tassou, S.A., Wrobel, L.C.,2003. Design and construction of a LiBr–water absorption machine. *Energy Conversion and Management*, 44(15), pp.2483–2508.

[5] Bermejo, P., Pino, F.J., Rosa, F., 2010. Solar absorption cooling plant in Seville. *Solar Energy*, 84(8), pp.1503–1512.

[6] Lizarte, R., Izquierdo, M., Marcos, J.D., Palacios, E., 2012. An innovative solar-driven directly air-cooled LiBr–H2O absorption chiller prototype for residential use. *Energy and Buildings*, 47, pp.1–11.

[7] Monné, C., Alonso, S., Palacin, F., Serra, L., 2011. Monitoring and simulation of an existing solar powered absorption cooling system in Zaragoza (Spain). *Applied Thermal Engineering*, 31(1), pp.28–35.

[8] Balghouthi, M., Chahbani, M.H. & Guizani, A., 2008. Feasibility of solar absorption air conditioning in Tunisia. *Building and Environment*, 43(9), pp.1459–1470.

[9] Yin, Y.L., Song, Z.P., Li, Y., Wang. R.Z., Zhai, X.Q., 2012. Experimental investigation of a mini-type solar absorption cooling system under different cooling modes. *Energy and Buildings*, 47, pp.131–138.

[10] Florides, G.A., Kalogirou, S.A., 2009. A solar cooling and heating system for a laboratory building. Proceedings of HPC'2009 Conference on Heat Power Cycles on CD-ROM, Berlin, Germany, pp.2–7.

IX. BIOGRAPHIES

Soteris A. Kalogirou was born in Trachonas, Nicosia, Cyprus on November 11, 1959. He is a Senior Lecturer at the Department of Mechanical Engineering and Materials Sciences and Engineering of the Cyprus University of Technology, Limassol, Cyprus. He received his HTI Degree in Mechanical Engineering in 1982, his M.Phil. in Mechanical Engineering from the Polytechnic of Wales in 1991 and his Ph.D. in Mechanical Engineering from the University of Glamorgan in 1995. In June 2011 he received from the University of Glamorgan the title of D.Sc. He is Visiting Professor at Brunel University, UK and Adjunct Professor at the Dublin Institute of Technology (DIT), Ireland. For more than 25 years, he is actively involved in research in the area of solar energy and particularly in flat plate and concentrating collectors, solar water heating, solar steam generating systems, desalination and absorption cooling.

He has 41 books and book contributions and published 264 papers; 109 in international scientific journals and 155 in refereed conference proceedings. Until now, he received more than 4000 citations on this work and his h-index is 35. He is Executive Editor of Energy, Associate Editor of Renewable Energy and Editorial Board Member of another eleven journals. He is the editor of the book Artificial Intelligence in Energy and Renewable Energy Systems, published by Nova Science Inc., co-editor of

the book Soft Computing in Green and Renewable Energy Systems, published by Springer and author of the book Solar Energy Engineering: Processes and Systems, published by Academic Press of Elsevier.

Fivos Frangou was born in Limassol (Cyprus), on July 30, 1989. He graduated from the Agia Phyla Lyceum, Limassol, and studied Mechanical Engineering and Materials of Science at the Cyprus University of Technology. He received the top overall performance in all 4 years of his study in university.

He works in his father company as a Mechanical Engineer but he is looking forward to work in the sector of oil and gas energy and with renewable energy.

Georgios Florides was born in Kaimakli, Nicosia, Cyprus on November 26, 1952. He was a Senior Lecturer and is now a researcher of the Department of Mechanical Engineering and Materials Science and Engineering. He received his basic degree in Mechanical Engineering from the Higher Technical Institute and he was awarded an MPhil and a PhD by Brunel University, London, UK. He was employed by the Higher Technical Institute from 1975-2007 in various posts, in the Mechanical Engineering Department and in the Engineering Practice Department. He used to teach the theory and practice of Welding, Machine-shop, Bench-fitting and Plumbing. His research activity focuses on the topic of Energy, which includes studies and analysis of the energy requirements of buildings, measures to lower building thermal loads, design of LiBr-water absorption machines, modelling and simulation of absorption solar cooling systems and earth heat exchangers and heat pumps. He also studies the thermal behaviour of reptiles and scientifically constructs models of extinct animals.

2nd Conference on Power Options for the Eastern Mediterranean Region
07-08 October 2013, Nicosia, Cyprus (Paper No. POEM13/168)

Energy Security in the Eastern Mediterranean Regional Security Complexes

Constantinos Adamides and Odysseas Christou

Abstract-- **This paper utilizes Regional Security Complex Theory (RSCT) in order to analyze developments in the trilateral securitization relations among Turkey, Israel and Cyprus. We use this set of relationships as a case study of the effects of energy as a referent object of securitization and as an exogenous parameter influencing the three states' securitization and security relationships. Furthermore, this paper argues that the increasing energy securitization dynamics among the three states poses a challenge for the RSCT. The emergence of patterns of security interdependence as a result of energy securitization among the three regional actors—Turkey, Israel and Cyprus—satisfies the criteria of subcomplex, yet violates the condition that a subcomplex is firmly embedded within a larger RSC. In fact, the triangle exists at the interstices of two RSCs and a major insulator state.**

I. Regional Security Complex Theory (RSCT) – A Brief Overview

THE concept of Regional Security Complexes (RSC) was first developed by Barry Buzan (1983) in the seminal *People, States and Fear* and advanced further in subsequent works (Buzan 1991; Buzan et al. 1998; Buzan and Waever 2003), focusing on the idea that the structure of international security could be understood better from a regional perspective. Originally Buzan (1983: 106) defined security complexes as 'a group of states whose primary security concerns link together sufficiently closely that their national securities cannot reasonably be considered apart from one another'. The concept developed by shifting emphasis towards securitization relations, resulting in the revised definition of 'a set of units whose major processes of securitization, desecuritization or both, are so interlinked that their security problems cannot be reasonably analyzed or resolved apart from one another' (Buzan et al. 1998: 201).[1] 'States' were substituted with 'units' – allowing for analysis beyond the state level – and the focus shifted to the interdependence of securitization processes rather than security interests (Huysmans 1998: 498).

States' involvement in security complexes under anarchy is not necessarily a negative development (Buzan 1991: 196-7). 'A security complex exists where a set of security relationships stands out from the general background by virtue of its relatively strong, inward-looking character, and the relative weakness of its outward security interactions with its neighbours' (ibid: 191). Thus, the driving force of security complexes is the enmity and amity relationships among states within the complex rather than the balance of power (Buzan 1998: 2). These relationships generate a number of possible formations ranging from regional conflict formation to regional security integration (Buzan 1991: 218). The distribution of power defines the polarity of RSCs (Buzan and Waever 2003: 55); however, the distribution of power within the RSC is determined by the perceptions of states within the complex (Buzan 2007: 161), which may be intensified by pre-existing amity and enmity relationships.

According to RSC Theory it is possible to study security in some or all four contexts: intra-state; inter-state (most often within the RSCs); between complexes; and on a global level (Buzan and Waever 2003: 51), but the focus remains on the regional level as 'most threats travel more easily over short distances than over long ones'. Thus, security interdependence is normally patterned into regionally-based clusters, or security complexes (ibid: 4). Buzan and Waever argue that there are numerous mutually exclusive regional complexes even though interaction across complexes is possible (ibid: 48). States do not limit their interactions to states within their complex; on the contrary, they may form security alliances or to counter disturbances in the balance of power. RSC interactions are separated into two distinct concepts: penetration and overlay. Penetration refers to cases where a state outside an RSC forms alliances with states within the complex. Such interactions link the two complexes without violating the exclusivity condition (ibid: 46). Overlay refers to cases where the influence of two or more great powers is so dominating that it does not allow the formation of an RSC (ibid: 61).

RSCs also co-exist with sub-complexes, insulator and buffer states as well as great and super powers. Sub-complexes are smaller complexes subsumed within larger RSCs. Insulator states are states located in an area where large security dynamics stand adjacent (ibid: 41), with Turkey being a prime example. Lastly, buffer states are states that are located at the center of strong patterns of securitization (ibid), but are not themselves actively involved in these securitization dynamics and cannot determine the outcome of the confrontations within the complex.

II. Energy Security and Energy Securitization

Energy security refers to the ability of states to maintain uninterrupted energy supply relative to demand at affordable and relatively stable prices without sudden and significant price increases (Winzer 2011; Deutch and Schlesinger 2006: 3; International Energy Agency[2] (IEA)). Energy insecurity,

Dr. Constantinos Adamides is a Lecturer at the Department of European Studies and International Relations, University of Nicosia and a Research Officer at the Research and Innovation Office.

Dr. Odysseas Christou is a Lecturer at the Department of European Studies and International Relations and a Postdoctoral Research Fellow at the Center for European and International Affairs at the University of Nicosia.

[1] See also Buzan 2007: 160 for a similar definition. Securitization is the intersubjective establishment of an existential threat that is salient enough to have significant political effects (Buzan et al. 1998: 25).

[2] http://www.iea.org/topics/energysecurity/

therefore, is the interruption of supply or sudden price fluctuations that could result from terrorism, oil nationalism and political instability in oil and gas producing regions such as the Middle East and the Caucasus (Kalicki and Goldwyn 2005, Mabro 2008). Energy security is further ensured through energy diversification so as to avoid overreliance on a single supplier and on a single form of energy (such as fossil fuels). Energy security, especially for industrialized states, inevitably entails a foreign policy dimension as observed by the meetings of George W. Bush and Vladimir Putin for more energy cooperation and those of China's President Hu Jintao with several African states' leaders and energy firms. Similarly, energy security also entails a military dimension as demonstrated by the ongoing US efforts to protect friendly energy-supplying regimes, such as Saudi Arabia, and energy routes such as the narrow Straits of Hormuz (Klare 2004).

In the securitization literature energy security remains a largely under-explored area with some notable exceptions (McGowan 2011; Kirchner and Berk 2010). Buzan et al. (1998: 116) characterized energy as an economic referent object, tradable in the global market and subject to market forces. Due to the relative abundance of this commodity, energy insecurity does not pose an existential threat beyond the economic sector. Others argue that energy security could be defined in political, military, technical and economic terms and theoretically examined in the associated sectors (Natorski and Herranz-Surralles 2008: 71).

Securitization theory claims that security threats are socially constructed and the outcome of an intersubjective process between securitizing actors and the relevant audiences. This approach to security allows for the development of a widened security agenda with multiple sectors and numerous potential referent objects and since its conception, the theory has been used to study security-related issues and processes in several areas.[3] The widened security agenda is divided into five sectors of specific security discourses. The five sectors, namely political, military, societal, economic and environmental have distinct referent objects, subject to empirical observations of securitization discourses in each area (Buzan et al. 1998). To this day however the widened security agenda is limited to the five original sectors, while the treatment of energy remains unclear.

Contrary to the Copenhagen School position that treats energy strictly as an economic referent object (Buzan et al. 1998: 116), we claim that energy could be a referent object in most the five sectors (Natorski and Herranz-Surralles 2008: 71). We argue that energy security's inherent characteristics - namely that the impact of energy insecurity could be both imminent and immediate - are important factors for securitization processes as they can simultaneously influence the securitization of non-energy referent objects in other sectors. Energy securitization rarely takes place independently of other security processes; on the contrary, it tends to be subsumed by political, economic and even military threat discourses, frequently acting as a multiplier on the existing securitization relations. Energy security therefore could best be analyzed using a cross-sectoral approach that also facilitates the examination of its impact on other referent objects in their respective sectors.

Energy security may also merit its own sector in the securitization framework. Indeed, it could be argued that if the existing sectors are identified by the frequency of relevant security discourses in that area, then energy may qualify as a sixth sector. We are skeptical of this argument given that energy-related threats are usually manifested in economic, political and military terms, which can already be sufficiently analyzed in the existing sectors. If energy insecurity is manifested through threat generation against state survival, it may be subsumed by the political and military sectors where the state is the referent object. A comprehensive approach to energy that encompasses all sectors will take into consideration the intertwined sectoral variables and securitization processes that take place. Such an approach is also necessitated by the aforementioned inherent characteristics of energy-related securitization: the imminence and the immediacy of such processes.

Imminence refers to the fact that energy insecurity can occur at any time and easily escalate from minor to existential threat. This escalation is likely to result from factors beyond economic considerations; indeed, political and military factors only tangentially relevant to energy frequently lead to energy insecurity. This characteristic differentiates energy from other economic referent objects which tend to be characterized by long-term processes of threat escalation or abatement. The Syrian crisis, or the frequently proposed sanctions on Iran, are indicative examples of how non-energy related issues could increase regional and global energy insecurity. Similarly, the reconfiguration of the political landscape in the post-Arab Spring Middle East could potentially lead to energy insecurity for states such as Israel due to changes in its political relations with Egypt, one of the main natural gas suppliers of Israel.[4] In such cases, energy insecurity that results from political or military actions is neither subject to nor rectifiable by market forces. Energy threats therefore are imminent and frequently unpredictable *because* they do not rely on economic rationale. On the contrary, economic benefits from potential energy agreements are frequently sacrificed for political and military considerations.

Energy insecurity is also unique because of the immediate and severe impact it can have on the functioning of a state. As demonstrated by the 2009 Russia-Ukraine gas dispute, energy insecurity had a direct and immediate impact on Ukraine as well as several EU member states, leading them into an energy crisis within a few days. The impact of energy-related threats quickly spills over from the economic sector into the political, given that energy insufficiency represents an existential threat to the entire state and not just the economy. Indicatively, the aforementioned event forced the EU Commission to treat the event as a political issue, warning Russia that their political relations could break down (Gow, 7/1/2009). As with the attribute of imminence, immediacy differentiates energy from other economic referent objects which are unlikely to represent existential threats to the state in the short-run.

Both characteristics may not necessarily be the outcome of a long-term intersubjective process between securitizing

[3] Indicative areas where securitization is used as an analytical tool are terrorism (Buzan 2006), immigration (Bigo 2002, 2005; Bigo and Walker 2002; Alexseev 2011), human security (Floyd 2007), the environment (Wishnick 2010) and women's rights (Hansen 2000).

[4] Indeed in 2012 Egypt, with the tumbling of the Mubarak regime, cancelled the 20-year contract to supply Israel with natural gas (http://www.theguardian.com/world/2012/apr/23/egypt-cancels-israeli-gas-contract)

actor and audience. The very nature of energy insecurity elevates securitization processes to high-stakes existential threats with a perceivable level of objectivity, which securitizing actors can easily choose to situate in multiple sectors. As a result, audiences can recognize and accept such threats and may grant extraordinary means without the necessity of extended negotiation.

Energy can also significantly influence cross-sector securitization through an intensification effect by reinforcing and broadening the existing securitization processes in the political, military and economic sectors. Specifically, in cases with securitized political and military sectors due to border or sovereign contestations – as is the case of Israel with Lebanon, Syria and the Palestinian authorities – energy becomes an additional contestation issue leading to the heightening of securitization in the two sectors. Conversely, where political and military securitization relations are relatively normalized – such as the case of Cyprus and Israel – or de-escalating – such as the case of Israel and Egypt – energy could reinforce desecuritization trends in the political and military sectors.

In addition, the nature of bilateral or multilateral energy agreements also contributes to cross-sectoral spillover, especially with respect to desecuritization. Energy agreements tend to be long-term and usually lead to significant interdependence among the actors involved, which tends to promote normalized relationships in all sectors, frequently leading to the development of strong alliances. Precisely for this reason, bilateral energy agreements – be they, for example, between Cyprus and Israel or Cyprus and Egypt – could be perceived as threats by third states, such as Turkey.

Where political relations are at a relatively low level of securitization, energy agreements are more likely to be achieved and can act as a reinforcing mechanism for the perpetuation of normalized relations. Conversely, where political relations are at a relatively high level of securitization energy is less likely to have similar impact; energy can only be a catalyst for desecuritization under certain conditions. Unless securitization in the political sector is less than or equal to securitization in the economic sector, then political considerations will trump economic ones, even to the point of foregoing the benefits of mutual cooperation. In other words, energy-related collaborations may normalize the economic but not the political sector in deeply securitized political relations. If the political sector is more securitized than the economic one, the establishment of energy collaborations and possible desecuritization processes in the economic sector will be impeded. However, in relatively normalized political environments, economic threats do not necessarily extend to political relations and securitization may be contained to the economic sector.

Economic collaborations in politically securitized environments may emerge when political securitization falls below a threshold level. A general criticism of securitization is that this level is not easily measurable; it may be determined and observed by public and elite audiences' reactions to proposed international agreements within highly securitized environments.

An indicative example is the case of Cyprus, where deeply securitized political relations eliminate any possibility for natural gas pipes from Cyprus to traverse through Turkey, despite the fact that this would be mutually beneficial. This would only be possible with a negotiated settlement to the ongoing dispute between the two states[5] or if it is perceived to serve the Cypriot national interest.[6] However, once such collaborations materialize, political securitization can be maintained at low levels if the benefits from cooperation are sufficiently high to counteract short-term elevations in political securitization. Energy is thus a special case in the sense that due to the characteristics outlined above – immediacy and magnitude of impact on securitization in multiple sectors – it can have political as well as economic relations, unlike other referent objects in the economic sector. Several case studies from the Middle East and North Africa demonstrate the aforementioned arguments.

III. Energy impact at the edge of the European and Middle Eastern RSC

The recently discovered natural gas reserves in the Eastern Mediterranean demonstrate how energy acts as an intervening variable of securitization in the political and military sectors. The exploitation of these resources in the EEZs of Israel, Lebanon, Syria and Cyprus indicates how energy exploitation is a significant factor in the shaping of the new Middle East. The prospects for energy exploitation exacerbated existing disputes over sovereignty such as the contestation of maritime borders, with the Palestinians, Syrians, Egyptians and Lebanese claiming that Israel is 'stealing their gas deposits' (Bahgat 2011; Shaffer 2011). The Lebanese and more specifically Hezbollah have intensified this contestation claiming that they will defend the country's natural resources (Bahgat 2011), forcing an Israeli response from the National Infrastructure Minister Uzi Landau, who warned that Israel will protect its national interests with 'all [its] ability' (Zacharia 2010). This demonstrates the confluence of the energy factor and the escalation of sovereignty disputes as securitization in the political sector. However, Minister Landau's response connotes that military relations subsumes threats to sovereignty in tandem with the threat to the ability to exploit national natural resources, thus intensifying securitization in the military sector (Shaffer 2011).

The prospects of energy exploitation need not always lead to intensified securitization relations. Israel and Cyprus for instance have realized the potential for mutual benefits to accrue from collaboration and quickly reached an agreement in 2010. The collaboration was possible however because of the desecuritized relationships of the two states, which not only maintained the (desecuritized) status quo, but also increased the prospects for bilateral alliances on political, economic and even military levels. Such energy-induced alliance formations however could also have inadvertent impact on regional security complexes by intensifiying securitization among other regional actors. For instance, the agreement between Israel and Cyprus regarding their EEZ and the prospect for natural gas exploitation led to the exacerbation of the already tense Israeli-Turkish relations following the 2010 Mavi Marmara incident.

While the relationship between Israel and Cyprus has remained devoid of conflict, the turbulent relationship between the Republic of Cyprus (RoC) and Turkey is deeply securitized because of the protracted Cyprus conflict. Turkey, which does not recognize the RoC, questions the

[5] http://www.cyprusgasnews.com/archives/1924

[6] http://www.financialmirror.com/news-details.php?nid=28669

validity of the agreement claiming that the rights of Turkish Cypriots are being violated. More importantly, Turkey perceives the improving Cyprus-Israeli relationship as a political and military challenge for Turkey (Bahgat 2011; Zaman 2012a). The magnitude of threat perception by Turkey is demonstrated by the recent claim that 20,000 Israeli commandos will be stationed on Cyprus for the protection of a growing Israeli contingent on the island and the planned natural gas processing plants (Hurriyet Daily News 20/5/2012). This claim was quickly rejected by the Cypriot government (Zaman 2012b). Such discourses demonstrate how energy-related issues can lead to securitization in the political and military sectors but not in the economic one.

From a RSC perspective the intensified relations among the three states is particularly interesting, as Cyprus and Israel are located in two different complexes, while Turkey is a major insulator state. Cyprus politically lies squarely – albeit geographically at the margins – in the European RSC, while Israel is at the heart of the Middle Eastern one. Turkey on the other hand is an insulator state located at the margin of three RSCs, the two aforementioned ones and the former Soviet one. The emergence of patterns of security interdependence as a result of energy securitization among the three regional actors – Turkey, Israel and Cyprus – satisfies the criteria of a subcomplex, yet violates the condition that a subcomplex is firmly embedded within a larger RSC (Buzan and Waever 2003: 51).

The existence of this triangle poses a challenge to the theory, which claims that there can be no overlap of RSCs. More importantly however the energy factor intensifies de/securitization among the three states, making Turkey a much more active actor in the region which is inconsistent with the expected behavior of insulator states. The example of Turkey highlights the limitation of RSCT that the regionalist assignment of borders does not provide the analytical tools to explain the simultaneous existence of bilateral or multilateral securitization relations across multiple RSCs by the same state.

Another shortcoming of RSCT is that it ignores the linkages between domestic politics and foreign policy decision-making (Diez 2012: 52), thereby ignoring a fundamental concept of securitization theory that securitizing acts are typically elite-driven and target domestic audiences. The existing bilateral securitization relations among the three actors of the subcomplex demonstrate enduring patterns of enmity and amity being affected by the introduction of the energy factor, which may further affect political decision-making even in the absence of securitizing acts as has been the case between Cyprus and Israel. In other words, securitizing acts are not a necessary condition for alterations in patterns of amity and enmity among states of the subcomplex.

The issue of penetration is analytically significant to the theory because it bridges the global and the regional levels of analysis. Typically penetration is analyzed merely as power projection with no differentiation among different types. In actuality penetration may take different forms – ranging from military intervention to alliance formation to economic collaborations and antagonisms – leading to different outcomes. The theory does not consider the duration of penetration, which is dependent on the referent object of that particular form. Where the referent object is energy, penetration tends to create durable patterns of interaction between global penetrating powers and regional actors. Additionally, securitizing or desecuritizing tendencies that may result from such patterns of penetration take place in a cross sectoral manner.

The analysis of the Israel-Turkey-Cyprus case is revealing of the impact of penetration on RSCs and exemplifies the fact that different actors will engage in different forms of penetration. The American intervention for the normalization of the Turkish-Israeli relationships over the Mavi-Marmara incident is indicative of a penetration aimed at desecuritizing relations between the two states in order to best serve American interests. The interest of energy Multinational Corporations (MNCs) in the region is another indicative form of penetration, where the actors involved do not explicitly represent state interest, but their presence alters or limits the range of claims of regional securitization.t.

IV. References

[1] E. H. Miller, "A note on reflector arrays," *IEEE Trans. Antennas Propagat.*, to be published

[2] Albert M and Buzan B (2011) Securitization, sectors and functional differentiation. Security Dialogue 42(4-5): 413-425.

[3] Alexseev M (2011) Societal security, the security dilemma, and extreme anti-migrant hostility in Russia. Journal of Peace Research 48(4): 509-523.

[4] Bagge Laustsen C and Wæver O (2000) In Defense of Religion: Sacred Referent Objects for Securitization. Millenium 29(3): 705-739.

[5] Bahgat G (2010) Israel's energy security: the Caspian Sea and the Middle East. Israel Affairs 16(3): 406-415.

[6] Bahgat G (2011) Israel's energy security: regional implications. Middle East Policy 18(3): 25-34.

[7] Bahgat G (2012) Preliminary assessment of Arab Spring' impact on oil and gas in Egypt, Libya. Oil & Gas Journal (Jan. 9, 2012): 58-63.

[8] Bigo D (2002) Security and Immigration: Towards a Critique of the Governmentality of Unease. Alternatives 27: 63-92.

[9] Bigo D (2005) Frontier Controls in the European Union: Who is in Control?. In: Didier B and Elspeth G (ed.) Controlling Frontiers: Free movement into and within Europe. Aldershot: Ashgate.

[10] Buzan B (1983) People, States and Fear: The National Security Problem in International Relations. Chapel Hill: University of North Carolina Press.

[11] Buzan B (1991) People, States, and Fear: An Agenda for International Security Studies in the Post-Cold Era (2nd ed.). Boulder: Lynne Rienner.

[12] Buzan B (2006) Will the 'global war on terrorism' be the new Cold War?. International Affairs 82(6): 1101–1118.

[13] Buzan B (2007) People, States, and Fear: An Agenda for International Security Studies in the Post-Cold Era. ECPR Press.

[14] Buzan B and Wæver O (2003) Regions and Powers: The Structure of International Security. Cambridge: Cambridge University Press.

[15] Buzan B, Wæver O and De Wilde J (1998) Security: A New Framework for Analysis. Boulder, CO: Lynne Rienner.

[16] Byman D (2011) Israel's pessimistic view of the Arab Spring. The Washington Quarterly 34(3): 123-136.

[17] Deutch J and Schlesigner J.R. (2006) National Security Consequences of U.S. Oil Dependency. New York: Council of Foreign Relations, Independent Task Force Report No. 58.

[18] Diez T (2012) Insulator, Bridge, Regional Center? Turkey and Regional Security Complexes in Ebru Canan-Sokullu ed. Debating Security in Turkey: Challenges and Changes in the Twenty-First Century. Plymouth: Lexington Books, 45-57.

[19] Floyd R (2007) Human Security and the Copenhagen School's Securitization Approach: Conceptualizing Human Security as a Securitization Move. Human Security Journal 5 (Winter): 38-49.

[20] Gow D (2009). Russia-Ukraine gas crisis intensifies as all European supplies are cut off. The Guardian, 7 January.

[21] Hansen L (2000) The Little Mermaid's Silent Security Dilemma and the Absence of Gender in the Copenhagen School. Millenium: Journal of International Studies 29(2): 285-306.

[22] Klare M (2004) Blood and Oil: The Dangers and Consequences of America's Growing Dependency on Imported Petroleum. New York: Metropolitan Books.

[23] Kirchner E and Berk C (2010) European Energy Security Co-operation: Between Amity and Enmity. Journal of Common Market Studies 48(4): 859-880.
[24] Mabro R (2008) On the security of oil supplies, oil weapons, oil nationalism and all that. Opec Review 32(1): 1-12
[25] McGowan F (2011) Putting Energy Insecurity into Historical Context: European Responses to the Energy Crises of the 1970s and 2000s. Geopolitics 16(3): 486-511.
[26] Natorski M and Herranz-Surrales A (2008) Securitizing Moves to Nowhere? The Framing of the European Union's Energy Policy. Journal of Contemporary European Research 2(2): 70-89.
[27] Shaffer B (2011) Israel – New natural gas producer in the Mediterranean. Energy Policy 39: 5379-5387.
[28] Winzer C (2011) Conceptualizing Energy Security. EPRG Working Paper 1123. Cambridge Working Paper in Economics 1151
[29] Wishnick E (2010) Dilemmas of securitization and health risk management in the People's Republic of China: the cases of SARS and avian influenza. Health Policy and Planning 25(6): 454-466.
[30] Zacharia J (2010) Offshore gas discoveries in Israel prompt squabbling over royalties. Washington Post, 29 August.
[31] Zaman (Ankara) (2012a) Greek Cyprus, Israel draw closer, presenting challenges for Turkey. Zaman, 16 February.
[32] Zaman (Ankara) (2012b) Greek Cyprus denies Israeli plans to deploy commandos. Zaman, 22 May.

2nd Conference on Power Options for the Eastern Mediterranean Region
07-08 October 2013, Nicosia, Cyprus (Paper No. POEM13/169)

The Cypriot Hydrocarbons and the European Financial Crisis

Christina Ioannou and Achilles C. Emilianides

Abstract-- **The aim of this paper is to address the significance of the Cypriot hydrocarbons within a European framework, identify the political challenges associated with the exploration of Cypriot hydrocarbons and argue that the Cypriot hydrocarbons, or indeed any credible European policy on hydrocarbons, may be a source of tackling future financial crises, only if the Union aims at further political integration, rather than merely integration at a monetary and technical level.**

Index Terms: Hydrocarbons, Financial Crisis, Energy Roadmap

I. The 2013 EP Resolution on the Energy Roadmap 2050

THE pillars of EU Energy policy are sustainability, security of supply and competitiveness. On 14 March 2013 the European Parliament (EP) adopted a Resolution on the Energy Roadmap 2050, a future with energy (herewith "the 2013 EP Resolution").[i] The 2013 EP Resolution was a follow-up to the 2011 Commission Communication,[ii] and the EP Resolutions of 15 March 2012[iii] and of 21 November 2012.[iv] The 2013 EP Resolution emphasizes that it is in the interests of Member State to reduce their dependency on energy imports with volatile prices and to diversify energy supplies and states the importance of taking into account adequate policies and instruments which might re-industrialize the EU economy. The aim of introducing the Energy Roadmap 2050 was to alleviate uncertainties that lead to tensions amongst states and to decrease market inefficiencies.

The 2013 EP Resolution proposes the 'adoption, within the spirit of solidarity, of a strategy that allows Member States to cooperate under the Roadmap in a spirit of solidarity - the creation of a European Energy Community'.[v] It further highlights the 'importance of the EU's energy policy amidst the economic and financial crisis; emphasizes the role that energy plays in spurring growth and economic competitiveness and creating jobs in the EU'.[vi] Understandably, the energy policy of the EU is considered as part of the wider aim to increase the competitiveness of Member State economies on the global market. It is the view of the EP that in order to achieve this goal, Member States should co-operate on the basis of common objectives and that national policies should be co-ordinated, so as to reach, where appropriate, a common 'European approach'.[vii] It is moreover stated that these goals will never be reached, 'unless the EU takes its responsibilities and fulfills a key role in the transition'.[viii] Whereas the financial crisis 'has made it more difficult to attract the required investment to finance the transformation of the energy system',[ix] the EP argues that the crisis should be used as an opportunity, rather than as a drawback; an opportunity to 'transform the EU model of society towards a highly energy-efficient, fully renewables-based and climate-resilient economy'.[x]

Within this framework the 2013 EP Resolution underlines the importance of natural gas in the 'transformation of the energy system, since it represents a relatively quick and cost-efficient way of reducing reliance on other more polluting fossil fuels; stressing the need to diversify natural gas supply routes to the European Union'.[xi] It further recognizes the potential of natural gas as 'a flexible back-up for balancing variable renewable energy supply alongside electricity storage, interconnection and demand-response'.[xii] The EP thus stresses that there is 'an urgent need to put in place a comprehensive EU policy on oil and gas drilling at sea; believes that emphasis should be put on potential hazards and on the delineation of exclusive economic zones (EEZs) for the Member States concerned and relevant third countries in accordance with the UNCLOS Convention, to which all Member States, and the EU as such, are signatories'.[xiii] Recognizing that the granting of licensing rights for drilling and the delineation of EEZ's may well become a source of friction with third countries, it is considered that 'the EU should maintain a high political profile in this respect and seek to preclude international discord; underlines that energy should be used as a motor for peace, environmental integrity, cooperation and stability'.[xiv] The 2013 EP Resolution further stresses that 'the solidarity between Member States called for in the EU Treaty should apply both to the daily working and the crisis management of the internal and external energy policy; calls on the Commission to provide a clear definition of ''energy solidarity'' in order to ensure that it is respected by all Member States'.[xv]

II. The Cypriot Hydrocarbons and the Energy Roadmap 2050

The Mediterranean region is of extreme significance for energy security purposes, since Egypt, Libya, Syria and Algeria have energy reserves and are hydrocarbon exporters, while countries such as Morocco and Tunisia are significant transit countries. The importance of the Mediterranean countries for the energy policy and security of the EU should not be underestimated.[xvi] EU demand for oil and gas is projected to rise within the next few years, whilst the domestic production of EU countries is in general projected to fall. Cyprus thus has the potential in the near future to

Christina Ioannou is Assistant Professor of European Politics at the University of Nicosia. She holds a PhD and an MA in European Politics from the University of Manchester and a BA in Economics from the University of Warwick. Email: ioannou.ch@unic.ac.cy
Achilles C. Emilianides is Associate Professor and Head of the Department of Law, University of Nicosia. He holds a PhD and an LLM in Law from the Aristotle University of Thessaloniki, as well as an LLM from the University of Leicester. Email: emilianides.a@unic.ac.cy

become a major net energy exporter of oil and gas.[xvii] This would fit within the parameters of the Energy Roadmap 2050 addressed above and would have the potential of enhancing the competitiveness of Cypriot economy, which was recently hit hard by austerity measures and the unprecedented haircut of bank deposits decided in the Eurogroup meeting on 24-25 March 2013.

The emergence of the Republic of Cyprus as an active actor in the exploitation of the energy potential of the Eastern Mediterranean is the result of forging strategic alliances with its neighbouring countries, despite the fact that such countries have competing interests and, sometimes, direct hostility towards one another. As already argued, forming long-term partnerships with Israel and countries like Egypt and Lebanon *at the same time* is not a simple task, as the major partners of the Republic of Cyprus are at odds with each other.[xviii] Within the wider context of stressed Arab-Israeli relations, Israel and Lebanon have been formally at war and devoid of diplomatic relations; the 2006 Lebanon war was the culmination of a period of stressed relations which have prevented the two countries from agreeing on a delimitation of their EEZs. The two countries have vowed to uphold their full sovereignty and economic rights over their territorial waters and EEZ and to exploit their natural resources, warning each other that they shall not tolerate any violation of their rights.[xix]

Whereas Egypt – the other major player in the region – has established diplomatic relations with Israel since 1980, this should not imply that the relations between the two countries are not strained. The Egyptian Revolution of 2011 resulted in a continuous conflict and instability at the Israeli-Egyptian border. The Turkish-Israeli relations are also strained. Whereas Turkey was the first Muslim country to recognize the state of Israel, relations between the two countries deteriorated following the 2008-2009 Gaza War and the 2010 Gaza Flotilla Raid; Turkey downgraded diplomatic ties with Israel on September 2011, recalled its ambassador from Israel and expelled Israel's ambassador. On the other hand, Turkey has signed a memorandum of understanding with Egypt to improve and enhance military relations and co-operation and to collaborate on the implementation of a natural gas agreement. Not surprisingly, relations between Cyprus and Turkey constitute the most difficult challenge for Cypriot hydrocarbons, as Turkey arbitrarily continues to argue that the Republic of Cyprus is not a sovereign state and that it has no power to sign delimitation agreements with its neighbouring states.[xx]

Within this turbulent framework, the Republic of Cyprus has tried to maintain a sensitive balance with its neighbouring countries concerning the exploration of reserves in the Eastern Mediterranean. The Republic of Cyprus is called upon to act as a mediator and maintain co-operation with countries which continue to have competing interests in the area. A good example is the 2010 increased strategic alliance forged between the Republic of Cyprus and Israel over the exploitation of the reserves. The two countries reached an agreement over their maritime boundaries in December 2010, which was ratified by Cyprus in February 2011. This resulted in protests by Lebanon which argued that the zone defined in the Israel-Cyprus 2010 Agreement, albeit consistent with the 2007 Lebanon-Cyprus Agreement, was inconsistent with the views of Lebanon. The strategic alliance with Israel has been a development of extreme significance, which presupposes however the continuation of the strategic partnership with Egypt and the eventual agreement with Lebanon over the delimitation of the respective maritime boundaries.

III. Lessons from Monetary Union: Revisiting the Spillover Effect

The inability of the EU to effectively tackle and provide solutions to issues pertaining to the financial stability and survival of its member states and citizens is the direct result of an unjustified optimism that monetary union would inevitably lead to enhanced political integration. In order to appreciate the short-sightedness of European technocrats at the time of the creation of the EMU one has to go as far back as the early 1990s and the Treaty of Maastricht. The Treaty laid down the foundations for a monetary union - modelled around a European Central Bank (ECB) - in the profound absence of an economic union, in terms of both fiscal and banking union, both of which are deemed to be essential attributes of any sound economic model. Despite the label '*EMU*' (Economic and Monetary Union) given to the new project, there was a clear absence of a strictly coordinated economic policy; hence '*EMU*' ended up being a huge misnomer.

The underlying assumption was that economic union (and thus further political integration) would inevitably follow. This rationale is in line with neofunctionalist predictions on European integration, which argue that the latter can be self-sustaining. The theoretical basis for this rests on the concept of spillover (functional and political spillover), which suggests that initial steps towards integration carry a dynamism, which may trigger endogenous economic and political dynamics, that can lead to further cooperation. The underlying assumption was that: *'integration within one sector will tend to beget its own impetus and spread to other sectors'.*[xxi]

This assumption was fundamentally flawed in the case of the EMU, as this automatic mechanism that could create a spillover from a monetary union to an economic union was seriously lacking. What's even worse is that the EMU also lacked the basis for an institutional mechanism that could restore economic stability in times of crisis and attract capital investments in times of market uncertainty. The question was how member states, and the system at large, would react when confronted with the first major financial crisis. It is a fact that the experience so far (a few years into the crisis) has shown that the Union is not willing to take steps towards a fiscal union, or a political union at large, but has rather focused on further institutional integration in terms of completing its banking union.

When the system was thus put to the test for the very first time, when the first major financial crisis hit the continent, Member States opted to integrate less politically, confirming that the establishment of monetary union does not necessarily lead to political union.[xxii] This would require both a banking union and a fiscal union. The former entails, at a very minimum, an integrated system of supervision in the form of a single supervisory mechanism for banks, based on a single rulebook; at a maximum, a single resolution mechanism to handle bust banks, funded by levies on the sector itself (even though this is difficult as the EU Treaties provide no base for such mechanism). A fiscal union, on the other hand, entails sacrificing state sovereignty on fiscal management. The latter seems the least likely of the two scenarios and the EU has thus focused on redressing the

anomalies and institutional weaknesses emanating from the foundations of the EMU structure. It is however unlikely that technical integration suffices for a comprehensive EU policy.

The recent Eurozone crisis has challenged the realities of the ideal of solidarity and has proven a major blow for supporters of a common European idea.[xxiii] The recent Eurogroup decision on Cyprus has further confirmed that national interests continue to reign supreme.[xxiv] The construction of an EMU lacking a true political union was initially considered as an unqualified success, with statements being nearly euphoric;[xxv] collapse however soon ensued, not the least due to lack of genuine political solidarity.[xxvi] The same could well happen to any attempt to construct a comprehensive energy policy on a technical level, with complete disregard to hard political realities and the need to genuinely achieve solidarity and political co-ordination in external affairs, beyond mere rhetoric.

The drafters of the EU have long considered that market economy might properly function by securing a closer economic integration. The EU's internal market sought to guarantee the free movement of capital, goods, services and people within its Member States; it was considered that a common market and the drive towards economic integration could occur without the necessity of similar progress in political integration. It is argued that this deification of market economy, the view that it might effectively function on its own, irrespective of its political framework, is flawed.[xxvii] Politics and economy are interwoven and a common market may not properly function in the long term, unless there is also a political framework securing its proper growth.

IV. Intergovernmentalist Approaches to European Integration

The extent to which member states are willing to pursue a political union at the expense of national control over certain policy areas, remains at the heart of the discussion. Intergovernmentalist analyses of European integration can shed light on this, as they emphasize the centrality of the nation state in the process of integration. The focus is on State actors and the dominant concept of national sovereignty and security in interstate relations.[xxviii] Intergovernmentalist theories stress that power is in the hands of member states, and it is their national governments which essentially control the degree and the speed of European integration. Initially proposed by Stanley Hoffmann[xxix], intergovernmentalism maintains that the potential strengthening of the supranational level - through more delegations of power to that level - is the result of decisions that are taken at the national governmental level. Hoffmann proposed the logic of diversity, which sets limits to the degree which the 'spillover' process can limit the freedom of action of the governments. '*The implications of the logic of diversity are that on vital issues of common interest, losses are not compensated by gains on other issues*'.[xxx]

Most notable among IR intergovernmental literature is the work of Moravcsik. Moravcsik[xxxi] historically stretches his research grid from Messina and the conclusion of the Treaties of Rome to the negotiations at Maastricht, looking at the evolution of some key policy areas (notably monetary policy, trade policy and agricultural policy). He tries to assess the factors that brought the treaties about and the dynamics that have driven European integration in the process. The core argument that emerges is that when national interests and preferences converge, then supranational co-operation moves forward. Moravcsik's liberal intergovernmentalism has three essential elements which combine: (a) a liberal theory of national preference formation, (b) an intergovernmentalistic analysis of interstate negotiation and (c) the assumption of rational state behaviour. Thus the ceding of power to the supranational level involves a set of rational choices by national leaders:

'European integration resulted from a series of rational choices made by national leaders who consistently pursued economic interest – primarily the commercial interests of powerful economic producers and secondarily the macroeconomic preferences of ruling governmental coalitions – that evolved slowly in response to structural incentives in the global economy. When such interests converged, integration advanced'.[xxxii]

In other words, Moravcsik clearly elevates the power of the national level in the process of European integration, arguing that '*domestic preference formation*' and '*interstate bargaining*' are driving the process. So if it is to the states' best interest, then integration will progress. Clearly then, this explicitly points to a nationalistic driver for European integration. This nationalistic driver is also in line with Milward's[xxxiii] history of European integration, which also advances the central role of national governments and national leaders. The process of European integration started in the post-war period because it was to the economic interest of nation states: '*The basis of the rescue of the nation-state was an economic one, and it follows that the Europeanization of its rescue had also to be economic*'.[xxxiv]

In the process of Europeanisation then, '*the states will make further surrenders of sovereignty if, but only if, they have to in the attempt to survive*'.[xxxv] Milward clearly rejects the argument that Europeanisation of policies necessarily usurps national democratic control, as this '*treats the abstract concept of national sovereignty as though it were a real form of political machinery*'.[xxxvi]

The notion of national interest driving the European integration process is central in the intergovernmentalist approach. The rationale of Milward's argument builds on the following puzzle:

'*How, in a world of such nationally dominated conceptions, apparently justified by the remarkable economic prosperity which attended them, could integration and the surrender of national sovereignty be born? Not as the intellectual counter-current to European nationalism, which it is so often said to represent, but only as a further stage in the reassertion of the role of the nation-state*'.[xxxvii]

The intergovernmentalist assertion is that the process of European integration has a nationalistic element involved, which is driving member states into a supranational surrender of powers, when (and if) it is to their best interest. The intergovernmentalist rationale points to the nationalist intent for integration. This is a distinction that we could explicitly make in the case of a more integrated and comprehensive EU policy on offshore drilling and hydrocarbons, as the argument dominating our discussion will project the idea that, even though the exploration of Cypriot hydrocarbons by the EU or any credible European policy on hydrocarbons could potentially serve as a source of tackling future financial crises, the Union seems to be dwelling on the idea of more integration. Even though the

issue seems to have an immediacy that could facilitate the formulation of a common hydrocarbon policy, the question is whether the Union is ready for taking a step leading to political union, which would make a coordinated policy on hydrocarbons much more comprehensive and, essentially, successful.

V. Politics, Energy and Finance: Connecting the Threads

The urgent need to put in place a comprehensive EU policy on oil and gas drilling at sea, as envisioned in the 2013 EP Resolution, is relevant in the case of the exploration of Cypriot hydrocarbons. The potential dangers acknowledged by the EP, predominantly the friction between EU Member States and third countries over the delineation of EEZ's, are applicable in the case of Cyprus. Even more troubling is the fact that Turkey, a country seeking membership in the EU, continues to threaten the Republic of Cyprus and to undermine the effect of its bilateral agreements. Turkey further calls upon all companies and neighbouring countries to refrain from any endeavour that would be contrary to Turkish interests. It suggested that any viable energy policy regarding the exploration of hydrocarbons in Cyprus, or indeed in the Eastern Mediterranean as a whole, is dependent upon political considerations.

The 2013 EP Resolution stressed that the EU should maintain a high political profile and should seek to preclude international discord. It further called upon all Member States to apply the principle of solidarity in the daily working and crisis management of the internal and external energy policy, so as to preclude international discord and to address financial problems through the energy roadmap. Whereas these are venerable goals, the reality of the situation is that a European comprehensive energy policy requires more than just technical integration and wishful thinking. The EU remains without a common external policy, especially with regards to the Middle East; the 2013 Syrian crisis is a good example of the EU failing to be a frontrunner in international affairs, because of differing views of its Member States. EU policy towards Turkey, especially with respect to its non-recognition of the Republic of Cyprus, is another obvious example which is of paramount importance in the case of Cypriot hydrocarbons.

It is suggested that a comprehensive energy policy should be based upon a comprehensive political framework enabling such policy to be applied. The 2013 EP Resolution appropriately acknowledged this inter-relationship between politics, economy and energy and called upon the EU to maintain a high political profile and to identify the notion of common energy solidarity. The case of the Cypriot hydrocarbons is a distinct case where any comprehensive energy policy will remain unfinished, unless it can be applied within the framework of a common political energy policy. It is therefore suggested that any credible European policy on hydrocarbons may be a source of tackling future financial crises, only if the EU aims at further political integration, rather than merely integration at a monetary and technical level. This might occur only if national actors actually opt to co-operate at the political level, even in the profound absence of formalised increased political integration.[xxxviii]

If the liberal depoliticised market ideal has not managed to avoid an unprecedented financial crisis, there is little evidence to suggest that a depoliticised comprehensive energy policy might be more successful in a politically loaded subject-matter, such as the exploration of hydrocarbons and the delineation of EEZ's.[xxxix] It is therefore suggested that a comprehensive energy policy on hydrocarbons requires more than merely technical integration. The main challenge, however, is how to convince Member States to trust European integration, when the so-called European ideals of solidarity have failed to inspire a comprehensive '*European*' policy for tackling the financial crisis.

---

[i] 2012/2103 (INI).
[ii] Energy Roadmap 2050 COM (2011) 885.
[iii] On a Roadmap for moving to a competitive low carbon economy in 2050.
[iv] On the industrial, energy and other aspects of shale gas and oil and on environmental impacts of shale gas and shale oil extraction activities.
[v] Resolution on the Energy Roadmap 2050, 14/3/2013, para. 1.
[vi] Ibid, para. 6.
[vii] Ibid, para. 14.
[viii] Ibid, para. 18.
[ix] Ibid, para. 47.
[x] Ibid, para. 23.
[xi] Ibid, para. 66.
[xii] Ibid, para. 67.
[xiii] Ibid, para. 77.
[xiv] Ibid, para. 78.
[xv] Ibid, para. 83.
[xvi] For a detailed analysis of the energy relations between the European Union and Mediterranean countries see S. Haghighi, *Energy Security: The External Legal Relations of the European Union with Major Oil and Gas Supplying Countries*, Oxford: Hart Publishing, 2007: 358 – 371.
[xvii] See in general A. Emilianides, P. Focaides, 'The Exploration of Hydrocarbons in Cyprus. Implications, Problems and Perspectives' (2008) 7 *Cyprus and European Law Review*: 91-108, S. Kassinis, 'Exclusive Economic Zone of the Republic of Cyprus: From Theory to Practice' in V. Kikilias (ed), *EEZ: Exclusive Economic Zone. From Strategic to Financial Solution*, Athens: Kastaniotis, 2012: 59ff (in Greek), G. Pamporides, *The Hydrocarbons of the Republic of Cyprus*, Nicosia, 2012 (in Greek), H. Faustmann, A. Gürel, G. Reichberg (eds), *Cyprus Offshore Hydrocarbons: Regional Politics and Wealth Distribution*, Oslo: Prio and Friedrich Ebert Stiftung, 2012, Tasssos Papadopoulos Research Centre, *The Geopolitical Situation in Eastern Mediterranean after the Discovery of Hydrocarbons*, Nicosia: 2012 (in Greek).
[xviii] A. Emilianides, P. Focaides, 'The Exploration of Hydrocarbons in Cyprus. Implications, Problems and Perspectives' in Power Options for the Eastern Mediterranean Conference Proceedings, Limassol, 2010, POEM 12/146: 1-4.
[xix] M. Wahlisch, 'Israel-Lebanon Offshore Oil & Gas Dispute-Rules of International Maritime Law' (2011) 15, 31 *Insights of the American Society of International Law*, available at http://www.asil.org/pdfs/insights/insight111205.pdf

[xx] For a rebuttal of the Turkish arguments see A. Jacovides, *International Law and Diplomacy*, Leiden: Brill, 2011, P. Athanassiou, 'State and Government Recognition and the 2011 Cyprus-EEZ Demarcation and Exploration Dispute: Some Reflections' [2012] *Cyprus Yearbook of International Law*: 19-32, as well as A. Emilianides, 'The Exploration of Hydrocarbons and Turkish Objections' (2013) 10 (4) *In Depth*, available at http://www.cceia.unic.ac.cy/index.php?option=com_content&task=view&id=336&Itemid=336. See further A. Emilianides, *Constitutional Law in Cyprus*, The Hague: Kluwer, 2013, Idem, *Beyond the Constitution of Cyprus*, Thessaloniki: Sakkoulas, 2006 (in Greek), K. Chrysostomides, *The Republic of Cyprus: A Study in International Law*, The Hague: Martinus Nijhoff, 2000: 117ff.

[xxi] J. Tranholm-Mikkelsen, 'Neo-functionalism: Obstinate or Obsolete? A Reappraisal in the Light of the New Dynamism of the EC' (1991) 20 (1) *Journal of International Studies*: 4.

[xxii] C. Johnson, *One Currency, One Country*, London: Federal Trust, 2000: 13.

[xxiii] V. Borger, 'How the Debt Crisis Explores the Development of Solidarity in the Euro Area' (2013) 9 (1) *European Constitutional Law Review* 7-36. See also Open Society Initiative for Europe, 'Europeans back Solidarity over National Self-Interest to Get out of Crisis' 2/4/2013, available at http://www.opensocietyfoundations.org/press-releases/europe-stands-firm-europeans-back-solidarity-over-national-self-interest-get-out

[xxiv] See C. Ioannou, 'From Bust Bank Bail-Ins in Nicosia to a Banking Union in Frankfurt: Can the EU Move Forward? (2013) April, *In Depth*, available at http://www.cceia.unic.ac.cy/index.php?option=com_content&task=view&id=316, A. Emilianides, 'Paradigm Shift. The EU and the Role of Academics' (2013) April, *In Depth*, available at http://www.cceia.unic.ac.cy/index.php?option=com_content&task=view&id=318,

[xxv] J. Van Overtveldt, *The End of the Euro*, B2 Books, Chicago, 2011.

[xxvi] See C. Douzinas, *Philosophy and Resistance in the Crisis: Greece and the Future of Europe*, Polity Press: Cambridge, 2013, H. Patomaki, *The Great Eurozone Disaster: From Crisis to Global New Deal*, Zed Books: London, 2013, J. Habermas, *The Crisis of the European Union: A Response*, Polity Press, Cambridge, 2012.

[xxvii] For a discussion see for instance J. Spero, *The Politics of International Economic Relations*, London: George Allen, 1977.

[xxviii] S. West, Liberal Intergovernmentalism, 2004, available at http://www.nyegaards.com/yansafiles/liberal%20Intergovernmentalism.ppt

[xxix] S. Hoffmann, 'Obstinate or obsolete? The Fate of the Nation State and the case of Western Europe', (1966) 95 (3) *Daedalus*: 862-915.

[xxx] Ibid: 882.

[xxxi] A. Moravcsik, 'The Choice for Europe: Social Purpose and State Power from Messina to Maastricht' London: Routledge, 1998.

[xxxii] Ibid: 3.

[xxxiii] A.S. Milward, *The European Rescue of the Nation-State*, London: Routledge, 2000.

[xxxiv] Ibid: 44.

[xxxv] Ibid: 436.

[xxxvi] Ibid: 436.

[xxxvii] Ibid: 44.

[xxxviii] The latter approach would, however, continue to remain dependent upon the good will of the Member States.

[xxxix] V. Paipais, 'Greek Expectations: Broaching the Case for a European Exclusive Economic Zone, available at http://blogs.lse.ac.uk/eurocrisispress/2013/03/14/greek-expectations-broaching-the-case-for-a-european-exclusive-economic-zone/ has argued that: '*Greek politicians use the EEEZ discourse opportunistically as a tool of diffusing domestic tension and mobilising popular support. Greece may have very good chances to be back on the energy map but not because the country's largely discredited political elite prematurely invests on a European EEZ. Unless a well-devised and credible European energy plan is put in place including the Mediterranean hydrocarbon reserves within a wider European geopolitical response to the crisis, there are few reasons to be optimistic*'.

2nd Conference on Power Options for the Eastern Mediterranean Region
07-08 October 2013, Nicosia, Cyprus (Paper No. POEM13/170)

The Feasibility and Impact of the Turkish-Israeli "Rapprochement" on the Geopolitics of the Eastern Mediterranean

Dr.Theodoros Tsakiris

Abstract-- The aim of this paper is to address the significance of the Cypriot hydrocarbons within a European framework, identify the political challenges associated with the exploration of Cypriot hydrocarbons and argue that the Cypriot hydrocarbons, or indeed any credible European policy on hydrocarbons, may be a source of tackling future financial crises, only if the Union aims at further political integration, rather than merely integration at a monetary and technical level.

Index Terms: Hydrocarbons, Financial Crisis, Energy Roadmap

I. Introduction

THE informal apology extended by Israeli Prime Minister Benjamin Netanyahu to his Turkish counterpart in April 2013 regarding the Mavi Marmara incident tends to create the erroneous impression that Turkish-Israeli relations are about to return (or are in the process of returning) to the point that they were before Israeli commandoes stormed the abovementioned Turkish vessel in the early hours of June 1st 2010. According to this line of thought the rapprochement between the two states is a "done deal"[1] that is already reconfiguring regional geopolitics in ways that are pushing Israel:

(i) to revise Israeli relations with Cyprus and Greece,

(ii) force Tel Aviv to revise or unilaterally annul the Exclusive Economic Zone (EEZ) agreement it signed with Cyprus in December 2010 and

(iii) force Delek and probably Noble to withdraw from Cyprus, unless Nicosia concedes to the construction of a gas export pipeline to Turkey that would carry Cypriot and Israeli gas from respectively the Aphrodite and Leviathan fields.

In case Cyprus refuses such an arrangement, which is promoted by Turkey regardless of the talks on the resolution of the Cypriot Question, Delek would withdraw from the development of the Vassilikos LNG terminal thereby making it financially unattainable. Other proponents of this argument are viewing the construction of the Turkish-Israeli pipeline as an opportunity to resolve the Cyprus Question by committing Cypriot gas to the construction of an underwater pipeline from Leviathan to Ceyhan arguing that this would be to the benefit of Greek-Cypriots despite the obvious commercial and political deficiencies of such a prospect.

Before we analyze the specific geopolitical parameters that would affect the viability of a Turkish-Israeli gas pipeline we need to (a) assess the status quo of Turkish-Israeli relations, and (b) estimate the range and potential significance of their aligned interests while analyzing the progress made between the two states since Netanyahu's "apology" five months ago.

II. The Geopolitical Context

A more accurate analysis of what has actually occurred in Turkish-Israeli relations since April is a credible indication to what may actually happen in the near future and constitutes a more accurate benchmark for measuring the actual progress of their rapprochement. Contrary to the perception of re-acquired normalcy, Turkey and Israel are only making the first steps in an effort to restart their rapprochement. Ankara and Tel Aviv are essentially negotiating the terms of how to negotiate their rapprochement. The end-result of this process is not a return to the strategic alliance of the 1990s or the more troubled alliance of the previous decade especially since Prime Minister Erdogan recognized Hammas as the government of the Gaza Strip in 2006 in clear contradiction of US and EU policy who have both characterized Hammas as a terrorist organization.

What lies at the end of this process, at least from the Israeli point of view, is the full restoration of diplomatic relations at the ambassadorial level and –on an ad hoc basis- the gradual restart of arms exports. From a political point of view the Turkish-Israeli pipeline would act as a confidence building measure or at least this is the principal Israeli perspective. From the Turkish point of view the pipeline's political usefulness is far more ambitious and relates to Ankara's efforts to neutralize Cyprus' progress regarding the development of its hydrocarbon resources.

The gap in the Israeli and Turkish perception of what is the political instrumentality of the pipeline is a first indication of divergence in what should be a process of convergence. In essence Turkey is likely to demand from Israel far more than what Tel Aviv may be willing to concede in order to act as a market for Israeli gas exports. In addition to this important policy divergence there are serious disagreements on several parts of the preconditions Turkey had set in order to re-establish full diplomatic relations with Israel.

For almost three years after the Mavi Marmara incident Erdogan demanded three pre-requisites from the Israelis in order to re-normalize Turkey's bilateral relationship with its

Dr. Theodoros Tsakiris, Assistant Professor Geopolitics of Hydrocarbons, University of Nicosia & Programme Director, Energy & Geopolitics, ELIAMEP (Hellenic Institute for Foreign & European Studies)

[1] Daniela Hubner & Natalie Tocci, Behind the Scenes of the Turkish-Israeli Breakthrough, Instituto degli Affari Internatiozali, Working Papers #13, (April 2013), p.1.

former ally: (a) that a formal apology is issued by the Israeli Prime Minister, (b) that the victims of the incident are compensated and (c) that the blockade of Gaza. From these preconditions, Tel Aviv did not agree to the third one, agreed in principle with the second and partially fulfilled the first. There has been no lifting whatsoever of the Gaza blockade. Tel Aviv is offering to pay $100,000 to the families of each victim provided that all civil and criminal charges against its soldiers and the State of Israel are dropped in Turkey's courts and the apology Mr. Erdogan got was as informal as it could have been. In effect multiple indications suggest that Netanyahu did not call Erdogan but granted Obama's request as a gesture of goodwill in order to break the ice in his own personal relationship with the recently re-elected –at the time-U.S. President during Obama's first visit to Israel. What the Israeli PM did after he talked to Erdogan speaks volumes of his decision to keep the rapprochement process going at a glacial pace, estimating that the Turkish Prime Minister would do something provocative enough to stop the process in its own tracks.

Mr. Erdogan's announcement on June 27th that he would be visiting Gaza on July 5th, as well as the recent statements (02/07/2013) by Turkey's Vice-Premier Bulent Arinc that the Jewish Diaspora was behind the anti-AKP demonstrations that rocked Turkey in June 2013 undercut the efforts of the Israeli diplomats who want to keep the rapprochement process alive. Most importantly though, Mr. Erdogan's sensational accusations that Israel orchestrated the coup d'état which overthrew Mohammed Morsi from the Presidency of Egypt in August 2013, seem to confirm Israel's worries that Turkey has Neo-Ottoman ambitions in the Eastern Mediterranean. These ambitions are bringing Ankara closer to the Muslim Brotherhood parties that have sprung around the Middle East since the revolutions of 2011 and in direct confrontation with the Wahabis of Saudi Arabia and the Military cast of Egypt.

Statements like the ones by Erdogan and Arinc, or plans to break the Gaza blockade, play into Netanyahu's hands regarding his decision to block the rapprochement process without losing face in Washington. Netanyahu's tactics are essentially pragmatic if one considers the entrenched diversity of Turkish-Israeli interests throughout the Middle East with the partial exception of Syria and Iran. The need\ to keep a united front over Syria has been the principal role for the continued US pressure behind the Turkish-Israeli rapprochement. Although the prospective partition of Syria along ethnic lines and the danger of WMD proliferation as a result of Assad's collapse will bring Turkey and Israel closer together, what would the ramification of this alignment be for Cyprus and the region's energy geopolitics? How viable, how solid, and how long-term could such an alignment prove to be? Can an anti-Assad tactical rapprochement prove to be the basis for a Turkish-Israeli rapprochement? Can Syria actually constitute the "glue in Turkish-Israeli relations"?[2]

The short answer is no because Turkey's role in a post-Assad Syria cannot guarantee any vital Israeli interests in Syria. To start with, it is quite unclear what would be the operational content of an anti-Syrian alignment for Turkey and Israel. It is true that neither side wants to remain idle as Syria's ethno-religious war spreads into Lebanon and increases the likelihood that Assad's bio-chemical weapons fall into the hands of Salafist zealots which are growing more powerful as the civil war continues but Tel Aviv and Ankara give different answers on the critical question of regime change. Israel would prefer stability and would not like to see Syria transformed into a battleground between Salafists, elements of the Muslim Brotherhood and whatever Shi'a/Christian coalition survives the potential fall of the Asad regime.

The risk of this development after the fall of Mubarak in Egypt is too significant for Tel Aviv to take and here lies the fundamental difference in the Turkish and Israeli perspective: the fall of Mubarak was a strategic accident of the first degree for Tel Aviv, but from Mr. Erdogan's point of view it was an opportunity for the promotion of his Neo-Ottoman agenda who forced him to stand by Mr. Morsi even as the Egyptian military was uprooting the Muslim Brotherhood's government from power.

Both Turkey and Israel would welcome –although for different reasons- the drastic curtailment of Iranian influence in Lebanon through the isolation of Hezbollah, a development that would make relations between Ankara and Shi'a controlled Baghdad even more hostile. Israel has already indicated twice that it would unilaterally intervene in the Syrian civil war whenever it deems it necessary for the protection of its national interest. Tel Aviv has attacked twice -in January and May 2013- convoys of Iranian weaponry that were allegedly en route to Hezbollah[3] and selectively bombed installations of Assad's Armed forces related to the regime's alleged WMD programme even before the Civil War started. Israel is remaining selectively neutral in the Syrian civil war without putting any real pressure against the Asad regime and without –of course- aiding the rebels in any tangible way. This is a major difference in the way Tel Aviv and Ankara view the continuing civil war in Syria. If Asad survives, Turkey looses all influence, at least for the foreseeable future. If Asad survives Tel Aviv will be more comfortable in dealing with the "devil it knows" rather than having to face a new unstable regime that is more likely to be closer either to the Wahabis of Saudi Arabia or the Egyptian Muslim Brotherhood.

Turkey is in essence powerless to guarantee any Israeli interest in a theoretical post-Assad regime for several years to come. The reasons are straightforward. What would succeed Asad in Syria is chaos, probably larger than Iraq's chaos in 2003 given the de facto partial regionalization of the war following Hezbollah's active engagement in the battle of al-Qusayr. After the chaos –if Syria is not partitioned along ethnic-religious lines- any government that would emerge is highly unlikely to be more pro-Israeli than Assad's regime. To the contrary, even if the Salafist elements of the SLA (Syrian Liberation Army) are somehow sidelined, the new government, even if it is a secular one, would be prone to use the only national card able to unite the various factions and this card can only be the Golan Heights issue. Ankara is unlikely to be able to influence such a government towards a settlement with Israel even if it wanted to.

Turkey, under the leadership of Mr. Erdogan and his Foreign Minister Dr.Ahmet Davutoglou, has invested most of its diplomatic capital in the Middle East in its efforts to

[2] Hubner & Tocci, ibid, p.7

[3] Yoel Guzansky, "Thin Red Lines: The Syrian and Iranian Contexts", Perceptions, Vol.16/Iss.2 (August 2013), The Institute for National Security Studies-INSS, p.25

drive Assad from power but it is not likely to be the most powerful foreign player in any post-Assad regime even if Asad collapses. Although Turkey has been the principal conduit for arms and supplies to the SLA, Saudi Arabia and Qatar remain the SLA's major financiers and will vehemently oppose any efforts on the part of Mr. Erdogan to either use its military forces to drive Assad out of power or turn the post-Assad regime into a Turkish protectorate. Consequently, whatever benefits Israel would want to secure from a post-Assad regime, such as the resolution of the Golan issue or the elimination of Hezbollah, Turkey cannot simply provide, even if it wanted to.

More importantly Turkey is unlikely to provide any tangible military support to Israel if it decides to attack Iran unilaterally, a prospect that remains highly unlikely as long as Barack Obama remains the occupant of the White House. As long as Turkey would continue to oppose the utilization of its territory as a platform for a pre-emptive strike against Iranian nuclear cites there is no real ground for a Turkish-Israeli rapprochement that would reverse the existing hostility between the region's principal U.S. allies and force Israel to make strategic concessions to Turkey vis-à-vis Greece and Cyprus like the ones described in the preface of this article.

There is no serious indication whatsoever that Israel would be ready or willing to revise its pro-Greek (energy) policy vis-à-vis Cyprus or withdraw from the Republic's energy development. As it was clearly manifested by the visit of Ministers Kassouledes (Foreign Affairs) and Lakotrypes (Energy) to Jerusalem (April 2013) and the visit of President Anastasiades in May 2013, Tel Aviv will continue to defend the validity of the 2010 EEZ agreement and fully support the active participation of the Delek Group in the development of the Aphrodite gas field, although it may not commit at this stage any gas resources to the Vassilikos liquefaction plant from the Leviathan field.

In the military level, Israel did not neutralize or annul its cooperation agreement with Cyprus that allows it to deploy Apache helicopters in Cypriot military bases. On 20-21 March 2013, U.S., Israeli and Greek naval assets conducted for a third consecutive year the combined Noble Dina exercises in the international waters within Cyprus' EEZ. There is also no indication from the Knesset or the Israeli cabinet regarding the lifting of the arms embargo which was imposed on Turkey in 2010 while on 22-25 April 2013 Israel sent five ships including a gun ship to Larnaca in order to conduct joint anti-terrorist exercises with the limited assets of Cyprus' navy. Israel is also in the process of planning joint Search & Rescue exercises with Greece and Cyprus in October 2013.[4] Israel may also be willing to take a larger share of the responsibility for the protection of the Vassilikos LNG terminal as long as there is a stronger show of support and commitment from Greece, Italy and France, which is increasing its naval military presence in the region in view of the possibility of western military action against Asad.

The potential sale of two L'Adroit type corvettes to the Cypriot Navy along the leasing of two OPV-class heavy patrol boats from the Israeli navy, as announced by Cypriot Defense Minister Fotiou in May 2013, would constitute a clear indication that a tripartite military alignment is under formation in order to protect Cypriot Hydrocarbon resources and their respective production/export infrastructure against asymmetric threats such as terrorism and strategic sabotage. This alignment is not of course directed against Turkey or the Turkish-Cypriots but it is necessary to guarantee the emergence of Vassilikos as a regional LNG export hub that could someday even export gas to Turkey.

The cumulative result of these developments was manifested by two major developments which attest to the deepening of Israel's energy relations with both Cyprus and Greece to the political detriment of the Turkish-Israeli pipeline:

(1) On 26 June 2013, Delek Drilling and Avner Oil & Gas signed a MoU with the government of Cyprus regarding the construction of the Vassilikos LNG terminal, almost 48 hours after the Israeli cabinet confirmed the decision of Prime Minister Netanyahu to export 40% of Israel's cumulative gas reserves equal to almost 380 bcm. The fact that the two Delek Group companies were the leading interlocutors and business proponents of the Turkish-Israeli pipeline on the Israeli side is indicative of the progress made so far by the champions of the Turkish-Israeli rapprochement.[5]

(2) On 8 August 2013, Israel signed with Cyprus and Greece a tripartite Memorandum of Understanding that committed all three sides to work together in all sectors of the hydrocarbons industry including the development and transportation of oil & natural gas. Although no specific gas export project was mentioned in the MoU the agreement was characterized as historic by all sides. At the very least its signing attests to the deepening cooperation of the three East Mediterranean states.

The apparent commitment of Delek to the Vassilikos terminal essentially excludes Cyprus (and its EEZ) as a potential route for the Turkish-Israeli gas pipeline and increases the pressure on the Israeli government to send the majority of Leviathan's exports for liquefaction in Cyprus. Delek's decision does not exclude the construction of a pipeline to Turkey. It excludes the possibility that such a pipeline would cross via Cyprus' EEZ as long as the Cyprus problem is not resolved. Nevertheless it is important to note that what Delek does not seem to have fully understood is that any export option to Turkey would exclude it from the development of Aphrodite at essentially Ankara's behest. From a political point of view it would be impossible for Delek (and Noble) to export gas to Turkey and simultaneously participate in the development of Aphrodite, given Ankara's decision to block any commercial cooperation with any IOCs (International Oil Companies) that operate in Cyprus' upstream sector**.**

It should be noted though that if Nicosia succeeds in getting Woodside on board the Vassilikos LNG consortium, then the commercial case for the Israeli government may prove too difficult to overlook, especially if Greece, Italy and France would increase their naval presence within Cyprus' EEZ and fully utilize the Republic's military installations which were constructed during the 1990s within the framework of Greece's United Defense Doctrine with Cyprus. Should this be the case, Netanyahu may overrule the recommendation of the Zemach Committee to not build any gas export infrastructure outside Israeli sovereign territory (including its EEZ).

[4] http://famagusta-gazette.com/cyprus-greece-and-israel-to-conduct-search-and-rescue-exercises-p19636-69.htm (accessed on 23/8/2013)

[5] The main champion of the Turkish-Israeli pipeline on the Turkish side is the TURCAS energy company.

III. The Geopolitical Parameters: Structural Obstacles along all possible Routes

An Israeli export pipeline to Turkey, regardless of its size and route, will also need to overcome a series of major geopolitical impediments that relate not only to the region's increasing volatility but also to the political preconditions necessary to construct a multibillion USD investment which will need to operate for decades. Moreover there are commercial considerations that need to be taken into account regarding the size of the exported volumes. Any meaningful long-term contract of Israeli exports to Turkey would represent a minimal volume of 10 bcm/y for a period of 15-20 years equal to around 40%-50% of Israel's entire export potential.

Would Israel accept to commit over a period of 15-20years such a large portion of its known export potential towards a country with which it has no practical diplomatic relations since 2010? If Turkish-Israeli relations would return to a status of hostility within the life expectancy of the Leviathan-Ceyhan pipeline, can Israel find readily available alternative export destinations in case Turkey cancels its own imports or stops the transit of Israeli gas through its territory even if such a transt were economically viable? The answer is probably no.

Gas pipelines do not get build in a matter of months. LNG liquefaction capacities are not constructed in a matter of months. The structure of the international gas market is too inflexible to allow an exporter to find alternative clients in case its principal market destination is lost, especially if this market was serviced through pipelines and represented such a large portion of its entire export capacity.

Let us now examine the alternative export options from a geopolitical point of view.

Leviathan-Ceyhan Pipeline 1: Onshore via Syria/Lebanon: The first theoretical route of such a pipeline would essentially bypass both Cyprus and Lebanon by crossing to Turkey via Syria probably along the route of the Trans-Arab Gas pipeline. Turkey and Syria were months away from completing the construction of a smaller capacity (3-5 bcm/y) gas interconnector before the civil war of 2011 errupted.

Apart from the evident problems of stabilizing and reconstructing Syria, the post-Asad regime is likely to have higher priorities than to facilitate the transit of Israeli gas especially as long as the Golan issue remains unresolved. It may prove a rather impossible exercise to convince Noble, Delek and more importantly Woodside to invest billions of USD in the construction of a 10-15 bcm/y pipeline through so volatile a place as post-Asad Syria.

LCP 2: Offshore Bypassing Lebanon via Cypriot EEZ: the second theoretical route of such a pipeline would essentially bypass Lebanon by crossing through Cyprus' EEZ and in particular Blocks 12, 9, 13 and 3 before it enters Turkish and "Turkish-Cypriot" territorial waters either via Syria's undetermined EEZ or via the arbitrarily defined EEZ of the occupied northern parts of Cyprus which is solely recognized by Turkey as the TRNC (Turkish Republic of Northern Cyprus). Such a solution would be impossible in the absence of a comprehensive resolution of the Cypriot Problem and Nicosia has said that it would not link its gas export options with the inter-communal talks which are set to begin in October.

Israel is unlikely to proceed with the de facto recognition of the TRNC a possibility it refused to consider even at the apex of its strategic alliance with Turkey during the second half of the 1990s. Noble and Delek are currently committed to the development of Aphrodite and the Vassilikos LNG terminal and are highly unlikely to jeopradise their investments in Cyprus for any Turkish Pipeline that would especially violate Cypriot sovereignty.

LCP 3: Offshore Bypassing Cyprus via Lebanese EEZ: The third and most likely alternative from a political point of view would essentially bypass Cyprus but would have to go through Lebenase territorial waters or Lebanon's EEZ. The difference would be very significant in terms of cost since it could increase the cost by a factor of 2,5 times. Given the existing state of war between Israel and Lebanon and their more recent friction over an area of 854km^2 that has frozen the development of the Alon F & Alon C blocks, it is unlikely that the Israelis can bypass both Cyprus and Lebanon when considering an underwater pipeline connection to Turkey.

For reasons of geography the pipeline would pass either through Cyprus' EEZ or through the area of the Lebanese EEZ, which is adjacent to the area of Israel's EEZ that is contested by Beirut. Moreover, a serious consideration of a Turkish-Israeli pipeline would make the ratification of the 2007 Cyprus-Lebanon EEZ agreement much more likely. In that case the construction of a Turkish-Israeli pipeline would become even more difficult. Even in the highly unlikely case that Turkey and Israel could reach an accomodation with Lebanon they would have to cross either Syrian territorial waters or Syria's EEZ which are undefined with both Lebanon and Turkey.

Cyprus-Lebanon-Israel Maritime Boundary Proposals

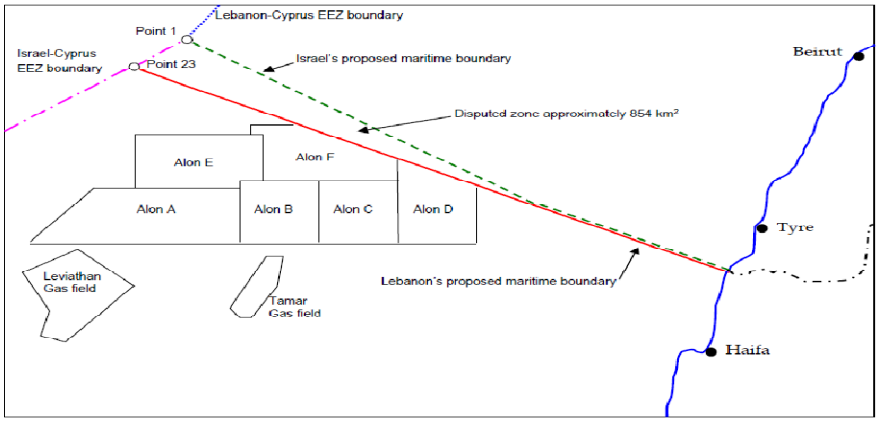

Source: *The Daily Star*.

2nd Conference on Power Options for the Eastern Mediterranean Region
07-08 October 2013, Nicosia, Cyprus (Paper No. POEM13/171)

Escapades at sea: sovereignty, legality and machismo in the Eastern Mediterranean

Dr. Costas M Constantinou

Abstract-- The latest episode of the Cyprus conflict - a dispute over the exercise of sovereignty at sea and the delimitation of sea zones between Turkey and Cyprus - highlights the role of political machismo in the practice of sovereignty, disregarding international law and further undermining prospects for a peaceful settlement of the conflict.

The Cyprus conflict is rapidly spreading to the seas. Clashing cartographies and owner-ship claims have begun circulating through the mass media. Natural-gas-speak is in the air. Accusations, protestations, veiled and naked threats abound. Noble Energy has begun drilling in Cypriot Sea Block 12 (south of the island), renamed Aphrodite, by positioning an extraction platform that goes by the name of Homer. Political reality is intertwined with mythology; epic narratives are about to unfold. Politicians are preparing themselves to do heroic deeds for 'our' sake and once again take up the role of 'our' mythical guardians.

I. Introduction

THE latest episode of the Cyprus conflict - a dispute over the exercise of sovereignty at sea and the delimitation of sea zones between Turkey and Cyprus - highlights the role of political machismo in the practice of sovereignty, disregarding international law and further undermining prospects for a peaceful settlement of the conflict.

The Cyprus conflict is rapidly spreading to the seas. Clashing cartographies and ownership claims have begun circulating through the mass media. Natural-gas-speak is in the air. Accusations, protestations, veiled and naked threats abound. Noble Energy has begun drilling in Cypriot Sea Block 12 (south of the island), renamed Aphrodite, by positioning an extraction platform that goes by the name of Homer. Political reality is intertwined with mythology; epic narratives are about to unfold. Politicians are preparing themselves to do heroic deeds for 'our' sake and once again take up the role of 'our' mythical guardians.

Sovereignty games have always entailed male bravado and machismo. From Jean Bodin to Ronald Reagan, the exercise of sovereignty has been symbolically narrated in terms of the paramountcy of male authority and what men can and should be allowed to do –and get away with – in everyday life. For Bodin, the 16th century theorist of sovereignty, 'the absolute and perpetual power' of the sovereign was akin to that 'admirable' power which the Roman pater familias had over his slaves, children and wife. For Reagan, the Cold War icon and 'great communicator' of the 20th century, the violent exercises of state sovereignty were justified and aestheticized as a playful exchange of male adolescents. 'Oh well, boys will be boys!', he remarkably understated, when informed about the Israeli air strikes against the Iraqi reactor in 1981.

Dr. Costas M Constantinou, Professor of International Relations
University of Cyprus

Cynical tautologies of this kind are not only puzzling but dangerous. They leave the manly, arbitrary and abusive power of the state unquestioned. They do this by avoiding reflection on the main feature of modern state sovereignty, namely its ability to use the law to go beyond the law or take exception from the law, including the decision to define the enemy and justify the use of force against him. Or to put this in more simple (Reaganian) terms, it would be like saying that the boys can do what they fancy, freely engage in their neighbourhood fights and harassments while still – and that is the important thing – being able to employ the law to justify their actions. What is legal, what is just, is what the macho boy does and desires.

If we were to apply these untimely meditations to the current situation in Cyprus, one can easily picture the big boys and small boys fighting in the neighbourhood. Clearly the physical and bullying abilities of the big and small boys differ, yet machismo in various degrees characterizes all. Big boy Turkey parades its naval gadgets in the Eastern Mediterranean to warn and intimidate the smaller boy Cyprus not to exploit its seabed unless and until the big boy says so. Small boy Cyprus cavalierly rejects EU calls for negotiation and ultimately adjudication by the International Court of Justice (ICJ), recklessly conflating its lawful right to exploit its seabed (which no one apart from Turkey questions) with its obligation to delimit its Exclusive Economic Zone (EEZ) west and north of the island as well. The big boy is unhappy about the call for adjudication anyway, and bitterly complains, given its physical ability to enforce what it considers to be 'right' and 'just',which makes it even more perplexing to understand why the small boy dismisses such procedure. In short, political machismo is in full display over this issue, with those speaking in the name of sovereignty making totalizing pronouncements whilst selectively using the law and legal principles, and erasing the inconvenient provisions, nuances and due processes of international law.

Two issues are especially problematic. First**,** how most politicians and the mass media in Cyprus and Turkey popularly treat the EEZ as if it were an area over which coastal states have territorial sovereignty, i.e. of the same kind they have over land. Nothing is further from the truth. On the contrary, the historical development of the concept of the EEZ was an explicit attempt to obviate the territorial sea claims of certain states up to 200 nautical miles (mostly Latin American countries, which arbitrarily re-appropriated the safety zone established under the 1939 Panama Declaration for neutrality during the WW II). In the 1972 Declaration of Santo Domingo, however, 15 Caribbean states drew a distinction between 'territorial sea' and 'patrimonial sea' – in the 'territorial sea' states could have full sovereignty whereas in the 'patrimonial sea' states could only have economic rights, with its delimitation occurring

through peaceful means and adjudication, not through declaration and appropriation.

Significantly, the Santo Domingo Declaration was made a year before the beginning of the negotiation of the new Law of the Sea Convention (1973-1982), and it effectively divided the Latin American states between the 'territorialists' and the 'patrimonialists'; basically between those aspiring for hard masculinity (i.e. declaration of sovereignty and appropriation up to 200 nautical miles) versus those promoting soft masculinity (i.e. that a coastal state has limited rights up to 200 miles and it has to negotiate with others whereand how to exercise these rights). In the 1982 Law of the Sea Convention, soft masculinity in the form of the EEZ won the day. The Convention clarifies that states possess and can exercise sovereignty only over their Territorial Sea– up to 12 miles; whereas over their EEZ (up to 200 miles) and Continental Shelf (under certain conditions up to 350 miles) they can only have 'sovereign rights'.

The point that coastal states only have 'sovereign rights' – not 'sovereignty' – over their EEZ is not pedantic legalism but a deliberate insertion by the drafters of the Convention (a Convention which took 9 years to painstakingly negotiate). It was calculated to deflate unilateral and totalizing territorial claims over the sharing of EEZ resources that could lead to interstate conflict, which the soft 'patrimonialists'feared and we currently face in the Eastern Mediterranean. The EEZ was thus designated as a 'specific legal regime' where the 'rights and jurisdiction' of the coastal state and the 'rights and freedoms' of all other states 'are governed by the relevant provisions of this Convention' and therefore states in exercising their rights must 'act in a manner compatible with the provisions of this Convention' (Articles 55 and 56). That is to say, they are granted rights of exclusivity and exploitation by the Convention beyond their territory on condition that they adhere to the provisions of the Convention and behave in a compatible manner to it. The EEZ constitutes an entirely separate regime outside the sovereign state, beyond Land Territory and Territorial Sea, and where states only have specific competencies. Although states have exclusivity over their EEZ under no circumstances can they treat it as a regime of territorial sovereignty.

The second issue over which there seems to be considerable misunderstanding by politicians and the mass media in the region concerns the delimitation of a coastal state's EEZ. They wrongly assume or deliberately misinform the public that EEZ can be unilaterally delimited. That is simply illegal, if there are opposite or adjacent coastal states at less than 400 nautical miles. In fact, according to the 1982 Law of the Sea Convention coastal states have a special obligation to delimit the EEZs of opposite or adjacent coasts (Article 74) and cannot avoid that obligation (indeed the Republic of Cyprus duly followed that obligation with Egypt, Israel and Lebanon - the latter agreement yet to be ratified; moreover the Republic of Cyprus in acceding to the Convention has accepted the settling of disputes by international arbitration or adjudication, if agreement with the neighbouring coastal states proves elusive).

The simple matter is that an EEZ between opposite or adjacent coastal states legally existsonly when and where it has been duly delimited, either by bilateral agreement or through binding international adjudication. The principle that guides delimitation under the 1982 Convention is that of an 'equitable solution' (Article 74), not merely a question of equidistance from the coastal baselines of states. As mentioned, the Republic of Cyprus has duly delimited its EEZ over its south and south-eastern seas (by bilateral agreements with Egypt and Israel, and potentially Lebanon), and that is why there is no legal basis for Turkish protests concerning its right to drill in Block 12 (Aphrodite). In this area, Cyprus has fulfilled its obligations to the Convention so as to exercise its 'sovereign right' to exploit the specific seabed and thus there is nothing to negotiate or adjudicate over.

However, over the western and northern seas of the island, i.e. the seas adjacent to the southern coast of Turkey, neither Cyprus nor Turkey can legally exercise their 'sovereign right' over the EEZ that they both have. They can make political claims as to the extent of the EEZ but maps that have been circulating showing the 'Cypriot' and 'Turkish' EEZs have no legal standing whatsoever in international law. They are simply used by both sides for irresponsible political statements, bad public diplomacy and highly dangerous brinkmanship.

The procedure under the 1982 Law of the Sea Convention is very clear. States with adjacent or opposite coasts have to seek a negotiated agreement over the limits of their respective EEZs 'within a reasonable period of time'. In lieu of a negotiated settlement, then they have to resort to Part XV of the Convention (Articles 279-299), which includes compulsory acceptance to resort to binding adjudication, among other options, to the International Tribunal for the Law of the Sea or the International Court of Justice (though, there is a possibility under Article 298 of a state opting out of this compulsory procedure, if it makes a declaration upon signature or accession to the Convention and meets certain other conditions for conciliation).

Unfortunately and irresponsibly, over this issue both Cypriot and Turkish governments flag their undisputed 'sovereign right' (to an EEZ in the case of Cyprus or Continental Shelf in the case of Turkey) in their adjacent seas and bypass their obligation to duly and properly delimit the area within which that'sovereign right' ought to be exercised. This conflation of issues is totally counterproductive, fuels tension, and serves as an exemplar of hard masculinity. Also counterproductive is the deliberate mixing from the Turkish side of the'sovereign right' of the Republic of Cyprus to exploit its resources with the position that the Greek-Cypriot community cannot be the exclusive beneficiary of these resources as the Republic of Cyprus is officially bicommunal. The Cypriot government seems willing to consider the latter view (sharing in principle the benefits with the Turkish Cypriots) and rightly rejects the former (negotiating or suspending its sovereign right to exploit its EEZ).

There is a paradoxical logic and great irony in the official Turkish discourse. Turkey that has occupied the northern part of the island since 1974 and sponsored a secessionist and unrecognized state there since 1983: (a) demands the resources share of the Turkish-Cypriot community that seceded from the Republic of Cyprus, from within the sea area that the seceding community does not control or even claim; (b) does not recognize the same right of the Greek-Cypriot community over the share of resources under the de facto control of the TRNC with which Turkey has signed an illegal maritime agreement. If the Turkish-Cypriot

community has a legal share in the Republic of Cyprus (being a constituent community when it was established), then the legality of the Republic of Cyprus and its'sovereign right' to exploit its resources in the areas that it controls – and even in the areas currently controlled by the Turkish-Cypriot authorities –cannot be disputed.

In sum, in the current debate, yet again, the sovereigns and politicians are invariably using the law for their escapades while deliberately being selective or not paying due regard to the legal provisions that they are employing to persuade us that they are right. If I were asked to recommend a way to defuse the current crisis, I would suggest the following

1. The Republic of Turkey and the Republic of Cyprus should start immediate negotiations for the maritime delimitation of their respective EEZs and the Greek-Cypriot and Turkish-Cypriot communities to discuss the share they should have from the exploitation of any natural resources from the Cypriot EEZ on condition that if there is no agreement within a specific timeframe in either or both cases, then the matter in dispute to be taken before the International Court of Justice (ICJ) for a binding decision.
2. If the case goes to the ICJ, I would ask the Court for the following: (a) to delimit the maritime border between Turkey and Cyprus west and north of the island in its entirety; (b) to determine the share that the Turkish Cypriots should get from any exploitation of natural resources at sea; and (c) whether they should get this share before or after the settlement of the Cyprus Problem.

I understand that certain issues and qualifications need to be taken into account:

- I realize, for example, that Turkey has not signed the 1982 Law of the Sea Convention. Interestingly, Turkey is referring to its provisions and in any case the substantive rules of the Convention have become customary international law and thereby binding also for states that have not signed and ratified it. Moreover, as painful as this may sound to some ears, there is no other way that Turkey can legally delimit its southern EEZ than by agreeing the extent of its maritime border or adjudicating it with the internationally recognized Republic of Cyprus. Unless Turkey does that it cannot legally exploit its southern seabed resources beyond its Territorial Sea or sign agreements with foreign companies that have a secure legal basis; neither can the Republic of Cyprus do that in the adjacent seas to Turkey, i.e. west and north of the island).
- I also realize that Turkey prefers to refer to Continental Shelf delimitation rather than EEZ delimitation, assessing that the former will be in its favour if somehow the 1958 Continental Shelf Convention applied (but I think this is not legally sustainable following the 1982 Law of the Sea Convention, whereby EEZ claims incorporate and can supersede the Continental Shelf ones, see for example the rationale in the Case of Libva vs. Malta before the ICJ in 1985, and they were notably delimiting Continental Shelves in that case. The natural prolongation of the Continental Shelf matters in claims over 200 up to 350 nautical miles from each adjacent coast; yet this could not be applied in the Eastern Mediterranean when the distance between the Turkish and Egyptian coastal baselines is less than 400 nautical miles and the other interested parties in the region have already claimed and bilaterally delimited EEZs).
- I also realize that Turkey does not recognize the Republic of Cyprus (but the Republic of Cyprus has a locus standi before the ICJ, and as a matter of fact there have been international legal cases between Cyprus and Turkey before, namely interstate cases before the European Court of Human Rights. Given that there are clear common interests in legally delimiting their respective EEZs and also, presumably, common interests in maintaining international peace and security in the region, this is the rational and procedurally correct way to go, if there is no negotiated agreement. Note that compulsory referral to the ICJ is also something that the Security Council can call upon UN member states to accept, under Article 33 of the UN Charter).
- Finally, I realize that the Republic of Cyprus has already begun exploratory drilling in an area where it has duly delimited its EEZ, exercising its sovereign right, though it has not delimited its EEZ in areas adjacent to Turkey or settled the other issues mentioned above (but there is still enough time to negotiate pending issues, and if there is no agreement, commit in advance to refer the case before the ICJ and make its ruling binding, and if necessary retroactive).

I believe that this is an effective way to deflate the dangerous political rhetoric and calm down the sovereignty anxieties and excesses that are very likely to intensify if this maritime issue remains unresolved. If properly managed, it could even be an opportunity for intercommunal and regional cooperation that is urgently needed, bringing 'unity at sea', supporting peace settlement efforts in Cyprus and leaving open the possibility of reunification – if not for current, at least for future generations – rather than cementing partition. Perhaps, even the boys may grow up and be boys no more, or no less publicly exposed as the untrustworthy, hypocritical and insecure males that do not deserve to lead us.

2nd Conference on Power Options for the Eastern Mediterranean Region
07-08 October 2013, Nicosia, Cyprus (Paper No. POEM13/173)

European Roadmap for Energy and the Role of Cyprus Hydrocarbons

Dr.Paris Fokaides

Abstract-- The recent developments in the exploitation of hydrocarbons in Cyprus are growing the need for strategic targeting of the actions of the Republic in this field. The Republic of Cyprus need to determine in a clear way the context in which the procedure of the exploitation of its mineral wealth must proceed. Having joined the European Union in 2004 mainly for security reasons, the Republic of Cyprus should consider at this stage the basic principles governing the European policy on energy, understand the origin of these principles and lead its strategy as a member Union towards a compatible target

This article aims to present the basic principles governing the European strategy on energy issues. Through the directives and regulations of the European Union, this article aims to present the main focus of Europe's energy policy, as well as the specific quantitative and qualitative targets to achieve them. A comprehensive assessment of the opportunities both for Cyprus and for Europe the potential exploitation of Cyprus deposits is also attempted. This study comes up with concrete strategy suggestions in relation to the proposed targeting of Cyprus' policy on the exploitation of its mineral deposits.

Index Terms: European energy policy, Cypriot hydrocarbon reserves

I. I Introduction

The affordable access to energy resources has been since the industrial revolution in the 19th century one of the main initiatives of the European states. This is due to the fact that both the cost and quantity of available energy determine critical economic indicators of societies , including the cost of goods in all three economic sectors (primary, secondary and tertiary) comprising in this way the thresholds for establishing conditions of economic development or recession. A commonly accepted fact is that all the disputes and conflicts in recent decades in the Middle East are related to the control of the energy resources of this region. A constant attempt is observed in various ways to intervene in oil-producing countries to ensure primarily the presence of governments which serve their goals and interests, which in the case of the Middle East, this coincides with the smooth supply of energy resources

The struggle for uninterrupted and affordable power supply is a key strategic priority of the European policy in the field of energy. The European Union's efforts focused in recent decades to ensure those conditions to create those facilities which will ensure energy independence at a low cost. This effort becomes more imperative given the fact that today 80 % of its energy resources are imported, mostly coming from socially and economically unstable regions of North Africa and the Middle East. Under these conditions the European energy strategy aims at ensuring the required resources that would ensure energy independence of the European area.

This strategy came to strengthen the environmental concerns content which expresses substantiated concerns for nearly two decades, about the negative effects of continued use of fossil hydrocarbons, which contribute and intensify the greenhouse effect. The main expression of this phenomenon is the climate change, halting of which requires large amounts of capital and therefore large investments and hence large outflows from the state funds. These flows do not seem to attach the short term, therefore, not considered in immediate economic gains of European states.

II. Main Parameter European energy strategy

Given the above realities , the European Union has come to adopt a multifaceted and integrated strategy for the rational use of energy. This strategy, which is summarized in the context of related communication on the European energy roadmap for 2020 is summarized in the following five policy axes:

1. Efficient use of energy
2. Free transport of energy
3. Safe and affordable energy
4. Supporting research and development in the energy sector
5. Development of strong international cooperation

The implementation of a policy which is based on the above lines is able to secure cheap and uninterrupted power supply in Europe.

Efficient use of energy

In the field of energy efficiency, energy conservation efforts are integrated. In the electricity sector these efforts are translated into efficient cycles and energy conversion processes and in buildings into conservation policies through efficient building services, efficient building shells and better energy management. In transport, the efficient use of energy is focused mainly on efficient engines with lower emissions.

Free transport of energy

The free transport of energy expressed through the development of trans-European networks, both for the transmission of electricity and for transport of liquid and gaseous fuels is supported. More choices can be ensured in distribution and therefore energy management, overcoming in this way issues of deferred production and demand.

Safe and affordable energy

This parameter is satisfied both with the use of technologies that can potentially reduce the cost of energy as well as with

P.A Fokaides is with School of Engineering and Applied Sciences, Frederick University, Cyprus (e-mail: eng.fp@frederick.ac.cy).

the energy independence through the use of local energy sources. Renewable energy is an excellent example which combines both criteria, and furthermore its utilization has minor impact to the environment. This is the main reason why the applications of renewable energy technologies flourish in recent years in Europe and are supported by a series of policies and measures.

Support for research and innovation

This policy is embodied in European research programs to support development in the energy sector. The topics in the energy sector in this region target both the further development of renewable energy technologies through new materials and the efficient use of conventional energy resources. In this context initiatives on gasification of conventional energy sources and hydrogen production are included, a technique which is gaining more and more ground in the use of fossil energy resources.

Development of strong international cooperation

This parameter consists of all the efforts of European countries to remote produce and transfer energy from outside the European Union in regions with rich energy potential , which can potentially produce energy efficiently and cheaply (e.g. utilization of solar energy in North Africa).

It is clear from the presentation of the main aspects of European policy in the energy sector that it has horizontal multifaceted nature and it is not limited to individual policies and initiatives, but sets a framework that meets the real needs of European societies.

III. THE ROLE OF THE CYPRIOT HYDROCARBONS IN EUROPEAN ENERGY POLICY

The existence of deposits in the sea area between Cyprus, Egypt and Middle East has been known since the 70's and particularly since 1978. Intensified dialogue, however, to exploit these resources started in 2001 with the conclusion of the government and the Minister of Trade agreement with Egypt on the delimitation of the common maritime space of the two countries. The years that followed the process of exploration and exploitation of resources took its course, with the following governments to add their stepping stone in helping realize , resulting to clear timelines for the time extraction and exploitation of the resources. The question which arises is whether the use of Cypriot hydrocarbon deposits is compatible with European policy in the field of energy and whether it can follow some of the European policy axes. A comparative statement of the European policy agenda on energy, with the potential that opens up the exploiting of Cypriot hydrocarbons, indicates the particular importance of Cyprus hydrocarbons within the European area.

The storage and transport of hydrocarbons will require the creation of trans-European transport network, and the integration of the infrastructure in existing networks in the case of transfer of a liquefied natural gas. This offers the opportunity to Cyprus to join existing networks, feeding these networks with its own gas. Such a prospect would ensure greater stability of the network and thus cement the principle of trans-European transport. It will give the opportunity to Cyprus to take advantage of both the power and the use of gas, which is clearly more efficient than the liquid fuel which is used today. Such a development, will lead to increased efficiency of the energy system of Cyprus, satisfying in this way and the first pillar of European energy policy, namely that the efficient use of energy.

The supply of European networks with Cypriot natural gas is also expected to have a positive impact on security of supply and the cost of energy. The Cypriot political and social environment is much more stable compared with those in the Middle East and North Africa. Therefore both the uninterrupted supply, and the predictable price, is expected to be the main feature of the possible participation of Cyprus in the European gas networks.

Alongside the latest developments in the exploitation of Cyprus deposits have revealed a new collaboration, that between Greece, Cyprus and Israel. Therefore Cyprus government meets through this process implicitly the requirement of the EU energy strategy for developing international synergies with reliable states, where in this case the state is Israel. Along with the laying of submarine cable power transmission of 2GW between the three countries, the requirement is also fulfilled at another level.

Finally noteworthy is the fact that through the development of initiatives in the field of exploitation of hydrocarbons in Cyprus, a new market is expected to arise, which the academic world of Cyprus rushed to support through a range of new academic and research programs. This development is expected to raise the level of proficiency and research object in Cyprus, and thus support the European effort to promote research and development issues in the energy sector.

The above analysis shows that the exploitation of the Cypriot exploration potential can be fully compatible with European authorities in the field of energy.

IV. THE " EUROPEAN CHOICE " EXPLOITATION OF CYPRIOT DEPOSITS

The strategic dilemma which the Cyprus at this stage will need to answer is whether it would name its deposits as European and will integrate them into the wider energy balance of the continent, or whether it will proceed in search of other markets for disposal of its deposits. For the first option the framework is already defined and predicted: the Cyprus acts as a European state, safeguarding the interests of offering deposits in mainland Europe, earning in this way reasonable and expected economic benefits and becoming a factor of energy security in the region. Additionally, the hard core of Europe will raise its supervisory custody on the Cypriot deposits and will ensure their smooth exploitation and disposal in the sense of mutual benefit. This framework ensures the safe exploitation of the deposits and seamless transfer from the southeastern Mediterranean in southern and central Europe, in existing networks. This scenario also seems the most reasonable, with Cyprus being a full member of the European Union, to adopt the common European policy and to define its goals and initiatives in a given framework.

This question also gains another dimension when safety issues and the ongoing threat of Turkey are considered, which will not compromise with the idea that the "Greek South" will have a greater role in the energy scene. The joint collaboration with the European family deprives the argument of Turkey but also makes it particularly skeptical to possible aggressive moves towards Cyprus. Along with the framework of the Euro- Turkish relations are very clear and largely determined based on the principles of the acquis communautaire , the position of Cyprus will be less risky.

V. CONCLUSIONS

This paper has attempted to analyze and demonstrate a strategic choice of the Republic of Cyprus to exploit its energy reserves, that of integration into the European energy system. This work demonstrated and analyzed through the European communication on European energy vision for 2020 the main axes strategists in Europe in the energy sector. At a reasonable comparative quote, this work demonstrated the absolute compatibility of the exploitation process of Cypriot hydrocarbons with the European strategy in the energy sector. This identification is complete and meets all the parameters, namely the following:

1. Promoting trans-european energy networks
2. Ensuring affortable and reliable energy
3. Ensuring synergies with third countries (Israel)
4. Improving the efficiency of energy system
5. Promoting research and innovation in the energy sector.

This work also demonstrated and analyzed the significant benefits from the pooling of Cypriot deposits with the European core in a relationship of mutual benefit. Finally this study analyzed the ensuring of Cyprus against Turkish threats through the integration of Cyprus reserves into the wider energy balance of the European continent.

2nd Conference on Power Options for the Eastern Mediterranean Region
07-08 October 2013, Nicosia, Cyprus (Paper No. POEM13/183)

From Sensors and Measurements to Data and Applications in Power Systems

Irina Ciornei, Petros Mavroeidis, Georgia Pieri and Elias Kyriakides

Abstract-- **This work is a comprehensive overview from sensors and measurements to data and applications in power systems. The focus lies on current technologies in the market, the penetration range at present in the power industry, as well as the trends for different types of technologies. Various sensors will be presented in terms of their characteristics, measurement quantities and ICT capabilities. Special attention will be given to the data produced by these sensors and measurements, and the applications built on top of them. The latter, are related to the operation, monitoring and control as well as power quality in distribution and transmission systems. In addition to traditional measurements, such as current and voltage transformers, new technologies have emerged, such as optical measurements and satellite measurement technologies. On top of that, the nature of the new ICT enabled capabilities will be demonstrated and their effect on applications from state estimation to post-mortem analysis will be presented. Future trends of measurements and applications development and deployment are discussed from an engineering perspective.**

Index Terms—**data, distribution system, measurements, power systems, sensors, transmission system, power system monitoring, power system control.**

I. Introduction

Advancements in metering technology and mainly in ICT have enabled a paradigm shift in how power systems could be designed, monitored, controlled and operated [1]. Many of these advancements are already incorporated or in the process of deployment in power systems such as novel sensors, phasor measurement units (PMU) [2] and advanced measurement infrastructure (AMI) [3]. However, due to the high level of required investments, the progress of this change has been rather slow. In addition, many of the aspects of this new, smart grid are still under debate [4], and far from standardization; this discourages long term investments. However, it is expected that this paradigm shift will materialize by necessity. The latter relates with a financial tight environment, deregulation, and the need for sustainability expressed largely by the demand for renewable energy penetration and energy efficiency. It will be in the engineering community's shoulders that this transition will be performed efficiently, timely and sustainably.

Power systems are vast in size and the aggregation and presentation of measurements in a meaningful way is a task in itself. Traditionally this is achieved by means of SCADA systems: centralized monitoring and control systems where measurements across vast geographical areas are gathered and the state of the power system at the transmission level is estimated in terms of voltages and power flows. Control actions, including dispatching, are taken accordingly. The advance of ICT technology and the empowerment of synchronized measurements by the use of GPS signals, has provided with new capabilities both in the measurements themselves, the aggregation of the produced data and the applications built on top of them. In the transmission system level, these technologies enable an enhanced situational awareness that further makes possible innovative monitoring and control applications. In the distribution system level, such sensors and technologies support many applications that drive benefits, including improved reliability, energy efficiency, power quality, reduced maintenance costs, and increased operational awareness. In some cases sensor measurements directly drive analysis and control applications. Sensors are also fundamental to distribution network state estimation, which is fast becoming a prerequisite for smart grid functionality [5].

Advancements and new technology deployment are occurring more extensively at the transmission level than at the distribution (e.g., wide-area monitoring systems, dynamic line rating), especially due to the criticality of the equipment involved as well as their implied economics. Traditionally, there is no visibility in the distribution network below the substation (SCADA). At present, there is a trend in gathering information and developing solutions for monitoring and control for the distribution networks due to a change in consumer status from consumer to prosumer (assumes the role of consumer and producer) as well as due to bidirectional power flows at the distribution level (called active networks due to energy generation at the distribution level) [6].

Technologies such as PMUs, intelligent electronic devices (IED) and advanced metering infrastructure (AMI, which includes also the smart meters) are the front page novelties of an enhanced or smart grid [7]. The above technologies provide an abundance of data in real time that enable new capabilities regarding awareness, monitor and control. They also create the challenge of storing, handling, transmitting and taking action upon this huge amount of data across vast geographical areas. Moreover, they introduce new kinds of vulnerabilities that relate with ICT such as cyber threats, but also with the interdependence of the power system and ICT infrastructure [8]. Although the sensors and ICT technologies are mature, there is still a long way to go in terms of applications deployment [9].

In this work, a comprehensive approach toward

This work was funded by the Republic of Cyprus through the Research Promotion Foundation (Project ΠΡΟΣΕΛΚΥΣΗ/ΝΕΟΣ/0311/34)

Irina Ciornei (e-mail: ciornei.irina@ieee.org), Petros Mavroeidis (e-mail: mpetros@ucy.ac.cy), Georgia Pieri (e-mail: pieri.georgia@ucy.ac.cy and Elias Kyriakides (e-mail: elias@ucy.ac.cy) are with the KIOS Research Center, Department of Electrical and Computer Engineering, University of Cyprus, CY-1678, Nicosia, Cyprus.

measurements in transmission and distribution systems is followed. Section II focuses on the sensors used in transmission and distribution systems. In Section III the attention lies on the data produced by measurements and the applications built on top of them. A discussion is conducted in Section IV with respect to the future trends in sensors, measurements and relevant applications, and the paper is concluded in Section V.

II. Measurements and Sensors in Power Transmission and Distribution Systems

Measurements or quantifying signal inputs in power systems are collected using measurement instruments. In the history of power transmission and distribution systems, instrumentation devices can range from simple sensing and measurement units (e.g., direct reading thermometers) to complex multiple type sensing and multi-variable process analyzers (e.g., power quality analyzer). In recent years, the power industry is showing a clear modernization trend where the adoption of digital electronics in metering (especially automatic meter reading via a variety of communication channels at large customers) are the front page improvements [7]. A picture that describes the past and present status of instrumentation at distribution and transmission level is presented in Figure 1.

Instrument Transformers (IT) are the backbone of metering applications in power transmission and distribution systems. They are used for billing purposes or transactions and the economic management of industrial loads. ITs are designed to convert high currents or voltages into low values that can be utilized by other low voltage instruments such as meters, relays (standard is 5 Amps/155-120 Volt) or other equipment used in protection control. In the metering applications, they play the role of extending the measurement range of the meters connected to them and differ from other instrument transformers used in protection applications by the accuracy range.

Traditionally, voltage is measured using inductive instrument transformers or capacitive voltage dividers. Capacitive voltage transformers/dividers have a good accuracy on narrow frequency band only, while the inductive voltage transformers suffer from harmonic frequency resonances between winding inductances and stray capacitances. There is a recent trend, following the traditional class of instrument transformers, in developing high accuracy Resistive Capacitive Voltage Dividers (RCVD) [10]. The RCVDs have the advantage of measuring harmonics with accuracy better than 1% in a range from DC up to 20 kHz and a phase displacement less than 1 degree, making them a good option in the smart grid era, where power quality plays an important role in the power system business sustainability.

By means of the current SCADA system, measurements, automatically collected by the Remote Terminal Units (RTUs) are either telemetered (e.g., every 10 seconds) or transmitted spontaneously when changes in the measurements exceed the threshold values. Data collection includes analogue measurements (such as active and reactive power, voltage, current, frequency, transformer tap position), switching equipment status data and alarm data, as well as energy meter readings (e.g. from participants in the electricity market which takes place twice a day in Romania [11]).

The traditional class of instrument transformers have been state of the art for many decades, however they also have a number of disadvantages:

- they are heavy and space consuming equipment (with weights of up to several tons at the highest voltage levels)
- need for separation between the main circuit carrying the current to be measured and the control circuit in which the measured signal will be utilized
- the measuring sensor needs to be shielded and galvanic insulated due to electromagnetic interference
- the previous two points result in complex and massive structures (high costs)

Within the last twenty years the trend is to develop alternative sensing technologies to overcome these obstacles. Different approaches are observed within which predominantly are the optical sensing and the signal

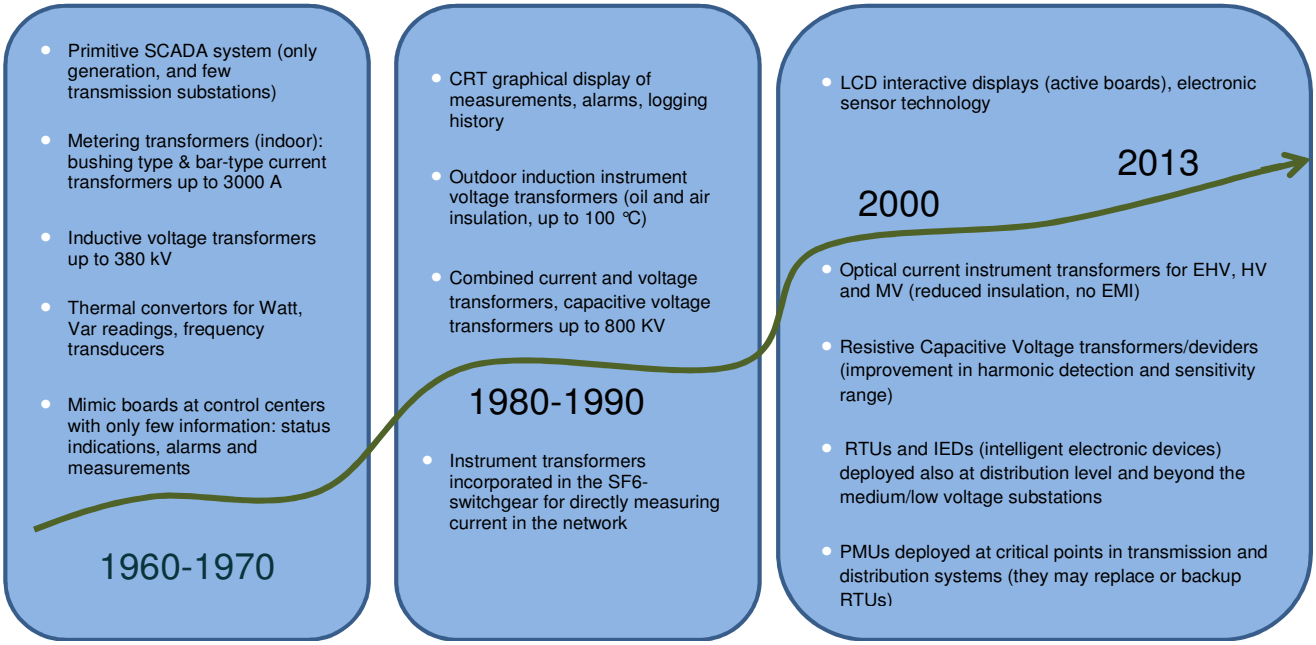

Fig.1. Evolution of instrumentation and control in the power transmission and distribution system

transmission techniques [12]. Advantages of optical voltage sensors over conventional voltage transformers include:

- higher fidelity and accuracy (e.g., due to their wider bandwidth, larger dynamic range and absence of effects like ferroresonance)
- smaller weight and size due to inherent galvanic isolation of secondary electronics from high voltage
- reduced environmental impact (e.g., no risk of oil spills)
- their output is readily compatible with the modern digital equipment for substation control and protection.

In addition to improvements in conventional sensors, a number of innovative power system instrumentation are being developed. Indicatively, some of the novel sensors are summarized in Table I together with the basic physical principle of their operation, some of their possible applications in power and transmission systems and the current status of their deployment [13],[14].

To accurately measure the desired quantity, novel measurement instruments are equipped with abilities such as time stamping, storage, communications and intelligence in terms of acting or enabling actions. The most prominent examples of deployment are phasor measurement units (PMUs) and smart meters (SMs). A PMU is a multichannel digital device that measures voltages and currents at a fast rate (e.g., in the order of 60 times per second) and time-stamps each measurement. The time is acquired by GPS, providing a high precision common time reference across geometrically distant measurements. The latter feature enables the computation of phase angles in addition to the magnitudes of the measured signals. A PMU measuring

TABLE I
NOVEL SENSORS FOR APPLICATIONS IN POWER TRANSMISSION AND DISTRIBUTION SYSTEMS

Sensor type	Physical principle	Application	Current status
Giant magnetoresist-ance	Change in electrical resistance of some materials (e.g., magnetic metallic multilayers, such as Fe/Cr and Co/Cu, separated by nonmagnetic spacer layers of a few nm thick) in response to an applied magnetic field.	Measuring the magnetic field intensity and other derived measurements (e.g., current, voltage)	Not yet applied to power systems
Faraday optical sensor	Current flowing in a conductor induces a magnetic field that rotates the plane of polarization of the light traveling the sensing path enclosing the conductor. The accumulated rotational displacement is proportional to the current traveling the conductor.	Optical voltage and current transducers for HV and MV overhead lines	Commercial devices available on the market from different vendors
Pockels optical sensor	Linear change in the refractive index of a material/crystal proportional to the electric field is applied to it.	Optical voltage and current transducers for HV and MV overhead lines	Experimental
Hall-effect sensor	Change in electrical resistance of semiconductor devices in response to the incident magnetic field	Power quality, voltage, current measurements	Commercial three phase power analyzers available on the market
Satellite measurement technologies	Differential global positioning method (DGPS)	Determine the sag of the overhead transmission lines	Experimental
Mechanical	CAT-1 system based on a conglomerate of thermal and mechanical sensors, together with data processing	Transmission line dynamic rating (correction in transmission line parameters for state estimation)	Commercially available
	Measurement of displacement proportional to the acoustic noise	Determine the loading in power transformers	Demonstration phase
Lab on chip	Integration of microprocessors and additional low cost sensors (e.g., chemical sensors) to determine other variables (pseudo-measurements) that would be available and ready for data collection.	Ozone or severity of impurities detection for determining the state of the insulators	Experimental
Video technology	Remote visual inspection	Visual inspection of electrical equipment for maintenance purposes, for double checking the status of some equipment (e.g., breakers)	Experimental
		Condition based maintenance instead of time interval maintenance	
Radio Frequency (RF)	RF communication of different sensors	Wireless communication and interoperability for meshes of sensors deployed in a substation	Commercially available
	Harvest of RF energy	Power harvesting and storage for powering the sensors	Experimental

system includes the voltage and current transformers, connection cables and filters that introduce potential errors in measurements. Additional errors might be introduced by the computational logic of the A/D converter. A proper calibration of a measurement system that incorporates a PMU is essential to take full advantage of its measurement accuracy. It is also important to note that, currently, the cost of a PMU installation is prohibitive for a complete observability of the power system network by PMUs.

A smart meter (SM) employs digital technology to measure and record electrical parameters (e.g., power, voltage, and energy) at the consumer side and it has communication ports linked to central control and distributed loads. It is intended to replace the traditional electric energy meter used for billing purposes. The smart meter is intended to be used as an enhancement in the distribution management system (DMS) due to its frequent reading and communication capability (provides consumption data to both consumer and supplier, and in some cases, switches loads on or off). Their significance in the DMS is way beyond the billing purpose as they may actually enable multiple applications towards efficiency and reliability (fault detection, load balance, shedding and control, etc).

The current status in smart metering deployment around the world is presented in Table II. The data was collected from [3],[15]-[17].

Sensors for the distribution power system have primarily focused on the measurement of current and voltage, and have calculated parameters based on these measured quantities. These measurement devices support a number of operational applications including distribution management systems (DMS), Volt-VAR, CVR, and Fault Location. Analogous to the substation and transmission environment, there exists a set of additional measurements that may yield value in the areas of asset management, particularly in the areas of failure prediction, detection, and prevention.

TABLE II
DEPLOYMENT STATISTICS OF THE SMART METERS

Country/Region	Number of SMs deployed/%from the total metered population
USA	37 300 000
Canada	800 000 (as of 2007)
Italy	27 000 000 (as of 2006) / 94%
UK	4.7%
France	4.5%
Germany	1.6%
Spain and Portugal	7.7%
Central and Eastern European	2.9%
China	139 000 000 (units purchased in 2011)
Korea	185 000 for industrial consumers (as of 2000)

Measurements such as temperature, vibration, partial discharge, and others, coupled with existing precise and accurate measurements of voltage and current will potentially yield solutions that provide an entirely new set of benefits [18].

The desire to operate distribution systems efficiently and reliably is causing utilities to consider methods for increasing the number of monitoring points on their distribution feeders. Traditionally, installing metering-class current transformer (CTs) and potential/voltage transformers (PTs) on the distribution lines to monitor selected points on feeders was standard practice. Vendors have now developed high accuracy current and voltage sensors and some sensors that combine both measurements - namely the line-post sensors, which monitor distribution level power flow and are easier to install than traditional CTs and PTs.

The line-post sensor provides two low ac, continuous voltage outputs proportional to the line current and phase voltage at the point of application along the distribution feeder. The per-phase installation of sensors supports the typical power measurements for voltage, current, active power and reactive power on a per-phase basis to address the variant nature and imbalance of the distribution loads along the radial distribution feeder [19]. The direct ac input to the remote terminal unit (RTU) from the sensor supports fault detection and power quality measurements including harmonic content. The RTU exposes the detection of the fault current when the phase current input exceeds the fault current threshold and the duration of the fault current exceeds the time threshold.

III. DATA AND APPLICATIONS

In general, data are a source of information and knowledge. They can be either directly retrieved or deduced from other data. In power systems, they relate to the measurements and sensors described above; in addition by applications, such as state estimation, further data are produced, leading to enhanced system awareness and enabling potential actions towards reliable, secure and efficient operation. Due to their interdependence, data and applications will be jointly presented.

The nature of data is important; they may be on-line or off-line. In power systems there are also synchronized and conventional data. Synchronism is enabled by a GPS common time reference; synchronized data are also characterized by high measurement rates. Conventional data refer to those sent by RTUs. The nature of data imposes different requirements on the ICT and power infrastructure. Moreover, it relates with different perspectives from operations to post-mortem analysis and planning [1],[9]. Applications may be distributed or centrally executed. The latter is an important characteristic of implementation designs as it relates to the notion of scalability; distributed designs are more scalable. On the other hand, central designs have better performance in certain occasions [20].

A prerequisite for any application towards a more stable and reliable power system is the knowledge of its state, either as a whole or locally. Thus, state estimation, was primarily given most of the attention concerning the exploitation of PMU measurements. Currently, the high installation cost is prohibitive for a full observability of a

power system solely by PMUs. In addition, state estimation solely by PMUs would be vulnerable in case of a GPS failure [21]. Thus a lot of research has been conducted for the optimal placement of PMUs [22]. Initial focus is placed on observability [23]. Further goals/constraints include a better dynamic monitoring, topology and measurement errors identification. Present techniques of state estimation incorporate measurements by PMUs and pseudo-measurements to the state estimator that includes conventional measurements. Pseudo-measurements are bus states that are computed from adjacent bus measurements and the application of Ohm's and Kirchhoff's laws.

The high measurement rate of PMUs can improve dispatching in power systems especially where there is a high penetration of renewables sources. Solar irradiation and, to a greater extent, wind are of high variability and difficult to forecast. Moreover, renewables are connected at the distribution system voltage level that is out of reach of the traditional SCADA system and state estimators that monitor the transmission system. PMUs enable a real time monitoring of energy production. Combined with demand side management and especially demand response schemes [24] they also enable a more efficient match of generation and demand and a reduction of the amount of spinning reserves. Demand response mainly relates to automation schemes that enable the switching of loads on or off with respect to dispatch issues, stability issues and energy efficiency issues. Higher efficiency is accomplished by achieving an as flat as possible energy production curve that allows for reduced cost per MWh. As will be discussed below, synchronized measurement technology, by addressing the associated stability problems, allows for increased renewable penetration and reduced spinning reserves; thus, it further improves energy efficiency and sustainability.

Another important application category is stability monitoring. There are various manifestations of instability in power systems: angle swings, inter-area oscillations, voltage magnitude stability. These instabilities are the result of faults and of equipment failures in a given power system topology, available control devices, power flows and generating capacity. It has to be noted that the optimal configuration of protection schemes differs between a healthy and an unhealthy power system condition (notions of dependability and security [25]). Small signal detection aims at identifying small disturbances. An example of such an approach is Prony analysis [26]. Other approaches for a better dynamic assessment of the power system include Kalman filters, Decision Trees, and neural networks [22]. Lyapunov energy functions may be used to identify rotor angle instability before it even occurs. Stability monitoring is also performed by static approaches, such as the well-established PV and QV curves and the use of the Jacobian matrix and sensitivities at the point of bifurcation [27]. It must also be noted that, when monitoring a power system, a contingency analysis must be present to assess the potential stability in the case of probable contingencies. PMUs enable a real-time monitoring of stability measures, enhancing the stability awareness and enabling the development of innovative approaches in stability enhancement discussed below.

As a means towards stability enhancement, the use of synchronized measurement technology (SMT) increases the situational awareness in the system and enables fast actuation of remedial measures. A voltage stability enhancement method usually requires the sensitivities of the voltage stability margin with respect to different control parameters such as the generation rescheduling, switching of reactive power devices, changing transformer taps, adjusting phase shifter angles, or load shedding to determine the correct amount of change in control action needed to drive the operating point away from a potentially dangerous situation. Adaptive relaying is the approach of on-line changing the settings of the protection schemes in accordance with the state – healthy or not – of the power system as diagnosed by the tools discussed in the previous section. Controlled islanding is the process of separating the grid in distinct stable islands to avoid a wider blackout. It presents many challenges, mostly related to the presence of distributed generation, and the necessity to meet power flow and power quality requirements. Novel protection schemes, similarly to state estimation and stability monitoring, are characterized by two different approaches: either to estimate, monitor and control in a local substation level, or to aggregate all the data, make estimations and take decisions centrally. The local approach has the distinct advantage of scalability, while the wide area approach has the advantage of flexibility, manageability and the implementation of more complex protection schemes. In addition, the wide area approach has, in certain cases, a better performance.

There are also important offline applications. A great source of inaccuracies in power system simulations and estimations originates from the models used to represent components such as generators, transmission lines and loads [28]. Data from measurements enable the validations of the models and the accuracy of the involved parameters. Moreover, synchronized measurements, due to their high measurement rate enable the validation of dynamic models, which is an important element of stability studies. Better models enable better secondary data: data based on measurements and computations that, for example, enable better model validation. Another important offline application is post mortem analysis. The use of synchronized measurements enables a faster analysis of the sequence of events and an identification of causes and effects. A relevant example is the analysis of the 2003 North America blackout.

Last, but not least, power system restoration is another important application. After blackouts or major loss of loads or generators, bringing the power system to its normal state is a tedious process. Re-connecting transmission lines and loads has to be sequential and careful. Synchronized measurement technology leads to increased confidence of such operations as both the magnitude and phase of voltages are measured, thus avoiding connecting buses with great phase angle differences.

State estimation is a horizontal enabler that makes many of the other applications possible. There are also other issues to be considered across the various applications. Common data modeling and data integration, for example, from low voltage to transmission voltage level, and the necessary ICT

TABLE III
INDICATIVE APPLICATIONS IN POWER SYSTEM TRANSMISSION AND DISTRIBUTION SYSTEMS

Application	Description
State Estimation	Real time computation of voltage phasors and power flows
Stability Monitoring and Stability Enhancement	Stability margins are calculated, oscillations are identified, contingencies are examined
Adaptive Control	Protection schemes are adapted to the state of the system in terms of dependability and security
Controlled Islanding	The process of separating the grid in distinct stable islands to avoid a wider blackout
Power System Restoration	After islanding or a blackout has occurred, the process of bringing the power system back to its normal state of operation
Post-mortem Analysis	Post-disturbance or post-blackout analysis of the sequence of events
Model, Parameter, Measurement Topology and Data Validation	By algorithms incorporating measurements, models, computations and simulations, the models, measurements, topologies and accuracies are validated and/or improved

infrastructure to support the abundance of data and applications are a prerequisite for the further deployment of the above novel concepts in power system monitoring and control. The corresponding business models must be developed accordingly towards customer-oriented functionality and better smart grid project management; potential lack of ICT expertise by electric utilities should also be taken into account.

IV. DISCUSSION ON FUTURE TRENDS

"Smart" has been the buzz-word adjective when proposing various innovative schemes for measurements and applications. However, the content of "smart" is not clear in many cases. What is also missing are well developed roadmaps and business plans for the deployment of these sensors and applications [9]. Another important aspect is to address cyber security issues from the beginning and not in a remedial manner [8],[29]. Last but not least, standards must be developed timely to enable the deployment of applications that incorporate the above described technologies.

It must also be noted that progress is not only a matter of available technology and engineering knowledge; it is related to financial and business constraints, policies and regulations, targets and objectives. Environmental sustainability is a political decision to make. Aggregation of resources for investments is related to governmental and legislative actions, and the expectations and perceptions of the private sectors with respect to costs, benefits and risk. An engineering point of view cannot address issues of political economy. However, it must be able to translate societal needs in well described technical solutions, it must be able to quantify the impact of the various contingencies, and finally to justify the relevant investments. The above process will define the rate of progress in the transition between the current and future power grids. A higher degree of renewable energy penetration and energy efficiency is expected, enabled both by advances in technology of renewables and by the above described measurements and applications.

Most of the application development and novel sensor technology deployment typically takes place at the transmission level, where reliability of equipment and the network as whole has a high economic impact. Therefore, upgrades at the transmission substations incorporate adoption of advanced instrumentation and communication technologies (e.g., optical voltage and current transformers, fiber optic communication between substations and the central control room, PMU placement at critical substations, video inspection for maintenance purposes, etc.). At the distribution level, the main adoption of novel sensor technologies is the deployment of smart meters as well as placement of PMUs below the medium voltage substation.

In the future, new digital communication technologies, combined with advanced digital meters and sensors, will support more complex measurements. Further, they will accommodate direct interaction between the service provider and the consumer.

V. CONCLUSION

In this work a comprehensive overview from sensors and measurements to data and applications in power systems has been presented. The focus lied on current technologies on the market, the penetration range at present in the power industry, as well as the trends for different types of technologies. Various sensors were presented in terms of their characteristics, measurement quantities and ICT capabilities. Additional attention was given to the data produced by these sensors and measurements, and the applications built on top of them. The latter, are related to the operation, monitoring and control as well as power quality in distribution and transmission systems.

VI. REFERENCES

[1] M. Kezunovic, V. Vittal, S. Meliopoulos, and T. Mount, "The Big Picture: Smart Research for Large-Scale Integrated Smart Grid Solutions," *IEEE Power and Energy Magazine,* vol. 10, no. 4, pp. 22-34, July 2012.

[2] S. Chakrabarti, E. Kyriakides, B. Tianshu, C. Deyu, and V. Terzija, "Measurements get together," *IEEE Power and Energy Magazine,* vol. 7, no. 1, pp. 41-49, Feb. 2009.

[3] S. Depuru, L. Wang, and V. Devabhaktuni, "Smart meters for power grid: Challenges, issues, advantages and status," *Renewable and Sustainable Energy Reviews,* vol. 15, no. 6, pp. 2736-2742, Aug. 2011.

[4] Z. Erkin, J. R. Troncoso-Pastoriza, R. L. Lagendijk, and F. Perez-Gonzalez, "Privacy-preserving data aggregation in smart metering systems: an overview," *IEEE Signal Processing Magazine,* vol. 30, no. 2, pp. 75-86, Mar. 2013.

[5] R. Singh, B. C. Pal, and R. A. Jabr, "Choice of estimator for distribution system state estimation," *IET Generation, Transmission & Distribution,* vol. 3, no. 7, pp. 666-678, July 2009.
[6] O. Samuelsson, S. Repo, R. Jessler, J. Aho, M. Karenlampi, and A. Malmquist, "Active distribution network - Demonstration project ADINE," *IEEE PES Innovative Smart Grid Technologies Conference Europe (ISGT Europe),* Gothenburg, Sweden, pp. 1-8, 11-13 Oct. 2010.
[7] K. Mauch and A. Foss, "Smart Grid Technology Overview," *Meeting of Canadian Experts and R&D Contributors for Smart Grids,* pp. 1-41, 27-28 Sept. 2005.
[8] D. Kirschen and F. Bouffard, "Keeping the lights on and the information flowing," *IEEE Power and Energy Magazine,* vol. 7, no. 1, pp. 50-60, Feb. 2009.
[9] D. Novosel, V. Madani, B. Bhargava, V. Khoi, and J. Cole, "Dawn of the grid synchronization," *IEEE Power and Energy Magazine,* vol. 6, no. 1, pp. 49-60, Feb. 2008.
[10] G. Crotti, D. Giordano, and A. Sardi, "Development of a RC medium voltage divider for on-site use," *Conference on Precision Electromagnetic Measurements (CPEM),* Daejeon, South Korea, pp. 655-656, 13-18 June 2010.
[11] T. E. Roman, "GNSS Services for Power grid," *1st SPARC Workshop, Space Threats and Critical Infrastructures: towards a common outlook,* Pisa, Italy, pp. 1-28, 26 March 2013.
[12] S. Wildermuth, K. Bohnert, H. Brändle, J.-M. Fourmigue, and D. Perrodin, "Growth and Characterization of Single Crystalline Bi4Ge3O12 Fibers for Electrooptic High Voltage Sensors," *Journal of Sensors,* vol. 2013, pp. 7, 2013.
[13] J. W. Stahlhut, G. T. Heydt, and E. Kyriakides, "Innovative Sensory Concepts for Power Systems," *38th North American Power Symposium (NAPS),* Carbondale, IL, pp. 397-404, 17-19 Sept. 2006.
[14] A. Phillips and L. van der Zel, *Sensor Technologies for a Smart Transmission System*, EPRI Wite Paper, Dec. 2009.
[15] X. Fang, S. Misra, G. Xue, and D. Yang, "Smart Grid - The New and Improved Power Grid: A Survey," *IEEE Communications Surveys & Tutorials,* vol. 14, no. 4, pp. 944-980, Oct 2012.
[16] SENTEC. "European market for electricity smart meters," Sept, 2013;[Online]: Available: www.sentec.co.uk/assets/download/471.
[17] EIA. "How many smart meters anre installed in the U.S. and who has them?," Sept, 2013;[Online]: Available: http://www.eia.gov/tools/faqs/faq.cfm?id=108&t=3.
[18] EPRI. "Distribution Systems," Sept., 2013;[Online]: Available: www.portfolio.epri.com/ProgramTab.aspx?sId=pdu&rId=265&pId=7644.
[19] G. L. Clark "Line Intelligence Feeds the Smart Grid," *T&D World Magazine*, Oct. 2010.
[20] J. W. Stahlhut, G. T. Heydt, and E. Kyriakides, "A Comparison of Local vs. Sensory, Input-Driven, Wide Area Reactive Power Control," *IEEE Power Engineering Society General Meeting,* pp. 1-7, 24-28 June 2007.
[21] M. Asprou and E. Kyriakides, "A constrained hybrid state estimator including pseudo flow measurements," *7th Mediterranean Conference and Exhibition on Power Generation, Transmission, Distribution and Energy Conversion (MedPower),* Agia Napa, Cyprus, pp. 1-6, 7-10 Nov. 2010 2010.
[22] B. Singh, N. Sharma, A. Tiwari, K. Verma, and S. Singh, "Applications of phasor measurement units (PMUs) in electric power system networks incorporated with FACTS controllers," *International Journal of Engineering, Science and Technology,* vol. 3, no. 3, pp. 64-82, March 2011.
[23] S. Chakrabarti and E. Kyriakides, "Optimal Placement of Phasor Measurement Units for Power System Observability," *IEEE Transactions on Power Systems,* vol. 23, no. 3, pp. 1433-1440, Aug. 2008.
[24] P. Palensky and D. Dietrich, "Demand Side Management: Demand Response, Intelligent Energy Systems, and Smart Loads," *IEEE Transactions on Industrial Informatics,* vol. 7, no. 3, pp. 381-388, Aug. 2011.
[25] J. De La Ree, V. Centeno, J. S. Thorp, and A. G. Phadke, "Synchronized Phasor Measurement Applications in Power Systems," *IEEE Transactions on Smart Grid,* vol. 1, no. 1, pp. 20-27, June 2010.
[26] J. C. H. Peng and N. K. C. Nair, "Adaptive sampling scheme for monitoring oscillations using Prony analysis," *IET Generation, Transmission & Distribution,* vol. 3, no. 12, pp. 1052-1060, Dec. 2009.
[27] P. Kundur, *Power System Stability and Control*: McGraw-Hill, 1994.
[28] M. Asprou, E. Kyriakides, and M. Albu, "The Effect of Instrument Transformer Accuracy Class on the WLS State Estimator Accuracy," *IEEE Power and Energy Society General meeting,* Vancouver, Canada, pp. 1-5, July 2013.
[29] P. D. Ray, R. Harnoor, and M. Hentea, "Smart power grid security: A unified risk management approach," *IEEE International Carnahan Conference on Security Technology (ICCST),* pp. 276-285, 5-8 Oct. 2010.

VII. BIOGRAPHIES

Irina Ciornei is with the KIOS Research Center for Intelligent Systems and Networks. She holds a PhD (2011) in Electrical and Computer Engineering from the University of Cyprus, and two MSc (2003) degrees in Energy and Environment form the University of Poitiers, France and from the Technical University of Iasi, Romania. Her research interests are in the area of research optimization techniques with application to power systems and smart grids ranging from computational intelligence algorithms such as GAs, PSO, NNs to stochastic dynamic programming. Other research interests cover smart cities from a business value perspective, integration of RES into the main grid, modeling and application of electrical devices in power systems.

Petros Mavroeidis was born in Athens, Greece in 1980. He holds an MEng and a PhD in Electrical and Computer Engineering awarded from the Aristotle University of Thessaloniki, Greece, in 2002 and 2010 respectively. He is also equipped with a BSc in Economic Sciences awarded by the National and Kapodistrian University of Athens, Greece in 2012. He has extensive laboratory experience both in conducting experiments and in analysing and interpreting experimental data. His research work includes air and surface discharges with an emphasis on composite insulation. Currently, he focuses on power systems monitoring and stability enhancement. Petros is a member of IEEE since 2001 (S'01, M'10) and a member of the Technical Chamber of Greece since 2003.

Georgia Pieri has received her Diploma in Electrical and Computer Engineering (Dipl – Ing) from the National Technical University of Athens (NTUA), Greece, in 2012. She is currently a Ph.D student in the Department of Electrical and Computer Engineering at University of Cyprus. She is also working as a researcher at the KIOS Research Center for Intelligent Systems and Networks. She has been a graduate student member of the IEEE since 2012. She is also a member of the Cyprus Scientific and Technical Chamber (ETEK). Her research interests include distribution system state estimation, power system operation and control, renewable energy resources, Distributed Energy Resources (DER), Microgrids and Smart Grids.

Elias Kyriakides received the B.Sc. degree from the Illinois Institute of Technology in Chicago, Illinois in 2000, and the M.Sc. and Ph.D. degrees from Arizona State University in Tempe, Arizona in 2001 and 2003 respectively, all in Electrical Engineering. He is currently an Assistant Professor in the Department of Electrical and Computer Engineering at the University of Cyprus, and a founding member of the KIOS Research Center for Intelligent Systems and Networks. He served as the Action Chair of the ESF-COST Action IC0806 "Intelligent Monitoring, Control, and Security of Critical Infrastructure Systems" (IntelliCIS) (2009-2013). His research interests include synchronized measurements in power systems, security and reliability of the power system network, optimization of power system operation techniques, and renewable energy sources.

2nd Conference on Power Options for the Eastern Mediterranean Region
07-08 October 2013, Nicosia, Cyprus (Paper No. POEM13/184)

A Power System Controlled Islanding Scheme for Emergency Control

Jairo Quirós-Tortós, *Student Member, IEEE*, and Vladimir Terzija, *Senior Member, IEEE*

***Abstract*--During major system disturbances, uncontrolled separation of the power system may take place, leading to further network stability degradation and likely a large-scale blackout. Intentional controlled islanding has been proposed as an effective approach to split the power system into several sustainable islands and prevent cascading outages. This paper proposes a novel methodology that determines suitable islanding solutions for minimal power imbalance or minimal power flow disruption while ensuring that only coherent generators are in each island. It also enables system operators to exclude any branch from islanding solutions, i.e. from its disconnection. In real applications, the actual power flow data and the prior-identification of the coherent groups of generators are required. The proposed methodology is illustrated using the IEEE 9-bus test system. Simulation results demonstrate the effectiveness and practicality of the proposed methodology to determine an islanding solution.**

***Index Terms*--Intentional controlled islanding, power flow disruption, power imbalance.**

I. Introduction

INTERCONNECTED power systems very often operate close to their stability limits [1] increasing the probability of cascading outages [2]. Recent blackouts across the world [3-6] highlighted the need to propose effective and efficient solutions to avoid the socio-economic consequences that cascading blackouts can cause [7].

Intentional Controlled Islanding (ICI) has been proposed as a last resort to attempt to save the power system when vulnerability analysis indicates that it is threatened by cascading outages [1], [7]. The islanding of a power system must be performed in a very limited timeframe [8-12] as system operators have only a few seconds to respond and attempt to save the power system. Thus, determining an islanding solution in real-time, i.e. quickly enough to ensure effective islanding within a limited timeframe, is an extremely complex analytical and practical problem [8], [9].

The objective of ICI methods is to determine the set of transmission lines that must be disconnected to create stable and sustainable islands [7]. When finding the solution, multiple constraints, such as generator coherency, load-generation balance, thermal limits, voltage and transient stability, must be considered [11]. Nevertheless, it would be impractical to attempt to find a solution including all of these; thus, only a set of selected constraints is usually taken into consideration when finding an islanding solution; therefore extra corrective measures [1], [7] are required in the post-islanding stage to retain the stability of the islands.

The existing ICI methods can be classified based on the objective function used. Two major classes are: *a*) minimal power imbalance or *b*) minimal power flow disruption. While methods for the former minimize the load-generation imbalance within the proposed islands, reducing the amount of load to be shed in the post-islanding stage [8], [9], methods for the latter minimize the change of the power flow pattern within the network following system islanding, reducing the possibility of overloading the branches in the created islands [11-13].

Overall, the existing methods have focused on solving the ICI problem for a single objective function, whilst the constraints are limited to ensure that only dynamically coherent generators are in each island [8-12]. For example, methods based on ordered binary decision diagrams (OBDDs) [8], [9], tracing power flows [14] and metaheuristic algorithms [15], [16] have been used to find islanding solutions for minimal power imbalance. Moreover, to determine an islanding solution for minimal power flow disruption, spectral clustering [10], [11] and multi-level kernel k-means algorithms [17] have been proposed.

Even though the existing ICI methods can determine suitable islanding solutions, these can only cope with a given single objective function. For example, spectral clustering algorithm cannot be used to find a solution for minimal power imbalance [11]. Hence, a more flexible method which allows system operators to change the objective function for different system scenarios is needed. This paper proposes a novel islanding methodology that is computationally efficient and can determine islanding solutions for any of the abovementioned objective functions while ensuring that only coherent generators are in each island. The methodology initially uses the topological characteristics of the electrical network to find "suitable islanding solutions", defined in this paper as solutions that split the power system into the given number of islands, while guaranteeing generator coherency. The optimal islanding solution is finally defined by computing either the power imbalance or the power flow disruption and the cutset with the minimum value is selected as the final solution.

The main advantage of the proposed methodology is its flexibility to cope with any objective function, allowing system operators to change this, based on their criteria and experience, while maintaining the efficiency of it. Moreover, it can provide various islanding solutions to prevent wide-area blackouts. The methodology demonstrates to be capable

This work was supported in part by The Office of Internationals Affairs and External Cooperation of The University of Costa Rica and the Engineering and Physical Science Research Council (EPSRC) in the U.K.

J. Quirós-Tortós and V. Terzija are with the School of Electrical & Electronic Engineering, The University of Manchester, Manchester, M13 9PL, U.K. (e-mail: jairoquirostortos@ieee.org, terzija@ieee.org).

of handling unexpected systems changes and to be able to constrain branches to be excluded from islanding solutions.

The proposed methodology is illustrated using the IEEE 9-bus test system and simulations are used to discuss in detail its benefits and limitations. This paper focuses on steady-state studies only and it is assumed that the coherent groups of generators are known in advance, e.g. obtained using existing algorithms [18], [19].

The paper is organized as follows. Section II presents the preliminaries and the proposed methodology to determine islanding solutions. Simulation studies using the IEEE 9-bus test system are presented in Section III. Finally, concluding remarks are provided in Section IV.

II. Proposed Methodology for Intentional Controlled Islanding

A. Preliminaries

An electrical power system with n buses and l branches (transmission lines and transformers) can naturally be represented as a graph $G = (V(G), E(G))$ [20]. The graph consists of a pair of sets $(V(G), E(G))$. When there is no scope of ambiguity, the letter G from graph theoretic symbols is omitted and V and E are used instead of $V(G)$ and $E(G)$. The elements of $V = \{v_1, v_2, \ldots, v_n\}$ are the nodes, or vertices, and the elements of $E \subset V \times V = \{e_1, e_2, \ldots, e_l\}$ are the edges, or links, in the graph G, respectively. The sets V and E represent the buses and branches of the power system, respectively. Due to the nature of power systems, the graph G can be assumed to be simple, i.e. no multiple edges and no loops are allowed.

If the edges have a direction associated with them, e.g. power flow direction, the graph is called *directed graph* or digraph, otherwise the graph is called *undirected graph*. For a digraph, the edge $e_k = (v_i, v_j) \in E$, $i, j = 1,2,\ldots,n$, is an ordered pair of vertices indicating that the edge e_k $k = 1,2,\ldots,l$, is incident to vertices v_i and v_j, where v_i and v_j are called the *tail* and the *head*, respectively. A similar definition can be drawn for undirected graphs by ignoring the direction of the edge, that is, $e_k = (v_i, v_j) = (v_j, v_i) \in E$, $i, j = 1,2,\ldots,n$.

Since the functional information about the system cannot be captured by the topological structure of the graph, we use weight factors associated with the edges. An *edge-weight* is a function $\omega: V \times V \rightarrow \mathbb{R}^{\geq 0}$ such that $w_k = \omega(e_k)$. To accommodate network losses, the value of w_k is calculated as follows.

$$w_k = \begin{cases} \dfrac{|P_{ij}| + |P_{ji}|}{2} & \text{if } e_{ij} \in E; \\ 0 & \text{otherwise.} \end{cases} \quad (1)$$

In (1), P_{ij} and P_{ji} represent the active power-flow in the branch from bus i to bus j, and from bus j to bus i, respectively.

B. Proposed Methodology

The ICI problem can be modeled as a constrained combinatorial optimization problem and its complexity increases exponentially with the size of the system [8], [9]. This combinatorial problem can be solved for the status of the branches (connected/disconnected) or the location of the buses in the islands (island number). The existing methods [8], [9] have attempted to solve the ICI problem for the status of the branches. Nevertheless, determining whether a branch requires to be disconnected or not to create islands is computationally more demanding as the number of branches is commonly larger than the number of buses ($l > n$).

Having identified the advantage of solving the combinatorial problem for the location of the buses, this paper aims to identify suitable islanding solution by defining the location of the buses first. This information then determines whether a branch needs to be disconnected or not. If a line connects two buses in the same island, this line should not be disconnected; however, the line must be disconnected if the buses are located in different islands.

This paper represents the results of the combinatorial problem in the matrix B. For a given number of islands, the matrix B is the $n \times c$ matrix, where c is the total number of combinations that can be obtained with the nodes (see example below). After solving this combinatorial problem, the methodology then provides a label (a number 1 or 2) to each node in G for each possible combination. For a given combination, the label of the node v_i indicates the number of the island at which that node should belong.

To illustrate the approach, consider the digraph shown in Fig. 1. The digraph will be split into two subgraphs G_1 and G_2. Mathematically, there are 16 possible combinations to split this graph into two subgraphs (see (2)). In other words, the matrix B will be of size 4×16. However, some combinations are not suitable, that is, they do not actually split the graph, or the number of subgraphs induced by the cutset is larger than two. We highlight in (2) the solutions that are not suitable. Furthermore, it must be noted that some combinations, e.g. $comb_2$ and $comb_{15}$ will produce the same cutset. The suitable cutsets can be defined by evaluating the *rank* of the graph induced by the corresponding cutset.

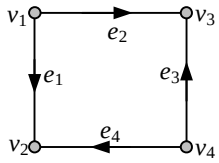

Fig. 1. Digraph with four nodes and four edges to exemplify the combinatorial problem to be solved.

$B^T =$

	v_1	v_2	v_3	v_4
$comb_1$	1	1	1	1
$comb_2$	1	1	1	2
$comb_3$	1	1	2	1
$comb_4$	1	1	2	2
$comb_5$	1	2	1	1
$comb_6$	1	2	1	2
$comb_7$	1	2	2	1
$comb_8$	1	2	2	2
$comb_9$	2	1	1	1
$comb_{10}$	2	1	1	2
$comb_{11}$	2	1	2	1
$comb_{12}$	2	1	2	2
$comb_{13}$	2	2	1	1
$comb_{14}$	2	2	1	2
$comb_{15}$	2	2	2	1
$comb_{16}$	2	2	2	2

(2)

Our methodology can also constrain certain nodes to

belong to a given island. For example, we assume that node v_1 must be allocated in the island 1 and node v_4 in the island 2. The nodes v_2 and v_3 can be assigned to any island. Since two islands can be created, four combinations can be obtained (3). Again, we evaluate whether a cutset is feasible or not by computing the *rank* of the resulting digraph. For this particular case, the four solutions are suitable in the sense that these split the graph into two subgraphs.

$B^T =$

	v_1	v_2	v_3	v_4
$comb_1$	1	1	1	2
$comb_2$	1	1	2	2
$comb_3$	1	2	1	2
$comb_4$	1	2	2	2

(3)

When the matrix B is computed, the cutset for each possible combination can be determined. These cutsets can be computed by using the incidence matrix M associated with the digraph [20]. The possible cutsets are represented in the matrix $C = B^T M$. The ik-th entry of C is -1, 0 or 1. The sign depends on the orientation of the edge, respect to the cutset orientation [20]:

$C =$

	e_1	e_2	e_3	e_4
$cutset_1$	0	0	1	1
$cutset_2$	0	-1	0	1
$cutset_3$	-1	0	1	0
$cutset_4$	-1	-1	0	0

(4)

As noticed in (4), if we implement the first combination, the lines represented by the edges e_3 and e_4 will have to be disconnected The matrix C is used to determine a solution for minimal power imbalance. To find a solution for minimal power flow disruption, we ignore the direction of the edges, and thus, we create the matrix C_U:

$C_U =$

	e_1	e_2	e_3	e_4
$cutset_1$	0	0	1	1
$cutset_2$	0	1	0	1
$cutset_3$	1	0	1	0
$cutset_4$	1	1	0	0

(5)

To identify the splitting strategy, we then compute a row vector w which contains in the k-th row the average power flow (1) in the branch k (represented by the edge e_k).

Then, by simply multiplying the matrix C, or C_U, by this row vector w, the power imbalance, or power flow disruption, induced by each cutset can be determined. Then, the islanding solution is determined by minimizing the value of the cut, i.e. min (*cut*), where the cut for minimal power imbalance (*cut* (MPI)) and the cut for minimal power flow disruption (*cut* (MPFD)) are computed as follows.

$$cut(MPI) = |C \cdot w|$$
$$cut(MPFD) = C_U \cdot w \quad (6)$$

III. Illustration of the Proposed Islanding Methodology

We illustrate the proposed methodology using the IEEE 9-bus test system [21]. Fig. 2 and Fig. 3 show the topology of the system and the equivalent digraph representation. The weight factors associated with the edges are obtained by computing the power flow solution using MATPOWER [22]. Note that the direction of the edges is based on the power flow results. Simulations are performed using MATLAB 7.10 (R2010a) [23] on an Intel® Core™ 2 Duo CPU E7500 @ 2.93 GHz, 4 GB of RAM.

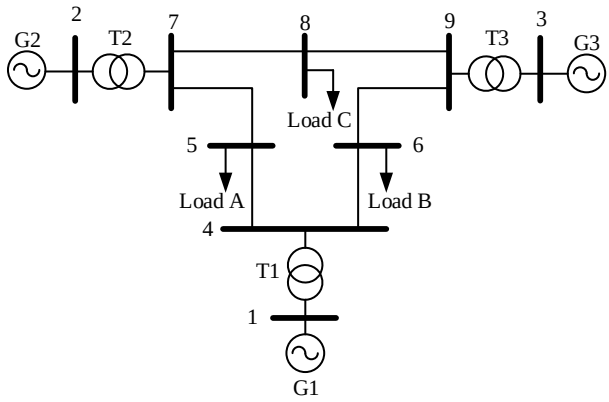

Fig. 2. Single line diagram of the IEEE 9-bus test system.

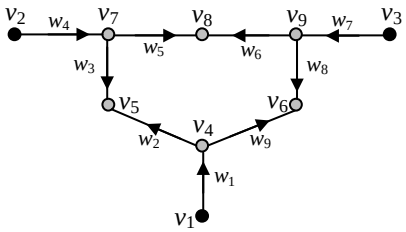

Fig. 3. Directed graph of the IEEE 9-bus test system.

As previously mentioned, the number of coherent groups of generators defines the number of islands to be created. In this paper, we assume that there exist two the coherent groups of generators: group 1: {G1} and group 2: {G2,G3}. Therefore, to compute the matrix B, we label the nodes v_1, v_2 and v_3 as 1, 2 and 2, respectively. Moreover, since bus 4 is connected to bus 1 through a transformer, an operational constraint is given to the edge e_1; thus, the node v_4 will be assigned to the same island as node v_1, i.e. the label associated with the node v_4 will be 1. Similar conclusion is drawn for nodes v_7 and v_9.

By implementing the previous operational constraints (transformer cannot be disconnected to create electrical islands), it can be noticed that the searching area is reduced from the entire power system to a single area which is shown in Fig. 4. Considering the case of two islands and the coherent groups of generators previously mentioned, it can be noticed that there are three nodes (v_5, v_6 and v_8) that can be assigned to Island 1 or 2.

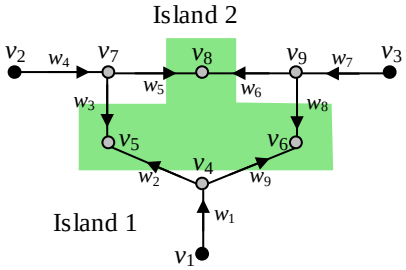

Fig. 4. Reduced searching area for the IEEE 9-bus test system

We compute matrix B and eight possible combinations are obtained (see (7)). We then use (7) and the incidence matrix M (not shown in this paper) to create the matrix C.

We then use the obtained matrix C to evaluate whether the cutsets included in C are suitable or not. We compute the

rank of the digraph induced by each cutset and we notice that the node v_8 must be labeled 2. Therefore, the matrix C with suitable islanding solutions is found to be as in (8). The area in the system with suitable solutions is shwon in Fig. 5.

$B^T =$

	v_1	v_2	v_3	v_4	v_5	v_6	v_7	v_8	v_9
$comb_1$	1	2	2	1	1	1	2	1	2
$comb_2$	1	2	2	1	1	1	2	2	2
$comb_3$	1	2	2	1	1	2	2	1	2
$comb_4$	1	2	2	1	1	2	2	2	2
$comb_5$	1	2	2	1	2	1	2	1	2
$comb_6$	1	2	2	1	2	1	2	2	2
$comb_7$	1	2	2	1	2	2	2	1	2
$comb_8$	1	2	2	1	2	2	2	2	2

(7)

$C =$

	e_1	e_2	e_3	e_4	e_5	e_6	e_7	e_8	e_9
$cutset_1$	0	0	1	0	0	0	0	1	0
$cutset_2$	0	0	1	0	0	0	0	0	-1
$cutset_3$	0	-1	0	0	0	0	0	1	0
$cutset_4$	0	-1	0	0	0	0	0	0	-1

(8)

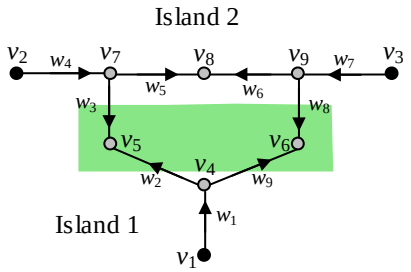

Fig. 5. Suitable searching area after reducing the number of possible cutsets by studying the rank of the digraph induced by the cutsets

We then compute the row vector w which contains in the k-th row the weight factor associated with the edge e_k:

$w =$

w_1	71.6
w_2	40.8
w_3	85.5
w_4	163.0
w_5	76.2
w_6	24.1
w_7	85.0
w_8	60.2
w_9	30.6

(9)

By using the vector w, we then compute the value of the *cut* for each cutset shown in (8). As mentioned above, the final islanding solution depends on the objective function.

We use the matrix C and the vector w for minimal power imbalance. Therefore, the value of the cut for minimal power imbalance for each possible cutset is:

$$cut(MPI) = \begin{bmatrix} 145.7 \\ 54.9 \\ 19.4 \\ 71.4 \end{bmatrix}. \quad (10)$$

As noticed, the first cutset, i.e. $\{e_3, e_8\}$, produces a load-generation imbalance of 145.7 MW in each island. We conclude from (10) that the optimal islanding solution is represented by the edges $\{e_2, e_8\}$ and it produces a power imbalance of 19.4 MW in each island.

The runtime of the methodology for this scenario was less than 0.5 ms. Fig. 6 shows the two electrical islands for minimal power imbalance.

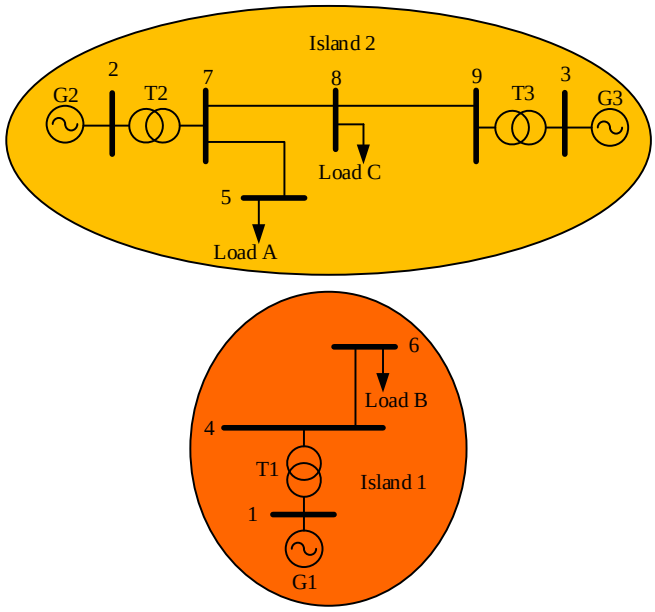

Fig. 6. Islanding solution for minimal power imbalance

We use the proposed methodology to determine the optimal islanding solution for minimal power flow disruption. We create the matrix C_U and use the vector w to compute the value of the *cut* for each cutset. The power flow disruption induced by each cutset is shwon (11).

The methodology finds that the cutset that produces minimal power flow disruption is across the edges $\{e_2, e_9\}$. After approximately 0.5 ms, the two islands created for minimal power flow disruption (see Fig. 7) are found to be represented by the subsets $V_1 = \{v_1, v_4\}$ and $V_2 = \{v_2, v_3, v_5, v_6, v_7, v_8, v_9\}$.

$$cut(MPFD) = \begin{bmatrix} 145.7 \\ 116.1 \\ 101.0 \\ 71.4 \end{bmatrix} \quad (11)$$

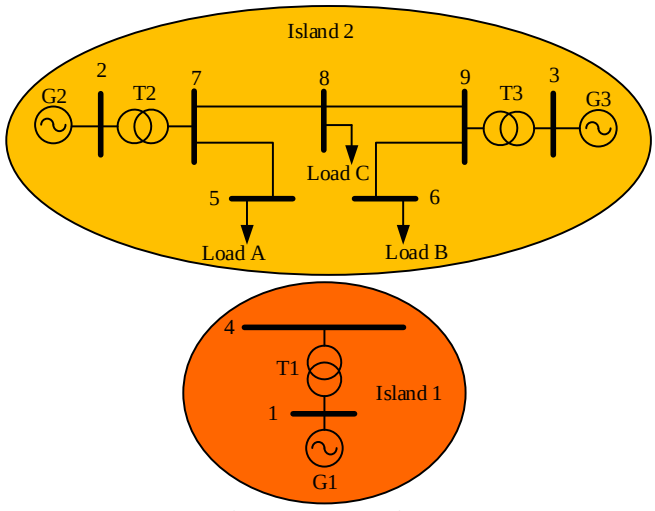

Fig. 7. Islanding solution for minimal power flow disruption

The simulations shown above demonstrate the effectiveness of the proposed methodology and clearly demonstrate that different objective functions can be used using our new approach. Moreover, they show that different objective function produces different islanding solution. The methodology is more flexible than the existing methods in

the sense that system operators can change the criteria to find islanding solution based on experience and operational features, for example, different load levels.

This paper presents results on a small test system and the results clearly demonstrate the efficiency and the potential benefits of the proposed methodology. Further studies in large-scale system must be carried out. In comparison to existing methods, we found that our approach identifies similar results. For example, the islanding solution shown in Fig. 6 is similar to that one obtained with the OBDD-based method [8], [9] and the solution shown in Fig. 7 is similar to the solution achieved using the method introduced in [11].

IV. Conclusions and Future Work

This paper presents a novel controlled islanding methodology that is computationally efficient and determines a set of suitable islanding solutions to be used for the purpose of intentional controlled islanding. In comparison to existing approaches, the methodology presents the significant advantage that it can find an optimal islanding solution for minimal power imbalance or minimal power flow disruption while ensuring that only coherent generators are in each island. This important advantage allows system operators to change the objective function based on system operating points and experience. The methodology considers the inherent topology of the network to find multiple islanding solutions. The optimal islanding solution, for any of the objective function, is then evaluated in the last step of the methodology. The proposed methodology was illustrated using the IEEE 9-bus test system. Simulations results demonstrate the efficiency and effectiveness of the new approach on small test systems. We are now planning to test and evaluate the performance of the new methodology on large-scale power systems.

V. Acknowledgment

The authors would like to thank the organizing committee of the Conference on the Power Options for the Eastern Mediterranean Region (POEM) for inviting us to present this paper. In particular, we would like to thank Dr. Elias Kyriakides for encouraging us to submit part of the research carried out at The University of Manchester.

VI. References

[1] G. Andersson, *et al.*, "Causes of the 2003 Major Grid Blackouts in North America and Europe, and Recommended Means to Improve System Dynamic Performance," *IEEE Trans. Power Syst.*, vol. 20, no. 4, p. 19221928, 2005.

[2] J. Quirós-Tortós, M. Panteli, V. Terzija, and P. Crossley, "On Evaluating the Performance of Intentional Controlled Islanding Schemes," presented at the IEEE PES General Meeting, Vancouver, 2013.

[3] U.S.-Canada Power System Outage Task Force, "Final Report on the August 14, 2003 Blackout in the United States and Canada: Causes and Recommendations," Apr. 2004.

[4] Swiss Federal Office of Energy (SFOE), "Report on the blackout in Italy on 28 September 2003," Nov. 2003.

[5] UCTE, "Final Report System Disturbance on 4 November 2006," Jan. 2007.

[6] "Report of the Enquiry Committee on Grid Disturbance in the Northern Region on 30th July 2012 and in Northern, Eastern & North-Eastern Region on 31st July 2012," Ministry of Power, New Delhi16th August 2012.

[7] P. Kundur and C. Taylor, "Blackout experiences and lessons, best practices for system dynamic performance, and the role of new technologies," IEEE Task Force Report2007.

[8] K. Sun, D. Zheng, and Q. Lu, "Splitting strategies for islanding operation of large-scale power systems using OBDD-based methods," *IEEE Trans. Power Syst.*, vol. 18, no. 2, pp. 912-923, May 2003.

[9] Q. Zhao, D. Zheng, J. Ma, and Q. Lu, "A study of system splitting strategies for island operation of power system: A two-phase method based on OBDDs," *IEEE Trans. Power Syst.*, vol. 18, no. 4, pp. 1556-1565, Nov. 2003.

[10] L. Hao, G.W. Rosenwald, J. Jung, and C.C. Liu, "Strategic power infrastructure defense," *Proceedings of the IEEE*, vol. 93, no. 5, pp. 918-933, May 2005.

[11] L. Ding, F. Gonzalez-Longatt, P. Wall, and V. Terzija, "Two-step spectral clustering controlled islanding algorithm," *IEEE Trans. Power Syst.*, vol. 28, no. 1, pp. 75-84, Feb. 2013.

[12] J. Quiros-Tortos and V. Terzija, "Controlled Islanding Strategy Considering Power System Restoration Constraints," in *Proceedings of the IEEE PES General Meeting*, San Diego, 2012, pp. 1-8.

[13] V.E. Henner, "A network separation scheme for emergency control," *Int. J. Electr. Power Energy Syst.*, vol. 2, no. 2, pp. 109–114, Apr. 1980.

[14] C. Wang, *et al.*, "A novel real-time searching method for power system splitting boundary," *IEEE Trans. Power Syst.*, vol. 25, no. 4, pp. 1902-1909 Nov. 2010.

[15] L. Liu, W. Liu, D.A. Cartes, and I.Y. Chung, "Slow coherency and Angle Modulated Particle Swarm Optimization based islanding of large-scale power systems," *Advanced Engineering Informatics*, vol. 23, pp. 45-56, 2009.

[16] M.R. Aghamohammadi and A. Shahmohammadi, "Intentional islanding using a new algorithm based on ant search mechanism," *Int. J. Electr. Power Energy Syst.*, vol. 35, no. 1, pp. 138–147, Feb. 2012.

[17] A. Peiravi and R. Ildarabadi, "A fast algorithm for intentional islanding of power systems using the multilevel kernel k-means approach," *J. of Applied Sciences*, vol. 9, no. 12, pp. 2247-2255, 2009.

[18] M. Jonsson, M. Begovic, and J. Daalder, "A new method suitable for real-time generator coherency determination," *IEEE Trans. Power Syst.*, vol. 19, no. 3, pp. 1473-1482, Aug. 2004.

[19] M.A.M. Ariff and B.C. Pal, "Coherency identification in interconnected power system—an independent component analysis approach," *IEEE Trans. Power Syst.*, vol. 28, 2, May 2013.

[20] W.K. Chen, *Graph theory and its engineering applications* vol. Vol. 5,. Singapore: World Scientific Publishing, 1997.

[21] P.W. Sauer and M.A. Pai, *Power System Dynamic and Stability*. New Jersey: Prentice Hall, 1998.

[22] R.D. Zimmerman, C.E. Murillo-Sánchez, and R.J. Thomas, "MATPOWER: Steady-state operations, planning, and analysis tools for power systems research and education," *IEEE Trans. Power Syst.*, vol. 26, no. 1, pp. 12-19, Feb. 2011.

[23] MATLAB R2010a: Natick, Massachusetts: The MathWorks Inc., 2010.

VII. Biographies

Jairo H. Quirós Tortós (S'08) was born in Limón, Costa Rica. He obtained the B.Sc. and Licentiate degree with honours in Electrical Engineering from the University of Costa Rica, San Pedro, Costa Rica in 2008 and 2009 respectively. Currently he is a Ph.D. student at The University of Manchester, working on power system restoration and intentional controlled islanding for power system. His main research interests are application of intelligent methods to power system restoration, and intentional controlled islanding, development of solutions for future Smart Transmission Grids power system monitoring, protection and control, and power system dynamics.

Vladimir Terzija (M'95, SM'2000) is the EPSRC Chair Professor in Power System Engineering in the School of Electrical and Electronic Engineering, The University of Manchester, where he has been since 2006. From 1997 to 1999, he was an Assistant Professor at the University of Belgrade. In 1999, he was awarded a prestigious Humboldt Research Fellowship. From 2000 to 2006, he was with ABB AG, Germany, working as an expert for switchgear and distribution automation. His main research interests are application of intelligent methods to power system monitoring, control, and protection, switchgear and fast transient processes, as well as DSP applications in power systems.

2nd Conference on Power Options for the Eastern Mediterranean Region
07-08 October 2013, Nicosia, Cyprus (Paper No. POEM13/185)

Measurement Data Aggregation in Power Systems – Challenges and Opportunities

Ana Maria Dumitrescu, Mihai Calin, Mihaela M. Albu

***Abstract*— Despite the increased use of distributed energy resources and of the active distribution networks, power systems are still modeled as operating in steady state at quasi-constant frequency, with bulk generation and constant power loads. For achieving a real time control, enabling a higher efficiency of energy transfer, a detailed model is required together with associated algorithms for information retrieval. Measurements are presently able to give insight to such details, communication channels are in place but the information has to be structured in a new way. Presently there are in use aggregation algorithms inherited from power quality standards like the IEC 61000-4-30 set. A discussion of the time- and space- aggregation is proposed in the paper, based on an analysis performed on voltages and frequency measurements; recommendations for the data aggregation algorithms are given for quantities which are not presently commonly considered for power systems monitoring. Data delivered by PMUs with a reporting rate of 50 frames per second is used to highlight the effect of aggregation algorithms.**

***Index Terms* – synchronized measurements, power quality, phasor measurement unit, smart metering, root mean square, data aggregation.**

I. Nomenclature

AMI - Advance Metering Infrastructure
AMR - Automatic meter reading
CT - Current transformer
DER - Distributed Energy Resources
DMS - Data Management System
DSM- Demand Side Management
DR –Demand Response
DSO – Distribution System Operator
EMS - Energy Management System
GIS - Geographic Information System
IED - Intelligent Electronic Device
ICT - Information and Communication Technology
LV- low voltage
LAN - Local Area Network
MA – moving average
MV- medium voltage
MDMS - Meter Data Management System
PDC - Phasor Data Concentrators
PMU Phasor Measurement Unit
PQ - Power Quality
PLC - Power Line Communication
RMS – Root Mean Square
ROCOF - Rate of Change of Frequency
SCADA - Supervisory Control and Data Acquisition
SM - Smart Metering
TSO - Transmission System Operator
VT – Voltage transformer
WAMCS - Wide Area Monitoring and Control System
WAN - Wide Area Network
WASA - Wide Area Situational Awareness
WAMS – Wide Area Measurement System

This work was supported by the Exploratory research project PN-II-ID-PCE-2011-3-0693 (Romania), Active Distribution Grids. Model Identification and Analysis Using Synchronized Measurements – ActiveDGModel and by "The use of telecommunications and GPS technology for the real-time wide-area monitoring and control of power systems", Project financed by Cyprus Research Promotion Foundation.

A.M. Dumitrescu is with Electrical Engineering Faculty, Politehnica University of Bucharest, Romania (Email: anamaria.dumitrescu@upb.ro)

M. Calin is PhD student at Politehnica University of Bucharest, Romania (Email: calinmihai@ieee.org)

M. Albu is with Electrical Engineering Faculty, Politehnica University of Bucharest, Romania (Email: albu@ieee.org)

II. Introduction

THE presently emerging power systems – known mostly as intrinsically included in the smart grids paradigm –reflect the synthesis of an unique technological evolution: on one side, the increased complexity of the active distribution grids are demanding the use of more elaborate models of the grid infrastructure: intermittent generation, prosumer - type loads with patterns highly variable in time (constant impedance, constant active power, profiled reactive power), and mobile storage units require new control algorithms, which have to rely on different models for the energy transfer itself: a relevant example is given by hybrid microgrids. On the other side, the evolution of the ICT-enabled solutions had a direct impact on both the customers and signal-processing techniques embedded in commercially available data acquisition systems.

A first consequence of the evolution of the grid infrastructure is the reduction in available inertia, mainly due to the an increased share in the generation mix of the power electronics interfaced generation units and to the dominance of the rectifier-based loads connected at ever-increasing voltage levels. This translates into one order of magnitude lower constant times associated to power transfer in both steady-state and dynamic operation: from seconds to tens of milliseconds.

A second consequence of the ICT-enabled power system infrastructure is the availability, at ever-reducing costs, of digital measurement equipment, designed for sampling rates of at least 10 kHz per channel, including synchronous sampling for multiple channels and high accuracy of analogue-to-digital conversion. Moreover, the applications based on the existing GIS systems enable the deployment of synchronized measurements, for the first time becoming possible accurate angle measurements (and not only estimation) over large geographical areas (WAMS and WAMCS). Apparently these solutions have a convergent effect towards meeting the previously announced

requirements of "zooming" the power systems signals on the time axis.

A third contribution to this apparently convergent technology evolution is given by the customers themselves, who cannot avoid a constantly re-invented world shaped in time by communication (with a daily life enabled by ever lower time constants) and in space by the information ubiquity (revolutionized by cloud computing and big data storage).

Simultaneously one can observe a lack of compatibility between the three above-mentioned phenomena and the daily practice in power engineering, which is framed by standards devoted to the classical power system. Some initiatives consider useful to analyze in greater detail the energy transfer at both LV and MV networks. An example is the "translation" of monitoring and control strategies developed for the transmission systems toward lower voltage levels. State estimation is one of the main applications that can be used in distribution networks, for providing the best estimation of the voltage magnitude and phase for all network nodes based on the network topology information, the network parameters, and available measurement data. Further, a specific task of distribution networks control is the power flow management providing direct benefit on deferral of investments due to network congestions. The increase use of smart metering and of the associated services like demand response (DR) and demand side management (DSM) contributes to the development of a quasi-real time responsiveness scheme for monitoring and control of the distribution networks. It is expected that features like automatic alarming of LV network outages will improve network reliability.

However, monitoring the power transfer in LV and MV networks is mainly done in the power quality (PQ) framework. In this case, monitoring (and control) is to be equally determined by the quality of measurement system and of the measurement results processing (acting as information /coding /retrieval). Standards [1] are silently assuming steady state operation with nearly constant frequency. The upper limitations for deviations of frequency and voltage (rms values) are applied to values obtained from a successive aggregation of measurement data obtained from long-term observation. A compromise between the end-user needs for information and the amount of data resulting from averaging over one period of the observed quantities waveforms is given by data aggregation over the time axis.

Meter Data Management (MDM) refers to a key component in the Smart Grid infrastructure that is in the process of being evolved and adopted by utility companies. An MDM system performs long-term data storage and management for the vast quantities of data that are now being delivered by smart metering systems. This data consists primarily of usage data and events that are imported from the head end servers that manage the data collection in Advanced Metering Infrastructure (AMI) or Automatic meter reading (AMR) systems. An AMI is the infrastructure relating to electric metering and communications, including meters capable of two-way communication. Currently, utilities are focusing on developing AMI to implement residential demand response and to serve as the main mechanism for implementing dynamic pricing. It consists of the communications hardware and software and associated system and data management software (DMS) that creates a two-way network between advanced meters and utility business systems, enabling collection and distribution of information to customers and other parties, such as competitive retail suppliers or the utility itself.

A direct consequence of new operational model of the distribution grids is a fast grow of the amount of data transferred among the stakeholders, and an analysis of the appropriate compression rate able to ensure the transfer of needed information is required. One method to decrease the amount of transferred data is its aggregation, which in PQ framework is defined as a time- averaging algorithm recommended in power quality – related measurement standards for data concentration [2].

III. Aggregation in Time

A first example of formalizing the information concentrators in power systems – in the sense of data compression -is given by the use of rms values for describing quantities with [quasi-] sinusoidal variation (currents, voltages, active and reactive powers):

$$X = \sqrt{\frac{1}{T}\int_{t_0}^{t_0+T} x^2(t)dt} \tag{1}$$

where $x(t)$ is the periodical (period T) quantity mapped into a single point X, its rms value. This method has been successfully applied by analogue voltage and current measurements – using the so-called true-rms measurement equipment – and then implemented on the numerical signals obtained after analog-to-digital conversion in modern digital measurement systems. However, the rms algorithms can be implemented in either synchronous way or using a moving window with pre-defined width (usually half of the fundamental period or one period). The algorithm of computing rms values on non-overlapping windows with fixed length (N samples) is a powerful compression method, with compression rate equal to the sampling rate used by the A/D conversion (today 10^4 Hz). In [3] it is shown that such algorithms are equivalent to low-pass filtering and more information on the actual implementation is required in cases where the response time of the monitoring process is less than tens of ms. In case of moving average algorithms for which the window advances with N_s samples, the compression rate becomes $f_s/(f_s/N_s)=N_s$ and in extreme case ($N_s=1$) the algorithm is losing the capability of data aggregation.

Further, the numerical signal (the rms values) needs to be compressed with as little loss of useful information as possible. In the PQ framework, where the energy transfer is assumed to follow a quasi-stationary regime, there are standardized [1, 2] several schemes of aggregation in time; they can be applied to two signal classes and for several levels of quality of the signal analysis: class A, class B and class S.

The first scheme is applied to voltages and currents (and extended also to voltage asymmetry index) – quantities for which the traditional description is done by the rms value.

According to [1]: "The basic measurement time interval for parameter magnitudes (supply voltage, harmonics, interharmonics and unbalance) shall be a 10-cycle time

interval for 50 Hz power system. Measurement time intervals are aggregated over 3 different time intervals". The aggregation time intervals are 3s (150 cycles), 10min, and 2h (Fig.1). The aggregation on level L_p+1 uses a quadratic norm of the vector containing the M_{Lp} values computed in the precedent aggregation step (L_p):

$$X^{A}_{(L_P+1)} = \sqrt{\frac{\sum_{k=1}^{M_{L_P}} \left(X^{2}_{(L_P)}\right)_k}{M_{L_P}}} \qquad (2)$$

where M_{Lp}= 10; 15; 200; 12 for the 200ms; 3s; 10min and 2h aggregation intervals respectively [4].

It is supposed that information is carried by the sampled signal (i.e. appropriate anti-aliasing filters and "perfect" measurements are available, adequate to the power system infrastructure, for which also a fully adequate model is known).

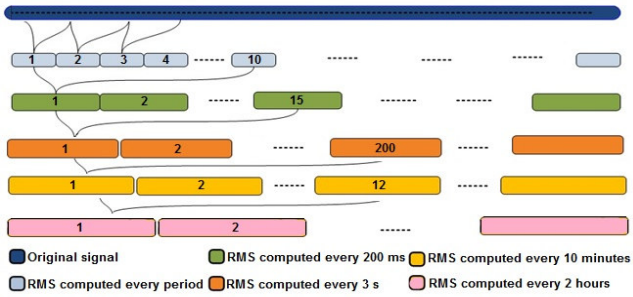

Fig. 1. Aggregation process as proposed in [1] for voltages, currents, voltage asymmetry

This aggregation process can be described mathematically by an additional filtering performed on the results of the rms calculation. It is interesting to observe that, if time reference is available, performing an *s-rms* algorithms followed by the time aggregation is equivalent to performing a moving –average rms algorithm (*m-rms*) followed by an decimation filtering (factor M_{Lp}), while the first option is providing a higher compression rate, by a factor (f_s/N_s).

Fig. 2 shows the amplitude characteristics of decimation filters applied to the rms aggregation proposed in [1].

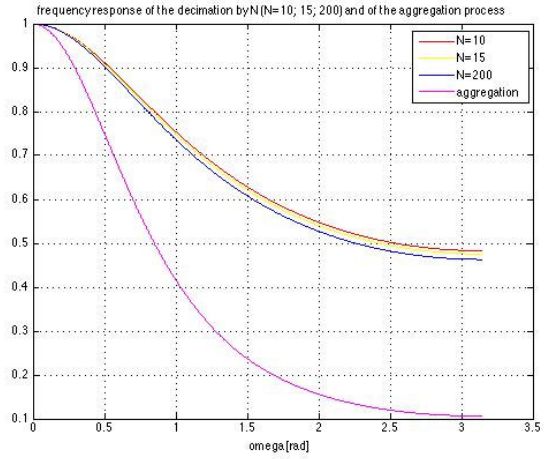

Fig. 2. Amplitude response of individual decimation filters used in the aggregation process and the response of the aggregation process (level 4)

For frequency it is proposed a different aggregation algorithm. For Class A instruments, there are only two levels recommended, corresponding to base intervals of 200ms and 10s. Although the frequency, like rms-values of voltages and currents or asymmetry factors has only *positive values*, a simple averaging algorithm is proposed. The reasons might lie in the paradigm of slow-variations of frequency (as this algorithm can run faster but the equivalent filter has a longer time response than the rms-norm, as one can see form Fig.3).

$$f_{(L_P+1)} = \frac{M_{L_P}}{\sum_{k=1}^{M_{L_P}} T_k^{L_P}} \qquad (3)$$

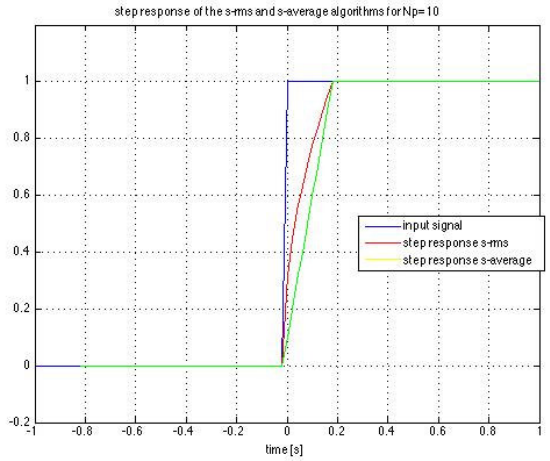

Fig. 3. Step response of the s-rms and the s-average filters used in the aggregation process proposed in [1]

Fig. 4 b shows the results of successive aggregation in time for frequency signal monitored in a Romanian DSO installation (Fig. 4a) and for which several aggregation algorithms have been applied [5].

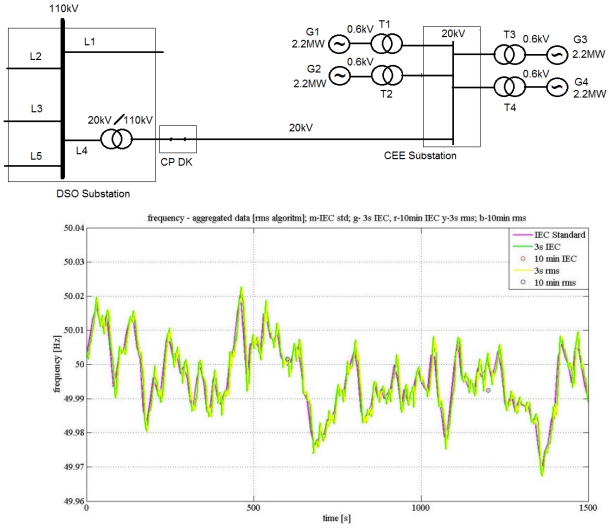

Fig. 4. a) MV distribution system used as test bench - single-phase equivalent diagram; b) Frequency variation in Babadag - aggregation results using the IEC and rms -averaging algorithm for 3s and 10 min [5]

Also, it is worth to mention that, although the information carried by the rate of change of frequency (ROCOF) signal is more and more useful in grid-control algorithms, there are no guidelines related to the time-aggregation. Considering that ROCOF can have both positive and negative values, an rms- time aggregation algorithm might be useful. However,

a simple averaging of the absolute values is less computationally complex and still is able to characterize the grid supply. Figure 5 shows the results of the aggregation process applied for ROCOF in the same case as Fig. 4.

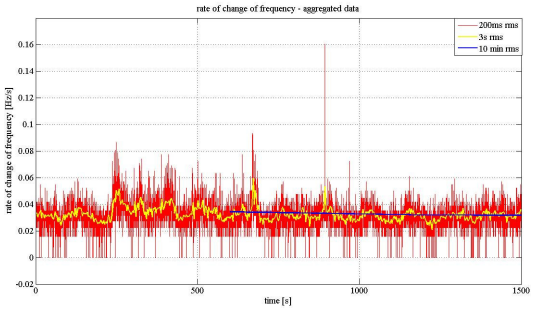

Fig. 5. Rate of change of frequency variation - aggregation results for 200ms, 3s, 10 min [5]

IV. Aggregation in Space

In the Smart Grid world, an "Aggregator" is related to the services provided for either DSOs or TSO and integrating the individual prosumers activity in terms of electrical energy exchanged within the Aggregator entity network limits. It relies on Energy Management Services (EMS), it uses dedicated communication protocols with various types of infrastructure (PLC, LAN, WAN etc. [6]).

However, with the advent of GIS-based measurement set-ups, aggregation in space denotes an algorithm to encode network information provided by sensors located in various nodes of a network for which accurate models are available. A geographic information system (GIS) is a system designed to capture, store, manipulate, analyze, manage, and present all types of geographically referenced data. In the simplest terms, GIS is the merging of cartography, statistical analysis, and database technology. Applications based on measurement information retrieved from several nodes of the system need a synchronization protocol. The required clock precision is dependent on the application, the standards maturity and available technology. Presently, SCADA is the reference for the space-aggregated measurements provided by IEDs. However, emerging control algorithms (like the ones included in WAMCS - Wide Area Monitoring and Control System) need higher level of synchronization of measurements, which is achieved by the use of Phasor Measurement Units (PMUs), integrated in a so-called Wide Area Measurement System (WAMS). Moreover, an emerging field is Wide Area Situational Awareness (WASA), consisting in monitoring and display of power-system components and performance across interconnections and over large geographic areas in near real-time. The goals of situational awareness are to understand and ultimately optimize the management of power-network components, behavior and performance, as well as to anticipate, prevent, or respond to problems before disruptions can arise.

WAMS can provide synchronized and time-tagged voltage and current phasor measurements to any protection, control, or monitoring function that requires measurements taken from several locations, whose phase angles are measured against a common, system wide reference. This is an extension of simple phasor measurements, commonly made with respect to a local reference. Present day implementations of many protection, control, or monitoring functions need access to the phase angles between local and remote measurements.

WAMS delivers information on the state of the power system timely and accurately. Newly defined PMU requirements [7] makes possible that WAMS provides synchronized observation of the dynamics of the power system which helps to manage the power system in a more efficient and responsive way and support the application of wide area control and protection schemes.

From practical point of view, data from the PMUs are collected with the help of a Phasor Data Concentrator (PDC). State Estimation programs based on phasors require all Phasor sources to be synchronized. In such scenario, it is PDC's responsibility (Fig. 6) to provide phasor data aligned to the same time-tag. These data can then be appended to the most updated real-time SCADA data.

This SCADA data time skew is a big problem for State Estimation programs based on data provided by Phasor sources since, due to the fact that phasors rotate at a rate that is proportional to the frequency deviation from nominal, this time skew will lead to phase-angle differences which are not real and useless in any case.

For the State Estimation point of view, to accurately align the phasor samples into an output snapshot is more critical than to provide data snapshots at a really high frequency. Due to that, it appears useless for the PMUs to transmit phasor data at reporting frequencies higher than ten frames per second for State Estimation purposes, if this data has to be correlated with SCADA-information. In the same way, the highest PDC output reporting frequency to be considered for monitoring purposes would be one frame per second. The PDC receives data streams from PMUs and other PDCs and correlates them in real-time into a single data stream that is locally stored and transmitted to the SCADA/EMS and to another PDC, if required.

As long as all Phasor sources reporting rates are fixed and equal to each other, all measurement sets obtained from every input stream could be exactly correlated on time since all measurement samples are equally time-tagged according to C37.118 standards [7-8].

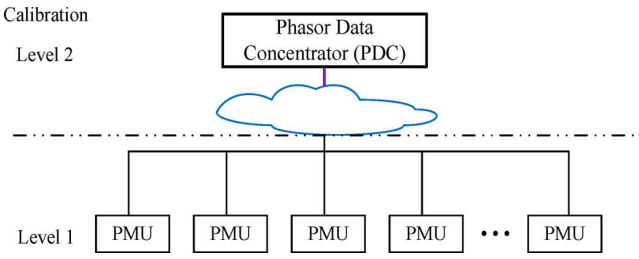

Fig. 6. Architecture of PDC Systems

V. Dual Aggregation

VI. Today, state estimations run typically every 2 -3 minutes and they take the most updated data registered in the SCADA System which usually update every 4 seconds. A good model of the dual aggregation is given by synchronized measurements. Such a platform encompasses multiple mobile PMUs from different vendors, full control over the measurement chain and its associated uncertainties,

a reliable communication infrastructure, and a data hub (PDC) as the underlying layer for concentrating the data and the environment for extracting, managing and processing the data. In order to have control over the measurement chain and its associated uncertainties, detailed information on the instrument transformers, rated voltages and currents of the monitored element has to be provided. In addition, a communication infrastructure independent from that of the substations has usually to be put in place, concentrating the synchrophasor data into a central server. For example, in [9] is described the set-up dedicated to near-real time monitoring of an active distribution network in Romania. The communication layer makes use of the extensive 3G-coverage area and is secured at three different levels: authentication through certificates, encryption and firewalling. Another unique feature of the architecture is that the PMUs do not have public IPs, therefore minimizing the number of possible backdoor entries into the system. After the PMU measurements are transmitted to the PDC according to the IEEE C37.118 standard [8], data are extracted from the PDC through a Java EE6 application. This enhances the PDC with additional functionality, like including information related to the CT and VT maximal uncertainty, while keeping the data processing layer separate from the actual PDC, therefore maintaining its level of reliability. Examples of features of the application are keeping track of PMU deployments and the technical details of their connection to the grid, defining customized data extraction queries for particular power system applications, time alignment and .CSV extraction for an easy post-processing experience and automatically filtering out the unnecessary data for storage space optimization. For example, typical data size is 17MB for 13min of registrations from one PMU in the "Basic" mode (50 frames/sec) and 2 GB for a 20 hours monitoring. This platform has been tested against five simultaneous connections extracting data from three different geographical locations, but the system is scalable for many more connections, as the code has been implemented according to the robust enterprise Java EE 6 Standards, aiming for optimized interactions between the business logic and persistence layers, concurrent access, transaction management, security, etc. Such an environment can be seen as a complex coding application (in space and time) for which a minimal standardization effort is required. PDC-related standardization (space-related data aggregation) is on-going [12], while for time aggregation only the PQ algorithms are standardized.

VII. Conclusions

If we term *adequacy* the ability of an electric power system to supply the aggregate electric power and energy required by the customers, under steady-state conditions, then the associated models of energy transfer have to be adequate as well. A measure of adequacy is obtained only by appropriate monitoring. The level of detail is limited by technical constraints given by the control algorithms. In this paper a discussion of the existing recommendations and standards related to measurement data aggregation in time and in space is presented, using as information reference the PMUs- based synchronized measurement systems. The PQ-framed aggregation algorithms have to be extended for achieving better information compression rates while preserving the ability to reflect the relevant phenomena in power systems.

VIII. References

[1] IEC 61000-4-30 ed2.0, Electromagnetic compatibility (EMC) Part 4-30: Testing and measurement techniques - Power quality measurement methods, 2008

[2] EN50160 - Voltage characteristics of electricity supplied by public distribution systems, 1999

[3] Mihaela M. Albu, G.T. Heydt, On the Use of RMS Values in Power Quality Assessment, IEEE Transactions on Power Delivery, vol. 18, nr. 4, Oct. 2003, pp.1586-1588

[4] Mihai Calin, Ana Maria Dumitrescu, Markos Asprou, Elias Kyriakides, Mihaela Albu, **2013**, Measurement Data Aggregation for Active Distribution Networks, *Proc. of IEEE Applied Measurements for Power Systems AMPS2013, Aachen*, 25-27 Sept. 2013

[5] Mihai Călin**,** Ana-Maria Dumitrescu**,** *„Stationarity Hypothesis in Power Systems Data Aggregation. Verification Algorithm"*, Proceeding of ATEE 2013, Bucharest, Romania, May, 2013, ISBN: 978-1-4673-5978-8

[6] S. Renner, M. Albu, s.a., European Smart Metering Landscape Report, SMART REGIONS project: Promoting smart metering best practices in EU. Online: http://www.smartregions.net /default.asp?SivuID=26927

[7] C37.118.1-2011 - IEEE Standard for Synchrophasor Measurements for Power Systems

[8] C37.118.2-2011 - IEEE Standard for Synchrophasor Data Transfer for Power Systems

[9] Mihaela Albu, *Extending OpenPDC into a versatile Data Concentrator for synchronized measurements*, presented (co-author Alexandru Nechifor) at Wide View - The use of telecommunications and GPS technology for the real-time wide-area monitoring and control of power systems Seminar, 11-16 March 2013, Nicosia, Cyprus.

[10] Ana-Maria Dumitrescu, Mihaela Albu, "Opportunities for updating the power quality standards following the large scale availability of synchronised measurements", FP7 Stargrid Workshop, Parliament Palace, Bucharest, 11 Sept. 2013

[11] FP 7 European Project – Pan European Grid Advanced Simulation and State Estimation – PEGASE "D6.3 –Part 1.2 Demonstration report for Phasor Data Concentrator Prototype"- online http://www.fp7-pegase.com/pdf_ddl/D6.3_part1.2.pdf.

[12] IEEE Std C37.242™-2013, IEEE Guide for Synchronization, Calibration, Testing, and Installation of Phasor Measurement Units (PMUs) for Power System Protection and Control

IX. Biographies

Ana-Maria Dumitrescu was born in Bucharest, Romania in August 1979. She graduated as an engineer in Electrical Engineering in 2003 and received the Ph.D. title from the Politehnica University of Bucharest in 2012. She started as Teaching Assistant at the Electrical Machines, Materials and Drives Department of the same University in 2005, becoming lecturer in 2013. Her area of interest includes: Control strategies, power quality, power electronics, electrical measurements. Ana-Maria is an IEEE member since 2009 and Vice-Chair of Romanian Chapter of Instrumentation and Measurements Society since 2013.

Mihai Calin was born in 1986, in Romania. He received the engineering degree and MSc degree in electrical engineering from the Politehnica University of Bucharest in 2009 and 2011, respectively. Since September 2009 he is member of MicroDERLab, being actively involved in several research projects. One task consisted in the development of a Matlab based algorithm for controlling a smart inverter system in order to emulate a Synchronous Generator, which also included extensive experimental work. Since March 2011, he is a PhD student at UPB and benefits from an EC-funded scholarship.

Mihaela M. Albu (M'96, SM'07) is from Craiova, Romania. She graduated from Politehnica University of Bucharest in 1987 and holds the Ph.D. degree (1998) from the same university. Since 2002 she is a Professor of Electrical Engineering and head of the MicroDERLab Group at UPB. Her research interests include instrumentation for power grids, active distribution networks, DC grids, power quality and remote experimentation embedded within on-line laboratories. Dr. Albu was spending a leave at Arizona State University as a Fulbright Fellow 2002 – 2003 and in 2010.

2nd Conference on Power Options for the Eastern Mediterranean Region
07-08 October 2013, Nicosia, Cyprus (Paper No. POEM13/186)

Dynamic Fault Studies of an Offshore Four-Terminal VSC-HVDC Grid Utilizing Protection Means Through AC/DC Circuit Breakers

Melios Hadjikypris, *Student Member*, *IEEE*
Department of Electrical Energy and Power Systems
The University of Manchester
Manchester, United Kingdom
Melios.Hadjikypris@postgrad.manchester.ac.uk

Vladimir Terzija, *Senior Member*, *IEEE*
Department of Electrical Energy and Power Systems
The University of Manchester
Manchester, United Kingdom
Vladimir.Terzija@manchester.ac.uk

***Abstract*—The concept of utilization of multi-terminal DC grids is a promising solution for integrating distant renewable energy sources and offshore wind farms into onshore AC networks. Protection of such networks is one of key factors ensuring their reliability and continuity of service. This paper addresses the dynamic behavior and sensitivity of a typical multi-terminal DC grid under faulty conditions, observing the severe impacts these could have on the entire hybrid AC-DC system. Protection measures will be introduced in the form of DC circuit breakers (CBs) to isolate the faults and recover system's normal operation. The study concludes the feasibility in using DC-CBs in a multi-terminal VSC-HVDC network serving as fault protection and stability recovery tool when DC-CBs are located in an optimally distributed way. The simulation work depicting the various scenarios has been performed using DigSILENT PowerFactory environment.**

***Index Terms*--DC Circuit Breakers, DC Fault, DC Protection, MTDC, VSC-HVDC**

I. INTRODUCTION

High Voltage Direct Current (HVDC) technology has proved to be an efficient, cost effective and reliable way of transmitting electrical power over long distances as compared to the classic and traditional AC transmission [1]. Especially the use of Voltage Source Converter (VSC) based HVDC has provided a number of benefits compared to the classical Current Source Converter (CSC) HVDC, in terms of enhanced flexibility in independent control of active and reactive power [2].

Up to date, several installations of HVDC transmissions have been installed world-world [1], [3], utilizing both VSC and CSC technologies. However, the vast majority of them concerns point to point transmissions. A few years back, the first Multi-Terminal DC (MTDC) grid configurations started to come into light, and it mainly targeted the reinforcement of national networks [4], [5] and, less frequently, formed power sharing platforms between countries such as the Sardinia-Corsica-Italy (SACOI) connection [6].

Due to the significant economic and environmental benefits that MTDC grids have to offer, a constant interest started to grow towards the expansion of these networks aiming the integration of distant renewable energy sources, such as offshore wind farms to inland AC grids. Since then, a considerable amount of studies have been undertaken addressing technical issues regarding the operation and control of MTDC systems utilizing VSC technology. These were mostly focused for an economic and efficient importation of wind power into onshore power systems [7]-[12].

Protection measures however, securing the combined AC/DC systems from faults and disturbances forms an important system, highly affecting the smooth and robust operation of the overall network. Some initial studies have been conducted concerning DC protection in MTDC grids [13]-[15]. The most recent ones concentrate on the location and isolation of DC faults relying on AC-CBs and fast DC switches [15]. However, this methodology requires temporal system unavailability since fault clearance heavily depends on functioning of AC-side circuit breakers, which sets the entire DC network out of service. This short gap in system's availability could have severe consequences on the overall network, as well as the interconnected sub-grids. This is especially true when large DC grids are considered interconnecting heavily loaded AC networks, such as the future European Supergrid [16], which will form the core of the power sharing platform of Europe.

Consequently, a selective and reliable protection scheme providing continuous and online security of MTDC networks against DC faults and disturbances is crucial, utilizing decent DC-CBs technologies [17] capable of instantly interrupting DC fault currents without affecting system's availability and performance.

The authors gratefully acknowledge the RCUK's Energy Programme for the financial support of this work through the Top & Tail Transformation programme grant, EP/I031707/1 (http://www.topandtail.org.uk/).

In this work, a four-terminal VSC-MTDC grid is used to interconnect four individual AC power networks through bipolar connections. The system is equipped with DC-CBs distributed along every transmission line, ensuring that in the unfavorable event of a permanent DC fault on a line, that faulted line will be immediately selectively disconnected and system's stability will be re-established. This is a highly favorable scenario that will be seriously taken into account during future developments of offshore MTDC grids.

The purpose of this study is to gain an initial experience regarding the dynamic behavior of the AC/DC system under permanent (ac/dc) faults, observing how these affect the stability of the system. The second part of this work, introduces the application of DC-CBs used as protection measures tackling the faults (dc-side), and hence re-establishing stability. The study concludes by confirming the feasible use of DC-CBs in a VSC-MTDC grid, serving as a guard to fault events whereas at the same time contributing to fast recovery of system's stability.

The test system considered in this paper can realistically reflect the first stages of an evolutionary development of a multi-terminal (under-sea) DC network, such as in the area of North Sea, forming the core (also known as the critical point) of the European Supergrid.

II. TEST SYSTEM

Figure 1 illustrates a single-line diagram of the proposed system. Each tie-line represents a bipolar connection realizing power transmissions under positive and negative DC voltages.

A. *Power System Architecture*

The topology of the MTDC network comprises the properties of ring (Lines 1-4) and meshed (Line 5) connections, enabling the system to comply with a wide variety of DC network configurations. Transmission lines 1-5 have a total length of 100km, 50km, 100km, 50km and 120km respectively. These are typical values representing offshore wind power integration to onshore AC grids. Figure 1 also depicts the DC-Circuit Breakers (CBs) distributed along the network with appropriate labeling.

B. *Control Strategy*

Converter terminal VSC1 is set to $\boldsymbol{Q\text{-}V_{dc}}$ control mode (Figure 2). This serves into controlling the reactive power ($\boldsymbol{Q}$) exchanged between external grid AC1 and the converter. Additionally, it maintains the DC voltage ($\boldsymbol{V_{dc}}$) of the network to a constant value. VSC1 acts as a slack bus to the system by balancing the power flows in the DC grid and adequately preserving a constant voltage level. The rest of the converters are all set to the $\boldsymbol{P\text{-}Q}$ control mode (Figure 3), establishing constant active power flows ($\boldsymbol{P}$) in the grid, as well as regulating the reactive power ($\boldsymbol{Q}$) exchanged between the AC grids and converter terminals.

C. *Power Sharing Plan*

The active power exchanged between the converter terminals (and hence the AC grids) is managed according to the following plan: Terminal VSC3 transmits a constant flow of 10MW to the DC grid, whereas terminals VSC2 and VSC4 each receive a constant amount of 10MW. Converter VSC1, acting as a slack bus in the system, compensates for the rest of active power needed including the grid power losses, by transmitting a total amount of 10.95MW. The reactive power transmissions, as controlled by each converter terminal, are all set to zero. The nominal voltage of the interconnected AC grids is set to 400kV (Line-Line) whereas the corresponding voltage of the DC grid is set to 320kV (Line-Ground).

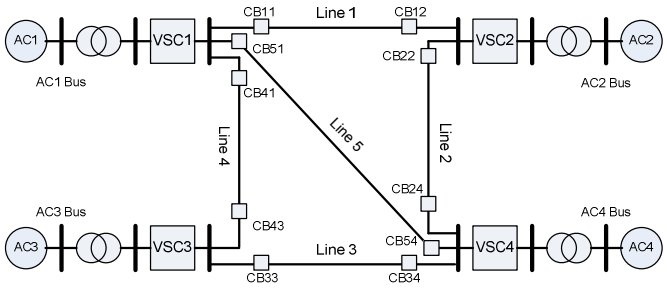

Figure 1. Single-line diagram of the mixed AC/DC test system

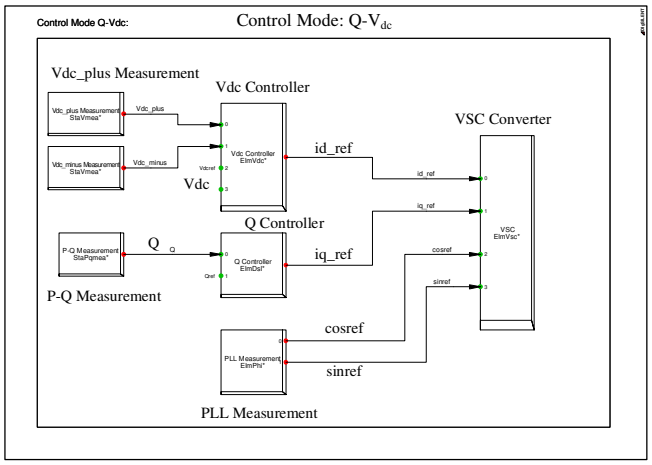

Figure 2. Control design of the converter terminal VSC1operating in V_{dc}-Q control mode and used to maintain a constant DC voltage level in the system

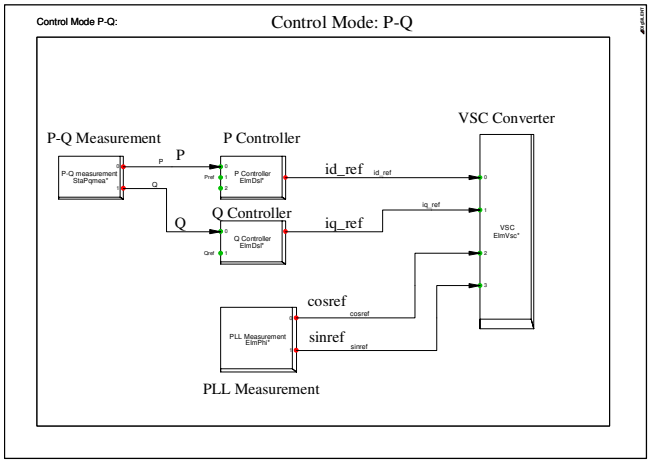

Figure 3. Control design of converter terminals VSC:2-4 operating in *P-Q* control mode which use to maintain constant active and reactive power streams in the system

III. SIMULATION STUDIES

In this section, two different scenarios will be considered. In the first scenario, a permanent AC/DC (short circuit) fault will be initiated on the given system presented in Figure 1, aiming to record its natural response and to the extent to which it is affected following the disturbance. With respect to the second scenario, the primary focus will be on the DC-side disturbance and how this can be eliminated, since AC-side faults are widely known and well addressed so far. Here, protection measures in the form of DC circuit breakers will be applied on the system, targeting the isolation of the dc short circuit fault. This in turn will result in system's stability recovery. This part verifies the feasible application of DC-CB's on VSC-MTDC grids for system protection and stability issues.

A. *Case Study 1*

DC Fault

Here, a permanent DC fault of impedance 0+j0 Ohms is applied on the positive voltage (DC+) pole of line "Line 5", at the time instant of 2 seconds. The obtained results depicting the system's behavior are presented on Figure 4 (a)-(b), where it is illustrated how the active powers (a), and DC voltage magnitudes (b), (as recorded on the positive terminal (DC+) of each converter), respond to the fault. It is important to note that identical results would have been obtained in the case where the fault would have simulated at the negative (DC-) pole of the transmission line while observing the negative terminals of each converter. Moreover, it is worthwhile making clear that the initial values of the active powers as shown on Figure 4 (a) are half the magnitude provided in section II-Part C. This is expected since we only consider the positive (DC+) terminal of each converter here, keeping in mind that the total active power transmitted or absorbed by each converter is equally split between its positive and negative terminals.

It is evident from Figure 4, that the permanent existence of the DC fault on the positive pole of the transmission line will have severe impacts on the entire network, causing the active power flows and DC voltages on the positive terminals to collapse. This will further cause significant overloading effects on the negative terminals of the converters in response to the high disturbance, and finally resulting in the instability of the overall VSC-MTDC grid.

Consequently, this first part of case study 1 underlines the increased importance of a continuous online security system safeguarding against the occurrence of dc fault disturbances in a multi-terminal AC/DC grid. This should provide a fast and uninterrupted protection against DC faults, securing the system from undesired consequences of this kind.

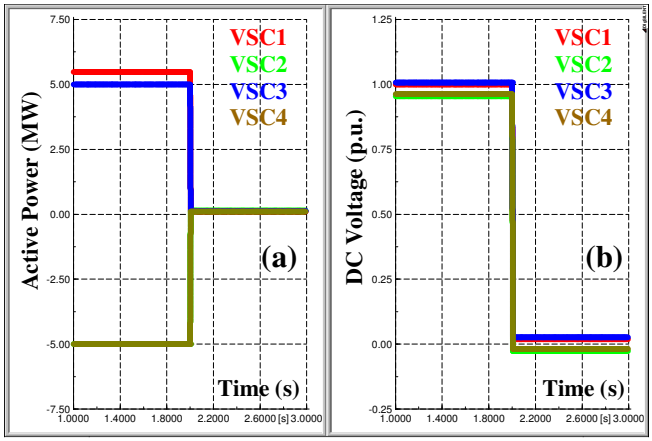

Figure 4. (a) Active power and (b) DC Voltage responses as recorded on the positive voltage terminals of each converter (VSC1-4) following a permanent DC fault disturbance

AC Fault

Lastly, case study 1 concludes by the investigation of a permanent bolted AC fault (impedance: 0+j0 Ohms) initiated on the AC side of our test system (bus AC1 Bus), at the time instant of 2 seconds. The purpose of this study is to observe how such a disturbance will propagate through the DC-side of the system and what consequences this could have on the entire network. The result of the study will determine whether control/protection actions, such as AC circuit breakers, are necessary for addressing such kinds of AC-side irregularities in a mixed AC/DC network. The simulation results realizing this scenario, are presented on Figure 5 (a)-(b), where likewise Figure 4 (a)-(b), the active powers and DC voltages are the chosen variables to reflect this condition.

According to Figure 5-(a), it is observed that at the instant of the fault the active power flowing through converter VSC1 is instantaneously reversed in direction, which is now flowing towards the fault and feeding the short circuit current (for just a fraction of a second), and immediately after drops to zero as expected. This loss of active power from converter VSC1 to the MTDC grid, has a direct consequence on the transmitted power by VSC3, which now increases to compensate for that loss. A part of it is injected into the DC network (which is then extracted by VSC2 & VSC4), while the rest of it is used to feed the short circuit current at AC1 Bus. Another impact of the zero power injection by VSC1 is the reduction of absorbed power by the converter VSC4. The reason behind this is because VSC4 was extracting active power from the grid directly from VSC1 and VSC3 (see Figure 1). A reduction in VSC1's transmitted power it will clearly be noticeable by VSC4's absorbed power. The less sensitive terminal to the AC disturbance, as Figure 5 suggests, is VSC2 which maintains its pre-fault power condition.

A similar effect is also depicted by the DC voltage profiles of the converters. As can be seen, the most highly affected voltage point in the DC grid is that of terminal's VSC1 which is the closest to the AC fault. This is reflected by a steep step decrease from its original value. The rest of the converter terminals also suffer a reduction in their voltage magnitudes, however the degree of that depends on their geometrical distance from the fault.

To summarise, an AC fault disturbance introduced in a multi-terminal VSC-HVDC network, has significant impacts on the DC-side of the system which can be represented by either the power or the voltage profiles of the system. In either way, it can be seen that the fault's effects are more pronounced closer to the affected AC network. However, it is important to note that a total black-out of powers and voltages was avoided, as compared to Figure 4, which shows that the DC grid merely takes shield actions. Despite that, continuity in service of the combined AC/DC network is an uncompromised priority and hence AC-side protection measures are necessary to establish this requirement.

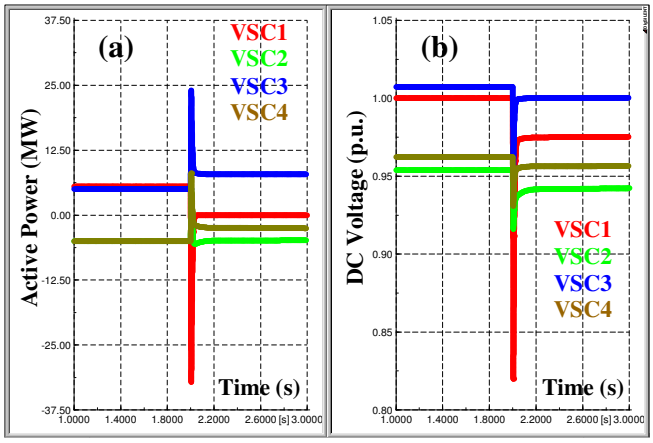

Figure 5. (a) Active power and (b) DC Voltage responses as recorded on the positive voltage terminals of each converter (VSC1-4) following a permanent AC fault disturbance

B. *Case Study 2 - **AC Fault Clearance***

In this second part of our simulation work, we examine how the VSC-MTDC grid recovers from faulty conditions and re-establishes stability and operational mode when appropriate control/protections actions are taken. These will take the form of AC and DC circuit breakers aiming to tackle the severe disturbances initiated on both the AC and DC sides of the system respectively.

Initially, we will begin by looking how the AC-CBs installed on network AC1 will operate at the location of AC1-Bus to clear/isolate the fault, and hence re-establish overall system stability. The installations of the AC-CBs however, are not marked on Figure 1 for reasons of simplicity, and bearing in mind that the focus of the paper is on DC-CBs. Tackling faults through AC-CBs in an AC grid is a well-known technology that has been extensively addressed in the field of electrical engineering. Consequently, a short description will be made here summarizing the post-fault behaviour of the system when the action of AC-CBs is introduced. This is shown on Figure 6 (a)-(b), which illustrates how the active powers and dc voltages of the converters evolve in time-domain following the fault. Here, the AC-CBs are triggered to isolate/clear the faulted sector of network AC1, 200ms after the fault is initiated (i.e. at 2.2 seconds).

As Figure 6 suggests, the introduction of CBs on AC1 works effectively as a shield to the AC disturbance, ensuring that the faulted sector is disconnected from the rest of the network, assisting into system's recovery to its pre-fault operational mode. This is confirmed by the active powers and dc voltages, both of which converge to their pre-disturbance equilibrium points as soon as the fault is cleared.

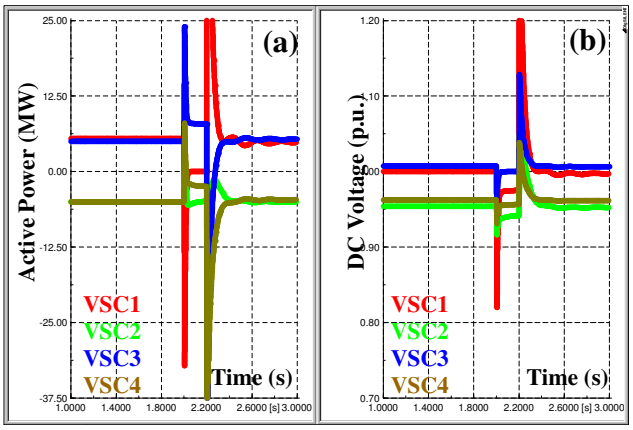

Figure 6. (a) Active power and (b) DC Voltage profiles of the four converters (as recorded on their positive voltage terminals) of the MTDC grid following an AC fault clearance through AC-CB's action

DC Fault Clearance

This last part of the simulation study, examines the feasibility in applying DC circuit breakers on the DC-side of the grid. This has a significant effect on the capability of these breakers in effectively interrupting DC fault currents (by tripping the appropriate faulted line), as well as providing support to the system to re-establish stability.

Here, the same (dc) fault scenario from Case study 1 – DC Fault is preserved, with the same characteristics and location. However now, the corresponding DC-circuit breakers (CB51 and CB54 – see Fig. 1) of the corresponding faulted line (Line 5) will be activated to clear the fault. This will be done by tripping the corresponding line out of operation 200ms after the fault event, i.e. at 2.2 seconds. The simulation results will determine whether the DC-CBs are capable of isolating/clearing such kinds of DC disturbances, while at same time preventing the system from losing stability. Figure 7 depicts this scenario, where the same variables (power, dc voltages) considered in the previous cases were chosen.

It can be seen from Figure 7 (a)-(b) that the use of the DC-CBs on the system efficiently tackle the DC disturbance (by clearing the fault in between 200ms), while at the same time assisting the network to return to its operational mode as soon as the fault is cleared.

With respect to active powers, it can be seen that up to 2.2 seconds a pattern similar to Figure 4-(a) can be seen. This indicates a stable power flow to/from the dc network and a sudden drop of zero power during the fault existence. However, immediately after the DC fault has been cleared by the DC-CB action, the active power flows quickly rise to their steady-state pre-fault values resuming the operational mode.

A similar scenario can also be observed from the voltage profiles. It is clear that during the fault all converters' voltages are severely affected by implementing significantly low values as compared to their initial (pre-fault) ones. Similarly here, once the fault has been resolved the voltages recover back to a stable mode.

Another important observation (besides the stability verification), is that the loss of a transmission line (through the operation of the tripping scheme) results in a reduction in overall capacity of the dc network as can be partially observed by Figure 7-(a). This has a direct consequence on the remaining "healthy" lines of the grid as they may overload and this may in turn result in an overvoltage effect on all terminals as can be observed by Figure 7-(b).

The impact of such phenomena however, could be dramatically decreased when larger/heavier VSC-MTDC grids are considered combining numerous assisting terminals interconnected with stronger AC networks. Additionally, it is also a matter of the novelty and sophistication of the control/protection algorithms adopted in the power system. Finally, it is also important a well-designed structure of the system (interconnections, complexity) providing enhanced robustness and flexibility.

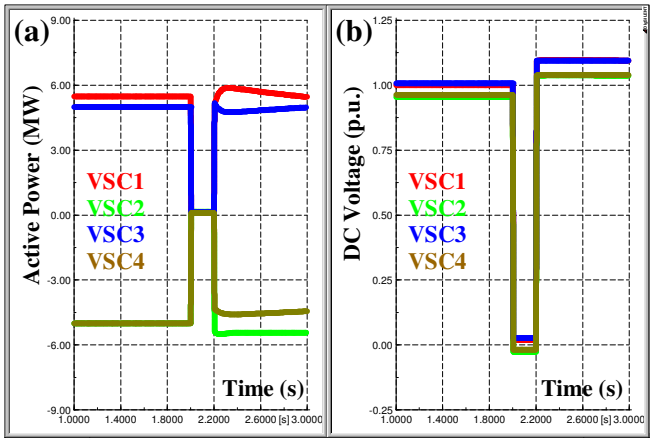

Figure 7. (a) Active power and (b) DC Voltage profiles of the four converters (as recorded on their positive voltage terminals) of the MTDC network following a DC fault clearance through the DC-CBs's action

IV. CONCLUSION

Summarizing the overall work, this study attempted to provide answers to some open questions regarding the behavior of VSC-MTDC grids under different types of disturbances (permanent/transient - AC/DC short circuit faults), and what impact these have on a part of or the entirety of the system depending on their location and nature.

Based on these, the study has been extended to include security/protection solutions providing isolation/clearance of the various faults based on the mature technology of AC CBs and the promising DC CBs.

Firstly, our results have shown that the initiation of a permanent DC fault on the system could have severe consequences on the entire VSC-MTDC network, resulting in total black outs. This was verified by both zero power injections and dramatically high voltage drops, both of which indicate the significance of a prompt protection action. On the other hand, an AC fault was shown to have considerable impact on the system which also needs mitigation strategies. However, total black outs were not observed, and it was shown that the severity of the fault was more pronounced closer to the fault (i.e. closer to the faulted AC network). This means, each of the four converter terminals of the network were affected to a degree analogous to their geometrical distance from the fault.

The second part of this study, attempted to tackle the AC/DC disturbance in the system as well as curbing propagation/distribution of these disturbances along the network, i.e. from AC to DC side and vice versa.

This was achieved by optimally spreading AC/DC circuit breaker devices along the network, covering both the AC and DC sides of the system. Once a fault is detected on a transmission line, the corresponding CBs of the faulted line open disconnecting the line from the rest of the network.

According to our simulation results, this method has proved very effective in successfully addressing the fault. In both fault cases (either of AC or DC nature), the corresponding CB devices (AC or DC respectively) were immediately triggered and isolated that fault in a time period of 200ms in both sides of the mixed AC/DC network. In addition to this, the termination of the short-circuit disturbance contributed in the recovery of system stability and hence the re-establishment of pre-fault operational mode.

Key outcome from this work, is the feasible use of an optimally combined protection scheme consisting of AC and DC circuit breaker technology applied into VSC-MTDC grid, which serves as an online guard securing the system from AC/DC fault events, while at the same time assisting the overall network regain stability and operation mode. This enhances the overall security and robustness of the transmission system to high disturbances such as instabilities and system paralysis, caused by short circuit phenomena.

It is a great advantage the fact that it is a relatively straight forward and robust protection solution, which can be directly applied to the offshore VSC-MTDC networks to be installed around the globe, forming the primary protection layer of the transmission medium.

REFERENCES

[1] R. Rudervall, J. P. Charpentier, and R. Sharma, “High voltage direct current (HVDC) transmission systems technology review paper,” in *Energy Week 2000*, Washington, D.C, USA, March 2000.

[2] Flourentzou N., Agelidis V. G., and Demetriades G. D., "VSC-based HVDC power transmission systems: An overview," *Power Electronics, IEEE Transactions on*, vol.24, no.3, pp.592-602, March 2009.

[3] Agelidis V. G., Demetriades G. D., Flourentzou N., "Recent advances in high-voltage direct-current power transmission systems," *Industrial Technology, 2006. ICIT 2006. IEEE International Conference on*, vol., no., pp.206-213, 15-17 Dec. 2006.

[4] G. Morin, L. X. Bui, S. Casoria, and J. Reeve, “Modeling of the Hydro-Quebec - New England HVDC system and digital controls with EMTP,” *IEEE Trans. Power Delivery*, vol. 8, no. 2, pp. 559–566, April 1993.

[5] T. Nakajima and S. Irokawa, “A control system for HVDC transmission by voltage sourced converters”, Power Engineering Society Summer Meeting, IEEE 1999.

[6] M. Hausler, “Multiterminal HVDC for high power transmission in Europe,” in *CEPEX99 conference*, Poznan, Poland, March 1999.

[7] W. F. McNichol, J. Reeve, J. R. McNichol, R. E. Harrison, J. P. Bowles, “Considerations for implementing multiterminal DC systems,” *IEEE Transaction on Power Apparatus and Systems*, Vol. PAS-104, September 1985.

[8] T. M. Hailesalassie, M. Molinas, T. Undeland, “Multi-terminal VSC-HVDC system for integration of offshore wind farms and green electrification of platforms in the North Sea,” *NORPIE 2008*, Espoo, Finland, 9 - 11 June, 2008.

[9] Lie Xu, W. Williams, Liangzhong Yao, “Multi-terminal DC transmission systems for connecting large offshore wind farms,” *Power and Energy Society General Meeting – Conversion and Delivery of Electrical Energy in the 21st Century*, 2008 IEEE, 20-24 July, 2008.

[10] T. Haileselassie, K. Uhlen, T. Undeland, “Control of multiterminal HVDC transmission for offshore wind energy,” *Nordic Wind Power Conference*, 10 - 11.09.2009, Bornholm, Denmark.

[11] C. Dierckxsens, K. Srivastava, M. Reza, S. Cole, J. Beerten, R. Belmans, “A distributed DC voltage control method for VSC MTDC systems”, Journal on Electric Power Systems Research, Vol. 82, pp. 54– 58, September 2011.

[12] V. Mier, P. G. Casielles, J. Coto, and L.Zeni, “Voltage margin control for offshore multi-use platform integration”, International Conference on Renewable Energies and Power Quality (ICREPQ’12), 28th to 30th March, 2012.

[13] L. Tang and B.-T. Ooi, “Protection of VSC-multi-terminal HVDC against DC faults,” in *Proc. Power Electronics Specialists Conf.*, Jun. 2002, vol. 2, pp. 719–724.

[14] L. Tang, “Control and protection of multi-terminal dc transmission systems based on voltage-source converters,” Ph.D. dissertation, McGill University, Montreal, QC, Canada, 2003.

[15] L. Tang, and B.–T. Ooi, “Locating and isolating DC faults in multi-terminal DC systems,” *IEEE Transaction Delivery*, Vol. 22, No 3, July, 2007.

[16] F. Schettler, M. S. Balavoine, M. Callavik, J. Corbett, N. Kuljaca, V. S. Larsen, N. MacLeod and Björn Sonerud, “Roadmap to the supergrid technologies”, in *Friends of the SuperGrid*, Brussels, Belgium, March 2012.

[17] D. Jovcic and B. Wu, "Fast fault current interruption on high-power DC networks," *Power and Energy Society General Meeting, 2010 IEEE*, vol., no., pp.1-6, 25-29 July 2010.

2nd Conference on Power Options for the Eastern Mediterranean Region
07-08 October 2013, Nicosia, Cyprus (Paper No. POEM13/187)

Experimental investigation of the thermosiphonic phenomenon in domestic solar water heaters

Soteris A. Kalogirou, Gregoris P. Panayiotou, Georgios A. Florides, George Roditis, Nasos Katsellis, Andreas Constantinou, Paraskevas Kyriakou, Yiannis Vasiades, Thomas Parisis, Alexandros Michaelides and Jan Erik Nielsen

Abstract-- The deeper understanding of the 'thermosiphonic phenomenon' and the identification of the key parameters affecting it, is the main aim of a research project currently in process in Cyprus. In this work a review of the existing standards and scientific knowledge concerning domestic solar water heaters is presented. The first preliminary results of the experimental investigation of the 'thermosiphonic phenomenon' in domestic solar water heaters are also presented. For this purpose a special test rig was set up and equipped with all sensors necessary to measure all parameters that are most likely to affect the 'thermosiphonic phenomenon'. All tests were conducted according to ISO 9459-2:1995(E). At first, the solar collector was tested according to EN12975-2:2006 in order to determine the thermal performance characteristics at a flow and operation conditions specified by the standard. Consequently, the efficiency of the collector operating thermosiphonically was calculated based on quasi-dynamic approach. Finally, a series of correlations were attempted using the data acquired when the collector is operating themosiphonically which are the following: (i) the temperature difference of the water at the outlet and the inlet of the collector (ΔT) with the solar global radiation, (ii) the water mass flow with the solar global radiation, (iii) the water mass flow with the temperature difference of the water at the outlet and the inlet of the collector (ΔT). The results of the data analysis showed that these parameters are very well correlated between them since the coefficient of determination (R^2) is over 0.91 in all cases.

***Index Terms*-- Cyprus, Solar water heaters, Thermosiphonic phenomenon.**

S. A. Kalogirou is with the Cyprus University of Technology, (e-mail: Soteris.Kalogirou@cut.ac.cy).
G. P. Panayiotou is with the Cyprus University of Technology, (e-mail: Gregoris.Panayiotou@cut.ac.cy).
G. A. Florides is with the Cyprus University of Technology, (e-mail: Georgios.florides@cut.ac.cy).
G. Roditis is with the Applied Energy Centre, (email: gro.cie@cytanet.com.cy)
N. Katsellis is with the Applied Energy Centre, (email: nk.cie@cytanet.com.cy)
A. Constantinou is with the Applied Energy Centre
P. Kyriakou is with the Cyprus Institute of Energy, (email: pke.cie@cytanet.com.cy)
Y. Vasiades is with the Cyprus Organisation for Standardisation, (email: y.vassiades@cys.org.cy)
T. Parisis is with TALOS RTD, (email: tp@talos-rtd.com)
A. Michaelides is with TALOS RTD, (email: am@talos-rtd.com)
J.E. Nielsen is an Individual Researcher, (email: jen@solarkey.dk)

I. Introduction

CYPRUS has no natural oil resources at the moment and relies entirely on imported fuel for its energy demands.

The only natural energy resource available is solar energy. Cyprus has a very sunny climate with an average annual solar radiation on a horizontal surface of 5.4 kWh/m^2-day.

Solar water heating units are extensively employed in Cyprus. In fact the total number of units installed, are such that constitute Cyprus to be the leading country in the world in this area. These units are mostly of the thermosiphonic type. This type of solar water heater consists of two flat-plate solar collectors having an absorber area between 3 to 4 m^2, a storage tank with capacity of 150 to 180 litters and a cold water storage tank, all installed on a suitable frame. An auxiliary electric immersion heater and/or a heat exchanger, for central heating assisted hot water production, are used in winter during periods of low solar insolation.

Because the manufacturing of solar water heaters and mainly that of the thermosiphon type has expanded rapidly in Cyprus, there is a need to study in depth and model this type of systems. It is also required to validate the model using simple physical experiments. In this way the model can be used to investigate the effect of design changes and therefore improve the solar water heater performance.

II. Literature Review

There have been extensive analyses of the modelling, analysis and performance of thermosiphon solar water heaters, both experimentally and analytically by numerous researchers [1]. Some of the most important are shown here.

Close [2] made the first published analysis of thermosiphon solar water heater circuit. He has presented a mathematical model where mean system temperature and water mass flow rate can be predicted by testing two thermosiphon systems with different characteristics. The results conformed well to those predicted.

Desa [3] considered the water heater system on the whole and by equating the incident energy received to the sum of the heat losses from it and the heat gained by the water, predicted the mean water temperature variation throughout the day for a natural circulation flow system.

Gupta and Garg [4] modified the model of Close [2] to take into account the heat exchange efficiency of the collector absorber plate and thermal capacitance. They have improved on Close's analysis by incorporating a plate

efficiency factor to account for the thermal efficiency of the plate and approximating ambient conditions using Fourier's series expansions for ambient temperature and radiation intensity. So they developed a model for thermal performance of a natural circulation solar water heater with no load and presented solar radiation and temperature with Fourier series. They also found experimentally that the flow rate of a thermosiphon water heater can be increased by increasing the relative height between the collector and storage tank, but the efficiency is not increased. The efficiency can be increased by reducing the loop resistance.

Ong [5,6] evaluated the thermal performance of a thermosiphon solar water heater. He used a small system with five thermocouples on the bottom surface of the water tubes and six thermocouples on the bottom surface of the collector plate. The six thermocouples were inserted into the storage tank and a dye tracer mass flow meter was employed. His studies were the first detailed ones on a thermosiphonic system. Ong [5] extended the work of Close [2] and Gupta and Garg [4] as he presented a finite difference method of solution to predict the mean system temperature and water mass flow rate in a solar water heater operating under thermosiphon flow conditions. The experimental results presented, showed that the mean collector plate temperature, the average water temperature in the storage tank and the mean water temperature in the collector tubes were not equal. Furthermore, the tank temperature distribution was non-linear. All these were contrary to the theoretical assumptions that the mean temperatures were equal, corresponding to a single mean system temperature and that the tank temperature distribution was linear. In [6] he wanted to improve the theoretical assumptions made previously in [5], in order to obtain a more satisfactory agreement between experimental data and prediction. Therefore, in [6], an improved theoretical model was presented to predict the thermal performance of a natural-recirculation solar water heater system.

Shitzer *et al*. [7] made experiments with a flat plate solar water heating system in thermosiphonic flow and observed linear temperature distributions both along the collectors and in the storage tank when no hot water consumption was allowed. They also found that water flow rate essentially follow solar radiation and reached a maximum of 0.95 l/min which is about 33% smaller than the value they predicted by an analytical model. However, they observed that by shutting the system off during the afternoon hours, when losses to the environment increases, might increase the efficiency of the system.

Morrison and Ranatunga [8] investigated the response of thermosiphon systems to step changes in solar radiation. Measurement of the transient flow rate was obtained using a laser Doppler anemometer and a mathematical model was developed to simulate the transient performance. Results shown that although there are long time delays associated with the development of the thermosiphon flow the energy collection capability is not affected by thermosiphon time delays.

Hahne [9] calculated the efficiency and warming up time of flat plate water collector under steady state and transient state conditions. Comparison of collector performance in summer and winter shows the importance of collector inclination and the effect of pipe spacing.

Morrison and Sapsford [10] investigated the performance of 6 thermosiphon solar water heaters while they were supplying typical domestic hot water loads. The performance of the solar systems was rated by comparing the auxiliary energy consumption with the energy consumed by a conventional electric system. In contrast to forced circulation systems the performance of thermosiphon systems was found to be best if a morning peak load pattern was used. Their results showed that the performance of thermosiphon solar water heaters is a function of the way the system is operated and that significant variations of performance exist between different systems configurations.

The results from the two previous studies have been used by Morrison and Tran [11] to develop a simulation program for thermosiphon solar water heaters supplying various domestic energy demand patterns. Morrison and Tran [11] presented a finite element simulation model for prediction the long term performance of thermosiphon solar water heaters. The simulation results indicate that the performance of a solar water heater with an in-tank booster improves as the flow rate through the collector is reduced. Also found that the efficiency of a thermosiphon system with in-tank booster is slightly higher than an equivalent pumped circulation system, due to better stratification in the storage tank in the thermosiphon system.

Kudish *et al*. [12] used a standard Israeli solar collector consisting of eight cooper tube risers connected to two cooper tube headers. They studied the effect of the height of the thermosiphon head on the flow rate. The rate of thermosiphon flow was measured periodically throughout the day during the sunshine hours so they determined the instantaneous collector efficiency through a day. They measured the thermosiphon flow rate directly by adapting a simple and a well known laboratory technique, using a constant level device to a solar collector in the thermosiphon mode. The data for the thermosiphon flow were used to construct a standard efficiency test curve so as to prove that this technique can be applied for collector testing as a standard laboratory technique. The correlation between the thermosiphon flow and the global insolation was observed to be linear in all cases studied.

Morrison and Braun [13] studied system modelling and operation characteristics of thermosiphon solar water heater with vertical and horizontal storage tank. They found that system performance is maximized when the daily collector volume flow is approximately equal to the daily load flow. Very important is the fact that they found that the system with vertical tank can perform better than the horizontal one. They found good agreement between the simulation results and experimental data as they compared an efficient numerical simulation model for thermosiphon solar water heaters for two locations. The model they used has also been adopted by TRNSYS simulation program.

Hobson and Norton [14] made the characteristic curve for an individual directly–heated thermosiphon solar energy water heater obtained from data of a test period of 30 days. Using this curve they calculated the annual solar fraction which agreed well with the corresponding value computed from the numerical simulation. They produced a simple but relatively accurate design method for direct thermosiphon solar water heater.

Tiwari and Lawrence [15] studied a transient analysis of a closed loop solar water heater with heat exchanger under a thermosiphon mode with analytical expressions for fluid

temperature in the flat plate collector and storage tank temperature.

Shariah and Shalabi [16] studied optimization of design parameters for a thermosiphon solar water heater for two regions in Jordan through the use of TRNSYS. Their results indicate that the solar fraction of the system can be improved by 10-25% when each studied parameter is chosen properly. Using the optimum or recommended values of the design parameters for a thermosiphon system could reduce the price of the system as well as improving the performance. However, solar fraction of a system installed in hot climate is less sensitive to some parameters than in mild climate. Shariah *et al*. [17] presented a comprehensive assessment of the impact of most of the design parameters on the performance of the thermosiphon water heating system and provide guidance on the `optimum' value for each. They used TRNSYS program to simulate the annual performance of thermosiphon water heating systems with meteorological data for Los Angeles.

Kalogirou and Papamarkou [18] studied the modelling of a thermosiphon solar water heating system with a simple model validation in Nicosia, Cyprus. They used two flat plate collectors with an area 2.7 m^2 and a storage tank of 150 l modelled using TRNSYS so to have a detailed analysis and a long term system performance. They found that the annual solar contribution of the simulated system was 79% and during the summer months no auxiliary heating is required as the solar contribution of the simulated system was 100%. This means that the solar fraction reached 100%. However, during the summer months the demand for hot water from storage tank was reduced. Experimentally they found that there is a decrease in solar radiation during May because of special conditions to the development of clouds encountered in Nicosia. They also made an economic analysis which they found that the pay-back time of the system is 8 years and the present worth of life cycle savings is equal to 161 Cy pounds (€275).

Chuawittayawuth and Kumar ([19] presented details of experimental observation of temperature and flow distribution in natural circulation solar water heating systems. They found that the temperature values at the riser tubes the collector inlet are generally much higher than those at the other risers on a clear day, while on cloudy days the temperature is uniform. They concluded that the temperature of water in the riser depends on its flow rate. They also carried out the measurements of the glass temperature.

Jiang *et al*. [20] found that the thermal performance of a solar thermosiphon system for water heating depends on its design characteristics and manufacturing quality so they analyzed four characteristic parameters which helped them to assess not only the solar thermosiphon system performance but also the direction for system performance improvement.

Runsheng *et al*. [21] constructed and tested two sets of water in glass evacuated tube solar water heaters. Both systems were identical in all aspects but had different collector tilt angle from the horizon with the one inclined at 22° and the other at 46°. Experimental results showed that the collector tilt angle of solar water heater had no significant influence on the heat removal from solar tubes to the water storage tank; both systems had almost the same daily solar thermal conversion efficiency but different daily solar and heat gains and climatic conditions had a negligible effect on the daily thermal efficiency of systems due to less heat losses of the collector to the ambient air. This fact shows that to maximize the annual heat gain of such solar water heaters, the collector should be inclined at a tilt angle for maximizing its annual collection of solar radiation. A year before [22] they studied a thermosiphon domestic solar water heater with flat plate collectors at clear night and found that thermosiphon domestic solar water heater flat plate collectors with a non solar selective absorber might suffer from freezing damage.

Riahi and Taherian [23] presented a detailed review of other studies and made a detailed analysis by discussing and comparing their results with other studies. They have used the hydrogen bubble method to measure the flow rate as shown by Bannerot [24]. They collected data for several sunny and cloudy days. Also they studied dynamic response of the system to variations in solar insolation. It was found that such systems can provide ample energy to satisfy the demand for hot water.

Okonkwo and Nwokoye [25] made an experimental investigation of the performance of a thermosiphon solar water heater for a period of six months measuring the solar radiation, water mass, relative humidity and wind speed using special equipment.

Sakhrieh and Al-Ghandoor [26] made an experimental investigation of overall performance, efficiency and reliability of five types of solar collectors as used in the local Jordanian market. The five types that they studied are blue coated, black coated, cooper, aluminum and with evacuated tube. They observed that the outlet temperature (T_{out}) of the five types increases during the day and reaches the peak at about 2.00 p.m. and then starts to decrease. The efficiency curve against time has the same shape as the T_{out} curve. They concluded that evacuated tube solar collector has the highest efficiency followed by black and blue coated solar collectors. The aluminum collector comes in the fourth place as the lowest efficiency is reserved for the copper collector.

III. European Standards

In April 2001 CEN started publishing a series of standards related to solar collectors and systems testing. With the publication of these European standards all national standards, related to the same topic and having conflicting provisions were (or have to be) withdrawn by the nations of the European Community. Some of these standards were revised in 2006 and are now under their second 5-year systematic review. A complete list of these standards is as follows:

EN 12975-1: 2006 +A1: 2010. *Thermal solar systems and components - Solar collectors - Part 1: General requirements*. This European standard specifies requirements on durability (including mechanical strength), reliability and safety for liquid heating solar collectors. It also includes provisions for evaluation of conformity to these requirements. (A1: 2010 in the standard reference number denotes a minor amendment which was made in 2010 to change the scope of the standard so as to extend its application for concentrating collectors as well).

EN 12975-2: 2006. *Thermal solar systems and components - Solar collectors - Part 2: Test methods.* This

European standard establishes test methods for validating the durability, reliability and safety requirements for liquid heating collectors as specified in EN 12975-1. This standard also includes three test methods for the thermal performance characterization for liquid heating collectors.

EN 12976-1: 2006. *Thermal solar systems and components - Factory made systems - Part 1: General requirements.* This European standard specifies requirements on durability, reliability and safety for factory made solar systems. This standard also includes provisions for evaluation of conformity to these requirements.

EN 12976-2: 2006. *Thermal solar systems and components - Factory made systems - Part 2: Test methods.* This European standard specifies test methods for validating the requirements for factory made solar systems as specified in EN 12976-1. The standard also includes two test methods for the thermal performance characterization by means of whole system testing.

EN 12977-1: 2012. *Thermal solar systems and components - Custom built systems - Part 1: General requirements for solar water heaters and combisystems.* This European standard specifies requirements on durability reliability and safety of small and large custom built solar heating and cooling systems with liquid heat transfer medium in the collector loop for residential buildings and similar applications. The standard also contains requirements on the design process of large custom-built systems.

EN 12977-2: 2012. *Thermal solar systems and components - Custom built systems - Part 2: Test methods for solar water heaters and combisystems.* This European standard applies to small and large custom built solar heating systems with liquid heat transfer medium for residential buildings and similar applications, and specifies test methods for verification of the requirements specified in EN 12977-1. The standard includes also a method for thermal performance characterization and system performance prediction of small custom built systems by means of component testing and system simulation.

EN 12977-3: 2012. *Thermal solar systems and components - Custom built systems - Part 3: Performance test methods for solar water heater stores.* This European standard specifies test methods for the performance characterization of stores that are intended for use in small custom built systems as specified in EN 12977-1.

EN 12977-4:2012. *Thermal solar systems and components - Custom built systems - Part 4: Performance test methods for solar combistores*. This European standard specifies test methods for the performance characterization of stores which are intended for use in small custom built systems as specified in EN 12977 1. Stores tested according to this document are commonly used in solar combisystems.

EN 12977-5:2012. *Thermal solar systems and components - Custom built systems - Part 5: Performance test methods for control equipment*. This European standard specifies performance test methods for control equipment as well as requirements on accuracy, durability and reliability of the control equipment.

EN ISO 9488: 1999. *Solar energy - Vocabulary (ISO 9488: 1999).* This European - International standard defines basic terms relating to solar energy and has been elaborated in common with ISO.

The elaboration of the above standards has been achieved through a wide European collaboration of all interested parties such as manufacturers, researchers, testing institutes and standardization bodies. Furthermore, these standards will promote a fair competition among producers of solar energy equipment on the market, since low-quality/low-price products will be easier to identify for the customers based on uniform test reports comparable throughout Europe.

The increased public awareness on environmental aspects will be reinforced from these standards, which will ensure the quality level for the consumer and will give him more confidence in the new solar heating technology and the products available.

IV. Solar Water Heaters Performance Evaluation

Many test procedures have been proposed by various organizations in order to determine the thermal performance of solar water heaters which include, integrated collector storage, thermosiphon and forced circulation systems, both custom and factory built. Testing of the complete system may serve a number of purposes. The main one is the prediction of the system long-term thermal performance. System testing may also be used as a diagnostic tool to identify failure and causes of failure of the system performance. Other purposes include the determination of the change in performance as a result of operation under different weather conditions or with a different load profile.

International Organization for Standardization (ISO) published a series of standards ranging from simple measurement and data correlation methods to complex parameter identification ones. International Standard ISO 9459 has been developed by the Technical Committee ISO/TC 180 – Solar Energy, to help facilitate the international comparison of solar domestic water heating systems. Because a generalized performance model, which is applicable to all systems, has not yet been developed, it has not been possible to obtain an international consensus for one test method and one standard set of test conditions. Therefore, each method can be applied on its own.

A total of five parts comprise ISO 9459 on solar domestic water heater performance testing as described below with their current status:

ISO 9459-1: 1993-*Solar heating - Domestic water heating systems. Part 1: Performance rating procedure using indoor test methods.* →ACTIVE

ISO 9459-2: 1995-*Solar heating - Domestic water heating Systems. Part 2: Outdoor test methods for system performance characterization and yearly performance prediction of solar-only systems.* →ACTIVE (referenced in EN 12976)

ISO 9459-3: 1997- *Solar heating - Domestic water heating systems. Part 3: Performance test for solar plus supplementary systems.* →WITHDRAWN in 2005

ISO/DIS 9459-4-*Solar heating - Domestic water heating systems. Part 4: System performance characterization by means of component tests and computer simulation.* →UNDER DEVELOPMENT, ISO/FDIS 9459-4 published October 2012 (FDIS=Final Draft International Standard)

ISO 9459-5: 2007-*Solar heating - Domestic water heating systems. Part 5: System performance characterization by means of whole-system tests and computer simulation.* →ACTIVE (referenced in EN 12976)

V. Standardisation Work in Progress

A. Modifications in existing standards

Currently the two standardization technical committees are discussing modifications in the various published standards. At European level, CEN/TC 312 is now working on the amendment of EN 12975-1, EN 12976-1 and EN 12976-2. At European and International levels, both CEN/TC 312 and ISO/TC 180 are co-operating to review EN 9488 and ISO 9806 (Solar Energy-Solar thermal collectors-Test methods). The latter, will include all the provisions and requirements of EN 12975-2 and will be published as a European-International EN ISO standard replacing all three existing parts of ISO 9806 as well as EN 12975-2.

B. New standards proposed or under development

A new draft standard has been developed by CEN/TC 312 concerning the determination of the long term behaviour and service life of selective absorbers for use in solar collectors working under typical domestic hot water system conditions. This will form one of the parts of the new standard EN ISO 22975 - *Solar Energy-Collector Components and materials*. Under the approval of the two committees is also a proposal for the development of two more parts to be included in the standard:

- *Evacuated tubes – Durability and performance*
- *Heat pipes for evacuated tubes – Durability and performance*

Furthermore, ISO/TC 180 is also developing ISO/DIS 9459-4 (now available as ISO/FDIS) which has already been described in previous sections.

VI. Standards related to thermosiphonic systems

It is clear from the above review that there is no standard related to the testing of flat-plate collectors, for the purpose to determine its characteristics and most important weather the collector is able to generate the thermosiphon effect, so as to indicate that such a collector is suitable for use in a thermosiphon system. Concerning the system testing, as the performance of the system is determined by measurements made irrespective of the type of system, the existing standards are considered adequate to be used to the thermosiphon systems as well.

VII. Description of the Test Rig

The thermosiphon test rig used for the experimental procedure, shown in Fig. 1, was assembled by the staff of Applied Energy Laboratory of the Cyprus Ministry of Commerce, Industry and Tourism and consists of three main components namely the Test Rig, the Cylinder and the Heat Sink which are described below.

The Test Rig is made out of galvanized steel and it was designed to adjust the angle of collector. For the adjustment of the angle of the collector, a fully automatic pneumatic stroke is installed. The angle of the collector is measured with an inclinometer. In addition, the Test Rig is designed so that the height between the collector and the Cylinder can be adjusted. Additionally, a pyranometer is attached on the Test Rig, in order to measure the global radiation during the test period.

The Cylinder is made out of copper and it is insulated with natural mineral wool. Sensors are attached on the cylinder, for recording the temperature of the water such as:

1. Inlet Temperature (2 x PT100)
2. Outlet Temperature (2 x PT100)
3. Draw off inlet and outlet (2 x PT100)
4. Mixing temperature (2 x PT100)
5. Stratification temperature (5 x Thermocouple)
6. Inlet and Outlet of the Heat Exchanger (2 x PT100)

Fig. 1 Front view of the test rig

A pneumatic ball valve is attached at the draw off outlet in order to regulate the flow at the draw off period. In addition, a mixing pump is attached at the back of the cylinder. Furthermore, the cylinder is equipped with a magnetic flow meter for measuring the flow at the exit of the collector, and a second portable ultrasonic flow meter is attached at the inlet pipe of the collector. It has also a differential pressure transmitter for measuring the pressure drop of the collector.

A supply tank is used as Heat Sink, which provides water to the system. At the exit of the supply tank, there is a three-way valve with an actuator, and a pump. This allows regulating the temperature and flow of the water which is provided to the system.

VIII. Methodology

The data analysed in this paper were recorded using Agilent data acquisition equipment between the 29th of May and the 13th of June. The data were recorded from 07:30 to 18:45. The area of the collector used for the experiments was 1.36m^2, its orientation was south and its inclination

angle was constant at 45°, which is the angle used by most solar water heating systems in Cyprus.

Initially, the solar collector was tested according to EN12975-2: 2006 in order to determine the thermal performance at a flow and operation conditions specified by the standard. According to the standard, the experimental parameters needed to compute the collector's efficiency under constant inlet temperature and mass flow during a test period, are the water temperature at the collector inlet, water temperature at the collector outlet, water mass flow, solar global radiation, ambient temperature and wind speed. Subsequently, the test was repeated with the collector operating thermosiphonically.

Several correlations were attempted as follows:

(i) temperature difference of the water at the outlet and the inlet of the collector (ΔT) with the solar global radiation,

(ii) water mass flow with the solar global radiation,

(iii) water mass flow with the temperature difference of the water at the outlet and the inlet of the collector (ΔT).

All tests were conducted according to ISO 9459-2:1995(E).

IX. Results and Discussion

The results concerning the thermal performance of the collector according to EN12975 and under thermosiphonic operation are depicted in Fig. 2. It can be observed that the thermal performance according to EN12975 is slightly higher than that of the thermosiphonic operation, which is rather logical due to the fact that the flow during the thermosiphonic operation is lower than the one according to EN12975 since it is naturally created as a result of the temperature difference between the inlet and the outlet water of the collector (thermosiphonic phenomenon). The equation of the performance of the collector according to EN12975 is:

$$h = 0.7025 - 4.3377\frac{T_m - T_a}{G} - 0.1630\frac{(T_m - T_a)^2}{G} \quad (1)$$

The results correlating the solar global radiation (G) with the temperature difference between the water inlet and outlet of the collector (ΔT) are depicted in Fig. 3 where, as can be observed, they are very well correlated since the coefficient of determination (R^2) is 0.9571. This result is rather logical since when the incident solar radiation, being the motive power of the thermosiphonic phenomenon, is higher, the temperature difference between the water inlet and outlet also increases. The equation describing the relation between them is the following:

$$\Delta T = -1.02x10^{-5}(G)^2 + 0.02579(G) - 1.63097 \quad (2)$$

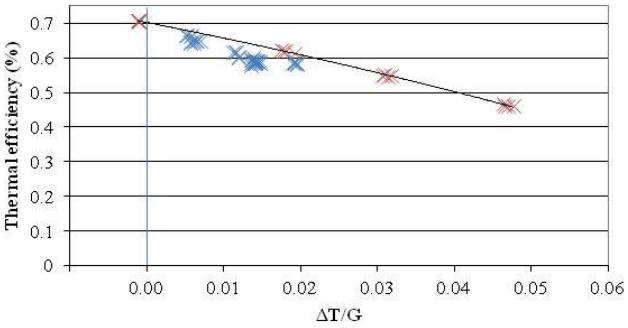

Fig. 2 Efficiency of the solar collector according to EN12975 and under thermosiphonic operation

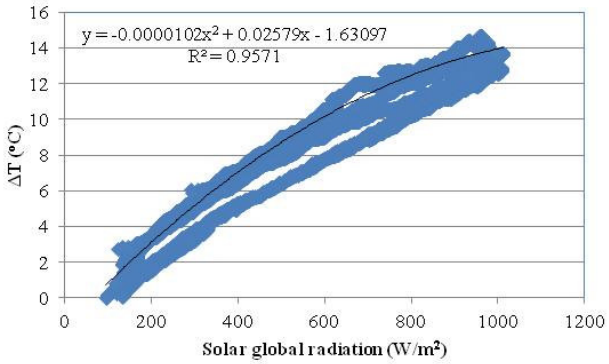

Fig. 3 Correlation of the solar global radiation to the temperature difference of the water in and out of the collector

As can be seen from Fig. 3, quite substantial temperature differences of the order of 15°C are developed in the collector, because of the action of solar radiation. The higher values, as expected, occur at the higher radiation input. It should be noted that by heat rejection the temperature in the storage tank was kept constant (to within 5-6°C) throughout the day.

The results correlating the solar global radiation (G) with the water mass flow (m) are presented in Fig. 4. It can be observed that they are also very well correlated since the coefficient of determination (R^2) is 0.9698.

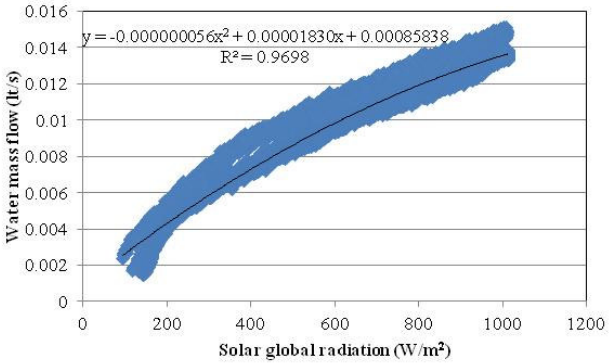

Fig. 4 Correlation of the solar global radiation to the water mass flow

From this result, it can be concluded that this water mass flow, which is naturally created from the temperature difference of the water at the outlet and the inlet of the collector (thermosiphon phenomenon), is directly correlated to the amount of the incident solar radiation on the collector. The equation describing the relation between them is the following:

$$m = -5.6x10^{-8}(G)^2 + 0.00001830(G) + 0.00085838 \quad (3)$$

As can be seen from Fig. 4 a flow rate of about 0.015 lt/s is created by the thermosiphonic effect at the higher radiation levels. By using the collector area of 1.36m^2, this gives a value of 0.011 lt/s/m^2, which is about half the flow rate specified by EN 12975 for testing the solar collectors (0.02 lt/s/m^2). This explains the slightly lower performance of the collector operating thermosiphonically shown in Fig. 2.

The results correlating water mass flow with the temperature difference between the inlet and the outlet water of the collector are depicted in Fig. 5. As can be observed they are also very well correlated since the coefficient of determination (R^2) is 0.9167. The equation describing the relation between them is the following:

$$m = 3.7x10^{-6}(\Delta T)^2 + 0.00096(\Delta T) + 0.0018962 \quad (4)$$

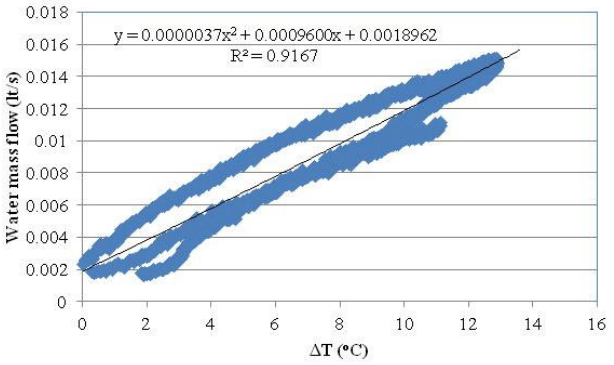

Fig. 5 Correlation of the water mass flow to the temperature difference of the water in and out of the collector

As expected the higher temperature differences create higher flow rates and vice versa. Both values depend on the input power, which is the solar radiation, so the higher values correspond to the higher values of solar radiation input on the collector.

X. Conclusions

This work constitutes the first preliminary data of a research project currently in process in Cyprus, which aims to gain deeper understanding of the 'thermosiphonic phenomenon' and the identification of the key parameters affecting it.

Specifically, a special test rig was set up and equipped with all sensors necessary to measure all parameters that are most likely to affect the 'thermosiphonic phenomenon'. All tests were conducted according to ISO 9459-2: 1995(E). The system was able to operate in various weather and operating conditions and could accommodate the change of inclination of the collector. Initially, the solar collector was tested according to EN12975-2: 2006 in order to determine the thermal performance at a flow and operation conditions specified by the standard. Subsequently, the efficiency of the collector operating thermosiphonically was calculated based on quasi-dynamic approach.

Finally, a series of correlations were attempted using the preliminary data acquired when the collector is operating thermosiphonically for the temperature difference of the water at the outlet and the inlet of the collector, the solar global radiation and the water mass flow.

The results of the data analysis showed that these parameters are very well correlated between them since the coefficient of determination (R^2) is over 0.91 in all cases. These results are very interesting since they give initial inside information of the relation between some of the main parameters that are most likely to affect the thermosiphonic phenomenon. The work is ongoing and the objective is also to find how the collector inclination and the distance between the top of the collector and the bottom of the storage tank affect the performance of the system. This work will lead to the suggestion of a new test procedure suitable for thermosiphonic units.

XI. Acknowledgment

This work was carried out as part of a research project co-funded by the Research Promotion Foundation (RPF) of Cyprus under contract ΤΕΧΝΟΛΟΓΙΑ/ΕΝΕΡΓ/0311(BIE)09 and the European Regional Development Fund (ERDF) of the EU.

XII. References

[1] Kalogirou S.A., (2009). Solar Energy Engineering: Processes and systems, Academic Press.
[2] Close D.J., (1962). The performance of solar water heaters with natural circulation, Solar Energy, Vol. 6, pp. 33.
[3] Desa V.G, (1964). Solar energy utilization at Dacca, Solar Energy, Vol. 8, pp.83.
[4] Gupta G.L., Garg H.P., (1968). System design in solar water heaters with natural circulation, Solar Energy, Vol. 12, pp.163-82.
[5] Ong K.S., (1974). A finite difference method to evaluate the thermal performance of a solar water heater, Solar Energy, Vol. 16, pp. 137-47.
[6] Ong K.S., (1975). An improved computer program for the thermal performance of a solar water heater, Solar Energy, Vol. 18, pp. 183-91.
[7] Shitzer A., Kalmanoviz D., Zvirin Y., Grossman G., (1978). Experiments with a flat plate solar water heating system in thermosiphonic flow, Solar Energy, Vol. 22, pp. 27-35.
[8] Morrison G.L., Ranatunga D.B.J., (1980). Transient response of thermosiphon solar collectors, Solar Energy, Vol. 24, pp. 55-61.
[9] Hahne E., (1983). Parameter effects on design and performance of flat plate solar collectors, Solar Energy, Vol. 34, pp. 497-504.
[10] Morrison G.L., Sapsford C.M., (1983). Long term performance of thermosiphon solar water heaters, Solar Energy, Vol. 30, pp.341-350.
[11] Morrison, G. L., & Tran, H. N. (1984). Simulation of the long term performance of thermosyphon solar water heaters. Solar Energy, 33(6), 515-526.
[12] Kudish A.I., Santamaura P., Beaufort P., (1985). Direct measurement and analysis of thermosiphon flow, Solar Energy, Vol.35, pp.167-73.
[13] Morrison G.L., Braun J.E., (1985). System modelling and operation characteristics of thermosiphon solar water heaters, Solar Energy, Vol. 34, pp. 389-405.
[14] Hobson P.A., Norton B.A., (1989). A design monogram for direct thermosiphon solar energy water heaters, Solar Energy, Vol. 43, pp. 89-95.
[15] Tiwari G.N., Lawrence S.A., (1990). A transient analysis of a closed loop solar thermosiphon water heater with heat exchangers, Energy Conversion and Management, Vol. 31, pp. 505-508.
[16] Shariah A.M., Shialabi B., (1997). Optimal design for a thermosiphon solar water heater, Renewable Energy, Vol. 11, pp. 351-61.
[17] Shariah A.M., Hittle D.C., Lof G.O.G., (1994). Computer simulation and optimization of design parameters for thermosiphon solar water heater, ASME-JSES-JSME International Solar Energy Conference, pp. 493-399.
[18] Kalogirou S.A., Papamarcou C., (2000). Modelling of a thermosiphon solar water heating system and simple model validation, Renewable Energy, Vol.21, pp.471-493.
[19] Chuawittayawuth K., Kumar S., (2002). Experimental investigation of temperature and flow distribution in a thermosiphon solar water heating system, Renewable Energy, Vol. 26, pp. 431-448.

[20] Jiang D.Y., He Wei, Hou J.X., Jei Ji, (2010). A new performance evaluation method for solar thermosiphon systems, International Journal for low carbon technologies, Vol.5, pp.239-244.
[21] Runsheng T., Yuqin Y., Wenfeng G., (2011). Comparative studies on thermal performance of water-in-glass evacuated tube solar water heaters with different collector tilt-angles, Solar Energy, Vol. 85, pp. 1381-1389.
[22] Runsheng T., Yanbin C., Maogang W., Zhimin L., Yamei Y., (2010). Experimental and modeling studies on thermosiphon domestic solar water heaters with flat- plate collectors at clear nights, Energy Conversion and Management, Vol. 51, pp. 2548-2556.
[23] Riahi A., Taherian H., (2011). Experimental investigation on the performance of thermosiphon solar water heater in the south Caspean sea, Thermal Science, Vol. 15, pp. 447-456.
[24] Bannerot R.B. et al., (1992). A Simple Device for Monitoring Flow Rates in Thermosiphon Solar Water Heaters, Journal of Solar Energy Engineering, Vol.1, pp. 47-51.
[25] Okonkwo G.N., Nwokoye A.O.C., (2012). Experimental investigation and performance analysis of thermosiphon solar water heater, Advances in Natural and Applied Sciences, Vol. 6, pp. 128-137.
[26] Sakhrieh A., Al-Ghandoor A., (2012). Experimental investigation of the performance of five types of solar collectors, Energy Conversion and Management – article in press.

XIII. BIOGRAPHIES

Soteris Kalogirou was born in Trachonas, Nicosia, Cyprus on November 11, 1959. He is a Senior Lecturer at the Department of Mechanical Engineering and Materials Sciences and Engineering of the Cyprus University of Technology, Limassol, Cyprus. He received his HTI Degree in Mechanical Engineering in 1982, his M.Phil. in Mechanical Engineering from the Polytechnic of Wales in 1991 and his Ph.D. in Mechanical Engineering from the University of Glamorgan in 1995. In June 2011 he received from the University of Glamorgan the title of D.Sc. He is Visiting Professor at Brunel University, UK and Adjunct Professor at the Dublin Institute of Technology (DIT), Ireland. For more than 25 years, he is actively involved in research in the area of solar energy and particularly in flat plate and concentrating collectors, solar water heating, solar steam generating systems, desalination and absorption cooling.

He has 41 books and book contributions and published 264 papers; 109 in international scientific journals and 155 in refereed conference proceedings. Until now, he received more than 4000 citations on this work and his h-index is 35. He is Deputy Editor-in-Chief of Energy, Associate Editor of Renewable Energy and Editorial Board Member of another eleven journals. He is the editor of the book Artificial Intelligence in Energy and Renewable Energy Systems, published by Nova Science Inc., co-editor of the book Soft Computing in Green and Renewable Energy Systems, published by Springer and author of the book Solar Energy Engineering: Processes and Systems, published by Academic Press of Elsevier.

Gregoris Panayiotou was born in Limassol, Cyprus on February 18, 1983. He graduated from the Technological Educational Institute of Athens first of his class as an Energy Technology Engineer in 2007. He had his MSc in Energy in Heriot-Watt University, Edinburgh where he graduated in 2008 with Distinction.

He is currently employed at Cyprus University of Technology as a Research Associate in a nationally funded project concerning the study and the deeper understanding of the thermosiphonic phenomenon that occurs in solar water heating systems that operate thermosiphonically.

In the past he had also worked in two research projects. The first project was funded by the Research Promotion Foundation of Cyprus and concerned the categorization of buildings in Cyprus according to their energy performance. The second project concerned the application and evaluation of advanced absorber coatings for parabolic trough collectors.

The main simulation tool he had used in most of his work is TRaNsient SYstem Simulation (TRNSYS) while he had also worked with HOMER and PVSyst.

He currently has 9 Journal publications and 12 Conference publications and his special fields of interest include wide range applications of Renewable Energy Sources systems and Energy Efficiency in buildings.

Georgios Florides is a Senior Lecturer in the Department of Mechanical Engineering and Materials Science and Engineering. He received his basic degree in Mechanical Engineering from the Higher Technical Institute and he was awarded an MPhil and a PhD by Brunel University, London, UK. He was employed by the Higher Technical Institute from 1975-2007 in various posts, in the Mechanical Engineering Department and in the Engineering Practice Department. He used to teach the theory and practice of Welding, Machine-shop, Bench-fitting and Plumbing.

His research activity focuses on the topic of Energy which includes studies and analysis of the energy requirements of buildings, measures to lower building thermal loads, design of LiBr-water absorption machines, modelling and simulation of absorption solar cooling systems and earth heat exchangers and heat pumps. He also studies the thermal behaviour of reptiles and scientifically constructs models of extinct animals.

Yiannis Vassiades was born in Nicosia, Cyprus. He graduated from the Mechanical Engineering department of the University of Manchester Institute of Science & Technology (UMIST) and he was awarded an honorary Bachelor's of Science degree. He continued his studies in the field of Refrigeration & Air-Conditioning at King's College London (KQC) and acquired a Master's of Science degree.

His previous professional experience includes working as a consultant Mechanical Engineer in both the private and the public sectors. He also worked in the mechanical contracting sector focused in the building construction industry.

Today, he holds the position of a Standards Officer at the Cyprus Organisation for Standardisation – CYS, promoting the application of European and international standards by Cyprus businesses. Frequently, he represents Cyprus in European Technical Committees of the European Organisation for Standardisation (CEN) for matters related to Mechanical Engineering. In addition, he acts as the Secretary of the national standardisation Technical Committee CYS/TC 13 "Thermal Solar Systems".

Thomas Parissis was born in Athens, Greece, on September 4, 1982. He holds a Diploma in Mining Engineering and Metallurgy from the National Technical University of Athens (NTUA) and an MSc in Metals and Energy Finance from Imperial College London for which he was awarded a scholarship by Eugenides Foundation in Greece.

During his career he held various positions in both production and commercial departments in industrial companies (ETEM S.A., Paperpack Tsoukaridis S.A.) and also offered consulting services regarding business development. At the moment he is working for RTD TALOS LTD as a Project Manager offering consulting and project management services to SMEs. In September 2011 he published his first book titled "Mine Expansion and Financial Implications" (ISBN 978-3845405643).

His special fields of interest include Energy, Mining, Metallurgy and Oil & Gas.

Alexandros Michaelides was born in Nicosia, Cyprus, on January 17, 1966. He holds a diploma in Mining Engineering and Metallurgy from the National Technical University of Athens (NTUA) and a Ph.D. degree in the sector of Metallurgy and Materials Technology of NTUA. During the period of 1990-1995 he worked as a researcher in the Laboratory of Physical Metallurgy of NTUA where he participated in a number of National and European research programs. Dr. Michaelides has presented his research work in numerous international conferences and he is the author/co-author of more than 15 research papers.

His employment experience includes the Cyprus Institute of Technology (CIT) where he was holding the position of the General Co-ordinator having under his supervision all of CIT's activities and RTD TALOS LTD, a development organisation dealing with technology and innovation issues, which was established by Dr. A. Michaelides in 2000.

His special fields of interest include Materials, Technology Transfer and Innovation.

Jan Erik Nielsen was born in Denmark on July 12, 1957. He graduated from the Danish Technical University in 1981. His employment experience include the Danish Technical University, the Danish Technological Institute, the private consultant company PlanEnergi and his own company SolarKey Int..

His special fields of interest are test methods, standards and certification for solar thermal systems and components and large scale solar thermal systems.

He is currently Operating Agent for IEA-SHC Task 43 "Solar Rating and Certification" and for IEA-SHC Task 45 "Large solar systems" (IEA-SHC is International Energy Agency – Solar Heating and Cooling).

2nd Conference on Power Options for the Eastern Mediterranean Region
07-08 October 2013, Nicosia, Cyprus (Paper No. POEM13/188)

Theoretical study of the application of Phase Change Materials (PCM) on the envelope of a typical dwelling in Cyprus

Gregoris P. Panayiotou, Soteris A. Kalogirou and Savvas A. Tassou

***Abstract*--In this work the application of Phase Change Materials (PCM) on the envelope of a dwelling in Cyprus is evaluated for the first time. The simulation process is carried out for a typical meteorological year using TRNSYS. Two types of simulations were carried out; the energy rate control and the temperature level control. The energy savings achieved by the addition of PCM compared to the base case (no insulation) ranged between 21.65-28.59%. When the PCM was combined with a common thermal insulation topology the maximum energy savings per year was 66.17%. In the second test the constructions containing PCM showed a better behaviour during summer conditions. Finally, the results of the optimum PCM case and the combined case were evaluated using Life Cycle Analysis. The results show that the PCM case is not yet considered to be very attractive due to the high initial cost.**

***Index Terms*--Cyprus, energy savings, free floating temperature, macroencapsulated, Phase Change Materials.**

I. Introduction

THE use of thermal storage in building envelopes is of great importance since it can smooth out daily temperature fluctuations and as a result lower the energy demand for heating and cooling. A way to increase thermal inertia of buildings is by integrating or including PCM on the buildings envelope and thus store energy in the form of latent heat. The main advantage of latent heat storage is that it has high storage density in small temperature interval [1]. The general principle of operation of PCM is that they store heat using their chemical bonds when they change phase from liquid to solid and release heat in the opposite way. The PCM that can be used in building applications should have a melting temperature range between 20-32^{o}C.

PCMs have been under study by many researchers around the world for over 30 years and thus many PCM are available in literature while some kinds are also commercially available by some companies such as BASF.

The main categories of PCM that can be used for this purpose are organic, inorganic and eutectics. In a very interesting and comprehensive work Cabeza et al. [1] reviewed all available PCM along with their classification, problems and possible solutions on their application in buildings. In their work Baetens et al. [2] also reviewed the state-of-the-art on the current knowledge of PCM applications in buildings.

In their work Tyagi and Buddhi [3] gave emphasis on the ways PCM can be applied in buildings such as PCM trombe wall, PCM wallboards, PCM shutters and PCM building blocks. Their results showed that there is a great potential on reducing the energy for covering heating and cooling demands.

A very promising application of microencapsulated PCM is their inclusion into construction materials such as concrete. This technology was studied in depth in the University of Lleida, Spain in 2004 but several drawbacks occurred. Consequently, Arce et al. [4] tried to overcome these problems. More specifically, the main drawback was the effect of the severe summer conditions (temperature and solar radiation) on the PCM that diminished their achievable potential benefits.

Although the inclusion of PCM into buildings materials such as concrete is considered to have numerous advantages it also has a very important drawback which lies to the fact that they can be used only in new buildings during the built up phase and not in existing buildings.

Additionally, in spite of the fact that a great number of studies have been performed for the incorporation of PCM in several construction materials only very few studies have been made for brick constructions. In his work, Alawadhi [5] numerically studied the application of PCM in bricks and obtained good results concerning the reduction of heat flow to the inner space during summer.

In a comprehensive work, Castell et al. [6] experimentally investigated the application of macroencapsulated PCM in two types of bricks namely conventional and alveolar brick. Their tests were performed under real conditions using five different cubicles located in Puigverd de Lleida. Two types of experiments were performed namely the free-floating temperature test and the controlled temperature test. The results showed good behavior, energy savings and technical viability. In spite of the promising results, a problem occurred during the experiments with the solidification of the PCM during night time. The authors suggested that this can be overcome by implementing a cooling strategy.

In this work the effect of the application of PCM in the thermal behavior of a typical dwelling in Cyprus will be theoretically investigated using several suitable models of the TRNSYS software library. Due to the complexity of the model used the simulations are carried out for a test cubicle and the results are then extrapolated for the typical dwelling.

G. P. Panayiotou is with the Department of Mechanical Engineering and Materials Science and Engineering, Cyprus University of Technology, (e-mail: Gregoris.Panayiotou@cut.ac.cy).

S. A. Kalogirou is with the Department of Mechanical Engineering and Materials Science and Engineering, Cyprus University of Technology, (e-mail: Soteris.Kalogirou@cut.ac.cy).

S. A. Tassou is with the School of Engineering and Design Brunel University, UK, (e-mail: Savvas.Tassou@brunel.ac.uk).

It should be noted that this is the first time the application of such materials is evaluated for Cyprus.

II. Model Design

The model design process is carried out using TRaNsient SYstem Simulation software (TRNSYS). The main component that simulates the PCM layer located in a structural element of a dwelling is Type1270. This is obtained from Thermal Energy System Specialists (TESS) Company and is described below. The other main component of this model is Type56 which simulates the building (test cubicle).

Type1270 is designed to interact with Type56 and can model a PCM located in any position in the thickness of a Type56 wall. The complete TRNSYS model developed is shown in Fig. 1. There are two options for setting the physical properties of the PCM the manual option and the built-in option. More specifically, in the manual option the user can specify the physical properties such as density, specific heat, melting temperature, freezing temperature, and latent heat of fusion. In the second option the user can utilize the built-in values of this component which concern a specific brand of PCM and the user may select a model number directly by setting a single parameter. It should be noted that Type1270 models a pure PCM (as opposed to a mixture of a PCM with an inert material). From a physical point of view, this means that the PCM is assumed to go through its freeze/thaw process at constant temperature, to have a constant specific heat in the solid phase and to have a constant specific heat in the liquid phase. This is done in order to simplify the analysis of the PCM by treating the phase change layer in bulk; it does not account for the wave front of freeze/thaw propagating through the material over time.

The PCM layer can be applied in any structural element of a house such as external walls, internal walls and roof. The selection of the structural element on which the PCM layer will be applied is very important since it changes the procedure of utilizing the model. Due to the specific weather conditions of Cyprus (hot dry summer) the model will only be applied to the external walls and the roof since this is considered to be much more important than applying the PCM on internal walls.

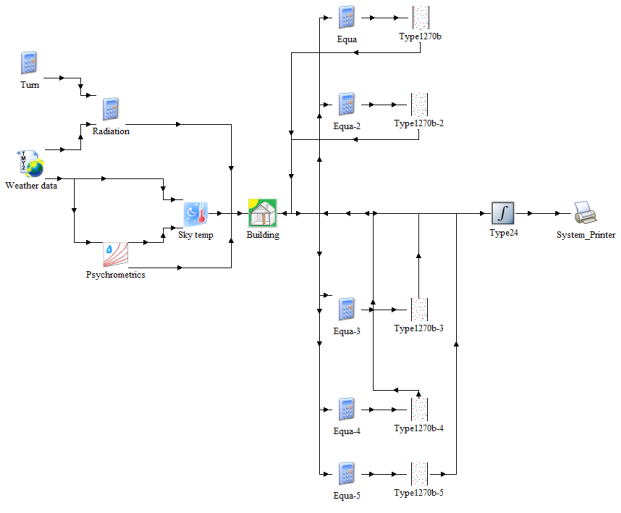

Fig. 1. Configuration of the complete TRNSYS model

III. Input Data

The dimensions of the test cubicle are 3m x 2m x 3m and the orientation of the various walls is depicted in Figure 2. As mentioned above the introduction of a direct airnode is necessary for the utilisation of Type 1270, thus in every orientation a direct airnode is introduced with a width of 0.01m as is also shown in Figure 2.

A. Position of the PCM layer

For the purposes of this work, the PCM layer is installed in three different positions in order to cover both existing and new dwellings. In the first one the PCM layer is placed in the middle of a double brick wall, which can be applied only in a new dwelling. In the second and third one, it is placed in the inner and the outer side of the wall between the brick and the plaster layer respectively and these can be applied in both new and existing dwelling). In all cases examined, the PCM layer applied on the roof of the building is positioned in the inner side of the concrete slab just behind the plaster. This is due to practical issues such as the protection of the material from walking on it and the fact that it cannot be placed inside the concrete slab in the form of this product; this can be done by using microencapsulated PCM as described in many articles in the literature.

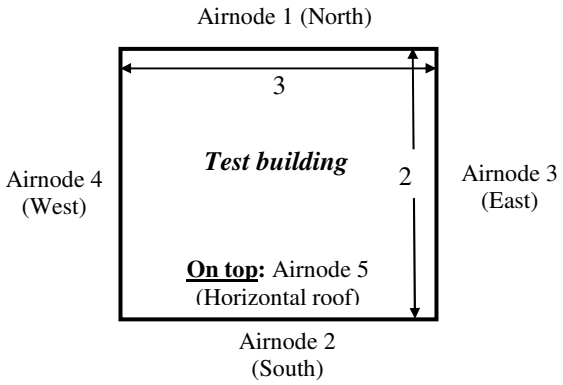

Fig. 2. Test building dimensions, orientation and adjacent airnodes

B. Physical properties and characteristics of the PCM used

During the simulation procedure the PCMs used were those of the built-in option. These PCMs concern specific commercial materials manufactured by Phase Change Energy Solutions Company and their series is BioPCmat™. These materials are the M27, M51 and M91 and their physical properties and characteristics are listed in Table I. These products are offered in four different melting temperatures namely 23, 25, 27 and 29°C.

TABLE I
PHYSICAL PROPERTIES AND CHARACTERISTICS OF THE PCM USED

Melting temperature*	29ºC		
Product	M27	M51	M91
Thickness (mm)	14		
Weight per unit area (kg/m^2)	2.49	3.56	6.15
Total unit thickness (mm)	6.35 - 8.89	10.16 - 15.24	25.4
Dimensions/Width (mm)	419.1		
Latent heat storage capacity (J/g)**	165 - 200		

As it can be seen, the main differences between these products is their weight per unit area (kg/m^2), which indicates the mass of the PCM within the product, and the total unit thickness. According to literature, the most commonly used melting temperatures for the application of PCM in hot environments is between 26-29ºC. Thus, in our case since Cyprus is a predominant hot weather environment the product with a melting temperature of 29ºC is employed.

IV. Methodology

Once the detailed model of the test cubicle is setup the simulation is carried for the 'basic case' where the building is considered to have no insulation installed in any structural element. The simulation is carried out for a complete typical year (8,760 hours) lasting from the 1st of January until the 31st of December.

For the definition of the optimum PCM layer case the energy rate control test is conducted with which the total energy demand for heating and cooling are estimated. More specifically, the results of each case examined are compared to the results of the 'basic case' in order to calculate the consequent energy savings. In this test the set temperature for heating and cooling are fixed to be 20ºC and 26ºC respectively while the power of the heating and cooling system is set to be unlimited in order to maintain comfort conditions at all times. The results are in the form of energy consumption per square meter per year (kWh/m^2/yr). As part of this work, the three different PCM products shown in Table I are evaluated in three different positions through modeling and simulation.

When the optimum case is defined then a second simulation is carried out using the temperature level control, which is a test showing the effect of applying the optimum PCM layer on the fluctuation of the mean air temperature of the cubicle. In this simulation the cubicle is considered to be unconditioned and thus the heating and cooling systems are both switched off. The results of this test are presented for the hottest day of summer which is the 26th of July according to the TMY2 for Nicosia, Cyprus.

Additionally, the temperature fluctuation of the test cubicle when it is insulated using common insulation materials used in Cyprus is presented. More specifically the insulation used is 3.5cm of thermal insulation plaster applied on the outer surface of the envelope of the test cubicle and 4cm of extruded polystyrene applied on the outer surface of the roof.

Finally, the insulated cubicle is combined with the optimum PCM case and the temperature fluctuation is calculated.

V. Results and Discussion

A. Energy rate control simulation

The results concerning the energy rate simulation are presented in Table II for all 9 PCM cases examined (3 types of materials times three positions examined). As it can be seen the optimum PCM case is that in position III with the 2991 material (29ºC melting temperature, material type 91) where the overall energy savings achieved is 28.59% (118.5 kWh/yr/m^2). Additionally, this case has the highest energy saving percentage in both heating and cooling which are 23.57% (62.585 kWh/yr/m^2) and 37.52% (55.925 kWh/yr/m^2) respectively. As expected, the energy savings in cooling are much higher than those of heating since essentially the PCM freezing/melting procedure is operating much better under the summer conditions. As aforementioned, the melting temperature of this PCM material is 29ºC and the only reason it is working in the winter is the fact that the space is conditioned and a part of the heat is absorbed by the PCM and released with a time lag and this is contributing to the decrease of the heating demand.

The reason for the superiority of this material against the others is that per unit area it has the higher weight and thus it contains a bigger amount of PCM material.

The results of the energy rate simulation concerning the insulated case and the combined case are presented in Table III where it can be observed that the combined (PCM and insulation) case achieves higher energy savings than the insulation case (66.17% instead of 60.95%) which is equal to 21.65 kWh/yr/m^2.

B. Temperature level control simulation

The results of the temperature level control simulation for the coldest day of winter (3-4th of February) and the hottest day of summer (26-27th of July) are depicted in Figures 3 and 4 respectively. In these figures the free-floating temperature for the base case (no insulation), the optimum PCM case, the insulation case and the combined case are plotted.

The optimum solution for the winter conditions is the insulation case followed by the combined case. The insulation case has a difference 2.5-3^{o}C when compared with the base case. The combined case has a difference between 0.8-1^{o}C when compared with the insulation case. When the combined case is compared with the base case shows a difference between 2-2.5^{o}C. The optimum PCM only case has a difference between -0.2-1^{o}C when compared to the base case. As can be seen between16:00-20:00 the mean air temperature of the PCM case is slightly lower (0.2^{o}C) than that of the base case a fact that can be attributed to the low response time of the PCM layer to the sudden rise of the temperature.

During summer time the optimum solution is the combined one where the PCM is combined with the insulation. It should also be noted that the mean air temperature of the test cubicle is much smoother than in all other cases and it is also 3-5ºC lower than the base case (no insulation). A very interesting thing to observe is the fact that the mean air temperature of the insulation case between 02:00-14:00 is exceeding the mean air temperature for the base case due to the fact that the heat that entered the space is trapped into the cubicle and it cannot escape. However, when a PCM layer is installed on the walls and roof this is not happening while this case is also slightly better than both insulation cases with a difference between 0.1-1.1ºC.

According to the results of both simulations the most attractive solution to be applied in a dwelling in Cyprus is the combined one, where the PCM is used together with thermal insulation and thus the benefits of using both materials are combined.

C. Life Cycle Analysis (LCA)

The LCA is carried out for a complete typical dwelling of Cyprus by extrapolating the results of the energy rate control

of the test cubicle. The typical dwelling used is that defined by Panayiotou [7] which is described below.

The typical dwelling is a single storey detached house located in Nicosia (Low mainland area) with a total area of 133 m^2. There are 4 occupants living in the dwelling and it does not have any kind of thermal insulation installed on its envelope. It consists of three bedrooms, a kitchen, a living room, a bathroom, and a dining room. For the production of DHW a solar water heating system is used while the heating and cooling energy demands are served by split type air-conditioning units. The windows of the dwelling are single-glazed with common aluminum frame; the main entrance door is made of wood while the kitchen door is made of aluminum frame and glass. Finally, the floor is in contact with the ground and is made of marble.

The cost of the optimum PCM case was estimated using the online calculator provided by the manufacturer [8] and was €22,490. According to the results of the LCA for the optimum PCM case (2991) the payback period of the investment is calculated to be 14 ½ years, the economic benefit at the end of the lifetime of the materials used, expressed as NPV, is €35,942 and the IRR is only 4%.

The cost of the combined case was calculated to be €23,259. The results of the LCA for the combined case showed that the payback period of the investment is calculated to be 7 ½ years, the economic benefit at the end of the lifetime of the materials used, expressed as NPV, is €110,416 and the IRR is 14%.

TABLE II
RESULTS OF THE ENERGY RATE CONTROL SIMULATION FOR THE PCMS EXAMINED

	PCM MATERIAL	**2927**		**2951**		**2991**	
		Q_{HEAT}	Q_{COOL}	Q_{HEAT}	Q_{COOL}	Q_{HEAT}	Q_{COOL}
POSITION I	Heating and cooling demand per m^2 (kWh/yr m^2)	224.88	99.89	224.82	99.57	224.73	99.28
	Total energy demand (kWh/yr m^2)	324.77		324.38		324.00	
	Heating and cooling energy savings per m^2 (kWh/yr m^2)	40.61	49.13	40.67	49.45	40.76	49.74
	Total energy savings (kWh/yr m^2)	89.74		90.13		90.51	
	Heating and cooling energy savings percentage per m^2 (% kWh/yr m^2)	15.30%	32.97%	15.32%	33.19%	15.35%	33.38%
	Total energy savings percentage (% kWh/yr m^2)	21.65%		21.74%		21.83%	
POSITION II	Heating and cooling demand per m^2 (kWh/yr m^2)	225.85	99.84	225.78	99.59	225.65	99.19
	Total energy demand (kWh/yr m^2)	325.70		325.37		324.84	
	Heating and cooling energy savings per m^2 (kWh/yr m^2)	39.64	49.18	39.71	49.43	39.84	49.83
	Total energy savings (kWh/yr m^2)	88.81		89.14		89.67	
	Heating and cooling energy savings percentage per m^2 (% kWh/yr m^2)	14.93%	33.00%	14.96%	33.17%	15.01%	33.44%
	Total energy savings percentage (% kWh/yr m^2)	21.43%		21.50%		21.63%	
POSITION III	Heating and cooling demand per m^2 (kWh/yr m^2)	203.01	93.42	202.97	93.26	202.91	93.10
	Total energy demand (kWh/yr m^2)	296.43		296.23		296.01	
	Heating and cooling energy savings per m^2 (kWh/yr m^2)	62.48	55.60	62.52	55.76	62.58	55.92
	Total energy savings (kWh/yr m^2)	118.08		118.28		118.50	
	Heating and cooling energy savings percentage per m^2 (% kWh/yr m^2)	23.53%	37.31%	23.55%	37.42%	23.57%	37.52%
	Total energy savings percentage (% kWh/yr m^2)	28.49%		28.54%		28.59%	

TABLE III
RESULTS OF THE ENERGY RATE CONTROL SIMULATION FOR THE INSULATION CASE AND THE COMBINED CASE

Examined case	**Insulation case**		**Combined case**	
	Q_{HEAT}	Q_{COOL}	Q_{HEAT}	Q_{COOL}
Heating and cooling demand per m^2 (kWh/yr m^2)	64.29	97.58	89.93	50.29
Total energy demand (kWh/yr m^2)	161.87		140.22	
Heating and cooling energy savings per m^2 (kWh/yr m^2)	201.20	51.44	175.56	98.73
Total energy savings (kWh/yr m^2)	252.64		274.29	
Heating and cooling energy savings percentage per m^2 (% kWh/yr m^2)	75.78%	34.52%	66.13%	66.26%
Total energy savings percentage (% kWh/yr m^2)	60.95%		66.17%	

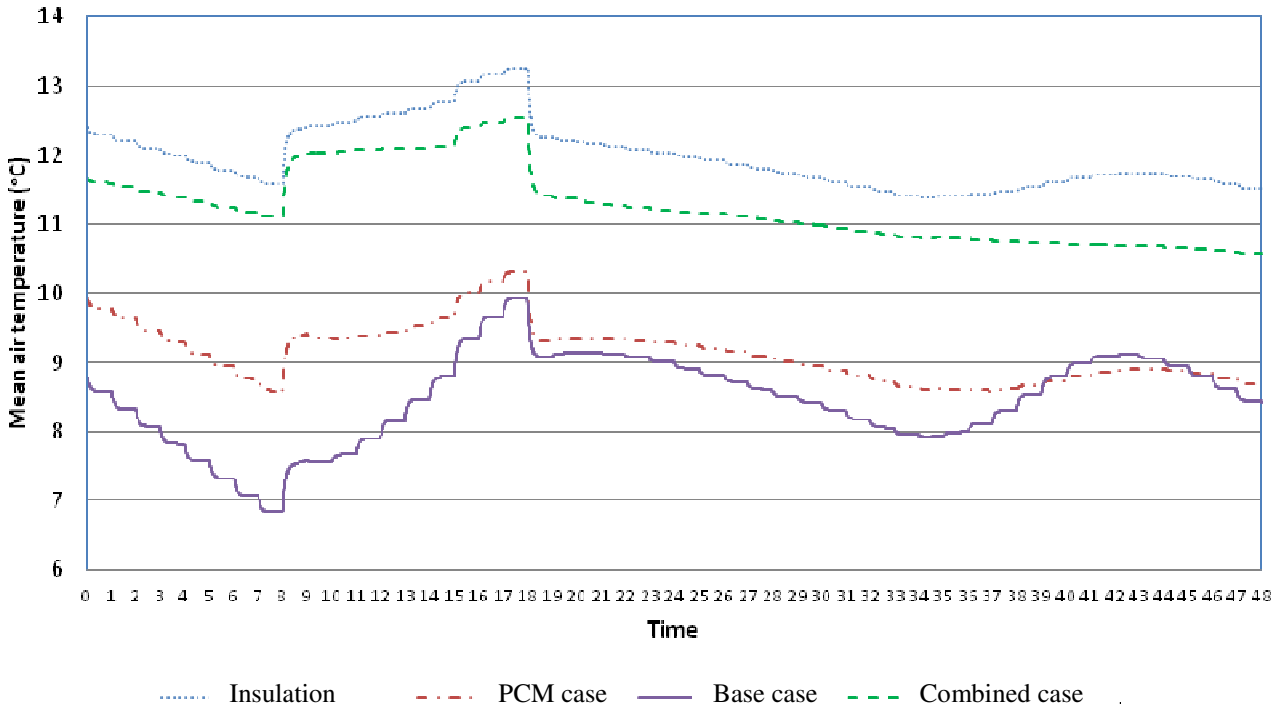

Fig. 3. Mean air temperature for all cases examined during the 3-4th of February

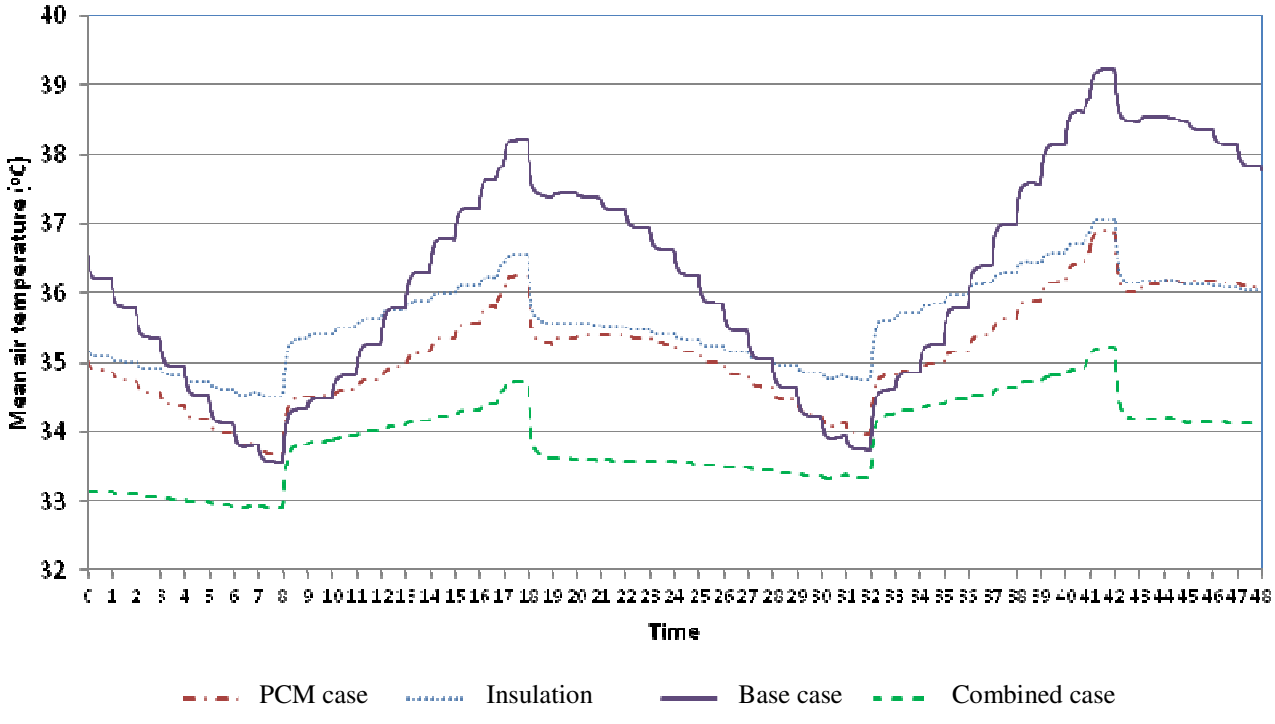

Fig.4. Mean air temperature for all cases examined during the 26-27th of July

VI. Conclusions

In this work the effect of the application of macroencapsulated PCM in the thermal behaviour of a test cubicle in Cyprus was theoretically investigated for the first time using a suitable model of TRNSYS software.

The results indicate that the application of such material in Cyprus is very attractive and advantageous since they operate very well in the specific weather conditions of Cyprus. More specifically, the optimum energy savings achieved by applying a PCM material with a melting temperature of 29ºC on the outer surface of a wall and inner side of the concrete slab just behind the plaster is 28.59% (118.5 kWh/yr/m^2). A very interesting option is when the PCM layer is used in combination with thermal insulation where the results showed that an energy saving of 66.17%

(274.29 kWh/yr/m^2) could be achieved while the energy savings achieved by the insulation alone is 60.95% (252.64 kWh/yr/m^2).

In the temperature rate control test the constructions containing PCM showed a better behaviour during the summer conditions, as expected, while during the winter conditions did not work very well. More specifically, during the winter conditions the optimum solution is the insulation only case followed by the combined case. The insulation case has a difference of 2.5-3^{o}C. When the combined case is compared with the base case the former show a difference between 2-2.5^{o}C. On the contrary during summer time the optimum solution is the combined case where the mean air temperature is 3-5ºC lower than the base case.

Finally, the results of the optimum PCM layer case and the combined case were economically evaluated using Life Cycle analysis (LCA) in order to define the IRR and the payback period of each investment. This is done by extrapolating the results of the test cubicle to a typical dwelling in Cyprus which as an area of 133 m^2. The results show that the PCM only case is not considered to be a very attractive solution, in monetary terms, due to the combination of the high initial cost and the annual money saving which result to a very long payback time which is estimated to be 14 ½ years and a rather low IRR (4%). This is changing when the PCM is used together with insulation where the payback period is reduced to 7 ½ years and the IRR is 13-14% respectively.

From the results of this work it can be concluded that the application of macroencapsulated PCM on the envelope of dwellings in Cyprus is considered to be a very attractive solution in terms of energy saving and comfort conditions while in monetary terms is not yet so attractive due to their high initial cost. Of course, this could change if the cost of PCM is decreased in the near future. It would be very interesting if in the near future an experimental unit is setup so as to validate experimentally the results of this work.

VII. References

[1] L.F. Cabeza, A. Castell, C. Barreneche, A. de Gracia, A.I. Fernández, Materials used as PCM in thermal energy storage in buildings: A review, Renewable and Sustainable Energy Reviews, vol. 15, pp. 1675-1695, 2011.

[2] R. Baetens, B. Petter Jelle, A. Gustavsen, Phase change materials for building applications: A state-of-the-art review, Energy and Buildings, vol. 42, pp. 1361-1368, 2010.

[3] V.V. Tyagi, D. Buddhi, PCM thermal storage in buildings: A state of art, Renewable and Sustainable Energy Reviews, vol. 11, pp. 1146-1166, 2007.

[4] P. Arce, C. Castellón, A. Castell, L.F. Cabeza, Use of microencapsulated PCM in buildings and the effect of adding awnings, Energy and Buildings, vol. 44, pp. 88-93, 2012.

[5] E.M. Alawadhi, Thermal analysis of a building brick containing phase change material, Energy and Buildings, vol. 40, pp. 351-357, 2008.

[6] A. Castell, I. Martorell, M. Medrano, G. Pérez, L.F. Cabeza, Experimental study of using PCM in brick constructive solutions for passive cooling, Energy and Buildings, vol. 42, pp. 534-540, 2010.

[7] Panayiotou G.P. (2013). Investigation of the energy behaviour of the residential building stock of Cyprus and application of commercial and innovative insulation materials towards to achieve a net-zero energy house. Unpublished Ph.D. Thesis, University of Brunel, London, UK.

[8] Phasechange. (2013), Retrieved May 01, 2013, from http://www.phasechange.com.au

VIII. Biographies

Soteris A. Kalogirou was born in Trachonas, Nicosia, Cyprus on November 11, 1959. He is a Senior Lecturer at the Department of Mechanical Engineering and Materials Sciences and Engineering of the Cyprus University of Technology, Limassol, Cyprus. He received his HTI Degree in Mechanical Engineering in 1982, his M.Phil. in Mechanical Engineering from the Polytechnic of Wales in 1991 and his Ph.D. in Mechanical Engineering from the University of Glamorgan in 1995. In June 2011 he received from the University of Glamorgan the title of D.Sc. He is Visiting Professor at Brunel University, UK and Adjunct Professor at the Dublin Institute of Technology (DIT), Ireland. For more than 25 years, he is actively involved in research in the area of solar energy and particularly in flat plate and concentrating collectors, solar water heating, solar steam generating systems, desalination and absorption cooling.

He has 41 books and book contributions and published 264 papers; 109 in international scientific journals and 155 in refereed conference proceedings. Until now, he received more than 4000 citations on this work and his h-index is 35. He is Deputy Editor-in-Chief of Energy, Associate Editor of Renewable Energy and Editorial Board Member of another eleven journals. He is the editor of the book Artificial Intelligence in Energy and Renewable Energy Systems, published by Nova Science Inc., co-editor of the book Soft Computing in Green and Renewable Energy Systems, published by Springer and author of the book Solar Energy Engineering: Processes and Systems, published by Academic Press of Elsevier.

Gregoris P. Panayiotou was born in Limassol, Cyprus on February 18, 1983. He graduated from the Technological Educational Institute of Athens first of his class as an Energy Technology Engineer in 2007. He had his MSc in Energy in Heriot-Watt University, Edinburgh where he graduated in 2008 with Distinction.

He is currently employed at Cyprus University of Technology as a Research Associate in a nationally funded project concerning the study and the deeper understanding of the thermosiphonic phenomenon that occurs in solar water heating systems that operate thermosiphonically.

In the past he had also worked in two research projects. The first project was funded by the Research Promotion Foundation of Cyprus and concerned the categorization of buildings in Cyprus according to their energy performance. The second project concerned the application and evaluation of advanced absorber coatings for parabolic trough collectors.

The main simulation tool he had used in most of his work is TRaNsient SYstem Simulation (TRNSYS) while he had also worked with HOMER and PVSyst.

He currently has 9 Journal publications and 12 Conference publications and his special fields of interest include wide range applications of Renewable Energy Sources systems and Energy Efficiency in buildings.

2nd Conference on Power Options for the Eastern Mediterranean Region
07-08 October 2013, Nicosia, Cyprus (Paper No. POEM13/189)

Experimental evaluation of Phase Change Materials (PCM) for energy storage in solar water heating systems

Soteris A. Kalogirou, Gregoris P. Panayiotou and Vasiliki Antoniou

***Abstract*-- In this paper the use of Phase Change Materials (PCM) in solar storage tanks is evaluated experimentally. Hot water storage tank is one of the main components of any solar water heating system. It is important to increase the storage capacity. The experimental investigations of the operation of the storage tank were carried out both during heating up and draw off phases. In all experiments the tanks with PCM show better performance than the tank without PCM. For the 50l tank used, two PCM canisters showed the optimum performance and a draw off profile up to 3 l/min. An additional experiment was performed with intermitted withdrawal of water from the storage tank so as to simulate the actual use. The results were also positive. It is concluded that the use of PCM improves storage capacity of such systems during draw-off.**

***Index Terms*—Cyprus, Latent heat, Paraffin, Phase Change Materials, Solar water heaters.**

I. Introduction

HOT water storage tank is the «heart» of any solar water heating system. For such systems it is important to keep the stratification, as this affects the effectiveness of the solar system operation. It is also true that the storage tank is not usually considered in the required detail during the system design. In this paper the use of Phase Change Materials (PCM) in solar storage tanks is considered in an attempt to improve the solar system operation. This should be done in such a way so as it will not change the production line of solar water heater manufacturers.

It is well known that PCMs have high latent heat of fusion and thus they are able to absorb energy during melting and release this energy during solidification. Therefore, the objective of this work is not only to improve the stratification characteristics of the storage tanks but also to reduce their volume by storing more energy in smaller volume.

For these tanks it is very important to create and keep the stratification both during heating up and during usage when there is a draw of water from the tank which is replaced by city mains cold water. This affects directly the effectiveness the solar system operation. With stratification it is possible to allow the hot water to "concentrate" at the top of the tank and the cold water at the bottom. As the water that returns to the solar collectors is from the bottom part of the storage tank, by keeping the stratification, relatively cold water is directed to the collectors and this increases their efficiency.

Many scientists have carried out research in this area. Cabeza et al. [1] used PCM to improve the stratification of a storage tank. In this work they investigated the choice of the right PCM for this application based on its thermodynamic and corrosive properties. They also studied the best configuration of the heat transfer vessel. Based on their experiments they found that the inclusion of a vessel with PCM at the top of the stratified storage tank there is an increase of the storage density at that area. The PCM used in this work had a melting temperature of 45°C and was contained in four small vessels.

Mazman et al. [2] in their work concluded that storage systems, separating the hot from the cold water through stratification, are very popular in applications of low and medium temperature. This happens because of the simplicity and low cost of these systems. With the inclusion of a PCM vessel at the top part of a stratified hot water storage tank, the storage density can be increased at this level, as well as the replacement of heat loss through the latent heat of solidification of the PCM. In this work the authors carried out experiments with a storage cylinder of 150 l capacity and a PCM vessel which has a diameter of 0.176 m and height of 0.315 m. They have also proved that a PCM with a mixture of paraffin and stearic acid (PS) gives the best results concerning the improvement of the thermal performance of the system.

Shmueli et al. [3] dealt with the numerical investigation of melting the PCM in a vertical cylindrical tube. The analysis aimed at an investigation of local flow and thermal phenomena by means of a numerical simulation which is compared to the previous experimental results. The numerical analysis is realized using an enthalpy–porosity formulation. The effect of various parameters of the numerical solution on the results is examined; in particular, the term describing the mushy zone in the momentum equation and the influence of the pressure–velocity coupling and pressure discretization schemes. Image processing of experimental results from the previous studies is performed, yielding quantitative information about the local melt fractions and heat transfer rates. The results showed quantitatively that at the beginning of the process, the heat transfer is by conduction from the tube wall to the solid phase through a relatively thin liquid layer. As the melting progresses, natural convection in the liquid becomes

S. A. Kalogirou is with the Cyprus University of Technology, (e-mail: Soteris.Kalogirou@cut.ac.cy).
G. P. Panayiotou is with the Cyprus University of Technology, (e-mail: Gregoris.Panayiotou@cut.ac.cy).
V. Antoniou is with University of Cyprus, (email: Va.antoniou@gmail.com)

dominant, changing the solid shape to a conical one, which shrinks in size from the top to the bottom.

Menon et al. [4] also studied the melting of commercial paraffin in vertical pipes using various values of the height of the PCM vessel. They have used copper pipes and the analysis was carried out using the Fourier, Stefan and Rayleigh numbers. A demonstration of melting was also carried out separately in a glass tube. They concluded that due to differences in density, the flow near the hot wall of the pipe was upward whereas the flow at near the cold interface of solid-liquid was downward.

Kousksou et al. [5] presented a numerical study for the use of phase change materials (PCMs) in solar-based domestic hot water (DHW) systems. The goal of the authors was to analyze the conditions under which there is no advantage of using PCMs in a DHW system and to propose improvements. The mathematical model considered describes the heat storage tank with PCM, collector, pump, controller and auxiliary heater. Realistic environmental conditions and typical end-user requirements were imposed. The authors concluded that the high sensitivity of the DHW system to the choice of first order design parameters, such as the PCM melting temperature, can lead to successful designs of PCM based DHW system that may be more efficient than a similar DHW system without PCM.

The objectives of the present work are to increase the storage capacity of a solar system or be able to reduce storage volume, thus increase the cost effectiveness of the system and to improve the formation and preservation of the stratification. For this purpose experimental investigations of the operation of the storage tank are carried out both during heating up and draw off.

II. Materials and Methods

In general, PCMs present high latent heat of melting or fusion. They absorb energy during melting and release this energy during solidification. For this purpose in the experiments we performed, paraffin is used with a melting temperature of 56°C. The latent heat of melting of the paraffin used is around 200 kJ/kg, which compared to specific heat capacity of water which is about 4.2 kJ/(kg.K) at the range of 20-60°C and dictates the amount of energy stored in water sensibly, offers 47 times more energy storage capacity than water.

The system consists of a storage tank 50 l in volume in which the PCM material was poured in liquid state in the special canister shown in Fig. 1. The canister can be inserted and hanged in a special attachment that is supported on a flange. The canister can hold about a liter of PCM material. This canister or a number of them (up to three) were hinged from the top of the tank on a special flange. This flange is of the type used in storage tanks to insert the immersion heater for auxiliary energy supply, thus its use is well known to the manufacturers of such storage tanks and is in line with their current practices.

To have regulated conditions an immersion electrical heater was used in the tank controlled by an immersion thermostat. During the experiments the temperature of the water entering the tank (make up water) and the temperature of the water outlet were continuously measured.

Fig. 1 Special container for the PCM and special flange used to insert the PCM-vessel in the tank.

The complete system is shown in Fig. 2. thermocouples are installed at inlet and outlets of the tank as shown to measure the temperature of the water flowing in and out of the system. As was mentioned above, for the testing of the system, the solar system is replaced by the immersion heater, used to heat the water to the required temperature.

Fig. 2 Tank with PCM equipped with thermocouples to measure temperature

The PCM used is the normal paraffin (wax), selected because of low cost, which has a fusion temperature of 56°C. This is chosen so to be near the safety temperature of 60°C for Legionella protection. An additional type of paraffin is also tried with a fusion temperature of 45°C.

III. Results and Discussion

A number of experiments were performed without and with PCMs installed in the tank. The numbers of experiments performed without and with PCM in the tank are shown in Tables 1 and 2 respectively. The maximum temperature is the setting of the immersion thermostat whereas the flow rate is the draw off flow rate during discharging. For the immersion thermostat a range of

temperatures are quoted as it was very difficult to achieve repeated similar settings when this value was changed manually. On the contrary it was relatively easy to use repeatedly the same flow rate controlled by a simple valve as shown in Fig. 2. In this case the water flow rate was measured with a measuring cylinder and a stop watch and could easily be slightly adjusted during the draw off process.

TABLE I EXPERIMENTS PERFORMED WITHOUT PCM IN THE TANK

Experiment No.	Maximum temperature (°C)	Flow rate (l/min)
1	80-85	6
2	70-75	6
3	80-85	1

TABLE II EXPERIMENTS PERFORMED WITH PCM IN THE TANK

Experiment No.	Maximum temperature (°C)	Flow rate (l/min)	No of PCM tanks
1	80 – 85	6	1
2	70 – 75	6	1
3	80 – 85	1	1
4	70 – 75	6	2
5	80 – 85	1	2
6	70 – 75	3	2
7	70 – 75	1	2
8*	80 – 85	1	1
Notes: * different PCM material with a fusion temperature of 45°C			

Fig. 3 Typical charging and discharging behaviour of the tank.

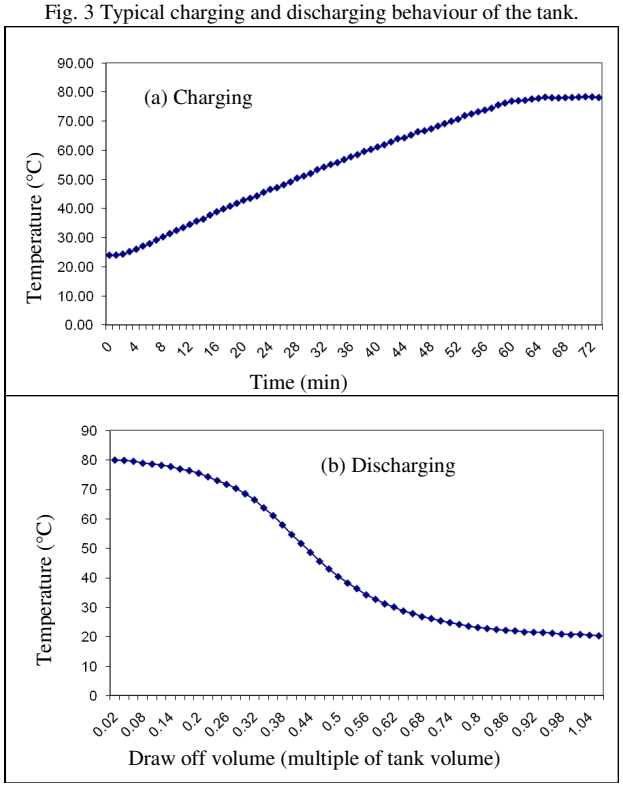

In all experiments carried at different initial storage temperatures, number of PCM canisters (1-3) and draw-off rates (1, 3 and 6 l/min) the tanks with PCM show superior performance than the same tank operating in similar conditions without PCM, as depicted from the results shown in the following figures. Typical charging (heating up) and discharging (draw off) performance is shown in Fig. 3.

What is of interest here is the temperature evolution of the water in the tank. During charging the temperature increases smoothly until the thermostat limit of the immersion heater is reached as shown in Fig. 3(a). During this time the PCM melts smoothly as the tank water temperature rises with a delay according to the mass of the PCM used. The discharge profile is of interest with respect to the amount of water drawn off before a useful temperature of about 40°C is reached. The more volume we get with water above this value the better is the draw off characteristics of the tank. The performance of the system presented in Fig. 3 is not very clear with respect to the enhancement achieved because of the use of the PCM. What is of interest is the comparison between the results from the different experiments. Most important are the comparative graphs during system draw-off for different flow rates of systems with and without PCM in the tank. It should be noted that in order to save space only a few typical results are presented in this paper.

The performance of the system during draw-off for initial water temperature of 85°C, draw off flow rate of 6 l/min without PCM (red line) and for initial water temperature of 75°C with 2 PCM vessels in the tank and same draw off flow rate (blue line), are shown in Fig. 4. The advantage of the system with PCM is obvious, despite the different initial temperature. The extra benefit in hot water volume at a minimum useful temperature of 40°C is shown with dotted lines.

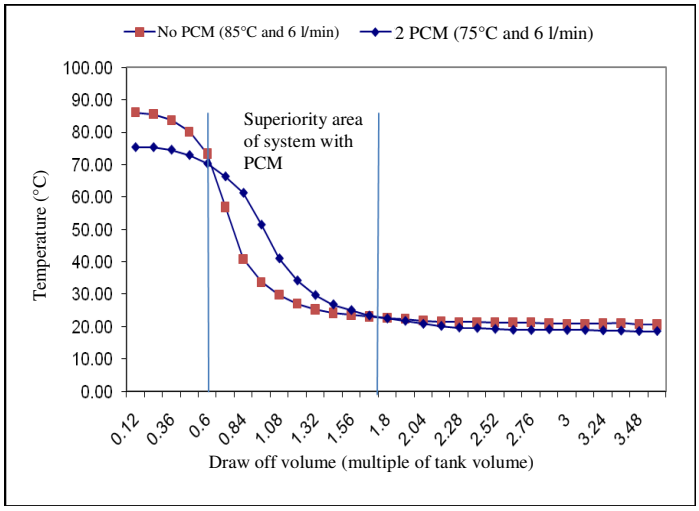

Fig. 4. Comparison of the performance without and with PCM in the tank for initial water temperature of about 80°C and flow rate of 6 l/min

The performance of the system during draw-off for initial water temperature of 80°C, draw off flow rate of 1 l/min without PCM (red line) and for initial water temperature of 71°C with 2 PCM vessels in the tank and same draw off flow rate (blue), are shown in Fig. 5. The advantage of the system with PCM is obvious, despite the different initial temperature. Again here the extra benefit in hot water volume at a minimum useful temperature of 40°C is shown with dotted lines and as can be seen there is a significant increase to what is shown in Fig. 4, which was at a higher draw off flow rate.

As can be seen from above, the draw off flow-rate effects the performance of the system drastically because if a high number is used the flow is very quick and reduced somewhat the effect of the PCM. The initial flow rate of 6 l/min is according to the relevant ISO standard. A comparison for the performance of the system for a flow rate of 1 (red line), 3 (blue line) and 6 (green line) l/min is shown in Fig. 6. As can be seen the system is capable of giving water of higher temperature for more time at low flow rates. Furthermore, the total volume of water is obtained for the higher initial temperature shown in Fig. 4 and it seems that a good compromise between the three flow rates is the middle one, i.e., the flow rate of 3 l/min. Additionally, it was found that the initial value of 6 l/min is not suitable for such a small volume tank.

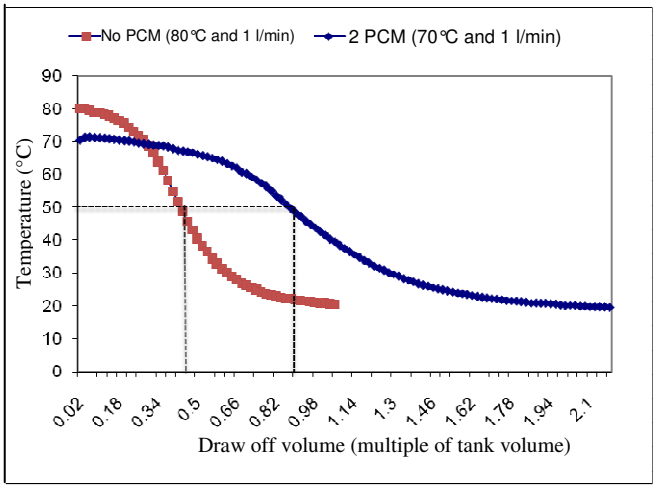

Fig. 5. Comparison of the performance without and with PCM in the tank for initial water temperature of about 77°C and flow rate of 1 l/min

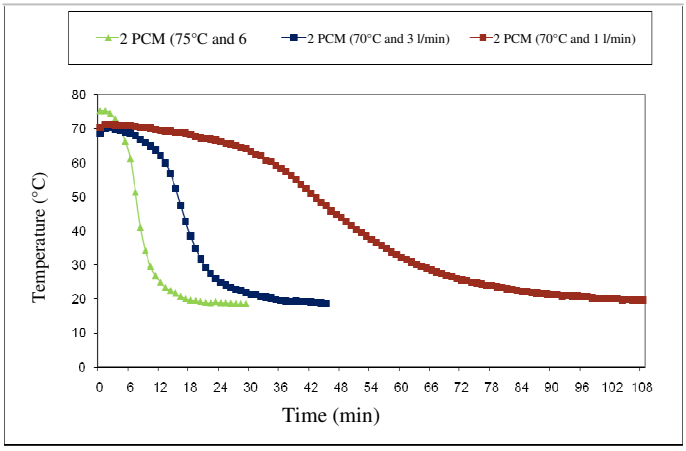

Fig. 6. Comparison of the performance of 2 PCM vessels in the tank for initial water temperature of about 70°C and flow rate of 6, 3 and 1 l/min

A comparison of the system with the same initial temperature of about 76°C and draw off flow rate of 6 l/min for 1 (blue line) and 2 (red line) PCM vessels in the tank is shown in Fig. 7. As can be seen the 2-PCM system is better.

It can be concluded from this work that for the tank used, which is of 50 liters capacity, the best performance is obtained with two PCM canisters and a draw off profile up to 3 l/min. The flow of 6 l/min seems to be excessive for small storage volume as the high flow rate does not allow the PCM to give its heat of solidification to the flowing water.

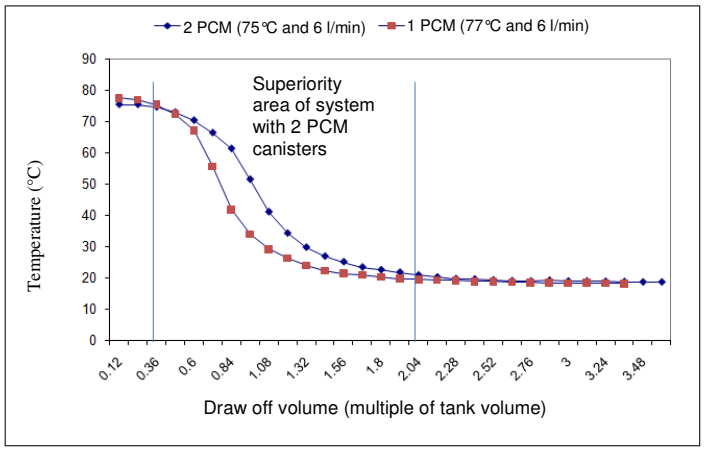

Fig. 7. Comparison of the performance of 1 and 2 PCM vessels in the tank for initial water temperature of about 76°C and flow rate of 6 l/min

Another comparative performance presented is the use of the different type of PCM as shown in experiment 8 in Table 2. The results are shown in Fig. 8 for a draw off flow of 1 l/min and about 80°C initial temperature. The performance of the new PCM is much lower than the PCM used in the experiments so far.

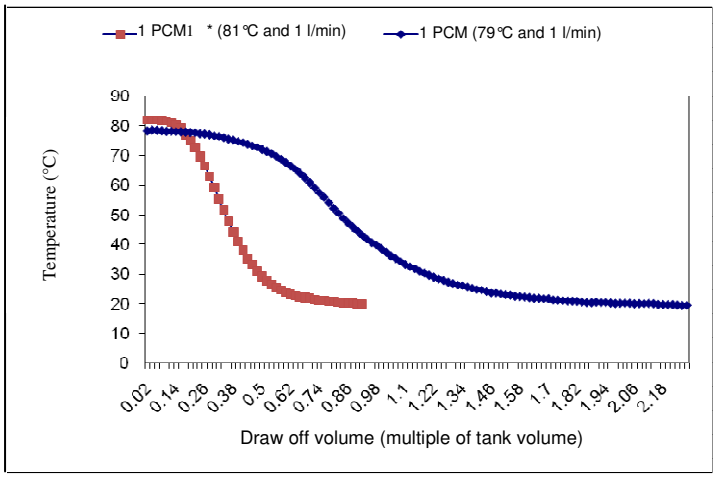

Fig. 8. Comparison of the performance of 1 PCM vessel in the tank of different type of PCM material for initial water temperature of about 80°C and flow rate of 1 l/min

Another experiment performed is the intermitted withdrawal of water from the storage tank so as to simulate the actual use. During this test a number of thermocouples were inserted in a special tube just outside the PCM canister so as to record the temperature of water at different heights in the tank. The locations of the thermocouples are shown in Fig. 9. The procedure was to warm the water in the storage tank and then apply a water draw off rate of 10 liters every 15 minutes.

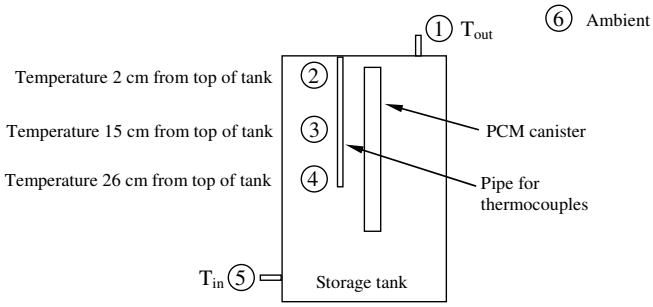

Fig. 9 Location of thermocouples for the intermitted draw off experiment

The results are shown graphically in Fig. 10. For this experiment one PCM canister was used. The draw off pattern can be seen clearly from the blue line which is the temperature of the water drawn from the tank. As can be seen when the water flow stops the energy contained in the PCM recovers somewhat the temperature of the water into the storage tank that would be much lower when the cold water replacing the hot water draw off is mixed with the water remaining into the storage tank after a few minutes. This is more clearly shown from line #4 which presents the temperature at the centre of the storage tank. Additionally, the temperature at point #2 at the top of the tank, shows that the PCM preserves stratification which is one of the main objectives in using PCM in storage tanks. This is proved by the fact that the temperature at this point is higher than the temperature of the water drawn from the cylinder (#1).

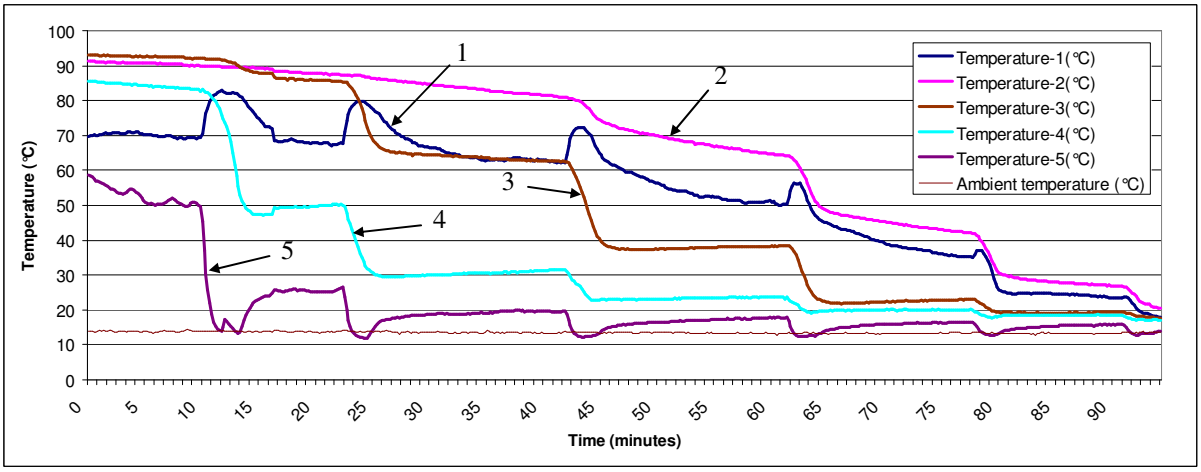

Fig. 10 Performance of the system at intermitted draw off (temperature numbers correspond to Fig. 9)

IV. Conclusions

The objective of this work is to increase the storage capacity of a solar system or to be able to reduce the storage volume and by doing so to increase the cost effectiveness of the system. It is also required to have better formation and preservation of stratification. The experimental investigations of the operation of the storage tank were carried out both during heating up and draw off.

From this work it is concluded that the use of PCM gives improved storage capacity of the system and considerable improvement of system behaviour during draw-off. This was done in a cost effective method without getting away from the production line of the manufacturers of storage tanks. Additionally, it was proved that the flow of 6 l/min seems to be excessive for small storage volume.

Another experiment performed was the intermitted withdrawal of water from the storage tank so as to simulate the actual use. The results were also positive and proved the effectiveness of the PCM to preserve stratification.

In the future, we plan to use 6 l/min flow in a larger volume cylinder and use the cylinder with PCM on a real solar water heating system to investigate its performance during real solar operation.

V. Acknowledgment

The authors are grateful to the EU COST Action TU0802: ‘‘Next generation cost effective phase change materials for increased energy efficiency in renewable energy systems in buildings (NeCoE-PCM)” for its sponsorship.

VI. References

[1] L.F. Cabeza, M. Nogues. J. Roca, M. Ibanez. PCM research at the University of Lleida (Spain), IEA,ECES IA Annex 17, 6th Workshop, Arvika, Sweden, 2004.

[2] M. Mazman, L.F. Cabeza, H. Mehling, M. Nogues, H. Evliya, H.O. Paksoy. Utilization of phase change materials in solar domestic hot water systems, Renewable Energy, Vol. 34, pp. 1639 – 1643, 2009.

[3] H. Shmueli, G. Ziskind, R. Letan. Melting in a vertical cylindrical tube: Numerical investigation and comparison with experiments, International Journal of Heat and Mass Transfer, Vol. 53, No. (19-20), pp. 4082-4091, 2010.

[4] A.S. Menon, M.E. Weber, A.S. Mujumdar. The dynamics of energy storage for paraffin wax in cylindrical containers, Canadian Journal of Chemical Engineering, Vol. 61, pp. 647-653, 1983.

[5] T. Kousksou, P. Bruel, G. Cherreau, V. Leoussoff, T. El Rhafiki. PCM storage for solar DHW: From an unfulfilled promise to a real benefit, Solar Energy, Vol. 85, No. 9, pp. 2033-2040, 2010.

VII. Biographies

Soteris Kalogirou was born in Trachonas, Nicosia, Cyprus on November 11, 1959. He is a Senior Lecturer at the Department of Mechanical Engineering and Materials Sciences and Engineering of the Cyprus University of Technology, Limassol, Cyprus. He received his HTI Degree in Mechanical Engineering in 1982, his M.Phil. in Mechanical Engineering from the Polytechnic of Wales in 1991 and his Ph.D. in Mechanical Engineering from the University of Glamorgan in 1995. In June 2011 he

received from the University of Glamorgan the title of D.Sc. He is Visiting Professor at Brunel University, UK and Adjunct Professor at the Dublin Institute of Technology (DIT), Ireland. For more than 25 years, he is actively involved in research in the area of solar energy and particularly in flat plate and concentrating collectors, solar water heating, solar steam generating systems, desalination and absorption cooling.
He has 41 books and book contributions and published 264 papers; 109 in international scientific journals and 155 in refereed conference proceedings. Until now, he received more than 4000 citations on this work and his h-index is 35. He is Deputy Editor-in-Chief of Energy, Associate Editor of Renewable Energy and Editorial Board Member of another eleven journals. He is the editor of the book Artificial Intelligence in Energy and Renewable Energy Systems, published by Nova Science Inc., co-editor of the book Soft Computing in Green and Renewable Energy Systems, published by Springer and author of the book Solar Energy Engineering: Processes and Systems, published by Academic Press of Elsevier.

Gregoris Panayiotou was born in Limassol, Cyprus on February 18, 1983. He graduated from the Technological Educational Institute of Athens as an Energy Technology Engineer in 2007. He had his MSc in Energy in Heriot-Watt University, Edinburgh where he graduated in 2008 with Distinction.

He is currently employed at Cyprus University of Technology as a Research Associate in a nationally funded project concerning the study and the deeper understanding of the thermosiphonic phenomenon that occurs in solar water heating systems that operate thermosiphonically. In the past he had also worked in two other research projects. The first one was a project funded by the Research Promotion Foundation of Cyprus, as a Post Graduate Associate, concerning the categorization of buildings in Cyprus according to their energy performance and the second one concerned the application and evaluation of advanced absorber coatings for parabolic trough collectors.

The main simulation tool he had used in most of his work is that of Transient System Simulation Software (TRNSYS) while he had also worked with HOMER and PVSyst.

He currently has 9 Journal publications and 12 Conference publications and his special fields of interest include wide range applications of Renewable Energy Sources and systems and Energy Efficiency in buildings.

Vasiliki Antoniou holds a Bachelors Degree in Mechanical Engineering and Materials Science and Engineering from Cyprus University of Technology (CUT). She graduated in 2011 with a tentative ranking to top 10%. In summer 2009, she represented CUT on a Renewable Energy Systems workshop (Erasmus Intensive Program) in Patra, Greece. During her final year undergraduate thesis, she worked on the use of phase change materials (PCM) for the improvement of energy storage in water heating systems. She is currently pursuing her Masters Degree in Petroleum Engineering at University of Cyprus.

2nd Conference on Power Options for the Eastern Mediterranean Region
07-08 October 2013, Nicosia, Cyprus (Paper No. POEM13/190)

Experimental investigation of the performance of a Parabolic Trough Collector (PTC) installed in Cyprus

Soteris A. Kalogirou and Gregoris P. Panayiotou

***Abstract*-- In this paper the performance of a Parabolic Trough Collector located at the Archimedes Solar Energy Laboratory is evaluated. It has an aperture area of 14.4 m^2, a concentration ratio of 13.7 and can be operated up to 200°C. The collector aperture is 1208 mm and the receiver pipe is stainless steel 304 L with a diameter of 28mm, coated with selective coating (absorptance: 0.93, emitance: 0.18). The collector in orientated with its axis in the E-W direction tracking the sun in the N-S direction. The advantages of this tracking mode are that very little collector adjustment is required during the day and the full aperture always faces the sun at noon. A programmable tracking system is responsible for keeping the collector focused at all times. The collector is connected to a 300 liters hot water storage tank. The water is pressurized to avoid boiling in the receiver. The performance obtained is very satisfactory and agrees with the performance curve given by the manufacturer.**

***Index Terms*—Concentrating collectors, parabolic trough collectors, performance testing, sun tracking.**

I. Nomenclature

A_a	Gross collector aperture area, m^2
A_r	Receiver area, m^2
C	Concentration ratio
c_1	First-order coefficient of the collector efficiency (W/m^2-°C)
c_2	Second-order coefficient of the collector efficiency (W/m^2-°C^2)
c_p	Specific heat capacity, J/kg-K
F_R	Heat removal factor
G_B	Solar beam radiation, W/m^2
m	Mass flow rate, kg/s
Q_u	Rate of useful energy collected, W
T_a	Ambient temperature, K
T_i	Collector inlet temperature, K
T_o	Collector outlet temperature, K
U_L	Overall heat loss coefficient, W/m^2-K

Greek

η	Collector thermal efficiency
η_o	Collector optical efficiency
ΔT	Temperature difference [$=T_i-T_a$], K

S. A. Kalogirou is with the Cyprus University of Technology, (e-mail: Soteris.Kalogirou@cut.ac.cy).

G. P. Panayiotou is with the Cyprus University of Technology, (e-mail: Gregoris.Panayiotou@cut.ac.cy).

II. Introduction

A parabolic trough collector (PTC), as shown in Fig. 1, is made by bending a sheet of reflective material into a parabolic shape. A metal black pipe, covered with a glass tube to reduce heat losses, is placed along the focal line of the receiver. When the parabola is pointed towards the sun, the parallel rays incident on the reflector are reflected and focused onto the receiver tube. The concentrated radiation reaching the receiver tube heats the fluid that circulates through it, thus transforming the solar radiation into useful heat. It is sufficient to use a single axis tracking of the sun and thus long collector modules are produced [1, 2].

The receiver of a parabolic trough collector is linear. Usually a tube is placed along the focal line to form an external surface receiver (see Fig. 1). The size of the tube, and therefore the concentration ratio, is determined by the size of the reflected sun image and the manufacturing tolerances of the trough. The surface of the receiver is typically plated with selective coating that has a high absorptance for solar irradiation but a low emittance for thermal radiation.

A glass cover tube is usually placed around the receiver tube to reduce the convective heat loss from the receiver, thereby further reducing the heat loss coefficient. A disadvantage, resulting from the use of the glass cover tube, is that the reflected light from the concentrator must pass through the glass to reach the receiver, adding a transmittance loss of about 0.9, when the glass is clean. The glass envelope usually has an anti-reflective coating to improve transmissivity. One way to further reduce convective heat loss from the receiver tube and thereby increase the performance of the collector, particularly for high temperature applications, is to evacuate the space between the glass cover tube and the receiver. The total receiver tube length of PTCs is usually from 25 m to 150 m.

Parabolic trough collectors are the most mature solar technology to generate heat at temperatures up to 400°C for solar thermal electricity generation or process heat applications. The biggest application of this type of system is the Southern California power plants, known as Solar Electric Generating Systems (SEGS), which have a total installed capacity of 354 MWe [3]. SEGS I is 14 MWe, SEGS II-VII are 30 MWe each and SEGS VIII and IX are 80 MWe each.

New developments in the field of parabolic trough collectors aim at cost reduction and improvements of the technology. In one system the collector can be washed automatically thus reducing drastically the maintenance cost, which is the mostly used process required [1].

Cyprus does not have any sources of energy and depends exclusively on imported oil for its energy needs. The only inexhaustible natural source of energy that Cyprus poses abundantly is solar energy. It is well known that other forms of renewable energy, like the wind energy, wave energy and biomass have limited potential in Cyprus. Solar energy can be converted directly to electrical energy using photovoltaic panels or to thermal energy using a large variety of thermal solar collectors. The type of collectors to use in each application depends on the operating temperature of the process to connect on the solar system. Cyprus Government decided to erect a solar thermoelectric power generation station with a capacity of about 50 MW, which is a very correct movement since the development of large scale photovoltaic parks would be a very expensive solution. The collector system to be used in this case is most probably the parabolic trough, so it is very important to have a collector of this type installed and examined under the prevailing weather conditions of the island.

The purpose of this paper is to present the collector erected at the premises of the Cyprus University of Technology and the performance evaluation of the collector. This is the first time a parabolic trough collector is installed on the island and the findings should prove valuable for future uses of this type of collector.

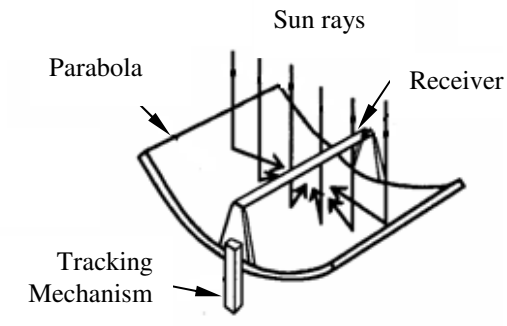

Fig. 1. Schematic of a parabolic trough collector

III. COLLECTOR SYSTEM DESCRIPTION

The collector is installed at the Cyprus University of Technology and in particular at the Archimedes Solar Energy Laboratory, which is located at the roof of the Mechanical Engineering Department of the university. The collector is supplied from the Australian company NEP-SOLAR and has the characteristics presented in Table 1.

The collector installed has a length of 12.2 m and consists of galvanized steel mounts, lightweight, stiff and precise parabolic reflector panels manufactured from reinforced polymeric material, a structurally efficient galvanized steel torque tube, a tubular receiver and an accurate solar tracking system.

TABLE I
CHARACTERISTICS OF THE COLLECTOR INSTALLED AT ARCHIMEDES SOLAR ENERGY LABORATORY

Parameter	Value
Collector Length	1993 mm
Collector width	1208 mm
Parabola focal distance	647 mm
Mirror reflectivity	93.5%
Receiver material	Stainless steel 304 L
Receiver external diameter	28 mm
Receiver internal diameter	25 mm
Glass tube transmittance	0.89
Selective coating absorptance	0.93
Selective coating emittance	0.18

The collector is orientated with its axis in the East-West direction. The advantages of this tracking mode are that very little collector adjustment is required during the day and the full aperture always faces the sun at noon. A dedicated computer-operated tracking mechanism is responsible for keeping the collector focused at all times. The motor of the tracking system is shown in Fig. 2, showing also the central support of the collector.

Photos of the collector installed are shown in Fig. 3. The photo at the left is with the collector at the focus position during operation and the photo on the right is for the collector at the park position. In this second photo the use of the flexible connectors at each side of the collector are clearly shown.

Fig. 2. Photo of the motor of the tracking system and central support of the collector (at park position).

Fig. 3. Photos of the PTC (a) on focus position , (b) at park position

The collector is connected to a hot water storage tank which has a capacity of 300 litres. The collector fluid used in the tests is water, which is pressurized to avoid boiling in the receiver. The complete plumbing circuit schematic is shown in Fig. 4 whereas a photo of the storage tank is shown in Fig. 5. As can be seen provisions are made to connect the system to the storage tank and to any other process for future experiments planned.

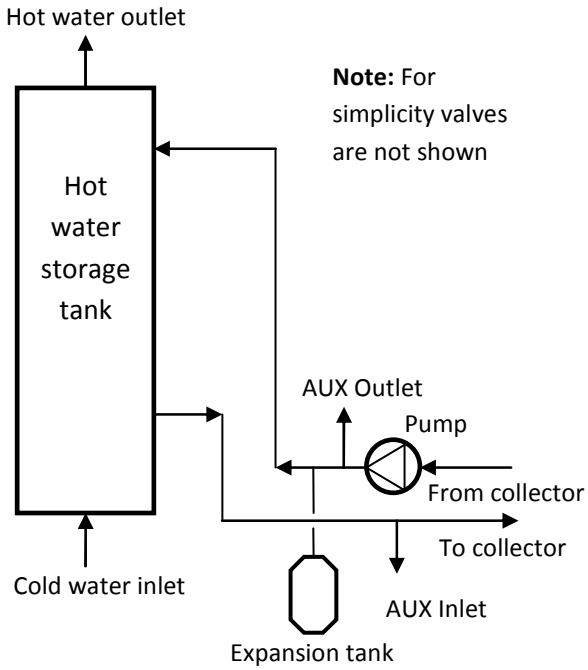

Fig. 4. Schematic diagram of the collector circuit

Fig. 5. Photo of the storage tank

IV. Collector Thermal Efficiency

The thermal performance of solar collectors can be determined by experimental performance testing under control conditions. In general, experimental verification of the collector characteristics is necessary in order to determine the thermal efficiency of the collector.

There are a number of standards, which describe the testing procedures for the thermal performance of solar collectors. The most well-known are the ISO 9806-1:1994 [4] and the ANSI/ASHRAE Standard 93:2010 [5]. These can be used to evaluate the performance of both flat-plate and concentrating solar collectors. The thermal performance of a solar collector is determined partly by obtaining values of instantaneous efficiency for different combinations of

incident radiation, ambient temperature and inlet fluid temperature. This requires experimental measurement of the rate of incident solar radiation falling onto the solar collector as well as the rate of energy addition to the transfer fluid as it passes through the collector, all under steady state or quasi-steady state conditions.

ISO 9806-1:1994 and ASHRAE Standard 93:2010 give information on testing solar energy collectors using single-phase fluids and no significant internal storage. The data can be used to predict the collector performance in any location and under any weather conditions where load, weather and insolation are known.

For steady state testing, the environmental conditions and collector operation must be constant during the testing period. For the concentrating collector tests, the following parameters need to be measured:

- Beam solar irradiance at the collector plane, G_B
- Ambient air temperature, T_a
- Fluid temperature at the collector inlet, T_i
- Fluid temperature at the collector outlet, T_o
- Fluid flow rate, $\dot{m}$

In addition, the gross collector aperture area, A_a, is required to be measured with certain accuracy. The collector efficiency, based on the gross collector aperture area is given by:

$$\eta = \frac{\dot{m}c_p(T_o - T_i)}{A_a G_B} \tag{1}$$

The collector performance test is performed under steady-state conditions, with steady radiant energy falling on the collector surface, steady fluid flow rate and constant wind speed and ambient temperature. When a constant inlet fluid temperature is supplied to the collector, it is possible to maintain a constant outlet fluid temperature from the collector. In this case, the useful energy gain from the collector is calculated from:

$$Q_u = \dot{m}c_p(T_o - T_i) \tag{2}$$

The useful energy collected from a concentrating solar collector is also given by [1]:

$$Q_u = F_R\left[G_B\eta_o A_a - A_r U_L(T_i - T_a)\right] \tag{3}$$

Moreover, the thermal efficiency is obtained by dividing Q_u by the energy input (A_aG_B). Therefore:

$$\eta = F_R\eta_o - \frac{F_R U_L(T_i - T_a)}{CG_B} \tag{4}$$

It should be noted that in concentrating collectors the beam radiation is used G_B as these collectors can utilize only this type of radiation [2].

For a collector operating under steady irradiation and fluid flow rate, the factor F_R and U_L are nearly constant. Thus, Eq. (4) plots as a straight line on a graph of efficiency versus the heat loss parameter $(T_i - T_a)/G_B$ as shown in Fig. 6. The intercept (intersection of the line with the vertical efficiency axis) equals to $F_R\eta_o$. The slope of the line, i.e., the efficiency difference divided by the corresponding horizontal scale difference, equals to $-F_RU_L/C$.

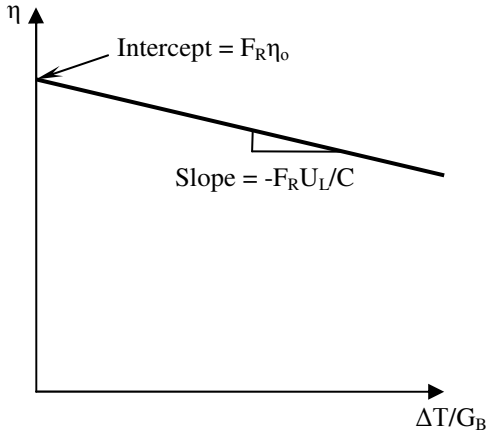

Fig. 6. Typical performance curve of a concentrating solar collector

If experimental data of collector heat delivery at various temperatures and solar conditions are plotted, with efficiency as the vertical axis and $\Delta T/G_B$ is used as the horizontal axis, the best straight line through the data points correlates the collector performance with solar and temperature conditions. The intersection of the line with the vertical axis is where the temperature of the fluid entering the collector equals the ambient temperature, and collector efficiency is at its maximum. The results of this experimental procedure for the collector installed are shown in Fig. 7. As can be seen the first order performance equation obtained is given by:

$$\eta = 0.6481 - 0.4832\frac{\Delta T}{G_B} \tag{5}$$

It should be pointed out that the slope of the concentrating collector performance curve is much smaller than the one for the flat plate ones. This is because the thermal losses are inversely proportional to the concentration ratio, C, as shown in Eq. (4). This is the greatest advantage of the concentrating collectors, i.e., the efficiency of concentrating collectors remains high at high inlet temperature; this is why this type of collectors is suitable for high temperature applications.

In reality, the heat loss coefficient U_L in Equation (4) is not constant but is a function of collector inlet and ambient temperatures. Therefore:

$$F_R U_L = c_1 + c_2(T_i - T_a) \tag{6}$$

Applying Equation (6) in Equation (3) we have:

$$Q_u = F_R\left[G_B\eta_o A_a - A_r c_1(T_i - T_a) - A_r c_2(T_i - T_a)^2\right] \tag{7}$$

Therefore, the efficiency can be written as:

$$\eta = F_R\eta_o - \frac{c_1(T_i - T_a)}{CG_B} - \frac{c_2(T_i - T_a)^2}{CG_B} \tag{8}$$

By applying this method of testing the curve obtained is as shown in Fig. 8.

As shown in Fig. 8 the second order performance equation of the collector is:

$$\eta = 0.6289 - 0.1887\frac{\Delta T}{G_B} - 2.7069\frac{\Delta T^2}{G_B} \quad (9)$$

As can be seen from both Figs 7 and 8 the testing is not performed at high collector inlet temperatures, so these results can be considered as preliminary. The circles shown in Fig. 8 represent the values given by the manufacturer, so the performance of the collector can be considered as valid and in conformity to the performance equation given by the manufacturer.

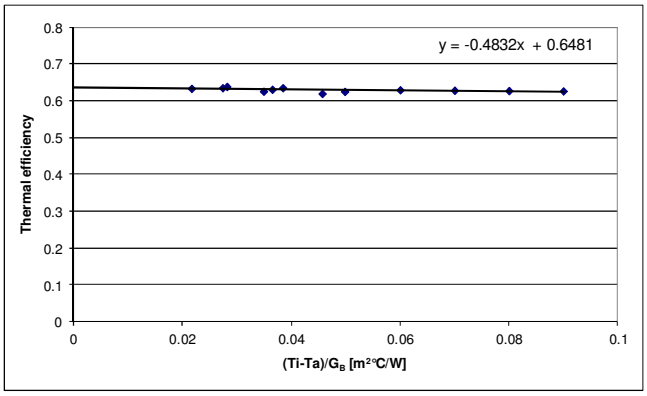

Fig. 7. First order performance curve of the collector installed at Archimedes Solar Energy Laboratory

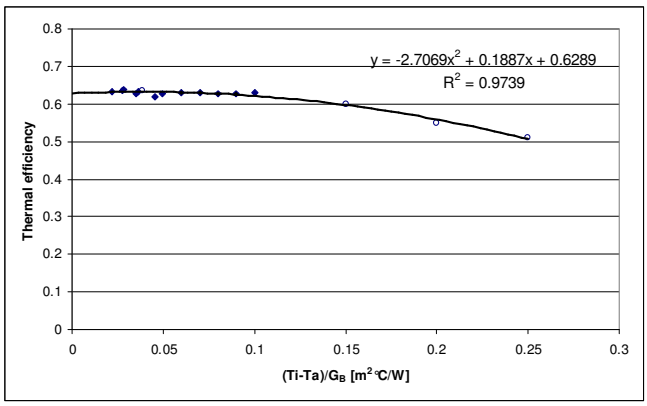

Fig. 8. Second order performance curve of the solar collector installed at Archimedes Solar Energy Laboratory

V. Conclusions

The collector installed at the Archimedes solar energy laboratory is first presented as well as the complete plumbing system. The measurements performed concern the instantaneous values of solar beam radiation, ambient temperature, collector inlet and outlet temperatures, and mass flow rate. It should be noted that this type of collector, because of the concentration, utilize only beam radiation. The collector performance was obtained by estimating the collector efficiency at various inlet fluid temperatures. By plotting the collector efficiency against the temperature rise (inlet minus ambient temperature) divided by the beam solar radiation, a straight line is obtained. The basic parameters obtained from this performance testing are the intercept and slope of the collector performance line. A second order performance curve is also obtained from the same results. Both show a satisfactory performance.

VI. References

[1] S.A. Kalogirou, 2009. *Solar energy engineering: Processes and systems*, ISBN: 978-0-12-374501-9, Academic Press, Elsevier Science.

[2] S.A. Kalogirou, Solar thermal collectors and applications, *Progress in Energy and Combustion Science*, Vol. 30, No. 3, pp. 231-295, 2004.

[3] D.W. Kearney, H.W. Price, Solar thermal plants - LUZ concept (current status of the SEGS plants), *Proceedings of the 2nd Renewable Energy Congress*, Reading UK, Vol. 2, pp. 582-588, 1992.

[4] ISO 9806-1:1994, Test Methods for Solar Collectors – Part 1: Thermal Performance of Glazed Liquid Heating Collectors Including Pressure Drop, 1994.

[5] ANSI/ASHRAE Standard 93:2010. Methods of Testing to Determine the Thermal Performance of Solar Collectors, 2003.

VII. Biographies

Soteris A. Kalogirou was born in Trachonas, Nicosia, Cyprus on November 11, 1959. He is a Senior Lecturer at the Department of Mechanical Engineering and Materials Sciences and Engineering of the Cyprus University of Technology, Limassol, Cyprus. He received his HTI Degree in Mechanical Engineering in 1982, his M.Phil. in Mechanical Engineering from the Polytechnic of Wales in 1991 and his Ph.D. in Mechanical Engineering from the University of Glamorgan in 1995. In June 2011 he received from the University of Glamorgan the title of D.Sc. He is Visiting Professor at Brunel University, UK and Adjunct Professor at the Dublin Institute of Technology (DIT), Ireland. For more than 25 years, he is actively involved in research in the area of solar energy and particularly in flat plate and concentrating collectors, solar water heating, solar steam generating systems, desalination and absorption cooling.

He has 41 books and book contributions and published 264 papers; 109 in international scientific journals and 155 in refereed conference proceedings. Until now, he received more than 4000 citations on this work and his h-index is 35. He is Deputy Editor-in-Chief of Energy, Associate Editor of Renewable Energy and Editorial Board Member of another eleven journals. He is the editor of the book Artificial Intelligence in Energy and Renewable Energy Systems, published by Nova Science Inc., co-editor of the book Soft Computing in Green and Renewable Energy Systems, published by Springer and author of the book Solar Energy Engineering: Processes and Systems, published by Academic Press of Elsevier.

Gregoris P. Panayiotou was born in Limassol, Cyprus on February 18, 1983. He graduated from the Technological Educational Institute of Athens first of his class as an Energy Technology Engineer in 2007. He had his MSc in Energy in Heriot-Watt University, Edinburgh where he graduated in 2008 with Distinction.

He is currently employed at Cyprus University of Technology as a Research Associate in a nationally funded project concerning the study and the deeper understanding of the thermosiphonic phenomenon that occurs in solar water heating systems that operate thermosiphonically.

In the past he had also worked in two research projects. The first project was funded by the Research Promotion Foundation of Cyprus and concerned the categorization of buildings in Cyprus according to their energy performance. The second project concerned the application and evaluation of advanced absorber coatings for parabolic trough collectors.

The main simulation tool he had used in most of his work is TRaNsient SYstem Simulation (TRNSYS) while he had also worked with HOMER and PVSyst.

He currently has 9 Journal publications and 12 Conference publications and his special fields of interest include wide range applications of Renewable Energy Sources systems and Energy Efficiency in buildings.

2nd Conference on Power Options for the Eastern Mediterranean Region
07-08 October 2013, Nicosia, Cyprus (Paper No. POEM13/191)

Optimization of Thermosiphon Solar Water Heaters working in a Mediterranean Environment

Soteris A. Kalogirou and Rafaela A. Agathokleous

***Abstract*-- Cyprus is currently the leading country in the world with respect to solar water heaters installations. The increase of the thermosiphon solar water heaters usage over the last years makes this subject to be very important for further investigation. The main objective of this study is to investigate the parameters affecting the system's performance in order to find the optimum design to increase the performance of the system. For this purpose, a number of riser and header tube diameters were considered ranging from 6 mm to 35 mm, slopes from latitude from 20° to 90°, distances between the top of the collector to the bottom side of the storage tank ranging from -30 to +20 cm and the vertical or horizontal tank position. The system is modelled using TRNSYS and simulated with the Typical Meteorological Year (TMY) of Nicosia, Cyprus.**

It was observed that, the current typical system is not the optimum case and its operation can be further improved. The optimum system obtained from the simulations has a flat plate collector with header pipe of 22 mm and 20 riser pipes of 8 mm diameter, sloped at 40° and the distance between the top of the collector and the bottom of the storage tank is -20 cm. These findings should prove valuable for the collector and systems designers and manufacturers.

***Index Terms*— thermosiphon, flat plate collector, riser tubes, solar water heater, optimization, solar thermal.**

I. Nomenclature

A_c	Area of the collector (m^2)
F_R	Heat removal factor
I	Solar radiation (W/m^2)
Q_u	Rate of useful energy (W)
T_a	Ambient temperature (K)
T_{fi}	Inlet fluid temperature (K)
U_L	Overall heat loss coefficient (W/m^2K)
Greek	
τ	Transmittance of the cover plate
α	Absorbance of the absorber plate

This work was carried out as part of a research project co-funded by the Research Promotion Foundation (RPF) of Cyprus under contract ΤΕΧΝΟΛΟΓΙΑ/ΕΝΕΡΓ/0311(ΒΙΕ)09 and the European Regional Development Fund (ERDF) of the EU.

S. A. Kalogirou is with the Department of Mechanical Engineering and Materials Science Engineering, Cyprus University of Technology, Cyprus (e-mail: soteris.kalogirou@cut.ac.cy).

R. A. Agathokleous is with the Department of Mechanical Engineering and Materials Science Engineering, Cyprus University of Technology, Cyprus (e-mail: rafaela.agathokleous@cut.ac.cy).

II. Introduction

As the energy crisis escalates and the price of gas and electricity increase, there is an inevitable shift to solar energy, which can be considered to be a unique opportunity to create a new clean energy economy. There are several solar energy technologies such as the solar thermal systems for heating, cooling and water heating, solar photovoltaics for electricity generation, solar architecture and artificial photosynthesis. Solar technologies tap directly into the infinite power of the sun and use that energy to produce heat and power. Lately, solar power systems are experiencing a rapid growth worldwide and mostly in the countries with high amount of solar radiation. Studies show that the worldwide leader country for the use of solar water heating systems per capita is Cyprus [1].

Solar radiation maps from all over the world show that Cyprus is between the countries with the highest amount of solar radiation. The mean daily global solar radiation varies from about 2.3 kWh/m^2 in the cloudiest months of the year December and January, to about 7.2 kWh/m^2 in July [1]. The graph in Figure 1 presents the solar thermal capacity of glazed water collectors in operation per 1000 inhabitants by the end of 2011 in the world. As can be observed, Cyprus is the leader country in terms of installed capacity of water collectors in operation per 1000 inhabitants. Between the EU countries, Cyprus had the highest installed collector capacity with 541.2 kWth/1000 inhabitants and then Austria and Greece with 355.7 kWth/1000 inhabitants and 268.2 kWth/1000 inhabitants, respectively. On the other hand, UK seems not to use those systems very much, as their installed capacity in 2011 was only 7.3 kWth 1000 inhabitants [1].

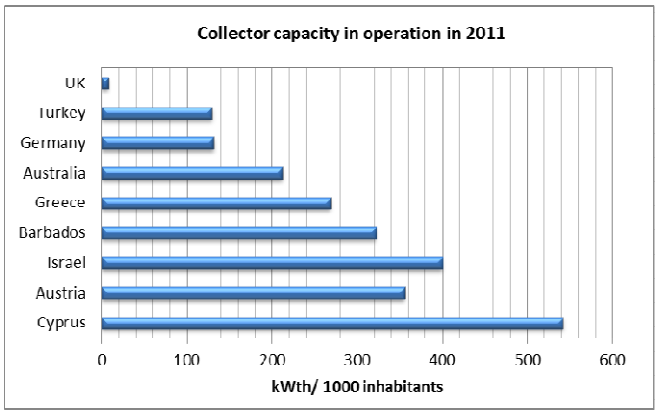

Fig. 1. Solar thermal capacity in operation per 1000 inhabitants in 2011 in Europe [1]

III. System under investigation

The majority of the systems installed in Cyprus are of the thermosiphon type. Consequently, this study is focused on the performance of SWH systems, which operate thermosiphonically with natural circulation of water, in the Mediterranean environment of Cyprus. A typical system in Cyprus uses 3 m^2 of flat plate collectors, 160 lt storage tank, its collectors are usually inclined at 45° from horizontal. The collector has 10 copper riser tubes of 15 mm diameter, header tubes with a diameter of 28 mm and its absorber plate is also made from copper [2]. The storage tank was used to be vertically installed in the past few years while in the new systems is installed horizontally.

The characteristics of the flat plate collector considered in this study for the typical thermosiphon system, are shown in Table I.

TABLE I
THE CHARACTERISTICS OF A FLAT PLATE COLLECTOR FOR THERMOSIPHON SYSTEM IN CYPRUS.

Parameter	Characteristics
Riser pipe diameter	15 mm
Riser tubes material	copper
Number of riser pipes	10
Header pipe diameter	28 mm
Absorber plate thickness	0.5 mm
Glass type	4 mm low iron glass
Collector insulation	Fiberglass 30 mm sides
	Fiberglass 50 mm back
Glazing	Low iron glass
External casing material	Galvanized sheet

The general aim of this study was to investigate the design parameters affecting the performance of the SWH systems operating thermosiphonically. However, the main objective of this paper is to investigate through modeling and simulation possible configurations of the thermosiphonic system, which will optimize the performance of the system. For this purpose, the following parameters are investigated:

- Number of riser tubes
- Riser tube diameters from 6 mm to 28 mm
- Header tube diameters from 8 mm to 35 mm
- Slopes from 20-90°, 5° step size
- Distances between the top of the collector and the bottom side of the storage tank, from -30 to +20 cm
- Horizontal or vertical storage tank
- Length of the riser and header pipes in different collector's shapes

The investigation of the thermosiphonic system will allow us to propose a new improved system design with higher efficiency than the existing systems.

Initially, the system was modelled using TRNSYS and simulated with the Typical Meteorological Year (TMY) of Nicosia, Cyprus. To achieve the objectives mentioned above, each of the design parameters under investigation needs to be examined separately. This is because in this way, the effect of each parameter on the system's efficiency will be recorded.

IV. The performance of the collector

The basic performance parameter is the collector thermal efficiency. The solar collector thermal efficiency is defined as the ratio of the useful thermal energy leaving the collector to the usable solar irradiance falling on the aperture area given by:

$$\eta = \frac{\dot{Q}_u}{A_c x I} \tag{1}$$

Where $\dot{Q}_u$ = Rate of useful energy output (W)
A_c= Area of the collector (m^2)
I= Solar irradiance falling on the collector's area (W/m^2)

However, it is more convenient to express the collector performance in terms of the fluid inlet temperature. This equation is known as the classical Hottel-Whillier-Bliss (HWB) equation to predict the collector performance as follows:

$$\dot{Q}_u = A_c F_R \left[(\tau\alpha) I - U_L (T_{fi} - T_a) \right] \tag{2}$$

Where τ= Transmittance of the cover plate
α= Absorptance of the absorber plate
T_a= Ambient temperature (°C)
U_L= Overall heat loss coefficient ($W/m^2 \cdot K$)
T_{fi}: Inlet fluid temperature (°C)
F_R: Heat removal factor

From Eq. (2), the collector efficiency in terms of the heat removal factor is given by:

$$\eta = \frac{\dot{Q}_u}{A_c I} = F_R \left[(\tau\alpha) - U_L \frac{T_{fi} - T_a}{I} \right] \tag{3}$$

Heat removal factor of the collector, F_R is affected only by the solar collector characteristics, the fluid type and the flow rate through the collector. Consequently, from the equation of fluid temperature distribution, the heat removal factor can be expressed as:

$$F_R = \frac{\dot{m} C_p}{A_c U_L} \left[1 - \exp\left(\frac{A_c U_L F'}{\dot{m} C_p} \right) \right] \tag{4}$$

Where F′is the collector efficiency factor, a measure of how enhanced the heat transfer is between the fluid and the absorber plate. The collector efficiency factor F' is given by the following equation and all the dimensions are illustrated in Figure 2.

$$F' = \frac{\frac{1}{U_L}}{W \left[\frac{1}{U_L (D + (W - D) F)} + \frac{1}{C_b} + \frac{1}{\pi D_i h_{fi}} \right]} \tag{5}$$

Where F is the standard fin efficiency given by:

$$F = \frac{\tanh\left[m\frac{(W-D)}{2}\right]}{m\frac{(W-D)}{2}} \quad (6)$$

Where C_b= Bond conductance (W/m K)
k= thermal conductivity of the absorber (W/m K)
h_{fi}=convective heat transfer coefficient between the fluid and tube wall (W/m^2·K)

And the factor *m* is given by:

$$m = \sqrt{\frac{U_L}{k\delta}} \quad (7)$$

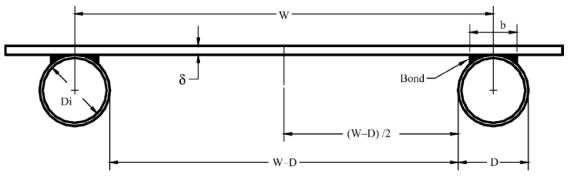

Fig. 2. Flat plate and tube configuration [3]

Morrison and Braun [4] studied the modeling and operation characteristics of thermosiphon solar water heaters with vertical or horizontal storage tanks. They found that the system performance is maximized when the daily collector volume flow is approximately equal to the daily load flow, and the system with horizontal tank did not perform as well as that with a vertical one. This model has also been adopted by the TRNSYS simulation program. According to this model, a thermosiphon system consisting of a flat-plate collector and a stratified tank is assumed to operate at a steady state. The system is divided into N segments normal to the flow direction, and the Bernoulli's equation for incompressible flow is applied to each segment. For steady-state conditions the sum of pressure drop at any segment is:

$$\Delta P_i = \rho_i g h_{fi} + \rho_i g H_i \quad (8)$$

And the sum of the pressure changes around the loop is 0; that is,

$$\sum_{i=1}^{N} r_i h_{fi} = \sum_{i=1}^{N} \rho_i H_i \quad (9)$$

where
ρ_i = density of any node calculated as a function of local temperature (kg/m^3).
h_{fi} = friction head drop through an element (m).
H_i = vertical height of the element (m).
For each time interval the thermosiphon flow rate must uniquely satisfy Eq. (9).

The friction head loss in pipes is given by:

$$H_f = \frac{fLv^2}{2dg} + \frac{kv^2}{2g} \quad (10)$$

where
d = pipe diameter (m).
v = fluid velocity (m/s).
L = *length* of pipe (m).
k = fitting loss coefficient.
f = friction factor.

The friction factor f, is equal to:

$$f = 64 / Re \text{ for } Re < 2000 \quad (11)$$
$$f = 0.032 \text{ for } Re > 2000$$

An estimate of the thermosiphon head may be found based on the relative positions of the tank and the flat-plate collectors as shown in Fig. 3. The thermosiphon head generated by the differences in density of fluid in the system may be approximated by making the following assumptions:

1. There are no thermal losses in the connecting pipes.
2. Water from the collector rises to the top of the tank.
3. The temperature distribution in the tank is linear.

Therefore, according to the dimensions indicated in Fig. 3, the thermosiphon head generated is given by:

$$h_T = \frac{1}{2}(S_i - S_o)\left[2(H_3 - H_1) - (H_2 - H_1) - \frac{(H_3 - H_5)^2}{(H_4 - H_5)}\right] \quad (12)$$

Where S_i and S_o is the specific gravity of the fluid at the collector inlet and outlet respectively. Here only direct circulation thermosiphon systems are considered in which water is the collection fluid. The specific gravity according to the temperature (in °C) of water is given by:

$$S = 1.0026 - 3.906\text{x}10^{-5}T - 4.05\text{x}10^{-6}T^2 \quad (13)$$

Therefore, as can be observed from the above equations, the performance of a SWH system depends on many factors such as the construction of the collector and the arrangement of the system, mainly with respect to the distance between the top of the solar collector and the bottom of the storage tank and the solar collector slope, which affects both the energy collected and the hydrostatic pressure of the system.

V. Technical Work Preparation

As already mentioned, the considerations of the parameters that affect the performance of the thermosiphon solar water heater have been made using TRNSYS simulation program through the use of component Type 45. There have been many attempts in the literature to model thermosiphon solar water heaters and most of them have failed to accurately represent the system [5]. However, the only program available and used by most researchers in this field is the TRNSYS Type 45. One such validation which concerns Cypriot manufactured units is from Kalogirou and Papamarcou in 2000 [6].

The various configurations evaluated, concerning header and riser pipes diameters are shown in Table II. As can be seen, riser pipe diameters vary from very small up to one size smaller pipe diameter than the header pipe.

Table II
Header and Riser Pipe Diameter Variations

Header diameter (mm)	Riser diameters (mm)
15	6, 8, 10, 12
22	6, 8, 10, 12, 15
28	6, 8, 10, 12, 15, 22
35	6, 8, 10, 12, 15, 22, 28

Although all the parameters affecting the system's performance were conducted using TRNSYS environment, there was a need to define previously some inputs needed for the program for each case under investigation. For the collector, those parameters are the heat removal factor of the collector F_R, the collector heat loss coefficient U_L, the slope of performance curve ($F_R \cdot U_L$) and the intercept of the efficiency curve F_R (τα). After the estimation of the inputs needed for the program, the design parameters were examined one by one and their effect in the performance of the system was recorded.

It is important to mention that the effect of the variations of a parameter on the system's efficiency was conducted by comparing the efficiency of the system every time that a change in the design was simulated.

A. *Calculation of the Heat Removal Factor - F_R*

Initially the collector performance characteristics were used to estimate the heat removal factor (F_R), the overall heat loss coefficient (U_L) and he transmittance absorptance product (τα) of the collector. The heat removal factor depends on the collector efficiency factor, which depends on the heat loss coefficient, diameter of the riser tubes, distance between the riser tubes, collector fin efficiency and the internal riser pipe convection heat transfer coefficient. The heat transfer coefficient depends on the flow rate and is estimated from the Nusselt number, which is a function of the Reynolds number that determines the type of flow in the riser tubes.

Subsequently, the new heat removal factor is estimated for the corresponding riser pipe internal diameter as well as the number of riser tubes, which is determined by trial and error so as the resulting type of flow (Reynolds number) to remain the same in order to have an adequate circulation of water in the collector. By using this new heat removal factor the input parameters $F_R(\tau\alpha)$ and $F_R U_L$ were calculated as well as the number of riser tubes, which are used in the various simulations. The values obtained from these calculations are shown in Table III. The bold letters show the specifications of the collectors at the typical thermosiphonic system with vertical storage tank.

TABLE III
MODIFIED COLLECTOR CHARACTERISTICS AND NUMBER OF RISER TUBES USED IN SIMULATIONS

Riser Diameter (mm)	**Number of riser tubes**	**F_R (τα)**	**$F_R U_L$ (kJ/hr m^{2o}C)**
6	29	0,836	25,263
8	20	0,825	24,94
10	16	0,817	24,685
12	13	0,807	24,395
15	**10**	**0,792**	**23,94**
22	7	0,765	23,13
28	5	0,731	22,103

Subsequently, the simulations started firstly by defining the efficiency of the typical system without any modifications. This will then be compared to the efficiency of the system each time that a different parameter is tested.

B. *Typical system with vertical storage tank*

The system set as typical in Cyprus that simulated at the beginning has a total aperture are 3 m^2 (2 panels), with storage tank capacity 160 lt installed vertically. The collector slope angle for this system was taken to be 45°. The collector for the typical system has 10 riser pipes made of copper with 15 mm diameter and header pipes with diameter 28 mm. As mentioned before, the slope of performance curve ($F_R U_L$) and the intercept of the efficiency curve F_R (τα) for this system, are shown in bold letters in Table III.

The simulations carried out for the typical system with vertical tank, showed that the efficiency of the system was 40.13%.

This system is going to be the basis for comparison for the next simulations. Every parameter under investigation was applied on this system, one each time, and the best result selected to be remain constant for the next simulation to find the optimum design at the end.

Then, the typical system was simulated with the various combinations of the header and riser pipes diameters in order to identify the best combination of riser and header pipes diameter and the required number of riser diameters that gives the higher system's performance.

C. *Riser and Header pipes diameter and number of risers*

The data from Table III were used as inputs to the program for each size of header diameter and its related riser pipes number and diameter as presented in Table II in order to record the efficiency of the system for each situation. The simulations have been separated in four sets of runs for header diameters 15 mm, 22 mm, 28 mm and 35 mm for the appropriate sizes of riser tubes in each group.

It is important to mention that the tested system was the typical one with 45° slope of the collector and the bottom of the tank was in the same height with the top of the collector as shown in Fig. 3. The only variables in each simulation were the size of the riser and header tubes and the number of riser tubes to keep constant the flow of the water. Consequently, the performance for each simulation was recorded and the highest one was selected to be kept constant for the next simulations.

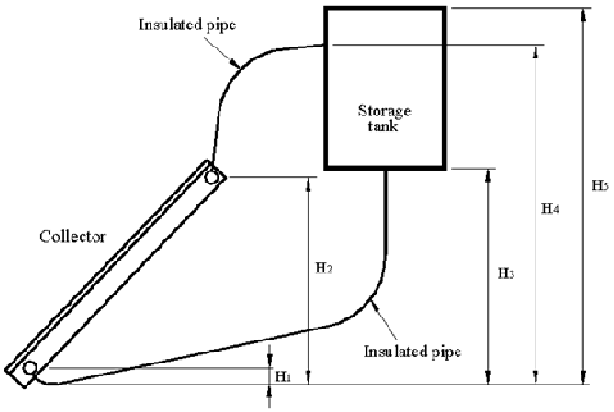

Fig. 3. Schematic diagram of a thermosiphon solar water heater.

In this way we were able to find the combination of the number of riser pipes and their diameter size as well as the header diameter that give higher performance of the system.

The results from the simulations are shown in Fig. 4 and as can be observed, a small riser diameter of 8 mm is the optimum. The smallest pipe of 6 mm is not selected because the systems employed in Cyprus are usually open, circulating the water supplied to the user directly into the collector, which may create scaling problems. A header diameter of 22 mm is selected in terms of performance because this is the same diameter as the connecting pipes between the collector and storage tank, which makes the installation easier.

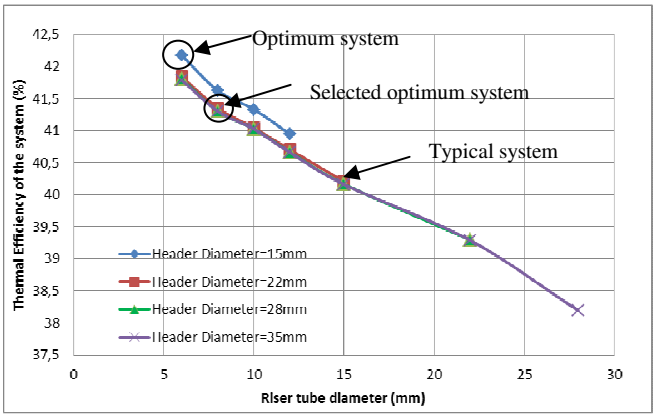

Fig. 4. Performance of the system for the tested collector's construction variations.

The improved system with the selected parameters has 2% higher efficiency than the typical system presented in the previous section.

After the selection of the optimum design parameters of the collector, those parameters were kept constant in order to investigate other parameters of the system such as the slope of the collector or the height of the storage tank. Step-by-step improvements on the system's design will allow us to have a new improved system at the end of the project.

D. Thermosiphonic system with horizontal storage tank

In the past years the storage tank of the thermosiphonic systems used to be vertically installed while in the recent years is being installed horizontally for the purpose of reducing the overall height of the unit. The two configurations are shown in Fig. 5.

Fig. 5. SWH system with horizontal storage tank (left) and SWH system with vertical storage tank (right)

After the definition of the dimensions of the connecting pipes and tank configuration in the program, the system with the horizontal tank was simulated and its efficiency was found to be 38.94%. It was observed that, the typical system with the vertical tank was 2% more efficient than the system with the horizontal tank. This is the same conclusion as Morrison and Braun found in 1985 [4].

As done for the typical system with the vertical tank, the selected parameters for the collector concerns the number of riser tubes and the diameter of the riser and header pipes were applied for this system and simulated. The outcomes from the simulation showed that the efficiency of the system was improved by 2.1%.

From now on, in the investigation of the rest of parameters the two systems are going to be presented the same time in order to have the opportunity to compare them and see the change in their efficiency for every modified parameter.

E. Slope of the collector

When constructing and installing a SWH it has to be assured that circulation of the heat carrying fluid (water) does occur. The circulation of the water in the collector depends in many factors such as the material of the pipes, the diameter of the pipes and the height that the water needs to be transferred. This height is depended with the slope of the collector. The lower is the height more easily the water moves.

The slope of the collector is very important for the system's performance so the system was simulated and tested in slopes from 20-90° at steps of 5°.

Figure 6 shows the results from simulations for slopes 20-90° for the selected number of risers and tubes diameters (from the previous section) for vertical storage tank configuration, for vertical height between the collector and the tank to be zero.

As can be observed, the optimum angle for this system is not the 45º that is used for the typical systems in real life so far. The chart in Fig. 6 shows that the typical systems with vertical tank perform slightly better in slopes of the collector around 35º-40º.

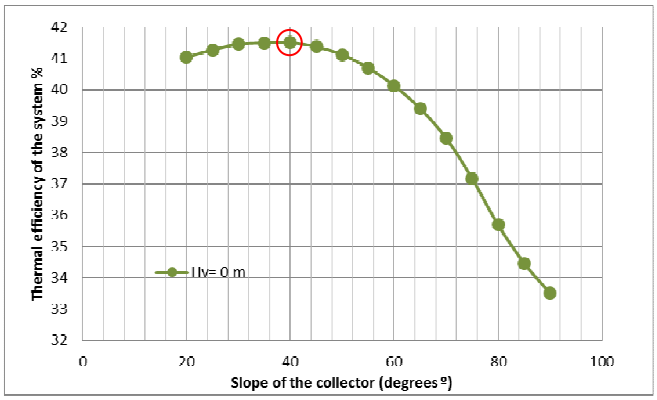

Fig. 6. Performance of the typical system with the improved collector characteristics for slopes 20-90°

Figure 7 shows the outcomes of the simulations for angles of the collector from 15º to 90º for a system with horizontal tank and the collector characteristics as selected from section C.

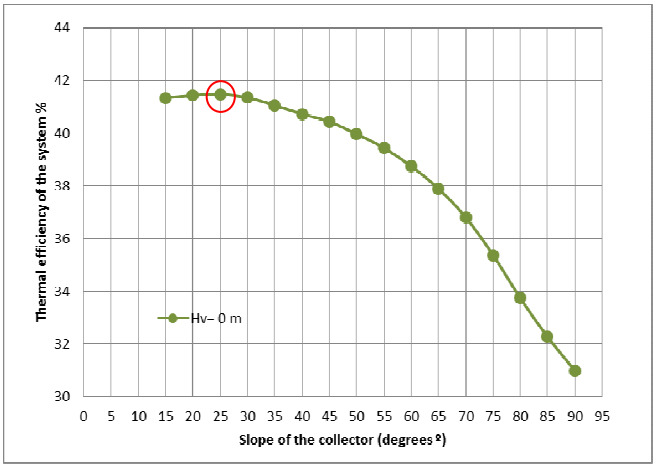

Fig. 7. Performance of the system with horizontal storage tank with the improved collector characteristics for slopes 15-90°

Figure 8 shows a comparison of the system performance between the vertical and horizontal tank configurations. A height between the collector top and the storage tank bottom of -20 cm is chosen as it shows more clearly the difference between the two arrangements. It is obvious that this system performs better in lower slope of the collector around 25º-35º. This outcome is very interesting if we consider that in real life, those systems are being installed in smaller angles but nobody ever said the reason for this. This outcome can somehow confirm the installation of those systems. From the results presented here it can be concluded that the system with horizontal tank performs better in lower inclination of the collector and this is the first written evidence which ensures that there is a reason for the way of their installation. It is now proved that their installation in lower slope, which was probably selected by experience and the outcomes from the simulations, agree.

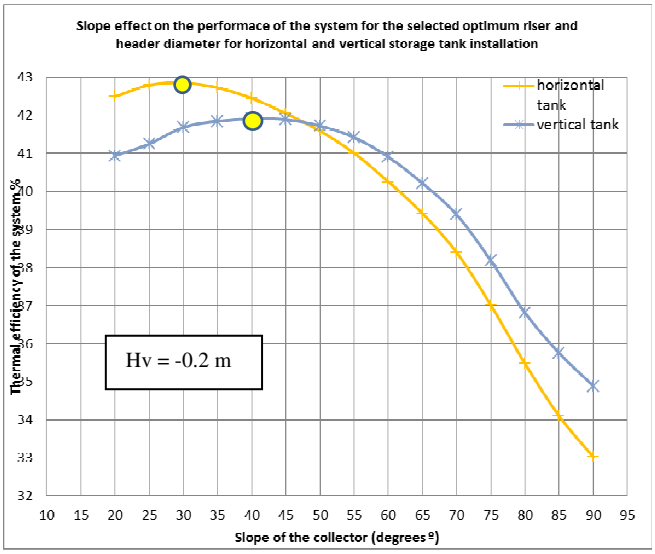

Fig. 8. Comparison of the performance of the system with vertical and horizontal storage tank

It is important to mention that the curves in Fig. 8 are not for the typical system with the tank and the collector at the same height. For the typical systems with the tank's bottom to be at the same height with the collector's top, the system with vertical tank is more efficient than the system with horizontal tank and the efficiencies of both of them are not higher than 41% as presented in previous sections. The graphs in Fig. 8 show an example of the slope's effect in systems with the bottom of the tank to be 20 cm below the top of the collector.

As can be observed, the bigger is the slope of the collector, the lower is the performance of the system. This is logical because we know that the circulation of the water depends on the dynamic forces ρ (density), g (gravity of earth), h (height). Consequently, the lower is the slope the lower is the height, thus the lower are the forces that need to circulate the water and the higher is the efficiency.

F. Height between the collector top and the tank bottom

Figure 3, presented before, shows schematically the typical thermosiphon system showing the bottom of the tank and the top of the collector to be at the same height. In this study, some different cases of this vertical distance were investigated, for the tank to be below or above the collector's top.

Six cases of this height difference were investigated, for vertical distance between the top of the collector and bottom of the tank -30 cm, -20 cm, -10 cm, 0 cm, 10 cm and 20 cm. The negative sign means that the tank's bottom is below the collector's bottom. Subsequently, the positive sign means that the bottom of the tank is above the top of the collector while zero distance means that they are in the same height level.

Figure 9 shows the results from 96 simulations for a thermosiphonic system with vertical storage tank for the six cases of heights discussed before, for slopes of the collector from 20º-90º. The results illustrated in Figure 9, show that the system with vertical tank performs better when the vertical distance between the top of the collector and the bottom of the tank is negative. That means that the system's efficiency is higher when the bottom of the tank is placed below the collector's top surface level. However, this doesn't mean that the tank should be placed on the ground level because in that case there will be a problem in the circulation of the water.

Additionally, as can be observed, the slope of 40° is the optimum for all the cases so this is the selected value to simulate the new selected parameters.

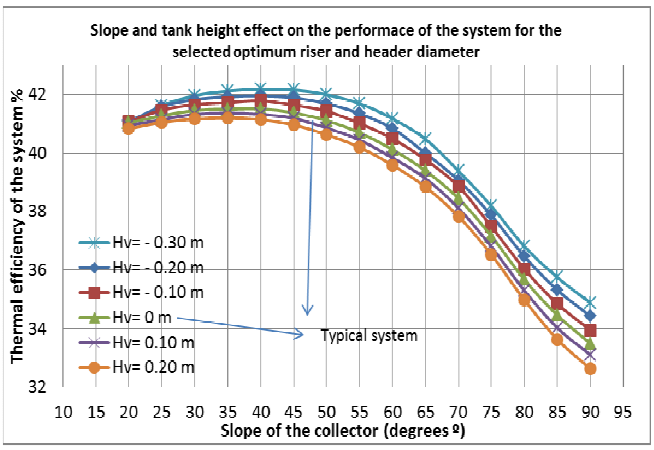

Fig. 9. Efficiency of the thermosiphon system with vertical tank in terms of the collector's slope and the height difference of the collector's top and the tank's bottom.

The efficiency of the system with vertical storage tank was improved by 0.5% with the changes in the slope of the

collector and the height of the tank. In addition with the changes made in the collector's design characteristics presented in section C there is a totally 2.4% improvement from the typical system.

Figure 10 shows the outcomes from 96 simulations for 6 cases of vertical height between the collector and the tank for slopes between 15° and 90° for the system with horizontal storage tank. As can be observed the lower is the tank placed above the collector's top, the higher is the system's efficiency.

Additionally, it is clearly shown that the system with horizontal tank performs better in lower slopes of the collector than the one with vertical tank as shown previously in Fig. 8.

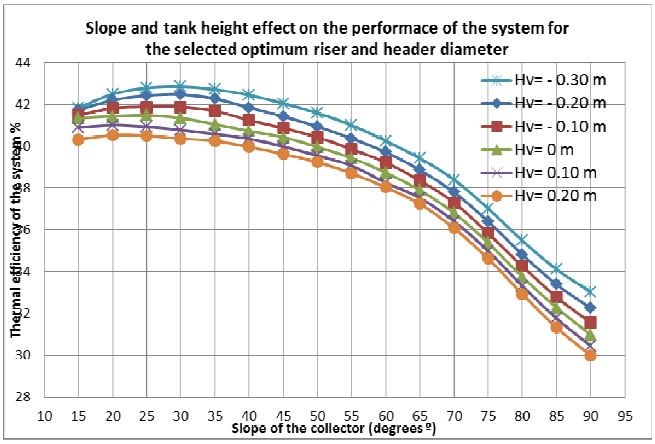

Fig. 10. Efficiency of the thermosiphon system with horizontal tank in terms of the collector's slope and the height difference of the collector's top and the tank's bottom

Accordingly for the system with horizontal storage tank, the slope of 30° was selected as optimum, and the height of the tank selected to be the 20 cm below the top of the collector. Then the selected parameters so far for the system with horizontal tank were simulated and the outcomes from the simulations showed that the performance of the system was 43.29% while before applying these changes it was 41.04%. This means that the changes in the collector achieved a 2.1% efficiency increase as mentioned in section D and the changes in the slope of the collector and the height of the tank improved the efficiency of the system by more 2.3%. In total we achieved to improve the system with the horizontal tank by 4.4 %.

G. Different shape of the collector

The design characteristics of the collector were investigated before but the shape of the collector was the same for every parameter tested so the length of the header and riser pipes was always the same. This section will show some other shapes that the collector could be manufactured. The aim is to prove whether those shapes are more efficient than the typical collector's shape. Consequently, the typical system with collector slope 45° and collector outlet to tank outlet vertical distance 0 m was taken as the basis in order to modify the shape of the collector and the related properties of its components to examine the system's efficiency in different shapes of the collector.

The length of the riser and header pipes depends on the shape geometry of the collector panel. Accordingly, a different shape of the collector for the same area (long distance to be the width instead of height that is the usual case), would require different length of riser and header pipes as well as different size diameters of the tubes in order to keep the flow constant.

This section, will describe the consideration of the dimensional characteristics of the collector's components and every shape tested will be compared with the collector of the typical system with 10 riser tubes of 15 mm and header tubes 28 mm. The typical collector has area of 1.5 m^2 where its length is 1.5 m and its width is 1 m which means that the length of the riser pipes was around 1.5 m each and accordingly the length of the header pipes was 2 m (2 pipes x 1 m each).

Four cases of different shapes of collector have been investigated in this study as follow:

1. Length= 1.5 m, Width= 1 m, Risers= 10 (typical)
2. Length= 1.15, Width= 1.30 m, Risers=13
3. Length= 1.875, Width= 0.8 m, Risers=8
4. Length= 1, Width= 1.5 m, Risers=15

The number of risers is estimated by considering that the distance between the riser tubes remains equal to 10 cm, as in the typical system, where the width is 1 m and there were 10 risers.

As can be observed, the Case 1 represents the typical system as described in section B with efficiency 40.13%. The results from the simulations of using a modified collector in the typical system are presented in Fig. 11.

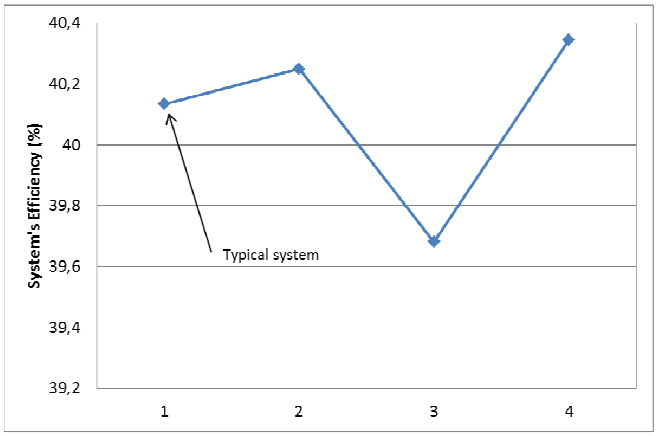

Fig. 11. Performance of the system in the four cases of collector's shapes

It is clearly shown that the Cases 2 and 4 are more efficient than the typical system but the difference between their efficiency is minimal. The efficiency of the system with collector from Case 1 differs from the efficiency of the Case 2 by less than 0.2% while the lower from the higher efficiencies presented in the diagram (Case 4) differs only by 0.66%. Case 3 with the taller collector seems to be the worst case.

Consequently, these parameters do not worth to be changed in the typical system, as their effect on the system's efficiency is almost zero.

VI. General Outcomes

After the examination of all the parameters and the analysis of their effect on the thermosiphonic system's performance, this section will recapitulate the outcomes of the changes and their effects.

Figure 12 shows that in the typical form the system with vertical tank is more efficient than the system with the horizontal tank. Firstly, the collector's design characteristics have been changed and they improved the efficiency of the system by 2% for the system with vertical tank and by 2.1% for the system with horizontal tank.

Afterwards, the changes selected to be done on the height of the tank and the slope of the collector improved the system with the vertical tank by 0.5% and the system with horizontal tank by 2.3%.

These last changes overturned the results and the system with the horizontal tank is more efficient than the system with the vertical tank. This has the added advantage of reduced overall system height and should be the preference of the manufacturers.

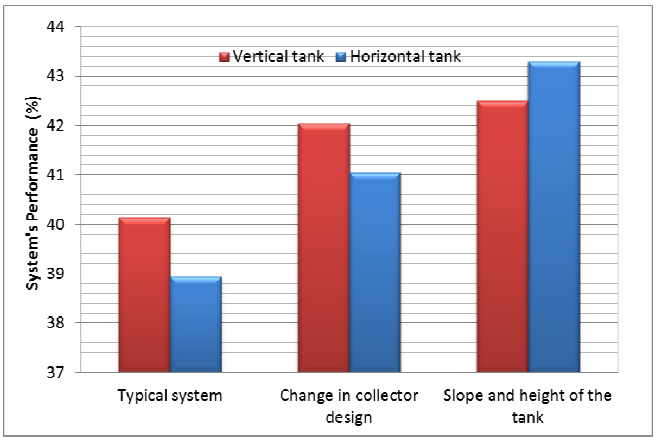

Fig. 12. Step by step improvements made on the systems with vertical and horizontal storage tank.

VII. References

[1] Mauthner, F., Weiss, W. (2011) Solar Heat Worldwide, Markets and Contribution E. H. Miller, "A note on reflector arrays," *IEEE Trans. Antennas Propagat.*, to be published.

[2] Kalogirou, S. (2005) 'Solar Water Heaters in Cyprus: Manufacturing, Performance and Applications', Proceedings of the 4th Congress on Energy Conservation in Buildings and Renewable Energy on CD-ROM, Tehran, Iran.

[3] Kalogirou, S.A. (2009) *Solar Energy Engineering: Processes and Systems.* 1st ed. Academic Press.

[4] Morrison, G.L. and Braun, J.E. (1985) 'System modeling and operation characteristics of thermosiphon solar water heaters', Solar Energy, 34 (4-5), pp.389-405.

[5] Abdunnabi, M.J.R., Loveday, D.L. (2012) 'Optimization of Thermosiphon Solar Water Heaters using TRNSYS', International Conference on Future Environment and Energy, vol. 28, IACSIT Press, Singapore.

[6] Kalogirou, S.A. and Papamarcou, C. (2000) 'Modelling of a Thermosyphon Solar Water Heating System and Simple Model Validation', Renewable Energy, 21(3-4), pp. 471-493.

VIII. Biographies

Soteris Kalogirou was born in Trachonas, Nicosia, Cyprus on November 11, 1959. He is a Senior Lecturer at the Department of Mechanical Engineering and Materials Sciences and Engineering of the Cyprus University of Technology, Limassol, Cyprus. He received his HTI Degree in Mechanical Engineering in 1982, his M.Phil. in Mechanical Engineering from the Polytechnic of Wales in 1991 and his Ph.D. in Mechanical Engineering from the University of Glamorgan in 1995. In June 2011 he received from the University of Glamorgan the title of D.Sc. He is Visiting Professor at Brunel University, UK and Adjunct Professor at the Dublin Institute of Technology (DIT), Ireland. For more than 25 years, he is actively involved in research in the area of solar energy and particularly in flat plate and concentrating collectors, solar water heating, solar steam generating systems, desalination and absorption cooling.

He has 41 books and book contributions and published 264 papers; 109 in international scientific journals and 155 in refereed conference proceedings. Until now, he received more than 4000 citations on this work and his h-index is 35. He is Deputy Editor-in-Chief of Energy, Associate Editor of Renewable Energy and Editorial Board Member of another eleven journals. He is the editor of the book Artificial Intelligence in Energy and Renewable Energy Systems, published by Nova Science Inc., co-editor of the book Soft Computing in Green and Renewable Energy Systems, published by Springer and author of the book Solar Energy Engineering: Processes and Systems, published by Academic Press of Elsevier

Rafaela Agathokleous was born in Limassol, Cyprus on June 1990. She graduated from the Ayias Fylaxeos Lyceum in 2008 and studied Mechanical Engineering and Materials Science Engineering at Cyprus University of Technology until 2012. In 2012 she participated as a last year undergraduate student in a competition organized by the Research Promotion Foundation in Cyprus and she earned first prize praise. By 2013 she studied for the degree of Masters of Science in Sustainable Energy Technologies and Management at Brunel University London.

Rafaela is a student member at the Chartered Institution of Building Services Engineers and member at the Cyprus Scientific and Technical Chamber.

She is currently employed as a Research Assistant at Cyprus University of Technology, and soon she will do her PhD in the field of Energy. Her special fields of interest are sustainability, sustainable and renewable energy technologies, sustainable building design, energy efficient buildings, and solar energy.

2nd Conference on Power Options for the Eastern Mediterranean Region
07-08 October 2013, Nicosia, Cyprus (Paper No. POEM13/192)

Increase of the energy efficiency of 25 low-income houses in Cyprus - a holistic approach

Gregoris P. Panayiotou, Anthi Charalambous, Savvas Vlachos, Orestis Kyriacou, Elisavet Theofanous and Thomas Filippou

***Abstract*-- ELIH-Med project aims to identify and implement innovative technical solutions to improve energy efficiency in low-income housings in the Mediterranean area. In this study the results of the Cyprus pilot projects concerning 25 houses all over Cyprus are presented. The specific objective of this project is to achieve at least 30% decrease in energy consumption or at least improvement of the energy class by two categories in all houses. Initially, an onsite energy audit was carried out and accordingly energy efficiency measures were proposed for each house. Additionally, a smart meter is installed in all houses while in several cases net-metering PV systems are installed for the first time in Cyprus. The results are in perfect compliance with the aim of the project. It is important to note that the first results of the net-metering PV systems reveal a very promising perspective for the application of these systems in Cyprus since a reduction of >95% is achieved on the net electricity consumption.**

***Index Terms*-- ELIH-Med, Energy efficiency, low-income houses, net-metering, PV, thermography**

I. Introduction

A great share of the final energy consumption, over 40%, in the EU-27 is consumed by the existing building stock. Residential buildings are of great importance since they account for 63% of the latter value [1] where according to EuroACE [2] 57% of the consumed energy is used for space heating, 25% for the production of domestic hot water (DHW), 11% for electronic devices and lighting and 7% in electric ovens and cookers. Thus, the consequent need to increase the energy performance of the houses is an important instrument in the efforts to lessen Europe's dependency on energy imports as well as carbon dioxide emissions. As a result the European commission prepared a number of legislative tools, one of which is the 2002/91/EC, so as to facilitate the 2020 target of 20% energy saving.

According to the Housing Statistics in the European Union [3] the total number of houses in the EU-27 is about 204 millions distributed accordingly in the following countries: 19.59 % in Germany, 13.22 % in Italy, 13.2 % in France, 12.32 % in UK, 8.18 % in Spain, 6.52 % in Poland, 3.57 % in the Netherlands the rest of the houses, around 23.4 %, belongs to the remaining European countries. Uihlein and Eder [4] state that the total residential building stock of Europe will increase by 2.5 times in 2060, compared to 2000 levels. This is a very important fact to consider due to the consequent increase in total energy consumption in this sector.

The dwelling stock in Cyprus at the end of 2007 reached 357,870 units and 63.3% of the houses were located in urban areas thus it becomes apparent that the energy behaviour of the average house in Cyprus plays a significant role to the energy consumption of the building sector. The built environment in Cyprus is characterized by low density city centers, which led to sprawl town phenomenon, where the multi-storey family buildings became the dominant house. In the suburbs the dominant house is the detached single-family house, which accounts for the largest share in the total dwelling stock of Cyprus [5].

In order to propose energy efficiency measures for the improvement of the energy performance of the existing houses a deeper understanding of the way the existing residential building stock of Europe behaves in terms of energy should be gained. This has been investigated in a number of studies during the last decade and the most important of which are presented below. It should be noted that the method used to evaluate and assess the energy performance of the existing residential building stock has been a subject for debate between researchers across Europe and thus many different approaches appear in literature.

The effect of thermal insulation, age and condition of heating system on the energy consumption for space heating and the resulting environmental impact is studied by Balaras *et al.* [6]. In their study they used a sample of 349 residential buildings in seven European countries following the INVESTIMMO methodology The data concerning the heating energy consumption came from 193 European residential buildings from five European countries namely Denmark, France, Greece, Poland, and Switzerland which participated in the project. The results showed that 38% of the audited buildings have higher annual heating energy

This work was financially supported by ELIH-Med project under the MED Programme. The PV systems installed were a kind courtesy of the following companies: L. Zotiades Trading & Consulting Ltd, Trikkis Energy, Solar Technologies Ltd, Neon Energy Cyprus Ltd, Andi Solartech Solutions Ltd, Savco Solar Ltd, Metartec, Lanitis Green Energy Group, Enfoton Solar Ltd and Johnsun Heaters Ltd. Finally, the installed smart meters were a kind courtesy of the Electricity Authority of Cyprus (EAC).

G. P. Panayiotou is with the Cyprus University of Technology, (e-mail: Gregoris.Panayiotou@cut.ac.cy).

A. Charalambous is with the Cyprus Energy Agency, Nicosia, Cyprus (email: anthi.charalambous@cea.org.cy).

S. Vlachos is with the Cyprus Energy Agency, Nicosia, Cyprus (email: savvas.vlachos@cea.org.cy).

O. Kyriacou, is with the Cyprus Energy Agency, Nicosia, Cyprus (email: orestis.kyriakou@cea.org.cy).

E. Theofanous is with the Cyprus University of Technology, (e-mail: et.theofanous@edu.cut.ac.cy).

T. Filippou is with ENERES C.P.M. Ltd, Limassol, Cyprus, (email: eneres.cpm@cytanet.com.cy).

consumption than the European average which is equal to 174.3 kWh/m^2.

The improvement of energy performance of existing houses can be achieved by applying several energy efficiency measures the most effective of which are the following along [7]: improve the thermal insulation of the houses' envelope, savings 33-60 %; achieve weather proofing of the openings so as to minimize the losses and gains during heating and cooling periods respectively from the ambient environment, savings 16-21 %; install windows of better performance than singe-glazing, i.e. double or triple glazing with inert gas filling in the gap, savings 14-20 %; implement regular maintenance of the central heating boiler, savings 10-12%.

In their work D'Orazio *et al.* [8] focused on the effects of thermal insulation of roofs during summer period by analyzing experimental data of a pilot unit in Italy. The results indicated that the installation of a thicker insulation layer on the roof lowers the effectiveness of passive cooling as result of thermal separation of the internal space and the top layers of the roof.

Dylewski and Adamczyk [9] defined the optimum type and width of thermal insulation that results to the maximum net present value. The analysis they used is the life cycle cost analysis and the results showed that the types of insulation with the most beneficial effects on the energy behavior of the building is those of polystyrene foam and ecofiber.

Florides *et al.* [10] described the evolution of domestic houses in Cyprus during the twentieth century with respect to their heating and cooling requirements. Additionally, the methods of construction employed and materials used were presented. The environment of TRNSYS was used for the modeling and simulation procedures. The results showed that the temperature variations inside a traditional house are similar with the variations in a well insulated modern house. More specifically, the variations for the traditional house range between 16–20°C for winter and 25–35°C for summer compared to 11–20°C for winter and 33–46°C for summer for a non-insulated house with a flat roof.

In a very comprehensive work Florides *et al.* [11] studied the energy flows of modern houses and examined measures to reduce the thermal load using TRNSYS. The measures examined were natural and controlled ventilation, solar shading, various types of glazing, orientation, shape of buildings, and thermal mass. The results of this work showed that a maximum reduction of annual cooling load of 7.7% for maintaining the house at 25^{o}C is achieved by ventilation. The saving in annual cooling load may be as much as 24% when low emissivity double glazing windows are used. Additionally, when overhangs of 1.5 m are used over windows about 7% of the annual cooling load can be saved for a house constructed from single walls with no roof insulation. The results showed that the elongated shape shows an increase in the annual heating load, which is between 8.2 and 26.7% depending on the construction type, compared with a square-shaped house. In respect to orientation, the best position for a symmetrical house is to face the four cardinal points and for an elongated house to have its long side facing south. Finally, the analysis of the results showed that the roof is the most important structural element of the buildings in a hot environment. The life-cycle cost analysis has shown that measures that increase the roof insulation pay back in a short period of time, between 3.5 and 5 years.

In another study Kalogirou *et al.* [12] investigated the effects on the heating and cooling load resulting from the use of building thermal mass in Cyprus. For this purpose a typical four-zone building with an insulated roof in which the south wall of one of the zones has been replaced by a thermal wall was modeled using TRNSYS. The results of the simulation showed that there is a reduction in the heating load requirement by about 47%, whereas at the same time a slight increase of the zone-cooling load is exhibited.

In this study the work carried out for the definition of the current energy efficiency and the proposition of innovative technical solutions for 25 low-income houses all over Cyprus is presented as part of Cyprus pilot projects under ELIH-Med project.

II. Characteristics of the Sample

As aforementioned the sample of the Cyprus' pilot project consists of 25 low-income households located in 14 Municipalities and Communities in Cyprus from which 10 are urban and 4 rural (5 coastal, 1 mountainous, 2 semi mountainous and 6 urban). More specifically, the sample reflects 32% population coverage (270.000 people) and 90.000 households. The participating municipalities and communities along with their population, total number of households and the number of pilot projects (households) chosen are listed in Table I.

TABLE I
PARTICIPATING MUNICIPALITIES, COMMUNITIES AND NUMBER OF PILOT PROJECTS

Municipality	Population	Households	Number of Pilot Projects
Strovolos	67,565	25,706	3
Agios Athanasios	13,965	3,234	2
Parallimni	14,946	5,107	2
Latsia	16,570	5,987	1
Dali	10,574	3,430	2
Polis Chrysochou	2,021	758	1
Aradippou	19,594	5,800	2
Larnaca	51,232	19,539	1
Lakatamia	38,770	12,676	3
Egomi	18,219	6,696	1
Yeri	8,450	2,749	1
Psimolofou	1,686	529	1
Ergates	1,792	547	1
Lefkara	826	292	2
Cyprus Land Development Organization	-	-	2

The selection procedure for the definition of the sample was initiated by a public call for interest released on 2 April 2012 and carried on through a series of publicity actions that included announcements on websites, advertises on national

newspapers and interviews of the personnel of CEA in a number of both television and radio channels. The application period ended on The selection procedure for the definition of the sample was initiated by a Public call for interest released on 2nd of April 2012 and carried on through a series of publicity actions that included announcements on websites, advertises on national newspapers and interviews of the personnel of CEA in several both television and radio channels. The application period expired at 31st of April 2012 and the submitted applications were evaluated by a responsible committee on the 5th of May 2012. The results of the evaluation were accordingly to the applicants.

The selection criteria were the following: the gross annual salary of the household depending on the number of occupants, the location of the household (eligible municipalities), the total area of the house (apartments below 100 m^2, and single houses below 150 m^2), the year of construction of the house (1970-1995) and the ownership of the house.

III. Methodology

The methodology for the assessment of the energy performance of each house was performed in two stages where during the first stage a preliminary visit was made by the personnel of CEA and the second stage concerned an extended energy audit performed by the experts of ENERES CPM Ltd. During the energy audit all required data were obtained from the owner of the house through a questionnaire specially formulated for this project while also an infrared thermography of the house was conducted. The data collected concerned the characteristics of the construction of the house and the energy consuming systems and devices such as HVAC systems, lighting, DHW production systems etc. Additionally, the architectural plans of each house were collected and in the cases were this was not possible due to several reasons, the experts drew a sketch of the house using proper laser distance meter.

Accordingly, the data collected were analyzed and inserted into the dedicated software for the calculation of their energy performance. The software used for these purpose is the SBEM-Cy which is the dedicated software for the calculation of the energy performance of buildings approved by the Energy Service of Cyprus, Ministry of Commerce, Industry and Tourism. As a result the current energy performance of each house was calculated. Then by taking into consideration the current energy performance and the results of the thermography of the house potential energy efficiency measures were identified. Finally, the energy performance of each house was re-calculated by applying the proposed measures so as to evaluate their effect on its energy performance in order to be in compliance with the main aim of this project.

It should be noted that in two selected cases (PP.3 and PP.24) an energy analyzer will be installed on the electricity distribution board of the houses in order to record and break down the energy consumptions per use for a complete year. This will be done in order to record and examine the energy consumption and the energy behavior of the occupants before and after the energy refurbishment of their house and also define the energy consumption of the house per use (lighting, cooling, heating, electric devices, washing machine, cooking, etc). It is very important to note that this is the first time where the break down of the energy consumption of houses in Cyprus per use is attempted practically by installing a dedicated device.

Currently, the project is on the stage where the contract has been signed with the successful contractor and the energy refurbishment of the selected houses will initiate.

IV. Results & Discussion

The results of the energy assessment of each house are presented in Table II. More specifically, the results shown in this table consist of the current energy state of each house (EPC class and theoretical energy consumption), the improved energy state (new EPC class and new theoretical energy consumption) and the list of the proposed energy efficiency measures to be applied on each house. Additionally, the increase of the energy efficiency of each case is listed.

The selection of each energy efficiency measure was based on the specific characteristics and energy behavior of each house and resulted on the highest energy savings. Additionally, a very important factor for the selection of the appropriate measure to be proposed for each case was the results of the infrared thermography inspection. An example of these results is given in Fig. 1 were the thermal image together with the photograph of an exterior wall where the existence of a thermal bridge is revealed. These images were taken from PP.25 and assisted on the selection of the addition of thermal insulation plaster on the exterior envelope of the house so as to eliminate such phenomena. Also, in a different case (PP.16) the thermal image indicated the existence of very intense thermal bridges on the internal wooden ceiling due to the lack of thermal insulation (Fig. 2) in this case amongst other measures the installation of internal thermal insulation (5cm) above the wooden ceiling was proposed. In another case the existence of thermal bridges on the internal side of the flat roof of PP.20 was exposed (Fig. 3). Consequently, a number of measures were simulated for each case and the optimum ones were chosen.

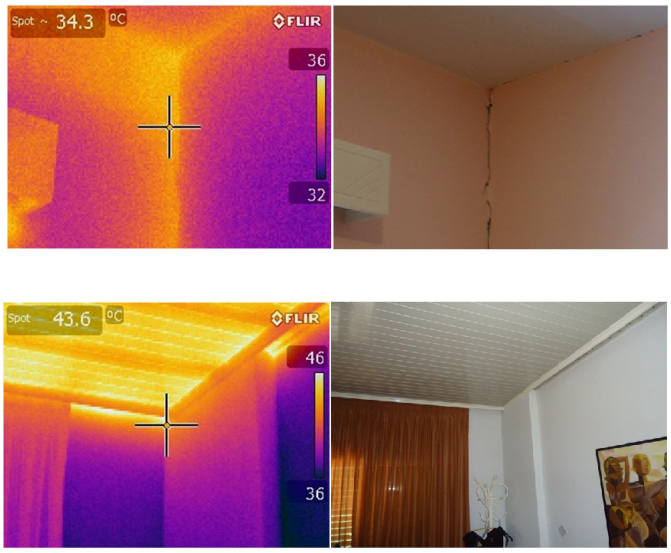

Fig. 1. Thermal Bridge on the exterior wall of PP. 25

Fig. 2. Thermal Bridges on the wooden ceiling of PP. 16

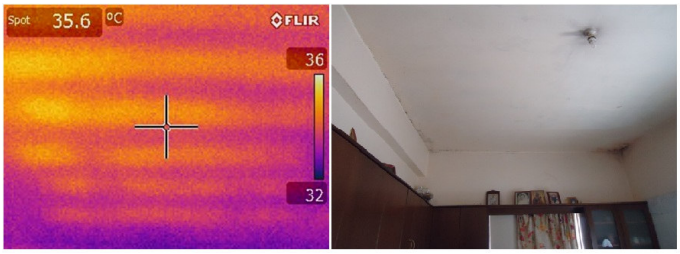

Fig. 3. Thermal bridges on the internal side of the flat roof of PP. 20

As it can be observed in Table II the most proposed measure was the replacement of the tungsten lamps (17 cases) followed by the installation of external insulation on the roof (15 cases) and the replacement of the existing damaged solar water heating system (11 cases). The replacement of old air conditioning units with new energy efficient and the addition of thermal insulation plaster on the envelope of the house were proposed for 6 cases. The replacement of single glazing with double glazing with thermal brakes in the aluminium frame was proposed for 5 houses while the addition of internal insulated plasterboard ceiling was suggested for 4 houses. The addition of 5 cm of thermal insulation on top of an internal ceiling was proposed for 3 cases. Finally, an energy efficient fire place (air module) was proposed for 2 cases and an energy efficient fire place (water module) and the addition of external blinds were proposed for 1 case.

The expected results were theoretically calculated and it can be clearly concluded that the specific aims of the project are fulfilled since the energy saving ranges between 18 to 76 % and also the increase of the EPC energy class in several cases exceeds the two class difference (i.e. PP. 15 and PP. 20 from G to C). In some cases the EPC energy class remains the same but the energy savings are higher than 30%.

Several cases (11) were selected for the installation of grid-connected net-metering PV systems of various capacities. The selection criteria were based on the number of available PV systems and the suitability and structure of the house. Additionally, a smart meter is are going to be installed in all houses so as to have a more specific picture of the energy consumption of the house especially in the cases where PV systems will be installed.

The first results of the net-metering PV systems installed in PP. 4 and PP. 18 are both very interesting and important. In the first case (PP.4) the net electricity consumption for the period between March-April 2013 was only 36kWh (11.64€) while the electricity consumption for the same period in 2012 was 1.836kWh (98% reduction). In the second case (PP.18) the net electricity consumption for the period between April-May 2013 was just 4kWh (3.55€) while the electricity consumption for the same period in 2012 was 840kWh (99.5% reduction).

V. Conclusions

In this study the definition and evaluation of the current energy efficiency and the proposition of energy efficiency measures for 25 low-income houses all over Cyprus are presented as part of Cyprus pilot projects under ELIH-Med project.

Initially, the current energy efficiency of the selected houses was evaluated through an extended energy audit while also the thermal imaging of the house was performed through infrared thermography inspection. The results of these two actions assisted on the proposition of the optimum energy efficiency measures suitable for each case. The proposed measures were focused on the improvement of the thermal insulation of the envelope of the house and also on the replacement of some of the devices that are energy consuming with energy efficient devices. Additionally, a smart meter is installed in all houses in order to improve their energy efficiency while in 11 cases PV systems of various capacities were installed so as to contribute to the increase of the energy efficiency of the house.

The expected results, which are theoretically calculated, are in perfect compliance with the aim of the project while in several cases exceed the expectations since the improvement of the energy class and the reduction of the energy consumption is much higher. More specifically, the energy saving ranges between 18 to 76 % and the increase of the EPC energy class in several cases exceeds two classes increase (i.e. PP. 15 and PP. 20 from G to C). In some cases the EPC energy class remains the same but nevertheless the energy savings are higher than 30%.

Finally, the first results of the net-metering PV systems installed are very interesting and important since a reduction of 98-99.5% on the net electricity consumption is achieved in comparison with the electricity consumption of the same periods in 2012. This is a very promising result especially in view of the newly launched Grant scheme for net-metering PV systems in Cyprus.

TABLE II
RESULTS OF THE ENERGY ASSESSMENT OF EACH HOUSE TOGETHER WITH THE PROPOSED ENERGY EFFICIENCY MEASURES

Pilot Project	Location	EPC class *Before	Energy consumption (kWh/m^{2}yr) *Before	List of energy efficiency measures	EPC class *After	Energy consumption (kWh/m^{2}yr) * After	Energy Efficiency Increase	PV system installed capacity (kW)
1	Dhali	E	397	• Installation of external thermal insulation (5cm width) on the flat roof • Replacement of old air conditioning units with new energy efficient	C	227	43%	1.2
2	Dhali	G	855	• Installation of external thermal insulation (5cm width) on the flat roof • Replacement of the old (damaged) Solar Water Heating system with new energy efficient	E	444	48%	-
3	Dhali	G	1021	• Installation of external thermal insulation (5cm width) on the flat roof • Replacement of tungsten bulbs with compact fluorescent lamps	G	553	46%	1.5
4	Larnaca	G	731	• Installation of external thermal insulation (5cm width) on the flat roof • Replacement of the old (damaged) Solar Water Heating system with new energy efficient • Replacement of tungsten bulbs with compact fluorescent lamps	E	352	52%	3
5	Poli Chrysochous	G	588	• Addition of thermal insulation plaster (2,5 cm) externally on the envelope of the house • Installation of external thermal insulation (5cm width) on the flat roof • Replacement of tungsten bulbs with compact fluorescent lamps	E	369	37%	1
6	Yeri	G	958	• Installation of external thermal insulation (5cm width) on the flat roof • Replacement of the old (damaged) Solar Water Heating system with new energy efficient • Replacement of tungsten bulbs with compact fluorescent lamps	F	541	44%	1
7	Lefkara	D	254	• Installation of new internal ceiling with thermal insulation (thickness 5cm) • Installation of new energy efficient fire place (air module) • Replacement of tungsten bulbs with compact fluorescent lamps	C	179	30%	-
8	Lefkara	C	289	• Installation of thermal insulation (5cm) above the internal wooden ceiling of the house • Installation of new energy efficient fire place and integration with the central heating	C	204	29%	-
9	Ayios Athanasios	G	1083	• Replacement of single glazing with double glazing with thermal brakes in the frame • Installation of external thermal insulation (5cm width) on the flat roof • Addition of thermal insulation plaster (2,5 cm) externally on the envelope of the house	F	603	44%	1
10	Ayios Athanasios	F	502	• Replacement of old air conditioning units with new energy efficient • Installation of external thermal insulation (5cm width) on the flat roof • Replacement of tungsten bulbs with compact fluorescent lamps	C	188	63%	3
11	Aradippou	E	432	• Installation of external thermal insulation (5cm width) on the flat roof • Replacement of the old (damaged) Solar Water Heating system with new energy efficient	C	281	35%	-
12	Aradippou	F	556	• Installation of external thermal insulation (5cm width) on the flat roof • Replacement of the old (damaged) Solar Water Heating system with new energy efficient • Replacement of old air conditioning units with new energy efficient	C	284	49%	-
13	Engomi	E	413	• Installation of new internal ceiling with thermal insulation (5cm width) • Replacement of tungsten bulbs with compact fluorescent lamps • Addition of thermal insulation plaster (2,5 cm) externally on the envelope of the house	D	282	32%	-
14	Strovolos	G	740	• Replacement of single glazing with double glazing with thermal brakes in the frame • Replacement of the old (damaged) Solar Water Heating system with new energy efficient • Replacement of old air conditioning units with new energy efficient • Replacement of tungsten bulbs with compact fluorescent lamps	E	385	48%	-

15	Strovolos	G	1127	• Installation of new internal ceiling with thermal insulation (5cm width) • Replacement of old air conditioning units with new energy efficient • Addition of thermal insulation plaster (2,5 cm) externally on the envelope of the house • Replacement of tungsten bulbs with compact fluorescent lamps	C	272	76%	-
16	Strovolos	F	604	• Installation of internal thermal insulation (5cm) above the wooden ceiling of the house • Replacement of single glazing with double glazing with thermal brakes in the frame (some) • Replacement of the old (damaged) Solar Water Heating system with new energy efficient • Replacement of old air conditioning units with new energy efficient • Replacement of tungsten bulbs with compact fluorescent lamps	D	354	41%	-
17	Paralimni	G	643	• Installation of external thermal insulation (5cm width) on the flat roof • Replacement of single glazing with double glazing with thermal brakes in the frame (some) • Replacement of tungsten bulbs with compact fluorescent lamps	F	457	29%	-
18	Paralimni	C	287	• Installation of external thermal insulation (5cm width) on the flat roof • Addition of thermal insulation plaster (2,5 cm) externally on the envelope of the house • Replacement of tungsten bulbs with compact fluorescent lamps	B	130	55%	3
19	Lakatamia	G	631	• Installation of external thermal insulation (5cm width) on the flat roof • Replacement of the old (damaged) Solar Water Heating system with new energy efficient • Replacement of tungsten bulbs with compact fluorescent lamps • Replacement of existing (old) hot water tank with new one	F	516	18%	-
20	Lakatamia	G	861	• Installation of external thermal insulation (5cm width) on the flat roof • Replacement of the old (damaged) Solar Water Heating system with new energy efficient	D	375	56%	1.5
21	Lakatamia	G	664	• Installation of internal thermal insulation (5cm) above the wooden ceiling of the house • Replacement of single glazing with double glazing with thermal brakes in the frame (some) • Replacement of tungsten bulbs with compact fluorescent lamps	E	502	24%	-
22	Ergates	C	313	• Installation of external thermal insulation (5cm width) on the flat roof • Replacement of the old (damaged) Solar Water Heating system with new energy efficient • Replacement of tungsten bulbs with compact fluorescent lamps	B	183	42%	3
23	Psimolofou	E	463	• Installation of new internal ceiling with thermal insulation (5cm width) • Replacement of old air conditioning units with new energy efficient • Replacement of tungsten bulbs with compact fluorescent lamps	C	274	41%	1.9
24	Ayios Athanasios	F	444	• Installation of new efficient fire place (air module) • Replacement of tungsten bulbs with compact fluorescent lamps • Installation of external blinds	E	315	40%	-
25	Strovolos	E	433	• Addition of thermal insulation plaster (2,5 cm) externally on the envelope of the house	C	281	35%	-

VI. REFERENCES

[1] European Commission, Doing more with less, Green Paper on energy efficiency 22.06.2005

[2] EuroACE, Towards Energy Efficient Buildings in Europe, final report June (2004).

[3] K. Dol, M. Haffner, Housing Statistics in the European Union, The Hague: Ministry of the Interior and Kingdom Relations, OTB Research Institute for the Built Environment, Delft University of Technology, (2010).

[4] A. Uihlein, P. Eder, Policy options towards an energy efficient residential building stock in EU-27, Energy and Buildings 42 (2010) 791-798.

[5] G. P. Panayiotou, S.A. Kalogirou, G.A. Florides, C.N. Maxoulis, A.M. Papadopoulos, M. Neophytou, P. Fokaides, G. Georgiou, A. Symeou, G. Georgakis, The characteristics and the energy behaviour of the residential building stock of Cyprus in view of Directive 2002/91/EC, Energy and buildings 42 (2010) 2083-2089.

[6] C.A. Balaras, K. Droutsa, E. Dascalaki, S. Kontoyiannidis, Heating energy consumption and resulting environmental impact of European apartment buildings, Energy and Buildings 37 (2005) 429-442.

[7] E.G. Dascalaki, K.G. Droutsa, C.A. Balaras, S.Kontoyiannidis, Building typologies as a tool for assessing the energy performance of residential buildings – A case study for the Hellenic building stock, Energy and Buildings 43 (2011) 3400-3409.

[8] M. D'Orazio, C. Di Pernab, E. Di Giuseppea, The effects of roof covering on the thermal performance of highly insulated roofs in Mediterranean climates, Energy and Buildings 42 (2010) 1619-1627.

[9] R. Dylewski, J. Adamczyk, Economic and environmental benefits of thermal insulation of building external walls, Building and Environment 46 (2011) 2615-2623.

[10] G. Florides, S. Tassou, S. Kalogirou, L. Wrobel, Evolution of domestic dwellings in Cyprus and energy analysis, Renewable Energy 23 (2001) 219-234.

[11] G.A. Florides, S.A. Tassou, S.A. Kalogirou, L.C. Wrobel, Measures used to lower building energy consumption and their cost effectiveness, Applied Energy 73 (2002) 299-328.

[12] S.A. Kalogirou, G. Florides, S. Tassou, Energy analysis of buildings employing thermal mass in Cyprus, Renewable Energy 27 (2002) 353-368.

VII. BIOGRAPHIES

Gregoris Panayiotou was born in Limassol, Cyprus on February 18, 1983. He graduated from the Technological Educational Institute of Athens first of his class as an Energy Technology Engineer in 2007. He had his MSc in Energy in Heriot-Watt University, Edinburgh where he graduated in 2008 with Distinction.

He is currently employed at Cyprus University of Technology as a Research Associate in a nationally funded project concerning the study and the deeper understanding of the thermosiphonic phenomenon that occurs in solar water heating systems that operate thermosiphonically.

In the past he had also worked in two research projects. The first project was funded by the Research Promotion Foundation of Cyprus and concerned the categorization of buildings in Cyprus according to their energy performance. The second project concerned the application and evaluation of advanced absorber coatings for parabolic trough collectors.

The main simulation tool he had used in most of his work is TRaNsient SYstem Simulation (TRNSYS) while he had also worked with HOMER and PVSyst.

He currently has 9 Journal publications and 12 Conference publications and his special fields of interest include wide range applications of Renewable Energy Sources systems and Energy Efficiency in buildings.

Anthi Charalambous was born in Paphos, Cyprus, on January 19, 1973. She is a Chemical Engineer by background, graduated from the National Technical University of Athens, and holds a MSc in Environmental Engineering, a Masters in Business Administration (MBA) and a MSc in Renewable Energy and Energy Management.

At the beginning of her career she worked abroad in environmental management, wastewater management and treatment and industrial pollution. From 2001 she began working in the field of Renewable Energy in Cyprus and Brussels. In 2007 she joined the European Commission Directorate General for Energy in the unit of renewable energy technologies. She is the Director of Cyprus Energy Agency since November 2008.

She participated in more than 60 conferences as invited speaker and she has released several publications and she is co-author of a number of papers.

Savvas Vlachos was born in Nicosia on February 12, 1983 and started his professional career in 2004. He graduated from the Polytechnic School of Crete, Greece, as an Environmental Engineer and he acquired his master degree on Civil Engineering at the Polytechnic Department of the University of Cyprus.

He is currently involved in studies related with energy efficiency in buildings, Sustainable Energy Action Plans and Renewable Energy Sources technologies including the follow up and supervision. He is trained for the use of several softwares related to Energy Management, RES and energy efficiency. Also, he acts as an information resource to public, businesses, authorities and suppliers and provides technical advice on Renewable Energy Sources technology and Saving Energy techniques. He participates in many European co-funded projects as technical expert. He is very familiar with the methodology of Sustainable Energy Action Plans (SEAP) and he is responsible for the preparation and implementation of SEAPs in Municipalities in Cyprus.

Orestis Kyriacou was born in Cyprus in 1984. He is a qualified electrical engineer graduated from the National Technical University of Athens in 2009 with specialization on electrical power. He started his career in 2009 and in 2010 he was employed by the Cyprus Energy Agency. He is responsible for energy management issues.

He is involved in studies and actions Promoting Renewable Energy Sources, rational use of energy, energy saving, energy efficiency and sustainable transport (electric vehicles and EVC). He participates in European co-funded projects as technical expert. He is familiar with the SEAP methodology and other tools e.g. RETSCREEN and DIALux.

Elisavet Theofanous Elisavet Theofanous was born in Limassol, Cyprus on November 6, 1989. In 2011 she was amongst the first graduates of the Cyprus University of Technology (CUT) where she graduated as a Mechanical Engineer. She then had her Master of Science (MSc) in the Department of Environmental Science and Technology in CUT in 'Environmental Biosciences and Technology' where she was the first graduate of the course in 2013. Since September 2012 she is employed as a Research Associate in a project funded by the Research Promotion Foundation of Cyprus concerning the investigation and the determination of the geothermal parameters of the lithologies in Cyprus, for the compilation of the geothermal map of the island.

She has 1 Journal publications and 4 Conference publications on aspects concerning the application of ground heat exchangers (GHE) installations.

The main simulation tool used in most of her work is FlexPDE while she had also worked with GLD. Her special fields of interest include applications of Renewable Energy Sources (RES) and especially Geothermal Energy.

Thomas Filippou was born in 1983 and holds a Degree in Mechanical Engineering from Technical Educational Institute of Athens, Greece and an MSc in Energy from Heriot-Watt University, Edinburgh, UK. He has 10 years of professional experience in energy sector with areas of competence being Energy Efficiency in industry and buildings, Renewable Energy Sources project development and assessment, Energy Management in industry and buildings, Energy audits and feasibility studies for EE & RES projects and Energy policy.

He has significant experience and knowledge in design, development and monitoring of Energy Efficiency and RES projects. He has also implemented significant number of energy audits in various types of buildings and industries. He has experience in evaluation of EE and RES institutional and policy frameworks and evaluation of EE and RES projects. He is familiar with data collection and analysis procedures and has also expertise in measurements of energy with various kinds of portable instrumentation. Furthermore he is familiar with simulation of RES and EE projects through dedicated software packages. He has wide expertise in this area in many countries of CEE and NIS. He holds advanced project management and planning, organisational, communication and report writing skills.

2nd Conference on Power Options for the Eastern Mediterranean Region
07-08 October 2013, Nicosia, Cyprus (Paper No. POEM13/193)

Promotion of PV Energy through net metering optimization (PV-NET project)

M. Hadjipanayi, G. E. Georghiou, P. De la Rosa, G. Papagiannis, P. Virtic, J. Oliveira, A. Charalambous and N. Poize

***Abstract*-- The project addresses the design of energy policies and strategies in the Mediterranean for cost-optimized utilization of renewable energy sources (RES). PV-NET involves optimizing smart energy management schemes, in particular net metering to provide an economically sustainable alternative to government feed-in-tariff subsidies. PV-NET proposes the implementation of pilot net metering schemes for a cross-section of buildings in Mediterranean countries. The involvement of electricity utilities, energy regulatory authorities and energy agencies in each country will allow access to consumption as well as pricing data for the study of economic advantages of different metering strategies. Metering schemes will be modelled and optimized using experimental data as feedback. In this way, the pilots will enable the demonstration of net metering benefits, validate the different models and help correct previous schemes' shortcomings. Through stimulating PV uptake in the region, PV-NET is expected to result in a reduction of electricity bills, better energy management, and promotion of sustainable development.**

***Index Terms*--photovoltaics, net metering, smart meters, energy management, pilot installations**

I. Introduction

The feed-in-tariff (FIT) scheme has been widely adopted by a number of EU countries and in the Mediterranean region as a cost effective measure to increase the number of installed PV systems, at a time when the technology was not competitive. Given the high solar resource in the Mediterranean and the fact that the area has already reached solar grid parity, the PV technology is no longer in need of any form of subsidization. Net metering schemes [1, 2] on the other hand offer a much more cost optimum-tool for the creation of a self-sustainable market.

The utilities in Europe are at the point where they have started looking at net metering in a more serious way and are trying to prepare for this transition. Therefore, the PV-NET project is highly timely and its objectives are in line with EU policies [3], targets [4] and guidelines. The activities of the project can effectively lead the way towards this transition to cost-effective and energy efficient implementation of RES in the Mediterranean and the EU as a whole.

In PV-NET, pilot installations will be implemented to collect data useful for improving energy efficiency and informing prosumers. The data analysis will lead to a parameterized model where local conditions will be considered in a successful rollout of smart net meters. A best pricing model will be produced for set of input parameters, resulting in a set of recommendations for best practices per country, driving a wider adoption of PV.

II. The PV-NET project

In this paper, we present the project entitled «Promotion of PV energy through net metering optimisation (PV NET)» which is financed by the European Regional Development Fund through the cross-border program MED.

A. The consortium

The participating countries span the whole of the Mediterranean region from East to West. Such a broad geographical span ensures the whole spectrum of different climatic and morphological aspects is covered, including both continental areas and islands. The whole countries of Cyprus, Slovenia and Greece participate as well as regions of Spain (Andalusia), France (Rhône-Alpes), and Portugal (Algarve). In particular, the partner institutions are: The University of Cyprus, the Instituto Andaluz de Tecnología, the Aristotle University of Thessaloniki, the University of Maribor, the Regional Agency for Energy and Environment in Algarve, the Cyprus Energy Agency, and the Agency for Energy and Environment in Rhone-Alpes. The outcomes of PV-NET are therefore applicable to the whole Mediterranean area and the plan is to diffuse and transfer them effectively in the region.

B. State-of-the-art

The countries of the Mediterranean have a high potential of solar irradiance, compared to Northern countries and one would have expected a higher penetration of PVs in their energy generation mixture. Moreover the current situation is that PV generation in the Mediterranean region is highly unevenly distributed. Figures for 2012 [5], [6] indicate that Italy leads the production with 16361 MW installed PV capacity, followed by Spain with 5166 MW and France with 4003 MW, while others such as Greece (1536 MW), Slovenia (198 MW) and Cyprus (9 MW) still lag behind. These figures are much lower compared to the EU leader in

This work is financed by the European Regional Development Fund through the cross-border programme MED.

M. Hadjipanayi is with the Department of Electrical Engineering, University of Cyprus (e-mail: hadjipanayi.maria@ucy.ac.cy).

G. E. Georghiou is with the Department of Electrical Engineering, University of Cyprus (e-mail: geg@ucy.ac.cy).

P. De la Rosa is with the Instituto Andaluz de Tecnologia (IAT), Spain (e-mail: pdlrosa@iat.es).

G. Papagiannis is with the Aristotle University of Thessaloniki, Greece (e-mail: grigoris@eng.auth.gr).

P. Virtic is with the University of Maribor, Slovenia (e-mail: peter.virtic@um.si).

J. Oliveira is with the Regional Agency for Energy and Environment in Algarve (AREAL), Portugal (e-mail: joliveira@areal-energia.pt).

A. Charalambous is with Cyprus Energy Agency (CEA), Cyprus (e-mail: anthi.charalambous@cea.org.cy).

N. Poize is with the Agency for Energy and Environment in Rhone-Alpes (RAEE), France (e-mail: noemie.poize@raee.org).

PV generation, Germany, which exhibits installed PV capacity of 32411 MW, although it has a lower solar potential than the Mediterranean. Moreover in countries like France only around 100 MW are installed in the Rhône-Alpes region, which is part of the Mediterranean region. These high discrepancies between the Mediterranean countries (and regions within the countries themselves) and countries with lower solar potential can be partly attributed to legal and bureaucratic barriers that exist in these countries but also to the lack of a consumer consciousness about the potential benefits of PV.

The promotion of the PV technology relies entirely on the FIT scheme, which is a heavy governmental subsidy. France and Spain constitute examples of countries which have recently successfully demonstrated the need to move away from subsidy schemes to open market conditions so that PV energy can continuous its growth in a sustainable way. Adding to this the fact that some countries in the Mediterranean have already reached grid parity (Cyprus) then it is an opportunity for them to lead this transition and set an example for other countries.

Despite the fact that smart net metering can alleviate administrative barriers in the most cost efficient way and make the transition from a subsidized to a market regulated situation, it has been adopted by very few countries (Italy and Spain). Energy agencies are participating in this project, with utilities and energy regulatory bodies as associate partners, demonstrating their willingness to push towards an implementation of the net metering scheme, once analysing the outcome of this project. The PV-NET will give a push towards achievement of the National Strategic Reference Framework (NSRF) [6] strategic objectives for all the participating counties, which include investments in production of their energy from RES.

C. The project objectives

The PV-NET project aims to address the issue of low implementation and grid integration of PV technology in the Mediterranean which is already reaching grid parity. It proposes the study of smart energy management schemes in particular net metering, and their optimization as a means of replacing costly subsidies. The specific objectives of the project are: (i) the promotion of initiatives to ensure that PV is implemented and used in the best cost-efficient way, and without the need for financial support, (ii) the appropriate handling of the energy generated by PV through smart management of supply and demand, (iii) that through this improved knowledge, both the utility and the final users of electricity will be able to better manage the energy generated by PV, (iv) the strengthening of public policy and strategy for PV.

Through stimulating PV uptake in the region, the project is expected to result in a reduction of citizens' electricity bills, better energy management and RES deployment, and promotion of sustainable development. Moreover, PV-NET will provide significant feedback and important lessons regarding smart net metering applicability to the whole of Europe given that the scheme can be readily implemented in the Mediterranean. PV-NET supports existing initiatives (smart cities, Covenant of Mayors) and EU policy on RES [2] by promoting increased RES deployment in the most cost-efficient way and a distributed, smart-grid electricity generation environment.

D. Pilot net metering installations

Pilot net metering schemes will take place in 3 countries (Cyprus, Slovenia and Portugal) for a cross-section of building types in the Mediterranean countries. This project will enable the quantitative analysis of the effect of tested schemes on electricity costs and efficiency. The involvement of electricity utilities, energy regulatory authorities and energy agencies in each country will allow access to consumption/pricing data for the study of economic advantages of different metering strategies and facilitate the network connection of installed PV. Metering schemes will be modelled and optimized using experimental data as feedback. In this way, the pilot installations will enable the demonstration of net metering benefits for both utilities and consumers in adopting optimized frameworks for renewables. The pilot installations will also serve for validation of the different models and help correct previous schemes' shortcomings.

E. Summary and expected results

PV-NET brings together a geographically diverse consortium to address the issues of electricity utilization efficiency and effective PV integration in the region. Collected data will be used to build typical end users consumption patterns for the development of transnational optimal net metering models, taking into account the intricacies of each country. The data and experiences exchanged among partners and 3rd parties will improve understanding of the impacts of local conditions in energy consumption/generation profiles and pinpoint cross-border barriers to the adoption of PV. Know-how will be transferred from more industrialized partners to less developed ones, particularly through development of the technical solutions for data management and RES grid integration. An improved interaction between local energy actors will enhance the prospect for future joint projects and reliable institutional and operational networks. Typical consumers will be educated, through access to their data, on the prospects of effective PV use and efficiency thereby creating more energy-conscious, 'smart' citizens. The smart net metering pilot schemes will encourage a transnational change of the energy mix by enabling PV to reach more competitive levels.

Therefore, PV-NET will lay the foundations for building knowledge-oriented, environmentally-friendly economies in the Mediterranean and the rest of Europe where smart territorial development and ample employment opportunities will be sustained.

III. References

[1] J. Hauff and D. Rendschmidt, SunEdison Report: "Enabling the European consumer to generate power for self-consumption", 2011

[2] EU policy on Renewable energy sources, EU Directive 2009/28/EC

[3] Smart Grids: from innovation to deployment, Communication from the Commission. COM (2011) 202.

[4] Smart Grid Mandate, European Commission, M/490 EN

[5] EPIA Report: Global Market Outlook for Photovoltaics 2013-2017

[6] H. Wirth, Fraunhofer Report: Recent Facts about photovoltaics in Germany, 2013

[7] EU Cohesion Policy 2007-2013, National Strategic Reference Frameworks (NSRF) 2008

2nd Conference on Power Options for the Eastern Mediterranean Region
07-08 October 2013, Nicosia, Cyprus (Paper No. POEM13/194)

Optimizing cultivation conditions of the estigmatophyte *Nannochloropsis salina* for enhancing growth and oil production

Nagwa G. Mohammady and Elsayed M .Ibrahim

Abstract-- **The problem of the unlimited increasing need for the unrenewable fossil fuels (petroleum) and its increasing price has urged scientists to use microalgae as a source for the production of biodiesel. The eustigmatophyte microalga *Nannochloropsis salina* has been cultivated under different laboratory conditions to increase its growth and potentiality for oil production. Results demonstrated that the maximum value of algal biomass (approximately 0.3 g/l) was obtained where the alga cultivated under light intensity of 1830 lux and 16:8 hrs light/dark regime. However oil content increased gradually with increasing light intensity under continuous light to reach the maximum value (0.12 g/l). The best nitrogen source and concentration that stimulate biomass downloading and oil production is 0.5g/l urea. In regard to nitrogen limitation, algal growth shows different responses towards the effects of nitrogen limitation. However, oil content of the starved algal cells was increased after adding urea with maximimum concentration of 0.26 g/l. Furthermore, algal cell number, biomass and oil content were increased under cultivation with sodium acetate and light conditions indicating that this organism can grow better mixotrophically rather than heterotrophically.**

Keywords: Biodiesel – Bio oil – Fatty acid- Growth- Heterotrophy- Light- Mixtrophy- *Nannochloropsis salina*- Nitrogen- Sodium Acetate.

I. Introduction

The concept of microalgae biomass production for conversion to fuels was first suggested in the early 1950s [1]. In view of the fact that algae have high photosynthetic efficiency, high biomass productivities, a faster growth rate than higher plants, highest CO_2 fixation and O_2 production, growing in liquid medium which can be handled easily, can be grown in variable climates and non-arable land including marginal areas unsuitable for agricultural purposes (e.g. desert and seashore lands), in non-potable water or even as a waste treatment purpose, use far less water than traditional crops, and do not displace food crop cultures; their production is not seasonal and can be harvested daily [2], [3]. However, not all microalgae strains are good candidates for biodiesel production purposes. Reference [4] addressed the characteristics deemed necessary for an organism to be considered for biodiesel fuel production as follow: 1- exhibit rapid growth rate. 2- Have appreciable lipid yields. 3- Demonstrate tolerance for the climatic conditions. 4- Possess a life cycle conductive to continuous culturing. *Nannochloropsis* algae have relative high intracellular lipid content [5]-[8] in comparison to other microalgae. Therefore, the genus is a good source for biofuel production [6], [9], [10]. In addition, *Nannochloropsis* showed a high tolerance against many different environmental stresses [11]-[14]. However, the amount of intracellular triglycerides of *N. salina* is relatively low [15]. In the framework to optimize biotechnological aspects involved in mass production of *Nannochloropsis salina* to enhance biomass and oil production, the algal cultivation was optimized under laboratory conditions, using different light intensities and light regimes, different nitrogen sources and concentrations, cultivation under different growth mode and nitrogen starvation stress were also applied.

N. G. Mohamady is with the department of Botany and Microbiology, Aelxandria university, Alexandria (e-mail: nagwa_phyco@yahoo.com).

E. M. Ibrahim is with the Department of Botany and Microbiology, Aelxandria university, Alexandria (e-mail: sm_sc_85@yahoo.com).

II. Technical Work

Biological material and culture maintenance: The eustigmatophyte *Nannochloropsis salina* Hibberd was obtained from the culture collection at phycology lab, Faculty of Science, Alexandria University. *Nannochloropsis salina* was grown batch-wise in BES (Boussiba's Enriched Seawater) [16]. Four light intensities were applied through 1, 2, 3, and 4 1m cool white fluorescent lamps measuring 740, 1000, 1830 and 2650 lux, respectively. The irradiance of these lamps was measured by HI 97500 Hanna portable Luxmeters. The light regimes (12: 12 hrs light/dark; 16: 8 hrs light/dark, and 24 hrs of continuous light) were applied.

Growth measurements: The growth of the examined alga was determined daily by cell count with haemocytometer slide using light microscopy. At least five replicas were taken to get the mean number of cells per ml culture. Growth rate: The growth rate coefficient (r) was calculated according the equation [17]: $r = \ln x_1 - \ln x_0 / t_1 - t_0$

Where x_0, and x_1 are the number of cells at time t_0, and t_1, respectively. r denotes the cell division per day. For biomass estimation, the optical density of algal suspension was determined spectrophotometrically at 625 nm, using Perkin Elmer Spectrophotometer, Lambada l. Biomass concentration was calculated accordingly [18].

Nitrogen source and concentration: Three different nitrogen sources (Potassium nitrate, Urea and Ammonium sulphate) were added in a concentration of 0.5, 1.0 and 1.5 g/l respectively.

Nitrogen limitation: The axenic cultures were grown in nitrogen limited-medium; After 7 days of nitrogen limited medium, a concentration of 0.5 g/l of above nitrogen sources used was added.

Carbon source: Two sets of axenic cultures were cultivated for 14 days with13.6 g/l of Sodium acetate, as a carbon source. The first set was grown mixotrophically under light intensity of 1830 lux and 16: 8 hrs light/ dark regime. However, the second set was grown heterotrophically, in complete darkness.

Lipid and oil extraction: At the end of the logarithmic growth phase (day 14), the cells were harvested by centrifugation and the lipid content was extracted with chloroform/methanol (2:1, v/v), [19]. On the other hand, algal oil was extracted using *n*-hexane [20].The average weight of total lipid and oil was calculated.

Fatty acid composition of algal oil: The crude oil, extracted from controlled cultures, was esterified [21] and analyzed in a Shimadzu gas-liquid chromatography (Kyoto, Japan), equipped with a flame ionization detector and Hp-5 column material (Agilent, Santa Clara, CA, USA). The carrier gas was nitrogen and the flow rate was 5 mm/min. Identification of the FAMEs was carried out by comparing their retention times with those of standards. Quantification was based on the internal standard method.

Statistical analysis: The standard deviation (SD) of three replicas was calculated. In addition, T-test was also applied to data obtained.

III. Results

Fatty acid methyl esters of algal oil: The composition of algal oil fatty acid methyl esters (biodiesel) of *N. salina*, grown under the basal conditions, is presented in (Table 1). Both saturated and unsaturated components were detected, besides some unknowns. The unsaturated fractions were identified as C16:1 (palmitoleic acid methyl ester, 16.7%), C18:1 (oleic acid methyl ester, 12.9%), C18:2 (linoleic acid methyl ester, 12.8%), C18:3 (linolenic acid methyl ester, 12%), C20:1 (gadoleic acid methyl ester, 9%), and C20:5 (eicosapentaenoic acid, EPA, methyl ester, 13.1%). On the other hand, the saturated ones are composed of C14:0 (myristic acid methyl ester, 4%), C16:0 (palmitic acid methyl ester, 6%), and C18:0 (stearic acid methyl ester, 7.5%). The amount of unsaturated to saturated fatty acids was approximately 4.4. A detailed characterization of biodiesel from *N. salina* was described [15].

Table I. Physical properties of fatty acid methyl esters composition of *N. salina* grown under controlled batch conditions.

FAME[a]	*Content (%)*[b]	*b.p. (˚C)*[c]	*Cetane number*[d]	*Kinematic viscosity*[e] *(mm^2/s)*	*HG*[f] *(kg cal/mol)*
C14:0 (myristic)	4	250.5	66.2	3.23	2254
C16:0 (palmitic)	6	350	74.5	4.32	2550
C16:1 (palmitoleic)	16.7	286	45	3.67	2657.4
C18:0 (stearic)	7.5	360	86.9	5.85	2696.12
C18:1 (oleic)	12.9	218.5	55	4.51	2828
C18:2 (linoleic)	12.8	215	36	3.65	nr[g]
C18:3 (linolenic)	12	230	28	3.14	Nr
C20:1 (gadoleic)	9	265	nr	5.77	3150
C20:5 (EPA)	13.1	nr	nr	nr	Nr
Unknowns	6	nr	nr	nr	Nr

[a]Fatty acid methyl esters (biodiesel).

[b]Values obtained from three parallel measurements with SD±1 for C14:0 and C16:0, and ± 0.2 for the remaining fatty acids.

[c]Boiling point data [22]- [24]

[d]Cetane number [24].

[e]Kinematic viscosity [25]- [27].

[f]Heat of combustion [22], [28].

Effect of different light intensities on growth of *N. salina*: Data at figure (1) showed a linearly increasing in the cell number of *N. salina* with increasing time till the day 15 from the beginning of culturing, where the organism entered its stationary growth phase. The cell number of *N. salina* increased progressively with increasing the light intensities from 740 lux to 2650 lux. The maximum increase was recorded at 1830 lux, followed by 2650 lux then 1000 lux. On the other hand the cell number recorded its maximum value under the light intensity of 1830 lux (14.17×10^6cells/ml) after 15 days.

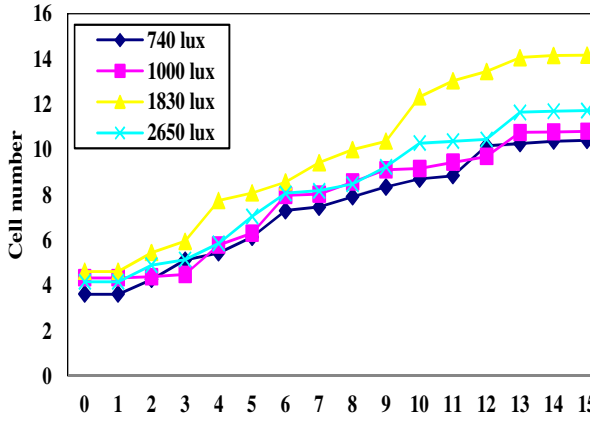

Fig. 1. Effect of different light intensities on the cell number of *N. salina* cultured under laboratory batch conditions.

Biomass based data (g/l) of *N. salina* were recorded in figure (2). It is noticed that the effect of different light intensities on the biomass increased progressively with increasing the light intensities from740 lux to 2650 lux, with maximum increase under 1830 lux followed by 2650 and 1000 lux respectively. On the other hand the biomass concentration recorded its maximum value under the light intensity of 1830 lux (0.291 g/l) after 15 days.

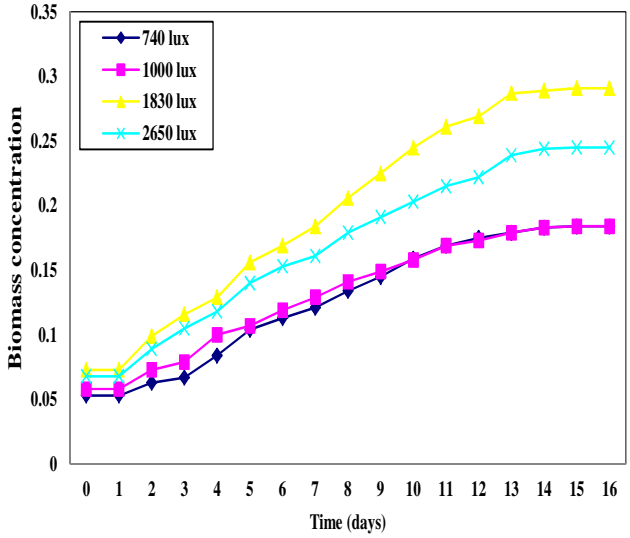

Fig. 2. Effect of different light intensities on the biomass concentration of *N. salina* cultured under laboratory batch conditions.

Figure (3) showed the influence of applied light intensities on the growth rate of the organism. The maximum growth rate was recorded at 740, 1000 and 2650 lux after 6 days from the beginning of culturing. These values were 0.12, 0.10 and 0.11 respectively. Meanwhile, the maximum growth rate at 1830 lux (0.13) was recorded after 4 days from culturing. It is noteworthy to mention that this maximum growth rate that recorded at 1830 lux was the maximum one of the four light intensities.

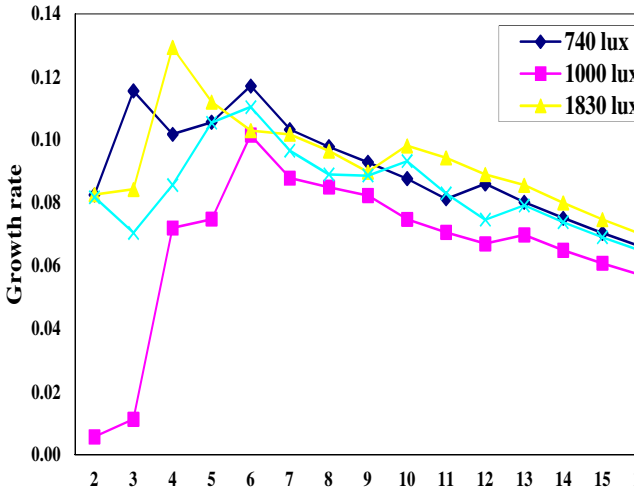

Fig. 3. Effect of different light intensities on the growth rate coefficient of *N. salina* cultured under laboratory batch conditions**.**

Effect of light intensities on oil production of *N. salina*: Data represent the effect of different light intensities (740, 1000, 1830 and 2650 lux) on the oil content of *N. salina* were shown in figure (4). These data cleared that oil content increased gradually with the increase of the light intensity. It can be noticed that the maximum value of oil content (0.116 g/l) was recorded when the alga was cultured under light intensity of 2650 lux.

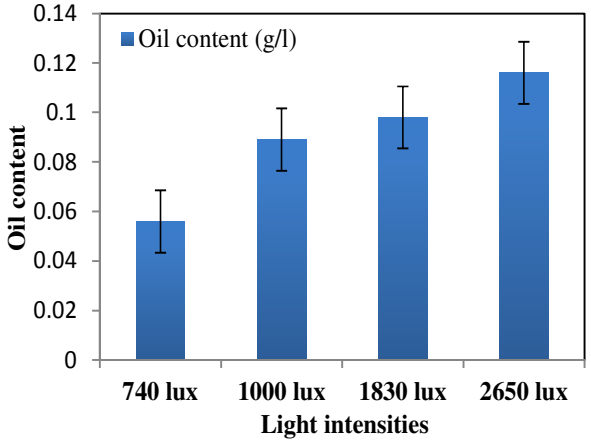

Fig. 4. Effect of different light intensities on oil content (g/l) of *N. salina* cultured for 14 days under laboratory batch conditions.

Effect of different light regimes on the cell number of *N. salina* cultured under laboratory batch conditions: The effects of different light regimes on cell number of *N. salina* cultured under light intensity of 1830 lux were recorded in figure (5). Generally the cell number of *N. salina* increased gradually with increasing time till the day 15, followed by a decrease in cell number with increasing the light period. On the other hand the cell number recorded its maximum value under the light regime of 12:12 hrs light/dark ($14.86*10^6$cells/ml) at the day 12.

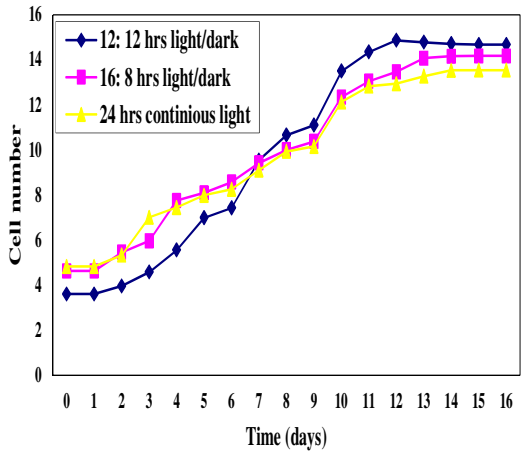

Fig. 5. Effect of different light regimes on the cell number of *N. salina* cultured under laboratory batch conditions.

Data obtained from the effect of different light regimes on the biomass concentration (g/l) of *N. salina* cultured under light intensity of 1830 lux were shown in figure (6). The biomass concentration of *N. salina* increased gradually with increasing time under all used light regimes tested till the day 15, and then no increase was noticed. Data obviously showed that *N. salina* preferred light regime of 16: 8 hrs light/dark, where the biomass concentration recorded its maximum value (0.291 g/l).

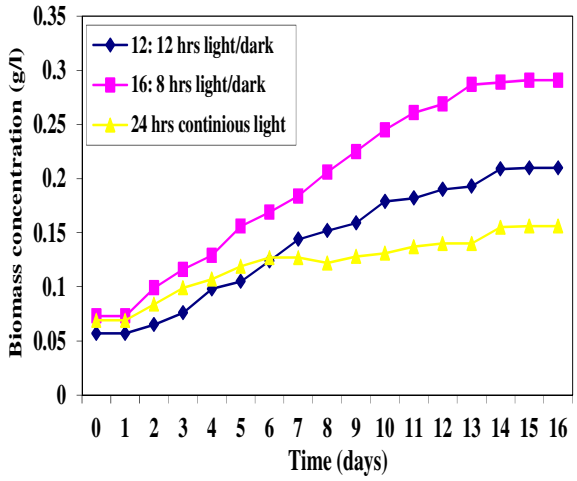

Fig. 6. Effect of different light regimes on the biomass concentration (g/l) of *N. salina* cultured under laboratory batch conditions.

Effect of different light regimes on the growth rate coefficient/day of *N. salina* cultured under laboratory batch conditions: Results Figure (7) showed that under 12: 12 hrs light/dark regime the growth rate recorded its maximum value (0.14) after 7 days. Under 16: 8h hrs light/dark regime the growth rate recorded its maximum value (0.13) after 4 days from culturing. Meanwhile, under 24 hrs of continuous light, the growth rate recorded its maximum value (0.12) after 3 days. It is noteworthy to mention that the maximum growth rate that recorded at 12: 12 hrs light/ dark regime was the maximum one of the three light regimes.

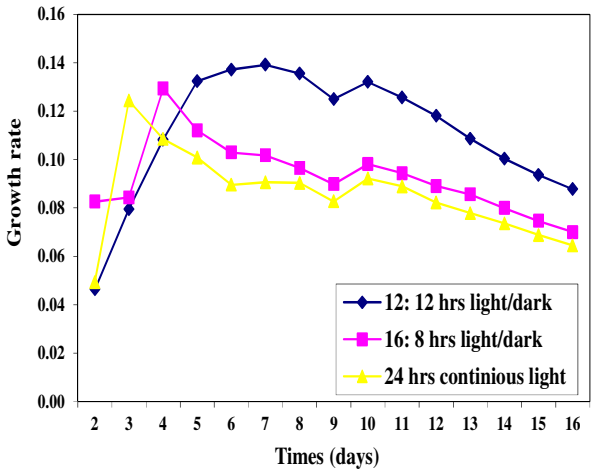

Fig. 7. Effect of different light regimes on the growth rate coefficient/day of *N. salina* cultured under laboratory batch conditions.

Figure (8) showed the effect of different light regimes on the oil content of *N. salina*. It is clear that oil content increased gradually with increasing the light period. Maximum oil content (0.129 g/l) was obtained at the continuous light.

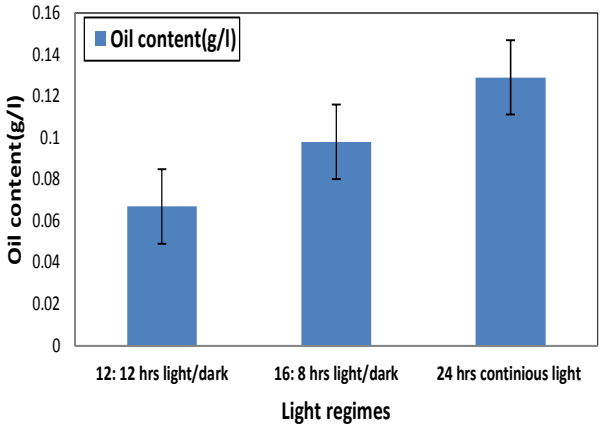

Fig. 8. Effect of different light regimes on oil content (g/l) of *N. salina* cultured for 14 days under laboratory batch conditions.

Effect of different nitrogen sources on the cell number of *N. salina* cultured for 14 days under light intensity of 1830 lux and light regime of 16: 8 hrs light/ dark: Results obtained for cell number of *N. salina* were recorded in figure (9). Data obtained showed that increase of potassium nitrate concentration from 0.5 to 1.0 g/l resulted in a decrease in the cell number (12.89 to 12.04×10^{6}cells/ml). On the other hand further increase of potassium nitrate concentration to 1.5 g/l led to the increase in the cell number (14.32×10^6 cells/ml). Regarding the effect of different concentrations of urea on the growth of *N. salina*, both 0.5 and 1.5 g/l showed lower cell numbers than 1.0 g/l. However, the cell number decreased gradually with increasing the concentration of ammonium sulphate from 0.5 to 1.0 and 1.5 g/l. On the other hand the cell number recorded its maximum value (14.32×10^6 cells) in the culture fed with 1.5 g/l of potassium nitrate.

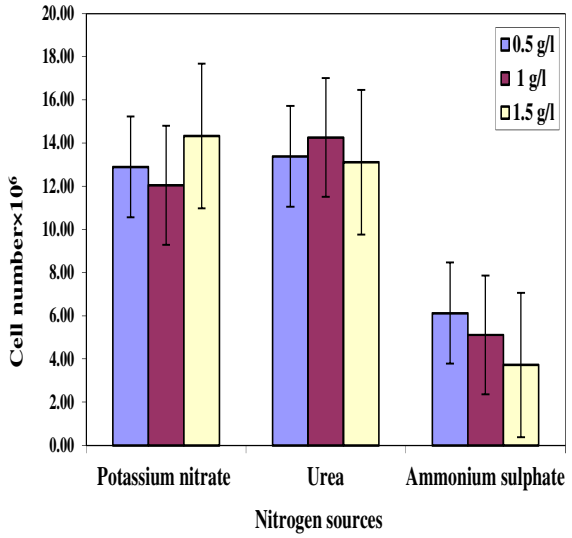

Fig. 9. Effect of different nitrogen sources on the cell number of *N. salina* cultured for 14 days under light intensity of 1830 lux and light regime of 16h light: 8h dark.

Effect of different nitrogen sources on biomass of *Nannochloropsis salina*. Data represent the effect of different nitrogen sources and concentrations on the biomass concentration of *N. salina* were recorded in figure (10). These experimental data showed that the increase in potassium nitrate concentration from 0.5 to 1.5 g/l led to gradual increase in the biomass concentration. However, the biomass concentration decreased gradually by increasing the concentration of both urea and ammonium sulphate from 0.5 to 1.5 g/l. The results also showed that the biomass concentration recorded its minimum value (0.055 g/l) when the culture was fed with 1.5 g/l of ammonium sulphate. On the other hand the maximum biomass concentration (0.190 g/l) was noticed in the culture fed with 1.5 g/l of potassium nitrate.

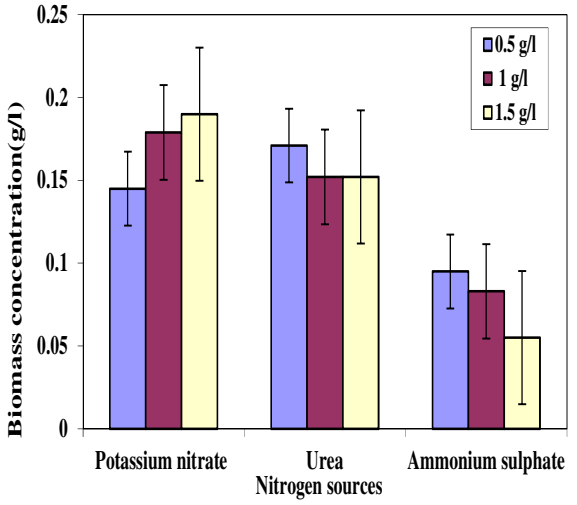

Fig. 10. Effect of different nitrogen sources on the biomass concentration of *N. salina* cultured for 14 days under light intensity of 1830 lux and light regime of 16: 8 hrs light/dark.

Data obtained from the effect of different nitrogen sources with different concentrations on oil content (g/l) of N. *salina* were recorded in figure (11). It can be noticed that the oil content decreased gradually with the increase of the concentrations of the three used nitrogen sources, potassium nitrate, urea and ammonium sulphate, from 0.5 to 1.5 g/l. However the oil content recorded its maximum value (0.123 g/l) in the culture fed with 0.5 g/l of urea.

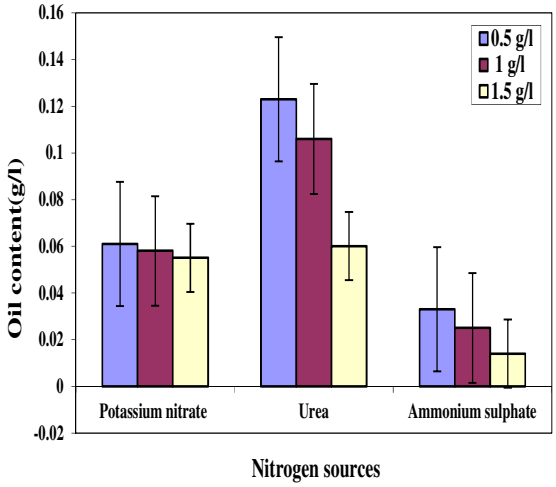

Fig. 11. Effect of different nitrogen sources on oil content of *N. salina* cultured for 14 days under light intensity of 1830 lux and light regime of 16: 8 hrs light/dark.

Table II showed that in the absence of nitrogen the cell number increased gradually till the 6th day (144hrs), where it reached 1.43×10^6 cells/ml, and then it decreased at the 7th day (168hrs) to be 1.4×10^6 cells/ml. With addition of potassium nitrate, urea and ammonium sulphate to the culture of nitrogen-free medium after the 168 hrs the cell number increased progressively till 194 hrs in all used nitrogen sources. It is also clear that the cell number recorded its maximum value (4.38×10^{6}cells/ml) after 24hrs of addition of potassium nitrate. After 28 hours from addition of the three nitrogen sources, the cell number showed a large drop to reach its minimum value (2.23×10^{6}cells/ml) in the case of potassium nitrate.

Table II. Effect of nitrogen limitation on the cell number of *N. salina* cultured for 7 days (168hrs) with nitrogen limited-medium, then adding 0.5 g/l of three nitrogen sources for four times intervals.

Treatments	Time (hours)	Cell number $\times 10^6$/ml		
		Potassium nitrate	Urea	Ammonium sulphate
Nitrogen limitation	0	0.63	0.63	0.63
	24	0.63	0.63	0.63
	48	0.74	0.74	0.74
	72	1.30	1.30	1.30
	96	1.43	1.43	1.43
	120	1.43	1.43	1.43
	144	1.43	1.43	1.43
	168	1.40	1.40	1.40
0.5 g/l	170	1.58	1.86	2.06
	182	2.49	2.73	3.13
	194	4.38	3.75	4.36
	218	2.23	2.91	2.93
P*.value			0.295	0.045*
				0.053*

P*.value was considered significant at p≤ 0.05 probability level according to paired t-test.

Table III. Effect of nitrogen limitation on the biomass concentration of *N. salina* cultured for 7 days (168hrs) with nitrogen limited -medium, then adding 0.5 g/l of three nitrogen sources for four times intervals.

Treatments	Time (hours)	Biomass concentration (g/l)		
		Potassium nitrate	Urea	Ammonium sulphate
Nitrogen limitation	0	0.030	0.020	0.017
	24	0.030	0.020	0.017
	48	0.042	0.022	0.018
	72	0.037	0.033	0.021
	96	0.055	0.048	0.042
	120	0.059	0.067	0.047
	144	0.064	0.085	0.052
	168	0.090	0.094	0.076
0.5 g/l	170	-0.005	-0.005	0.000
	182	-0.004	-0.010	0.009
	194	-0.006	-0.009	0.028
	218	0.029	0.076	0.043
P*.value			0.375	0.202
				0.165

P*.value was considered significant at p≤ 0.05 probability level a

- : means decrease from the value of the 7th day (168 h).ccording to paired t-test.

However, biomass concentration (table III) of *N. salina* increased gradually with time when it was cultured in nitrogen-free medium until the 7th day (168hrs). After 2 hours from the addition of both potassium nitrate and urea at the 7th day, the biomass decreased by 0.005 g/l (table 13), this decrease was continued for the next 12hrs and 24 hrs compared to the last day of nitrogen limitation (7th day). No change in the biomass concentration value of the alga was noticed after 2 hours in the case of addition of ammonium sulphate. However, when the alga was allowed to grow for longer time in the presence of this nitrogen source, its biomass increased gradually for the next 48 hrs to reach its maximum value (0.043 g/l).

The results obtained for the effect of nitrogen limitation on the oil content (table IV) showed that oil content increased with the addition of urea to reach its maximum value (0.261 g/l). Meanwhile, the addition of either potassium nitrate or ammonium sulphate led to the decrease in the oil content of the alga. The maximum decrement (0.068 g/l) was recorded after 2 hrs from the addition of ammonium sulphate.

Table IV. Effect of nitrogen limitation on the oil contents (g/l) of *N. salina* cultured for 7 days (168h) with nitrogen limited -medium, then adding 0.5 g/l of three nitrogen sources for four times intervals.

Treatments	Time (hours)	Oil content (g/l)		
		Potassium nitrate	Urea	Ammonium sulphate
Nitrogen starvation	168	0.04	0.007	0.08
0.5 g/l	170	-0.01	0.026	-0.068
	182	-0.02	0.082	-0.005
	194	-0.02	0.261	-0.004
	218	-0.02	0.251	-0.004
P*.value			0.023*	0.372
				0.034*

P*.value was considered significant at p≤ 0.05 probability level according to paired t-test

- : means decrease from the value of the 7th day (168 h).

Effect of sodium acetate on cell number: *N. salina* cultivated with sodium acetate was exposed to light and complete darkness conditions. The cell number, under light (16: 8hrs light/dark and light intensity of 1830 lux) and complete darkness were recorded in figure (12). The cell concentration increased gradually with increasing time till the 10th day then decreased in culture fed with sodium acetate under 16: 8hrs light/dark and light intensity of 1830 lux. On the other hand the cell number of *N. salina* increased gradually with the increase of time till the 4th day then decreased in culture fed with sodium acetate grown in complete darkness.

Effect of sodium acetate on biomass: Concerning biomass concentration figure (13), the results increased gradually with time till the 10th day then decreased under both light and complete dark conditions. On the other hand the biomass concentration showed higher values under mixotrophic conditions than under heterotrophic conditions. Also the biomass concentration reached maximum value (0.213 g/l) in the culture fed with sodium acetate under 16: 8hrs light/dark and light intensity of 1830 lux.

Effect of sodium acetate on oil content: figure (14) Showed that oil content recorded its maximum value (0.159 g/l) in culture fed with sodium acetate under 16: 8hrs light/dark and light intensity of 1830 lux.

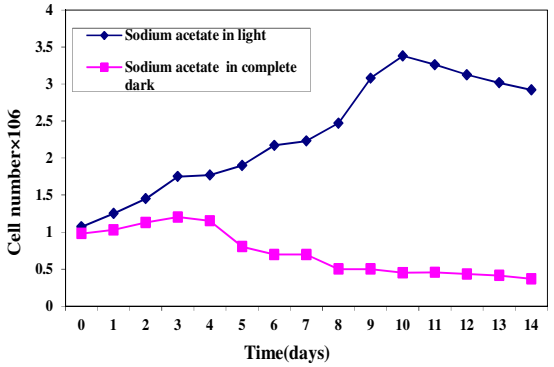

Fig. 12. Effect of sodium acetate on the cell number of *N. salina* grown under light regime of 16h light: 8h dark and light intensity of 1830 lux and under a complete darkness.

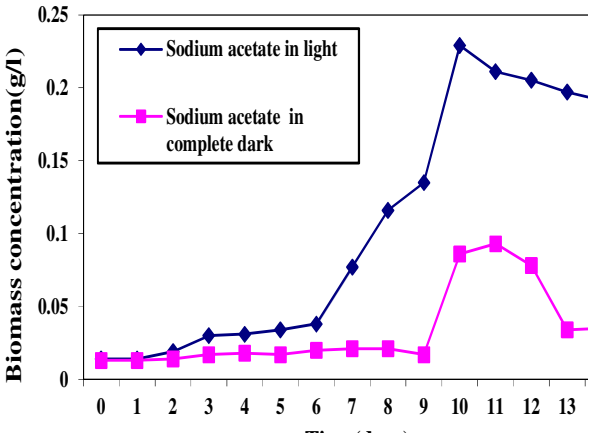

Fig. 13. Effect of sodium acetate on the biomass concentration of *N. salina* grown under light regime of 16: 8hrs light/dark and light intensity of 1830 lux and under a complete dark.

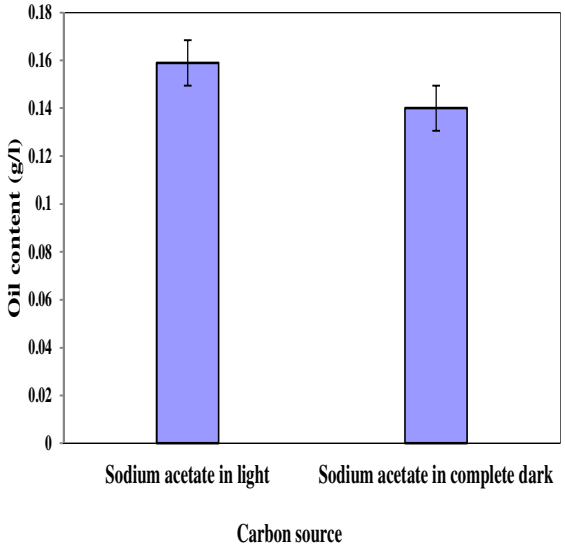

Fig. 14. Effect of sodium acetate on oil content of *N. salina* grown under light regime of 16: 8hrs light/dark and light intensity of 1830 lux and under a complete dark**.**

IV. Discussion

In the present work, fatty acid composition of *N. salina* was found to be in agreement with the general distribution pattern of fatty acids in other microalgae [29]. The characterization of fatty acid comprising biodiesel of *N. salina* was described in details [15]. However, although *N. salina* is described by many authors as a single cell lipid producer, the content of its TAG is relatively low [15]. For this reason, the study here looks to manipulate the cultivation conditions of *N. salina* to enhance the amount of oil production.

The results here showed relatively lower values of *N. salina*'s biomass. The slowly growth of the tested strain may be lower than expected results due to not enough agitation or the carbon dioxide being bubbled through the culture, which was the case in previous [4], [30], [31]. However, there is an increasing response of biomass of *N salina* towards different light intensities. A result goes in agreement with that obtained previously on *Nannochloropsis oculata* [32].

Results show a gradual increase of *N salina*'s oil content with increasing light intensity. Low light intensity causes the formation of polar lipids, particularly the membrane polar lipids that are associated with the chloroplast. However, high light intensity causes a decrease in the total polar lipid content with a concomitant increase in the amount of neutral storage lipids, mainly TAGs [33].

Exposure time of algal cell to light intensity, which is known as photoperiod, could affect its growth [30]. Adaptation of microalgae to fixed light regimes has received considerable attention and has provided detailed knowledge on the structure and functioning of their photosynthetic apparatus [34]. The optimal light/dark regimes have been found to vary from 12: 12 to 16: 8 light/dark cycles for most algae cultures [30]. In this connection, growth of *N. salina*, expressed as cell number, shows a positive response under 12:12 hrs light/dark regime cultivation, While the highest biomass was produced in cells grown under 16:8 hrs light/dark regime. A result indicating that exposure of *N. salina* to 16: 8 hrs light/dark regime with intensity of 1830 lux may stimulate the synthesis of some cellular biochemical compounds. As mentioned above, TAG is the mainly storage material associated with downloaded biomass. Therefore, in spite of a slowing of cell division at 12:12 hrs light/dark regime, biomass could still increase with light prolong time, due to net production of TAG [35]. On the other hand, the highest growth rate was found for cells grown under 12/12 hrs light/dark regime at the first 7 days, a result goes parallel with data of cell population density, since the growth rate in this study was calculated according to the cell number of the organism. Responses of algal growth rate to illumination are species-specific and depend on both the average light intensity and the period of light exposure [36]. In this study, 1830 lux was found to be the best light intensity that accelerates cell division, biomass downloading and the growth rate of *N. salina*. However, the continuous light showed a negative effect on cell number, biomass and growth rate of *N. salina*. An observation which was previously explained [37], since over illumination can cause photo-inhibition by photo-oxidative stress on the algae. Therefore, we can postulate that the preferred light cycle for the growth of *N. salina* is 16: 8 hrs light/dark regime, although the maximum growth rate was obtained at 12: 12 hrs light/dark cycle.

Although data in this study support the growth of the tested micralga under light/dark cycle, the production of the crude oil was stimulated in cells grown under continuous light. A result found in agreement with previous studies on other strains [38]-[41].

Reduction of biomass in cells growing under nitrogen limitation was previously explained [42]; it's a result of decreasing the intracellular chlorophyll content during the stationary growth phase. Decreasing in chlorophyll content in algal cell leads to minimize the size of the chloroplast [43]. Therefore, biomass yield is often inhibited in nitrogen-lacking situations [44].

Previous studies have long-established that lipid content in some micro algae strains could be increased by various cultivation conditions [45]. Among all the factors, nitrogen is known to have the strong influence on metabolism of lipids and fatty acids in various microalgae. In addition, nitrogen is easy to manipulate and is less expensive when compared to other factors. So it is critical to enhancing the lipid productivity for bio-fuel production [46]. Cells of *N. salina* fed with 0.5 g/l of urea gave approximately two and four folds of oil yield by the cells fed with the same concentration of nitrate and ammonium respectively. Therefore, we recommend urea as a nitrogen source for growing *N. salina* for biofuel purposes.

The lowermost growth values (cell density and biomass) of *N. salina* were detected in cells fed with ammonium sulphate. Declining of the growth in cells fed with ammonium sulphate was previously explained [47] high concentration of ammonium may cause a drastic pH drop in the growth medium of microalgae. Such conditions can have detrimental effect on algal photosynthesis [47]. In addition, the salt in the medium may play role in creating osmotic pressure that could affect cell viability [48]. However, the highest cell number was detected in cultures fed with 1g/l urea and 1.5 g/l potassium nitrate, both gave approximately the same population density. Based on biomass, the maximum growth values were in cultures fed with 0.5 g/l urea and 1.5 g/l potassium nitrate. Therefore, we recommend using of 0.5 g/l urea, as the best nitrogen concentration for *N. salina,* for its low price. Urea can be used as a very efficient nitrogen source for microalgae cultivation. Urea is very cheap compared to other nitrogenous nutrients available for microalgae which ultimately make it economically suitable for industrial production of microalgal fuel [49].

Nutrient limitation usually causes a decrease in cell division [50], [51]. In this study, no correlation between the effect of nitrogen limitation on cell number and biomass as a function of the growth was noticed. Perhaps, as a result of limitation conditions for 7 days, dead and non-valid cells were taken into consideration during cell counting. Therefore we will consider biomass data as a growth determinant. The maximum biomass of *N. salina* was achieved in cells fed with urea after 4-days of starvation conditions. Again, urea is the preferred nitrogen substrate for the growth of *N. salina*.

In this study, the maximum oil amount (0.261 g/l) was extracted from the N-starved cells after 24 hrs of feeding with urea. A result agrees with other studies [52], [53] and on

microalgae *Phaeodactylum tricornutum, Chaetoceros s*p., *Isochrysis galbana, Nannochloris atomus*, *Tetraselmis sp. Gymnodinum sp*. and *C. vulgaris*.

Further studies reported that lipid content can be enhanced by imposing nitrogen starvation leading to decreased cell division, if division was blocked, the rate of neutral lipid utilization would be slower than the rate of synthesis, so triglycerides would accumulate in the cells [50].

The algal cells specific growth rates, biomass concentrations and biochemical compositions were significantly influenced by the nutritional modes [54]. Most microalgal strains are well grown under autotrophic growth conditions; however, some spp have the ability to increase its biomass and lipid production under heterotrophic conditions [55]. Our results showed that supplementation of exogenous carbon sources such as sodium acetate could result in an increase in cell number and biomass yield. Under such conditions, carbon fixation through photosynthesis is greatly reduced and intercellular carbon will be mainly derived from acetate assimilation via the glyoxylate cycle. In the meantime, starch will be degraded to glucose through the glycolytic pathway to produce pyruvate, and thus triacylglycerols [56].

Our data showed a significant increase of oil production by *N. salina* grown under photoautotrophic and mixotrophic with sodium acetate, compared with heterotrophic conditions. *Chlorella protothecoides* can grow under photoautotrophic, mixotrophic and heterotrophic conditions [57]. The highest lipid accumulation was obtained under heterotrophy [55]. In mixotrophic and heterotrophic culture, the lipid content was much higher than that in the autotrophic culture. The same result was concluded [54] previsouly on *Chlorella vulgaris*.

Conclusion and future work: what was done previously at our lab demonstrates that *N. salina* is not a superior source for biodiesel manufacturing purposes; the amount of algal oil is relatively low, and the quality of biodiesel needs to be improved. To achieve our goal for enhancing the quantity of oil production, some of biochemical engineering work was carried out on *N. salina.* The response of algal cell showed positive results towards the cultivation under different stresses. Continuous high light intensity, feeding with urea as a nitrogen source, nitrogen limitation, mixotrophic nutritional mode; are all collectively enhancing the amount of oil produced by the examined strain. However, further applications of many other circumstances, e.g. mutation and other omics engineering, may positively contribute to our research. A compromise between high oil production while maintaining high cell division of *N. salina* is also an important target. In addition, we still need to correlate between the stress conditions applied in this study and the quality of biodiesel manufactured.

V. Acknowledgment

The authors gratefully acknowledge Mrs Anthi Charalambous from the Cyprus Energy Agency for their work to facilitate the project and Dr Ioannis Tzevenis from the National and Kapodistrian University of Athens.

VI. References

[1] R. L. Meier, "Biological cycles in the transformation of solar energy into useful fuels," In: Solar Energy Research, (Daniels, F. and Duffie, J. A. eds.), Madison University Wisconsin, 1955, pp. 179–183.

[2] C. J. Campbell, "The coming oil crisis Multi-science Publishing Company and petro consultants S.A, Essex, England, 210 pp.

[3] Y. Chisti, "Biodiesel from microalgae beats bioethanol. Trends in Biotechnology," vol. 26, pp. 126-131, Mar. 2008.

[4] J. Sheehan, T. Dunahay, J. Benemann, and P. Roessler, " A look back at the U.S. Department of Energy's Aquatic Species Program: biodiesel from algae. In Closeout Report NREL/TP-580-24190,U.S.Department of Energy's Office of Fuels Development, National Renewable Energy Laboratory, Golden, CO.

[5] S. Y. Chiu, C. Y. Kao, M. T. Tsai, S. C. Onq, C. H. Chen, and C. S. Lin, " Lipid accumulation and CO2 utilization of *Nannochloropsis oculata* in response to CO2 aeration," Bioresour. Technol., vol. 100(2), pp. 833-838, Jan. 2009.

[6] L. Gouveia, and A. C. Gouveia, "Microalgae as a raw material for biofuels production," J. Ind. Microbiol. Biotechnol., vol. 36, pp. 269-274, Feb. 2009.

[7] N. Zou, C. W. Zhang, Z. Cohen, and A. Richmond, "Production of cell mass and eicosapentaenoic acid (EPA) in ultrahigh cell density cultures of *Nannochloropsis* sp. (Eustigmatophyceae)," Eur. J. Phycol., vol. 35, pp. 127-133, May. 2000.

[8] Y. Suen, J. S. Hubbard, G. Holzer, and T. G. Tornabene, "Total lipid production of the green-alga *Nannochloropsis* sp. QII under different nitrogen regimes," J. Phycol., vol. 23, pp. 289-296, Apr. 1987.

[9] J. N. Rosenberg, G. A. Oyler, L. Wilkinson, and M. J. Betenbaugh, "A green light for engineered algae: redirecting metabolism to fuel a biotechnology revolution," Curr. Opin. Biotechnol., vol. 19(5), pp. 430-436, Oct. 2008.

[10] L. Rodolfi, G. C. Zittelli, N. Bassi, G. Padovani, N. Biondi, G. Bonini, and M. R. Tredici, "Microalgae for oil: strain selection, induction of lipid synthesis and outdoor mass cultivation in a low-cost photobioreactor," Biotechnol. Bioeng., vol. 102, pp. 100-112, Jan. 2009.

[11] N. G. Mohammady, Y. C. Chen, A. A. El-Mahdy, and R. F. Mohammad, "Temporal alterations of *Nannochloropsis salina* (Eustigmatophyceae) grown under aqueous diesel fuel stress," J. App. Phycol., vol. 17, pp. 161-170(10), Mar. 2005.

[12] L. M. Lubián, "Ultraestructura y pigmentos de algunas Chlorophyceae y Eustigmatophyceae planctonicas de morfologia similar," Collectanea Botanica., vol. 13, pp. 873-880, Dec. 1982.

[13] Y. Gonen-Zurgil, Y. Carmeli-Schwartz, and A. Sukenik, "Selective effect of the herbicide DCMU on unicellular algae-a potential tool to maintain monoalgal mass culture of *Nannochloropsis*," J. Appl. Phycol., vol. 8, pp. 415-419, Aug. 1996.

[14] I. Moreno-Garrido, J. Blasco, M. Gonzalez-Delvalle, and L. M. Lubian, "Differences in copper accumulation by the marine microalga *Nannochloropsis gaditana*, submitted to two different thermal treatments," Ecotox. Environ. Restoration, vol. 1, pp. 43-47, 1998.

[15] N. G. Mohammady, "Characterization of Fatty acid composition of *Nannocloropsis salina* as a determinant of biodiesel properties," Z. Naturforsch., vol. 66, pp. 328-332, Jul. 2011.

[16] S. Boussiba, A. Vonshak, Z. Cholen, Y. Avissar, and A. Richmond, "Lipid and biomass production by halotolerant microalga *Nannochloropsis salina*," Biomass, vol. 12, pp. 37-47, 1987.

[17] A. M. Wood, R. C. Everroad, and L. M. Wingrad, "Measuring growth rates in microalgae cultures," In: Andersen, RA (ed) Algal culturing techniques Elsevier, Amsterdam, 2005, pp. 429–538.

[18] A. S. Mirón, C. Garcia, F. G. Camacho, E. M. Grima, and Y. Chisti, "Growth and biochemical characterization of microalgal biomass produced in bubble column and airlift photobioreactors: studies in fed-batch culture," Enzyme Microb.Technol., vol. 31, pp. 1015-1023, Dec. 2002.

[19] E. G. Bligh, and W. M. Dyer, "Rapid method for lipid extraction," Can. J. Biochem. Physiol., vol. 35, pp. 911-915, 1959.

[20] X. Miao, and Q. Wu, "Biodiesel production from heterotrophic microalgal oil," Bioresour. Technol., vol. 97, pp. 841-846, Apr. Apr. 2006.

[21] S. S. Radwan, "Sources of C20-polyunsaturated fatty acids for biotechnological use," Appl. Microbiol. Biotechnol., vol. 35, pp. 421-430, Jul. 1991.

[22] R. Weast, (1986): Handbook of Chemistry and Physics, 66th ed. CRC Press, Boca Raton, FL, p. D272.

[23] F. Gunstone, J. Harwood, and F. Padley, (1994): The Lipid Handbook. Chapman and Hall, London.

[24] P. Schenk, S. Thomas-Hall, E. Stephens, U. Marx, J. Mussgnug, C. Posten, O. Kruse, and B. Hankamer, "Second generation biofuels: High-efficiency microalgae for biodiesel production," Bioenerg. Res., vol. 1, pp. 20-43, Mar. 2008.

[25] G. Knothe, J. Krahl, and J. Van Gerpen, (eds). (2005): The Biodiesel Handbook.AOCS Press, Champaign, IL.

[26] G. H. Knothe, and K. R. Steidley, "Kinematic viscosity of biodiesel fuel components and related compounds. Influence of compound structure and comparison to petrodiesel fuel components," Fuel, vol. 84, pp. 1059-1065, Jun. 2005.

[27] T. Gouw, J. Vlugter, and C. Roelands, "Physical properties of fatty acid methyl esters: VI. Viscosity," J. Am. Oil Chem. Soc., vol. 43, pp. 433-434, Jul. 1966.

[28] B. Freedman, and M. Bagby, "Heats of combustions of fatty esters and triglycerides," Am. J. Oil Chem. Soc., vol. 66, pp. 1601-1605, Nov. 1989.

[29] X. Meng, J. Yang, X. Xu, L. Zhang, Q. Nie, and M. Xian, "Biodiesel production from oleaginous microorganisms," Renew. Energ., vol. 34, pp. 1-5, Jan. 2009.

[30] R. A. Andersen, Algal culturing techniques. San Diego: Elseveier Academic Press.

[31] Y. Chisti, "Biodiesel from microalgae, "Biotechnol. Adv., vol. 25, pp. 294-306, Feb. 2007.

[32] S. Banerjee, W. Hew, H. Khatoon, M. Shariff, and F. Yusoff, "Growth and proximate composition of tropical marine *Chaetoceros calcitrans* and *Nannochloropsis oculata* cultured outdoors and under laboratory conditions," Afr. J. Biotechnol., vol. 10, pp. 1375-1383, Feb. 2011.

[33] Q. Hu, M. Sommerfeld, E. Jarvis, M. Ghirardi, M. Posewitz, M. Seibert, and A. Darzins, "Microalgal triacylglycerols as feedstocks for biofuel production: perspectives and advances," Plant J., vol. 54, pp. 621-639, May. 2008.

[34] P. G. Falkowski, and J. LaRoche, "Acclimation to spectral irradiance in algae," J. Phycol. vol. 27, pp. 8-14, Feb. 1991.

[35] I. Khozin-Goldberg, C. Bigogno, P. Shreshta, and Z. Cohen, "Nitrogen starvation induces the accumulation of arachidonic acid in the freshwater green alga *Parietochloris incisa* (Trebouxiophyceae)," J. Phycol., vol. 38, pp. 991-994, Oct. 2002.

[36] E. Litchman, "Growth rates of phytoplankton under fluctuating light," Freshwater Biol., vol. 44, pp. 223-235, Jun. 2000.

[37] R. Leon, and D. Galvan, "Interaction between saline stress and photo inhibition of photosynthesis in the freshwater green algae *Chlamydomonas reinhardtii*. Implication for glycerol photoproduction," Plant Physiol. Bioch., vol. 37, pp. 623-628, Aug.1999.

[38] S. V. Khotimchenko, and I. M. Yakovleva, "Lipid composition of the red alga *Tichocarpus crinitus* exposed to different levels of photon irradiance," Phytochemistry, vol. 66, pp. 73-79, Jan. 2005.

[39] M. R. Brown, G. A. Dunstan, S. J. Norwood, and K. A. Miller, "Effects of harvest stage and light on the biochemical composition of the diatom *Thalassiosira pseudonana*," J. Phycol., vol. 32, pp. 64-73, Feb. 1996.

[40] G. E. Napolitano, "The relationship of lipids with light and chlorophyll measurement in freshwater algae and periphyton," J. Phycol., vol. 30, pp. 943-950, Dec. 1994.

[41] A. Sukenik, Y. Carmeli, and T. Berner, "Regulation of fatty acid composition by irradiance level in the eustigmatophyte *Nannochloropsis* sp," J. Phycol., vol. 25, pp. 686-692, Dec. 1989.

[42] K. Yamaberi, M. Takagi, and T. Yoshida, "Nitrogen depletion for intracellular triglyceride accumulation to enhance liquefaction yield of marine microalgal cells into a fuel oil," J. Mar. Biotechnol., vol. 6, pp. 44-48, 1998.

[43] M. Vesk, and S. W. Jeffre, "Effect of blue-green light on photo synthetic pigments and chloroplast structure in unicellular marine algae from six classes," J. Phycol., vol. 13, pp. 280-288, Sep.1977.

[44] Y. Shen, Z. Pei, W. Yuan, and E. Mao, "Effect of nitrogen and extraction method on algae lipid yield," Int. J. Agric. and Biol. Eng., vol. 2, pp. 51-57, Mar. 2009.

[45] A. M. Illman, A. H. Scragg, and S. W. Shales, "Increase in *Chlorella* strains calorific values when grown in low nitrogen medium," Enzyme Microb. Technol., vol. 27, pp. 631-635, Nov. 2000.

[46] M. Takagi, K. Watanbe, K. Yamaberi, and T. Yoshida, "Limited feeding of potassium nitrate for intracellular lipid and triglyceride accumulation of *Nannochloris* sp. UTEX LB 1999," Appl. Microbiol. Biotechnol., vol. 54, pp. 112-117, Jul. 2000.

[47] N. F. Y. Tarn, and Y. S. Wong, "Effect of ammonia concentrations on growth of *Chlorella vulgaris* and nitrogen removal from media," Bioresour. Technol., vol. 57, pp. 45-50, Jul. 1996.

[48] S. Schuldiner, H. Rotenberg, and M. Avron, "Determination of change in pH in chloroplasts," Eur. J. Biochem., vol. 25, pp. 64-70, Jan. 1972.

[49] R. Goswami, and M. Kalita, "*Scenedesmus dimorphus* and *Scenedesmus quadricauda*: two potent indigenous microalgae strains for biomass production and CO2 mitigation - A study on their growth behavior and lipid productivity under different concentration of urea as nitrogen source," J. Algal Biomass Utln., vol. 2, pp. 42-49, 2011.

[50] M. Takagi, Karseno, and T. Yoshida, "Effect of salt concentration on intracellular accumulation of lipids and triacylglyceride in marine microalgae *Dunaliella* Cells," J. Biosci. Bioeng., vol. 101, pp. 223-226, Mar. 2006.

[51] N. G. Mohammady, C. W. Rieken, S. R. Lindell, C. M. Reddy, H. M. Taha, C. P. Ling Lau, and C. A. Carmichael, "Age of nitrogen deficient microalgal cells is a key factor for maximizing lipid content,". Res. J. Phytochem., vol. 6, pp. 42-53, 2012.

[52] K. I. Reitan, J. R. Rainuzzo, and Y. Olsen, "Effect of nutrient limitation on fatty acid and lipid content of marine microalgae," J. Phycol., vol. 30, pp. 972-979, Dec. 1994.

[53] A. Widjaja, C. C. Chien, and J. Yi-Shu, "Study of increasing lipid production from fresh water microalgae *Chlorella vulgaris*," J. Tai. Inst. Chem. Eng., vol. 40, pp. 13-20, 2009.

[54] W. Kong, H. Song, Y. Cao, H. Yang, S. Hua, and C. Xia, "The characteristics of biomass production, lipid accumulation and chlorophyll biosynthesis of *Chlorella vulgaris* under mixotrophic cultivation," Afr. J. Biotechnol., vol. 10, pp. 11620-11630, Sep. 2011.

[55] X. Miao, and Q. Wu, "High yield bio-oil production from fast pyrolysis by metabolic controlling of *Chlorella protothecoides*," J. Biotechnol., vol. 110, pp. 85-93, May. 2004.

[56] L. P. Lin, and T. Chen, "Factors affecting the mixotrophic maximum growth of *Chlorella pyrenoidosa*," J. Chin. Agric. Chem. Soc., vol. 32, pp. 91-102, Feb. 1994.

[57] N. Jiménez –Ruiz, M. D. C. Cerón –García, A. Sanchez- Mirón, E. H. Belarbi- Haftalaui, F. García –Camacho, and E. Molina-Grima, "Lipids accumulation in *Chlorella protothecoides* through mixotrophic and heterotrophic cultures for biodiesel production," New Biotechnol., vol. 2, pp. 25-266, 2009.

VII. BIOGRAPHIES

Nagwa Gamal Eldin Mohamady was born in cairo, Egypt, on October, 25, 1959. She studied at Alexandria University.

Her employment experience included both teaching for undergraduates, postgraduates and research as well.

She has been awarded Lucy mann research award from MBL, MA, USA, 2009 and the Man of the Year-representing Egypt-2009 from the American Institute of Biography, NC, USA.

Currently Dr Mohamady is a professor of phycology at Alexandria University, her research interest focus on microalgae as a source for biofuel production.

Elsayed Mohamed ibrahim was born in kafr-elsheik, Egypt, on septemberber, 9, 1985. He studied at Alexandria University.

His employment experience included both teaching for undergraduates, postgraduates and research as well.

Currently Mr Elsayed is an assistant lecturer of phycology at Alexandria University, his research interest focus on microalgae as a source for biofuel production.

2nd Conference on Power Options for the Eastern Mediterranean Region
07-08 October 2013, Nicosia, Cyprus (Paper No. POEM13/195)

Towards low carbon homes through energy renovations

Gregoris P. Panayiotou, Maria Ioannidou, Anthi Charalambous
Cyprus Energy Agency

***Abstract*--In this paper a description of the ERACOBUILD "Countdown to Low Carbon Homes" project along with the current progress to date in Cyprus is presented. This project began in 2012 and involves partners from three EU countries: Cyprus Energy Agency (Cyprus), Aristotle University of Thessaloniki (Greece), and Severn Wye Energy Agency (United Kingdom). Cyprus Energy Agency is undertaking this project in order to develop a one stop service for the sustainable energy retrofit of homes in Cyprus. This service aims to support anyone wishing to improve the energy efficiency of their home, by showing them low cost methods to maximise their return on investment, with long term benefits for the environment and their own family budget. In Cyprus twenty-one case studies of domestic sustainable energy retrofit have been selected while also two support groups have been created: the Regional Advisory Group and the Local Installers Group. Both groups meet on a regular basis to exchange information and opinions on the progress, implementation and outcomes of the project.**

***Index Terms*—Energy behavior, Financial, Low Carbon, Quantitative results, Retrofit, Smart meter, SMEs**

I. Introduction

Building upon workable local solutions provides the ideal basis for scaling up and cutting costs. Working within geographical communities in 3 member states (UK, Greece and Cyprus), the Countdown project aims to research, develop and communicate an integrated practical delivery approach to community scale retrofit of buildings, with a particular focus on homes and delivery by SMEs, and with the potential to contribute substantially to challenging carbon and energy saving targets within the EU. The project involves partners from three EU countries: Severn Wye Energy Agency-lead partner (United Kingdom), Aristotle University of Thessaloniki (Greece), and Cyprus Energy Agency, CEA (Cyprus).

Attention will be given to the whole 'retrofit journey', encompassing both demand and supply side action, including awareness-raising, bespoke advice, local installer groups and financing mechanisms, with a new financing programme established and trialled in one of the partner regions, to form the basis for an exchange of knowledge and experience with the other partners.

Following the sustainable development framework of 'engage, encourage, enable and exemplify', innovative aspects of the project include action research to draw lessons from the retrofit experience of both installers and households, engaging all key actors (home owners, installers, suppliers, advisers, and building and planning control) in co-learning, and engaging households themselves in post retrofit monitoring.

II. State of the Art

Current thinking on cost reduction and scaling up retrofit tends to focus on area-based approaches (limited area street by street) as the solution, to secure logistical benefits and scale economies, which depend on being able to carry out substantial works within a relatively short time. This may work for social housing, but application to private sector requires leverage of investment by property owners, as well as willingness to accept the disruption of building works which is common to all tenures. For high deprivation areas there may be enough subsidy and benefits in improvement in living conditions to overcome these barriers, but not elsewhere.

Our direct experience of working with owner occupiers and installers indicates growing concern about energy costs and climate change, and interest in improving energy efficiency, but many reasons in practice for a step by step approach to making improvements. There are also many barriers and opportunities, practical, financial, aesthetic, regulatory.

These details will be explored through researching knowledge and experience of key actors: home owners and the retrofit supply chain, in particular (mainly SME) builders and installers, planning/ building control, and local building suppliers. Little research has been done to engage this crucial sector (focussing rather on larger commercial and public sector market actors),or to document the real experience of home-owners in getting retrofit work done, making user adjustments post retrofit, and barriers and solutions to ensuring full benefits are realised.

Finally, the issue of how to finance deep carbon reduction retrofit (as opposed to quick return measures only) is highlighted in current debate, but only partly addressed, due to lack of detailed knowledge of real practical issues, costs and savings.

The high proportion of owner occupied homes in the EU makes this a significant issue to understand better in terms of scaling up retrofit, and reducing costs.

III. Proposed Solutions

Policy work is being done in UK to develop a 'Green Deal' retrofit framework, and many programmes here and in other countries support roll-out of single measures, but practical delivery of deep carbon cuts through retrofit is complex, and primarily delivered on a bespoke level by the local/regional supply chain.

This project has been co-funded by the National Framework Programme of Research Promotion Foundation, DESMI 2009-2012.

G. P. Panayiotou is an external expert of Cyprus Energy Agency, Nicosia, Cyprus (e-mail: Gregoris.Panayiotou@yahoo.com).

A. Charalambous is with the Cyprus Energy Agency, Nicosia, Cyprus (email: Anthi.Charalambous@cea.org.cy).

M. Ioannidou is with the Cyprus Energy Agency, Nicosia, Cyprus (email: Maria.Ioannidou@cea.org.cy).

Scaling up can be achieved by starting at this level and building on it, overcoming practical barriers step by step. This also has the benefit of supporting the local economy and increasing capacity, as opposed to 'cherry-picking' profitable measures by larger companies with no long term local presence.

Finance can be a major barrier for the private owner. Studies by SWEA and FEDARENE have reviewed existing finance products and note heavy reliance on public sector funding, with funds available diminishing. A knowledge exchange programme between partner regions will explore different approaches in use, such as the CERT/ECO in the UK, 'Exikonomo katikon – Saving energy at home' in Greece, and observe development in UK of a Revolving Loan Guarantee Fund, following the successful approach used in Hungary and Estonia.

The project will deliver:

- Valuable insights into barriers and solutions to retrofit of private housing, from perspective of key actors directly involved
- Quantitative results in terms of potential and actual savings, and evidence of user behaviour issues encountered
- Trialling, evaluation, documentation, communication of integrated local delivery model, including advice, supply, installation and behaviour support
- Knowledge exchange on retrofit finance between regions, including application of revolving loan guarantee fund to private housing in a western European country for the first time

This will provide a core delivery model which can be replicated to achieve retrofit on a large scale, building up from practical success at community level. Outputs will be disseminated at regional, national and EU level.

IV. Description of the Project

A. *Research and Development Actions*

The research and development part of the project aims to develop and trial a local delivery model and draw in knowledge and experience from key market actors and is separated in the following actions:

- Establishment of the Local Installers Group (LIG) and Regional Advisory Group (RAG).
- Implementation and evaluation of a co-learning programme.
- Recruitment of a Post-retrofit household group.
- Recruitment of a Pre-retrofit household group.

(1): Establishment of the Local Installers Group and Regional Advisory Group

The establishment of LIG in Cyprus is very important step towards the successful implementation of the project. The reason of establishing such group is to cover all the main technologies and techniques required for sustainable energy retrofit of homes in Cyprus. It is expected that the LIG should include the following specialities: Boiler installers, Chillers installers, Heating and Air Conditioning (HVAC) installers, Lighting improvements (designers and installers), Specialists on the Building envelope modifications (including the insulation materials, plasters, paints etc), Renewable technologies installers, Electricity utility including the smart metering, Domestic appliances sellers, Sellers and installers of double glazing and shading devices.

The number of persons that will be included in the LIG is expected to be 2 from each category. Approximately the Group will be consisted of 20 members.

The CEA will support this group as an identifiable service, at the same time as working with them to evaluate the barriers and solutions to retrofit from their perspective. The barriers related with the retrofit are usually (a) market barriers: consumer (demand Site) barriers and contractors (supply site) barriers, (b) financial, (c) Technology and (d) policy.

The objective of establishing the LIG is a win-win situation as the aim is that installers group should benefit from being part of the group, but also the CEA and the project would benefit as well from their experiences. The indicative list below describes the benefits of the LIG:

- cross-transfer of information and knowledge between providers and installers of different technologies
- possibility of Joint marketing of retrofit services and products
- Information on grants, planning, new technologies
- Arranging information and/or short training sessions according to interest, such as with suppliers and planning control officers
- Presenting examples of installations and barriers overcome in the local area
- Joint visits to see installations, or to trade fairs etc
- Collaboration on opportunities for join procurement, to save time and bring down costs
- Reviewing opportunities for other cooperative activities, to enable them to engage in new markets – such as training and accreditation

The LIG will meet 2 times together with the RAG. These meetings will be arranged in such a way as to be both convenient and attractive, offering information and exchange of views.

All activities and the reactions to them will be fully documented. The action research approach of action and reflection in series will be applied.

In addition, in Cyprus, a RAG will also be established to engage the key experts on the retrofit. This Group will come also in contact with the Installers Group as in Cyprus rarely key experts meet together with the Installers. In Cyprus for example, the aim is that the RAG will consist of 10 members, for example: Social housing providers e.g Cyprus Land Development Organization, a representative of the Cyprus Association of the Renewable Energy Enterprises, a senior planning control officer (e.g. Town Planning Department), a senior building control officer (e.g. ESCOs), a building supplies company representative (Associations of Energy Saving Enterprises), a research academic (Private and Public Universities).

(2): A co-learning programme

A co-learning programme will be implemented and evaluated, using case study (or 'exemplar') homes as the basis for study by groups consisting of all key actors, home owners, installers, building suppliers, building and planning control personnel and advisers. This will be fully documented and form the basis of written case studies. In particular the description of the actions will be implemented in Cyprus are the following:

- Find a number of home owners (the target will be 20) who are willing to undertake an energy renovation on their homes to improve energy performance.
- Agree with them to be case studies
- Advise and help them through the process, including technical advice, estimated energy savings, cost etc
- Set up some 'action learning' sets to involve the different actors involved – will for example include reviewing barriers and solutions to getting sustainable energy retrofit done, practical issues arising, user behaviour issues etc
- Write up the case studies as examples to form part of the report (this will also be used for advice and dissemination actions)

(3): Post retrofit household group

A group of households (target of 5 in Cyprus) will be recruited to work with over a period of 2 years. This will focus upon the user experience and behaviour, and the performance of buildings after retrofit. It will include the establishment of an 'energy diary' approach to self monitoring which will encourage the householder in the habit of monitoring consumption and actions or external factors that impact upon it .

The project partner will provide a monthly energy adviser visit to each home, so as to:

- take meter readings
- discuss and record any changes to usage behaviour
- discuss and record any changes to the building, works done etc

(4): Pre retrofit household group

This will focus upon the household experience of retrofit. Home owners will be recruited for assistance with retrofit and to participate in detailed documentation of their experience.

The project partner will provide an onsite energy visit and advice, with a written report on the energy performance of the house and recommendations for energy improvements. They will also provide follow on 'hand holding' advice to help to get works done, including finance and installers, with recording of the experience by both householder and adviser.

Focus groups will be held to draw out experience of the group, as well as each individually keeping a diary of experience.

Incentives will be provided to ensure participation (given at the end of the programme), the precise nature of these will be decided by each partner, but it could for example be a cash payment or a voucher for an energy efficient appliance.

B. Financing retrofit

This part of the project will involve two main elements:

- Finance for retrofit knowledge exchange:
- Implementation of Revolving Loan Retrofit Guarantee Fund

(1): Implementation of Revolving Loan Retrofit Guarantee Fund

This will be implemented only in the UK, and will be the first time that this has been established in a western European country. The work will be coordinated by Severn Wye Energy Agency in partnership with Stroud District Council (together with the other neighbouring partner local authorities) with expert support from sub-contractor GESB.

(2): Finance for retrofit knowledge exchange:

A programme of knowledge exchange on finance for retrofit within the UK and the other partner regions. This will be achieved by engaging the project partners (and other key actors identified by them) as observers in development of the RRGF in the UK, as well as through exchange communications regarding the range of finance products for retrofit employed in each of the partner countries. This exchange will be extended to other countries, through relevant EU networks as part of the dissemination programme.

C. Local retrofit delivery model

The results and learning from the previous actions of this project will be captured and presented as a basis for a replicable local retrofit delivery model. The detail of the content toolkit will be clarified and developed from the experience of the research program, but is likely to include the following general areas:

- typology of buildings, retrofitting measures, energy, carbon and cost calculations
- advice, information and support for home owners, installers
- financing the measures
- barriers and solutions in different building types
- connecting the local supply chain, so that advice and information, supplies, finance, installation expertise, and building permissions are all part of a coherent customer journey

V. Benefit for the Society and the Business Sector

The retrofit challenge is a major one for all countries in Europe, as reflected in EU wide policy on reducing emissions from existing buildings. Climate change agreements highlight the need to reduce carbon emissions, and there is concern about security of energy supplies to meet rising demand in the next decades. Energy poverty is on the rise and is a phenomenon increasingly recognised in EU countries, with consequences for health and well-being.

With economic downturn the rate of replacement of buildings has reduced drastically, increasing further the significance of achieving deep carbon retrofit. Loss of work in the construction sector is both an additional socio-economic concern, and risks loss of valuable skills.

Good quality and appropriate retrofit is a win-win solution, but is complex to achieve in practice, especially in private housing, where it relies on significant levels of own investment by home owners, as well as disruption and purchase of potentially unfamiliar new technologies. Most repair and refurbishment is done by SMEs, and they also face challenges and barriers. Other key actors in the supply chain are building suppliers, and local planning and building control personnel.

This project will view the sector from the perspective of these actors for the first time, bringing them together in a co-learning program. It will research and develop real practical experience, and produce evidence-based research conclusions and a practical guide for a local delivery model. This has the potential to kick-start an EU wide exchange on local retrofit of lasting benefit socially, environmentally, and economically.

The guarantee fund enables the scheme to run continually in the event of temporary default on repayments (as high as 5% can be accommodated). The loans funds can be derived from a range of sources and can be scaled up or down. We aim in this case to source European (Recovery Fund) funding for the guarantee fund, against which to interest commercial banks in offering loans to home owners. The scheme has been proven to be able to offer the highest leverage ratio (as high as 1:20) compared to other currently known finance mechanisms.

The exchange of knowledge on finance mechanisms will enable sharing of this crucial area of knowledge to enable retrofit across the EU

VI. Progress to Date in Cyprus

Currently, in Cyprus the LIG (Table I), the RAG (Table II) and the pre-retrofit household group have been formed and work with them is underway. Working with these groups enables us to identify opportunities and barriers for encouraging widespread take up of domestic energy improvements.

TABLE I
LOCAL INSTALLERS GROUP PARTICIPANTS

Installers/SMEs	Number
Boiler installers	3
Chillers installers	2
Heating and Air Conditioning (HVAC)	4
Lighting improvements	3
Building shell	7
Renewable technologies	11
Electricity utility & smart metering	1
Domestic appliances	-
Double glazing	1

TABLE II
REGIONAL ADVISORY GROUP PARTICIPANTS

Participants	Number
Policy Makers	2
Local Authorities	1
Energy Agencies	CEA
RES Associations	1
Other Association	2
Housing providers	1
Finance	1
Academia	3

The 1st meeting of the LIG was held on the 20th of December 2012 where the homeowners and the members of the RAG also participated. The LIG representatives presented their products and services. The aim of the meeting was to identify possible problems and barriers but also to find opportunities and solutions during the discussions with owners. For this purpose a specific questionnaire was formulated which included 6 different questions. The results of the completed questionnaires are graphically presented in Figs. 1-6 below.

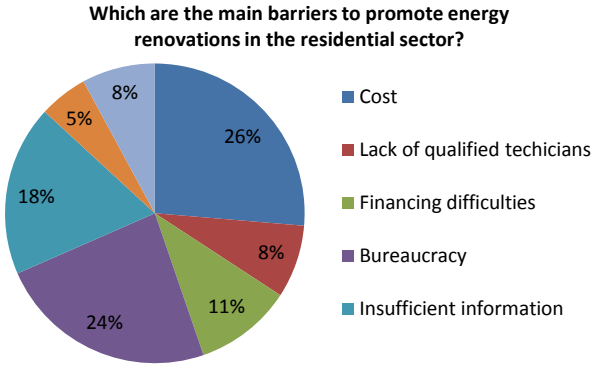

Fig. 1. The main barriers to promote energy renovations in the residential sector.

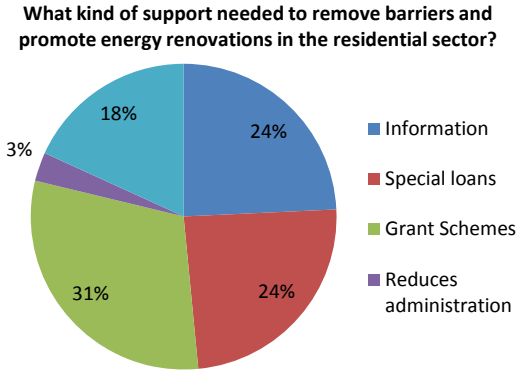

Fig. 2. The necessary kind of support required to remove barriers and promote energy renovations in the residential sector.

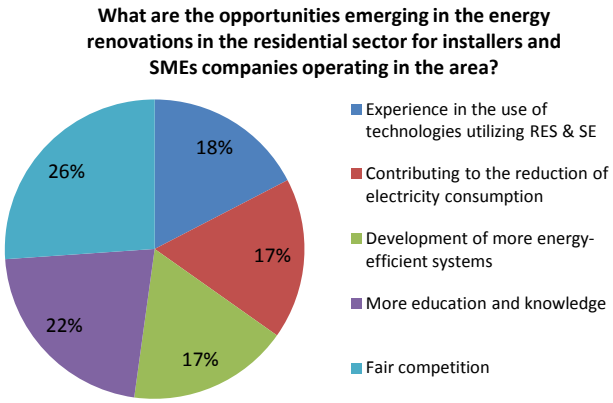

Fig. 3. The opportunities emerging in the energy renovations in the residential sector for installers and SMEs companies operating in the area.

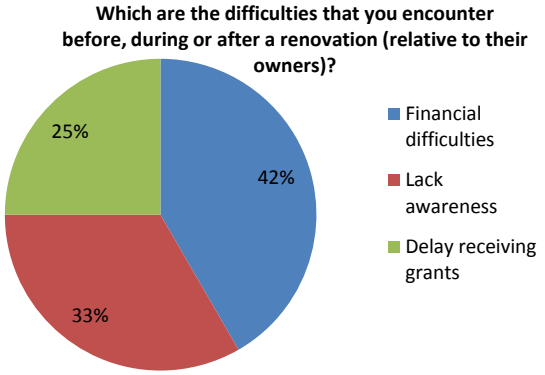

Fig. 4. The difficulties that the LIG encounter before, during or after a renovation (relative to their owners)

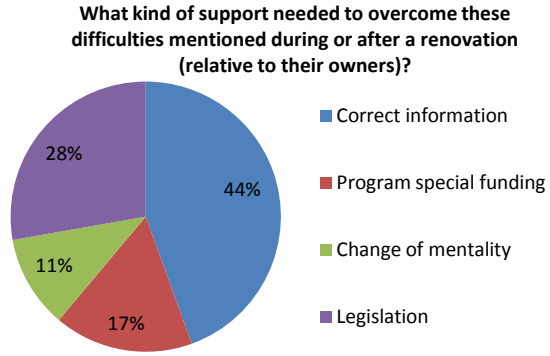

Fig. 5. The kind of support needed to overcome these difficulties mentioned during or after a renovation (relative to their owners).

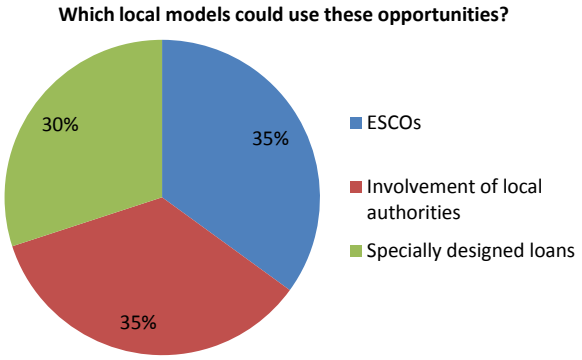

Fig. 6. The kind of local models to use these opportunities.

It is very interesting to notice that according to the LIG the main barrier to the promotion of energy renovations in the residential sector is their cost (26%) followed by bureaucracy (24%). The financial are also considered to be the main difficulties (42%) encountered before, during or after a renovation. Thus, the required support necessary to overcome these barriers and promote energy renovations in the residential sector in Cyprus are the deployment of new Grant Schemes (31%) and special loans by the banks (24%) and the correct information of the public (24%).

Twenty-one households, the location of which is shown in Fig. 7, have been selected to participate in the action research following a call for expressions of interest. The characteristics of the participating households are listed in Table III. The current energy status of these households will be evaluated through an onsite energy visit from energy experts in order to advise on possible measures and ways to reduce the current energy consumption and to calculate the Energy Performance Certificate (EPC). Additionally, in each household a smart meter has been installed (kind courtesy of CEA) in order both to log the energy consumption before and after the application of the proposed retrofit measures and also to assist the occupants of the house understand the main energy consuming devices and consequently help change their energy behaviour. The participating households have also been offered access to professionals, guidance for funding opportunities, as well as ongoing support both during and after their home energy improvements to ensure they reap the maximum benefits.

Fig. 7. Map of Cyprus showing the number of the selected households in each city of Cyprus.

TABLE III
CHARACTERISTICS OF THE PARTICIPATING HOUSEHOLDS

Year of construction				
1965-1980	1981-1990	1991-2000	2001-2010	<2011
7	4	6	6	0
Area of the household				
<100	101-150	151-200	201-250	251<
1	8	5	3	6
Type of the household				
Flat	Single house	Duplex house	Semi-	
3	10	9	1	
Occupants				
Single person	Couple	Family with	residents	
2	1	15	5	
Family annual income (thousand €)				
0-20	20–30	30-40	40-55	55-70	<70
1	5	3	8	5	1

Between March-July 2013 the CEA team has completed the onsite energy visits and has collected qualitative and quantitative data concerning the energy consumption of each household. The purpose of the visits was twofold; to collect data from owners through a constructive questionnaire which was specifically formulated for the needs of this project and also technical information and data such as the U-values of the external walls, measurements of humidity, temperature and where possible, infrared thermal imaging of the house.

Currently, the collected data and information are being evaluated and it is expected that by the end of autumn of 2014 the results will be completed and sent to the

homeowners in the form of a report. Additionally these results will be disseminated by the CEA through web pages, scientific articles, participation in conferences, workshops and seminars through the media.

VII. Initial Results of the Energy Visits

The initial results of the analysis of the data acquired during the completed energy visits for 5 houses reveal some very interesting facts. The energy class of all 5 houses is calculated to be G while none of them has any kind of thermal insulation installed on their envelope. On the contrary 4 of the houses have double glazing and all 5 have solar water heating system (SWH) installed. As a result of the absence of thermal insulation several thermal bridges occur on the envelope of these houses. The existence of the thermal bridges was revealed by using infrared thermal imaging of the house as shown in Fig. 8.

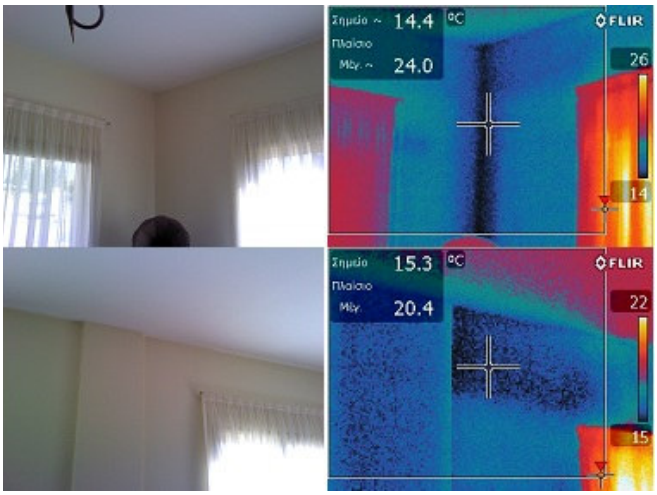

Fig. 8. Thermal images of the envelope of one of the selected households revealing the existence of thermal bridges.

The proposed measures included the following: replacement of tungsten lamps (1 case), installation of external insulation on the roof (2 cases), installation of internal insulation on top of the ceiling (1 case), replacement of old air conditioning units with new energy efficient (1 case) and replacement of single glazing with double glazing with thermal brakes in the aluminum frame (1 case).

The expected energy savings of each measure range between 8-40% while the consequent cost ranges between 150€ (replacement of the lamps) to 5,000€ (installation of external thermal insulation on the roof).

VIII. Conclusions

In this paper the ERACOBUILD "Countdown to Low Carbon Homes" project is presented along with its current progress to date in Cyprus. Cyprus Energy Agency is undertaking this project in order to develop a one stop service for the sustainable energy retrofit of homes in Cyprus.

In Cyprus twenty-one households have been selected to participate in the action research following a call for expressions of interest. An onsite energy visit from CEA energy experts has been carried out for all households in order to advise on possible measures and ways to reduce the current energy consumption and to calculate the energy performance certificate. Additionally, in each household a smart meter has been installed (kind courtesy of CEA) in order both to log the energy consumption before and after the application of the suggested retrofit measures and also to assist the occupants of the house understand the main energy consuming devices and consequently help change their energy behaviour.

The data collected during the energy visits are currently being evaluated and it is expected that by the end of autumn of 2014 the results will be completed and a report will be sent to the homeowners.

Additionally two support groups have been created: the Regional Advisory Group and the Local Installers Group. Both groups meet on a regular basis to exchange information and opinions on the progress, implementation and outcomes of the project.

During the 1st meeting of the LIG (20th of December 2012) a questionnaire was completed by the LIG members so as to identify the possible problems, barriers, opportunities and solutions concerning the energy renovations of the residential sector in Cyprus.

According to the results of the questionnaires the main barrier to the promotion of energy renovations in the residential sector is their cost 26% followed by the bureaucracy 24%. In the same manner the financial are considered to be the main difficulties by 42% encountered before, during or after a renovation. Thus, the required support necessary to overcome these barriers and promote the energy renovations in the residential sector are the development of new Grant Schemes 31%, the development of special loans by the banks 24% and the correct information of the public 24%.

IX. Biographies

Gregoris Panayiotou was born in Limassol, Cyprus on February 18, 1983. He graduated from the Technological Educational Institute of Athens first of his class as an Energy Technology Engineer in 2007. He had his MSc in Energy in Heriot-Watt University, Edinburgh where he graduated in 2008 with Distinction.

He is currently employed at Cyprus University of Technology as a Research Associate in a nationally funded project concerning the study and the deeper understanding of the thermosiphonic phenomenon that occurs in solar water heating systems that operate thermosiphonically.

In the past he had also worked in two research projects. The first project was funded by the Research Promotion Foundation of Cyprus and concerned the categorization of buildings in Cyprus according to their energy performance. The second project concerned the application and evaluation of advanced absorber coatings for parabolic trough collectors.

The main simulation tool he had used in most of his work is TRaNsient SYstem Simulation (TRNSYS) while he had also worked with HOMER and PVSyst.

He currently has 9 Journal publications and 12 Conference publications and his special fields of interest include wide range applications of Renewable Energy Sources systems and Energy Efficiency in buildings.

Anthi Charalambous was born in Paphos, Cyprus, on January 19, 1973. She is a Chemical Engineer by background, graduated from the National Technical University of Athens, and holds a MSc in Environmental Engineering, a Masters in Business Administration (MBA) and a MSc in Renewable Energy and Energy Management.

At the beginning of her career she worked abroad in environmental management, wastewater management and treatment and industrial pollution. From 2001 she began working in the field of Renewable Energy in Cyprus and Brussels. In 2007 she joined the European Commission Directorate General for Energy in the unit of renewable energy technologies. She is the Director of Cyprus Energy Agency since November 2008.

She participated in more than 60 conferences as invited speaker and she has released several publications and she is co-author of a number of papers.

Maria Ioannidou was born in Lefkosia in the Cyprus, on April 24, 1981. She holds an energy resources management degree graduated in 2005,

MBA and master on Environmental Education and Sustainable Development.

She is employed by the Cyprus Energy Agency since 2009. She is responsible for the development of educational material for primary and secondary education, and other target groups adults and public. She is entitled to visit schools in Cyprus (upon request) to present and demonstrate relevant materials including experiments for motivating and educating students on renewable energies, energy savings and sustainable transport as well to visit local communities to motivate and educate people on the field. Furthermore, she provides technical support in co-financed projects, she is an energy expert for buildings.

Organised by:

Electricity Authority of Cyprus

CYPRUS EMPLOYERS & INDUSTRIALISTS FEDERATION OEB

Η Πράξη συγχρηματοδοτείται από την Ευρωπαϊκή Ένωση (ΕΤΠΑ) και από Εθνικούς Πόρους της Ελλάδας και της Κύπρου

Πρόγραμμα Διασυνοριακής Συνεργασίας Ελλάδα - Κύπρος 2007-2013
ΕΠΕΝΔΥΟΥΜΕ ΣΤΟ ΚΟΙΝΟ ΜΑΣ ΜΕΛΛΟΝ

ΗΠΗΝ
Ηλιοθερμική Παραγωγή Ηλεκτρισμού και Νερού

Sponsored by:

ΕΤΕΚ

ecOiko.eu
Cyprus's Green Eco Directory

CYPRUS TOURISM ORGANISATION

Endorsed by:

The Cyprus Institute

cyprus energy regulatory authority

RES & EC special fund

AIMS Energy

cygas

University of Cyprus

CIPA
CYPRUS INVESTMENT PROMOTION AGENCY

Coordinated by:

easy CONFERENCES